

POST-IRRADIATION EXAMINATION AND
IN-PILE MEASUREMENT TECHNIQUES
FOR WATER REACTOR FUELS

The following States are Members of the International Atomic Energy Agency:

AFGHANISTAN	GHANA	NIGERIA
ALBANIA	GREECE	NORWAY
ALGERIA	GUATEMALA	OMAN
ANGOLA	HAITI	PAKISTAN
ARGENTINA	HOLY SEE	PALAU
ARMENIA	HONDURAS	PANAMA
AUSTRALIA	HUNGARY	PARAGUAY
AUSTRIA	ICELAND	PERU
AZERBAIJAN	INDIA	PHILIPPINES
BAHRAIN	INDONESIA	POLAND
BANGLADESH	IRAN, ISLAMIC REPUBLIC OF	PORTUGAL
BELARUS	IRAQ	QATAR
BELGIUM	IRELAND	REPUBLIC OF MOLDOVA
BELIZE	ISRAEL	ROMANIA
BENIN	ITALY	RUSSIAN FEDERATION
BOLIVIA	JAMAICA	SAUDI ARABIA
BOSNIA AND HERZEGOVINA	JAPAN	SENEGAL
BOTSWANA	JORDAN	SERBIA
BRAZIL	KAZAKHSTAN	SEYCHELLES
BULGARIA	KENYA	SIERRA LEONE
BURKINA FASO	KOREA, REPUBLIC OF	SINGAPORE
BURUNDI	KUWAIT	SLOVAKIA
CAMEROON	KYRGYZSTAN	SLOVENIA
CANADA	LATVIA	SOUTH AFRICA
CENTRAL AFRICAN REPUBLIC	LEBANON	SPAIN
CHAD	LESOTHO	SRI LANKA
CHILE	LIBERIA	SUDAN
CHINA	LIBYAN ARAB JAMAHIRIYA	SWEDEN
COLOMBIA	LIECHTENSTEIN	SWITZERLAND
CONGO	LITHUANIA	SYRIAN ARAB REPUBLIC
COSTA RICA	LUXEMBOURG	TAJIKISTAN
CÔTE D'IVOIRE	MADAGASCAR	THAILAND
CROATIA	MALAWI	THE FORMER YUGOSLAV REPUBLIC OF MACEDONIA
CUBA	MALAYSIA	TUNISIA
CYPRUS	MALI	TURKEY
CZECH REPUBLIC	MALTA	UGANDA
DEMOCRATIC REPUBLIC OF THE CONGO	MARSHALL ISLANDS	UKRAINE
DENMARK	MAURITANIA	UNITED ARAB EMIRATES
DOMINICAN REPUBLIC	MAURITIUS	UNITED KINGDOM OF GREAT BRITAIN AND NORTHERN IRELAND
ECUADOR	MEXICO	UNITED REPUBLIC OF TANZANIA
EGYPT	MONACO	UNITED STATES OF AMERICA
EL SALVADOR	MONGOLIA	URUGUAY
ERITREA	MONTENEGRO	UZBEKISTAN
ESTONIA	MOROCCO	VENEZUELA
ETHIOPIA	MOZAMBIQUE	VIETNAM
FINLAND	MYANMAR	YEMEN
FRANCE	NAMIBIA	ZAMBIA
GABON	NEPAL	ZIMBABWE
GEORGIA	NETHERLANDS	
GERMANY	NEW ZEALAND	
	NICARAGUA	
	NIGER	

The Agency's Statute was approved on 23 October 1956 by the Conference on the Statute of the IAEA held at United Nations Headquarters, New York; it entered into force on 29 July 1957. The Headquarters of the Agency are situated in Vienna. Its principal objective is "to accelerate and enlarge the contribution of atomic energy to peace, health and prosperity throughout the world".

IAEA-TECDOC-CD-1635

**Post-Irradiation Examination
and In-Pile
Measurement Techniques
for Water Reactor Fuels**

INTERNATIONAL ATOMIC ENERGY AGENCY
VIENNA, 2009

COPYRIGHT NOTICE

All IAEA scientific and technical publications are protected by the terms of the Universal Copyright Convention as adopted in 1952 (Berne) and as revised in 1972 (Paris). The copyright has since been extended by the World Intellectual Property Organization (Geneva) to include electronic and virtual intellectual property. Permission to use whole or parts of texts contained in IAEA publications in printed or electronic form must be obtained and is usually subject to royalty agreements. Proposals for non-commercial reproductions and translations are welcomed and considered on a case-by-case basis. Enquiries should be addressed to the IAEA Publishing Section at:

Sales and Promotion, Publishing Section
International Atomic Energy Agency
Vienna International Centre
PO Box 100
1400 Vienna, Austria
fax: +43 1 2600 29302
tel.: +43 1 2600 22417
email: sales.publications@iaea.org
<http://www.iaea.org/books>

For further information on this publication, please contact:

Nuclear Fuel Cycle and Materials Section
International Atomic Energy Agency
Vienna International Centre
PO Box 100
1400 Vienna, Austria
email: Official.Mail@iaea.org

**POST-IRRADIATION EXAMINATION AND IN-PILE
MEASUREMENT TECHNIQUES FOR WATER REACTOR FUELS**

IAEA, VIENNA, 2009
IAEA-TECDOC-CD-1635
ISBN 978-92-0-162709-4
ISSN 1684-2073
© IAEA, 2009
Printed by the IAEA in Austria
December 2009

FOREWORD

Taking into consideration the prospects of growing energy demands, dwindling supplies of fossil fuels and global warming, nuclear power seems to be the only economically feasible and carbon-free energy option for the near future. Safe operation of existing nuclear power plants and development of future reactor systems are to follow a long-term strategy driven by an optimal plant management and life extension policy, reinforcement of the safety and reliability, mature waste and resource management. Economic efficiency strives for fuel operation under more demanding duties that include higher burnup, longer fuel cycles, higher temperatures and transient regimes. Justification of these new challenging conditions, as well as new advanced materials and designs, require new techniques and methods for measurement and analysis. It is always necessary to prove that fuel safety margins have not been affected by higher duties that presume availability of sufficient information on nuclear fuel behaviour under normal, transient and accident conditions. The quality and quantity of required data are defined by the status of destructive and non-destructive methods and capabilities, availability of post-irradiation and in-pile examination facilities.

The cost of irradiated materials testing is continuously increasing, while the availability of test facilities has steadily decreased in the last decades, resulting in a need for their more efficient use, including international exchange of information and collaboration. The IAEA traditionally enforces co-operation exchange in this area through technical meetings (TMs) aimed at discussion of status, problems and perspectives of hot labs and material test reactors, development and application of new techniques for examination and characterisation of reactor materials.

Two such TMs were organized, on 27-30 November 2006 in Buenos Aires, Argentina (Hot Cell Post-Irradiation Examination Techniques and Poolside Inspection of Water Reactor Fuel Assemblies) and on 3-5 September 2007 in Halden, Norway (Fuel Rod Instrumentation and In-Pile Measurement Techniques). These two TMs were the sixth and the seventh in a series of the IAEA subject meetings held in 1981 and 1984 (Tokyo, Japan), 1990 (Workington, United Kingdom), 1994 (Cadarache, France) and 2001 (Dimitrovgrad, Russian Federation) upon recommendations of the Technical Working Group on Water Reactor Fuel Performance and Technology (TWGFPT). Co-ordinated Research Programmes on Examination and Documentation Methodology for Water Reactor Fuel (Part 1, 1994-1989, and Part 2, 1992-1995) resulted in the publication of two guidebooks (Technical Reports Series No. 322, 1991 and No. 385, 1997 respectively). All of these activities were found to be of value in advancing experimental methods and measurement techniques for better understanding of fuel behaviour.

The IAEA expresses its gratitude to all participants of both TMs for their contributions to this publication. The IAEA officer responsible for this publication was V. Inozemtsev.

EDITORIAL NOTE

This CD-ROM has been prepared from the original material as submitted by contributors. Neither the IAEA nor its Member States assume any responsibility for the information contained on this CD-ROM.

The use of particular designations of countries or territories does not imply any judgement by the publisher, the IAEA, as to the legal status of such countries or territories, of their authorities and institutions or of the delimitation of their boundaries.

The mention of names of specific companies or products (whether or not indicated as registered) does not imply any intention to infringe proprietary rights, nor should it be construed as an endorsement or recommendation on the part of the IAEA.

CONTENTS

Summary

PART 1. PROCEEDINGS OF THE IAEA TECHNICAL MEETING HELD IN BUENOS AIRES, ARGENTINA 2006

SESSION 1: PIE INTERNATIONAL EXPERIENCE

Post irradiation examination of water reactor fuel assemblies in India

S. Anantharaman, U.K. Viswsanathan, S. Chatterjee, E. Ramadasan, K. Unnikrishnan, J.L. Singh, ... K.S. Balakrishnan, P.M. Ouseph, H.N. Singh, R.S. Sriwastaw, P. Pishra, D.N. Sah

PIE results and new techniques applied for 55 GWd/t high Burnup fuel of PWR

T. Tsuda, Y. Yamaguchi, Y. Kosaka, T. Kawagoe, T. Kitagawa

Underwater fuel inspection for irradiated LWR fuels in the Republic of Korea

Y.B. Chun, D.K. Min, G.S. Kim, J.R. Park, J.Y. Park

Performance of HEU and LEU fuels in Pakistan Research Reactor-1 (PARR-1)

S. Pervez, M. Latif, M. Israr

SESSION 2. HOT CEL LABS AND PIE FACILITIES

PIE in hot cells and poolside: Facilities and techniques applied in Argentina

G. Ruggirello

Presence of DEA hot laboratories, with a focus on LECI

J.Y. Blank

Overview of post-irradiation examination techniques applied at PSI for light water reactor fuel characterization

G. Bart, J. Bertsch, D. Gavillet, I. Gunther-Leopold, Ch. Hellwig, H. Wiese

The LFR radiochemical facility

A. Stsankevicius

SESSION 3. PIE TECHNIQUES AND APPLICATIONS (PART-1)

Examination of the WWER-440 fuel after irradiation up to burnup 70 MWd/kg

Using electron probe microanalysis and scanning electron microscopy

F. N. Kryukov, S.V. Kuzmin, G.D. Lyadov, O.N. Nikitin, V.P. Smirnov

Burnup estimation of nuclear fuels with a gamma scanning test

Heemoon Kim, Hong-ki Lee, Byoung-ok Yoo, Jae-min Sohn, Bong-goo Kim, Yong-sun Choo, Kwon-pyo hong

Burnup determination in 20% enrichment uranium compounds

D. Devida, E. Gautier, D. Gil, A. Stankevicius

The chemistry of spent nuclear fuel from X-ray absorption spectroscopy

J.A. Forner, A. Jeremy Kropf, J.C. Cunnane

SESSION 3. PIE TECHNIQUES AND APPLICATIONS (PART-2)

Distortion measurement for fuel assemblies with ultrasonic technique

Xu Yuanhuan, Nie Yong

LWR fuel gas characterization at CEA Cadarache LECA-STAR hot laboratory

J. Noiroi, C. Gonnier, L. Desgranges, Y. Pontillon, J. Lamontagne

Development of a non-destructive post-irradiation examination technique using high-energy X-ray computer tomography

K. Katsuyama, T. Nagamine, Y. Nakamura

Modelling of V-HTR fuel elements and coated particles: Needs of PIE in support to the European "Raphael" and GEN-IV projects

G. Ruggirello, E.H. Toscano

Fracture surface analysis of an irradiated hafnium control rod by metallographic replicas

G. Domizzi, D. Ciriani, G. Vigna, E. Chomik, A. Iorio

Effect of irradiation and hydrogen concentration on fracture toughness of a hafnium control rod

G. Domizzi, G. Vigna, E. Chomik, D. Ciriani, A. Iorio

SESSION 4. INTERNATIONAL PROJECTS AND DATA BASE

The European HOTLAB project and its future with emphasis on its Internet catalogue

L. Sannen, W. Goll, J.Y. Blane, C. Verdeau

Status of the iNFCIS IAEA PIE facilities database

H.K. Jenssen

PART II. PROCEEDINGS OF THE IAEA TECHNICAL MEETING HELD IN HALDEN, NORWAY 2007

SESSION 1. IRRADIATION TESTING TECHNIQUES — EXPERIENCE AND DEVELOPMENT

Fuel irradiation testing technology at SCK•CEN: Experience and developments

L. Vermeeren, J. Dekeyser

Instrumentation and re-fabrication techniques used for fuel rod performance

Characterization in the Halden reactor

C. Helsingreen

Hard drilling technique for making a center hole of irradiated fuel pellets

F. Berdoula, k. Silberstein

Improving high-temperature and fission gas release measurements in irradiation experiments

J.F. Villard, D. Fourmentel, n.L. Hullier, T. Lambert, E. Muller

SESSION 2. IRRADIATION TESTING FACILITIES AND CAPABILITIES

Instrumentation techniques in NSRR experiments

Y. Muramatsu, Y. Udagawa

Test methods of WWER fuel with simulating transitive and emergency modes

In the MIR reactor

A.L. Izhutov, A.V. Burukin, V.V. Kalygin, V.A., Ovchinnikov, V.N. Shulimov

Irradiation facility project

O. Beuter, S. Halpert, A. Marajofsky, L. Vázquez

Remote on-line measurement of fission gas release during irradiation testing

F.C. Klaassen, M.A.C. van Kranenburg, K. Bakker, R.P.C. Schram

In-core measurements of fuel clad — Coolant interactions in the Halden reactor

P. Bennett

Flux mapping and channel temperature monitoring system for Tapp3&4

R.K. Patil

Design of the on-line fission gas release analysis system in the high flux reactor Petten

M. Laurie, A. Marmier, G. Berg, M.A. Fütterer

SESSION 4. HOT CELL FACILITIES AND PIE

RIAR hot cells material testing complex, methodical possibilities

Y.D. Goncharenko, V.N. Golovanov, A.E. Novoselov, V.D. Risovany

Diffusion of Xenon gas in nuclear fuels with oxygen potentials in 0.1 MWd/t-U of a Burnup

Heemoon Kim, Kwangheon Park, Bong Goo Kim, Yong Sun Choo, Woo Seog Ryu

Post irradiation examinations of a Pakistani fabricated fuel bundle irradiated at
Karachi nuclear power plant

M.S. Zaheer

SESSION 5. PRACTICAL USES OF IN-PILE AND PIE DATA

Fuel failure and reconstitute in Qinshan nuclear power plant

Xue Xincui

A negative void reactivity PHWR fuel element for extended Burnup: Design, modelling,
experimental support and a proposal for an irradiation test

A.C. Marino, D.O. Bransnarof, H.A. Lestani, P.C. Florido

SUMMARY

Today nuclear technology plays an increasingly important role in our everyday lives, i.e. in energy, industry, medical and environmental applications. Faced with the immediate world's problems of economics, greenhouse gas emissions and water scarcity, as well as the future demand for electricity, nuclear power would provide a long term solution. However better reactor design is required to fulfil such objectives. Therefore, after its stagnation, nuclear engineering has been going through a revival which is reflected in the start of such international projects as Generation IV, INPRO, GNEP and others.

These development programs include consideration of a wide range of nuclear reactors of different types and purposes, from high temperature gas cooled and fast reactors with different coolant options to thermal water cooled ones which have both enhanced operating safety and efficient operation due to the optimal design and coolant parameters, etc. Requirements for enhanced reactor safety and efficiency make it necessary to perform precise in- and post-reactor experiments and, consequently, to use more up-to-date measurement equipment and analysis techniques, thus developing hot labs and research reactor facilities. Application of new techniques for measurement and analysis is also related to the consideration of advanced materials for future innovative nuclear reactors with challenging operational conditions that differ greatly from those of the existing nuclear reactors.

The necessity to use the most up-to-date precise equipment follows from the necessity to prolong the operating lifetime of the existing NPPs. The designed lifetime of units of many NPPs under operation is practically over. Since these units are in satisfactory condition and the construction of new NPPs is very expensive, it is reasonable to justify their lifetime more precisely and prolong it. However, it requires additional in- and post-reactor examinations.

The majority of the hot labs were designed in the 1960s when the construction of NPPs was being started. Evidently it can be assumed that infrastructure with basic unique equipments is old enough, both morally and physically, and needs to be up-graded or replaced.

Thus, a sharp increase of the hydrocarbon fuel cost, green-house effect, necessity to construct more safe and efficient NPPs, justification of the lifetime prolongation of the existing NPPs, moral and physical ageing of the hot labs and research reactors equipment lead to the strong necessity to develop more perfect and more precise methods and equipment to examine irradiated components of nuclear reactors, first of all the most expensive one – nuclear fuel.

Now the national hot laboratories and material testing reactors usually act as individual independent research establishments without any common and coordinated technical and business strategy towards the future needs and challenges.

Even if there are not many joint programs for the development of nuclear power engineering in different countries, the method base and accumulated experience of the in- and post-reactor experiments should be widely shared so as to decrease the cost of this base in each country and to enforce its development. Thus, both problems and results of the application of new techniques to examine nuclear reactor components, as well as the conditions of separate labs should be discussed at the international level.

The IAEA technical meetings are one of the most convenient means of arranging such discussion on the problems of the hot labs and research reactors development and application of new original techniques for examination of reactor materials properties.

This publication represents a summary and proceedings of the two technical meetings (TMs) organized by IAEA on the subjects of Hot Cell Post-Irradiation Examination (PIE)

Techniques and Pool Side Inspection of Water Reactor Fuel Assemblies and Fuel Rod Instrumentation and In-Pile Measurement Techniques. The first TM was held from 27-30 November 2006 in Buenos Aires, Argentina, while the second TM was organized on 3-5 September 2007 in Halden, Norway. The purpose of these technical meetings was to provide an overview of the status of in-pile and post irradiation techniques of water reactor fuel examination with an emphasis given to experimental methods applied to high burnup fuel. The majority of presentations made at the technical meeting in Argentina and at the sessions on post irradiation examination techniques in Norway either directly described the status of different national hot labs (methods, infrastructure) or described these labs by the examples of investigations carried out in and typical of these labs. Other papers presented at the meetings described the progress achieved in non destructive and destructive PIE techniques used for investigation of water reactor fuel. Recent practices in high burn up fuel investigation revealed the importance of advanced PIE techniques, such as 3-D tomography, secondary ion mass spectrometry and scanning electron microscopy, as well as advanced in-pile measurement techniques for better understanding of the mechanisms of fuel behaviour under irradiation.

TM-ARGENTINA-2006 HOT CELL POST-IRRADIATION EXAMINATION TECHNIQUES AND POOL SIDE INSPECTION OF WATER REACTOR FUEL ASSEMBLIES

This TM was hosted by the Comision Nacional de Energia Atomica (CNEA) and provided an overview about the status of post-irradiation examination (PIE) techniques for water reactor fuel assemblies and their components. On the last day of the meeting a technical visit to CONUAR-FAE and CNEA Hot Cell Laboratories was organized. The advanced PIE techniques applied to high burn up fuel including non destructive and destructive PIE techniques, fuel rod refabrication and instrumentation techniques for in pile experiments and poolside inspection methods were considered. That was the sixth TM in a series of IAEA subject meetings which have been held in 1981 and 1984 (Tokyo, Japan), 1990 (Workington, UK), 1994 (Cadarache, France) and 2001 (Dimitrovgrad, Russian Federation) upon the advice of the IAEA Technical Working Group on Fuel Performance and Technology (TWGFPT). As per recommendations of its meeting in 2005, the development status of the IAEA PIE facilities/techniques database was discussed and evaluated during this TM-2006.

Gabriel Ruggirello, Chairman of this meeting, welcomed the participants and thanked IAEA for providing this opportunity for international discussion. He called this meeting to strengthen the cooperation between twenty one participating countries. In his welcoming address, the importance of hot cell contribution was stressed to implement the new National Nuclear Plan.

The Scientific Secretary of the Meeting, Victor Inozemtsev from IAEA, presented the status of IAEA activities in the areas of fuel performance analysis and advanced nuclear materials development. In this presentation it was explained how the IAEA Nuclear Fuel Cycle & Material Section, Subprogram B.2 on Nuclear Power Reactor Fuel Engineering and the TWG on Fuel Performance and Technology respond to the current challenges and increasing demands on fuel materials.

In this TM, a total of eighteen papers were organised into four sessions. These papers were presented and discussed on the subjects of all aspects of non destructive (e.g. dimensional measurements, oxide layer thickness measurements, gamma scanning and tomography, neutron and X ray radiography, etc.) and destructive (e.g. micro structural studies, elemental

and isotopic analysis, measurement of physical and mechanical properties, etc.) PIE techniques and methods used for investigation of water reactor fuel. The ideas and discussion carried in this TM are summarised in this chapter.

SESSION 1: PIE International Experience

In Session 1 four papers were presented. Three of them demonstrated comprehensive PIE studies, hot cell laboratories and poolside facilities under operation in India, Japan and Republic of Korea respectively, whereas the fourth paper described the Pakistani activities on the poolside inspection of Material Testing Reactor (MTR) fuel.

The papers in Session 1 showed similarities and differences in the techniques applied in the different laboratories. In most cases, techniques are similar, but the applied methods are different and sometimes innovative depending on the level of the laboratories. The objectives of the tests are different in each case, depending on the needs to be addressed.

During the panel discussion at the end of the meeting the need for some standardisation in the field of PIE was pointed out, but it was concluded that standardisation is difficult due to long traditions in some laboratories and the difficulty arising from the need to license a new technique, as well as financial problems.

Sundaresan Anantharaman from Bhabha Atomic Research Centre, India, presented a paper on Post Irradiation Examination of Water Reactor Fuel Assemblies. India has two boiling water reactors (BWR), each with a capacity for the generation of 165 MWe and 12 pressurized Heavy Water Reactors (PHWR), ten of them with a capacity of 220 MWe and 2 PHWRs, each with a capacity of 540 MWe. The BWRs use enriched UO₂ fuel and PHWRs use natural UO₂ as the fuel. The fuel utilized in PHWRs is reprocessed to extract plutonium. This plutonium will be used in fast reactors, which is the second stage of the Indian nuclear power programme. As a part of the Pu recycling programme, MOX fuel will be used in the BWRs. This paper presented the salient features of the findings of PIE on some of the experimental MOX fuels and PHWR fuels that have been examined in the recent past. Trying to find out the reasons for damage of fuel elements at low and high fuel burn up, the Bhabha Atomic Research Centre demonstrated its capabilities to investigate the irradiated fuel assemblies with mixed uranium-plutonium oxide fuel. Methodical capabilities of the Centre are mainly associated with application of such methods as visual examination, gamma scanning, profilometry, fission gas analysis, autoradiography, metallography and mechanical tests on the cladding.

The PIE Results and New Techniques Applied for 55 GWd/t High Burnup Fuel of PWR was comprehensively presented and explained by Tomohiro Tsuda from Nuclear Development Corporation Japan. For post irradiation examination of irradiated fuel elements, for instance, up to 55 GWd/t the Nuclear Development Corporation, besides usual demonstration of its methodical capabilities (γ scanning was applied, measurements of dimensions, measurement of Fission Product (FP) gas release rate, measurements of cladding oxide film thickness and hydrogen content, as well as measurements of cladding mechanical properties), proposed two new original post irradiation examination methods, such as a tube-shape axial tensile test and a pellets density measurement method for high burn up fuels. The PIE was conducted at the fuel hot laboratory of the NDC to check the soundness of 55 GWd/t high burnup fuel and any effects of improved corrosion-resistant claddings and large grain-size pellets aimed at reducing the release of FP gas. The proposed methods make a good contribution to the methods used for measurement of mechanical properties of fuel element claddings and

irradiated nuclear fuel density. The main objective was the comparison among different cladding and fuel materials; Zry-4, MDA and Zirlo for cladding and standard, large grain size and pellet containing Gadolinia for fuel material. Particular emphasis was given to an improved method for the clamping jig of samples devoted to cladding mechanical testing and also to the fuel density determination. The obtained results permitted the verification of the improvement of the cladding corrosion resistance and the reduction of the fission gas release in the fuel pellet.

Y.B. Chun from Korea Atomic Energy Research Institute, Republic of Korea presented the results of Underwater Fuel Inspection for LWR Irradiated Fuel in Republic of Korea. Most of irradiated fuel assemblies are inspected in the pool of NPP sites during regular overhaul outages and some of them are selectively transported to the post-irradiation examination facility (PIEF) in KAERI for PIE to evaluate the irradiation performances as well as the fuel integrities. The data obtained from the PIE is used for the improvement of nuclear fuel performances and operation reliabilities. For instance, a comprehensive underwater fuel inspection system was developed and was used to confirm the integrities of the fuels to be reloaded in the next cycle of reactor operation. Recently, PIE activities focused on the oxidation condition of the cladding tube as well as the failure inspections to cope with the licensing requirements of fuel integrities under the highly extended burn up conditions. In order to provide appropriate underwater fuel examination technologies for the safeguard inspections, spent fuel management and fuel service activities, and in order to support nuclear R & D program in Republic of Korea, various kinds of underwater fuel examination technologies, such as fuel rod verification technology, exponential experiment, hold-down spring force measurement technology, image processing based dimensional measurement methods and burn up determination technology by underwater gamma spectroscopy were developed. The paper concludes that the developed and implemented examination techniques allowed assuring and improving the performance of the nuclear fuel during service in the NPP.

Showket Pervez, from Pakistan Institute of Nuclear Science and Technology (PINSTECH), presented the results of the in-pool visual inspection of the PARR-1 MTR fuel elements carried out within its transition from LEU fuel to HEU fuel. The inspection was made with a specially installed fuel failure detection system based on delayed neutrons. In addition, special tools were developed to repair fuel damaged during handling. The post irradiation visual inspection of both HEU and LEU fuels has never shown any damage to or distortion of the fuel, monitoring and water sampling of the reactor pool and the wet storage pool has never shown any signs of fission product release during operation as well as storage after irradiation. One HEU fuel element, which was partly damaged during fuel handling, was repaired and replaced in the core and it attained 28 % burn up without giving any problem. The fuel failure detection system has also recorded no incident of fuel failure during operation.

SESSION 2: Hot Cell Laboratories and PIE Facilities

In Session 2 six papers were presented. The hot cell laboratories and PIE facilities in the Russian Federation, France, Switzerland and Argentina were comprehensively described. In addition, a summary of post-irradiation studies on PHWR-components at CNEA hot cells in Argentina was presented.

Yury Goncharenko from the Research Institute of Atomic Reactors (RIAR), Russian Federation, explained the RIAR Hot Cells Material Testing Complex Methodical Possibilities.

The RIAR hot laboratory in Dimitrovgrad is the largest in the country and has been in operation for more than 40 years. The specialists have gained great experience in conducting examinations of irradiated materials, methods that are the most suitable for investigation of such materials have been selected. In this laboratory a complete characterization of fuel elements, fuel rods, fuel, absorber and structural material, including destructive and non destructive analysis, is currently being performed prior and after irradiation. The Russian hot laboratory is using intensively a large number of various methods of measurement and the analysis. For non destructive analysis of full scale fuel rods and fuel assemblies, measurements of fuel rod parameters, visual examinations, gamma scanning, vortex-current defectoscopy, etc were explained. For destructive analysis; fission products release, gamma scanning, metallography and micro-hardness, density and porosity, thermal conductivity and electric resistance, X ray analysis, dilatometry, TEM, SEM, EPMA, AES, SIMS, mechanical testing (tensile, compression, bending, impact, etc.) were taken into description. In addition, investigations are conducted in the field of radiation damage physics and the modelling of core materials and fuel elements.

Jean-Yves Blanc from CEA, France presented the main features of Hot Laboratories under CEA and mentioned the studies in LECA facility. After several years of optimization and refurbishing, a coherent set of laboratories was setup including several facilities in four locations:

- Fuel studies in the LECA-STAR facilities, in Cadarache: Possibilities range from classical non-destructive examinations, puncturing and metallography up to EPMA and SIMS analyses. Thermal treatments and long term storage tests on LWR fuels are also performed. Particular emphasis is given to micro-structural analyses and fission gas release studies.
- Plutonium and minor actinides fuels (GEN IV and MOX) in LEFCA are also studied in Cadarache.
- Reprocessing, partitioning and waste immobilization in ATALANTE, Marcoule: It ranges from theoretical chemistry to technological validation, as a support to La Hague industrial facilities and to address governmental issues on radioactive waste disposal, including partitioning and transmutation.
- Micro structural studies, corrosion analysis and mechanical testing in LECI, Saclay: LECI has all the panel of equipments for performing micro structural, corrosion analyses and mechanical testing characterization on irradiated metallic and ceramics materials (pressure vessel steels, fuel cladding and structure materials etc). Its equipments include non destructive examinations on short fuel rods, hydrogen pick-up measurement, spark machining, a corrosion loop with autoclaves, and micro structural analyses with EPMA, SEM, TEM and Raman. Its new building, started last year and includes twenty cells with up-to-date mechanical testing facilities (tensile, burst, creep, impact, toughness, IASCC tests).

These facilities cover the whole range of studies performed on fuel elements components and structural materials mainly for PWRs.

LECA-STAR and LECI are strongly connected to CEA fuel and material testing reactors. The radiation testing in France is performed at experimental reactors such as Osiris for a few more years, Phenix until its scheduled closure in 2009 and the JHR6 as of 2014. CEA R&D efforts targeting these two fast neutron systems would also bring innovations in fuel recycling. Osiris

and Phenix of today and JHR of tomorrow with fuel rod re-fabrication capacity include instrumented experiments.

At present, all four main French labs dealing with the development of nuclear power engineering and working with fissile materials are located in new buildings or reconstructed ones and have perfect methodical support.

Two papers were presented by CNEA representatives. The first one was entitled Summary of Post Irradiation Studies on PHWR Components at CNEA Hot Cells and the second one explained the The LFR radiochemical Facility. These two presentations covered all the activities in Argentina concerning hot cell laboratories and poolside activities. The poolside activities include visual examination and fuel inspection and disassembling as well as metallurgy of fuel elements and components (tubes and channels) and gamma spectroscopy. The hot cell facility is divided into two sections; the physical hot cells and the radiochemical hot cells covering visual examination, metrology, density, eddy current techniques, gamma scanning, metallography and ceramography, burnup determination and radiochemical analysis of different materials and solutions.

An expert from Paul Scherrer Institute PSI, Bart G., Switzerland presented the Overview of Post Irradiation Examinations applied at PSI for Light Water Reactor Fuel Characterization. Within long term cooperation agreements, the PSI Laboratory for Material Behaviour (LWV) in the Department for Nuclear Energy and Safety (NES) has characterized pathfinder PWR- and BWR fuel and cladding of the Swiss nuclear power stations, Gösgen (KKG) and Leibstadt (KKL) in many PIE sequences. Based on these pathfinder fuel pin and lead assembly tests, the fuel in these reactors has been continuously improved over the years and reaches a batch burn up today which is nearly twice as high as at the beginning of 1980. In addition to providing scientific analytical services with respect to accurate engineering fuel and cladding PIE data, PSI itself as a research organization, undertakes basic and applied scientific research. The Laboratory for Material Behaviour focuses on cladding corrosion, hydrogenation, mechanical aging mechanisms and the fission gas diffusion process in the fuel.

The PIE tools available at PSI consist of non destructive methods (visual examination, gamma scanning, profilometry and EC defect and oxide thickness measurements), puncturing and fission gas analysis, and destructive investigations of cut samples (metallography/ceramography, hydrogen hot gas extraction, electron probe micro-analysis (EPMA), secondary ion mass spectroscopy (SIMS), scanning and transmission electron microscopy (SEM and TEM). Recently, laser ablation inductively coupled plasma mass spectroscopy (LA-ICPMS), x ray absorption spectroscopy, and mechanical testing facilities are also included.

While commercial high burn up programs often request standard engineering data like cladding oxide thickness values and hydrogen contents or fuel pin fission gas release values, PSI has improved such analytical techniques. Additionally, as per presented talk, they have performed independent research in order to improve the fundamental understanding of the irradiation behaviour e.g. by elucidating the corrosion process with detailed characterization of the cladding metal-oxide interface using TEM, local fission product and actinide isotopic distributions in fuel cross sections with SIMS and LA-ICPMS or by studying the conditions for hydride reorientation in hydrogenated claddings.

The PSI PIE tools support the Swiss and international nuclear fuel industry in the best possible manner with scientific service work in their strive to develop high performance, high burn up fuel, which is economically attractive both with respect to reduced procurement and

waste volume costs, but for which the safety margins have also to be proven during the full life.

Last presentation comprehensively focussed on the LFR radiochemical facility. The Facility is designed and constructed with a hot-cells line, a glove-boxes and fume-hoods as per requirements of work with radioactive materials. This facility is being used for different research and development programs in the Nuclear Fuel Cycle field, such as the burn up determination, absolute burn up measurement, the radiochemical analysis of different materials and solutions, the evaluation of radioactive waste immobilization processes and researches on burnable poisons.

SESSION 3: PIE Techniques and Applications

Session 3 included ten papers on PIE techniques and applications. The burn up determination methods and evaluation of fuel after irradiation were focused in these presentations. Determination of burn up may be achieved by measurement (i.e. destructive and non destructive methods e.g. measurement of ^{148}Nd formation by mass spectroscopy, or gamma scanning) and by calculation methods using computer codes using irradiation histories etc.

In Hee-Moon Kim's paper (Korea Atomic Energy Research Institute), a non-destructive approach i.e. burn up of Nuclear Fuels with gamma scanning test was presented. In his presentation, he provided the comparison of burn up by code computation (ORIGEN-ARP) with the results deduced from gamma scanning using $^{134}\text{Cs}/^{137}\text{Cs}$ ratio. The results were good for PWR spent fuel, but showed a 15% discrepancy for HANARO-irradiated capsules. Attempts are being made to find a dedicated code for this research reactor. In this regard a preliminary method was proposed, that consists of using ^{137}Cs total counting with reference samples, calibrated by ^{148}Nd mass spectroscopy method. But it does not account for Cs migration and variation of $^{134}\text{Cs}/^{137}\text{Cs}$ ratio.

C. Devida, an expert from National Atomic Energy Commission, Argentina presented the Burn up determination in 20% enrichment uranium compound by destructive method. The ^{148}Nd burn-up determination has been implemented for the first time in Argentina, in the LFR laboratory of CNEA, by D. Gil and his colleagues. A series of dissolutions of MTR irradiated fuel was performed and determined its isotopic composition of Uranium, Plutonium and neodymium (as burn up monitor), by the thermal ionization mass spectrometry (TIMS). It was concluded that this technique of burn up measurement is powerful and accurate when properly applied, and allows validation of the calculation codes when isotopic dissolution is performed. It was used successfully on U_3Si_2 research reactor fuel using TIMS for isotopic analyses. The precision will be increased in the near future by introducing HPLC-ICP-MS on-line coupling, instead of TIMS after HPLC separation.

For high burn up fuel, a paper on the subject Examination of the WWER-440 Fuel after Irradiation up to Burn up of 70 MW•d/kg using Electron Probe Microanalysis and Scanning Electron Microscopy was presented by Y. Goncharenko from RIAR, Russian Federation. He showed the burn-up profile along a pellet diameter is obtained by Electron Probe Micro Analysis (EPMA) and measuring the Nd total creation. But the Xe-profile was found different from the burn-up, because Xe fission gas release depends on temperature and fuel microstructure evolution. This paper discussed the resolution of Xe measurement depending on the energy of electrons from EPMA, and compared to the observed microstructure.

Another technique was shown by Mr. Jeffrey from Argonne National Laboratory, USA, to study the evolution of spent fuel subjected to 10 year ground water leaching, to simulate

underground storage conditions. This highly technological method employs X ray absorption spectroscopy (XAS) using a synchrotron facility. This powerful system was developed specially for this purpose and adapted to irradiated samples. The results showed that U, Np and Pu are tetravalent in this fuel and that migration of Mo and Tc from the spent fuel is rather limited. The main purpose of this presentation was to show the usefulness of the X ray absorption spectroscopy using a synchrotron facility. However the cost of the synchrotron facility required to get the primary X ray emission is enormous and it cannot be compared even with the secondary ion mass spectrometry. Therefore, it is reasonable to use this method only in case of necessity and apply it to entities which have this synchrotron facility and can work at it with irradiated fuel samples.

This kind of TCM was a good place to discuss classical techniques among hot laboratories, which have used it for a long time, and new labs, which are trying to adapt it for their own needs. Even classical techniques can be improved (e.g. by modifying electronic energy level in EPMA, or changing TIMS by ICP-MS for ^{148}Nd measurement). New, highly technological methods (such as XAS on a last generation synchrotron) can be developed, even on irradiated samples, to get useful information.

Distortion Measurement for Fuel Assemblies with Ultrasonic Technique was presented by Yuanhuan Xu from Research Institute of Nuclear Power Operation, China. In this work, the ultrasonic technique with multi-channels data acquisition was used to measure the distance between a side face of fuel assembly and the reference plate holding ultrasonic probes. The measurement is performed while the fuel assemblies are transferred during unloading period. No tools or equipment touch the measured fuel assembly during the measurement process. The proper parameter of ultrasonic technique is confirmed to ensure the measurement precision. It takes only 3~5 minutes to measure one fuel assembly. Though this technique has been applied successfully at the Research Institute of Nuclear Power Operation (China), however, it may be difficult to directly use the algorithm applied at RINPO in other labs. The scheme of the experiment will be different in each case, and only the ultrasonic method of analysis will remain the same.

The sixth paper presented by LECA-STAR Hot laboratory (Cadarache CEA, France) was devoted to the complex application of modern methods of analysis (including secondary ion mass spectrometry and scanning electron microscopy) for investigation of gas fission products behaviour in irradiated nuclear fuel. First of all, the paper demonstrates that the application of the most up-to-date methods of analysis of irradiated fuel is very expedient. It also shows the advantages and disadvantages of each method, taking the examination of GFP behaviour as an example. It is shown that the application of only one method does not allow complete and reliable data to be obtained. It means, to obtain reliable information, e.g. on the distribution of fission gases in irradiated fuel, multiple methods would be employed (in this case for example, ceramography, SEM and SIMS).

The specialist from Japan Atomic Energy Agency highlighted the application of high resolution high energy X ray tomography for non destructive post irradiation examination of fuel assemblies. X ray CT images of different sections of a fuel assembly (with resolution up to several fractions of a millimetre) have been obtained. Thus, X ray CT images of different sections of a fuel assembly irradiated up to high burn ups were obtained for the first time in the world in the presence of strong gamma ray emissions from the irradiated fuel assembly, stated the presenter. Further development of the proposed method will allow non destructive examination of the fuel column state, fracture by the debris and fracture by the fretting corrosion. This technique using the X ray CT can eject destructive methods in many measurements. In addition, this technique can also be applied further to observation of high

density and high radioactivity specimens, such as high level radioactive wastes, activated equipment used in nuclear reactor and so on. Should the development of this method be successful, it will be in great demand, as it can be used for the non destructive control of fuel assemblies during the core reloading.

The paper presented jointly by the Joint Research Centre European Commission and Argentine CNEA-UATEN-CAE makes a preliminary selection of methods necessary for post irradiation examination of HTR micro fuel elements. It also indicates what additional methods are required by the existing hot labs involved in post irradiation examination of fuel elements and micro fuel elements of this promising reactor type. The fuel elements (spherical or compacts) of Very High Temperature Reactors (V/HTRs) are based on ceramic multilayer coated fuel particles, that represent the smallest constituent of the energy source in this type of reactors. In this context, the performance of the particle coatings (failure) and the consequent fission product release is of paramount importance.

The ninth paper of this session was presented by Domizzi G. CNEA, Buenos Aires, Argentina, and presented the fracture surface analysis of an irradiated Hafnium control rod by metallographic replicas. The replication technique was presented as an alternative to study fracture surface of a failed irradiated rod with inside-hot-cell SEM. The methodology of replicating fracture surface was developed on non-irradiated fractured specimens and implemented inside hot cell using tele-manipulators. In spite of the damage that irradiation produced on the cellulose and the resin material, the quality of the replica was good enough to allow the crack origin identification and some details of fracture surface. These methods for fabrication of replicas of high activity specimens may be very useful particularly for the hot labs, which do not possess shielded microscopes intended for investigation of irradiated materials. Besides, it allows replicas of hard to access sections, which are undesirable to dismantle.

Finally, the Argentinean specialist, made one more presentation on Effect of irradiation and hydrogen concentration on fracture toughness of Hafnium control rod. He highlighted the influence of irradiation and hydrogen concentration on fracture toughness of such control rod. From a methodical point of view, they demonstrated a possibility to prepare specimens from irradiated hafnium control rod for mechanical tests. With application of SEM after mechanical testing, common features and differences between the fractured surfaces of hydrogenated non-irradiated and irradiated specimens were discussed. It was concluded that the tensile and fracture test, performed on a 'hot' hafnium rod and a similar 'cold' rod hydride until different hydrogen concentrations, showed that the failure occurred by the combined embitterment effect produced by irradiation and hydride precipitation.

It was concluded at the end of this session that:

1. This kind of TM is a good place to discuss classical techniques between hot laboratories which have used it for a long time and new labs trying to adapt it for their own needs.
2. Even classical techniques can be improved (e.g. by modifying electronic energy level in EPMA, or changing TIMS by ICP-MS for ^{148}Nd measurement).
3. New, highly-technological methods (such as XAS on a last generation synchrotron) can be developed, even on irradiated samples, to get useful information.

SESSION 4: International Projects and Databases

In Session 4 two papers were presented. Mr J.Y. Blanc presented European HOTLAB project with the emphasis on its internet catalogue. This project demonstrated one of the possible

ways to unite different countries which have national hot labs so as to minimize the costs for designing new generations of NPPs and preserve the safety of the existing ones.

The PIE database was successfully implemented under the IAEA Integrated Nuclear Fuel Cycle Information System (iNFCIS) in early 2004. The iNFCIS database was given a new layout and it is also now possible for the facility coordinators to edit the PIE facilities data on the web page interactively. The number of visitors to the IAEA iNFCIS web site was 3350 and 4887 in 2004 and 2005 respectively. The number of visitors has nearly doubled since 15 November 2006. A similar PIE facilities database, but only on the European PIE facilities, was designed in 2005 at the LHMA-SCK-CEN hot laboratory in Belgium under sponsorship by the European Sixth Framework Programme and European Hot Laboratories Research Capacities and Needs. The export and import data from one database to another was suggested.

These two connected presentations showed the utility of shared databases for information exchange among facilities, researchers, and policy-makers. The high entry costs for specialized nuclear facilities and the common interest in safety, security, and availability of nuclear power across international boundaries provide impetus for sharing of information. Indeed, this idea of information sharing, in all the areas of nuclear technology, lies at the heart of the IAEA mission.

At this technical meeting the presentations of new techniques, instruments, capabilities, and interpretations of data, were discussed. However, a database and electronic forum for evaluating capabilities and sharing experiences with technologies and procedures provides greater flexibility and on-demand availability that no single meeting can hope to provide. Such databases may serve as a starting point of entry for those new to the nuclear field. Managers and decision-makers can use these databases to rapidly compare information and evaluate programs, identify collaborators, and make the case for needed upgrades and expansion.

Compared to the former sessions, where overviews were given over programs and equipment of the whole nuclear facilities, all the speakers in last part of session 4 introduced dedicated methods to solve specific applied questions of NPP utilities and/or fuel vendors (present LWRs and future third or fourth- generation systems):

- Y. Xu RINPO: How to measure without much delay the distortion and bending of LWR FAs to be reinstalled in power plants?
- J. Noriot, CEA: What fission gas ratio, from which reservoirs is released from LWR fuel and under what operational transient or accident conditions?
- K. Katsuyama, JAEA: Applying high-energy-pulsed X ray CT, what information can be extracted from an FBR FA non-destructively?
- E. Toscano, ITU: How to get information about fission product release from coated fuel particles under loss of forced coolant conditions in HTRs?
- G. Domizzi, CNEA: What was the damage mechanism of an Hf control rod from ATUCHA-1 power station?
- G. Domizzi, CNEA: How much information can be extracted out of replica from the control rod fractured surface in order to elucidate its damage process?

Two of the six presentations introduced new successful non-destructive test methodologies and it was discussed that these new tools were state of the art. It was clearly observed that efforts to introduce new NDT tools are important, as such techniques normally help to reduce the analytical costs, times and wastes produced and allow a larger numbers of items to be

analyzed. Thus the improvement would be possible for statistics of analyses and reliability of controlled systems.

Out of the two presented topics it became quite clear that in order to solve complex questions like fission gas detainment or release under accident conditions, a lab has to have access to a broad series of instrumental and analytical tools which supplement/complement each other. Such tools can be equal or only slightly modified compared to non-nuclear applications, sometimes the tools however are very specific, complex and need extraordinary radiological control efforts.

From the above it is clear that in the long term very few centres will have the opportunity to cover the full range of (continuously evolving) analytical tools to deal with all imaginable, emerging, complex questions of power reactor applications. However, some major tools exist (like visual inspection, some EC tools, gamma and mass spectrometry, metallography and sample preparation techniques) which are mandatory also in small HOTLABS if they have to support national nuclear programs. Thus they foster the local nuclear knowledge and help to improve the safety in local nuclear energy applications and indispensable goals.

It can be extrapolated that particularly smaller nuclear centres need to specialize and do forefront R&D in niches research areas where they have excellent chances to build up special knowledge, participate in international programs, add real value to the worldwide nuclear (growing) community and support, or even challenge, the key players.

Conclusions regarding present hot cell situation

Present hot cell scope of work encompasses a wide range of activities dedicated to the support of safe and efficient operation of nuclear power plants including initial work for new reactor systems. Emphasis is placed on work related to fuel cycle and lifetime assessment of structural core components (e.g. pressure vessel steel and steel internals).

Though the total number of hot cell laboratories in Europe has been substantially reduced, many laboratories are now indicating high levels of utilization of basic analytical techniques (e.g. optical microscopy, Transmission Electron Microscopy, Scanning Electron Microscopy, Microprobe Analysis (EPMA), X ray diffraction, etc). This implies that in such conditions, only a limited capacity would be available to absorb any significant increase in demand.

Outlook regarding future hot cell utilization

Near term utilization of hot cell laboratories will be characterized by a continuation of the present scope of work, since the techniques of commercial reactors will not change significantly. Nevertheless, efforts are constantly being made to improve the safety and economic efficiency of reactors resulting in an ongoing utilization of hot cell laboratories. On the other hand, one has to be aware that new programmes cannot be mathematically added to the old ones without balancing changes at the utilization level.

Long term utilization of hot cell laboratories is strongly dependent on research scenarios towards new reactor systems envisaged to supplement or replace the present fleet of commercial reactors. However, it should be taken into account that most of future programmes will be implemented on a worldwide basis, and not on a 'European only' basis, which implies sharing tasks with non European partners. It also means that future hot cell utilization is even more dependent on progressing technical and political developments.

The second presentation in Session 4 was made by Mr Victor Inozemtsev (Nuclear Fuel Specialist, International Atomic Energy Agency) and devoted to the Status of the INFCIS IAEA PIE Facilities Database.

Both the EU hot lab catalogue and the IAEA catalogue have a lot in common and both were designed to solve one and the same task. The first IAEA catalogue version became the basis for the European hot lab catalogue. The last IAEA catalogue version has been upgraded greatly based on the HOTLAB catalogue. However, these two catalogues are different. The European catalogue contains data on the European hot labs only, while the IAEA one is much broader. On the other hand, the IAEA catalogue does not contain a section about transport casks. In any case, it is necessary to further check the data similarity of the two databases to avoid confusion for the database users due to possible inconsistency of data for the same facility. The owners of the two databases should agree upon how to export and import data from one database to another and the reviewer's role in this situation could include communication of necessary actions to be performed.

TM-Norway-2007 FUEL ROD ROD INSTRUMENTATION AND IN-PILE MEASUREMENT TECHNIQUES

This Technical Meeting was hosted by the OECD Halden Reactor Project who provided a forum for the presentations and discussions on current methods and technologies being applied to fuel irradiation research. Focussing on advanced techniques being carried out for the understanding of high burn up fuel behaviour, this meeting also considered Post Irradiation Examination and power reactor techniques to acquire fuel performance information. The target of the meeting was to strengthen and widen the knowledge base of in-pile measurement techniques as applied to nuclear fuel rather than to exchange and present fuel properties and performance data. Innovative methods for testing fuel in non-rod configurations, re-fabrication techniques for irradiated fuel and ramp testing facilities, as well as more standard techniques for the measurement of temperature, fission gas release and dimensional changes were discussed at this TM. Experimental methods used to control the local power of fuel so that the test conditions would properly represent power reactor irradiations, including operational conditions such as transients or load follow, were described in several presentations.

The meeting complemented the series of IAEA meetings discussing PIE of water reactor fuel, providing a state of the art description of fuel experimentation and examination in support of operation. This meeting was held following recommendations of the IAEA Technical Working Group on Water Reactor Fuel Performance and Technology (TWGFPT) at its meetings in 2005 and 2006. The most recent PIE meeting was held in Argentina on November 2006. Prior to this 2006 TM, other meetings were held in 1981 and 1984 (Tokyo, Japan), 1990 (Workington, UK), 1994 (Cadarache, France) and 2001 (Dimitrovgrad, Russian Federation), respectively.

Twenty seven experts from fifteen countries and one international organisation participated at this Technical Meeting. A total of five technical sessions were organized in which seventeen research papers were presented covering irradiation testing techniques – experience and development, irradiation testing facilities and capabilities, on-line monitoring systems, hot cell facilities & PIE, and practical uses of In-pile and PIE Data. Each session was closed by expert discussions on the presented papers. Two technical visits were organised, one to the Halden instrumentation workshop and the second to the Halden Boiling Water Reactor facilities.

The Meeting was opened by Dr W. Wiesenack, Halden Project Manager, who welcomed the participants and described the history of the Halden Reactor Project (HRP) and its irradiation facilities. This project is hosted by Institute of Energiteknikk (IFE). The details of HRP have been given in later section of this document. The Agency representative, John Killeen, presented its work programme in the field of nuclear fuel cycle and material technologies and discussed the work carried out within the CRP FUMEX-II, which relied heavily on data provided by the Halden Project.

SESSION 1: Irradiation Testing Techniques – Experience and Development

In the first session of this TM, five technical paper presentations were given and a discussion of them was held. Two papers were presented by representatives of the Halden Reactor Project (IFE, Norway), one paper by an expert of SCK/CEN (Belgium) and remaining two papers were presented by experts from CEA (Cadarache and Saclay, France). This session described the state of art technologies applied for irradiation testing, covering innovative technologies for power determination, temperature and fission gas release monitoring during the reactor operation.

Dr Vermeeren from SCK/CEN Belgium described the Multipurpose Material Test Reactor BR2, its available research facilities and the work carried out there. He described the technique used for on-line fuel power determination. His method requires a thermal balance measurement as well as power distribution calculations using an improved procedure. The thermal balance measurement relies on a continuous measurement of enthalpy increase of the cooling water in the experimental arrangement to give a measured power. Corrections are made for radial and axial heat losses to give a total power deposited in the irradiation device. A further correction is made for the power produced in structural parts and the distribution of power over the rods to give the total power in each test fuel rod. Axial power profiles are calculated to give a maximum power generation rate in the test fuel rod. A three dimensional Monte Carlo computation (MCNP) tool was employed for all these calculations.

Dr Vermeeren explained how complementary data from self-powered neutron detectors (SPND) is used and provided a detailed model on the detector response using MCNP methodology. Both the fast and slow response SPNDs and the uncertainties for each type were discussed in this paper. The existing fuel instrumentation experience and developments at the BR2 reactor were also described.

In order to increase the flexibility and efficiency of the Pressurised Water Capsule (PWC) setup for fuel transient tests a new system is under design. It consists of two components: a variable neutron screen surrounding the PWC, realized by a variable concentration boric acid solution (baptized as VANESSA) and a system to rotate the complete device within a 200 mm BR2 channel (RODEO). VANESSA not only provides the variable thermal neutron absorption, but the fluid in the device will also evacuate the heat and will serve to determine the fuel rod power via the thermal balance method. In principle, an unlimited number of transients with amplitude up to a factor two can be achieved by VANESSA. However, in order to reduce the complexity of the out-of-pile installation and to limit the amount of boric acid needed (and the waste) VANESSA will be designed to be compatible with the RODEO system. The details of this system are given in the paper. A rotating plug in a 200 mm channel allows movement of the PWC (possibly within VANESSA) across the flux gradient of the channel, yielding a maximum power increase factor of about 4, depending on the BR2 configuration and on the boric acid concentration in VANESSA (assumed fixed). In this concept, VANESSA would serve to adjust the minimum power level and the ramp test would

be accomplished by RODEO only. Of course any number of transients is possible with this system. As compared to the He-3 based ramp test technology, there is almost no production of waste. There is no production of tritium and system availability problems linked to the tritium tightness are eliminated. The combination of VANESSA and RODEO allows the use of VANESSA to adjust base power level and perform a transient test with RODEO.

Dr C Halsengreen from IFE, Halden Reactor Project, explained the instrumentation and re-fabrication techniques for fuel rod performance characterization in the Halden reactor. The possibility of attaching in-core instrumentation to pre-irradiated and un-irradiated fuel rods and material samples from power reactors stand points is very important for the nuclear industry. In this regard, the Halden Reactor Project is refining its existing instrumentation and is working with development of new instruments on a continuous basis. Starting with a description of the Halden Boiling Water Reactor (HBWR), he described the HBWR capabilities that have been developed at Halden for performing fuel irradiations with in-core instrumentation for on-line monitoring of key parameters. For basic fuel studies, instrumentation for monitoring the thermal and mechanical behaviour of the fuel has been developed as well as for measuring fission gas release. Instrumentation for monitoring fuel pellet interaction with the cladding or for separately investigating the mechanical behaviour of the cladding can also be used. It was also explained how current instrumentation at Halden is being implemented for characterising the fuel performance and behaviour under different testing conditions.

For the future, he noted that the development of new instruments will focus on Linear Voltage Differential Detectors for high temperature applications (above 400°C), but will include on-line cladding corrosion detectors (potential drop, EIS / ECN), electrochemical sensors (ECP, conductivity etc.), in core Eddy-current techniques (e.g. for detecting cladding cracking / development of defects) and instrumentation for Generation IV applications (able to operate in liquid metals, supercritical 'steam', molten salt etc.).

Francis Berdoula from Cadarache, CEA, presented the results on the topic of Hard drilling technique for making a centre hole of Irradiated Fuel Pellets. The objective was to provide the information on central line temperature of fuel pellets during power transient and to study the fission gas releasing behaviour of high burn up LWR fuel rods. In this presentation, the techniques of hard drilling were described, showing enhancements of the tool material, geometry and drilling process parameters including cutting speed feed and gas flow. CEA-LECA hot-lab have established a hard drilling technique for making a centre hole in irradiated fuel pellets for thermocouple insertion, beginning in 1999. This hard drilling process offers an accurate technique for making a centre hole in fuel pellets, without altering the integrity of fuel pellets, and no significant metallographic changes have been observed. The hard drilling technique is now being improved to allow drilling of a central hole up to 100 mm in depth and 2.5mm in diameter with optimization of drilling conditions.

The Halden Project representative T. Tverberg explained the In-pile fuel rod performance characterisation in the Halden Reactor. Halden Reactor Project with its instrument capabilities has developed the direct measurements of following important parameters related to fuel in-pile behaviour.

- Fuel temperature
- Feedback from fission gas release and dimensional changes
- Dimensional stability
- Quantification of fuel densification and rate of fuel swelling
- Fission gas release behaviour

- Temperature onset as function of burn up
- Cladding strain
- Pellet cladding mechanical interaction (PCMI)
- The data provide for detailed modelling of LWR fuel
- Other measurements and techniques

Other measurement techniques including noise analysis (at steady state), fuel thermocouple provides information on fuel thermal conductivity and gap conductance (fission gas release), cladding elongation detector (state of contact between fuel and cladding (PCMI)), SCRAM data were considered in this paper.

In the last presentation of the session , J-F Villard from the Commissariat à l’Energie Atomique Saclay, France (CEA, Saclay), demonstrated the improvements in rod instrumentation capabilities which have been achieved at CEA, making possible the execution of high-performance irradiation experiments on advanced PWR fuels in OSIRIS reactor. He described that the CEA has been managing a large research program to develop and qualify innovative in-pile instrumentation for some years. Radiation measurement and measurement of parameters inside the irradiation rigs are the main scope of this research program. J-F Villard presented two examples of rod instrumentation. First, the new high-temperature thermocouples based on molybdenum and niobium thermo-elements. These have the propriety to remain nearly unchanged by neutron flux even during long-term irradiation, whereas in similar conditions, standard high-temperature thermocouples are altered by significant drift due to composition changes arising from neutron irradiation and the consequent material transmutations. For these reasons, this improvement is expected to have a significant impact on temperature measurement capabilities of future fuel irradiation experiments. The second example was the characterization of fission gas release. Successful results have been obtained for this purpose by measuring simultaneously the fuel temperature and the rod internal pressure, using a very accurate pressure sensor developed by CEA.

SESSION 2: Testing Facilities and Capabilities

Four papers were presented in this session. Pulse irradiation experiments in LWR were discussed to study the fuel behaviour under reactivity initiated accident (RIA) conditions. The developed instrumentation and installations for testing of WWER-type fuel at transient and project emergency conditions was also presented in the session. The information on capabilities of the irradiation facilities of the Halden Reactor in Norway and Petten facility were provided. The new proposed irradiation facility that is already under consideration in Argentina was also the subject of discussion.

Yasuyuki Muramatsu from Japan Atomic Energy Commission (JAEC) presented the Instrumentation techniques in NSRR experiments. The NSRR, research reactor, has been utilized since 1975 to perform experiments simulating accident conditions on light water reactor fuels. Over 1200 experiments on fresh fuel rods were performed to clarify fuel behaviour under RIA conditions and to obtain a fuel failure limit. More than seventy experiments have also been carried out on the modified NSRR facilities for high burn up fuel tests since 1989. Using accumulated experience and developed sensors, unique instrumentation techniques as spot-welding of thermocouple to cladding surface or water column velocimeter have been developed. It was mentioned that results obtained have been incorporated into safety evaluation guidelines for RIA in some other countries as well as in Japan. Further, it was described that safety research on NSRR is expected to support fuel

burnup extension and MOX fuel introduction. It was noted that the capabilities of the NSRR facility are being extended and improved to meet the current research requirements.

L. Izhutov from State Scientific Centre of Russia Research Institute of Atomic Reactors (RIAR) presented the topic of Test methods of WWER fuel with simulating transitive and emergency modes in the MIR reactor. He gave a full description of MIR, and the capability of the of MIR reactor was discussed for testing fuel element fragments and fuel assemblies of different nuclear power reactors under normal and emergency operating conditions. Several types of irradiation devices have been described for WWER-type fuel rods under steady state conditions. Presently, six test loop facilities are being operated i.e. two PWR loops, two BWR loops and two steam coolant loops. Most of the fuel tests are conducted for improving and upgrading the Russian PWR fuel. These test include: long term tests of short-size rods with different modifications of cladding materials and fuel pellets; further irradiation of NPP refabricated and full-size fuel rods up to 80 MW•d/kg U; experiments with leaking fuel rods at different burnup and under transient conditions; continuation of the RAMP type experiments at high burnup of fuel; in pile tests with simulation of LOCA and RIA type accidents. During the talk, it was mentioned that irradiation of LEU fuel of research reactor within the framework of the RERTR programme is also performed. The loop installations characteristics and their instrumental equipment were presented.

The upgrading of the gas cooled PG-1 loop with outlet temperature up to 1100 oC for in-pile investigations of HTGR fuel has been planned. The steam cooled PVP-2 loop with pressure up to 22.5 MPa for testing fuel materials of sub critical water-cooled reactor has also been scheduled.

O. Beuter from National Atomic Energy Commission of Argentina presented the features of proposed Irradiation Facility Project (IFP). The objectives and detailed description of the facility were provided in his presentation. To study fuel behaviour, this facility was installed in the RA-3 reactor to irradiate NPP fuel rods, under total or partial operating conditions. It has been planned to construct a full scale facility mock-up with electrical heater. The majority of the components will be the same as used in the in-pile facility. It was described that the facility will operate this mock-up in normal and some transient conditions to set up all of the involved systems i.e. Instrumentation & Control, SDCS and emergency. This idea was presented to the IAEA as a Technical Cooperation Project (which has been approved; ARG/4/087) and contemplates the design, fabrication and assembling of an irradiation facility loop.

F.C. Klaassen, from the Nuclear Research and Consultancy group (NRC) in the Netherlands, explained the remote on-line measurement of fission gas release during irradiation testing at the High Flux Reactor (HFR) at Petten. The fuel performance on the basis of fission gas release was highlighted. The innovative technique for measuring fission gas during irradiation but with the instrumentation maintained out of pile was discussed in this presentation. The procedures to implement this technique were given with special emphasis on the correct interpretation of the pressure data. It was concluded that accurate internal pressure and fission gas release can be measured very well outside the core by Iodine PSF experiment. The application of these out-of-pile pressure measurements can be easily extended to test the fission gas release in (light) water reactor nuclear fuels under various conditions.

SESSION 3: On-line Monitoring Systems

Three papers were presented in this session, two of them covering corrosion studies of plant materials and High Temperature Reactor (HTR) fuel irradiations for higher temperature and burnups. The third paper considered optimising the core, fuel capability and efficient operation which demand accurate and detailed information of core condition. To meet these requirements, flux mapping and channel temperature monitoring system for TAPP 3 and 4 (Tarapur Power Plant) were performed and presented in this session.

In the first presentation, Peter Bennett from the Halden Reactor Project described the details of the In-core measurements of fuel clad – coolant interactions in the Halden reactor. The control of thermal hydraulic and water chemistry conditions in the loop systems was discussed. The details of the techniques currently applied, to provide on-line, in-core corrosion and water chemistry monitoring data were also mentioned in this paper. It was concluded that loop systems allow tests to be conducted under LWR thermal-hydraulic and water chemistry conditions. The in-core, on-line instrumentation is flexible and can be used for several purposes for example, diameter gauges can be used to obtain creep data and to detect crud deposition of fuel cladding. Instrumentation developed for studies of corrosion of plant materials, for example electrochemical corrosion potential (ECP) electrodes are also valuable in fuel clad corrosion/crud studies where the water chemistry conditions have a large effect on fuel-coolant interactions.

In the second presentation, M. Laurie from European Commission described the design of the on-line fission gas release analysis system in the High Flux Reactor at Petten. Starting with the introduction and main objective of HTR fuel irradiation tests he explained the Sweep Loop Facility (SLF) which was designed to deal with a wide range of activities by modification of the distance between detectors and gas samples. Further, it was noted that each irradiation test connected to SLF needs to fulfil three tasks: firstly, the maintenance of constant irradiation conditions (temperature, hygrometry, gas flow etc.); secondly, the surveillance of fission gas release by purging capsules with inert gas, enabling qualitative and quantitative calculation of fission gas release rates; and finally monitoring of safety-relevant operating parameters (dose rate in the gas lines, glove boxes and working area). In case predefined thresholds are exceeded, automatic actions are triggered to put the installation into a safe configuration. The gas activity measurement technique, which allows qualitative and quantitative analysis of volatile fission products to be performed on-line, was specifically discussed. The newly developed data acquisition system allows for higher measurement frequencies when activity values are increased, thus enabling the follow-up of transients.

Indian specialist, R.K. Patil from Bhabha Atomic Research Centre, presented the Flux Mapping and Channel Monitoring System for TAPP 3 & 4 reactor core. The two core monitoring systems (i.e. flux mapping and channel temperature monitoring) were taken separately. First the full functioning (hardware, software) of the Flux Mapping System (FMS) was explained. The system requirements, configuration, hardware used at different levels of the FMS along with the dual, fault tolerant, optical link between various nodes of the system was discussed in the presentation. Further it was noted that this system helps the operator in core monitoring, its analysis and to predict the future core conditions. The well-designed graphical user interface helps the site engineers to analyse and evaluate core conditions under different operating conditions and fuel utilization. It was also stated that this online system eliminates the need for an off-line flux map code analysis. Further, the computerised Channel Temperature Monitoring System (CTM) was described. This system has evolved from a simple monitoring system to a safety related system, generating setback for NPP. The system has also used the advances in the technology to improve both hardware and software. The

hardware used in the system has evolved from 8 bit CPU (5MHz) at MAPS (Madras Power Station) to 32 bit CPU (20MHz) at TAPP. The software for TAPP-4 has been developed to the required quality standards for a safety related system (Class 1B).

SESSION 4: Hot Cell Facilities and PIE

This session presented three papers covering the given range of topics. These papers discussed the post irradiation experience of RIAR Material testing complex, Post irradiation annealing tests to obtain the Xe-133 diffusion coefficients in a UO₂, (Th,U)O₂ & SIMFUEL and PIE of Pakistani fabricated fuel bundles, irradiated at KANUPP and examined at Irradiation Examination facility of Pakistan Institute of Nuclear Science and Technology (PINSTECH).

Y.D. Goncharenko from Research Institute of Atomic Reactors (RIAR), the Material Science Complex, Russian Federation, presented the current methodical possibilities of RIAR Material testing complex. This complex is the biggest hot lab in Russian Federation and the details of its hot laboratories were described in this presentation. This complex houses 64 hot cells and 60 heavy-duty boxes (up to 2.2×10^{16} Bq) and consisted of three buildings with their following mandates.

1. For non-destructive analysis of full-scale fuel rods and fuel assemblies: The measurements of fuel rod parameters, visual examinations, gamma scanning and vortex-current defectoscopy are being performed in this building.
2. For destructive analysis where burn-up, fission products release, gamma scanning, metallography and micro-hardness, density and porosity, thermal conductivity and electric resistance, X ray analysis, dilatometry, TEM, SEM, EPMA, AES, SIMS, mechanical testing (tensile, compression, bending, impact etc.) are taken place.
3. For technological engineering programs:

Fission gas release is an important indicator of fuel behaviour and performance. Many models have been published to explain this mechanism. In these models, a diffusion coefficient is dominant factor for a fission gas release. Keeping the importance of the subject in view, Heemoun Kim from KAERI presented the results on Diffusion of Xenon Gas in Nuclear Fuels with Oxygen Potentials in 0.1 MW•d/t U of a Burn up. In his presentation, he proved that the xenon diffusion coefficients for the near stoichiometric single crystalline UO₂ agree well with the data of others. It was described that the xenon diffusion coefficients in the polycrystalline (Th,U)O₂ and SIMFUEL were lower than those in the polycrystalline UO₂ by one order of a magnitude and 3 times, respectively. It was noted in the talk that xenon diffusion in a fuel seems to be controlled by the cation vacancy concentration which is related to the melting point and valence of a matrix. Its diffusion coefficient in fuel increases with increasing oxygen potential of the ambient gas.

M. S. Zaheer from PINSTECH described the Post Irradiation Examinations of a Pakistani Fabricated Fuel Bundle Irradiated at Karachi Nuclear Power Plant. He presented the results of one bundle having its damaged end plates. This bundle had an irradiation history of about five years in reactor and had maximum burn-up of 6917 MW•d/Te U. The examinations comprised of visual examination, metrology, gamma scanning, fission gases collection, spectro-chemical analysis, metallography and autoradiography.

SESSION 5: Practical Uses of In-pile and PIE Data

This fifth and last session of the meeting presented two papers. The failure of fuel assembly has serious safety concerns as well as representing a significant economic loss. At Qinshan nuclear power plant, if one fuel assembly is not able to be refuelled due to failure, the other three fuel assemblies from core symmetrical locations are also not able to be reused. The root cause investigation and corrective actions for fuel failure of Qinshan nuclear power plant were described in the first paper presented by Xue Xincan from Qinshan Nuclear Power Company, China. Based on the fuel failure experience in Qinshan nuclear power plant, the major cause of fuel assembly defective was found to be debris fretting. To prevent future fuel failure, some corrective actions taken were described in this presentation.

The second paper was about the CARA fuel design for the Argentinian PHWR (Atucha I & II). Typically, the PHWR is fuelled with natural uranium which has positive void reactivity. CARA fuel has been designed to have a robust safety design, based on a negative void reactivity obtained through the use of SEU and burnable poison. The BaCo code ('Barra Combustible', Spanish expression for 'fuel rod') was developed at CNEA for the simulation of the behaviour of nuclear fuel rods under irradiation. The CARA fuel basic design, the BaCo code and the results of a code validation were described in detail. The restart of the Atucha II NPP project requires an updated safety system in agreement with the best international practices and broadly accepted design approaches. The participation in the CRP FUMEX II and the extensive use of the Halden irradiations tests were emphasized to show the demanding conditions of the designers and modellers before the preparation of an irradiation experiment.

Panel discussions

There were two panel discussion sessions during the meeting and there were involved debates on methods of fuel centre temperature measurements and techniques for determining helium and hydrogen gas migration in experimental fuel rods. A discussion on the reliability of experimental information, which provides confidence to nuclear regulatory authorities for the safety limits applied to fuel in commercial reactors, was also held. The final issue of the discussion was the monitoring of deliberately defected fuel, where issues of instrumentation calibration under such difficult environmental conditions were raised and how best to carry out on-line monitoring with options of using either in-core or out-of-core instrumentation.

Technical visits

The two technical visits were an important part of the meeting, and the Halden Project provided hands-on access to many of their instruments and their staff members were willing to discuss techniques and methods. The participants of the meeting were extremely interested in this opportunity, and took full advantage, both asking questions and also taking photographs to carry home.

Conclusions

This Technical Meeting was organised to allow discussion of irradiation testing techniques and the host organisation was extremely helpful in providing opportunities to see their facilities and to explain details of their techniques and the extent of their testing facilities.

The Halden Project is strongly supportive of IAEA initiatives, including support to TC projects and provision of data for the IAEA FUMEX CRPs.

**PART I. PROCEEDINGS OF THE IAEA TECHNICAL
MEETING HELD IN BUENOS AIRES, ARGENTINA 2006**

SESSION 1: PIE INTERNATIONAL EXPERIENCE

Chairpersons

G. Rusgirello (CNEA, Argentina)

V. Inozemtsev (IAEA)

POST IRRADIATION EXAMINATION OF WATER REACTOR FUEL ASSEMBLIES IN INDIA

S. Anantharaman, U.K. Viswanathan, S. Chatterjee, E. Ramadasan, K. Unnikrishnan, J.L. Singh, K.S. Balakrishnan, P.M. Ouseph, H.N. Singh, R.S. Sriwastaw, Prerna Mishra and D.N. Sah

**Post Irradiation Examination Division
Bhabha Atomic Research Centre
Trombay, Mumbai 400085, India**

ABSTRACT

The post irradiation examination facility at the Bhabha Atomic Research Centre has been in operation for more than three decades. Over these years, irradiated fuels from boiling water reactors, pressurized heavy water reactors and experimental fuel from research reactor irradiations have been examined in the hot cells of the facility. The burnups of the fuels ranged from 1,000MWD/TU to 25,000 MWD/TU. Many of these fuels had failed and the causes of failures have been identified in most of the cases. The techniques used are visual examination, gamma scanning, profilometry, fission gas analysis, autoradiography, metallography and mechanical tests on the cladding. The paper presents the salient features observed during the PIE of some of the fuels examined in the past five years.

INTRODUCTION

India has two boiling water reactors (BWR), each with a capacity for the generation of 165 MWe and 12 pressurized heavy water reactors (PHWR), each with a capacity of 220 MWe and 2 PHWRs, each with a capacity of 540 MWe. The BWRs use enriched UO_2 as the fuel and PHWRs use natural UO_2 as the fuel. The fuel utilized in PHWRs is reprocessed to extract Pu. This Pu will be used in fast reactors, which is the second stage of the Indian nuclear power programme. As a part of the Pu recycling programme, MOX (i.e. the mixed oxide of Pu and natural U) will be used in the BWRs.

In order to evaluate the performance of the MOX fuel, experimental fuel element clusters containing MOX (4% PuO_2 + 96% nat. UO_2) were irradiated in the pressurized water loop (PWL) of the research reactor CIRUS at Trombay, up to a burnup of about 16,000 MWD/T.

There is a need to increase the discharge burnup of PHWR fuels to reduce the cost of fuel and also reduce the volume of discharged fuel to be stored. With this in view, some of the PHWR fuels that have been irradiated to a burnup of around 15,000MWD/TU against the average discharge burnup of 7,000 MWD/TU to study their performance at extended burnup.

This paper presents the salient features of the findings of post irradiation examination (PIE) on some of the experimental MOX fuels and PHWR fuels that have been examined in the recent past.

PIE OF EXPERIMENTAL MOX FUELS

A series of fuel elements of the typical BWR design containing $\text{UO}_2 + 4\% \text{PuO}_2$ and $\text{ThO}_2 + 4\% \text{PuO}_2$ fuel in Zircaloy-2 free standing cladding have been successfully irradiated at linear heat ratings in the range of 400W/cm to 490 W/cm to burnups in the region of 16,000 MWD/T in the pressurised water loop of the CIRUS reactor. Pre-irradiation documentation of these fuel elements was thoroughly made. The non-destructive testing of these fuel elements after irradiation has indicated excellent in-pile behaviour except for a small amount of crud deposition. The results of the measurements of the released fission gas collected from these elements are given in the table-1. A detailed destructive examination is being planned to generate quantitative information on various aspects of mixed oxide fuel behaviour.

PIE OF PHWR FUEL

There are 14 PHWR's in operation, 12 of which are of 220MWe capacity and use the 19-element natural UO_2 fuel bundle. The other two PHWR's are of 540MWe capacity and utilize 37-element natural UO_2 fuel bundle. In all there is a 66-reactor year experience in the irradiation of PHWR fuel in Indian power reactors. The average discharge burn up of these fuels is 7,000MWD/TU. During these years there has been considerable improvement in the fuel performance with the fuel failure rate of <0.1%. Still some of the bundles fail at lower burnups than the average discharge burnup. To understand the cause of low burn up fuel failure, some of these failed bundles in the burnup range of 300 MWD/T to 4,725 MWD/T were subjected to detailed post irradiation examination, which included visual examination, leak testing, gamma scanning and metallography.

PIE of low burnup fuel

The 19-element fuel bundle has 12 fuel elements in the outer ring, 6 in the intermediate ring and one central fuel element. All the fuel elements are of equal diameter of around 15mm. The total length of the bundle is around 500mm.

The detailed results generated on a 19-element PHWR fuel bundle that had failed at a burnup of 387MWD/TU within 17 days of residence in the reactor are presented. Out of the low burnup fuels that had failed, this bundle alone had multiple cracks on two of the outer fuel elements extending up to the end plug. Ultrasonic testing of the end plug indicated a lack of fusion. The other 17 pins were intact, which was confirmed by leak testing by the liquid nitrogen-alcohol method. Fig.1a shows one of the cracks that was observed in one of the outer elements and the lack of fusion observed at the end plug weld by ultrasonic testing is given in fig. 1b.

Fission gas puncture tests were carried out on fuel elements from the outer ring, intermediate ring and the central ring. The collected gas did not have any Xe or Kr indicating that no fission gases were released during the period of service in the reactor.

One of the failed fuel elements was sectioned at several places along the failed region and detailed metallography was carried out. The results are given in figures 2 to 6. It can be seen from the metallographs (fig. 4) that the fuel had undergone restructuring. Based on the restructuring, the central temperature was estimated as 1760°C [1,2]. Many incipient cracks were observed in the cladding, both in the circumferential and the radial orientation, in addition to the through wall crack (figs. 5 and 6). Some of these cracks were in line with the cracks in the fuel. The fuel was found in contact with the clad at several places indicating

strong interaction with each other. These observations are typical features of the pellet-clad interaction/stress corrosion cracking (PCI/SCC) type of failure. Since the fuel burnup is very low, there would not have been sufficient inventory of iodine to promote SCC.

To examine this further, metallographic samples were taken from the adjacent intact fuel pin from the same bundle. The photo macrograph (fig.7) did not reveal any restructuring. An examination at a higher magnification (fig.8) revealed a microstructure of fuel containing intergranular pores. Based on the microstructure, the fuel centre temperature was estimated to be less than 1300°C [1,2]. This ruled out any power ramps that the fuel might have undergone during its loading into the reactor.

Based on the foregoing, the cause of failure has been identified as the lack-of-fusion defect in the end cap weld of this pin that had gone undetected during the manufacture of the element. This defect had opened up during the reactor operation leading to the ingress of water in this pin. The presence of steam in the fuel-clad gap would have severely affected the gap-conductance increasing the centre temperature of the fuel. The presence of steam also causes the oxidation of UO₂ leading to an increase in the volume of the fuel, stressing the clad at several places. This could have led to the formation of incipient cracks in the cladding that grew by the delayed hydride cracking as is evidenced by the presence of hydride platelets at the crack tip, fig. 9.

Failures observed in other low burnup fuel bundles

The failures observed in the other low burn up fuel bundles are given in figures 10a to 10d. The formation of a localised hydride blister that led to a pinhole in the clad is shown in fig 10a. The uprooting of the bearing pad, fig. 1b, during the fueling is the cause of the failure observed in one of the fuel bundles. Fig. 10c shows the end cap weld failures observed in a fuel bundle. Fig. 10d is the micrograph of the massive hydriding observed at the end cap welds.

Remedies

To avoid low burn up failures the following remedial actions have been taken up by the manufacturers:

1. Ultrasonic testing of end plug welds
2. Stringent control of moisture inside fuel element
3. Triple melting to avoid stringer defects in end plugs

PIE of high burn up fuel

Two 19-element natural UO₂ fuel bundles that had undergone a burn up of around 14,580MWD/TU were examined in detail with emphasis on fission gas release, pellet-clad interaction and cladding corrosion. All the fuel elements from these bundles were intact without any evidence of deterioration.

Fission gas puncture tests were carried out on fuel elements from the outer ring, the intermediate ring and the central ring. The results are given in table 2. The results indicate that the fission gas release from the out fuel elements is about 12 times higher than that from

the intermediate element. The measured gas release from the central element was negligible when compared with the release from the outer element.

The macrographs of the cross sections taken from the outer, the intermediate and the central element along with the corresponding β - γ autoradiographs are presented in fig. 11. The β - γ autoradiographs indicated that there is a considerable migration of fission products from the centre towards the periphery in the case of the outer fuel element as compared to that of intermediate and the central elements. Also a dark circular porous region is observed in the central region of the fuel pellet as shown in the macrograph of the outer fuel element, fig. 11, extending up to about half the pellet radius. The size of this region decreases in the case of the intermediate and the central fuel elements.

The metallographic features observed in the outer fuel element are shown in fig. 12. There is an increase in the grain size of the fuel from the periphery towards the centre. The grains at the centre of the fuel were decorated with bubbles at their boundary in the case of all fuel elements. The measured grain size at the central region of the fuel pellets and other parameters like radial pellet-clad gap, thickness of the oxide layers and the estimated central temperature from the metallographic cross sections are given in table-2.

Since the extent of clad corrosion and the crevice corrosion near the spot welds of bearing pads and other appendages are a cause of concern at high burnups for a PHWR fuel, these areas were examined. Fig.13 shows a section through the spot weld of the bearing pad, which indicates a uniform corrosion of the clad and the weld region without any evidence of crevice corrosion.

No abnormal features were observed on the fuel pins, implying that the PHWR fuel pins examined can operate up to such high burnups, which is twice the average discharge burnup, without failure under normal operating conditions. The higher release of fission gases from the outer elements will be of concern in the case of operation of such fuels under off-normal conditions, which will call for a change in the design to reduce its linear heat rating and the central temperature from its current value.

CONCLUSIONS

1. The experimental MOX fuel irradiated up to a burnup of 16,000MWD/T at a heat flux of 93W/cm² had a low fission gas release of less than 1%, compared to around 8% release of fission gases from the fuel elements irradiated at a heat flux of 110W/cm².
2. The primary cause of failure in the case of the low burn up fuel was the presence of a lack-of-fusion defect in the end cap weld of the fuel pins that led to the ingress of water and hence steam inside the fuel pin, increasing the fuel temperature, degradation of physical and chemical state of the fuel and cladding and severe fuel-clad interaction leading to the failure of the fuel pins.
3. The fuel in the failed pin was found to have experienced a centre temperature of more than 1700°C, which is at least 400°C more than the central temperature in an adjacent non-failed fuel pin.
4. The observed features like the cracks in the clad, high fuel centre temperature and associated restructuring of the fuel are only secondary effects.
5. The high burnup fuel bundle had performed well under normal operating conditions, without any detrimental fuel-clad interaction.

6. The fission gas pressure measured in the outer fuel elements was 28 kg/cm^2 at STP and the corresponding estimated release was in the region of 25%.
7. The maximum centre temperature of the fuel in the outer element during operation was estimated to be 1600°C . The consequent migration of fission gases towards the grain boundary and the grain growth had led to a higher release of the fission gases in the outer elements.
8. The maximum oxide layer thickness in the outer fuel element is found to be 3.7μ
9. PIE results indicate that suitable design modifications may be required to take care of high internal gas pressure due to high fission gas release observed in the outer fuel elements at the extended burnup.

REFERENCES

1. D.N.Sah, et. al., "Estimation of Centre Temperature from Microstructural Features in Irradiated Oxide Fuels," IAEA Specialists' meeting on Examination of Fuel Assembly for Water Cooled Power Reactors, Tokyo, Japan, Nov. 9-13, 1981.
2. K. Unnikrishnan and E. Ramadasan, "Microstructural Changes in the Fuel of TAPS during Irradiation," Proceedings, Symposium on Radiation Effects in Solids, BARC, Mumbai, Pages 221-234, Nov. 23-25, 1983.

Table-1. Released Fission Gas Measured from Experimental MOX Fuel Pins

Cluster ID, burnup & heat flux	Pin No.	Average pellet density, % TD	Post irradiation change in void volume, %	Fission gas produced, cm ³ at STP	Fission gas released, cm ³ at STP	Internal gas pressure, Atmospheres (G)	Xenon to krypton ratio	Fission gas released, %
AC2 16,265 MWD/Te 93 W/cm ²	TU8	94.56	(-) 3.1	47.03	0	0.3	0	0
	TP1	96.27	(-) 20.12	296.18	0.36	0.61	14.44	0.12
	TP2	96.34	(-) 19.53	287.39	0.29	0.56	13.90	0.10
	TP3	94.32	(-) 18.33	282.57	0	0.65	0	0
	TP4	96.26	(-) 19.35	288.16	0.45	0.60	16.38	0.16
	TP5	96.20	(-) 12.47	296.08	1.09	0.58	12.70	0.37
AC3 16,000 MWD/Te 110 W/cm ²	TP6	95.92	(-) 12.1	245.79	20.59	7.37	13.92	8.38
	TP7	95.57	(-) 10.2	245.75	25.88	8.30	13.98	10.53
	TP8	95.81	(-) 17.0	285.84	22.55	7.97	13.93	9.17

(-) Negative sign indicates decrease in void volume

Table-2 Results of PIE of high burn up fuel, burn up 14,580MWD/TU

Parameter	Outer element	Intermediate element	Central element
Fission gas release %	25	2	0.6
Fission gas pressure kg/cm ²	28	4.3	3.2
Estimated fuel centre temperature °C [1,2]	1600	1320	1150
Grain size μ	33	19	15
Pellet clad gap μ	32	27	16
Clad inner oxide layer thickness μ	5	Thin and discontinuous	0
Clad outer oxide layer thickness μ	2.7	2.4	2.4
Oxide thickness on bearing pad μ	3.7	Not measured	Not measured

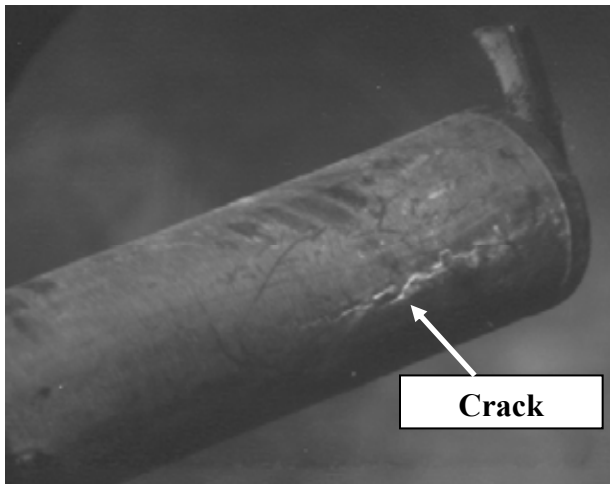


Fig.-1a. Crack observed on the cladding of the outer fuel element of the low burnup bundle

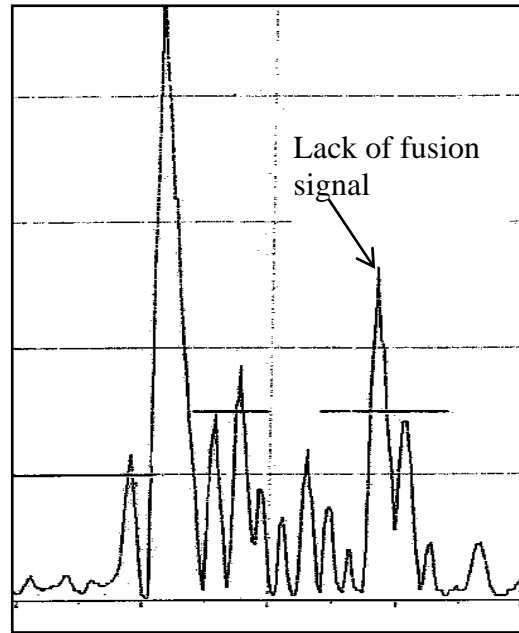


Fig.1b. Ultrasonic signal from a lack of fusion defect in the end-plug weld



Fig-2 As polished cross section of the failed fuel near the end plug

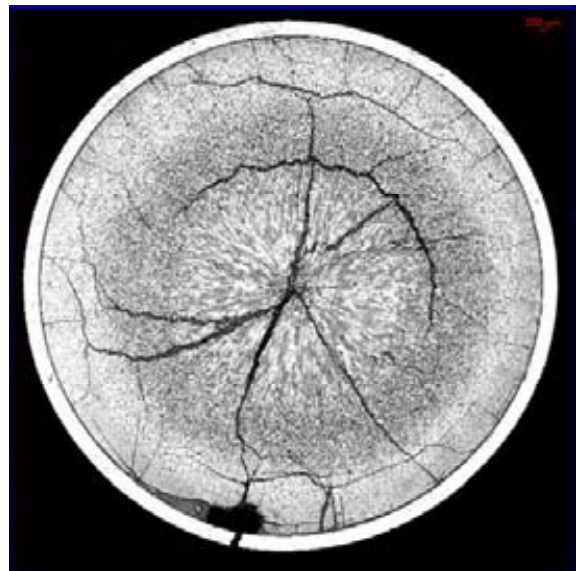


Fig-3 Etched cross-section of the fuel at the failed location

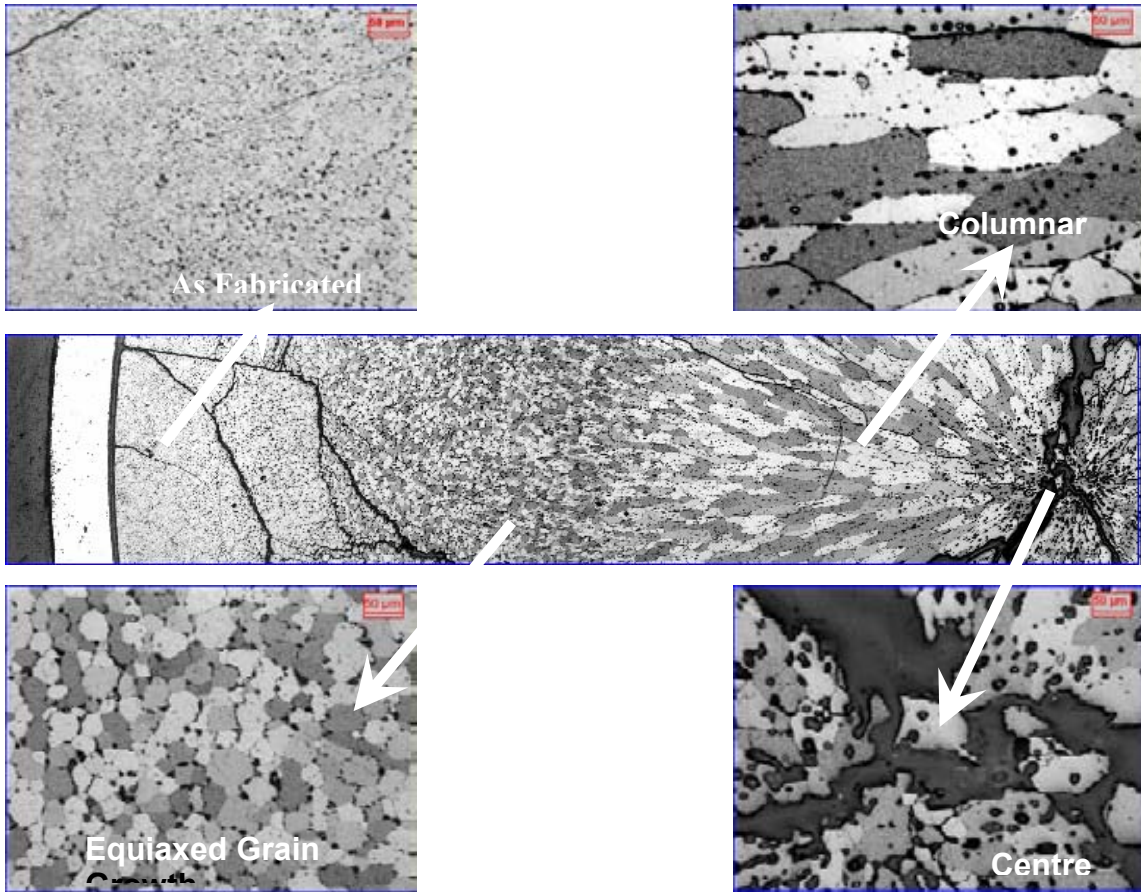


Fig.-4: Restructured zones from the periphery to the centre of the fuel pellet in the failed pin at the location of failure

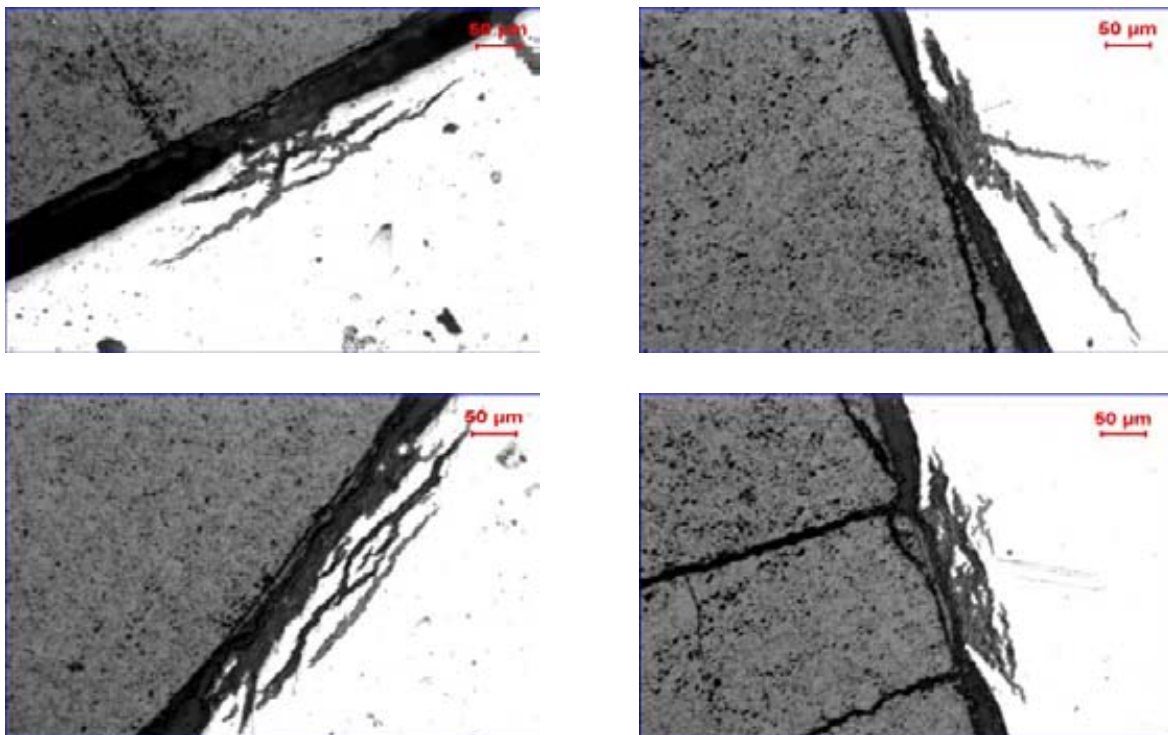


Fig.-5 Circumferential defect sites in the clad showing the contact of the fuel with the clad at some places

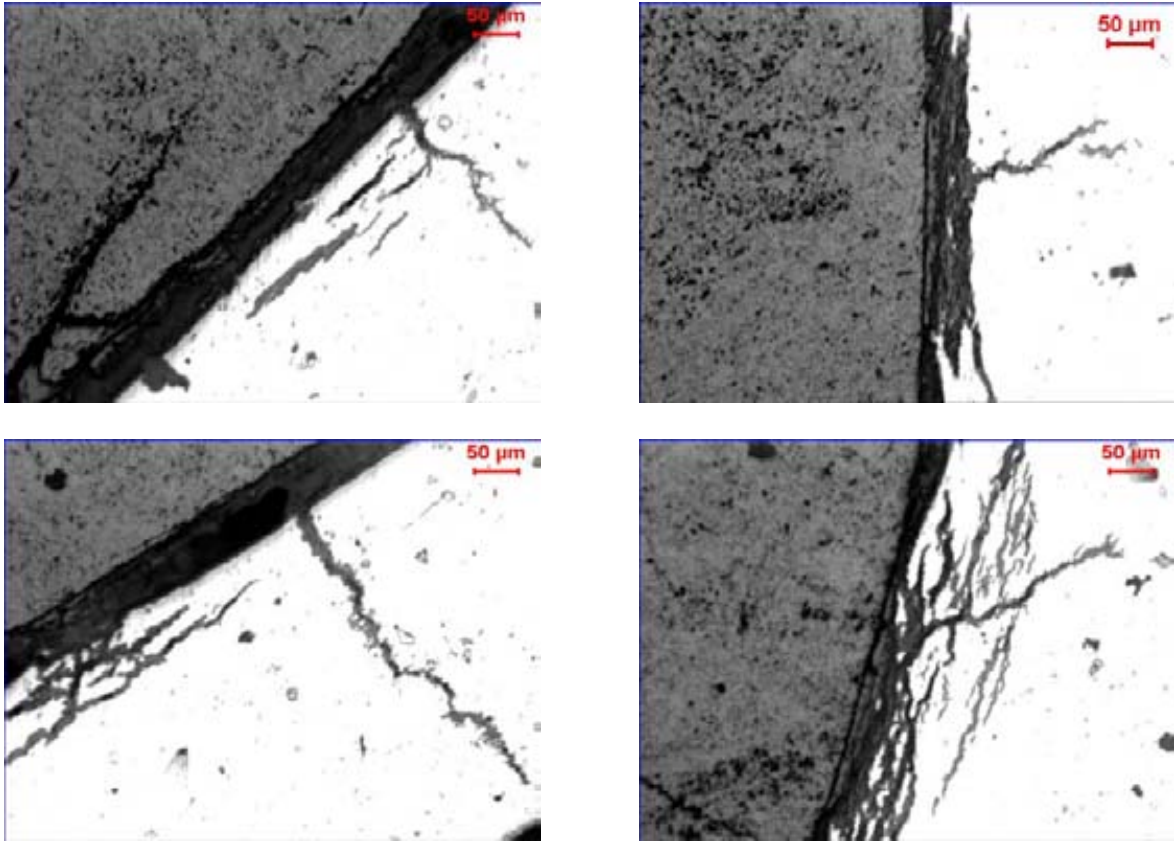


Fig-6 Mixed mode defect sites in the clad showing contact of the fuel with the clad at some places

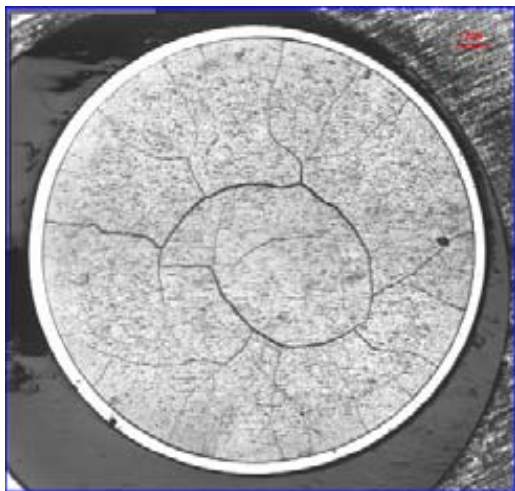


Fig-7: Photo-macrograph of the fuel cross-section in an un-failed adjacent pin at a similar distance as that of the failed pin

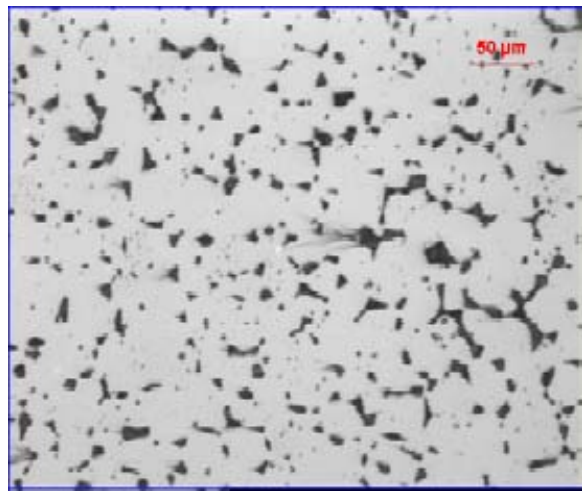


Fig-8 Microstructure at the central region of the sample shown in fig.7

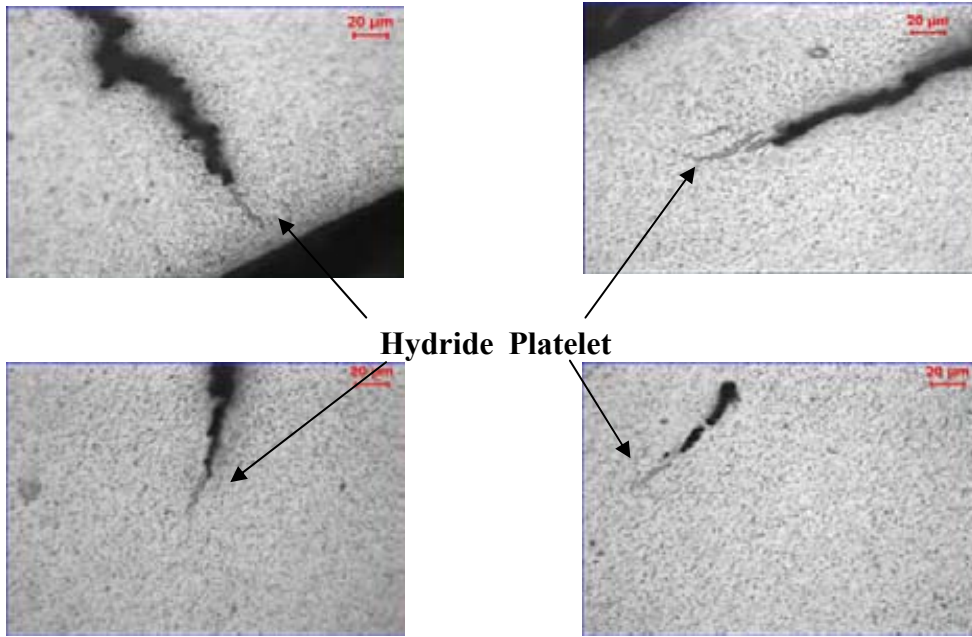


Fig.-9 Hydride platelet at the crack tips in the clad

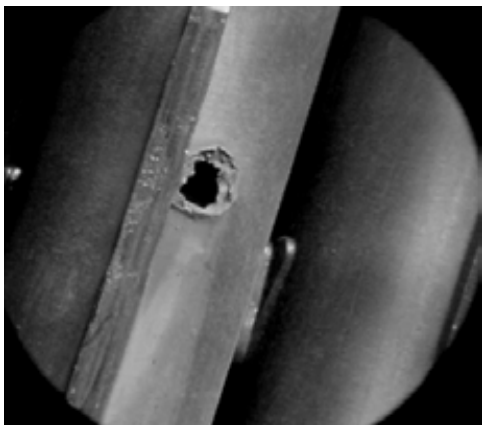


Fig. 10a Pinhole in the clad due to a hydride blister

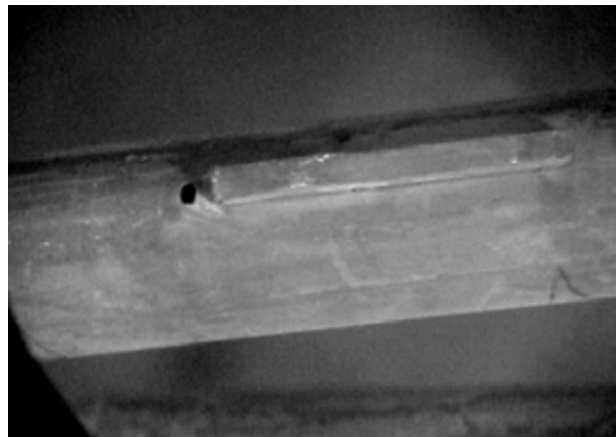


Fig. 10b Pinhole formed due to damage to a bearing pad

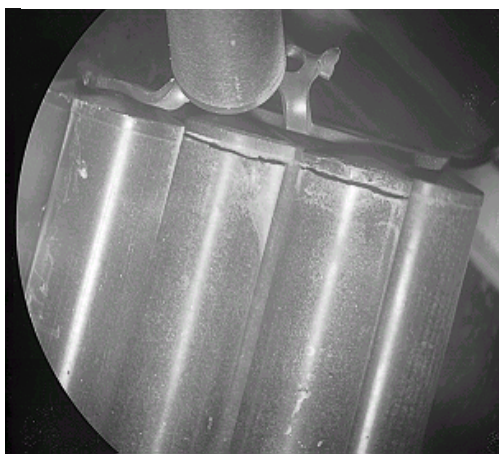


Fig. 10c Cracks at the end plugs

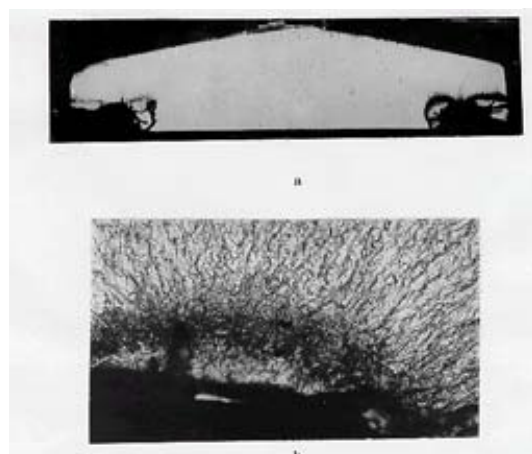
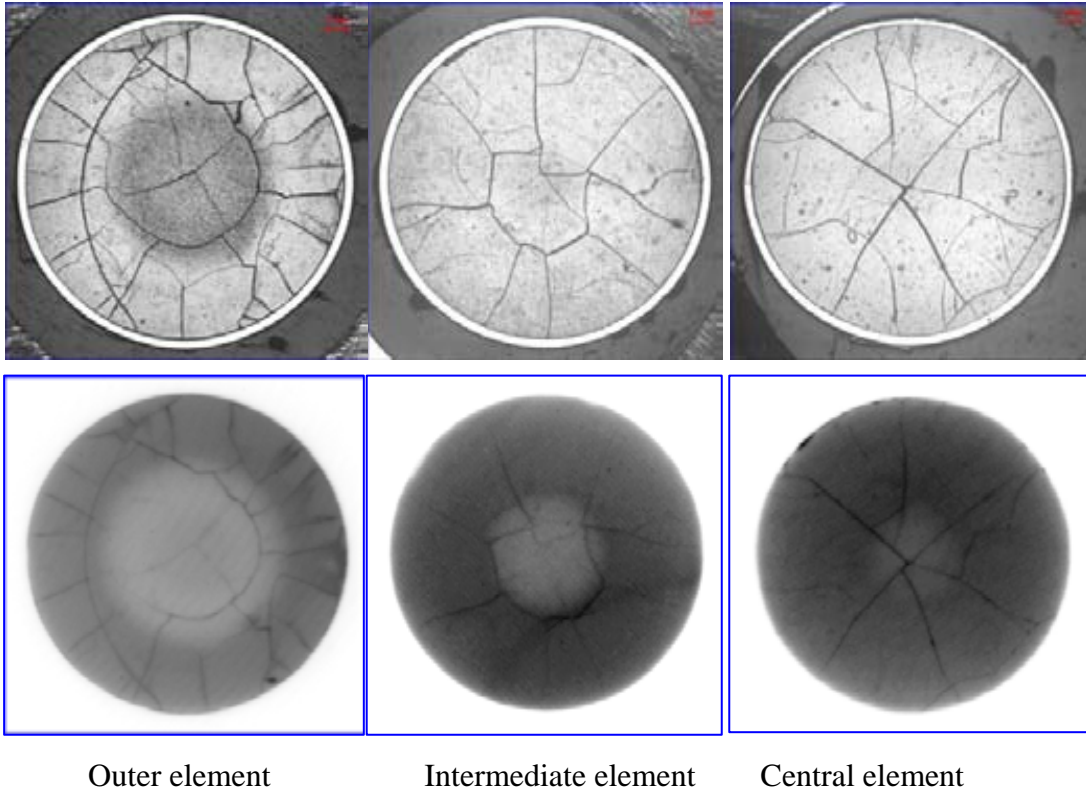


Fig. 10d Hydriding observed at the end plug

Fig.10. Some of the low burnup fuel failures examined at the PIE facility



Outer element

Intermediate element

Central element

Fig.-11. Photomacrographs and the corresponding β - γ autoradiographs of the high burnup fuel examined (Bundle 56504, Burnup 14, 580MWD/TU)

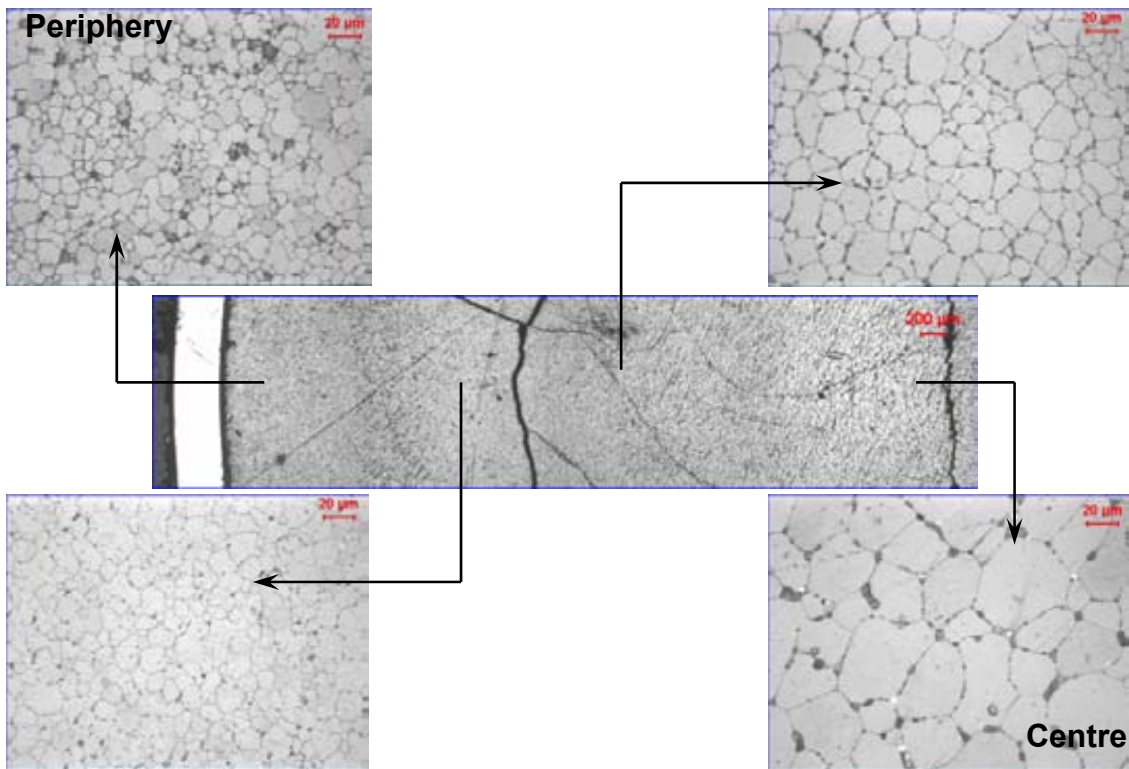


Fig. 12: Different microstructures observed from the centre to the periphery of the outer pin of the bundle 56504, burnup 14,580 MWD/TU

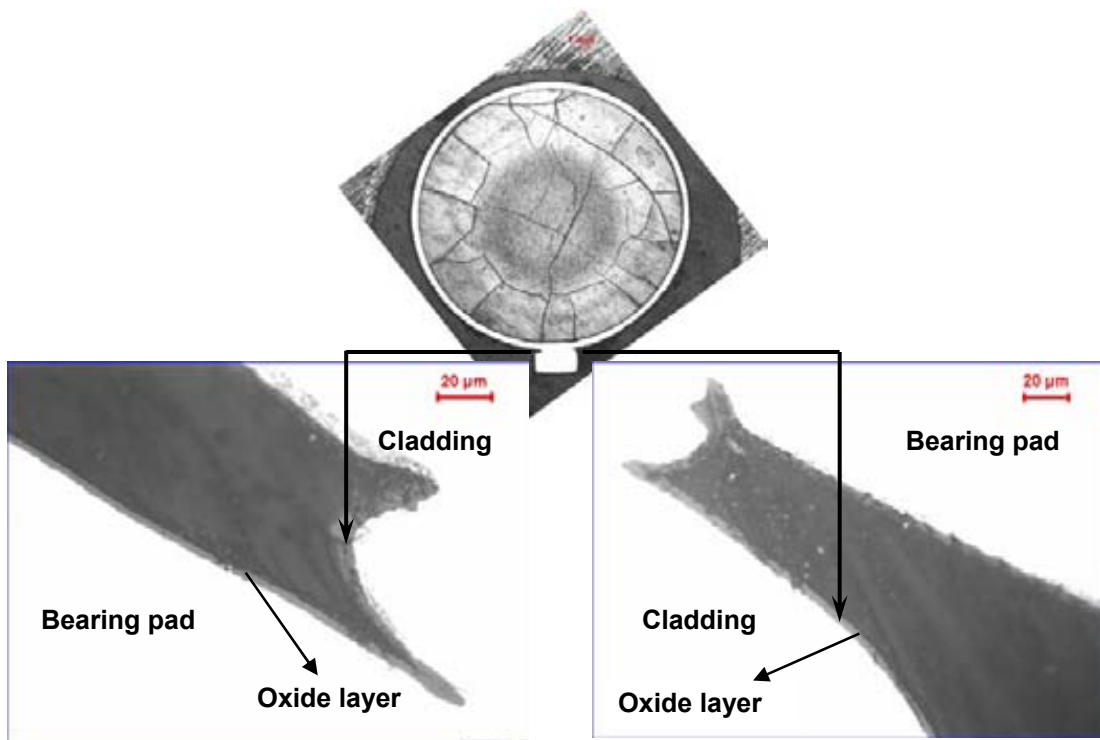


Fig. 13: Uniform corrosion observed at the crevice of the bearing pad of the outer element

PIE Results and New Techniques Applied for 55GWd/t High Burnup Fuel of PWR

Tomohiro Tsuda, Yoichiro Yamaguchi, Yuji Kosaka,

Nuclear Development Corporation, 622-12, Funaishikawa, Tokaimura, Ibaraki 319-1111, Japan

Toshiyuki Kawagoe, Takaaki Kitagawa

Mitsubishi Heavy Industries, LTD., 1-1-1 Wadasakicho, Hyogo-ku, Kobe 652-8585, Japan

ABSTRACT

Post-irradiation examinations (PIE) for 55GWd/t high burnup fuel which had been irradiated at a domestic PWR plant was conducted at the fuel hot laboratory of the Nuclear Development Corporation (NDC). In this PIE, such new techniques as the clamping for axial tensile test and the pellets density measurement method for high burnup fuels were used in addition to existing techniques to confirm the integrity of 55GWd/t high burnup fuel. The superiority of improved corrosion-resistant claddings over currently used current Zircaloy-4 claddings in terms of corrosion-resistance was also confirmed. This paper describes the PIE results and the advanced PIE techniques.

INTRODUCTION

Japanese PWR utilities are planning to increase the burnup of fuel from 48 GWd/t to 55GWd/t for the purposes of improving the fuel cycle economy and reducing the amount of spent fuel. In order to confirm the integrity of the fuel prior to the practical use of 55 GWd/t fuel, the present PIE was conducted at the fuel hot laboratory of NDC using 55 GWd/t fuel rods which had been spent for four cycles at a PWR plant in Japan.

In addition to confirming the integrity of conventional claddings and pellets, this PIE also checked the improvement effects of improved corrosion-resistant claddings and large grain-size pellets designed to reduce the released amount of FP gas. This paper introduces the data of the PIE which was conducted to confirm the integrity of conventional claddings and pellets and the improvement effects of improved corrosion-resistant claddings and large grain-size pellets.

In this PIE, advanced PIE techniques such as ① the tube-shape axial tensile test and ② the pellets density measurement method for high burnup fuels, had been applied in addition to conventional PIE items. This report explains these new techniques and these results .

1. PIE Result of 55GWd/t Burnup Fuel Using Conventional Techniques

1.1 Fuel Rods

Table 1⁽¹⁾ shows the specifications of the fuel rods used in this PIE. The average burnup of a fuel assembly was 52 GWd/t and 13 fuel rods were removed from the assembly for their transportation to a hot laboratory. The assembly was the 17 x 17 type with advanced fuel materials. That is three types of the claddings: ① Zircaloy-4 claddings, which are currently in use, ② MDA and ③ ZIRLOTM as improved corrosion-resistant claddings and three types of fuel pellets : ① pellets currently in use, ② large grain-size pellets aimed at reducing the released amount of FP gas and ③ pellets with added Gd₂O₃ at a rate of 10 wt% were contained.

1.2 PIE Results

(1) γ Scanning Measurement

The γ scanning measurement was conducted to confirm the burnup along the axial direction of the fuel rods and the migration of FP. Fig.1⁽¹⁾ shows the measurement results of the γ ray intensity of Cs-137 along the axial direction. The observed γ ray intensity showed an almost flat pattern except at the grid section and the upper and lower ends, confirming almost even burning along the axial direction.

(2) Measurement of Dimensions

Fig.2⁽¹⁾ shows the measurement results of the fuel rod length. The rod length changes was smaller with the improved corrosion-resistant claddings (MDA/ZIRLOTM) than current Zircaloy-4 claddings, presumably because of the different alloy constituents of these claddings. Meanwhile, the fuel rods containing large grain-size pellets showed a larger rod length changes, presumably because of the influence of PCMI.

(3) Measurement of FP Gas Release Rate

The puncture test was conducted to check the released amount of FP gas. Fig.3⁽¹⁾ shows the test results compared with the overseas data. While the FP gas release rate increased with increased burnup, the measurement results this time were lower than the overseas data due to its low linear heat rate/low temperature irradiation condition. The difference in the grain-size of pellets did not significantly affect the FP gas release rate.

(4) Cladding Oxide Film Thickness and Hydrogen Content

The oxide film thickness on the outer surface of the cladding was measured by the

eddy current method to check any positive effect of the improved corrosion-resistant claddings. Fig.4⁽¹⁾ shows the measurement results for the peak oxide film thickness and the corresponding data of an earlier study. The results indicate a better corrosion-resistance performance of the improved corrosion-resistant claddings than current Zircaloy-4 claddings.

Fig.5⁽¹⁾ shows the relationships between the measured hydrogen content and the oxide film thickness on claddings. In short, the hydrogen content of this study claddings was 400 ppm or lower.

(5) Cladding Mechanical Properties

The tensile test by using the dog-bone shape specimen was conducted at 385°C to identify the mechanical properties. Fig.6⁽¹⁾ and Fig.7⁽¹⁾ shows 0.2% yield strength and fracture elongation along with corresponding data of an earlier study. The results indicate that this study claddings have good mechanical properties performance in the high burnup region. The mechanical properties data of the improved corrosion-resistant claddings fall within the existing data range for the claddings currently in use.

2. PIE of 55 GWd/t Burnup Fuel Using New Techniques

2.1 Improvement of Clamping Jig for Cladding Tensile Test

The axial tensile test for a tubular specimen of a cladding is conventionally conducted to establish the mechanical properties of claddings. However, the obtaining of elongation data is difficult because of the fracture within not gauge length(GL) section but at the wedge grip type chuck section. To solve this problem, the method to clamp the specimen was changed from the wedge type chuck to the collet type chuck for the present PIE as shown in Fig. 8. Because of the lack of precedence of this method, it was necessary to find a suitable clamping force to prevent any slippage of the tubular specimen. A hydrogen-absorbed non-irradiated specimen for the tube axial tensile test was used to check this suitable force and it was found that the necessary clamping force was approximately 240 N.m. A clamping jig with a structure of a combination of gears was manufactured to enable clamping work by remote control. Fig. 9 shows the appearance of this jig. For the present PIE, this jig was used to clamp the specimen for the axial tensile test. The test results were that fracture took place within the GL of the tubular specimen and that the measured elongation data was reasonable results.

2.2 Examination of Density Measuring Method for High Burnup Fuel

To evaluate the densitication as well as swelling of fuel pellets due to irradiation the conventional method of density measurement is conventionally conducted using several pellet fragments extracted from the fuel rod. However, it was supposed that the collection of fuel

fragments by the conventional method would be difficult in the case of high burnup fuel because of the bonding between the cladding and fuel pellet. There was also concern in regard to adverse impacts of the volume of the remaining layer of pellets on the inner surface of the claddings after defueling on the pellet density value. For this reason, the conventional method and a new method were carried out in present PIE for high burnup fuel and the both results were compared. In the new method, the density of a cut piece (claddings and fuel pellets) and the density of the claddings after defueling are measured and then the pellet density is evaluated based on the above measured results. The specimen was produced by cutting the fuel rod by some 3mm in length. The weights were measured in air and in liquid based on the immersion method. Fig. 10 shows the density measuring results based on the conventional and the new methods, which indicates good agreement between the both measurement results. Accordingly, it is confirmed that the results of the new measuring method should be valid as those of the conventional measuring method are.

CONCLUSIONS

The PIE was conducted at the fuel hot laboratory of the NDC to check the soundness of 55 GWd/t high burnup fuel and any effects of improved corrosion-resistant claddings and large grain-size pellets aimed at reducing the release of FP gas.

Apart from the accumulation of integrity data for 55 GWd/t fuel, the results confirmed the superior corrosion resistance of improved corrosion-resistant claddings compared to the current Zircaloy-4 claddings which are currently in use.

The present PIE established new techniques regarding reliable axial tensile test method and density measuring and contributed to the soundness checking of 55 GWd/t high burnup fuel.

REFERENCES

- (1) T.Kitagawa,T.Takahashi,Y.Shinohara,M.Sugano,Y.Kosaka,T.Sendo, “Post Irradiation Examination of fuel rods in 55gwd/t Lead Use Assembly”,2005 Water Reactor Fuel Performance meeting

Table1 General specifications of fuel rods ⁽¹⁾

Fuel rods in LUA	
Cladding Material	MDA ZIRLO Low Tin Zircaloy-4
Outer Diameter	9.50mm
Inner Diameter	8.36mm
Pellet Material	Current UO ₂ Large grain UO ₂ 10wt%Gd ₂ O ₃ doped UO ₂
Diameter	8.19mm
Length	10mm
Density	95%T.D.
Enrichment	4.5wt% 2.0wt%(10wt%Gd)
Fuel Rod Fuel Stack Length	3.6m
Length	3.9m
Fuel Assembly Type	17x17
Grid Material	Inconel

* : Lead Use Assembly

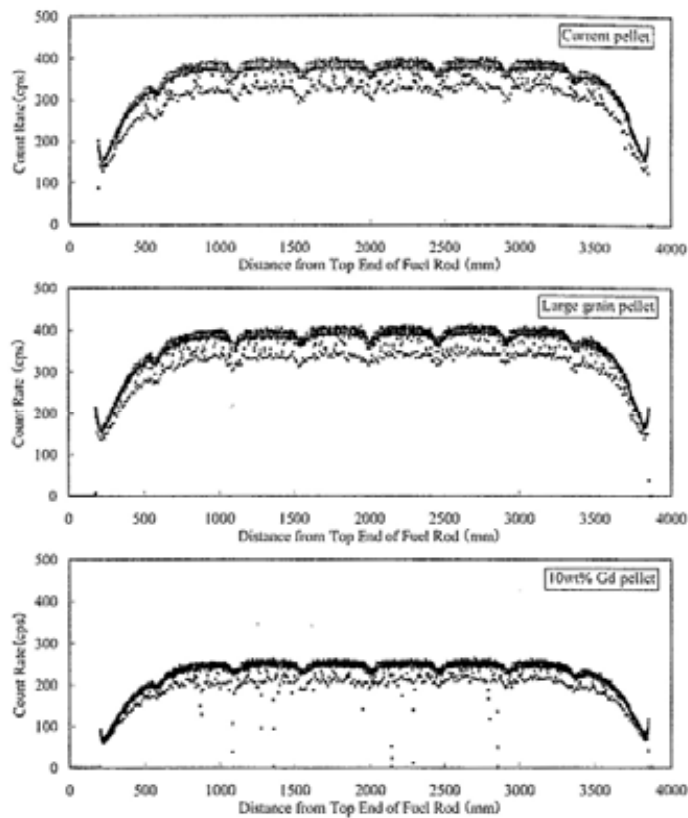


Fig.1 Axial Cs-137 gamma scanning trace ⁽¹⁾

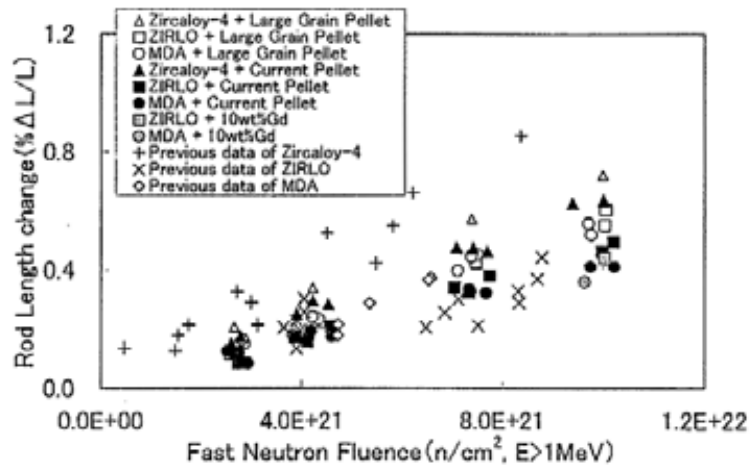


Fig.2 Relationship between Rod length change and fast neutron fluence⁽¹⁾

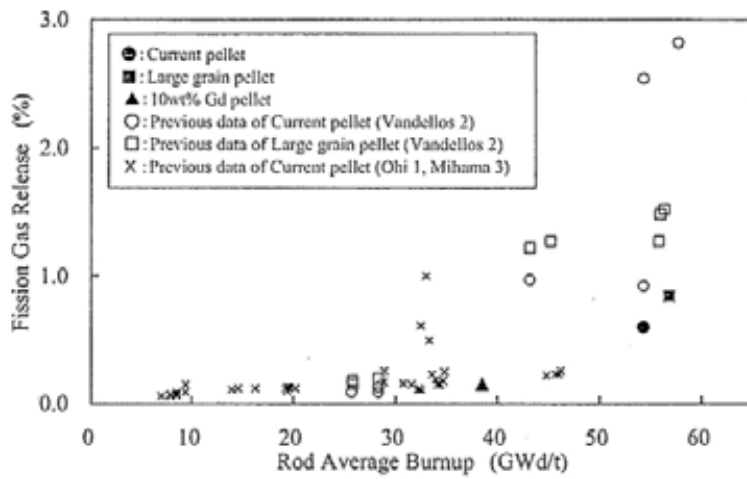


Fig.3 Comparison of fission gas release among the fuel pellet types⁽¹⁾

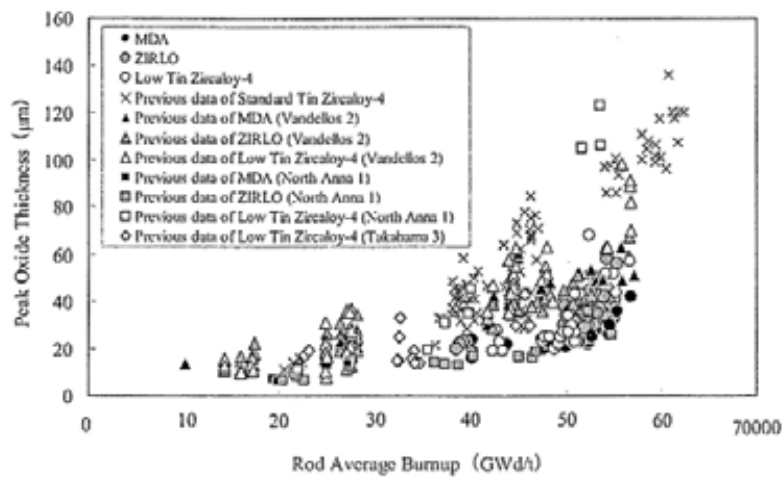


Fig.4 Measurement results of peak oxide thickness by ECT⁽¹⁾

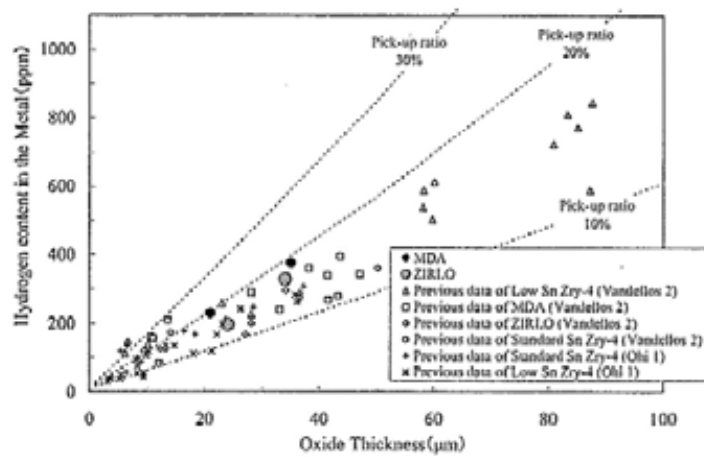


Fig.5 Relationship between oxide thickness and hydrogen content⁽¹⁾

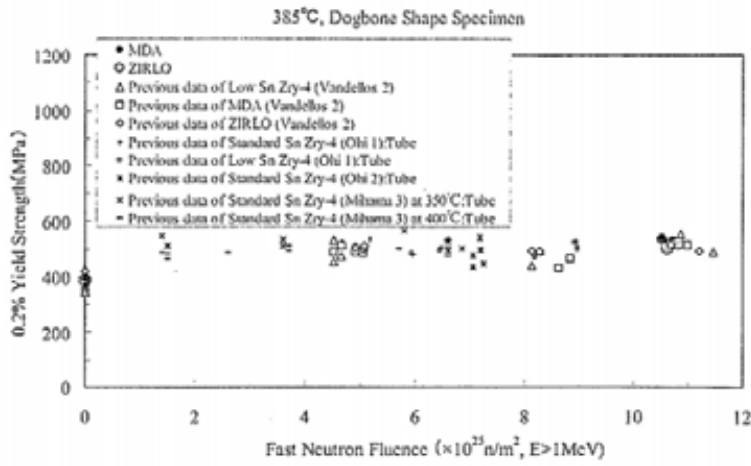


Fig.6 Relationship between fast neutron fluence and yield strength of the cladding⁽¹⁾

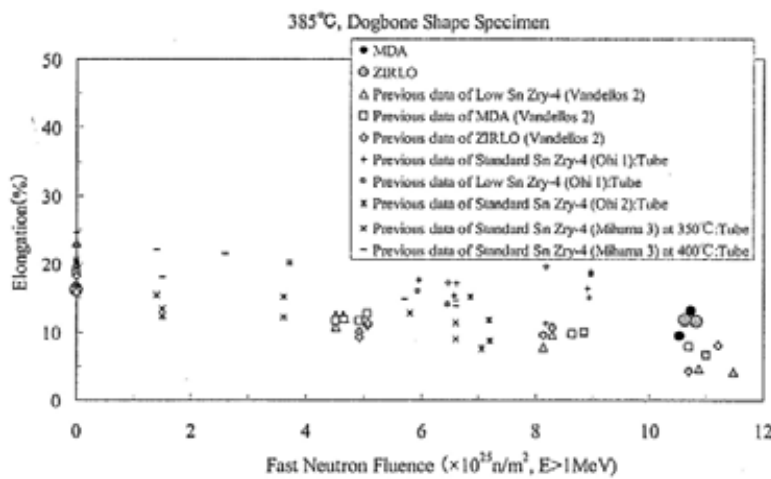


Fig.7 Relationship between fast neutron fluence and elongation⁽¹⁾

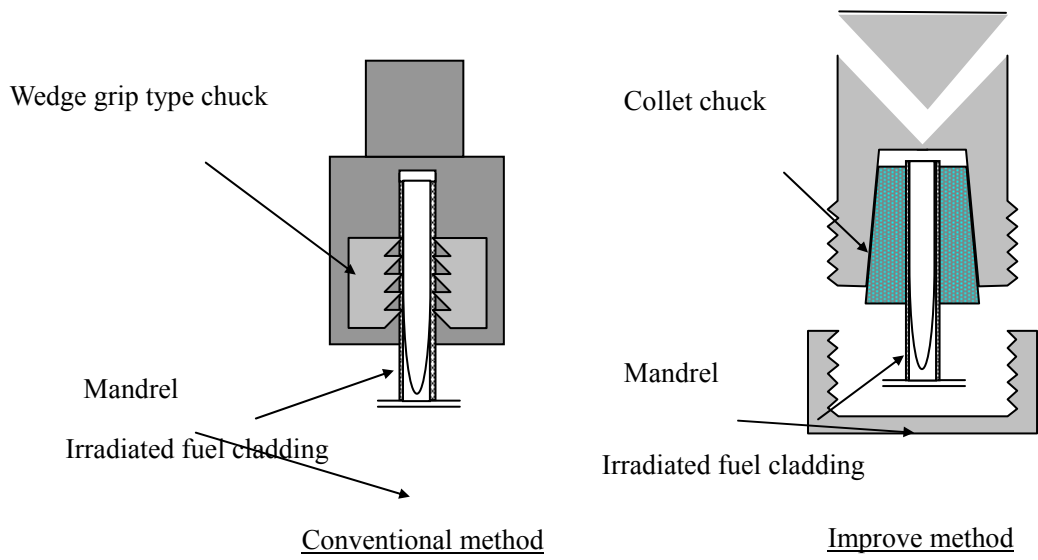


Fig.8 Clamping method

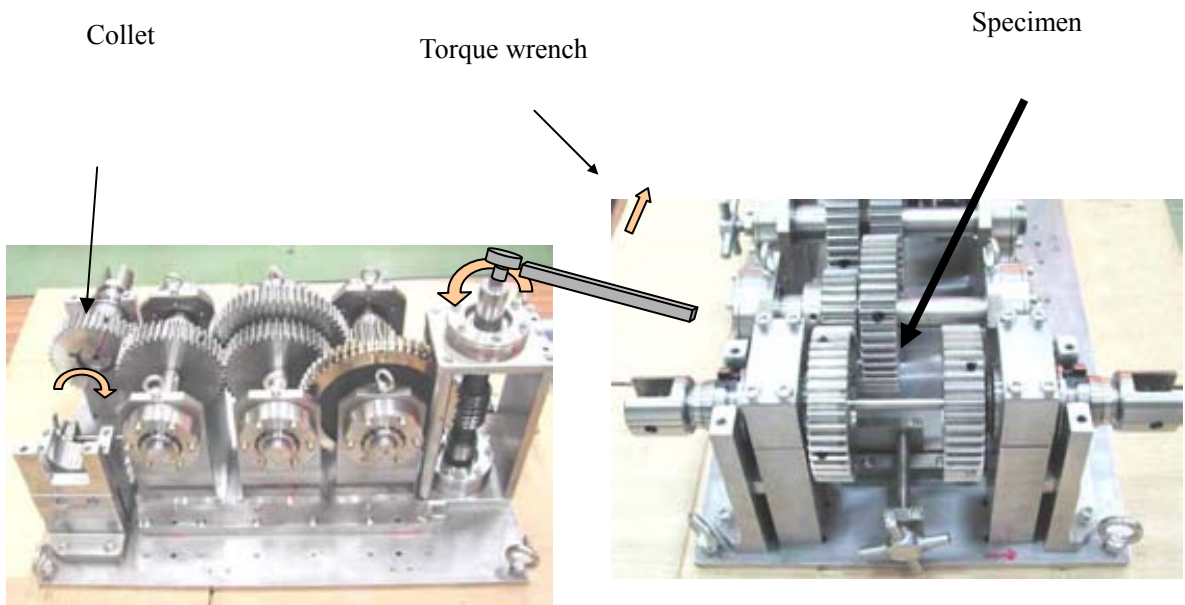


Fig.9 Appearance of clamping jig

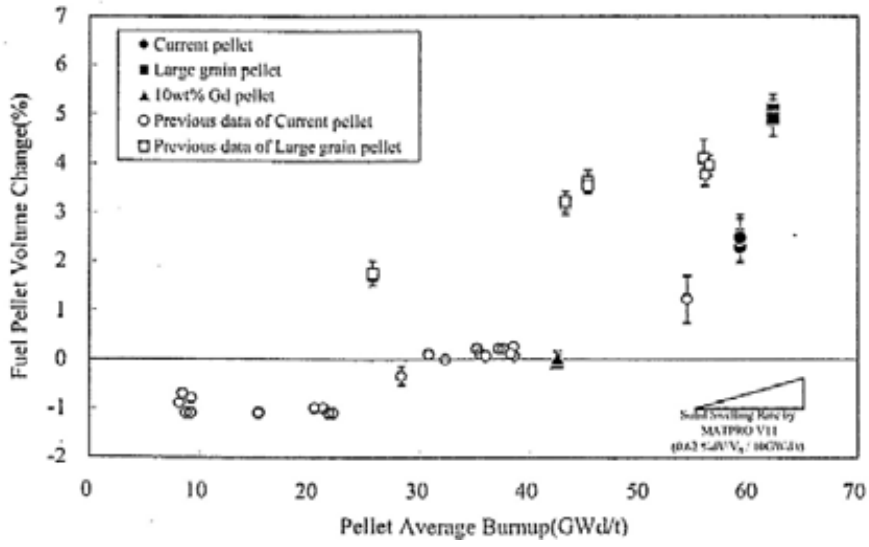


Fig. 10 Fuel pellet volume change with burnup⁽¹⁾

Underwater Fuel Inspection for Irradiated LWR Fuels in Korea

Y.B. Chun*, D.K. Min*, G.S. Kim*, J.R. Park**, J.Y. Park**,
J.M. Seo**, J.S. Lee**, J.C. Shin** and K.P. Hong*

*Korea Atomic Energy Research Institute
P.O.Box 105, Yusong, Taejon, Korea, 305-600
Tel: +81-42-868-2482, E-mail: ybchun@kaeri.re.kr

** Korea Nuclear Fuel Co., LTD

Abstract

A wide range of post-irradiation examination (PIE) for the nuclear fuels irradiated at NPPs with different design characteristics have been conducted in Korea. Most of irradiated fuel assemblies are inspected in the pool of NPP sites during regular overhaul outages and some of them are selectively transported to the post-irradiation examination facility (PIEF) in KAERI for PIE to evaluate the irradiation performances as well as the fuel integrities. The data obtained from the PIE is used for the improvement of nuclear fuel performances and operation reliabilities. A comprehensive underwater fuel inspection system is developed and has been used to confirm the integrities of the fuels to be reloaded in the next cycle of reactor operation. In this paper, the underwater fuel inspection activities conducted in Korea are introduced and described. Recently, PIE activities put great concentrations on the oxidation condition of the cladding tube as well as the failure inspections to cope with the licensing requirements of fuel integrities under the highly extended burn up conditions. The more precise hot cell examination results are incorporated to confirm the on-site inspection results and to improve the capabilities of the equipment, as well.

1. Introduction

Nuclear power has been one of the major sources of energy demands in Korea since the first commercial nuclear power operation in 1978. As of December 2005, 16 PWR type nuclear power plants and 4 PHWR (CANDU) are providing around 40 % of the national electricity demand with total capacity of 17,716 MWe. 14x14, 16x16 and 17x17 type fuels are used in PWR type reactors. According to the national energy program, nuclear energy will cover around 34.6 % of national energy demand that will lead to 26,640 MWe by 2016.

Table 1 and 2 show the electrical energy share as of 2005 and the present status of nuclear power plants in Korea, respectively.

Table 1. Electric Energy Production Share of Korea (x 10 MWe)

	Nuclear	Coal	LNG	Oil	Hydraulic	Others	Total
2005	1,772 (28.4)	1,797 (28.8)	1,637 (26.2)	471 (7.6)	388 (6.2)	177 (2.8)	6,241 (100)
2017	2,664 (30.3)	2,224 (25.3)	2,313 (26.3)	333 (3.8)	629 (7.1)	641 (7.3)	8,804 (100)

Nowadays, the fuel design groups and the utility groups put great efforts on extending the operation cycle to get higher burnup, higher power and high integrities of the fuels under severe conditions. To assure the safety of power plant, activities to improve fuel performances and safeties have been carried out, so far. Fuel inspection technologies, in this context, have been playing a great role in improving fuel performances and operation safety of the plants.

KAERI as a government sponsored research establishment, endeavored to develop fuel inspection technologies to support utilities as well as research activities by providing nuclear fuel performance data adequately. Table 3 shows the in-pool examination activities conducted in PIEF for underwater inspection of spent nuclear fuels at KAERI. Three large pools of KAERI enable full scale of underwater examinations for the PWR type of irradiated nuclear fuels. Figure 1 shows the plane drawing of post-irradiation examination (PIE) facility at KAERI. Three pools for CASK receiving & unloading, fuel storage, and inspection & dismantling of the fuel assembly have been in operation since 1985 to evaluate the fuel performances and to develop a series of underwater fuel examination technologies. Underwater inspection for the fuel assembly covers various examination items physically and/or mechanically, such as gamma spectroscopy for the fuel assembly and rod, visual inspection, dimensional measurement, geometrical change inspection, and hold-down spring force measurement, etc. And for the fuel rods, it covers the examination items such as oxide layer thickness, wear, diameter, ovality, fuel growth, and fuel defect identification, etc. Under the in-pool PIE technique development program, underwater dismantling and reconstitution technology were also developed. For dismantling of the assembly, various kinds of dismantling methods were developed and applied in the PIEF pool according to the

Table 2. Status of Nuclear Power Plants in Korea

NPP	Power (MWe)	Type	Supplier		Startup
			Reactor	Turbine	
Kori-1	587	PWR	<u>W</u>	G.E.C	'78.4
Kori-2	650	PWR	<u>W</u>	G.E.C	'83.7
Kori-3	950	PWR	<u>W</u>	G.E.C	'85.9
Kori-4	950	PWR	<u>W</u>	G.E.C	'86.4
Wolsung-1	680	PHWR	AECL	Parson	'83.4
Wolsung-2	700	PHWR	HANJOONG /AECL	HANJUNG (GE)	'97.6
Wolsung-3	700	PHWR	HANJOONG /AECL	HANJUNG (GE)	'98.7
Wolsung-4	700	PHWR	HANJOONG /AECL	HANJUNG (GE)	'99.6
YGN-1	950	PWR	<u>W</u>	<u>W</u>	'86.8
YGN-2	950	PWR	<u>W</u>	<u>W</u>	'87.6
YGN-3	1000	PWR	HANJOONG /KAERI(GE)	HANJUNG (GE)	'95.3
YGN-4	1000	PWR	HANJOONG /KAERI(GE)	HANJUNG (GE)	'96.1
YGN-5	1000	PWR	HANJOONG /KAERI/KOPEC	HANJUNG (GE)	'01.12
YGN-6	1000	PWR	HANJOONG /KAERI/KOPEC	HANJUNG (GE)	'02.12
Ulchin-1	950	PWR	FRAMATOME	ALSTOM	'89.9
Ulchin-2	950	PWR	FRAMATOME	ALSTOM	'88.9
Ulchin-3	1000	PWR	HANJOONG /KAERI(CE)	HANJUNG (GE)	'98.6
Ulchin-4	1000	PWR	HANJOONG /KAERI(CE)	HANJUNG (GE)	'99.6
Ulchin-5	1000	PWR	HANJOONG /KAERI(CE)	HANJUNG (GE)	'04.6
Ulchin-6	1000	PWR	HANJOONG /KAERI(CE)	HANJUNG (GE)	'05.6
Total	17,717				

Table 3. Underwater PIE Items of PIEF

Items	
Visual inspection	Underwater Camera
Dimensional Measurement	Encoder/XY table/ Image processing
Underwater Fuel Rod Verification	Gamma radiation collimation
Hold-down Spring Force Measurement	Load Cell/Encoder
Underwater Gamma Spectroscopy	
Exponential Experiment	



Figure 1. Plane Drawing of PIE facility at KAERI

design and fabrication types of the fuel. For the first generation nuclear fuels which were supplied for the beginning periods of NPPs of Korea, the dismantling was carried out by cutting the guide thimble tubes with a band saw or by milling out the welds between the tubes and top end piece (TEP). But now, reconstitutably designed fuels facilitate dismantling as well as maintenances. With very simple remote handling tools to remove the screws or lock tubes which assembles the guide tubes and TEP allows to access to the fuel rods to be extracted. For the selective extraction of fuel rods, fuel rod index is used in aligning the fuel extraction tool to the fuels to be extracted.

2. Status of fuel services

PIE facility was constructed and started its hot operation from 1985. The main activities of PIEF are to examine the irradiated nuclear fuels and evaluate the fuel performances. And, many efforts were put on the examinations to find the root causes of the defective fuels and preparing the remedies to improve the safety of the fuels. All type of indigenous irradiated PWR fuel assemblies were transferred to PIEF and examined. The fuel assemblies received full scale of underwater examinations and dismantled, then fuel rods were extracted selectively for furthermore in-pool and hot cell PIEs. For the underwater fuel inspection and examination, KAERI developed comprehensive transportable fuel inspection equipment with the start of the indigenous nuclear fuel development program of Korea. The equipment was developed for use at all type of NPP sites in Korea to verify fuel performances and integrities. It was used in fuel inspection during refueling outages to get the information of irradiation performance and reload flexibility of the fuels to be reloaded. Figure 2 and 3 shows the fuel inspection equipment developed by KAERI.

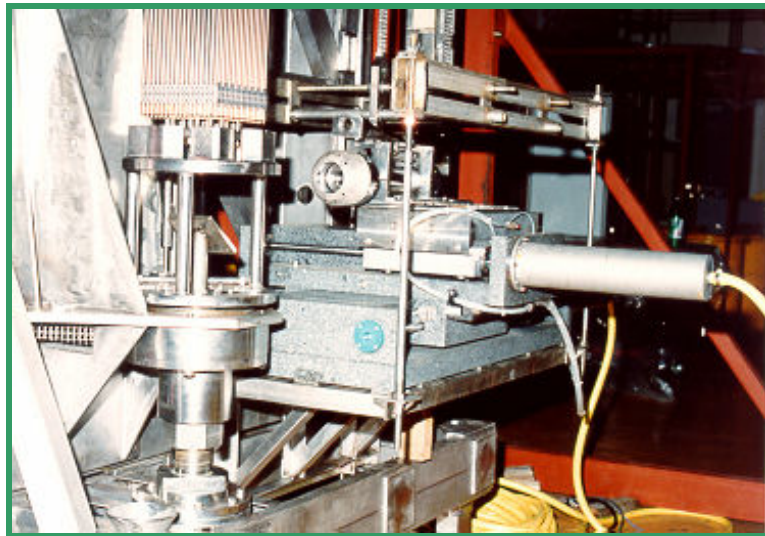


Figure 2. Measuring System mounted on the XY Table

Most of developed technologies were transferred to the utility service groups for the on-site fuel inspections at Nuclear Power Plants. Now, Korea Nuclear Fuel Co., Ltd. (KNFC) has extended the fuel fabrication capabilities and supplies all the type of nuclear fuels to the power plants in Korea. As a major fuel provider, KNFC runs nuclear fuel service team to guarantee the safety of the fuels and to cope with the growing needs of fuel services. At present, KNFC has developed a series of fuel service equipment and provides all of the nuclear fuel services.

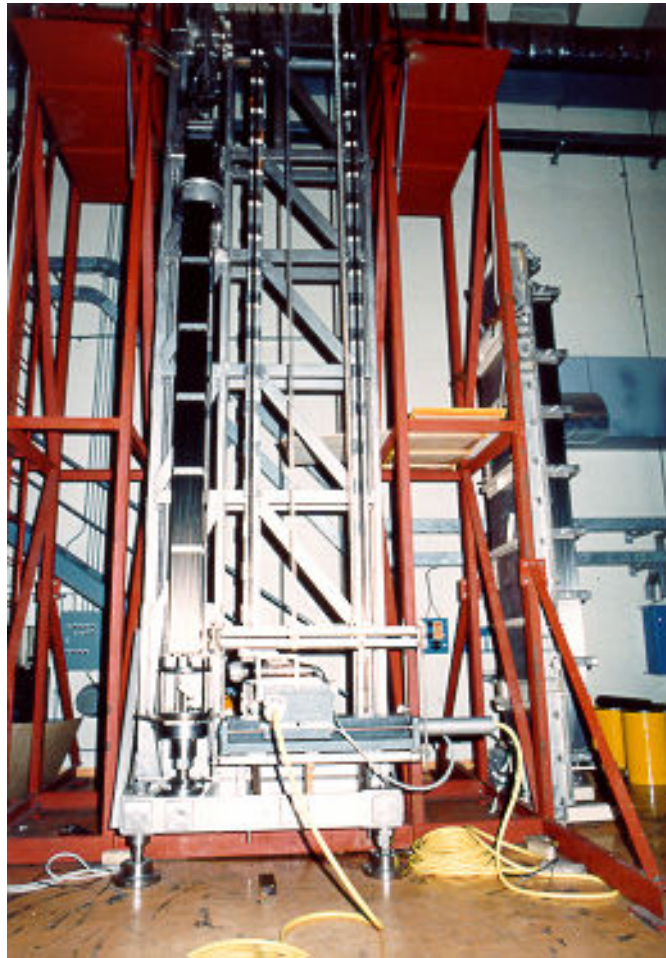


Figure 3. A Comprehensive Transportable On-site Fuel Inspection System

3. Fuel service activities

Since the first nuclear power plant, Kori unit-1, started its commercial power operation in 1978, various kinds of fuel failure and damage occurred. The first reported fuel failure events were due to baffle jet flow damages on the peripheral fuels in the vicinity of baffle joint of reactor vessels. Since then, various kinds of fuel damages, such as design oriented failures, debris induced defects, flow induced vibration-oriented fretting/wear, etc were occurred. Since the first big fuel repair campaign conducted by W fuel service team for the Kori unit-1 fuels damaged from baffle jet flow, Westinghouse, CE fuel service teams conducted fuel service activities in 1980's. Now, most of fuel service activities are carried out by KNFC fuel service team. With various inspection technology incorporated system, irradiation performance examination campaign against the fuels irradiated at various NPPs in Korea has been conducted successfully, so far. Recent considerations are put on the items

such as fuel component function test technology including spacer grid spring force measurement, grid cell dimension, rod dragging force from fuel assembly, guide tube oxide layer thickness measurement and crud sampling.

Another concentration is put on the fuel service technology development program for the Plus-7 and ACE-7 fuels to improve safety, reliability and economy of the fuel by improving the fuel components and fuel designs.

4. Underwater Post Irradiation Examination

4.1. Visual Inspection

A radiation resistant underwater camera mounted on the XY table is used for the visual inspection of the fuel assembly. Fuel assembly standing on rotary base plate of the visual and dimensional inspection stand is inspected as the rotary plate rotates the fuel assembly to expose all faces to a camera. The measuring head equipped with underwater cameras and detecting sensors is raised and lowered along the fuel assembly for inspection. Figure 4 shows the visual and dimensional inspection stand (stationary system) fabricated installed in PIEF pool at KAERI.

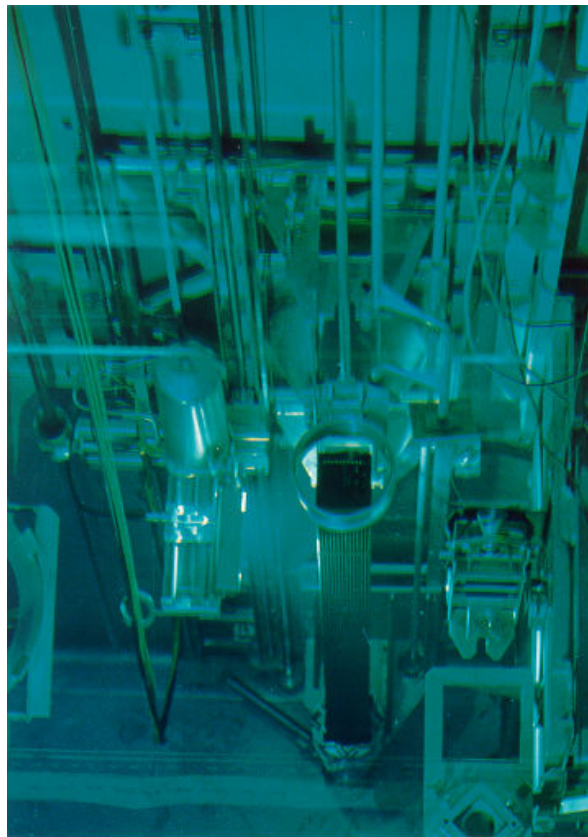


Figure 4. Visual and Dimensional Inspection Stand in PIEF Pool of KAERI

4.2. Dimensional Measurement

Fuel rod length, rod diameter, rod to rod gap, shoulder gap, assembly length, twist, bowing, grid location, etc are measured. Two ways of measurement are carried out. The first one is the original way of dimensional measurement in which the readings are taken using an underwater camera system by aligning the object surfaces with cross hairs superimposed on the monitor. Figure 5 shows the conventional dimensional measurement system panel. Another way of measurement is using image-processing methods in measuring. Figure 5 and 6 shows the image processing system incorporated with the VDIS and the images before and after image processing by this system.



Fig. 5. Control Panel, Display Monitor & Data Acquisition System of VDIS

4.3. Fuel Rod Verification Examination

This is to support IAEA inspection in verifying fuel rods located in the dismantled fuel assembly. After dismantling a fuel assembly, several fuel rods are extracted for furthermore specified PIE. The remaining fuel rods are to be inspected regularly by IAEA. To avoid unnecessary rod extraction, which is not supposed to be examined but designated to be extracted by IAEA for the verification, KAERI developed fuel rod verification system. The idea of this equipment is to use gamma spectrometry system in collecting gamma spectra emit from fuel rod pellets by collimating them with special alignment system. Fuel rod index were designed to align fuel rods selectively along with the collimator tube, which was incorporated with the HPGe detector. The gamma radiation emit from the fuel pellet come through this collimator tube is collected and analyzed. By comparing the collected data with the background around the system and the radiation intensities around the empty holes that was made by rod extraction, the designated fuel rod is verified. Figure 8 shows the in-pool fuel rod verification system installed in the fuel storage pool of PIEF at KAERI.

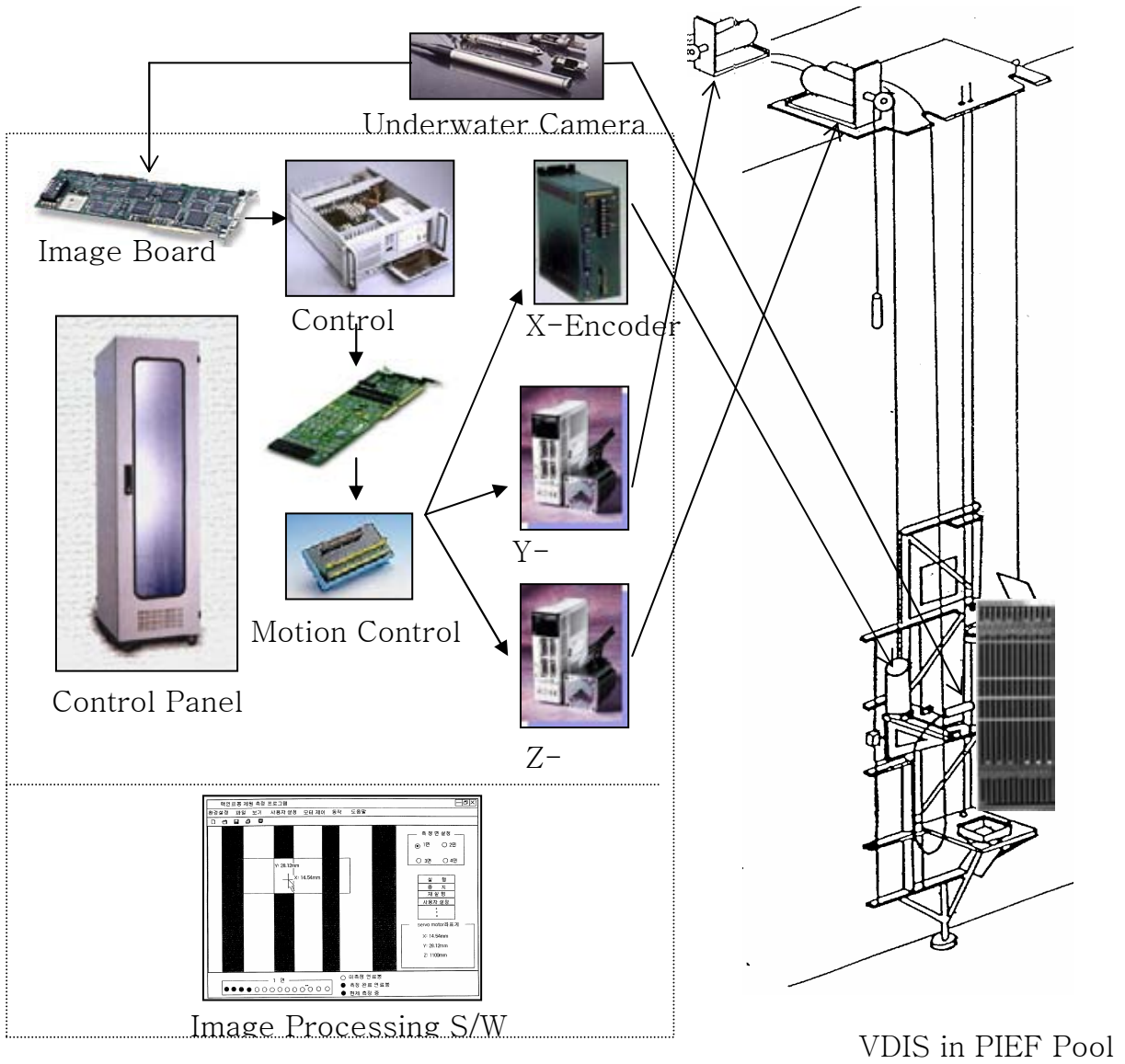


Fig. 6. Schematic View of Image Processing System Incorporated with VDIS

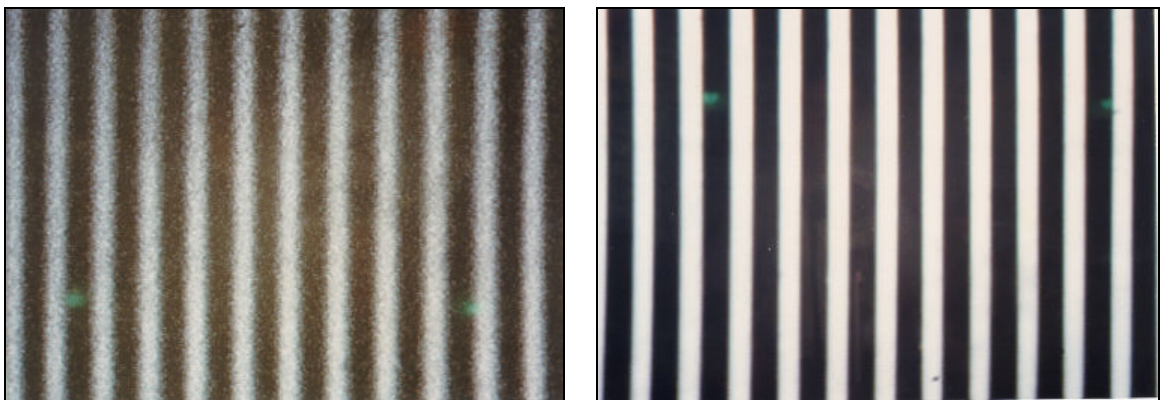


Figure 7. Fuel Rod Image before and after image processing

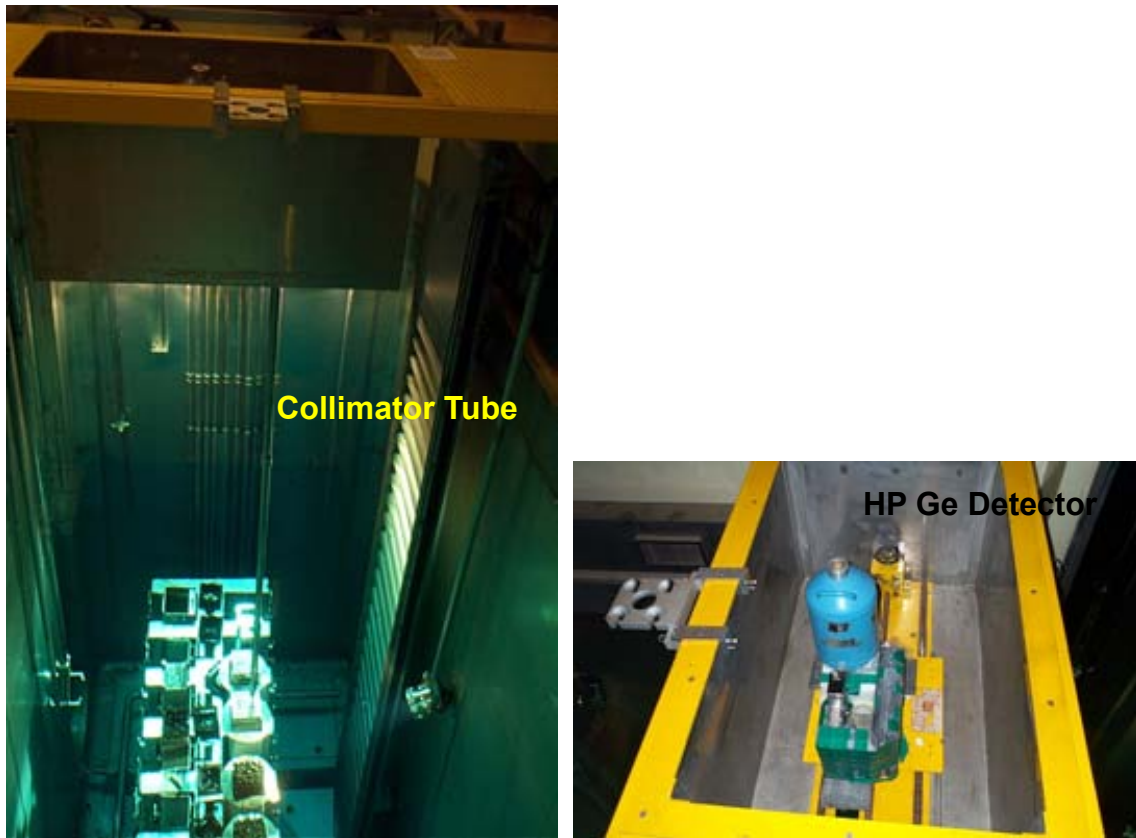


Figure 8. In-pool fuel rod verification system at KAERI

4.4. Hold-down Spring Force Measurement

The hold down spring is to suppress the fuel assembly against very strong and high speed of upstream coolant flows during the reactor operation. The capability to sustain a proper hold-down spring force during the reactor operation should be assured. The spring should have enough strength to suppress the fuel assembly and should not exceed the design strength during irradiation so as not to make any deflection or damage of the fuel assembly structures due to the thermal and irradiation growth of the assembly. To measure the hold-down spring forces of the PWR type nuclear fuels, a simple and transportable hold-down spring force measuring equipment was developed. The leaf spring of TEP of fuel assembly is pressed down and the load-displacement curve is obtained which reveals the spring characteristics after irradiation. This system was designed to avoid any excessive load put on the fuel structures during the suppression of the leaf spring. Figure 9 shows the hold-down spring force measuring devices.

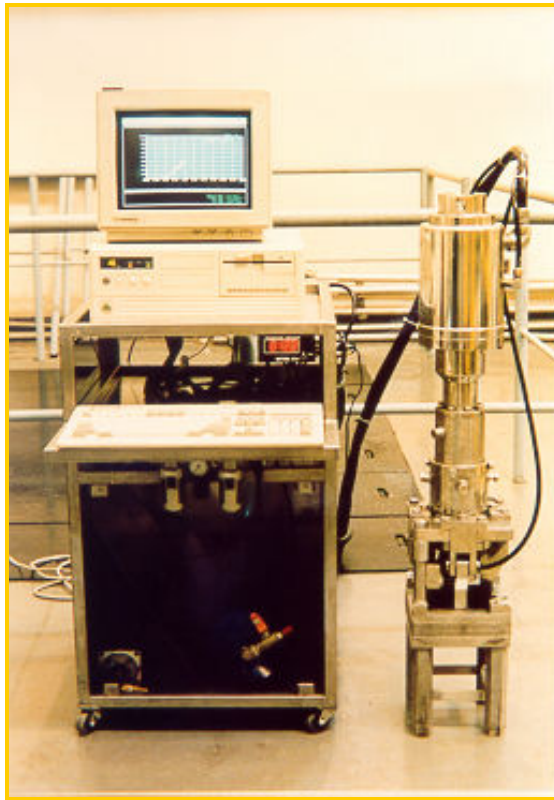


Figure 9. In-pool Hold-down Spring Force Measuring Equipment

4.5. Underwater Gamma Scanning

With the results obtained by measuring and collecting the gamma ray spectra emitted from the fuel assembly, average burnup, cooling time, and initial enrichment are evaluated. And by introducing and applying a burnup credit concept in the spent fuel management system, it is expected to improve the fuel criticality safety and spent fuel management economy. The burnup can be estimated within 5 % of error bound as compared with the result determined by chemical analysis methods. This system can be applied in obtaining an axial burnup profile as well as a horizontal burnup gradient for the fuel assembly.

4.6. Exponential experiment

Exponential experiment is introduced to predict the critical buckling by extrapolating the buckling of a small system, which is in an extremely sub-critical state. The experiment was applied to the sub-criticality estimation for LWR spent fuel and confirmed that the experiment can be used to obtain the neutron effective multiplication factor for the sub-critical system in order to validate criticality calculations. The exponential experiment system is installed in the PIEF pool at KAERI in order to determine the neutron multiplication factor for the PWR spent fuel stored in pool. The objectives of this experiment are to validate criticality calculation code and finally contribute to the implementation of the

actinide plus fission product burnup credit. The exponential experiment system was installed in PIEF storage pool as shown in Fig. 11-13. The system, which is composed of neutron detector, signal analysis system and neutron source, 10 mCi Cf-252 has been installed in the storage pool of PIEF at KAERI in order to experimentally determining neutron effective multiplication factors of PWR spent fuel assemblies.



Figure 10. Underwater Gamma Scanning System for Burnup Measurement

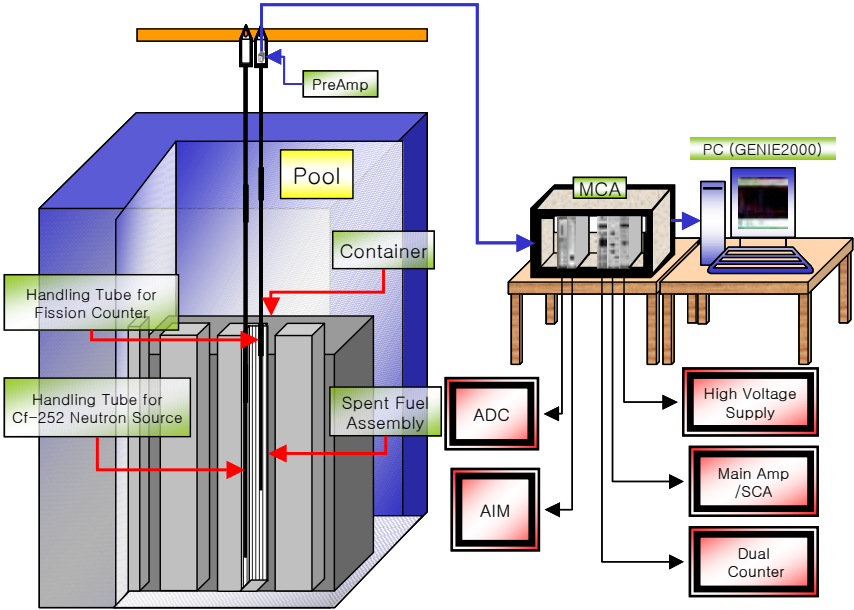


Figure 11. Exponential Experiment System Installed in the PIEF Pool.



Figure 12. Exponential Experiment for Spent Fuel Assembly in PIEF Pool

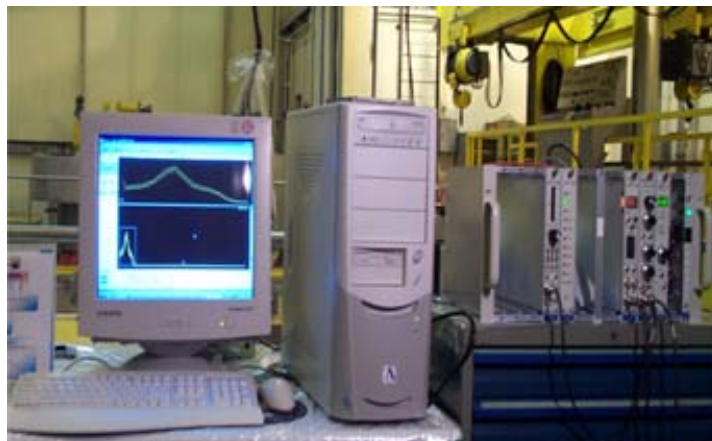


Figure 13. Exponential Experiment System

5. Conclusion

Underwater post irradiation examination technologies were developed and adopted to assure and improve the safety of nuclear fuels as well as nuclear power plants. Many of the developed technologies were put together with the fuel service technologies of the utility groups to provide proper fuel service activities. KNFC has developed and run a series of underwater fuel service technologies and now covers all of the fuel service demands in Korea. KAERI put many efforts on the development of in-pool PIE for the LWR fuels. In order to provide appropriate underwater fuel examination technologies for the safeguard inspections, spent fuel management and fuel service activities, and in order to support nuclear R & D program in Korea, various kinds of underwater fuel examination technologies, such as fuel rod verification technology, exponential experiment, hold-down spring force

measurement technology, image processing applied dimensional measurement methods, and burnup determination technology by underwater gamma spectroscopy were developed.

References

- [1] J.Y.Park, et. al., “Nuclear Fuel Poolside Inspection Technology Development”, KAIF/KNS Annual Conference, (2003)
- [2] Y.B.Chun, et. al., “Operation of Nuclear Fuel Cycle Research Facility”, KAERI/MR-369/2001, (2001)
- [3] E.K.Kim; Y.B. Chun, et. al., “ Nuclear Fuel Failure Analysis of Korean NPP”, KAERI/CR-78/99, (1999)
- [4] K.P.Hong; Y.B.Chun, et. al.,”Development of High Radioactive Materials Examination Techniques”, KAERI/RR-2319/2002, (2002)
- [5] C.B.Lee; Y.B.Chun, et.al.,”High Burnup Fuel Safety Tests and Evaluation Technology Development”, KAERI/RR-2314/2002, (2002)
- [6] Y.B.Chun, et. al., “Operation of Post-Irradiation Examination Facility”, KAERI/MR-348/2000, (2000)
- [7] Recent Developments in post-irradiation examination techniques for water reactor fuel, Proc. Tech. Committee Meeting, Cadarache, France, 17-21 October (1994)
- [8] S.G.Ro, et. al., “Status of the Art Report for Exponential Experiments for PWR spent Nuclear Fuels”, KAERI/OT-387/98, (1998)
- [9] H.S.Shin, et. al.,”Nuclear Characteristics Analysis of Spent Nuclear Fuel for Exponential Experiment”, KNS Spring Meeting, (2001)
- [10] Y.B.Chun, et. al., “Development of On-site Fuel Inspection Equipment”, ANS Winter Meeting, the 39th Conference on Remote Systems Technology, (1991)

Performance of HEU and LEU fuels in Pakistan Research Reactor-1 (PARR-1)

Showket Pervez, Mujahid Latif, Muhammad Israr

Nuclear Engineering Division,
Pakistan Institute of Nuclear Science and Technology (PINSTECH),
Nilore, Islamabad, Pakistan

ABSTRACT

Pakistan Research Reactor-1 (PARR-1) a swimming pool MTR type 5 MW research reactor went critical in 1965 with HEU fuel. The reactor was operated with HEU fuel for about 30,000 hours in 25 years and produced about 93,000 MWh energy. The reactor was then converted to LEU fuel and its power upgraded from 5 MW to 10 MW to meet the demand of higher neutron flux and compensate the penalty in neutron flux due to conversion from HEU to LEU. The reactor went critical with LEU fuel in 1991. The operation with LEU fuel in the last 14 years has been about 10,000 hours and the energy produced is about 66,000 MWh. The performance of both HEU and LEU fuels has been excellent during the long operation history. The average and maximum burn up with HEU fuel was 34 % and 49 % respectively whereas that with LEU fuel has been 42 % and 48 % respectively. No signs of fission product release in pool water have ever been observed thus establishing full integrity of the fuel. Post irradiation visual inspection of the fuel has revealed no abnormality. No signs of geometrical distortion, corrosion or any other damage to the fuel have ever been observed. A fuel element got damaged during fuel handling which was repaired and replaced in the core and it achieved 28 % burn up without causing any problem. To establish the quality of the new fuel, a fuel failure detection system has been installed. This system is based upon monitoring the delayed neutrons emitted from fission products leaking into the primary coolant as a result of any clad failure. No incident of fuel failure has even been recorded by this system.

1. Introduction

Pakistan Research Reactor-1 (PARR-1), a swimming pool, MTR type research reactor went critical on 21 December 1965 and attained full power of 5 MW on 22 June 1966 with 93 % Highly Enriched Uranium (HEU) fuel. The reactor is cooled and moderated by light water. Light water and graphite act as the reflector. The reactor was operated with HEU fuel for about 30,000 hours in 25 years producing about 93,000 MWh energy. Eighty four HEU fuel elements were used. The average and maximum burn up in HEU fuel was 34 % and 49 % respectively.

The reactor was shut down in 1990 for core conversion to commercially available Low Enriched Uranium (LEU) fuel. During the process of core conversion the reactor power was also upgraded to 10 MW to meet the demand of higher neutron flux and to compensate the penalty in neutron flux due to conversion from HEU to LEU fuel. Most of the reactor systems including primary and secondary heat transport systems were renovated and several additional systems were installed. IAEA also provided technical assistance for the completion of this project. PARR-1 went critical with < 20 % LEU fuel on 31 October 1991 and attained the upgraded power level of 9 MW on 07 May 1992. The reactor power was raised to 10 MW on 27 February 1998 after enhancing the primary flow rate.

During the last 14 years, the reactor has been operated with LEU fuel for about 10,000 hours producing about 66,000 MWh energy. Maximum burn up of 48 % has been achieved in LEU fuel whereas the average burn up is 42 %. Since its commissioning, PARR-1 has been mainly utilized for studies in solid state physics, neutron diffraction, nuclear structures and fission

physics, neutron activation analysis, radioisotope production and training of scientists, engineers and technicians.

2. Post irradiation examination of the fuel elements

The performance of both HEU and LEU fuels has been excellent during the long operation history. During operation, pool water sampling, dose measurements and gamma activity measurements by N-16 channels have never shown any signs of fission product release in the pool thus establishing full integrity of the fuel. Continuous dose monitoring and water sampling of the wet storage pool have also never shown any unusual results. Post irradiation visual inspection of the fuel has revealed no abnormality. No signs of geometrical distortion, corrosion or any other damage to the fuel have ever been observed.

3. Post repair irradiation and performance evaluation of a damaged fuel element

One of the HEU standard fuel elements, S-55, got damaged on 02 August 1982 during fuel handling for assembling core [1]. The element got hit and one end of the lifting pin sheared off the side plate and broke off (Fig. 1). The other welded end of the pin also got damaged and

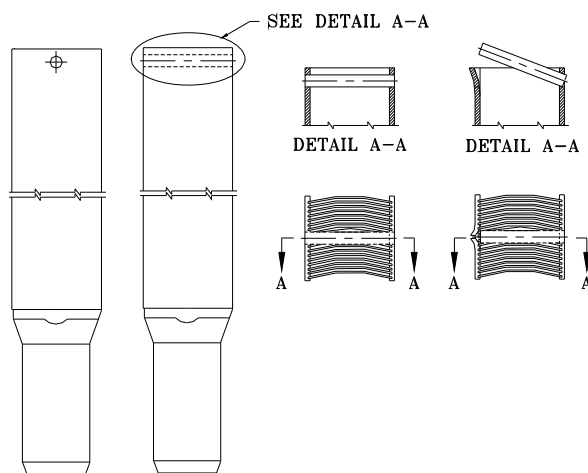


FIG. 1. Details of damaged fuel element.

the pin got detached from the element. The damaged fuel element was placed in the fuel rack. The repair of the element was planned in August 1983 after one year cooling.

Two special tools were designed and fabricated to straighten the side plates of the element. The broken Aluminium pin of the fuel element was replaced with a newly designed and fabricated stainless steel pin (Fig. 2). The pin was originally welded to the inner side of the side plates but welding of the new pin was not possible. Therefore, a collar was provided on one side of the new pin, that could seat on the inner side of the side plate, and a lock pin hole was provided on the other side of the new pin to accommodate an Aluminium locking pin that could be just adjacent to the inner side of the opposite side plate.

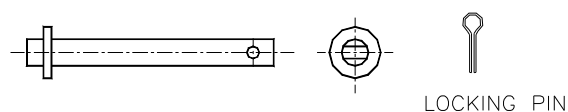


FIG. 2. New lifting pin and locking pin for damaged fuel element.

The affected side plate was straightened with the help of special tools (Fig. 3). New lifting pin was held in a tong and placed in position with its ends inside the holes of the opposite side plates. The damaged side plates were straightened to the maximum possible extent but still they were not perfectly straight and had slight curvature. The repaired fuel element was lifted with the help of standard fuel element handling tool and loaded in grid plate positions B-1 and then in D-1 and then placed back in the fuel rack. The fuel rack was raised in the pool to 1 m below the pool water level and the lifting pin and side plates were observed. They were found unaffected. Then the element was loaded in the grid plate position D-4 where it seated about half an inch above the original position. The element was placed in the fuel rack and observed raising the rack under water. It was observed that the lifting pin was slightly oversized on the locking end due to curvature present in the side plates which was obstructing the neighbouring elements and did not allow the repaired element to seat properly. The lifting pin was removed and its collar thickness and length were reduced by 0.5 mm each. The lifting pin was again installed in its position and locked. The element was again loaded in the grid plate position D-4 where it seated properly. It was also loaded in the grid plate positions B-4 and B-5 and then again placed back in the fuel rack. The rack was raised as before and the element was observed. It was ensured that the side plates and the lifting pin were intact.

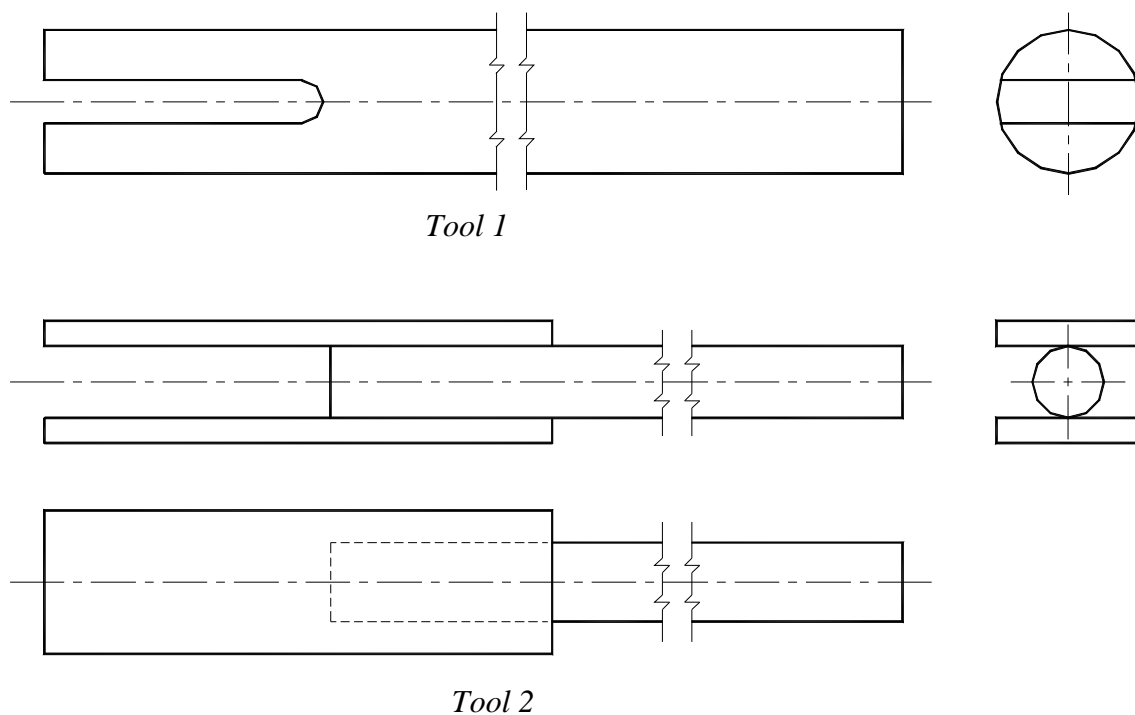


FIG. 3. Tools used for straightening the damaged side plate of the fuel element

The reactivity effect of using a stainless steel lifting pin instead of the original Aluminium lifting pin was negligible. Also there was no danger of activity release while using the repaired fuel element as the damaged part of the element was in the dummy region almost 3 cm above the active fuel region. The loading of the element in the core was approved by Nuclear Safety Committee PINSTECH on 21 November 1983. The element was loaded in the core position E-6 for use. The element was tested at reactor power 80 kW for one hour with forced flow. Primary water activity was kept under observation. The element was then tested at higher reactor powers of 1 MW, 3 MW and 5 MW for more than an hour. Then the reactor was run for 82 hours at full power. No abnormality was observed.

The repaired fuel element was kept under continuous monitoring. No physical distortion or damage was ever observed. During operation, the pool water sampling never showed any unusual results thus ensuring integrity of the fuel element. The element achieved 28 % burn up without causing any problem. After being retired, the element was stored in the wet storage bay and is under continuous surveillance along with other stored elements.

4. Fuel failure detection system

To establish the quality of the new fuel, a fuel failure detection system has been installed [2]. This system is based upon monitoring the delayed neutrons emitted from fission products such as ^{87}Br , ^{88}Br , ^{137}I , ^{138}I etc. leaking into the primary coolant as a result of any clad failure. The detectors are placed near the outlet coolant pipe in the valve pit (Fig. 4). A high background of neutrons and gamma activity is present in the valve pit, therefore the system has been properly shielded. Lead bricks are used for gamma shielding and polyethylene/paraffin shielding has been provided to reduce background neutrons mainly from scattering. Graphite blocks have been used to increase the system sensitivity by thermalizing the delayed neutrons emitted from precursors. Two BF_3 neutron detectors monitor the delayed neutrons emitted from fission products in case of a pin hole type fuel failure while one NaI gamma detector detects the gamma energy of delayed neutron precursors in the event of pin hole type and slow leak type fuel failures. The background neutron count rates at various levels of reactor power in steps of 100 kW were obtained and alarm was set at three times the background count rate. No incident of fuel failure has even been recorded by this system.

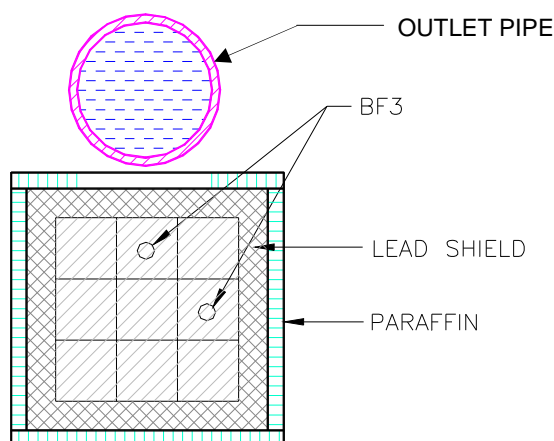


FIG.4. Fuel failure detection system

5. Conclusions

The post irradiation visual inspection of both HEU and LEU fuels has never shown any damage to or distortion of the fuel. Monitoring and water sampling of the reactor pool and the wet storage pool has never shown any signs of fission product release during operation as well as storage after irradiation. One HEU fuel element, that got partly damaged during fuel handling, was repaired and replaced in the core attained 28 % burn up without giving any problem. A fuel failure detection system has also recorded no incident of fuel failure during operation.

REFERENCES

- [1] PAKISTAN INSTITUTE OF NUCLEAR SCIENCE AND TECHNOLOGY, 'Repair of standard fuel element S-55', Technical Report, PINSTECH/NED-120, December 1983.
- [2] PAKISTAN INSTITUTE OF NUCLEAR SCIENCE AND TECHNOLOGY, 'Delayed neutron monitoring system for fuel failure detection at PARR-1', Technical Report, PINSTECH-131, July 1993.

SESSION 2: HOT CELL LABS AND PIE FACILITIES

Chairpersons

E. Toscano (European Commission)

F. Iorio (CNEA, Argentina)

PIE in Hot Cells and Poolside: Facilities and Techniques applied in Argentina

A brief overview

Gabriel Ruggirello ruggirel@cnea.gov.ar

CNEA, Argentina

Argentina has covered a wide range of activities concerning PIE, visual inspection of Fuel Elements (FE), internal components of NPP and Research Reactors (RR). These activities are performed both in the Poolside Bay (Spent Fuel Pool) at each nuclear power plant and in external Hot Cell Laboratories.

Argentina has two PHWR power reactors (one CANDU type at C.N.Embalse and other KWU prototype at C.N.ATUCHA 1) which have started operation in the early 80's and 70's respectively. Argentina has also one 10 MW research reactor (RA-3) for radioisotope production for more than 40 years ago. The PIE activities have covered the basic requirement for the controls and improvements of the FE and the surveillance programs for the behavior assessment of the critical internal components of the NPP (pressure vessel or tubes, control rods, guide tubes etc) consistently.

PIE activities for FE were begun with the application techniques to evaluate the fission product release in the primary circuit and localization of failed FE in the core, on-line Sipping Test and exhaustive underwater visual inspection including metrology of the dimensional changes of the components. In some cases it was necessary to make available the equipment for disassembling the fuel element for further analysis. The other cases involved the studies including the determination of the cause of the primary failure to discriminate among fabrication flaws or flaws related to PCI or with the operation outside the design range.

The Hot Cells Laboratory is divided in two installations i.e. the Physical Hot Cells and the Radiochemical Hot Cells

The Physical Hot Cells (CELCA) consist of one beta-gamma cell for structural materials with five working positions and two alpha tight boxes for fuel material testing with four working positions. An Optical Microscopy bench and Scanning Electronic Microscope are also exited in these cells.

The following destructive tests for PIE are available:

- **Metallurgical Test**
Metallurgical specimens' preparation according to ASTM standards
Universal tensile machine for tensile and fracture testing and Charpy (impact) tests
- **Gamma Scanning**
Discrete gamma-ray spectrum analysis for the characterization of the existed radio nuclides and its activity profiles in the sample performed with high and medium resolution detectors with different types of collimators.
- **NDT, Eddy Current Technique**
Volumetric inspection of rod, tubes and plates for defects and Oxide layer thickness on non-ferrous metal
- **Visual Examination, Metrology and density determination**
Inspection by optical instruments, measurement of length, inner and outer diameter, thickness and gap with precision calipers and LVDT

- The density determination is performed by immersion method and digital balance.
- **DT, Metallography**
 - Samples preparation by cut-off wheel for rod specimens and punching device for plate specimens;
 - Specimen impregnation and semiautomatic grinding and polishing equipments

The Radiochemical Hot Cells Facility (LFR) consists of three alpha tight boxes with four simple tele manipulators working positions. The sample dissolution is performed for radiochemical analysis and burn-up determination of fuel material by means of ICP mass spectrometer attached to the hot cells line

The main works being performed up to now are

- Metallurgical test of steel specimens from the Pressure Vessel of C.N.ATUCHA 1 reactor.
- Characterization test of C.N.ATUCHA 1 internal reactor components: control rod, fuel channels, tubing and foils.
- Metallurgical test of C.N.Embalse Pressure Tubes.
- PIE of FE irradiated at the RA-3 RR

Some of the ongoing works are:

- PIE of High Density Uranium compound (UMo and silicide), mini-plates and FE for RR.
- Assessment of failure in Fuel Elements from NPP

PRESENTATION OF CEA HOT LABORATORIES, WITH A FOCUS ON LECI

Jean-Yves BLANC, DEN/DSOE, Bâtiment 121, CEA/Saclay,
F-91191 Gif-sur-Yvette Cedex,
France

ABSTRACT

After several years of optimisation and refurbishment, CEA presents a coherent set of hot laboratories for fulfilling R&D and industrial needs. Fuel studies are concentrated in Cadarache, where the LECA-STAR performs all post-irradiation examinations on LWR fuel rods from NPP. Possibilities range from classical non-destructive examinations, puncturing and metallography up to EPMA and SIMS analyses. Thermal treatments and long term storage tests on LWR fuels are also performed. A particular emphasis is given on micro-structural analyses and fission gas release studies. LEFCA, on the same site, is preparing plutonium-based fuels possibly including minor actinides for Generation IV and MOX studies and can characterize these products. In Saclay, LECI has all the panel of equipments for performing micro-structural, corrosion analyses and mechanical testing characterization on irradiated metallic and ceramics materials (pressure vessel steels, fuel cladding and structure materials). Its equipments include non-destructive examinations on short fuel rods, hydrogen pick-up measurement, spark machining, a corrosion loop with autoclaves, and micro-structural analyses with EPMA, SEM, TEM and Raman. Its new building, started last year, includes twenty cells with up-to-date mechanical testing facilities (tensile, burst, creep, impact, toughness, IASCC tests). In Marcoule, ATALANTE performs R&D on reprocessing, partitioning and vitrification. It ranges from theoretical chemistry to technological validation (with tests involving up to 15 kg of LWR-irradiated fuel), as a support to La Hague industrial facilities and to address governmental issues on radioactive waste disposal, including partitioning and transmutation. LECA-STAR and LECI are strongly connected to CEA fuel and material testing reactors: Osiris and Phenix today, and JHR tomorrow, with fuel rod re-fabrication capacity, including instrumented experiments. This paper presents this set of hot laboratories with an emphasis on LECI new possibilities, and some illustrations on the refurbishment accomplished in LECA and LECI to reach the latest safety and R&D requirements.

1. INTRODUCTION

As in many other countries in Europe, the fleet of hot laboratories belonging to CEA was mainly built in the sixties, to deal with the expansion of nuclear industry. As years were passing by, it became a necessity to update this tool. The incentives were on the one hand to adjust the tool to the customers' needs and on the other hand to satisfy more stringent safety rules. During the last ten years, CEA has accomplished a very important adaptation of its hot laboratories, and present today a coherent set of facilities to perform its programmes and answer its customers' demand. The optimisation of CEA laboratories included a reduction of the total number of facilities:

- Some facilities were shutdown, such as RM2 in Fontenay-aux-Roses and more recently LAMA in Grenoble in 2002, because they were situated on research centres where nuclear activities were decreasing;
- In Saclay, post-irradiation examinations were performed inside two different facilities. It was decided to close one (the LHA in 2003) and to gather all equipments inside the other one (the LECI), which implied the construction of a new building [1];

- In Cadarache, some activities are also transferred to other facilities in order to close the COMIR facility next year.

Two large refurbishment programmes were undertaken to upgrade LECA and LECI to the current safety standards. This included decreasing the source term of both facilities by evacuating all rod samples coming from ancient research programmes, decontaminating cells and improving confinement, seismic resistance, fire hazard resistance and so on.

In order to increase the synergy between teams and to reduce transport of nuclear materials and wastes, this optimization was driven along by gathering:

- Fuels studies in Cadarache inside LECA-STAR and LEFCA facilities,
- Structure material studies in Saclay within the LECI,
- Fuel cycle and waste studies in Marcoule within ATALANTE.

This choice was made according to the necessary connexion between a Material Testing Reactor and a hot laboratory. CEA MTR is currently Osiris, started in 1966 and located in Saclay near the LECI, and in the future it will be the Jules Horowitz Reactor, to be built in Cadarache near the LECA-STAR and expected to start in 2014. Hence, fuel research activities will be completely transferred from Saclay to Cadarache, when Osiris will be shutdown.

The result of this optimization is now a very coherent set of laboratories, which are described below. The Post-Irradiation Examination (PIE) techniques on water reactor fuel are mainly concentrated in the LECA-STAR and in the LECI. As the detailed capabilities of LECA are presented in another paper [2], this paper will give more focus on LECI techniques.

2. LECI IN SACLAY

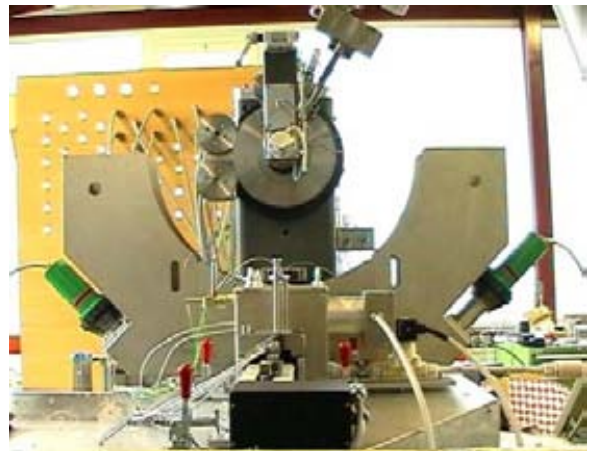
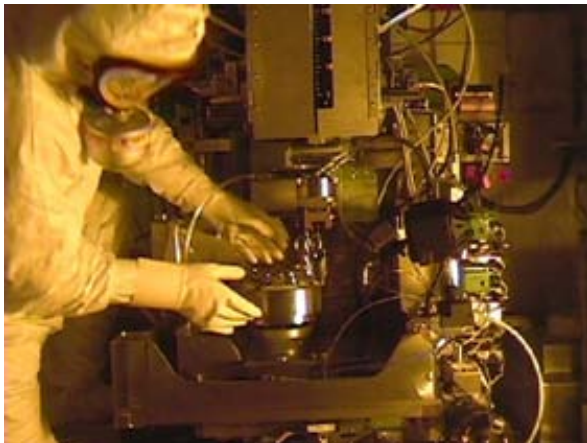
As explained above, the LECI is specialized on structural materials under irradiation. The facility includes the main building, which was completely renovated and a new one, started in October 2005. Its 40 shielded hot cells are operated by a staff of around 70 people, not including trainees and PhD students.



Figures 1 & 2 show the M line, its working area and its transfer area during construction.

The strong points of LECI are as follows:

- Mechanical testing, with a complete set of new equipments in the new building:
 - o *Machining (conventional, ram and wire spark erosion machines)*
 - o *Tensile testing: 10, 25 and 100 kN, -170 to 1000°C (1800°C), dynamic capacities (0.5 m/s), rapid heating (induction and Joule effect)*
 - o *Fracture toughness (100 and 250 kN, -170 to 1000°C),*
 - o *50 J and 350 J Charpy testing,*
 - o *Burst machine coupled to tensile testing machine,*
 - o *Axial creep tests,*
 - o *Internal pressure creep tests,*
 - o *Burst and creep under iodine.*
- Microstructural analysis, with shielded new optical microscope with microhardness, SEM, TEM, EPMA, X-ray diffractometry, a Raman microscope and density measurement.
- Corrosion, with a new loop of three autoclaves (360°C, 220 bar, one coupled to a slow tensile testing) to be commissioned by 2007, and a hot vacuum extraction furnace to measure of hydrogen content in fuel cladding (or other metals).
- Support to the Osiris reactor for LWR fuel ramp testing [3] and material irradiations. This includes the capability to realise small fuel rods (“Fabrice”) or creep specimens, with non destructive equipment (metrology, eddy current, X-ray radiography), machining (lathe, milling machine) and welding (TIG and laser).



Figures 3 to 6 show ram spark erosion machining (upper left), the new optical microscope (upper right), dynamic tensile test machine (bottom left) and instrumented Charpy for sub-size specimen before installation inside the new cells (bottom right).



Figures 7 & 8 present the corrosion loop with the autoclaves (now inside the hot cell) and its regulation system.

To show some applications of the LECI capabilities, we have selected two illustrations.

- Ring testing for Reactivity Initiated Accident (RIA) simulation on cladding materials

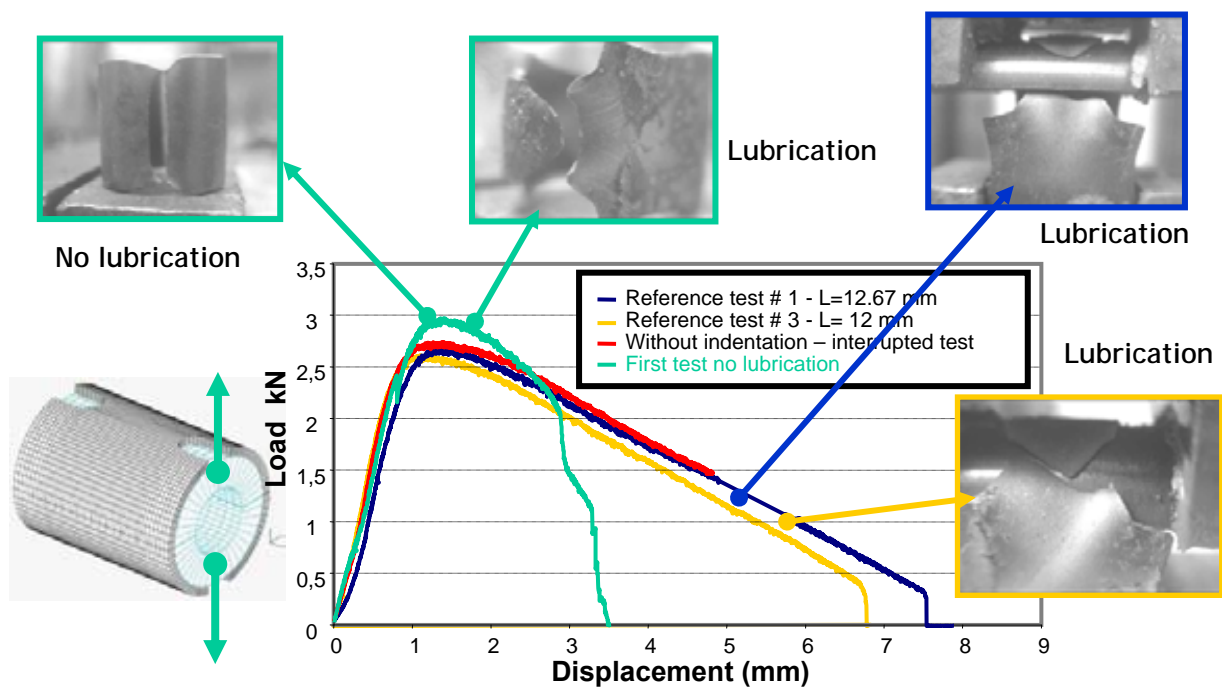


Figure 9: Tensile testing of cladding ring samples of Penn State type.

To simulate the stress created on fuel cladding during a transient occurring during a RIA, tests are conducted on ring samples. The claddings have been previously de-fuelled using chemical dissolution of pellets in the Atalante facility. Several types of ring samples have been used. The following illustration shows samples of Penn State type, submitted to an optimisation of the test, with or without lubrication. Without lubrication, failure occurs out of the gage section and noticeable differences can be detected when compared to other tests on fresh Zircaloy-4. As high friction levels are expected on irradiated samples, the specimen could fail out of the gage section. Another interesting feature of these tests is the use of computer code to model these tests.

SEM observations of Iodine – Stress Corrosion Cracking (SCC):

This method is used to observe a PWR fuel rod after it had been submitted to a ramp test in the nearby Osiris reactor. If a rod rupture has occurred, it is necessary to check if the failure has been initiated by SCC. In order to reveal this phenomenon, a particular process is applied in hot cell (Figure 10). The failure is localized, the rod is cut longitudinally, in order to obtain two half claddings, with the failure in the middle. Then a half portion of cladding is pressed against a support (A); this process is conducted until a failure line is clearly visible (B) and finally a punch is used to get the final break in two parts of the cladding, in order to look at the fracture surface (C). Then it is possible to observe the cladding, to see the inter-pellet mark and finally, through SEM observation the typical I-SCC crack as shown on the figure.

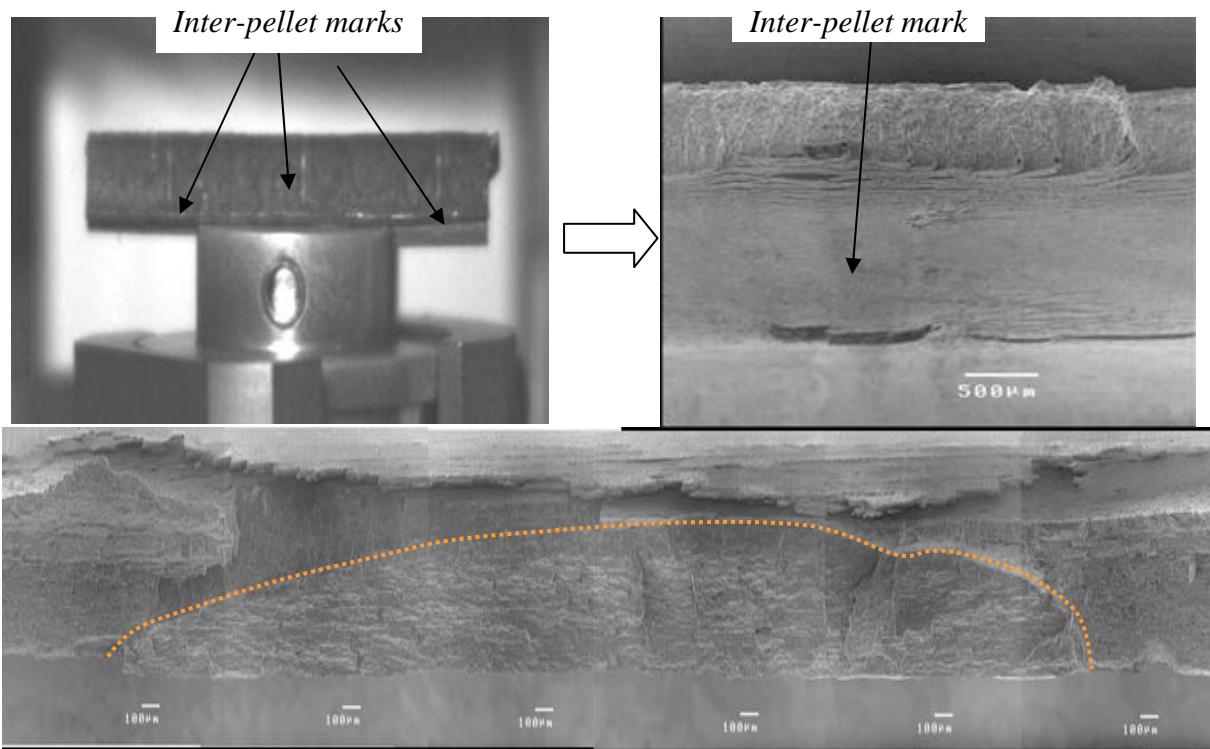
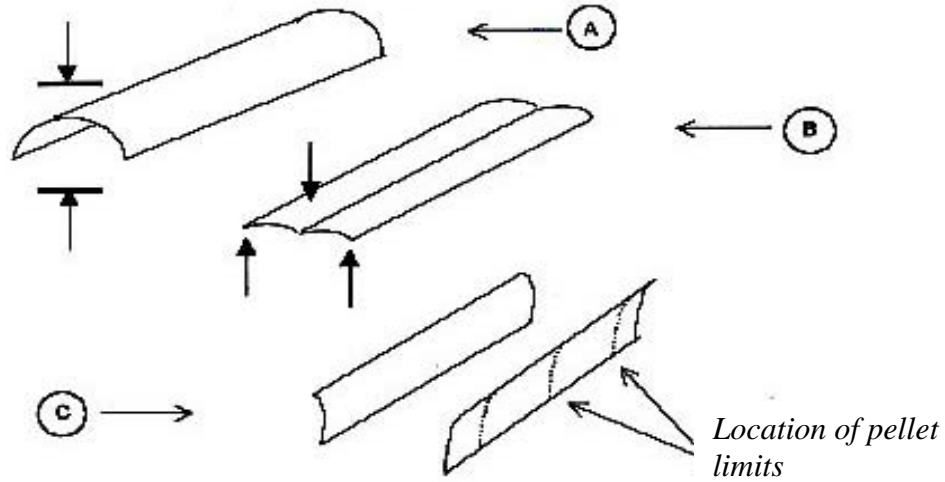


Figure 10: Method used to observe a clad coming from a ramp tested PWR fuel rod with a SEM. The picture at the bottom shows a typical I-SCC crack with a high elongation ratio in the axial direction comparatively to the cladding.

3. LECA-STAR IN CADARACHE

The LECA-STAR is the French facility for examination of irradiated fuel rods coming from nuclear power plant, mainly in the frame of surveillance programmes in cooperation with AREVA NP and EDF. It is also open to international programmes.

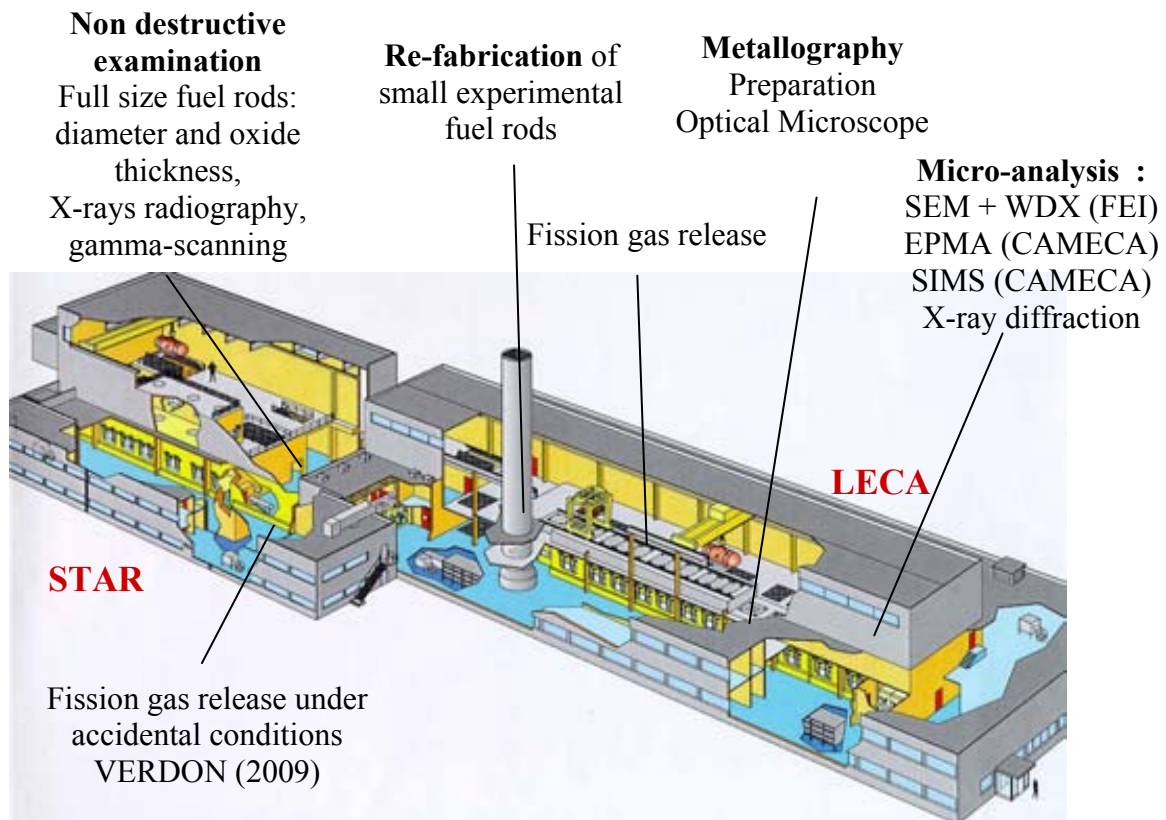


Figure 11: Scheme of LECA-STAR facility.

The LECA-STAR is a (nearly) completely refurbished laboratory, including 20 hot cells, mainly with concrete shielding. Its staff is of about 110 people, including a team for the reconditioning of fuel wastes coming from other facilities.

The refurbishment of the LECA-STAR [4] was a very important programme, launched in 1997 and aiming at:

- Improving confinement, by installing stainless steel boxes inside some cells and reducing cell leakages in all of them,
- Reducing source term, by decreasing fissile masses stored inside the facilities and cleaning the cells. Waste characterization & evacuation was also improved.
- Updating general safety features (fire protection, fire and radioactivity detection, changing power supplies, updating traveling cranes, ventilation systems, changing windows and manipulators),
- Improving seismic behavior, by strengthening buildings & cells. Hot cells that cannot be sufficiently strengthened are under deconstruction.

This renovation work will be terminated in mid-2007 (only some civil engineering work on seismic strengthening remains to be completed).



Figures 12 to 15: a stainless steel confinement box is inserted inside a LECA hot cell (upper left), a new window is put in place (upper right), civil engineering work to reinforce seismic resistance (bottom left), a new mobile hot cell has been constructed on the roofs of the concrete shielded line to improve confinement when opening cell roof (bottom right).

The strong points of LECA-STAR are:

- Non destructive PIE on LWR fuel rods (metrology, eddy currents for clad integrity control and oxide thickness, gamma-scanning, X-ray radiography) and puncturing, with several benches adapted to full length 1300 and 900 MWe PWR rods, small rods (e.g. for ramp testing in Osiris) and fuel plates. Examinations are carried out on UO₂ and MOX fuels.
- Fuel rod re-fabrication and instrumentation for MTR ramp tests.
- Long Term storage studies, with two furnaces for testing irradiated fuel rod (with or without clad defect) behaviour under transport or storage conditions.
- Micro-structural analysis with shielded SEM, SIMS, EPMA and X-ray diffractometry,
- Fission gas release studies with:
 - o a high frequency induction furnace to study fission gas release up to ~2700°C, with on-line gamma spectrometry and planned for early 2007;
 - o a HIP furnace to study fission gas release of irradiated fuel under simulated strain state encountered by grains inside fuel in case of high temperature transient (160 MPa, 1600°C) and planned for end 2007.

Two new hot cells (“VERDON”) to be constructed to study fuel behaviour and short-term fission product release under various severe accident atmospheres (steam, H₂ or air). The 10-

cm long re-irradiated, fuel segment is heated from room temperature up to fuel melting temperature in a high frequency induction furnace. This equipment is planned for 2009.

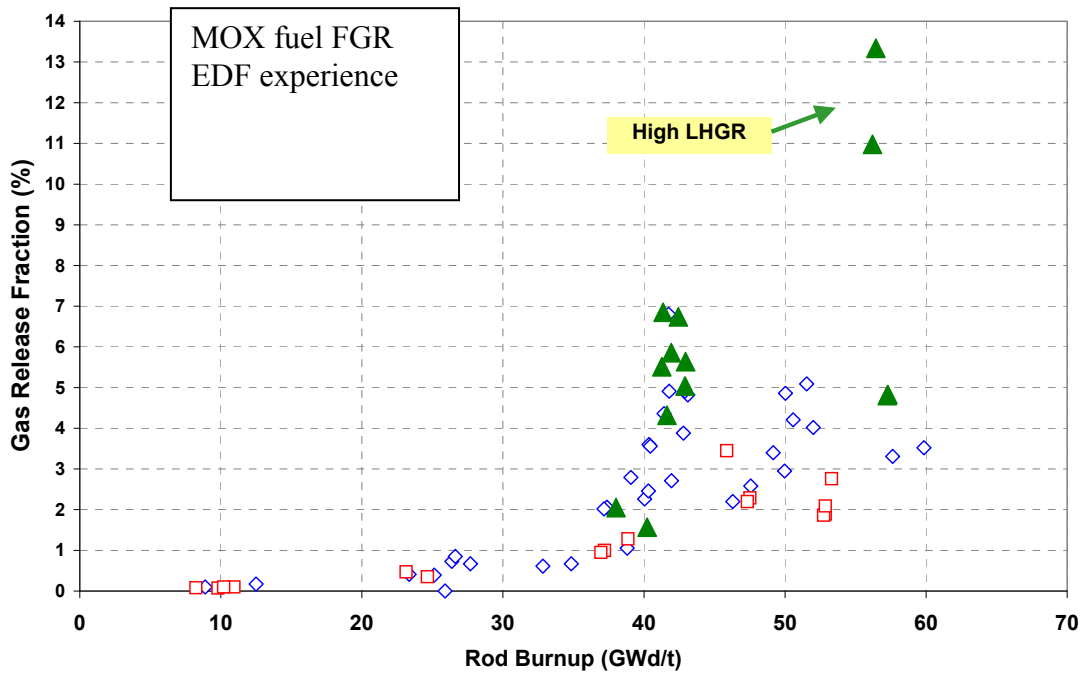


Figure 16: The release of fission gases in PWR MOX fuel rods from EDF power plants is measured in the LECA-STAR facility [5].

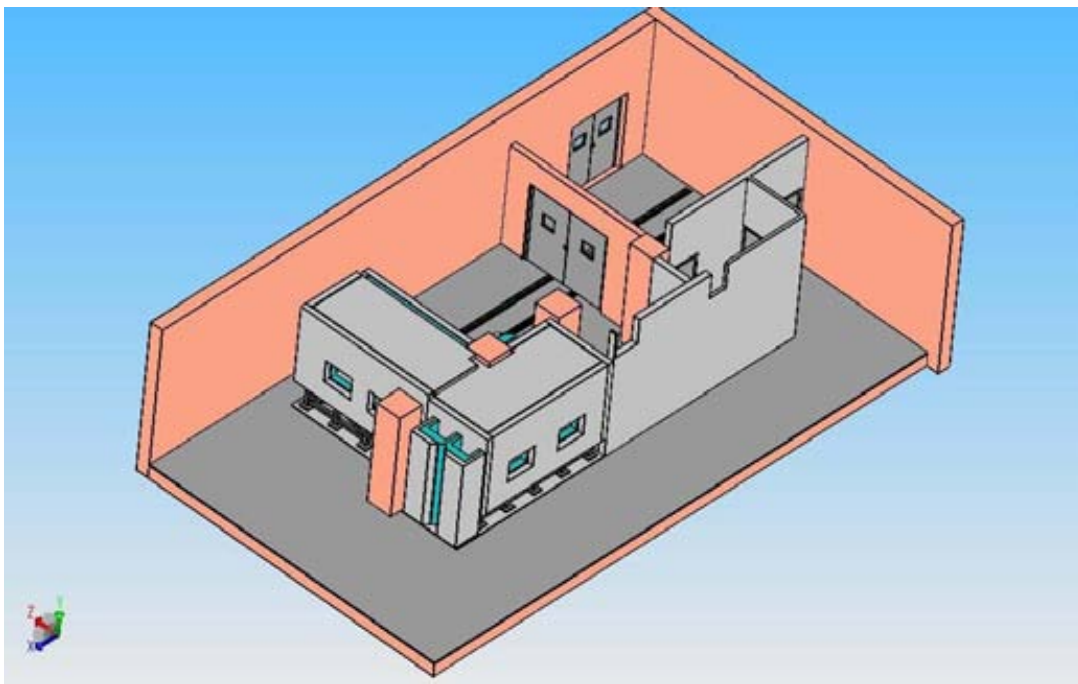


Figure 17: Scheme of the future VERDON facility devoted to study of fission gas release in severe accident conditions. This facility will include two lead shielded hot cells, with two windows each, and a high temperature furnace to heat a freshly re-irradiated fuel rod segment. Release of fission gases will be measured on line.

4. ATALANTE IN MARCOULE

Atalante is the largest CEA hot cell facility, with 19,000 m² of laboratories and a permanent staff of 210 people. Its programmes are oriented either to support the AREVA NC industrial facilities in La Hague in the fuel treatment area, or to support governmental decisions on transmutation & partitioning. It also works on Generation IV studies for developing new fuels for new reactor types (SFR, GCR & HTR) & new cycles (e.g. co-extraction, co-precipitation). Its specialities include:

- To improve reprocessing techniques of nuclear spent fuel, diminish their cost and further reduce their impact in terms of discharges and waste production,
- To prepare for reprocessing of new fuels (high burn-up UO₂ or MOX),
- Partitioning & transmutation of long life radio-nuclides, e.g. by preparing and characterizing “targets” from previously separated actinides,
- Immobilization of radio-nuclides inside ultimate waste packages, with containment matrices such as glasses, ceramics or glass-ceramics,
- To study the long-term behaviour of possible containment matrices for deep geological disposal or for long-term interim storage of waste packages,
- Future nuclear fuel cycles. Major issues facing back end of cycle include reprocessing new types of fuel with group separation and recycling of all actinides (uranium, plutonium and minor actinides).

The most interesting feature of Atalante is its capability to range from basic research inside glove boxes to demonstration experiments, e.g. inside the CBP shielded line that demonstrated actinide separation on a pilot scale with 15 kg of spent fuel. Emphasis is given on separation science and actinide chemistry. Another department investigates containment material science (glasses, etc). Concerning post-irradiation examinations of LWR fuels, after their non destructive examination in LECA-STAR, segments of fuel rods are shipped to Atalante for a chemical de-fuelling, to obtain claddings for mechanical tests in the LECI.



Figure 18: General view of ATALANTE in Marcoule

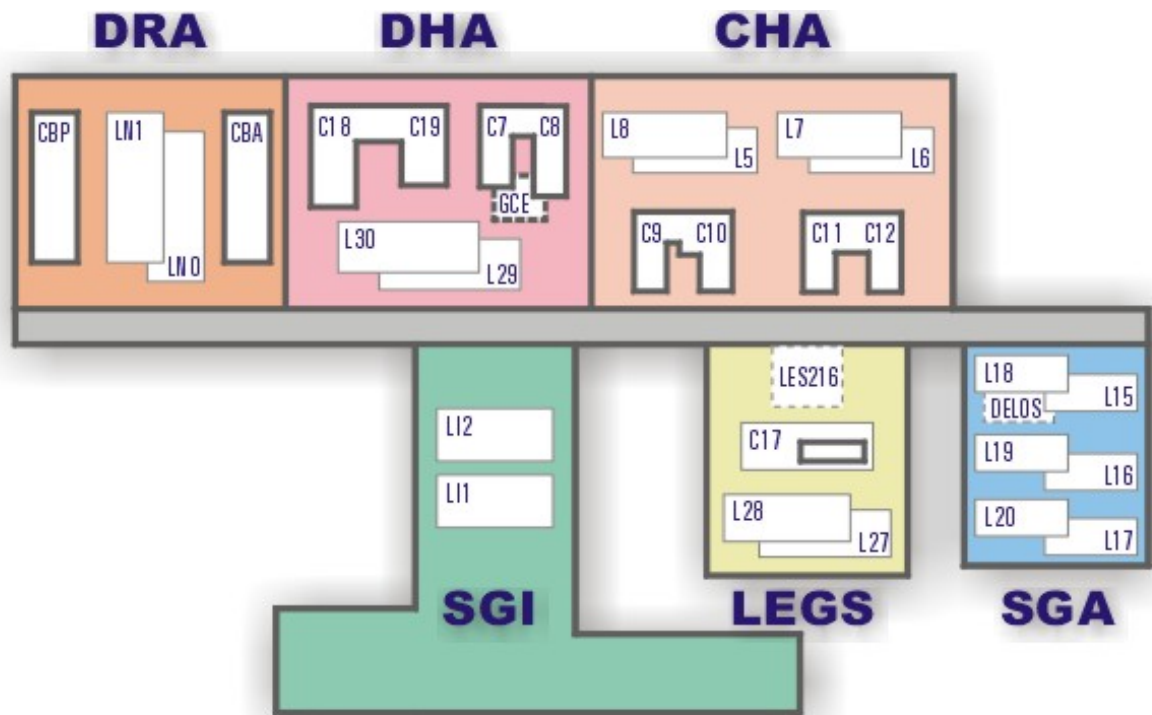







Figure 19: Layout of laboratories inside ATALANTE. Major equipments includes 7 shielded cell lines (labelled C on the figure) representing about 60 workstations, and 17 laboratories (labelled L on the figure) with radiochemistry equipment in glove boxes.

To illustrate the capabilities of Atalante, the figure below shows the preparation of pellets made of a mixed oxide of americium and plutonium for the FUTURIX experiment, to be irradiated in the Phenix fast breeder reactor, to study the transmutation of americium.

Three compounds $\text{Pu}_{0,8}\text{Am}_{0,2}\text{O}_2$, $\text{Pu}_{0,5}\text{Am}_{0,5}\text{O}_2$, $\text{Pu}_{0,2}\text{Am}_{0,8}\text{O}_2$ were obtained by continuous oxalic co-precipitation in a shielded line.

Pu,Am oxalate precipitate	Am,Pu oxide
	
	
Calcination under air, at 850°C, during 3h	
	
($\text{Am}_{0,5}\text{Pu}_{0,5}$) O_2 pellets	



Equipment for continuous precipitation (25 g of actinides produced in 2h30)

Figure 20: Manufacturing of fuel for transmutation experiment. The mixed oxide pellets of plutonium and americium were prepared for the FUTURIX-FTA experiment, by oxalic co-precipitation in a shielded line in Atalante [6].

5. LEFCA IN CADARACHE

LEFCA is a glove box research facility used for preparing U & Pu-based fuels (with the possibility to include a small amount of Am). Its programmes range from R&D on Generation IV fuels (nitride, carbide, oxide) to R&D on MOX fuel (as a support to Areva NP). This laboratory can prepare pellets (powder metallurgy) and experimental rods for irradiation in MTR (Osiris, Phenix, etc). It includes characterisation equipments such as SEM, EPMA and measurement of thermo-mechanical properties, especially thermal conductivity. It constitutes a very versatile facility, able to handle all plutonium isotopes and small quantities of americium. This facility is being upgraded for seismic hazard (e.g. fixation of glove boxes).

LEFCA is completed by a Uranium laboratory, located in another building. The Bernard François Laboratory can prepare custom-made fuels for R&D. Its tools include the capability to define new manufacturing processes, and then to characterize the fuel obtained by these processes. Programmes are ranging from LWR with studies to increase the burn-up of MOX fuels by a better homogenization of Pu, to fuels for experimental reactors such as UMO and U_3Si_2 , or to HTR as for example Triso-type micro-sphere fuels.

The next figure illustrates the R&D possibilities of LEFCA. In order to decrease the release of fission gases in MOX fuels during irradiation and also to limit the amount of Pu-rich agglomerates, new pellets containing doping elements were manufactured and further tested in reactor. In this example, addition of a small amount of Cr_2O_3 in the powder leads to a change in MOX fuel microstructure. It is called “reversed microstructure”: Pu-rich agglomerates occupy a very low volume, and so plutonium repartition is quasi homogeneous. Grain size is doubled. When irradiated, these samples release less fission gases than standard MOX fuel. In 2002, the CEA verified the homogenizing effect of chromium addition and, in 2004, MELOX made chromium-“doped” pellets on its test line.

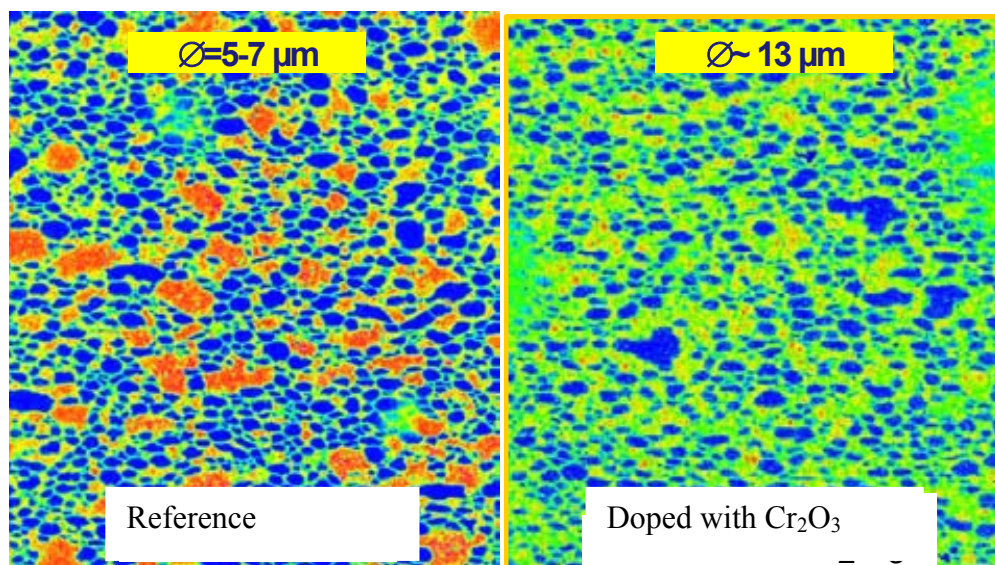


Figure 21: Electron microprobe image of two MOX pellets, the reference microstructure is shown on the left, whereas the pellet doped with chromium oxide is on the right [7].

6. THE EUROPEAN INTEGRATION

CEA hot laboratories are evolving inside a European context, in which some needs are really shared, such as economic and safety constraints, or needs to be connected one to another and to perform always better R&D inside limited budget. In this context, several actions have been and are currently taken to improve collaborative links between facilities. The annual European conference has been transformed in 2004 and 2005 into a successful HOTLAB project sponsored by the European Commission inside its 6th Framework Programme. Other actions, such as the ACTINET network for actinide sciences are also increasing this integration aspect. The idea is to improve diffusion of information, personnel exchanges, to organize round robins and share equipments to increase the global efficiency [8, 9 and 10].

7. CONCLUSION

After about ten years of refurbishment and optimisation, CEA has now a coherent set of hot laboratories, to perform its programmes. Fuel studies are concentrated in Cadarache, around LECA-STAR, LEFCA and the future Jules Horowitz material testing reactor; irradiated materials are mainly in Saclay with the LECI and its new M line; finally Atalante in Marcoule gathers fuel cycle studies. Improvement is going on with new fission gas release facilities to be built in LECA-STAR. These laboratories are open to European and international cooperation, such as the HOTLAB project, the ACTINET network in Atalante, or NFIR-EPRI programmes in LECA & LECI.

BIBLIOGRAPHY

- [1] Blanc J.-Y. et al., “Refurbishment of the LECI”, Proceedings of the International Topical Meeting on Hot Laboratories and Remote Handling, CIEMAT Serie Ponencias, 22-24 Oct. 2001, Madrid.
- [2] Noirot J. et al., “LWR fuel gas characterization at CEA Cadarache LECA-STAR Hot Laboratory”, IAEA Technical Meeting on Hot Cell Post Irradiation Examination Techniques and Poolside Inspection of Water Reactor Fuel Assemblies, 27-30 November 2006, Buenos Aires, Argentina.
- [3] Mougel C. et al., “Power ramping in the Osiris reactor: Data Base Analysis for Standard UO₂ fuel with Zy-4 cladding”, International Seminar on pellet-clad interactions with water reactor fuels, NEA/NSC/DOC(2004)8, Aix-en-Provence, 9-11 March 2004.
- [4] Lignini F. et al., “Démarche et travaux de rénovation dans le cadre de la réévaluation de sûreté du LECA”, Journée SFEN « Réévaluation de sûreté », Paris, May 4, 2004.
- [5] Blanpain P. et al., “Le MOX et ses évolutions futures”, Convention SFEN, 13-14 June 2006.
- [6] E. Brunon et al., “The FUTURIX-FTA experiment in Phenix”, Actinides and Fission Product Partitioning & Transmutation, 8th Information Exchange Meeting, Las Vegas, Nevada, USA, 9-11 November 2004.
- [7] Castelli R., “Areva’s MOX fuel experience: current status and future improvements”, Atomic Energy Society of Japan, 13-14 July, 2006.
- [8] Chaix P., “ACTINET Network for actinide sciences”, FISA-2006, Luxembourg, 13-16 March 2006.
- [9] Sannen L. et al., “HOTLAB - European hot laboratories research capacities and needs”, Conference Proceedings EUR 21026, FISA-2003, Luxembourg, 10-13 November 2003.
- [10] Sannen L. et al., “European Network on Hot Laboratories (HOTLAB)”, FISA-2006, Luxembourg, 13-16 March 2006.

INTERNATIONAL ATOMIC ENERGY AGENCY

TECHNICAL MEETING ON “HOCELL POST-IRRADIATION EXAMINATION TECHNIQUES AND POOLSIDE INSPECTION OF WATER REACTOR FUEL ASSEMBLIES”

27 - 30 November 2006
Buenos Aires, Argentina

OVERVIEW OF POST-IRRADIATION EXAMINATION TECHNIQUES APPLIED AT PSI FOR LIGHT WATER REACTOR FUEL CHARACTERIZATION

Bart G., Bertsch J., Gavillet D., Günther-Leopold I., Hellwig Ch., Wiese H.
Department for Nuclear Energy and Safety Research (NES), Laboratory for Materials Behaviour (LWV),
Paul Scherrer Institut,
5232 Villigen,
Switzerland

Abstract

Within long term cooperation agreements, the PSI Laboratory for Material Behaviour (LWV) in the Department for Nuclear Energy and Safety (NES) has characterized pathfinder PWR- and BWR fuel (meaning fuel and cladding) of the Swiss nuclear power stations Gösgen (KKG) and Leibstadt (KKL) in many PIE sequences. Based on these pathfinder fuel pin and lead assembly tests the fuels in these reactors has been continuously improved over the years and reaches today a batch burnup which is nearly twice as high as at the beginning of 1980. Additionally to providing scientific analytical services with respect to accurate engineering fuel and cladding PIE data, PSI itself as a research organization undertakes basic and applied scientific research. We focus in this environment in elucidating the cladding corrosion and hydriding mechanisms, the cladding mechanical aging processes and the fission gas diffusion process in the fuel.

The PIE tools available at PSI consist of non-destructive methods (visual examination, gamma scanning, profilometry and EC-defect and -oxide thickness measurements), puncturing and fission gas analysis, and destructive investigations of cut samples (metallography/ceramography, hydrogen hot gas extraction, electron probe micro-analysis (EPMA), secondary ion mass spectroscopy (SIMS), scanning- and transmission- electron microscopy (SEM and TEM), lately also laser ablation inductively coupled plasma mass spectroscopy (LA-ICPMS), x-ray absorption spectroscopy, and mechanical testing).

While commercial high burnup programs often request standard engineering data like cladding oxide thickness values and hydrogen contents or fuel pin fission gas release values, PSI has improved such analytical techniques. Additionally, we have performed independent research in order to improve the fundamental understanding of the irradiation behaviour e.g. by elucidating the corrosion process with detailed characterization of the cladding metal-oxide interface by TEM, by local fission product and actinide isotopic distributions in fuel cross sections with SIMS and LA-ICPMS or by studying the conditions for hydride reorientation in hydrided claddings.

The presentation gives an overview of the currently available fuel PIE logistics and tools at PSI, with their meaning, value, and limitations.

Introduction

The origin of the PSI post irradiation examination (PIE) experiments for LWR fuel dates back to 1982, where a 5 meter long hotcell was extended with a shielded backpack, in order to allow the nondestructive testing of 4 meter long, pressurized water reactor (PWR) fuel pins of the Swiss nuclear power station Gösgen (KKG). This station operated with high power ratings and showed unusual cladding corrosion phenomena at burnups of 20 – 30 MWd/kgHM. The problems were solved by the fuel vendor AREVA and the utility KKG, supported by PSI. Since then, KKG showed strong interest in increasing its core average discharge burnup. The impetus lying in reduced fuel procurement- and fuel cycle backend costs, as Swiss nuclear waste regulations request the power stations to pay per waste volume produced (and not per energy equivalent extracted from fuel). The thrust led to a significant long term alliance between the three mentioned partners, leading presently to a fuel core average burnup of 60 MWd/kgHM. A similar long term alliance developed also between the Swiss boiling water reactor operator Leibstadt (KKL), its main fuel vendor Westinghouse and PSI. Again the PIE questions started with corrosion damage analyses, this time due to reactor water chemistry induced spacer shadow corrosion problems. Also this second alliance turned into a long term cooperation between the three partners and resulted in significant burnup increase at KKL with present core average discharge burnups of 55 MWd/kgHM. This means that based on these pathfinder fuel pin- and lead assembly tests the fuels in these reactors has been continuously improved over the years and reaches today a batch burnup which is nearly twice as high as at the beginning of 1980. As example for the cooperation between KKG, AREVA and PSI the latest PIE campaigns are shown in figure 1. On the one hand the PSI work consists in providing scientific analytical services with respect to accurate engineering fuel and cladding PIE data. On the other hand, PSI itself as a research organization undertakes basic and applied scientific research. We focus in this environment in elucidating the cladding corrosion and hydriding mechanisms, the cladding mechanical aging processes and the fission gas diffusion process in the fuel. The present paper gives an overview on the available infrastructure and expertise of the PSI Laboratory for Material Behaviour (LWV) in the Department for Nuclear Energy, Safety (NES).

Logistics for PIE at PSI HOTLAB

The HOTLAB at PSI is divided into a radiochemistry wing where individual radioactive samples (fuel, cladding, structural materials) are characterized mainly by solid state and wet chemical analytical techniques, and a hotcell wing, where large components (fuel pins, fuel channel or control rod components as well as accelerator targets of PSI) are loaded into and are characterized non-destructively and dispatched later to the afore mentioned specialized hotcells. Fuel pins are transported on a truck/trailer to the hotcell wing, which is equipped with a 30 ton crane to transfer the fuel cask (typical container types are NCS-R-52, TRANSNUBEL-BG-18, AREVA-TN-106 etc.) from the trailer and to hook it to the port of the hotcell line. Apart from docking stations for small and large fuel flasks, the hotcell line is also accessible through removable roof plugs and side wall doors. Within the cell line, material movement between cells is performed by a power manipulator or a transport bin.

The PSI HOTLAB is identified as one of the Swiss nuclear installations and is governed by the Swiss atomic law and controlled by the Swiss Federal Nuclear Safety Inspectorate (HSK), which requests that all safety relevant activities are performed in accordance with a quality management programme. So from the very beginning of organizing and accepting a fuel transport to the

HOTLAB, all activities are performed under QA controlled conditions (transport, radioactivity control when handling the transport containers, fissile material safeguards and criticality control, etc.). Furthermore, the industrial partners (Swiss nuclear power plant operators and their fuel vendors as well as international research organizations) also request quality management procedures to be applied on PIE service work performed for them. In this context the LWV as main user and operator of the HOTLAB has installed its QA procedures by IQSOFT- software and is certified according to ISO-9001-2000 standards. Fissile material safeguards and criticality control are guaranteed with a customized software program KBUCH which provides several control options depending on whether a) the fissile material storage conditions are geometrically safe or b) the material is diluted with natural or depleted uranium. Apart from the mentioned controls, KBUCH also provides for complete sample description/identification and allocation over the full life time.

The LWR fuel pins (up to 23 MOX or 33 UO₂ pins) are loaded into a five meter long beta/gamma tight hotcell which serves for pin storage, non-destructive assessment, marking (for subsequent cutting), and (at the end of a PIE campaign) for encapsulation of the fuel segment remnants (into four meter long overcans, which are TIG (tungsten inert gas) arc welded), before loading again into a container for return transportation to the power plants (Figure 2). Although the NDT (non destructive testing) fuel cell (fit initially to accept 10⁵ Ci of Co-60) is not air tight in a strict sense, aerosol contamination towards the operator area is hindered by reduced cell pressure provided by redundant cell ventilators, which, for station black outs, are backed up with diesel electricity generators.

After finalizing the NDT measurements and marking of axial pin positions, the fuel pins are slid through a port into the adjacent hotcell where they are cut by diamond wheel and where the fuel can be drilled out if necessary (Figure 2). Individual fuel and/or cladding samples are then transported within shielded flasks (Figure 3) through double door systems into individual hot cells for metallography/ceramography, EPMA, SIMS, LA-ICP-MS, hydrogen hot gas extraction, cladding mechanical testing, fuel dissolution etc. Remnants from pin cutting on the other hand are overcanned individually, combined into 70 cm long steel cylinders and transferred by shielded cask into the fuel interim dry storage area next to the hotcell line (Figure 4). With this concept the individual cells (except the cutting cell which is refurbished about every 10 years) are kept quite clean and, if necessary, can be accessed by personnel for repair and service work relatively quickly after fuel segment or pin removal.

Review of experimental NDT results and fuel pin damage analyses

For non-destructive assessment, the pins are placed on a measuring bench which is computer controlled by LABVIEW software. The test equipment (periscopes, EC-defect probes, EC-oxide thickness probes, laser scanning profilometry tool or collimated gamma scanning equipment) are mounted (one at a time) at a fixed position close to the cell wall, while the pins are moved for the measurements. This is done by sliding the pins into a shielded hotcell extension device (Figure 4 gives the cell external view of this extension). The NDT measurements are performed according to customized protocols, defining measuring steps, times, angular rotations, measurement frequencies etc. Table I specifies the measuring equipments, typical process step intervals and measurement precisions.

Table I: Specifications and typical process parameters for NDT fuel pin analysis

	Equipment type, vendor	Steps mm / °	Bandwidth	Precision:	Comments:
MF-EC-oxide thickness	Co-Planar coil	>1,5 >15	0,5-30MHz	± 3 µm	Allows for subtraction of magnetic crud
EC-oxide thickness	Fischerscope Point probe	>0,5 >5	4,4 MHz	± 2 µm	Faster than MF-EC
EC-defect testing	EOR encircling coil	>0,3	10-10E6 Hz	-	Search for cladding cracks and pellet gap
Diametrical measurements a) mechanical probes b) laser scan	TESA LVDT	>0,3 >3	-	± 1,5 µm	Laser scan shows better resolution and repeatability. No wearing of probe tips meaning better calibration stability
	Mitutoyo/PSI		670 nm	± 0,5 µm	
Gamma scanning	Canberra MCA07-0469	>0,3 >3	0,1-2 MeV	± 0,5 keV	Axial or azimuthal

The NDT results are evaluated to answer the specific questions raised (and accessible) concerning the fuel pin behaviour (Figure 5) and as prerequisite for pin cutting to define the sample positions.

PWR fuel pins at the beginning of the 80ies showed rather strong homogeneous corrosion, reaching at highest fluence and high water temperatures corrosion layers of 50-100 µm at burnups > 30 MWd/kg. The claddings used were standard Zry-4 or thermo-mechanically improved Zry-4. Oxide spalling occurred at relatively thick oxide layers only. Many types of corrosion improved claddings were tested in the following years at KKG. Additionally fresh fuel was exposed to rather high power ratings of >300 W/cm for the first two yearly reactor cycles. Sub-cooled boiling was assumed to occur in the upper halves of the pins based on fuel behaviour modelling. Thus lithium enhanced corrosion was considered. SIMS lithium profiling through oxide layers was performed to check this assumption (see below). Hydrogen pickup and hydride orientation are also important issues and there was (and still is) a debate on, whether or not local hydride concentrations are detectable by EC-multi frequency measurement techniques and/or EC probes for defect testing. Another important issue has always been the analysis of the released fission gas and plenum pressure. Figure 6 shows trends in fission gas release which are clearly dependant on burnup, power ratings and fuel type, the MOX fuels always showing higher release values than the UO₂ fuels. Pin puncturing is always performed mechanically, leaks being checked for by vacuum loss and by gas mass spectroscopic analyses of nitrogen and oxygen in the released fission gas samples. In order to guarantee full evacuation of the fuel bed after puncturing, vacuum pumping for fission gas plenum pressure analysis is performed typically for 12-24 hours.

BWR fuel pin claddings in Zry-2 showed at the beginning of the 90ies nodular corrosion and enhanced corrosion in the spacer region. The overall corrosion layer thickness was less expressed than for PWR fuel pins, reflecting the lower operation temperatures of the BWR's. Since KKL had replaced very early the brass condenser, no copper induced local corrosion (CILC) phenomena were observed. As remedy against pellet-clad mechanical interaction (PCMI), some fuel was equipped with a soft internal zirconium layer. Such fuel with a primary e.g. fretting

defect, showed significant secondary corrosion and hydriding, resulting in axial splitting. Some of these pins were characterized, the focus being laid on fuel cladding metallography and hydride etching at the crack tip positions. Another question was raised in relation to altered water chemistry with Zn and Fe addition. The claddings suddenly revealed extremely large oxide thickness values in pool-side EC-oxide thickness measurements at KKL (Figure 7), and PSI at that time offered rapid PIE services to clarify the findings. Within one week from the first KKL call, two fuel pins, freshly unloaded from the reactor, were shipped to the hotcells and one week later the results of NDT profilometry, metallography and EPMA analyses were available, showing that the oxide thickness was regular (around 30 μm) but covered with a Zn containing crud layer of chemical composition typical for Zn-spinells (around 20 μm thick) (Figure 7). It then became clear that the EC-oxide thickness values were falsified by the magnetic crud layer. Subsequently, the EC-oxide thickness measuring procedure was improved by multi-frequency analyses, which allowed correcting the oxide thickness values for magnetic crud layers (Figure 8). In connection with the mentioned alterations in reactor water chemistry regimes however, another real case with severe enhanced spacer shadow corrosion occurred. We carefully characterized the spacer region non-destructively and by metallography and detailed hydrogen analyses in our hotcells. A detailed mapping of the EC-oxide thickness information in the spacer region revealed severely enhanced corrosion and spalling at spacer spring contact points (Figure 9). The problem at the power station was solved by controlling subsequently the Fe/Ni ratio in the reactor water.

Similarly to the PWR fuel, hydriding and fission gas release was also an issue for the BWR fuel where the hydrogen pickup rates were varying in dependence of the burnup. While PCMI failure cases under power ramping conditions were controlled in the 1990ies with the introduction of narrow operational ramp limits and the afore mentioned inner clad liners, new pin failures were discovered beginning of 2000 at KKL, again during a power ramp case, and the question was raised whether the ramp-rate limits were exceeded. While (by visual examination and EC-defect testing) no primary cracks were observable, neutron radiography and subsequent fuel ceramography did reveal missing pellet surfaces at the fuel pin height, at which the control rod was moving across, when fuel “swelling” occurred [Groeschel, Bart]. Later on, additional colour penetration tests gave indications about a primary defect. After finishing the experimental analysis of the pin positions and dimensions of the missing fuel pellet surfaces, it was shown by FEM analyses that the stresses due to these missing fuel surfaces were high enough to cause pin cracking during the ramp (Figure 10)

Overview of destructive fuel and cladding testing

Detailed instrumental characterization of high burnup fuel and cladding was performed both for engineering lead fuel test programs (and the afore mentioned fuel damage analyses) as well as for improving the mechanical understanding of the fuel and cladding aging phenomena. The applied PIE techniques and analytical goals for our research areas are listed as an overview in Table II.

Table II: Specifications and typical process parameters for destructive fuel pin analysis

	Equipment type, vendor	Type of analysis	Precision	Comments
EPMA	Cameca-Camebax SX50-R	Local fuel and cladding chemical composition analysis	Percent range for components ≥ 1 at% spacial Resolution 2 μm	Frequently used in combination with SIMS, LA-ICP-MS and ceramography/metallography
SIMS	Atomica-4000	Local (qualitative elemental) and relative isotopic analyses in fuel and cladding (chemical quantification possible with standards)	5 % range precision for components in ppm range, spatial resolution 5 μm	Sensitive down to the ppm wt. range of elements, applied for radial Gd-, fissile- and fission product distribution in fuel. Li distribution in ZrO ₂ layers
HPLC-ICP-MS	HPLC: DX-600, Dionex, ICP-MS: Neptune, ThermoElectron	Fuel burnup analysis	< 1 % range for actinides and fission products	Significantly reduced time consumption for BU analyses compared to offline chromatographic separation and TIMS analysis
LA-ICP-MS	LA: 266 nm Nd-YAG laser, CETAC; ICP-MS: Neptune, ThermoElectron	Fission gas composition and pressure in local fuel pores	10% range precision, spatial resolution up to 10 μm	Only available option to quantify fission gas pressure in high burnup fuel pores, detection limits in the ppb/cm ² range
Ceramography Metallography	Jeol Telatom-4	Observation of fuel rod cross-section (cladding and fuel); observation of highly structural materials	Optical magnification between 10x to 2000x	Allows the determination of oxide layer on cladding or structural material, porosity in fuel and phase distribution on etched surface.
Hydrogen hot gas extraction		Hydrogen concentration in cladding and ZrO ₂ layers	5% range for concentrations >50 ppm wt.	
Fuel density analysis		Hg-pyknometry		
Cladding mechanical testing		Fracture toughness, hydride reorientation and de-		

		layered hydride cracking Burst testing		
TEM		Microstructural analysis at Zr/ZrO ₂ interface, dissolution of spp's in cladding		
μ-XAS				

In the fuel research area PSI improved the burnup analysis procedures by coupling a high performance liquid chromatography (HPLC) to the nebulizer of an ICP-MS. With this technique the burnup analysis is achievable (after fuel dissolution/dilution) by chromatographic separation of the series of present actinides and lanthanides by HPLC, and subsequent online detection of the individual isotopes by ICP-MS (Figure 11). After some initial uncertainties, this technique has now definitely replaced the tedious, time consuming procedure applying offline chromatographic column separations for the elements and subsequent thermal ionization mass spectrometry [Guenther 1 und 2]. ICP-MS was also applied to measure average lithium concentrations in ZrO₂ layers, distinguishing between water and acid leachable lithium from non leachable lithium. Lately, LA-ICP-MS proved to be very powerful in estimating the pressure of fission gases in large, high burnup fuel pores (Figure 12).

A significant step in improving PIE techniques at PSI was the introduction and application of SIMS in combination with EPMA to analyse the isotopic concentrations of fissile materials and fission products across irradiated fuel pellets to validate radial fuel burnup modelling results [Zwicky, Grimm]. Applying this technique, it was for the first time possible to look precisely at the fuel periphery of UO₂ pellets where U-235 is depleted due to burnup and concentrations of Pu-isotopes are building up (Figure 13). These analyses often show quite significant gradients in azimuthal fuel burnup due to pin orientation towards Gd-rods, fuel element water holes or control rods. Having realized this, it became standard practice to define zero degree azimuth orientations of BWR-fuel pins when extracting them from fuel bundles in reactor pools for hotcell PIE. While SIMS per se provides elemental isotopic ratios only, SIMS in combination with EPMA (or ICP-MS) of the same fuel cross sections could be normalized to show true radial isotopic abundance values. Naturally the shielded PSI SIMS was also applied in fuel related topics such as fuel melt down studies, absorber rod analyses, fuel waste glass analysis etc. but these topics are not subject in this conference.

As mentioned before, significant efforts were made to characterize lithium concentration profiles across cladding ZrO₂ layers. This in connection with the findings that Zircaloy does show a corrosion rate increase in a lithiated water environment, while it does not so, if the pH of the reactor water is raised by NH₃ or KOH [Garzarolli, Portland ca. 1985]. (It shall however not be discussed here, whether lithium is the reason for, or result of enhanced corrosion, leading to a porous re-precipitated oxide, in which lithium under sub-cooled boiling conditions is accumulated). In respect to SIMS profiling of lithium, it was found and assumed that lithium, enhancing the corrosion rate, would have to show significant concentration levels in the oxide layer all the way down to the oxide metal interface, where the corrosion front moves into the bulk metal. Such profiles were rarely analyzed at PSI but were indeed found in oxide layers from some

heavily corroding cladding samples (Figure 14).

In connection with the corrosion process, significant work was performed to quantify microstructural findings by TEM at the metal/oxide interface of loop and in-pile tested zirconium alloys, showing improved corrosion resistance. While initially the samples for such tests were mechanically thinned and subsequently ion milled, the sample preparation procedure today relies on focused ion beam cutting (FIB). This technique allows to reproducibly prepare homogeneous TEM transparent metal-oxide interface samples of $\sim 10 \times 10 \times 0.2 \mu\text{m}$, in which we characterize the corrugation of the interface, the oxide grain shapes and texture, the crystal lattice transition from metal to oxide (by high resolution TEM) and, last but not least, the oxygen profile through the metal oxide interface. The oxygen profiles indeed seem to shed light into the corrosion process, showing stoichiometric ZrO_2 profiles at the M/O boundary for “normally corroding” alloys, while more corrosion resistant cladding variants reveal sub-stoichiometric oxides (Figure 15) [Abolhassani].

With respect to clad hydriding, several analytical approaches were followed. First the hot gas extraction routine with LECO analyzers was improved in order to sample crystal water and hydrogen from ZrO_2 in a first low temperature extraction step at $\sim 550^\circ\text{C}$ and then, in a second high temperature extraction step at $\sim 1900^\circ\text{C}$, the more meaningful hydrogen from the bulk metal phase (Figure 16) [Hermann01]. Metallographic etching is applied to characterize the localization, concentration and orientation of precipitated hydrides in cladding cross sections. Such characterisation is applied today in as received and thermo-mechanically treated samples in connection with hydride reorientation experiments under dry fuel transportation conditions (Figure 17) [Alam]. These tests are undertaken in order to define fuel pool handling procedures which do not lead to undesirable radial hydride orientation or delayed hydride cracking under dry long-term intermediate fuel storage conditions. Hydride reorientation is investigated by the Cladding Tube Deformation Test (CTDT), where a small cladding tube segment is elastically deformed at a high temperature (the temperature reachable within the evacuated fuel cask) and then (still under load) let the samples cool down slowly. The metallographic results are then evaluated by Finite Element Modelling (FEM) of the CTDT. Hydride analysis is also performed by neutron radiography, particularly in connection with fuel damage analysis with assumed heavy secondary hydriding (and when searching e.g. for cladding sections containing local hydride rims). This technique was quantified and has given accurate absolute hydrogen concentration profiles validated with local hot gas extraction results.

Again in connection with hydriding (and neutron embrittlement), PSI also performed cladding burst tests at room temperature and at 300°C . Subsequent micro structural analyses showed that even at a burnup of $\sim 60 \text{ MWd/kg}$ and hydrogen concentrations in the cladding of $>500 \text{ ppm wt}$ the claddings in the burst region still show ample ductility ($> 5\%$) [Yagnik, Hermann Gavillet]. However, such tests do not deliver any fracture toughness information. PSI therefore evaluated within an international round robin test also a cladding fracture toughness procedure [Bertsch]. As the cladding tubes do not show adequate geometrical conditions for standard fracture toughness analysis procedures, PSI developed an adapted procedure. It consists in straining defuelled notched cladding sections and measuring the energy necessary to progress the cracks, recording the crack propagation and applied force. This procedure was applied at room and elevated temperature (Figure 18). FEM is again needed to subtract friction forces of the experiment in order to estimate J-integral values of the samples.

Conclusions and outlook

The PSI PIE tools support the Swiss and international nuclear fuel industry in the best possible manner with scientific service work in their strive to develop high performance, high burnup fuel, which is economically attractive both with respect to reduced procurement and waste volume costs, but for which the safety margins have also to be proven during the full life.

At the same time PSI as research organization supports nuclear energy related applied research topics. Under these boundary conditions the PSI LWV is devoting significant efforts to elucidate the LWR cladding corrosion and hydriding phenomena, to improve the knowledge in cladding mechanical behaviour under normal operation and operational transient conditions (up to answering safety questions with respect to dry interim storage) and to understand the fission gas diffusion mechanism in fuel structures.

Significant steps in this context have been reached both in terms of covered fuel burnup spans (with highest LWR fuel burnups ever reached worldwide both for BWR's and PWR's) and of analytical process development and fuel aging process interpretation.

The Swiss nuclear power plant operators, represented by "swissnuclear", support the PSI HOTLAB infrastructure financially at a significant level. On the other hand, PSI is prepared to support the Swiss power stations immediately if they would need urgent HOTLAB support. Since nuclear power for electricity production in Switzerland will continue to be important (with presently 40% nuclear share in electricity production) this reciprocal support will be continued. At the same time the evolution of fuel assemblies with new fuel additives, modified cladding material or modified geometry is ongoing. Therefore PIE on new lead fuel pins will maintain an indispensable step for validating new assemblies.

The challenge for us lies in maintaining a high level of analytical possibilities and services and to identify areas of research which are of scientific and industrial interest and which ideally take advantage of the material science competence and analytical possibilities at PSI.

References

- [Hermann01] A. Hermann, H. Wiese, R. Bühner, M. Steinemann, G. Bart, „Hydrogen Distribution between Fuel Cladding Metal and Overlying Corrosion Layers“
Proceeding of ANS Int. Topical Meeting on LWR Fuel Performance, Park-City, Utah, Vol.1, 372-384, USA, April 2000.
- [Groeschel, Bart] F. Groeschel, G. Bart, R. Montgomery, S.K. Yagnik, “Failure Root Cause of a PCI Suspect Liner Fuel Rod”, IAEA-TECDOC-1345, Fuel failure in water reactors: Causes and mitigation, p.188-202, March 2003.
- [Abolhassani] S. Abolhassani-Dadras, R. Restani, T. Rebac, F. Groeschel, W. Hoffelner, G. Bart, W. Goll, F. Aeschbach, “TEM examinations of the metal-oxide interface of zirconium based alloys irradiated in a pressurised water reactor”, Zirconium in the Nuclear Industry: Fourteenth International Symposium, ASTM STP1467, p.467-493 2005.
- [Alam] A. Alam, C. Hellwig, “Stress Reorientation of Hydrides in Unirradiated Zircaloy-2 Tube Specimens”,
Proceeding of Fontevraud 6, International Symposium on Contribution of Materials Investigations to Improve the Safety and Performance of LWRs, Vol. 2, p 933-944, Fontevraud Royal Abbey, France. Sept. 18-22, 2006.
- [Günther 1] I. Günther-Leopold, B. Wernli, Z. Kopajtic “Characterization of spent nuclear fuels by an online combination of chromatographic and mass spectrometric techniques”
Proceedings of the 7th International Conference on Nuclear Criticality Safety, Tokaimura, Japan, 884 – 889, 2003.
- [Günther 2] I. Günther-Leopold, J. Kobler Waldis, B. Wernli, Z. Kopajtic (2005) “Measurement of plutonium isotope ratios in nuclear fuel samples by HPLC-MC-ICP-MS”
Intern. J. Mass Spectrom. 242, 197 – 202.
- [Bart 01] G. Bart, J. Bertsch “Zirconium Alloys for Fuel Element Structures”,
Chimia 59, ISSN 0009-4293, No. 12, 938-943, 2005.
- [Zwicky 01] H.U. Zwicky et al. “Enhanced Spacer Shadow Corrosion on SVEA Fuel Assemblies in the Leibstadt Nuclear Power Plant”
Proceeding of ANS Int. Topical Meeting on LWR Fuel Performance, Park-City, Utah, Vol.1, 459-469, USA, April 2000.
- [Zwicky 02] H.U. Zwicky et al. “Radial Plutonium and Fission Product Isotope Profiles in Mixed Oxide Fuel

Pins Evaluated by Secondary Ion Mass Spectrometry”
Journal of Nuclear Materials, Vol. 202, 65, 1993.

[Holzgrew]

F. Holzgrewe et al.
“Validation of CASMO-4 against SIMS measured spatial Nuclide
Distributions inside a 9 WT% GD BWR Pin”
Proceeding of ANS Int. Topical Meeting on LWR Fuel Performance, Park-
City, Utah, Vol.1, 595-607, USA, April 2000.

[Bart 02]

G. Bart et al.
“Experience in the Application of a Shielded Secondary Ion Mass
Spectrometer for Nuclear Material Research”
IAEA TECDoc~822, 337, 1995

[Gebhardt]

O. Gebhardt et al.
“SIMS Depth Profile and Line Scan Analyses at the Metal/Oxide Interface
of Corrosion Films on Zirconium Based Alloys”
Secondary Ion Mass spectrometry (SIMSX), John Wiley & Sons,
Chichester, 869, 1997.

[Garzarolli]

F. Garzarolli et al.
“Influence of Various Additions to water on Zircaloy 4 Corrosion in
Autoclave Tests at 350°C.”
Proceedings of IAEA Working Group on Water Reactor Fuel Performance
and Technology, Portland, Oregon, USA, p. 65-72, 1989.

THE LFR RADIOCHEMICAL FACILITY

A.Stankevicius, e-mail: stankevi@cae.cnea.gov.ar
Comisión Nacional de Energía Atómica, Argentina

ABSTRACT

The LFR Facility is a radiochemical laboratory designed and constructed with a hot-cells line, a glove-boxes and fume-hoods, all of them suited to work with radioactive materials. It is worth noticed the LFR capacity to carry on different research and development programs (R+D) in the Nuclear Fuel Cycle field, such as the burn up determination, absolute burn up measurement, the radiochemical analysis of different materials and solutions, the evaluation of radioactive waste immobilization processes, and researches on burnable poisons.

1. INTRODUCTION

The LFR Facility is sited in the Ezeiza Atomic Center of the National Atomic Energy Commission of Argentina. In the *Fig. 1*, it is possible to appreciate the internal distribution of the different sectors.

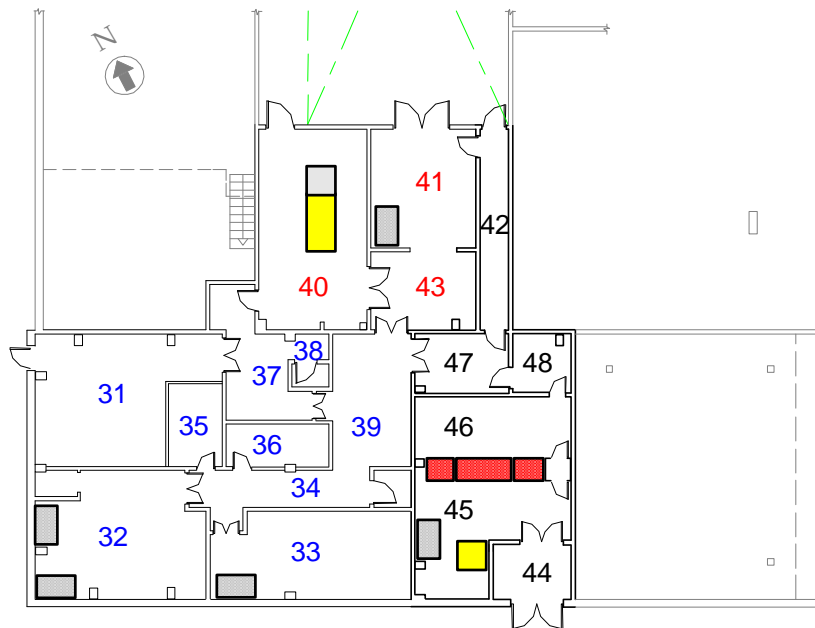


Fig. 1 – LFR Facility ground level.

The LFR ventilation system, so important in this kind of laboratories, includes an Injection Room, an Extraction Room and a Filtration Room all of them on first floor (*Fig. 2 and 3*).



Fig. 2 – LFR Extraction Room.



Fig. 3 – LFR Filtration Room.

The hot-cells line was built with 10cm thickness of lead-shielding, mounted with master-slave manipulators and remote handling tools, with HEPA filtration system and double door air tight transfer system between cells. Two of the cells, with sealed enclosures and with alpha tight protecting booting, are suited to work with open sources of radioactive materials (*Fig. 4, 5 and 6*).



Fig. 4 – Metallic frame for the shielding and internal sealed enclosures for cells numbers 1 and 2.



Fig. 5 – Frontal view of LFR hot-cells line (Supervised Area).

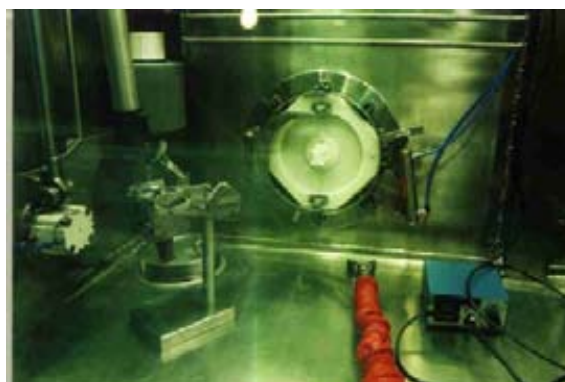


Fig. 6 – Internal view of hot-cell Number 2.

It's possible to operate as well with 10 Ci of Beta-Gamma fission products and with Alpha emitters materials. Inside Cell 2, there are two extra attached shielded containers. This containers storage active materials, and reduce the total dose rate applied to the rest of the components.

In the Controlled Area of the hot-cells there are two main components, the Glove-Box and the Fume-Hood, as well as the “Padirac” and “La Calhene” transfer systems (*Fig. 7 and 8*).



Fig. 7 – LFR Glove-Box with the HPLC system.



Fig. 8 – LFR hot-cells line, rear view (Controlled Area).

In these Glove-Box it is installed a high performance liquid chromatography (HPLC) system.

To make possible an α -tight operation with the manipulators it was necessary to exchange tongs and hands in the master-slave hot-cell operation system (*Fig. 9, 10 and 11*). In this way a gauntlet (booting) was internally attached to them, to improve the tightness of the system.



Fig. 9 – Telem manipulator “PAR” in hot-Cell N°1



Fig. 10 – Adaptation of tongs and hands (old vs. new)



Fig. 11 – Final adjust (old tongs and fingers vs. new tongs)

During the construction of the sector advocated primary to active waste studies and characterizations, was necessary to open news doors in the old building, install pneumatic

valves for the ventilation system and adjust the fume-hoods in their places (Fig. 12, 13 and 14).

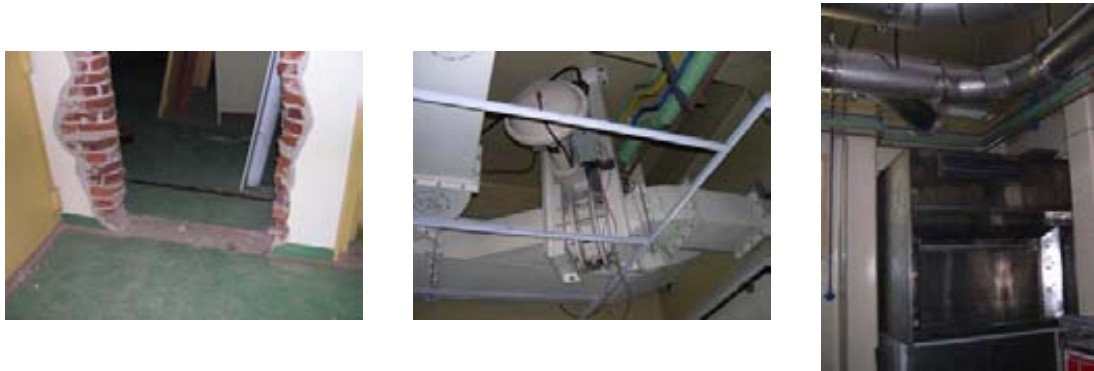


Fig. 12, 13 and 14 – Shallow view of LFR mounting operations

In the following figures, an overview of this LFR facility sector, were the fume-hoods, tables equipped with laboratory plastic fittings and glassware, the alpha and the beta-gamma spectrometer, the beta scintillation counter, the spectrophotometer and the precision balance, all of them are possible to appreciate.



Fig. 15 to 22 – An overview of one of the LFR facility sectors

The last one LFR sector that reach an operative condition was the ICP-MS laboratory. There were installed an inductive coupled plasma mass spectrometer attached to an a alpha tight glove-box, with an special flange that avoid radioactive leaks during the possible maintenance operation in the system.

In the following figures is possible to appreciate an overview during the setup of this another LFR facility sector, were radiochemical analysis of elements and their isotopes processes.



Fig. 23 to 28 – An overview of the ICP-MS Laboratory

The high temperature into the plasma (*Fig. 29*) destroy all chemical compounds and liberate their constituent elements. The mass-spectrometer included in the equipment permit the elemental and isotopic determination of them.

Due to the small quantities of materials required in this type of assay, the total dose to the operators is reduced. In case of high activity materials, is possible to dilute or remove a small fraction of them, into de hot-cells or in their glove-box or fume hood (*Fig. 30*).



Fig. 29 and 30 – Plasma high temperature without glass-shielding protection and glove-box and fume hood in the “Controlled Area” of the hot-cell line

2.- CONCLUSION

It is worth noticed and was shown the capability of the LFR facility for destructive assays in the characterization of irradiated nuclear fuels and materials, specially in the following areas.

- R&D in the Nuclear Fuel Cycle
- Burnup determinations
- Radiochemical analysis of materials
- Evaluations of radioactive waste immobilization processes

Acknowledgement

The authors wish to recognize the assistance and collaboration of D.A.Gil, M.Falcón and C.A.Devida, in the selection, buying and setup of the equipment and components of the LFR.

SESSION 3: PIE TECHNIQUES AND APPLICATIONS (PART-1)

Chairpersons

J. Y. Blanc (CEA, France)

Yong Bum Chun (Republic of Korea)

EXAMINATION OF THE WWER-440 FUEL AFTER IRRADIATION UP TO BURNUP 70 MWd/kg USING ELECTRON PROBE MICROANALYSIS AND SCANNING ELECTRON MICROSCOPY

F.N. Kryukov, S.V. Kuzmin, G.D. Lyadov, O.N. Nikitin, V.P. Smirnov
“State Scientific Center of Russian Federation Research Institute of Atomic Reactors”,
Ulyanovsk region, Dimitrovgrad, Russia

ABSTRACT

The change of structure of thermal reactor fuel is determined to a great extent by the generation and behavior of gaseous fission products. We studied the interaction of the fuel structure change with the content and distribution of xenon using a sample made from the WWER-440 reactor fuel rod irradiated for 6 fuel cycles. The fission products distribution was examined by the electron-probe X-ray microanalysis using the transversal cross-section of the fuel rod. The structure was examined by the scanning microscopy using the fuel rod section and fracture. At a fuel burnup of 70.2MWd/kg in the WWER-440 reactor the decrease of the xenon content in the fuel matrix was observed over the whole pellet cross-section as compared to that one resulted from irradiation. It is related to the complete or partial fuel restructuring that occurs, first of all, at the primary grain boundaries and is characterized by the generation of fine-grain structure together with submicron and micron voids.

The change of structure of thermal reactor fuel is determined to a great extent by the generation and behavior of gaseous fission products. We studied the interaction of the fuel structure change with the content and distribution of xenon using a sample made from the WWER-440 reactor fuel rod irradiated for 6 fuel cycles. We used a fuel rod cross-section with the maximal linear dose rate. The fission products distribution was examined by the electron-probe X-ray microanalysis using the transversal cross-section of the fuel rod. The structure was examined by the scanning microscopy using the fuel rod section and fracture. The measured values of the neodymium content along the pellet radius were used to calculate the local burnup and to plot the radial burnup profile. We used this profile to calculate the radial distribution of xenon resulted from irradiation. The comparison of the xenon content with the measured values gives us information about its redistribution under the operating conditions. The determination of xenon content in the irradiated fuel by the electron-probe X-ray microanalysis has some peculiar features: a part of gas can be found in voids, of which size and distribution influences the intensity of the characteristics X-ray line due to the difference in the interaction of the primary electron beam with a solid substance and gas. So, we can use the microanalysis as a structural sensitive method to examine the xenon behavior.

At microprobe electrons energy of up to 20keV we can register and perform quantitative measurements of a part of xenon containing in the solid solution and small voids with a diameter less than 0.01 μ m. At a higher energy we can register xenon containing in big voids and obtain a perfect picture of the xenon distribution in the surface voids (at the section).

Fig.1 presents the distribution of neodymium, burnup, xenon and cesium along the fuel pellet radius. The average burnup calculated by its radial distribution made up 70.2 \pm 1.3MWd/kg. The comparison of mass portions of the generated cesium and that one contained in fuel showed that temperature level was not sufficient for its migration.

The measured xenon content over the whole pellet radius was lower than the calculated one as a result of irradiation. The decrease of the xenon content in the fuel matrix in the pellet outer zone was determined by the generation of a typical edge zone and the release of xenon atoms from the grains into the voids (Fig. 2).

Xenon with a mass portion of 0.2-0.4% was also found in the oxide film on the cladding inner surface. Figure 3 shows the microstructure of fuel and maps of the xenon distribution near the pellet central hole. They evidence about the xenon release from the fuel matrix in the near-boundary grain zones and generation of grain boundary porosity. Regardless the energy of the micro-probe electrons, it is really difficult to reveal xenon in the grain boundary voids in case of its high content in a grain because of low effectiveness of the characteristics X-ray line in the gaseous phase.

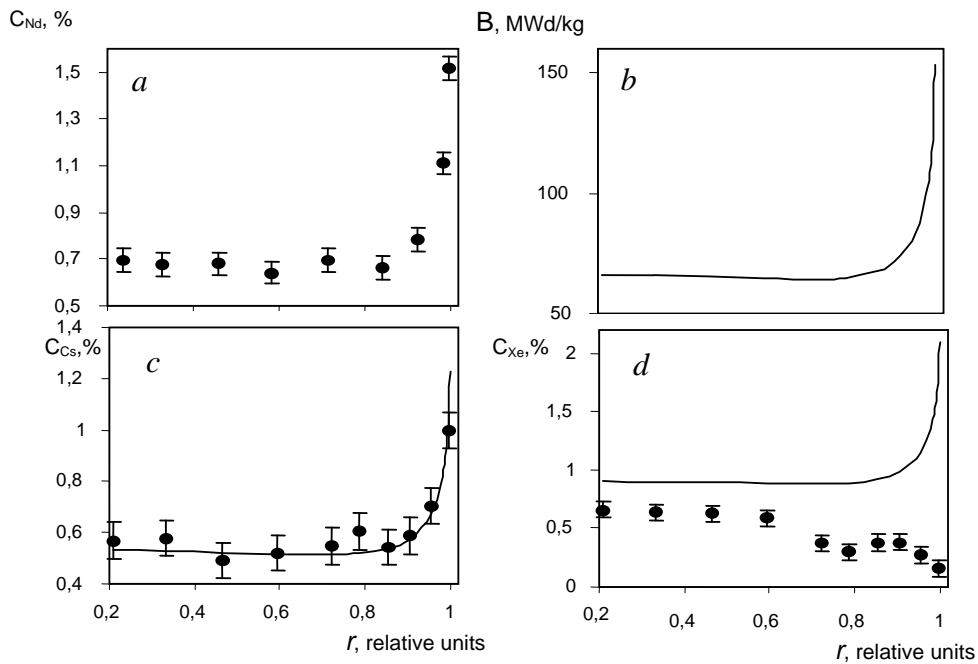


Fig. 1. Distribution of neodymium (a), burnup (b), cesium (c) and xenon (d) over the fuel pellet radius: — — calculation; • — experiment

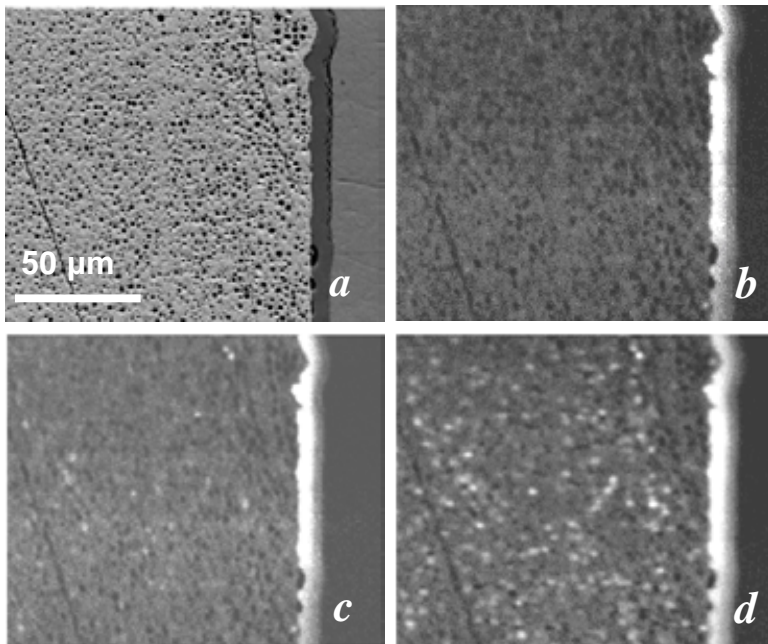


Fig. 2. Microstructure of fuel (a) and maps of xenon distribution near the pellet surface obtained at an accelerating stress of 15kV (b), 20kV (c) and 30kV (d).

So, Figure 3 shows only separate gas-filled voids located at the grain boundaries. Figure 4 presents the porosity distribution over the fuel pellet radius obtained by the microstructure images processing. One of the tasks set during the scanning electron microscopy of the fuel structure was to determine the mechanism of the grain boundary porosity formation out of the fuel pellet edge zone. We had to find out whether it was related to the fuel restructuring or determined by the xenon diffusion activated on the grain boundary without any structural changes of fuel. The fresh pellet fractures obtained by the scanning electron microscopy are presented in Figure 5. There are micron voids and uniform

submicron grains in the completely restructured edge zone near the pellet surface (Fig. 5, a, b). A fragment of the pellet transversal cross-section can be seen in Fig.5, a. Near the edge zone there is a relatively wide transient zone that represents a total of restructured areas and fragments of initial structure (Fig.5, c, d).

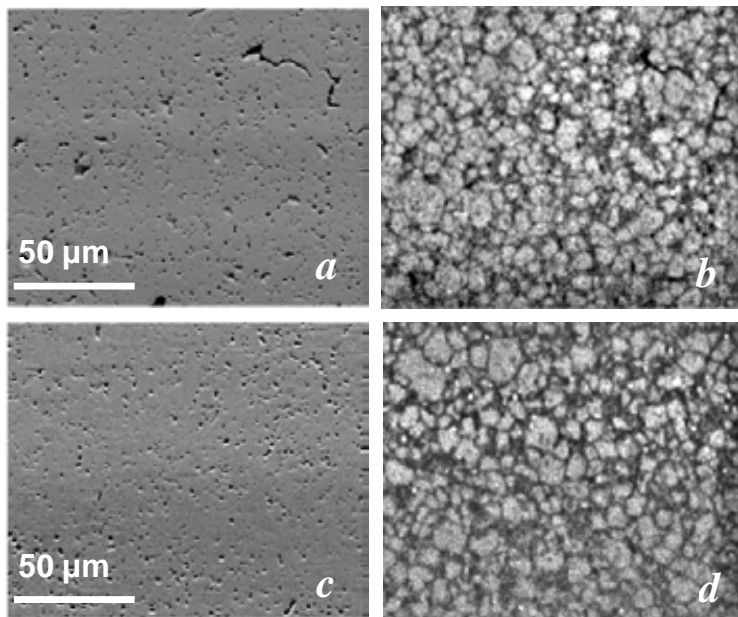


Fig. 3. Microstructure of fuel and maps of xenon distribution on the area of 0.6 of the radius (a, b) and near the pellet central hole (c, d), respectively

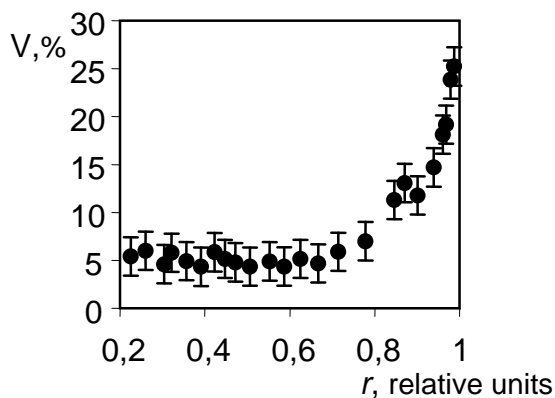


Fig. 4. Distribution of porosity over the fuel pellet radius

The number of restructured zones decreases as the distance from the pellet edge increases and these zones are located at the primary grain boundaries in the pellet inner area (less than 0.6 of the relative radius). These localized zones are inevitably related to the submicron and micron voids and can be found up to the pellet central hole.

Thus, at a fuel burnup of 70.2MWd/kg in the WWER-440 reactor the decrease of the xenon content in the fuel matrix was observed over the whole pellet cross-section as compared to that one resulted from irradiation. It is related to the complete or partial fuel restructuring that occurs, first of all, at the primary grain boundaries and is characterized by the generation of fine-grain structure together with submicron and micron voids.

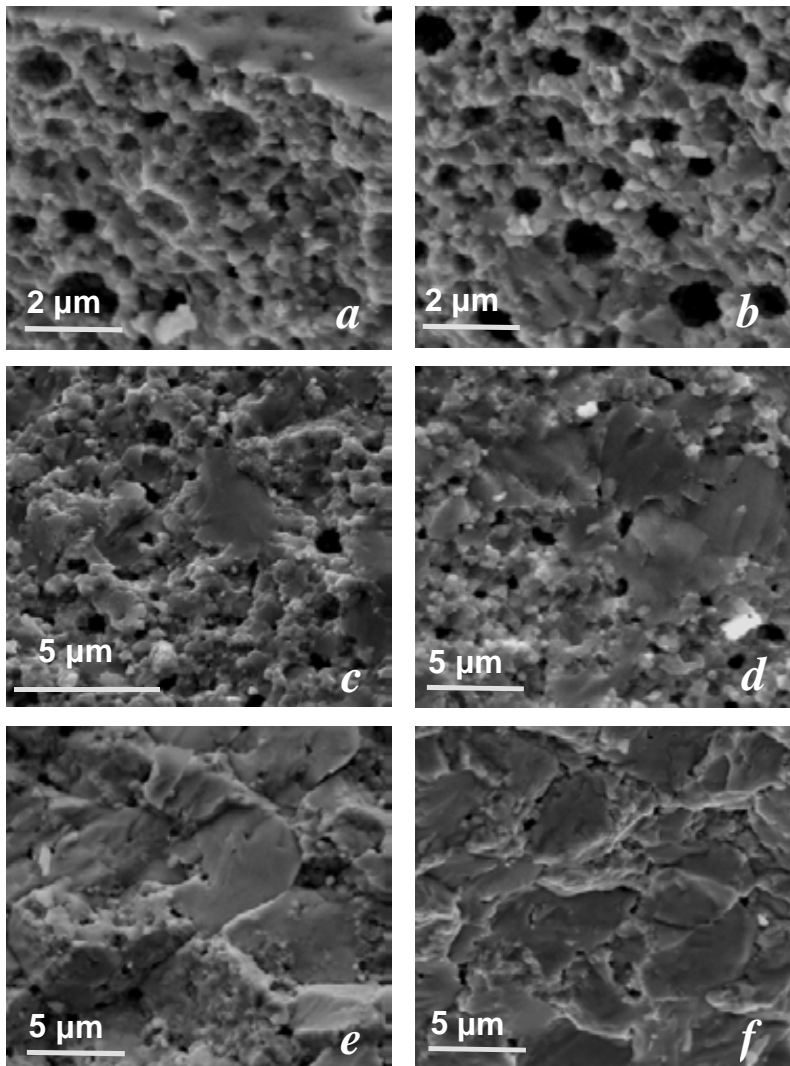


Fig.5. Fuel fractography over the pellet radius: a, b – 0.995, c, d, e, f– 0.95, 0.9, 0.6, 0.22 of radius, respectively

Burnup Estimation of Nuclear Fuels with a Gamma Scanning Test

Heemoon Kim, Hong-ki Lee, Byoung-ok Yoo, Jae-min Sohn, Bong-goo Kim, Yong-sun Choo,
Kwon-pyo Hong

Korea Atomic Energy Research Institute
150 Deokjin-dong, Yuseong-gu, Daejeon, 305-353, Republic of Korea
hkim1211@kaeri.re.kr

ABSTRACT

PWR spent fuel from a nuclear power plant and two irradiated fuel capsules were prepared for a burnup estimation. The former declared burnup was used for a preliminary test of the capsules. The latter was for a burnup estimation. Two fuel capsules(02F-11K, 03F-05K) containing three fuel rigs each were irradiated in the HANARO research reactor, then a gamma scanning was carried out. Three detection positions of each fuel rig in the capsules were selected, which were the first, third and fifth pellets from the top of the fuel rig while one point in the PWR spent fuel was selected. After setting up the detection points, the gamma scanings were performed for 3 hours at a each point and carried out three times at each point repeatedly to reduce the counting errors of the cesium isotopes. ORIGEN-ARP code was used to calculate the burnups which are related to the obtained atomic ratio of Cs-134/Cs-137 gamma peaks. The atomic ratio for a PWR spent fuel rod was 5.84×10^{-4} and the related burnup from ORIGEN-ARP was 39,500 MWd/t-U. It provided a good agreement when compared to the declared burnup of 40,000 MWd/t-U. In this case, the code library was correctly applied to the PWR spent fuel. The burnups calculated by HANAFMS were 5.9 MWd/t-U for 02F-11K and 5.6 MWd/t-U for 03F-05K. In the results of the gamma scanning, the burnups were 5.1 GWd/MTU for the 02F-11K and 4.8 GWd/MTU for the 03F-05K as a mean value. These results were lower than those of HANAFMS by 15% due to the CANDU library being applied to the ORIGEN-ARP incorrectly. It is necessary to develop a new library for the HANARO irradiation hole.

Keywords : gamma scanning, Cs-137, burnup, atomic ratio, ORIGEN-ARP

1. INTRODUCTION

Burnup is a basal parameter and therefore a burnup verification is important. Nondestructive tests have been performed on a spent nuclear fuel to verify burnup and cooling time data for safeguard purposes. Normally, for a measurement by a gamma scanning, Cs-137 is used as a monitoring nuclide for a burnup[1]. The additional fission products studied are Cs-134 and Eu-154, these isotopes dominate the gamma-ray spectrum of a spent fuel with a cooling time of 10-20 years[2].

To avoid a geometry correlation for a quantitative analysis, the activity ratios of the nuclides, which are fission products, have been introduced. Haddad calculated the cooling time of a fuel with the activity ratio of Nb-95/Zr-95[3]. Iqbal and et al. performed a gamma scanning to obtain the activity ratios of Zr-95/Cs-137 and Cs-134/Cs-137[4]. Especially, the activity ratio of Cs-134/Cs-137 is more readily available due to the same thermal migration behavior as well as relative long half lives, namely 30 years for Cs-137 and 2.06 years for Cs-134[5]. Furthermore, the activity ratio of Cs-134/Cs-137 shows a good linearity with the burnup.

To obtain the activity ratios of two isotopes which have different gamma energies, a calibration of a energy efficiency for the selected energy range has to be done prior to a gamma scanning for the target fuels. Standard sources have to be used in the energy calibration. In this study, the atomic ratio of Cs-134/Cs-137, instead of the activity ratio, is introduced by using a calibration of the energy efficiency with Cs-134.

For a burnup calculation using the atomic ratio, the number of fission events, the fission yield and the decay history of the mother and daughter nuclides must be considered. These days, the ORIGEN-ARP code is available to calculate all the considered parameters including the atomic ratio as mentioned above for a burnup calculation[6,7].

HANARO research reactor has performed fuel capsule irradiations for a few years. Whenever there are capsule irradiations in some test holes, HANAFMS, the reactor core calculation code for HANARO, has been used for the burnup calculation in each test hole. So, we attempted to compare this data with the data from a gamma scanning. In this study, two fuel capsules(02F-11K, 03F-05K) containing three fuel rigs each were irradiated in the HANARO research reactor and cooled down, then a gamma scanning was carried out for the burnup calculation.

2. EXPERIMENTAL

The PWR spent fuel had a declared burnup of 40,000 MWd/t-U and two irradiated fuel capsules were prepared. The former with a full active length(3.6 m) was cut into 10 pellets, and they were contained in a zircaloy tube. It was cooled down for 16.5 years until a gamma scanning. The latter, the capsules(02F-11K, 03F-05K) containing three fuel rigs each, were made for an irradiation and temperature test[8]. Each rig had 5 UO₂ pellets. Table I shows the properties of the rig and UO₂ pellet. 02F-11K was irradiated at the OR5 hole in the HANARO research reactor in March, 2003 and the 03F-05K in April, 2004. These capsules had a different linear power history for the full power days of 54 days and 60 days as shown in Fig.1, then they were cooled down for 20 months and 12 months, respectively.

The gamma scanning for all the fuels was performed with the geometry as shown in Fig. 2. The slit dimension of the collimator was 40 mm(W) x 0.5 mm(H) x 250 mm(L) and it was made of tungsten. The detecting distance was 160 cm due to a 100 cm wall thickness. HPGe detector for a high count rate was activated with a 16,000 channel MCA. After being cooled down, the capsules were dismantled to withdraw the fuel rigs. To measure the center temperature, 3 pellets from the top were drilled for a thermocouple. Three detection points of each rig were selected, which were the first, third and fifth pellets from the top of the rig based on a short-time scanning to obtain the pellet points as shown in Fig. 3, while one point of the PWR spent fuel was selected.

Fig.3 shows each pellet position in three rigs of 02F-11K by a short-time gamma scanning which was performed every 2 mm in the gap and for 600 sec of a detection time in each gap. After setting up the detection points, gamma scanings were performed with 3 hours of a detecting time at each point. They were carried out three times at each point repeatedly to reduce the counting errors of the cesium isotopes.

Table I. Properties of the fuel rig

Rig material	Zry-4	Pellet dia. (mm).	8.18
Rig outer dia.(mm)	9.5	Pellet density (TD)	95.8%
Rig thickness (mm)	0.57	Pellet grain size(μ m)	9.35
Rig length(mm)	250	Filled gas (atm)	Helium (1.2)
Gap size(μ m)	167	Enrichment (w/o)	2.42

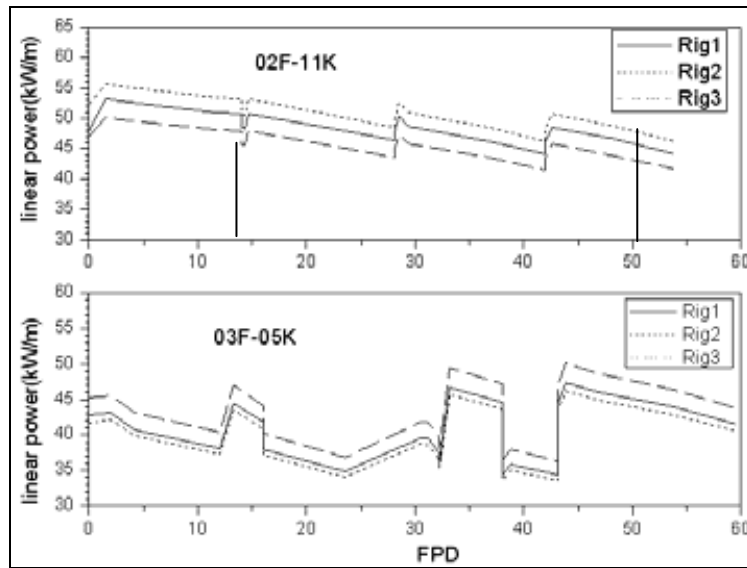


Fig. 1. Linear power history(02F-11K, 03F-05K) – Helios code calculation

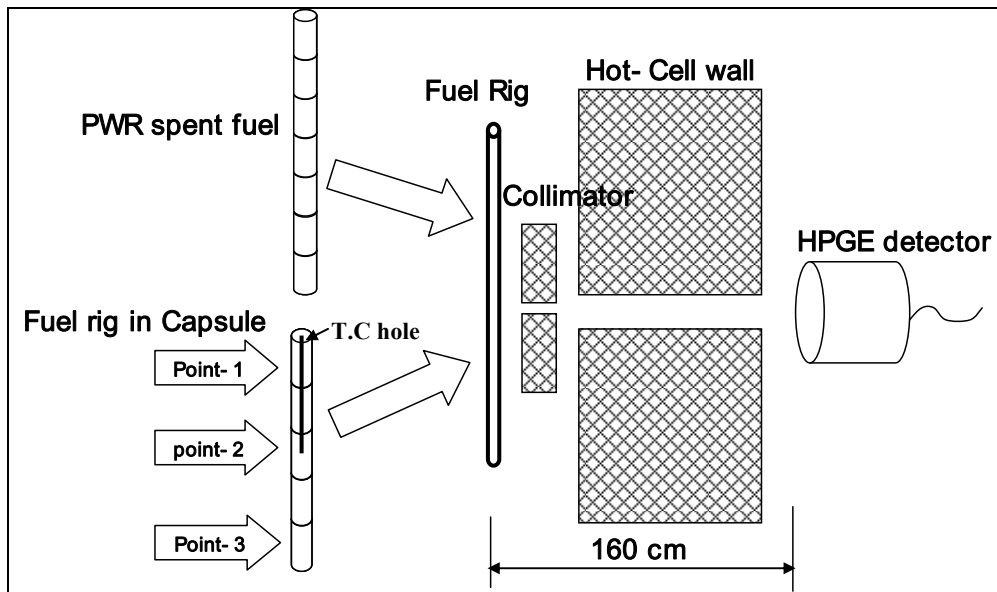


Fig. 2. The geometry of a gamma scanning.

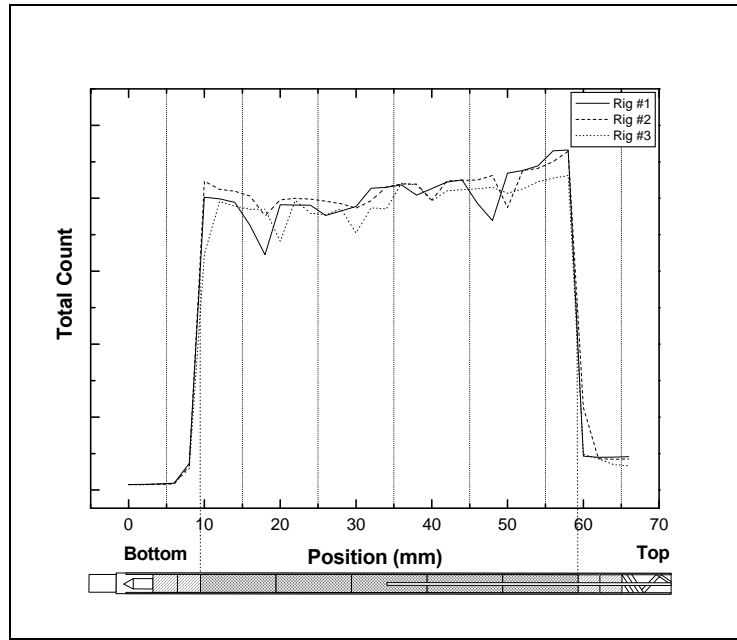


Fig. 3. Pellet positions by a gamma scanning.

3. RESULTS

Atomic ratio of Cs-134/Cs-137, instead of the activity ratio, was applied in this study, while the gamma peak of Eu-154 was too small for the fuel capsules due to a short irradiation time. To calculate the atomic ratio of Cs-134/Cs-137, the basic equation is as follows;

$$C(E_i) = \lambda NP(E_i)\varepsilon(E_i) \quad (1)$$

Where, C is the gamma counts(cps) at each energy, λ is the decay constant(s^{-1}), N is the atomic amount, P is the decay branch ratio, and ε is the energy efficiency. Here, λN is the radioactivity. Most papers have shown the activity ratio($\lambda_{134}N_{134}/\lambda_{137}N_{137}$), but we show the function of $N\varepsilon$ from a different viewpoint in this paper as shown in Eq.(2).

$$\frac{N_{134}\varepsilon(E_{134})}{N_{137}\varepsilon(662keV)} = \frac{C_{134}/(\lambda_{134}P_{134})}{C_{137}/(\lambda_{137}P_{137})} \quad (2)$$

From Eq.(2), the numerator in the left term can be changed to $N_{134}\varepsilon(662keV)$ by means of an interpolation of the plot of $N_{134}\varepsilon(E_{134})$ at 662 keV as shown Fig.4.

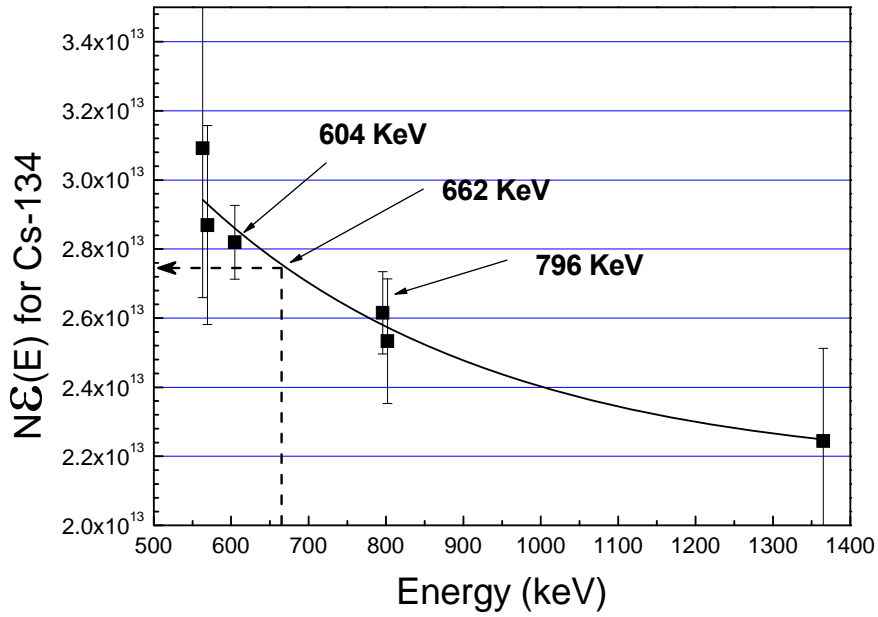


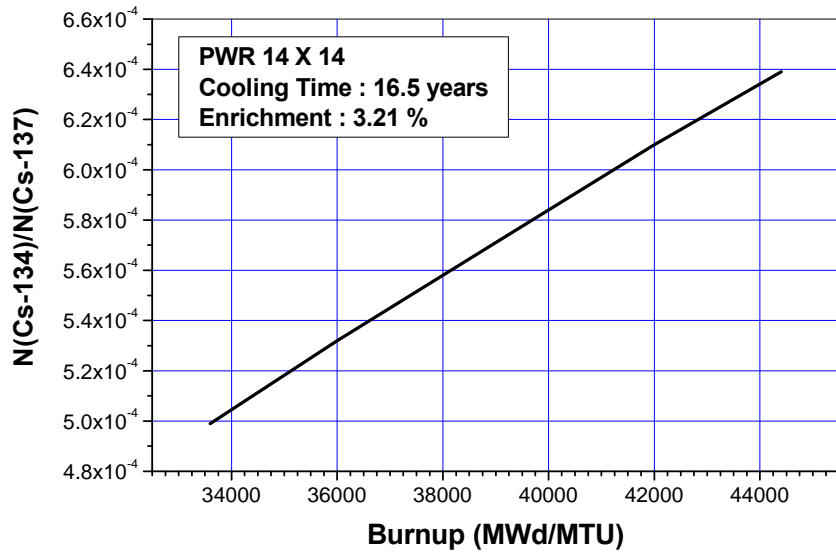
Fig. 4. plot of $N\epsilon(E)$. vs. E for Cs-134

But only two energy peaks of Cs-134, 605 keV and 796 keV, were available due to the low peaks of the others which have large systematic errors at over 20%. It is assumed that Cs-134 has another gamma ray at 662 keV, so the value of $N_{134}\epsilon$ at 662 keV is obtained by an interpolation between 605 keV and 796 keV. Finally, the detector efficiencies of the numerator and the denominator at the ratio are the same. Eq.(3) is shown as follows;

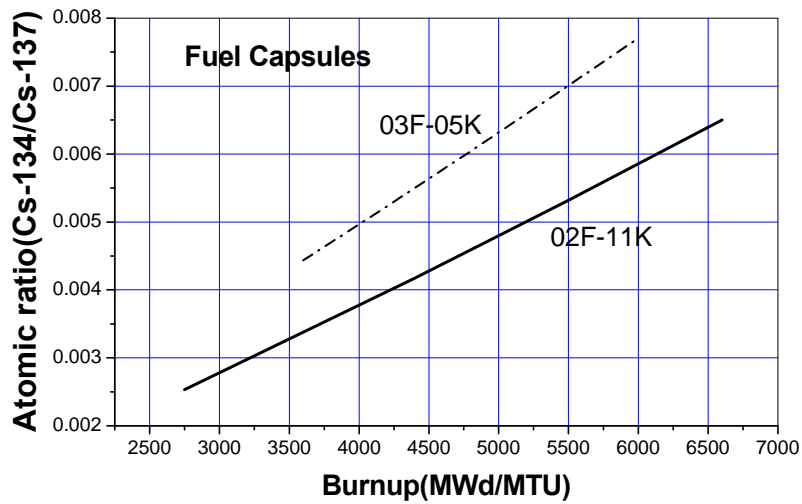
$$\frac{N_{134}\epsilon(662keV)}{N_{137}\epsilon(662keV)} = \frac{N_{134}}{N_{137}} = R_{exp} \quad (3)$$

Where, R_{exp} is the experimental ratio from a gamma scanning.

To estimate a burnup with an experimental value (R_{exp}), the ORIGEN-ARP code was used to obtain the calculated value (R_{cal}) with a burnup as shown in Fig.5. The ratio follows a linearity and the exact burnup of the fuel can be obtained.



(a)



(b)

Fig. 5. The plot of the atomic ratio with the burnup by ORIGEN-ARP ((a) is for spent PWR fuel and (b) is for fuel capsules).

The atomic ratio for the spent PWR fuel was 5.84×10^{-4} and the relevant burnup was 39,500 MWd/MTU based on the Fig.5(a). Table II shows the experimental ratio and the burnup at each point in the rigs in the fuel capsules. 5.4 GWd/MTU of an average burnup for the 02F-11K and 5.0 GWd/MTU of an average burnup for the 03F-05K were predicted except for some low burnup rigs which is assumed to be due to the fact that they were placed farther from the core. All of the rigs show the highest burnup at the upper positions due to the location of the core center which has a higher neutron flux.

Table II. The atomic ratios of Cs-134/Cs-137 and the burnups at each rig position in the fuel capsules

Position		Point-1	Point-2	Point-3	
02F-11K	Rod #1	R _{exp}	0.0055	0.0051	0.0050
		Bu	5.66	5.3	5.25
	Rod #2	R _{exp}	0.0055	0.0051	0.0050
		Bu	5.66	5.3	5.25
	Rod #3	R _{exp}	0.0044	0.0042	0.0042
		Bu	4.62	4.4	4.4
03F-05K	Rod #1	R _{exp}	0.0060	0.0053	0.0050
		Bu	4.7	4.2	4.0
	Rod #2	R _{exp}	0.0073	0.0065	0.0060
		Bu	5.75	5.15	4.79
	Rod #3	R _{exp}	0.0071	0.0061	0.0059
		Bu	5.58	4.9	4.7

Bu : GWd/MTU

4. DISCUSSION

In the gamma scanning for UO₂ in this study, gamma peaks of Eu-154 were not found due to a low irradiation for the fuel capsules. The peaks of Cs-134 and Cs-137, therefore, were used.

Most papers start with an equation such as Eq.(1) to obtain the activity ratio($N_{134}\lambda_{134}/N_{137}\lambda_{137}$) from a gamma scanning. But few papers have explained how to calibrate a energy efficiency(ϵ) in detail. It is assumed that a calibration of a energy efficiency would be established by using several reference gamma sources in advance or a gamma isotope emitting several gamma rays such as Cs-134. For a calibration of a energy efficiency with Cs-134, it was a difficult when using the gamma counts because all the energy peaks, except for 605 keV and 796 keV, were very low.

In this study, it is proposed that the value($N\epsilon$) for Cs-134 is obtained at 662 keV without knowing each value, N and ϵ , independently as mentioned in the above section. Finally, the atomic ratio of N_{134}/N_{137} was obtained. This atomic ratio can be compared to the calculated result from the ORIGEN-ARP to obtain a burnup.

Before the capsule was irradiated, the HANAFMS was used to estimate the linear power and the burnup for a safe irradiation condition[5]. This code is the application program for all the irradiation holes in the HANARO reactor as well as for the core calculation, which consists of the WIMS/VENTURE code. 3-D geometry construction of this code for a capsule in a hole is only one cell due to the minimum dimensions which cover the whole length of the fuel rig and the diameter of the hole.

The values of the average burnup from this code, therefore, were 5.9 GWd/MTU for 02F-11K and 5.6 GWd/MTU for 03F-05K, respectively. The burnup from the gamma scanning would be lower than that from the HANAFMS code by 10%, which would be due to the improper library of the ORIGEN-ARP code if the data of the HANAFMS code is correct. Neutron cross section data in ORIGEN-ARP that we used in this study was a natural fueled CANDU library. This probably causes an error because of the absence of a library for the hole in the HANARO reactor in the code. Thus, a construction of the relevant libraries in the code is very important as shown in Fig.6.

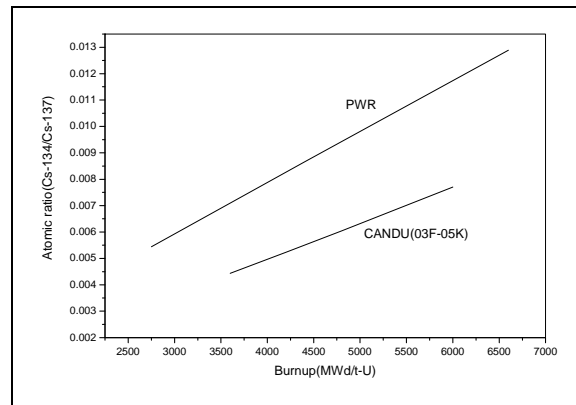


Fig. 6. Difference of the atomic ratio with the libraries in the ORIGEN-ARP code.

In the figure, depending upon the libraries, the same atomic ratio creates different burnup values by about two times. It is related to the neutron spectrum under an irradiation. Fig.7 shows the neutron spectrum of three types of reactors. It is assumed that the neutron spectrum of the HANARO research reactor is softer than those of the CANDU and PWR reactors based on a consideration of the library in the ORIGEN-ARP code.

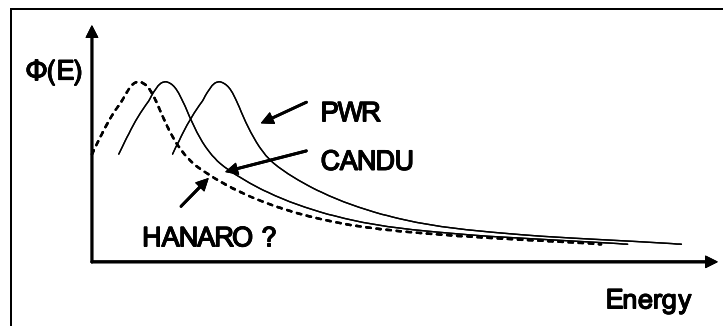


Fig. 7. The neutron spectrum for each reactor type.

But it is hard to say which one is the correct burnup between the values from the gamma scanning and that from the HANAFMS code. We need to undertake more verifications and we have to compare the results among the code calculation, the gamma scanning and the chemical analysis.

5. CONCLUSIONS

We started fuel capsule irradiations in the HANARO research reactor a few years ago. the Burnups of the fuel have been obtained from HANAFMS, but the results need to be verified. We tried to verify the code calculation by using a gamma scanning. The burnup(39.5 GWd/MTU) for the spent PWR fuel from a gamma scanning agreed with the declared burnup(40 GWd/MTU) following a setting up of the appropriate library in the ORIGEN-ARP code. Fuel capsules(02F-11K, 03F-05K) containing three 3 UO₂ fuel rigs were irradiated with a different linear power history in the HANARO research reactor for 54 days and 60 days, respectively. Gamma scanings were performed to obtain the Cs-134 and Cs-137 peaks for a burnup calculation. The atomic ratio would be better than the activity ratio in the case of a reduction of the procedures for a energy efficiency calibration. The atomic ratio of Cs-134/Cs-137 from the gamma scanings were compared to that from the ORIGEN-ARP code calculation. 5.1 GWd/MTU for the 02F-11K and 4.8 GWd/MTU for the 03F-05K were obtained. These results were lower than those of the core calculation code(HANAFMS) by 15% due to an inappropriate library in the ORIGEN-ARP.

ACKNOWLEDGEMENTS

This work has been supported by the Department of Irradiation Test for Fuel and Material and we deeply appreciate it.

REFERENCES

- [1] I.MATSSON, B.GRAPENGIESSER, "Development in Gamma Scanning of Irradiated Nuclear Fuel.", Applied Radiation and Isotopes, Vol.48, No.10-12, (1997) 1289-1298
- [2] J.R.PHILLIPS, T.R.BEMENT, et al., "Non-destructive Verification of Relative Burnup Values and Cooling Times of Irradiated MTR Fuel Elements", Los Alamos Scientific Laboratory, LA-7949-MS(1979).
- [3] KH.HADDAD, "Burnup effect on Nb-95/Zr-95 ratio-cooling time correlation.", J.Nucl.Mat.,345 (2005)86-88
- [4] MASOOD IQBAL, T.Mehmood, S.K.Ayazuddin, A.Salahuddin, S.Pervez, "A comparative study to investigate burnup in research reactor fuel using two independent experimental methods.", Annals of Nuclear Energy, 28 (2001)1733-1744
- [5] J.D.CHEN, R.B.LYPKA, D.G.ZETARUK, D.G. BOASE, "Non-Destructive Determination of Burnup by Gamma-scanning: An Assessment of Ce-134/Cs-137 Activity Ratio as a Fission Monitor in CANDU Fuels", AECL-6192(1978).
- [6] S.M.BOWMAN, L.C.LEAL, "ORIGEN-ARP: Automatic Rapid Process for Spent Fuel Depletion, Decay, and Source Term Analysis", Oak ridge national laboratory, NUREG/CR-0200,Rev. 6(2000)
- [7] I.C.GAULD, O.W.HERMANN, R.M.WESTFALL, "ORIGEN-S: Scale System Module to Calculate Fuel Depletion, Actinide Transmutation, Fission Product Buildup and Decay, and Associated Radiation Source Terms", Oak ridge national laboratory, NUREG/CR-0200,Rev. 7(2002)
- [8] B.G.KIM, et al., " Design Verification Test Plan and Safety Analysis of Instrumented Capsule (02F-11K) for Nuclear Fuel Irradiation in HANARO", KAERI/TR-2415, (2003).

BURNUP DETERMINATION IN 20% ENRICHMENT URANIUM COMPOUNDS

C, Devida, E. Gautier, D. Gil, A. Stankevicius
National Atomic Energy Commission – Argentina

ABSTRACT

In the hot-cells of the Radiochemical Laboratory (LFR) facility a series of dissolutions of MTR irradiated fuel was performed and determined its isotopic composition of Uranium, Plutonium and neodymium (this last as burnup monitor), by the thermal ionization mass spectrometry (TIMS). It is concluded that this technique of burnup measurement is powerful and accurate when properly applied, and permit to validate the calculation codes when isotopic dissolution is performed.

Principle

The burnup of the spent fuel is a very important parameter that indicates the energy produced by the fuel during irradiation in the reactor. It is defined as the percentage of the fissioned heavy metals (HM) with respect to the total preirradiated heavy metal; this is determined by measuring of the ^{148}Nd amount. ^{148}Nd is the most representative fission product as burnup indicator. The ^{148}Nd is selected for this analysis because it is a stable final fission product, has well known fission yield, and low absorption cross section for thermal neutrons, then the concentration of this nuclide is proportional to the total fission's number occurred, from which the burnup may be calculated.

Then, the burnup for uranium fuels is calculated by the following equation:

$$\text{Bu}\% = \frac{\text{number of fissioned atoms}}{\text{number of preirradiated heavy metals atoms}} \cdot 100$$

Where

$$\text{Number of fissioned atoms} = \frac{\text{number of } ^{148}\text{Nd atoms}}{^{148}\text{Nd yield}}$$

$$^{148}\text{Nd yield} = 0.017$$

and

Number of preirradiated HM atoms = remain uranium + fissioned uranium + activated uranium

Then,

$$Bu\% = \frac{\frac{^{148}\text{Nd atoms}}{\text{Yield}_{^{148}\text{Nd}}} \cdot 100}{\frac{\text{HM atoms}}{\text{Yield}_{^{148}\text{Nd}}}} = \frac{\frac{^{148}\text{Nd atoms}}{\text{Yield}_{^{148}\text{Nd}}}}{\frac{^{148}\text{Nd atoms}}{\text{Yield}_{^{148}\text{Nd}}} + U_{\text{total atoms}} + Pu_{\text{total atoms}}} \cdot 100$$

Since the determination is done from an aliquot of the dissolution of the fuel, it is only necessary to take into account the relative concentration of the ^{148}Nd and the total heavy metals in the dissolution.

$$Bu(\%) = \frac{\frac{g(^{148}\text{Nd})/g(\text{solution})}{148(g/\text{mol}) \cdot 0.017}}{\frac{g(^{148}\text{Nd})/g(\text{solution})}{148g\text{ mol}^{-1} \cdot 0.017} + \frac{g(U_{\text{total}} + Pu_{\text{total}})/g(\text{solution})}{238g\text{ mol}^{-1}}} \cdot 100$$

Procedure

The process flow sheet (Fig. 1) summarizes the fuel burnup material processing, in the LFR.

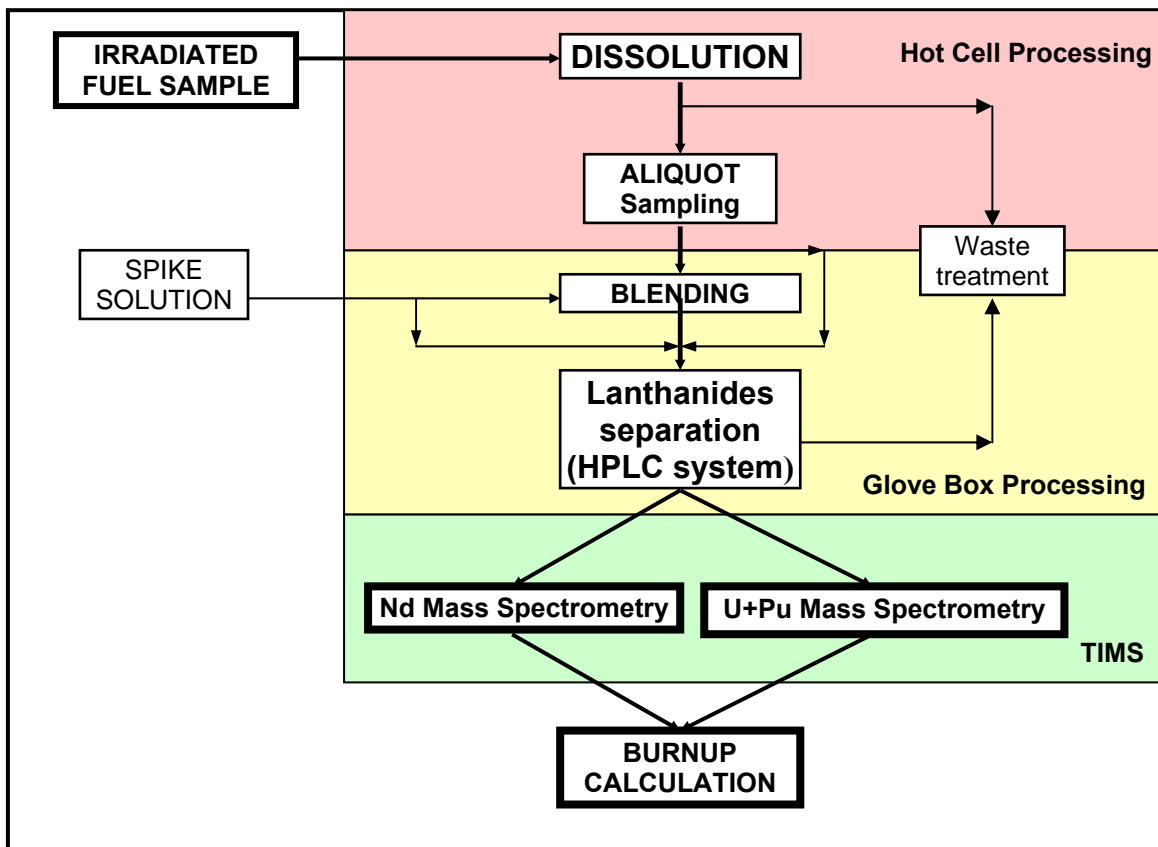


Fig 1 – Normal Processing of Material in the LFR

Nuclear fuel samples were dissolved in 10 mL 7M HNO₃, 0.5 mL HCl and 0.5 mL HF in a Hot Cell LFR facility by refluxing and the resulting solution was diluted with 1 M HNO₃. A small aliquot containing about 100 µg of fuel per gram of solution were transferred into the Glove-Box for further dilution, spiking and chromatographic separation of lanthanides and actinides.

The high performance liquid chromatography (HPLC) system is installed in the Glove-Box. The high pressure chromatographic pump, the post column reactor (PCR) and the UV-visible detector are mounted outside the box. The injection sample valve with a 100 µl sample loop, the switching valve for fraction collection, and the analytical column were placed inside. The column is packed with a C-18 reversed phase on a suitable support.

The separation of actinides has not been performed up to now, and due to it, an isobaric interference at masses 238 (U-Pu), decreases the confidence on the Pu results.

By means of this chromatographic technique it was possible to separate neodymium (as burnup monitor) from the other fission products, avoiding the isobaric interferences during the mass spectrometric analysis.

Fig 2 shows the separation of standards of natural lanthanides by the HPLC system, while

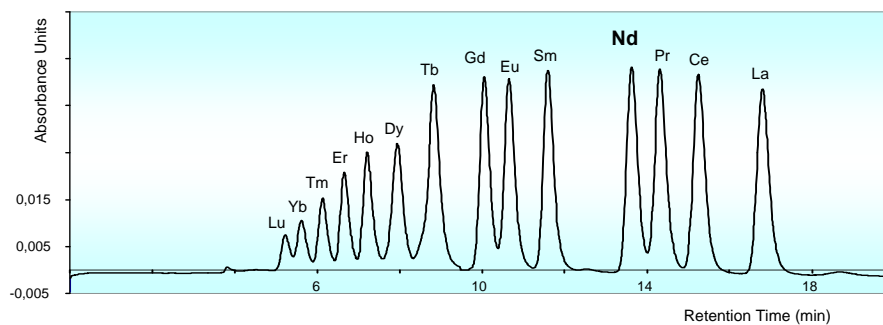


Fig 2 – Gradient Separation of the Lanthanides chromatogram

Fig. 3 shows the separation of U+Pu and Nd in a real sample by the same technique

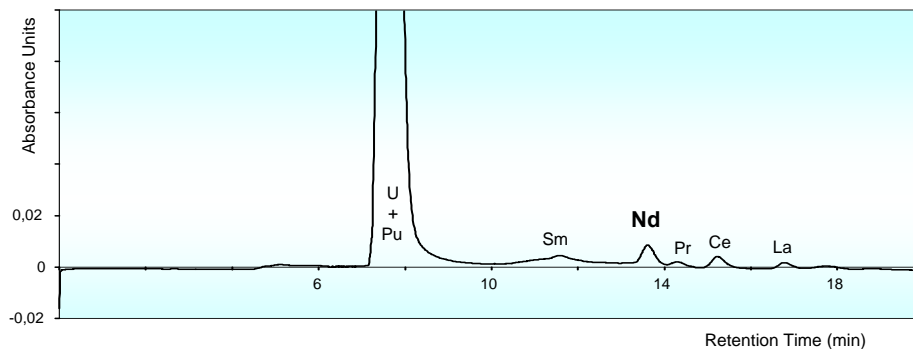


Fig 3 – Gradient Separation of Lanthanide Fission Products in Irradiated U-Si MTR Fuel

Both collected fractions (neodymium and also U+Pu) were loaded on different rhenium filaments for the subsequent thermal ionization mass spectrometry (TIMS) isotopic analysis.

Other samples, previous to the chromatographic run, were blended with known amounts of certified spikes of enriched ^{233}U and ^{150}Nd solutions. These isotopes are not present in significant quantities in the spent fuel. Due to isotopic dilution of the spikes produced by the isotopes present in the sample, it is possible to calculate the actual ^{148}Nd and U concentration, of the spent fuel sample.

Results and Discussion

As an approach of the burn up determination, the depletion of ^{235}U in the spent fuels was measured. In *table 1* it is possible to compare the isotopic composition of fresh and some samples of the two irradiated fuels.

Sample	U (% w)			Pu (% w)			
	^{234}U	^{235}U	^{236}U	^{239}Pu	^{240}Pu	^{241}Pu	^{242}Pu
Fresh Fuel	0.13	19.74	<0.020	-	-	-	-
A-10	0.11	15.44	1.02	88.7	9.3	1.9	0.1
A-11	0.11	13.89	1.29	88.3	11.1	2.4	0.2
A-20	0.11	14.83	1.12	87.1	10.1	2.6	0.2
B-29	0.11	7.27	2.39	70.8	18.7	8.9	1.6
B-30	0.12	7.78	2.28	72.1	18.8	7.8	1.3
B-31	0.12	11.51	1.61	82.4	13.4	4.0	<0.2

Table 1 – Isotopic composition of different samples

This work shows the capability of the LFR facility for destructive assays in burnup determinations of irradiated nuclear fuels.

In the near future HPLC-ICP-MS on-line coupling will be applied for the separation and determination of actinides and lanthanides. This method is optimized in the LFR to be used with spent nuclear fuel solutions for burnup determination.

Conclusions

- With these techniques it was possible to obtain the first spent nuclear fuel chemistry analysis in the LFR.

- These results were successful and permit a real personal training of LFR staff in this field.
- The LFR showed in this way their capability for the radiochemical spent nuclear fuel analysis.

The chemistry of spent nuclear fuel from x-ray absorption spectroscopy

Jeffrey A. Fortner, A. Jeremy Kropf, and James C. Cunnane

ARGONNE NATIONAL LABORATORY
9700 S. Cass Ave., Argonne, IL 60439 USA
Chemical Engineering Division

ABSTRACT

Present and future nuclear fuel cycles will require an understanding of the complex chemistry of trace fission products and transuranium actinides in spent nuclear fuel (SNF). Because of the unique analytical challenges presented by SNF to the materials scientist, many of its fundamental physical and chemical properties remain poorly understood, especially on the microscopic scale. Such an understanding of the chemical states of radionuclides in SNF would benefit development of technologies for fuel monitoring, fuel performance improvement and modeling, fuel reprocessing, and spent fuel storage and disposal. We have recently demonstrated the use of synchrotron x-ray absorption spectroscopy (XAS) to examine crystal chemical properties of actinides and fission products in extracted specimens of SNF. Information obtained includes oxidation state, chemical bond coordination, and quantitative elemental concentration and distribution. We have also used XAS in a scanning mode to obtain x-ray spectral micrographs with resolution approaching 1 micron. A brief overview of the technique will be presented, along with findings on uranium, plutonium, neptunium, technetium, and molybdenum in commercial PWR SNF specimens.

Research funded by U.S. Department of Energy, Office of Civilian Radioactive Waste Management, under contract W-31-109-ENG-38.

SESSION 3: PIE TECHNIQUES AND APPLICATIONS (II- PART)

Chairpersons

Gerhard Bart (Switzerland)

Y. Goncharenko (Russian Federation)

Distortion Measurement for Fuel Assemblies with Ultrasonic Technique

Xu Yuanhuan, Nie Yong

Research Institute of Nuclear Power Operation, China

ABSTRACT

The paper introduces an applied approach of using ultrasonic technique to measure exactly the bend and torsion of fuel assemblies on nuclear power plant. The ultrasonic technique with multi-channels data acquisition is used to measure the distance between a side face of Fuel Assembly and the reference plate holding ultrasonic probes position.

The measurement is performed on the road of transferring the fuel assemblies during unloading period. No tools or equipments touch the measured fuel assembly during the measurement process. 16 measure points corresponding to 16 ultrasonic probes are selected in the side face of each fuel assembly measured along the whole length direction. The fuel assembly is free or swing during the measurement with ultrasonic data acquisition. The proper parameter of ultrasonic technique is confirmed to ensure the measure precision.

The profile of each fuel assembly in addition to the bend and the torsion can be obtained through analyzing and calculating the distance result measured at the same time. And the result, the offset between the projection of up plate and one of down plate in the horizontal section of fuel assembly, can guide reloading fuel assembly so that the coordinate position of all of fuel assemblies in the core can be corrected to insert in easily. Only 3~5 minters is needed to measure one fuel assembly. The technique has been applied successfully in China.

1. General

The Fuel Assembly (*FA*) is the best important component located in core of reactor to produce nuclear fission and release the calories. A Fuel Assembly (*FA*) constitutes fuel rods arrayed with 15×15 or 17×17 grid, support framework, top plate, bottom plate and several layers of fixation trellis. Each Fuel Assembly (*FA*) is about 4 meters length.

A distortion will be produced because of the action of fuel assembly surroundings condition like high temperature, high pressure, strong neutron radiation, waterpower vibration, and adjacent rod extrusion. The distortion is usually represented with bend of fuel assembly and torsion of fuel assembly.

The distortion will directly result in the difficulties of reloading fuels and the extension of reloading period. So it is very necessary to know the detailed measurement value of the distortion.

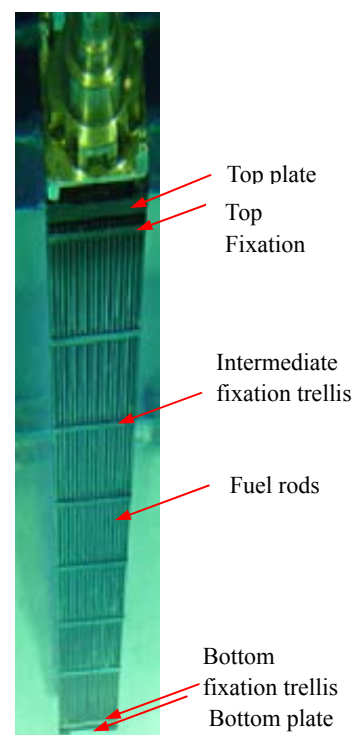


Fig. 1

Here the measurement approach and applied result are introduced using ultrasonic technique to measure exactly the bend and torsion of fuel assemblies on nuclear power plant. The measurement of FA bend is to measure the profile of fuel assembly and the offset between the top plate & bottom plate. The measurement of FA torsion means to measure the torsion between the top plate and bottom plate.

2. Measurement principle

In the normal instance, the top plate and bottom plate locate at the same projection position in the vertical direction. It is easy to load fuel assembly into reactor core grid through controlling the position of top plate. When a fuel assembly holds distortion, the projection of top plate in the vertical direction will not lap over entirely with one of bottom plate and trellis. The distortion results in the difficulty to reload fuel assembly on site.

So if or not the distortion appears, the estimation can be analyzed through measurement of relative position among top plate, bottom plate and intermediate fixation trellis.

The ultrasonic technique is used to measure the horizontal separation from one of side faces of fuel assembly to reference side face (examination side). Select two neighbor side face of fuel assembly, measure each of separation from the top plate, bottom plate, trellis of those selected side face to reference face holding ultrasonic probes position respectively. The results represent the interrelation of the top plate, bottom plate and the trellis. If each of the measured points is located inside a line which is parallel to calibration line, the Fuel Assembly will be considered as no distortion. When some points are out of the line, the distortion will appear in the corresponding positions from the points. The offset outside the line represents the distortion value. All the offset can give the profile of the fuel assembly.

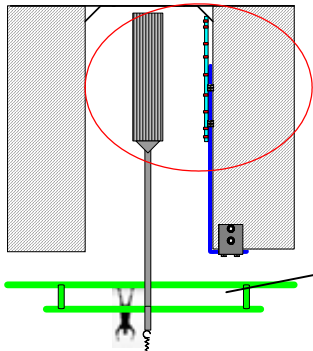
The ultrasonic technique with multi-channels data acquisition is used to measure the distance between a side face of Fuel Assembly and the reference plate holding ultrasonic probes position.

3. Measure system and measure mode

The measurement is performed on the road of transferring the fuel assemblies during unloading period. No tools or equipments touch the measured fuel assembly during the measurement process. 16 measure points corresponding to 16 ultrasonic probes are selected in the side face of each fuel assembly measured along the whole length direction. The fuel assembly is free or swings during the measurement with ultrasonic data acquisition. The proper parameter of ultrasonic technique is confirmed to ensure the measure precision.

The main measure system consists of:

- Mechanical measure tool
- Tomoscan-III 16 channels ultrasonic system
- Ultrasonic probe
- Data acquisition and analysis system

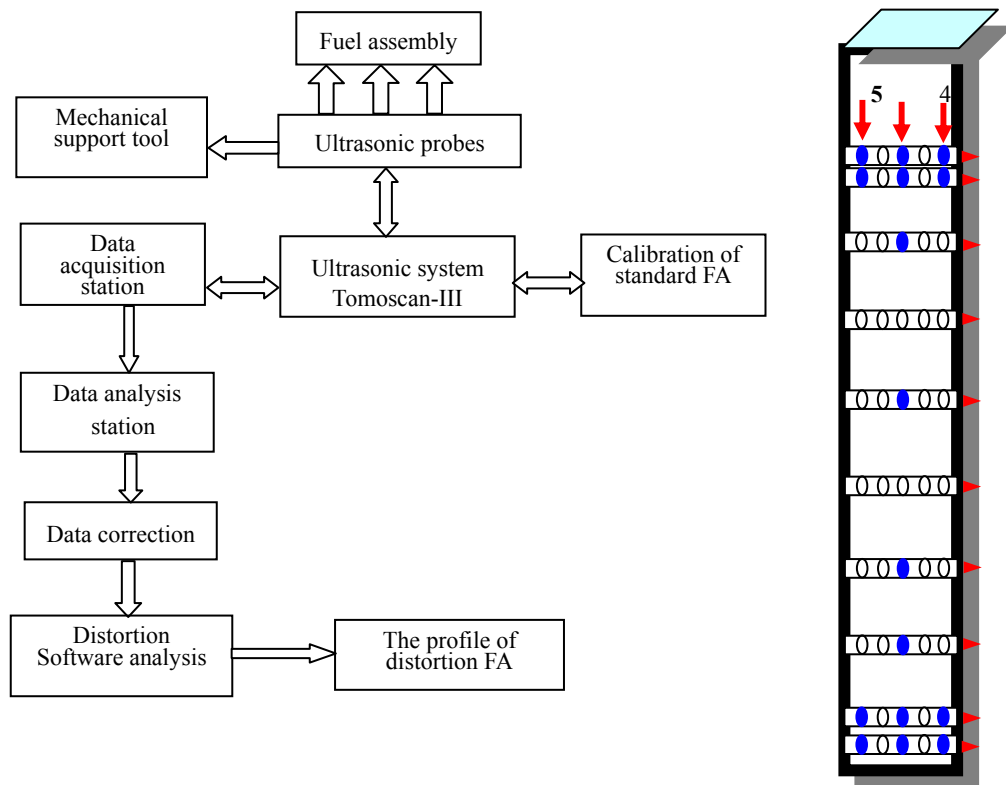


Mechanical measure tool



Ultrasonic probes

The chart of interrelation:



The mechanical measurement system is assembled beside the poolside of strobe channel. During unloading the FAs, the measurement is carried out on the road of transferring the fuel assemblies from reactor vessel to spent pool. While the fuel assemblies reach the strobe channel, fire the ultrasonic data acquisition system. After finishing the acquisition with several minutes later, continue moving the FA.

The measurement ultrasonic probes are fixed in the mechanical tool with a serial array. The center array probes are main measurement probes, the other probes provide the secondary data. The UT probe is immersion mode due to the water couplant.

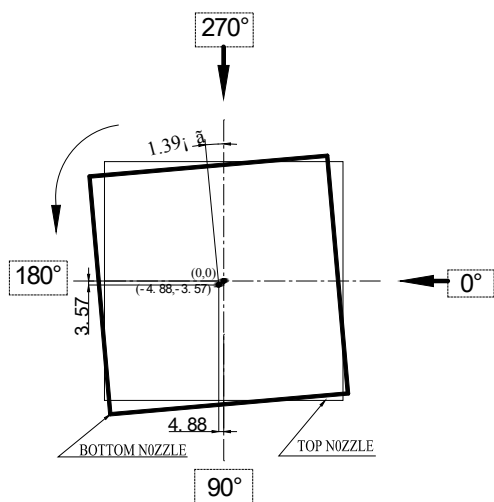
The TOMOSCAN-III multi-channels ultrasonic acquisition system is used with all channels. Usually the UT channels should be 16 channels at least, because more measurement points can be measured according to the available channels, so the results is more detail. The inner pulse mode of the encoder is used to fire all probes in a cycle at a very short time.

4. Calibration

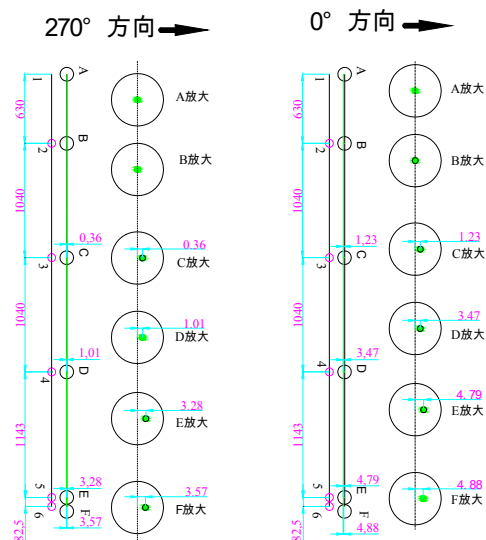
A calibration is carried out before measuring the fuel assemblies formally. A standard fuel assembly with no distortion is used to set up a reference basis. In the actual measurement, the measure result will be compared with the calibration basis. The calibration can adjust the ultrasonic probe delay of each measure point and set up a reference line. The calibration should be carried out while the standard fuel assembly is almost actionless/stock-still in the water.

5. Data process

The result obtained from the ultrasonic probe will be corrected with a special software through comparing with calibration data. The process software can set up a basis for each fuel assembly and can analyze and calculate the offset of each of measured point. The software can give the basic result of bend and the torsion value directly and profile of the fuel assembly like as:



projection of up plate and one of down plate in the horizontal section of fuel assembly



Profile of the fuel assembly

6. Conclusion

A effective method can be obtained with ultrasonic technique to measure the distortion of fuel assembly. The profile of each fuel assembly in addition to the bend and the torsion can be obtained through analyzing and calculating the distance result measured at the same time. And the result, the offset between the projection of up plate and one of down plate in the horizontal section of fuel assembly, can guide reloading fuel assembly so that the coordinate position of all of fuel assemblies in the core can be corrected to insert in easily. Only 3~5 minters is needed to measure one fuel assembly. The technique has been applied successfully on-site in China.

LWR FUEL GAS CHARACTERIZATION AT CEA CADARACHE LECA-STAR HOT LABORATORY

J. NOIROT, C. GONNIER, L. DESGRANGES, Y. PONTILLON, J. LAMONTAGNE

DEN/DEC/SA3C, CEA Cadarache

13108 Saint Paul Lez Durance, France

jean.noirot@cea.fr

ABSTRACT

The aim to improve LWR fuel behaviour led CEA to improve its PIE capacities in term of test devices and characterization techniques in the shielded hot cells of the LECA-STAR facility, located in Cadarache. A presentation of these capacities is made, focusing on gas characterization :

- annealing test devices used for transient simulations. These devices are test facilities allowing to simulate a very large range of conditions (temperature, atmosphere, pressure etc).
- characterization techniques :
 - o optical microscopy, for microstructure characterizations on polished samples
 - o scanning electron microscopy (SEM) used both on polished samples and on fractographs,
 - o Electron Probe Micro-Analyzer (EPMA) for quantitative elementary analysis and elementary mappings,
 - o Secondary Ion Mass Spectrometer (SIMS), for isotopic analysis, mapping depth profiles and gas measurements.

It shows an overview of their main applications for the study of fuel behaviour under nominal operating conditions but also under simulated accidental conditions and storage conditions. Two detailed examples of the use of these techniques working together on the same samples, are then presented, focusing on fission gas characterizations.

The first one is a 72 GW.d.t⁻¹ high burnup UO₂ PWR fuel for which detailed characterizations have been performed before and after a LOCA type condition annealing test.

The second one is a 35 GW.d.t⁻¹ UO₂ PWR fuel for which these characterizations have been done before and after a ramp test at 100 W.cm⁻¹.min⁻¹ up to a 90 s maximum power hold time at 520 W.cm⁻¹.

In both cases, the complementarities of these various techniques show the interest of such detailed characterizations.

1. INTRODUCTION

R&D work about fuel is conducted in order to investigate fuel properties and fuel behaviour. This work covers various domains such as :

- Nominal operating conditions : within this framework, studies deal with burn-up extension of standard UO₂ and MOX fuels, advanced fuel microstructures, fuel management schemes, new cladding materials,..
- Off-normal conditions and accidental conditions (improvement of our knowledge and studies of the impact of fuel evolution on safety aspects).
- Storage conditions (normal and off-normal situations).

Several domains can be investigated through hot cell experimentation and characterization. Therefore, the Fuel Studies Department (DEC), at CEA Cadarache Centre, operates or will operate experimental tools in order to investigate the different domains. Such large domains require several dedicated test facilities (annealing test devices [1]) and characterization techniques in the shielded cells of the LECA-STAR hot laboratory.

Generally speaking, investigations concern fuel coming from power reactors or experimental reactors. The first steps are Non Destructive Examinations (NDE : Visual examination, Gamma scanning, Eddy current measurement, Rod length and Diameter measurement, Zirconia thickness measurement, X-ray radiography).

Rod puncturing is then performed in order to determine and quantify gases within the cladding. A double depressurisation technique allows to evaluate the “free” volume within the cladding and therefore, the internal pressure of the rod [2]. The large range of “free volume” and “gas releases” (ranging from few hundreds cubic millimetres to few hundreds cubic centimetres) required several specific equipments.

Then the fuel rod is cut in order to provide samples to destructive examinations (optical microscopy, SEM, EPMA, SIMS, XRD) and to the test facilities. These two aspects will be described in the following sections.

In some cases, fuel spans are also used for fuel re-fabrication in order to perform in-pile investigation in specific reactors. A recent improvement of the equipment (the “CORALIE” bench) allows the re-fabrication of instrumented rods (with a fuel centreline thermocouple and a pressure transducer).

Fission gas behaviour is a key issue for global fuel behaviour, both during normal operation and during off normal situations. We will focus here on the way we investigate this gas behaviour in our facility.

In order to underline the complementarities of the different equipments, two examples will be finally described in the paper, one dealing with $72 \text{ GW.d.t}^{-1} \text{ UO}_2$ fuel behaviour under LOCA type conditions, the second one with $35 \text{ GW.d.t}^{-1} \text{ UO}_2$ fuel behaviour during a power ramp test.

2. ANNEALING TESTS DEVICES

Fuel qualification, improvement of our knowledge about fuel behaviour, and fuel testing under various conditions, require a set of furnaces which are already used or about to be used. The main characteristics of these furnaces strongly depend on the experimental objectives.

2.1. MERARG furnace

The “MERARG” facility capacities gives us the possibility to fulfil different goals :

- Fuel gas distribution characterizations
- Investigation of the mechanisms leading to fission gas release at high temperature
- Simulation of off normal irradiation conditions

This is done by operating this device in various chosen conditions :

- The gas distribution within the fuel (inter/intra granular position) is evaluated by performing Adagio type experiment [3]. It consists in an oxidation of the grain boundaries in order to measure the releases of the gas in inter-granular position, at a relatively low temperature (350 to 400°C). It is usually followed by a total oxidation of the fuel at 1400°C in order to measure the total gas inventory.
- Slow temperature ramps allow to discriminate the release mechanisms at high temperature by measuring the fission gas release versus time and temperature.
- fission gas release under accidental conditions such as LOCA or RIA can also be partially simulated with faster temperature increase.

The “MERARG” facility, presented in

Fig. 1, allows to investigate fission gas behaviour. It consists in a high frequency (50 kHz) induction furnace, located in a hot cell, coupled with an on-line gas release measurement.

The furnace consists in a metallic crucible (on the centreline of the coil) in which the fuel sample is located. It can be Pt crucible for tests with air (up to 1400 °C) or Mo /W crucibles for high temperature tests under inert atmosphere (up to fuel melting). Between the crucible and the coil, a quartz tube allows to keep the system tight and to collect all the released gases.

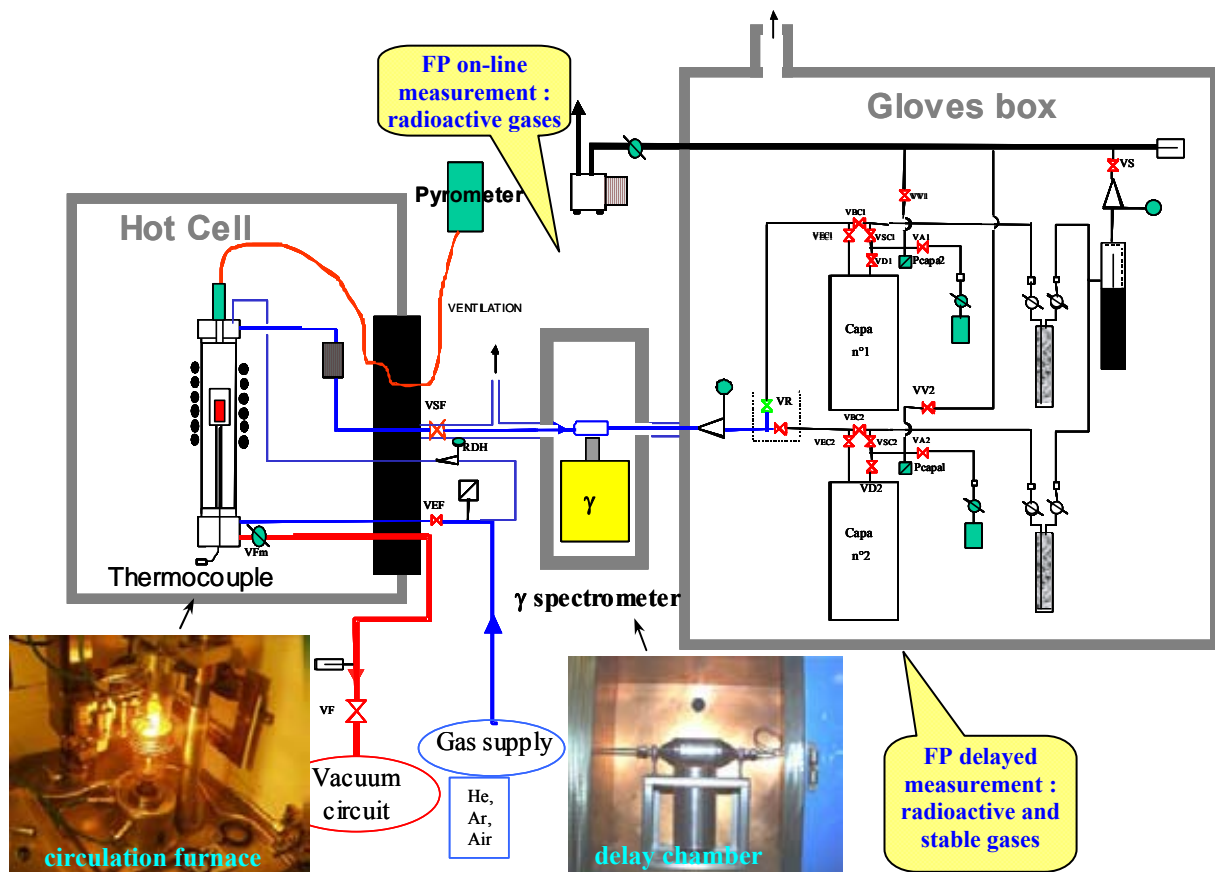


Fig. 1 : MERARG facility

A sweeping gas carries the released gases out of the hot cell so that it can be analysed in a glove box located behind the cell. Sweeping gas can be He for fission gas analysis or Argon for He release analysis.

Gas is stored in several collecting tanks, allowing a sequential storage of the experimental gas. Gas analysis is usually performed by the mean of gamma spectrometry measurement (in a counting chamber) that allows to monitor ^{85}Kr releases or other gas isotopes (such as ^{133}Xe for fresh re-irradiated fuel).

In order to also analyse stable gases, a micro gas-chromatograph will be installed on the outlet line. This apparatus will be particularly used to quantify He release or gases resulting from fuel thermal decomposition (carbide and nitride fuel for example).

Electrical power is high enough to reach $300\text{ }^{\circ}\text{C}\cdot\text{s}^{-1}$. On the other hand, the power control system has been adapted to allow low heat up rates ($0.05\text{ }^{\circ}\text{C}\cdot\text{s}^{-1}$).

Instrumentation used to monitor the experiment consists in one high temperature thermocouple, one optical pyrometer, two (inlet and outlet) flow-metres, one pressure transducer.

In order to enlarge the experimental capabilities, a gamma spectrometer will be installed in sight of the fuel. This equipment will allow to measure FP release from the fuel during thermal transient : cesium, iodine (in the case of test on re-irradiated fuel), ruthenium (during test with air).

The experimental capability is about 50 tests a year.

2.2. MEXIICO Furnace.

The MERARG facility allows to test fuel only at atmospheric pressure. It is proved that stresses within the fuel have an impact on fission gas behaviour [4] [5] (bubble growth, fuel swelling, fission gas release,...). These situations are particularly encountered during thermal transients such as power ramp or RIA which could lead to stresses up to 300 MPa. In order to investigate the impact of stresses

on FGR, decision was made to install a high pressure furnace in a hot cell : the MEXIICO furnace. Restraint state is then simulated by the mean of Argon at high pressure.

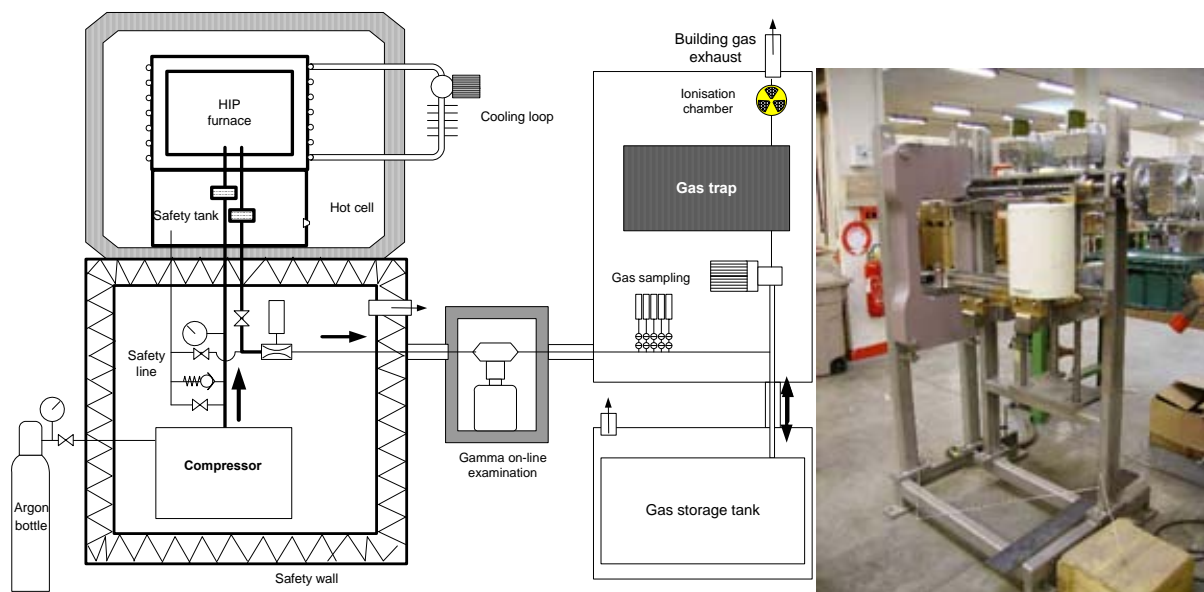


Fig. 2 : Schematic diagram of the future high pressure experimental loop ; view of the MEXIICO furnace (white colour) and its handling devices.

Nevertheless, technical constraints led to reduce the experimental capabilities to the following domain :

Maximum temperature / pressure : 1600 °C / 160 MPa (design : 1800 °C / 180 MPa) ; Maximum heat up rate : 1 °C.s⁻¹.

The standard fuel sample is a fuel pellet (a few grams).

Heating is provided by a resistor (molybdenum or graphite) installed within the pressure vessel. Thermal insulation is made with several molybdenum and graphite screens between the resistor and the pressure vessel.

The measuring system is a gamma spectrometer located on the outlet line. Argon pressurizing gas is used to transport the information in the outlet line. Gas is finally stored in a low pressure tank of about 2 m³ (initially under vacuum).

The main part of the components : the 2 steps of compressors, the safety valves, the pressure control system, the experimental filters,... are located out-of the cell. The only equipments located in the cell are the pressure vessel and the high efficiency safety filter. Pressure and temperature are separately controlled, allowing various type of experimental scenario.

The apparatus will be delivered for testing at the end of November 2006, first experiment with fuel is planned at the beginning of 2008.

2.3. VERDON facility

The two previous facilities are mainly dedicated to fission gas release measurement. There is a need to get information about FP release (not only gas) in the context of severe accident studies. Complementary to integral experiment such as Phebus FP program [6], several separate effect experiments were run in order to get detailed information about FP releases depending on type of fuel (MOX or UO₂), atmosphere (oxidizing or not), presence of control rod material,... Such experiments were performed particularly in the Vercors Facility which has been shut down in 2002. In order to enlarge the data base, a new facility "Verdon" will be built in the LECA-STAR hot cells. As in the Vercors experiments, the Verdon facility will consist in a high frequency furnace allowing to reach fuel melting temperature under representative conditions (steam, air , hydrogen, eventually neutral atmosphere). The characterization of the FP releases will be done by the mean of specific

instrumentations : filters to discriminate vapours and aerosols, impactors for particle sizing, thermal gradient tubes (TGT) to discriminate the gaseous species by the condensation temperature, iodine trapping and/or ruthenium trapping device, gas capacity to measure noble gases,....

Several gamma spectrometers will be used for the on-line monitoring of the experiment : one focusing on the experimental fuel, one focusing on the filter or TGT located at the furnace outlet, one focusing on the gas tank, and one focusing on the trapping device. Tests will be run with irradiated fuel but also with re-irradiated samples in order to get information about short half-life FP behaviour and to increase the number of detectable FP.

As far as the furnace is concerned, it comprises, from the inside to the outside, the crucible containing the sample, a stack of dense zirconia and/or hafnia sleeves. The corresponding external channel receives the susceptor, a double-layer heat insulator (porous zirconia and hafnia), the quartz tube constituting the furnace chamber, and the inductor.

This new facility will take benefit of the Vercors feedback, using an improved design of the loop which will allow more tests per year, but also an improved shielding allowing to perform future tests on new fuel type and fuel of new reactor type. (improved gamma shielding and neutron shielding). As in the Vercors facility, tests will be run with various fuel geometry : "rod geometry" or "debris bed". The maximum length in rod geometry is 10 cm but the standard tests will be run with only one fuel pellet.

The technology of the furnace and the circuit are rather complex. The experimental capabilities depend on the type of test : it is foreseen to perform 3 test campaigns a year ; one campaign can be one test in the case of a circuit heavily instrumented or 3 tests in the case of simplified tests (instrumentation reduced to one filter downstream the furnace). In the last type of test, it is foreseen to use 3 samples coming from the same re-irradiated segment in order to have very comparable fuel samples for the 3 tests.

The four first tests will be performed within the framework of the "Source Term Project". One will be devoted to high burn-up UO₂ fuel, two to MOX fuel, and one to UO₂ fuel in case of air ingress

2.4. Other furnaces

In addition to the annealing test devices described in this paper, and used for fission gases studies, another set of furnaces is dedicated to fuel behaviour evaluation under transport and storage conditions [7]. They are operating at rather low temperature (200 to 500 °C) but on long periods of time :

- Fuel behaviour under standard storage conditions is studied in the so called "Esterel" furnace. Short rods, with various internal pressure are heated at 380 °C in an Argon atmosphere. They are periodically unloaded for NDE, and furnace atmosphere is also periodically analysed in order to detect a possible clad failure (helium detection). Rods will be definitively unloaded for destructive examinations at end 2007 and 2008 (after about 1000 effective heating days). The main objectives concern helium behaviour as well as fuel and cladding evolution.

- In case of incidental conditions with air ingress in a dry storage container, fuel of defective rods could oxidize. Two types of experiments are run :

- Oxidation kinetics is studied at 200 °C under air by the means of regular sample weightings and micro characterization. Note that during the oxidation process, weight evolution is not only due to oxidation but also to fission gas releases that make more complicated the interpretations.

- Crocodile is an "integral test" on a defective short rod. Maximum temperature of the furnace is 500 °C, atmosphere is controlled (inert gas, air, air with pollutant such as NO_x,...) at 1 bar. Rod is located in a quartz tube with filters at both ends. A visual bench allows examinations, oxidation kinetics is characterized by weightings. The objectives are to analyse oxidation process versus gas atmosphere, type of fuel, temperature, but also size and shape of the defect.

3. CHARACTERIZATION TECHNIQUES

Within the framework of a huge renovation of the LECA-STAR facility, the small lead cells that were used for most of the work on small samples, such as the optical microscopy, the annealing tests and the sample preparation for microanalysis, have been closed and are being decommissioned. This was

decided because of earthquake resistance considerations. Therefore, we had to move to other hot cells and took this opportunity to try to improve our devices.

For ceramography and metallography, this led to improve :

- the impregnation / embedding device. With the new device, we can use both epoxy resins and low melting point metallic alloys (these last ones being mainly used for SEM, EPMA and SIMS examinations for a good electrical charge evacuation) with a sequence first under vacuum then under pressures up to 0.5 MPa. This device is also used in the density measurement processes, for liquid penetration in open porosity.
- the grinding and polishing, with the possibility to prepare 3 samples at the same time (one with a 50 mm diameter and two with a 25 mm diameter embedding holder).
- the optical microscope with a Vickers device is a LEICA DMR modified for hot cell operation with the help of Defi System. A special care was taken to design a sample holder allowing to keep the sample orientation whatever the sample manipulation could be. This was done together with an evolution of the image data base and acquisition software so that the location of the detailed area and the acquisition conditions are stored together with the image itself. It is used together with image analysis and chemical etchings to evaluate the microstructural changes in the fuel: cracks, gap evolution, bubbles formation, grains and grain boundaries evolutions, precipitations, clad corrosions, hydrides formation in the cladding, dishing and chamfers evolutions etc.

Our Scanning Electron Microscope (SEM) is a homely shielded Philips XL30 with a Microspec WDX detector, a SIS ADDA system for 4096×4096 pixels image acquisition, a KE developments Centaurus Back Scattered Electron (BSE) detector, and a SIS image analysis software. It is used both on polished samples and on fractographs for microstructural, precipitates and bubbles characterization. Its work is closely linked to the optical microscopy, the EPMA and the SIMS work.

The Electron Probe Micro-Analyzer (EPMA) is a shielded Camebax microbeam (CAMECA), with a SAMx acquisition system. Part of its electronic has just been replaced by a SAMx MASH system. It is used both for local quantitative analysis and for elementary mappings. One of the main particularities of EPMA for fission gas measurement is that it is mainly used to detect the existence and amplitude of gas precipitation into bubbles. Indeed, as the EPMA measurement only involves a ~0.6 μm thick layer, and as the gas that is precipitated into bubbles is released when these bubbles are opened during the preparation, part of the gas cannot be measured. This part depends on the amount of gas in the bubbles and on the size of the bubbles [8] [9]. The larger the bubbles, the higher the lack in the measurement. These lacks in the measurements are then first a confirmation of a gas bubble formation which, usually was previously detected by ceramography, often after chemical etching. It can nevertheless be the sign of true gas release, but it then needs a confrontation with the SEM and SIMS results. Of course EPMA is not used only for gas measurement and it can be used for local burnup determination, fission products and actinides movements characterization etc. [10] [11] [12].

The Secondary Ion Mass Spectrometer (SIMS) is a CAMECA IMS 6f. Its installation was presented at the last equivalent meeting in 2001 [13]. Some work using this SIMS have already been published [14] [15] [16] [17] [18] [19] [20] [21] [9]. Applications on volatile elements, low abundant elements, isotopic analysis and gas measurements are quite valuable.

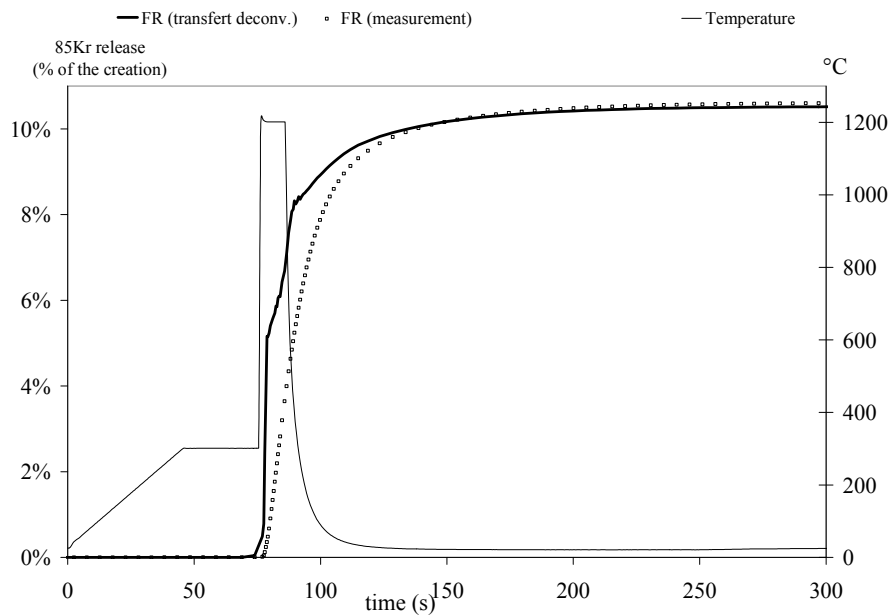
4. APPLICATION EXAMPLES

The examples chosen hereafter have been performed within the framework of a collaboration between Areva, Electricité de France (EDF) and CEA.

4.1. First application example: fuel behaviour under LOCA type conditions

With the objective to allow increasing burnup for nuclear power plant fuel, very high burnup fuels were examined both for MOX fuel and for UO₂ fuels. Moreover, simulated LOCA type condition tests

characterizations performed before the test (Gaspard program [22]). As an example, a thermal transient test was performed on a $71.8 \text{ GW.d.t}^{-1} \text{ UO}_2$ fuel. At this burnup, the fission gas release was 5.2 % of the created gases. During this transient, a $20 \text{ }^\circ\text{C.s}^{-1}$ temperature increase rate led to a maximal temperature of $1200 \text{ }^\circ\text{C}$ that was held for 10 min. During this test, the fission gas release of ^{85}Kr was measured and the result of these measurements are given on Fig. 3. The overall release during the test was 11.6 % of the created ^{85}Kr . Fig.1 shows the temperature profile during the thermal transient, the measured release of ^{85}Kr (cumulative and instantaneous) as well as the result of a transfer deconvolution. This transfer deconvolution takes into account the delays between the release of the gas and its measurement in the spectrometry chamber as well as the dilution in the furnace. This transfer deconvolution results exhibit a few imperfections in case, like here, of high temperature increase rates. The quality obtained for lower increase rate transients is much better. This deconvolution process is one of the points we are working on to improve its accuracy. Nevertheless, it already gives, even in this difficult case, quite valuable information on the events occurring during the test. It first shows that about half of the release occurs very quickly around the end of the temperature increase and that this release is a very short event. This burst release is understood as the release of the gas accumulated in grain boundaries during the PWR base irradiation. It is followed by a much slower event occurring during the $1200 \text{ }^\circ\text{C}$ plateau.



a

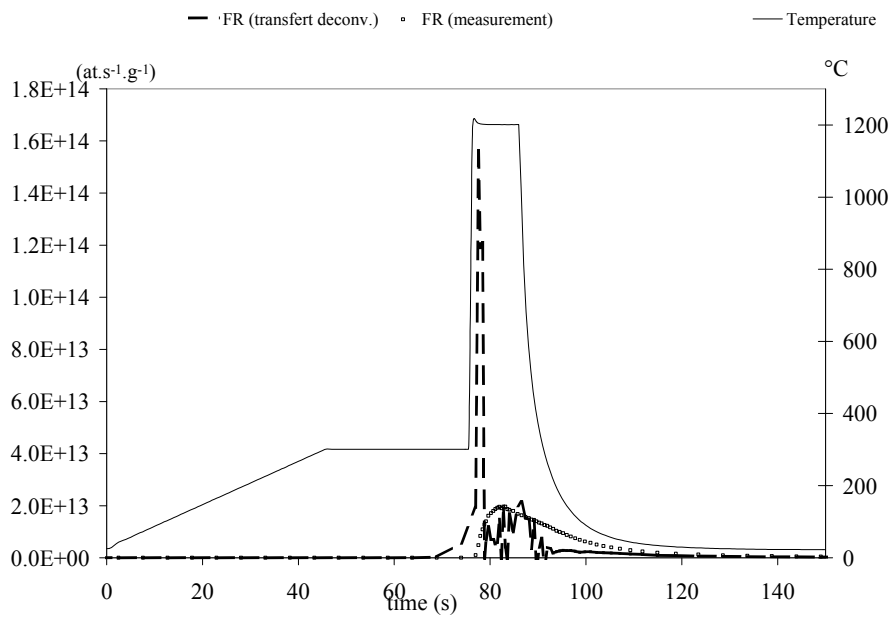


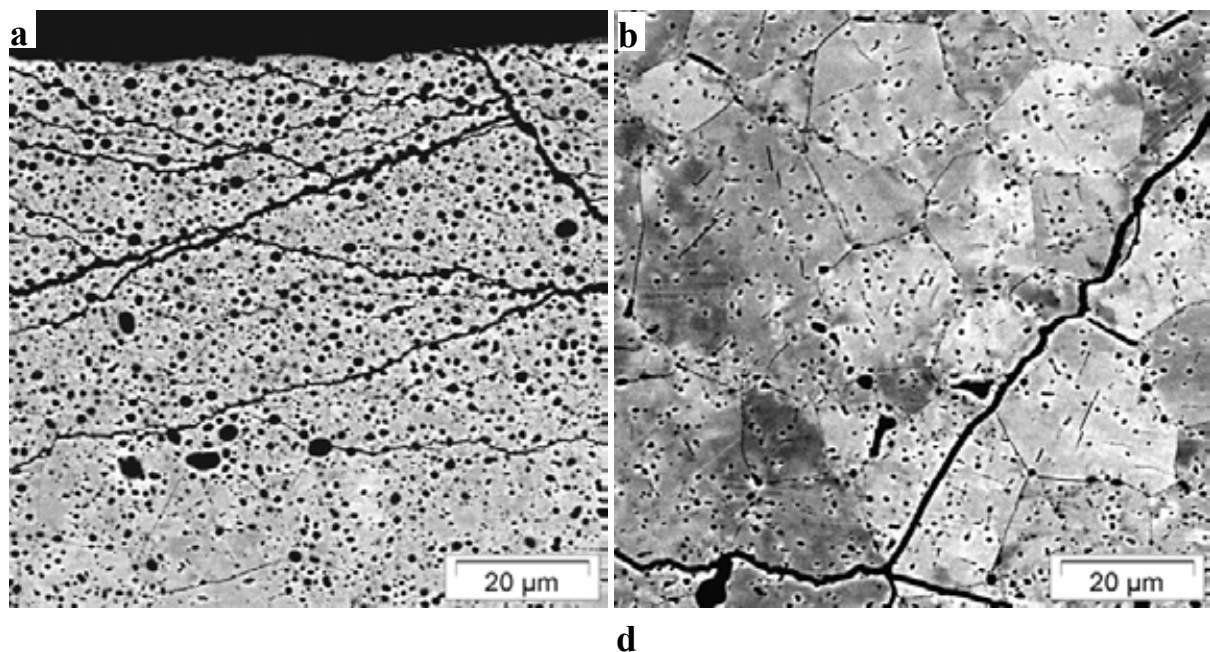
Fig. 3 : ^{85}Kr release kinetics during a 20 °C.s^{-1} increase up to a 10 min plateau at 1200 °C , on a 71.8 GW.d.t^{-1} UO_2 fuel. **a** cumulative values, **b** instantaneous release. Direct measurement and result of the transfer deconvolution.

In order to have some information on the intergranular / intragranular distribution of the released gas, a 8 days 9 W.cm^{-1} re-irradiation had been performed in the OSIRIS MTR reactor before the tests. The ^{133}Xe was also measured and, by a release of 1.3 % showed that most of the gas released during the thermal transient is intergranular gas.

Previously, for this fuel, the intergranular / intragranular gas distribution had been evaluated thanks to the « adagio » experiment allowing to discriminate between the intergranular release obtained by the opening of the grain boundaries during the oxidizing process (that is the majority) and the unwanted intragranular release. In this case, the part of intergranular gas for the whole section of the fuel deduced from this "adagio" experiment was 23 %.

In the simulated LOCA type condition test of such a fuel, it is therefore measured that about half of the intergranular gas has been released.

SEM post test examination are presented Fig. 4 after an image processing allowing some contrast enhancement.



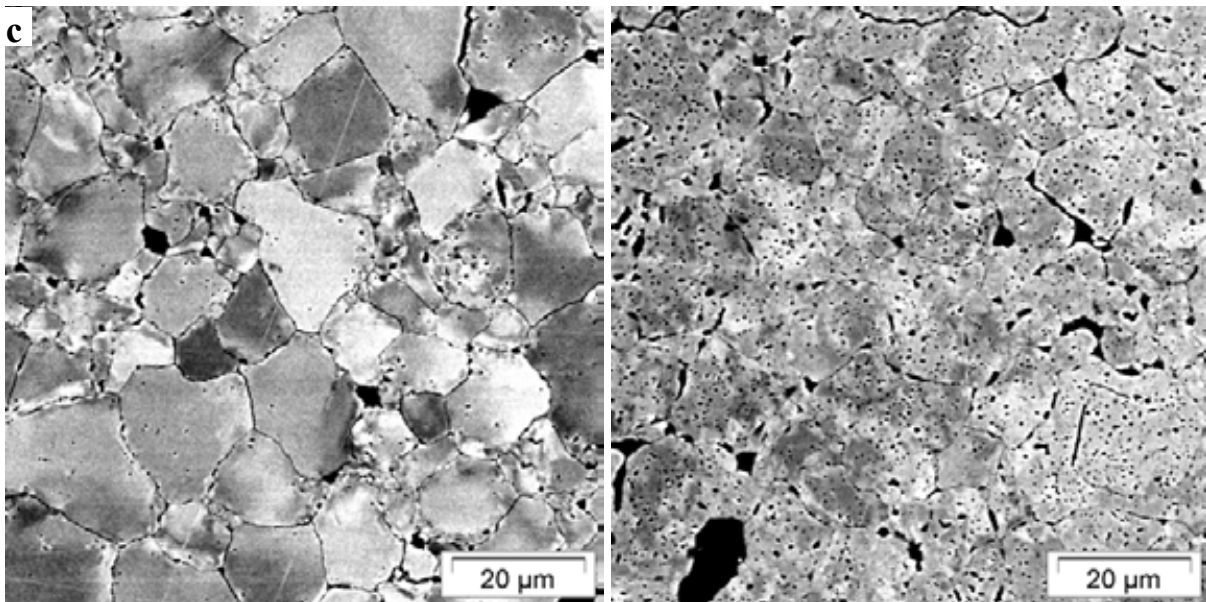


Fig. 4 : SEM images of a 71.8 GW.d.t^{-1} UO_2 fuel after a $20 \text{ }^\circ\text{C.s}^{-1}$ increase up to a 10 min plateau at $1200 \text{ }^\circ\text{C}$. **a** at periphery (1R), **b** at 0.97R, **c** at 0.4R, **d** at the centre, with high contrasts enhancements.

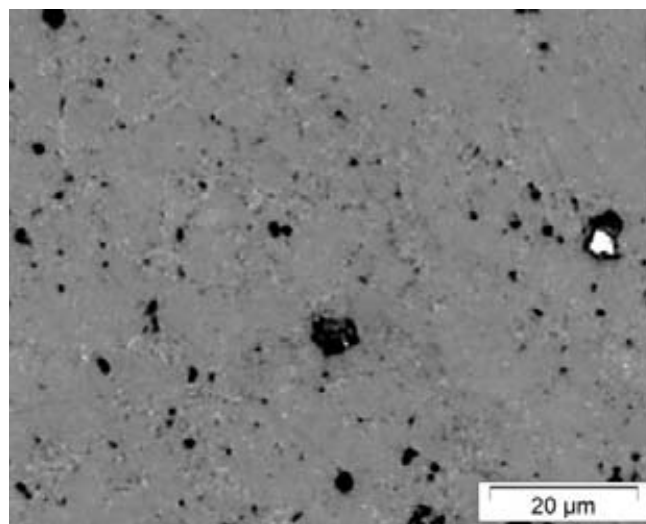


Fig. 5 : Optical microscopy of a 71.8 GW.d.t^{-1} UO_2 fuel after a $20 \text{ }^\circ\text{C.s}^{-1}$ increase up to a 10 min plateau at 1200°C , at 0.75R with contrast enhancement.

In the rim area, Fig. 4 **a** shows a very high fracturation that clearly induced some fission gas release. Nevertheless, the release of the gas from most of the rim bubbles is not obvious. However, SIMS xenon measurements on quite similar areas, within the framework of other programs showed that the bubbles of the rim area have completely lost their xenon after equivalent tests. Once this point is known, the SEM detailed examination of the rim surface after polishing shows that many grain boundaries of the HBS sub-grains are, after the thermal transient, visible as dark lines, without any etching.

At the back of the rim area (Fig. 4 **b**), the main result of the SEM examination is the observation of most of the grain boundaries as dark lines. The main part of the intergranular gas that was in these boundaries must have been released during the burst release. In a few cases, the dark line is not so clear, especially when some micrometric bubbles are observed along the grain boundaries. These few bubbles are likely to have retained their gas. The other modification, at this position, is the apparition of the planar defects [23]. Though they existed before the test, they were only visible after an etching.

Moreover their length increased during the test. This is the only clear intragranular effect of the test visible with SEM.

At 0.4R (Fig. 4 **c**), just outside the central precipitation area, again, most of the grain boundaries are seen as dark lines. Optical microscopy (Fig. 5) did not allow to detect this phenomenon, even after image processing.

At the centre of the cut (Fig. 4 **d**), though some of the grain boundaries are visible the same way, many of them are not.

Post test examinations show therefore that the intergranular gas released during the test includes the gas coming from the HBS bubbles and that the intergranular gas still retained within the fuel must be in the few grain boundaries that remain apparently unmodified on SEM images during the test. Outside the central part it was seen that these grain boundaries are probably those where the gas was already widely gathered into micrometric bubbles. It may also be the case in the central area where many grain boundaries remain less visible than elsewhere, where a large amount of intergranular gas is expected after base irradiation and in which the difference between base irradiation temperature and the maximum temperature during the test is the lowest.

4.2. Second application example : fuel behaviour under a power ramp test

The second example shown hereafter is a comparison between fuel before and after a ramp test. The fuel is a $38.8 \text{ GW.d.t}^{-1} \text{ UO}_2$, irradiated with local average linear powers of 178, 260 and 214 W.cm^{-1} during the 3 cycles of the irradiation. A rodlet refabricated from the nuclear power plant complete rod in our facility was then submitted to a ramp test in the Osiris test reactor. This ramp rise rate was $100 \text{ W.cm}^{-1}.\text{min}^{-1}$. The maximum power, 520 W.cm^{-1} , was held during 90 s. During this ramp test, without failure, the additional fission gas release was 3.8 % of the created gas whereas the release at the end of the irradiation was only 0.39 % for the entire rod (see ref. [19] for more details). Fig. 6 shows the xenon measurement results along a radius of a pellet on a reference sample of the same rod before the ramp test and on a sample after the ramp test, close to the maximal power position during the ramp test. These measurements have been performed both with the EPMA and the SIMS. A few examples of the SIMS xenon depth profiles are shown on the right side of Fig. 6. The radial position corresponding to these depth profiles are indicated with arrows on the radial profiles

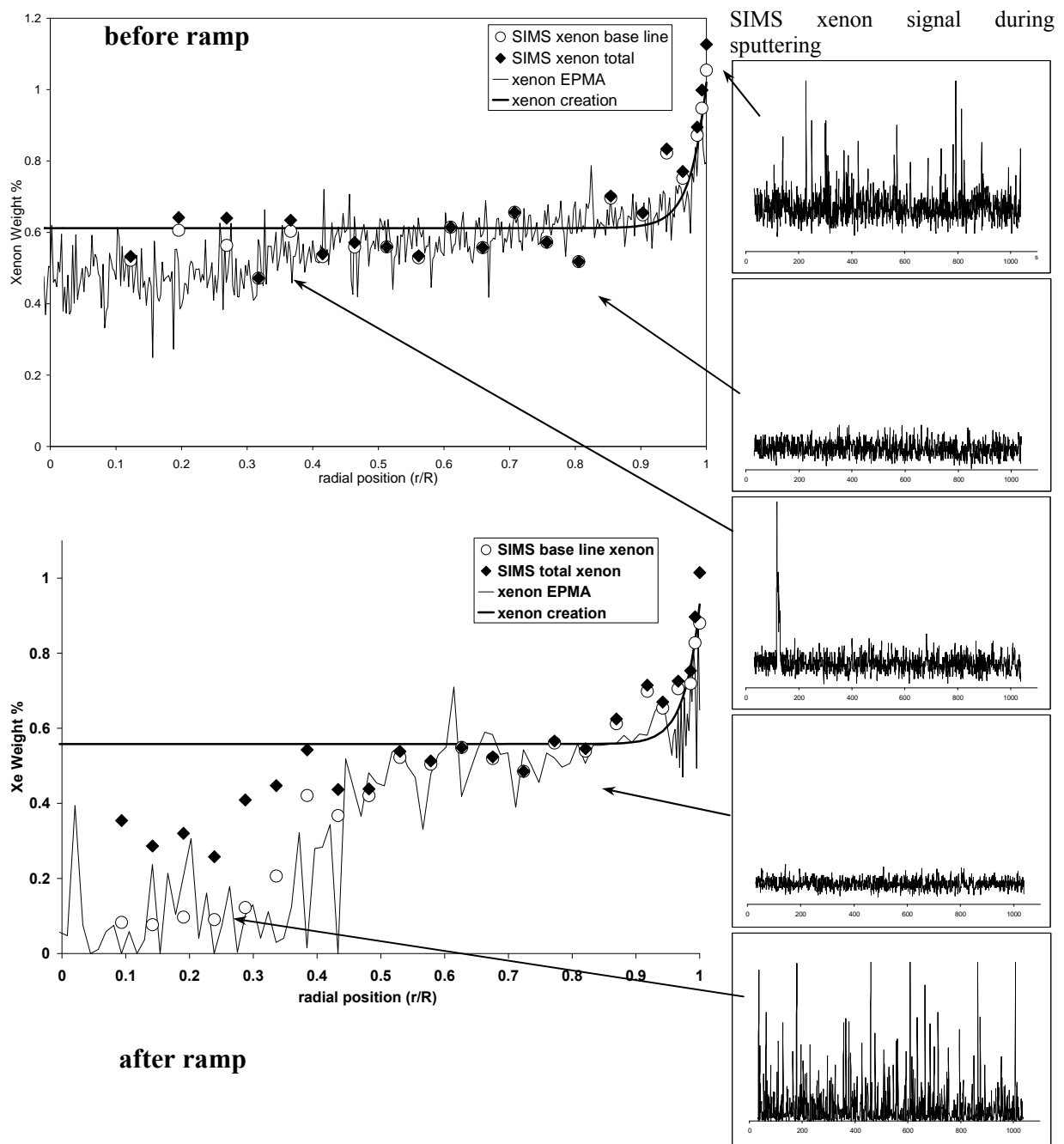


Fig. 6 : Xenon measurements with EPMA and SIMS before and after the ramp test.

. These xenon SIMS depth profiles are the intensity of the measured signal for xenon during the sputtering time. On these profiles, the base line comes from the solid solution xenon or from the xenon in nanobubbles or very low content bubbles. The peaks come from the opening of bubbles during the sputtering. On the radial profiles, for each measurement position, two values are plotted for the SIMS. First the empty circles are deduced from the base lines of the xenon depth profiles, then the solid squares are deduced from the total signal including the peaks. That is to say that the lowest points are the level of xenon in solid solution or in nanobubbles and that the highest ones are the total xenon concentration, including the bubbles. All along the SIMS radial profiles, differences are observed between the measurements even between points that could be expected closer. These differences are due to differences between the volumes of the sputtered material in spite of identical experimental conditions. These volume differences come from the effect of the grain lattice orientation on the sputtering speed. The 30 μm diameter craters do not include enough grains for these differences to lead to an average behaviour. One of the improvements foreseen in a close future is the volume

measurement of each one of the craters for a correcting of the amount of xenon measured according to these volumes.

Before the ramp, as the fission gas release is only 0.39 % of the created gas, most of the gas is still in the fuel. Nevertheless, EPMA xenon measurement is, in the central part of the pellet, clearly lower than the local creation. Between 0R and 0.5R, the EPMA mean value is 14 % lower than the local creation, so that the participation of this central part to the total release would be about 3.4 % of the created xenon on this section. In fact, this is not an actual release, most of this gas being trapped into bubbles. This is deduced from the SIMS xenon measurements. Indeed, whereas the presented xenon depth profiles show that around 0.7R no presence of gas bubbles can be detected, at the very periphery and in the central part, these profiles exhibit peaks. At the periphery, these peaks are the sign of the beginning of the formation of the rim High Burn-up Structure (HBS), which is not yet detected properly by EPMA.

In the central part, differences are detected between the base line and the total signal, that is to say that, as it was expected by the comparison between the EPMA result and the low total fission gas release, part of the gas, which is not measured by EPMA, is actually into bubbles. The uncertainties on the SIMS measurements mainly due in this case to the sputtered volumes variations do not allow to deduce the actual local release from the SIMS measurements in case of low release. Moreover, the depth profiles in this central area show that in fact, unlike at the periphery, the bubbles are rare but contain a large amount of xenon. SEM images explain this point. In this area, no intragranular bubbles are detected with SEM, only intergranular. These last are more likely to be partly interconnected and to gather large amounts of fission gases, as well as completely escaping to EPMA measurements.

After the ramp test, no major change can be found between 0.5R and 1R. Between 0R and 0.5R, on the contrary, a great decrease in the EPMA xenon concentrations shows large effects of the ramp test on the fission gases distribution. On this area, only 36 % of the locally created gas is still measured (only 19 % between 0R and 0.3R). This implies that about 15 % of the gas created at this level of the rodlet is missing in the bulk of the material. This is much more than the 3.4 % of release due to the ramp test, even adding the initial 0.39 % base irradiation release and taking into account the location of the sample, close to the peak power level of the ramp test that implies that the local release at this level is expected higher than the mean rodlet release. Consequently a large amount of fission gas must still be into large bubbles. This is what is seen on EPMA X-ray mappings, where some bubbles containing xenon can be seen under the surface of the sample, and on SEM images of the surface where intragranular and intergranular bubbles are clearly the consequence of the ramp test (Fig. 7). With EPMA or SEM, no global quantification of the amount of gas in these bubbles is possible. The SIMS central measurements confirm the presence of a high amount of gas in bubbles and allow some quantification of the phenomenon. The SIMS base line, after the ramp and in the central part of the pellet, are very low and quite consistent with the EPMA measurements, confirming the evaluation of the amount of gas still in solid solution or in nano bubbles of the oxide. The depth profiles show the presence of a large number of bubbles opened during sputtering. The amount of gas still missing, once both the base line and the peaks are taken into account, is only 6 % of the total creation at this rodlet level, which is more consistent with the total release from the rodlet fuel. This evaluation could be improved with the sputtered volumes determination. Moreover part of the retention may still escape to the measurement if it is in cavities larger or of the same magnitude as the depths of the sputtered volumes.

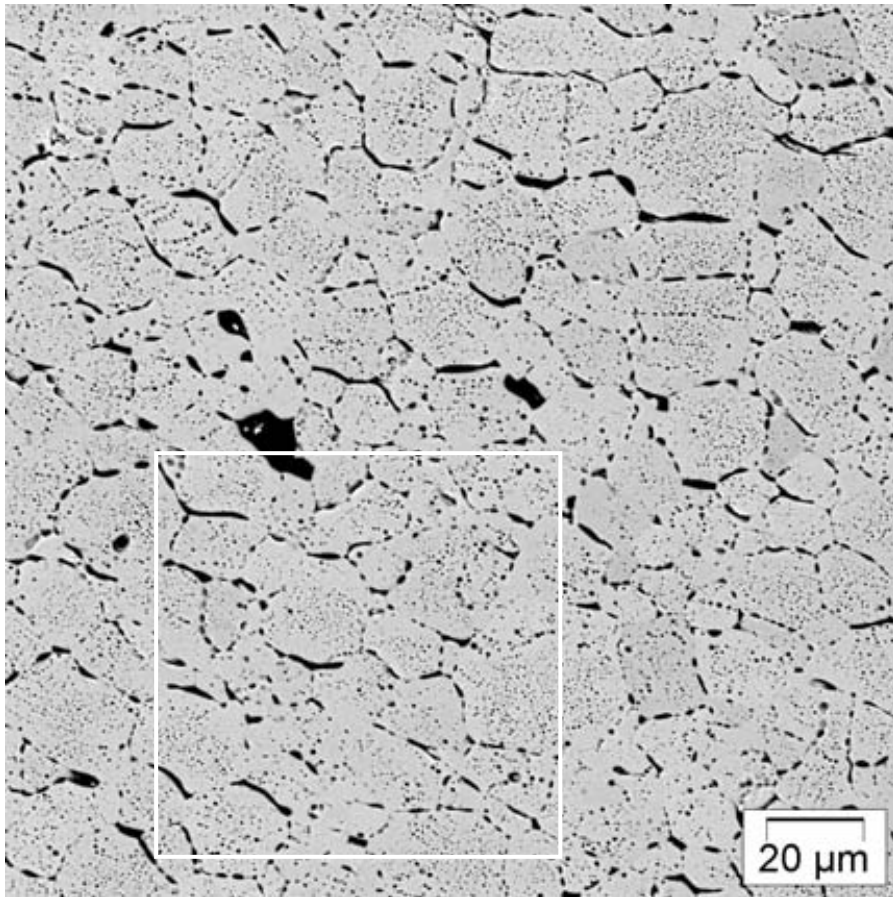


Fig. 7 : SEM image for image analysis of the porosity at the centre of the pellet after the ramp test

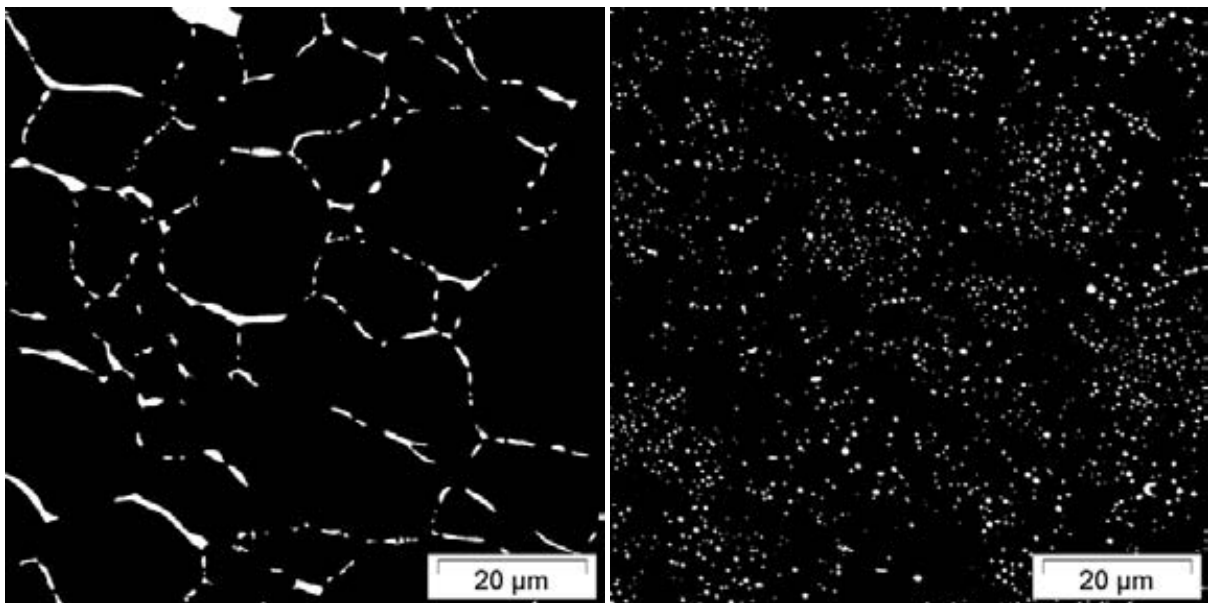


Fig. 8 : intergranular and intragranular distribution of the porosity after the ramp test, extracted from Fig. 7.

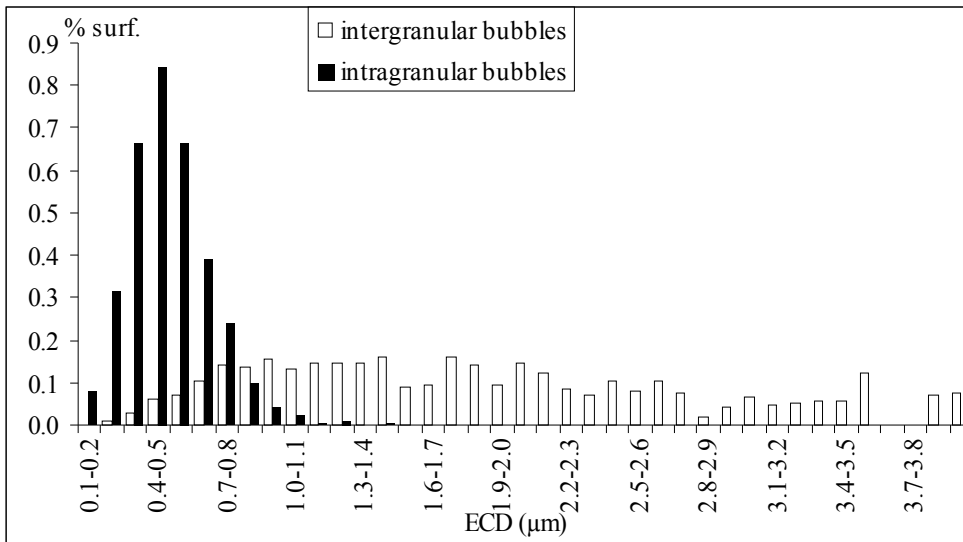


Fig. 9 : size distribution of the Equivalent Circular Diameter (ECD) of the inter and intragranular bubbles at the centre of the ramped fuel.

SEM examination gives some additional information. Fig. 7 to Fig. 10 show that in addition to the preexisting large pores and intergranular porosity, in the central part, a large intergranular porosity appeared during the ramp test. It covers about 4 % of the surface. The intragranular porosity with much smaller bubbles, covers about 3.5 % of the surface of the grains. According to the shape, size and amount of intergranular bubbles, one could expect a large interconnection of these cavities and therefore that most of the gas detected into bubbles by SIMS would be in intragranular position.

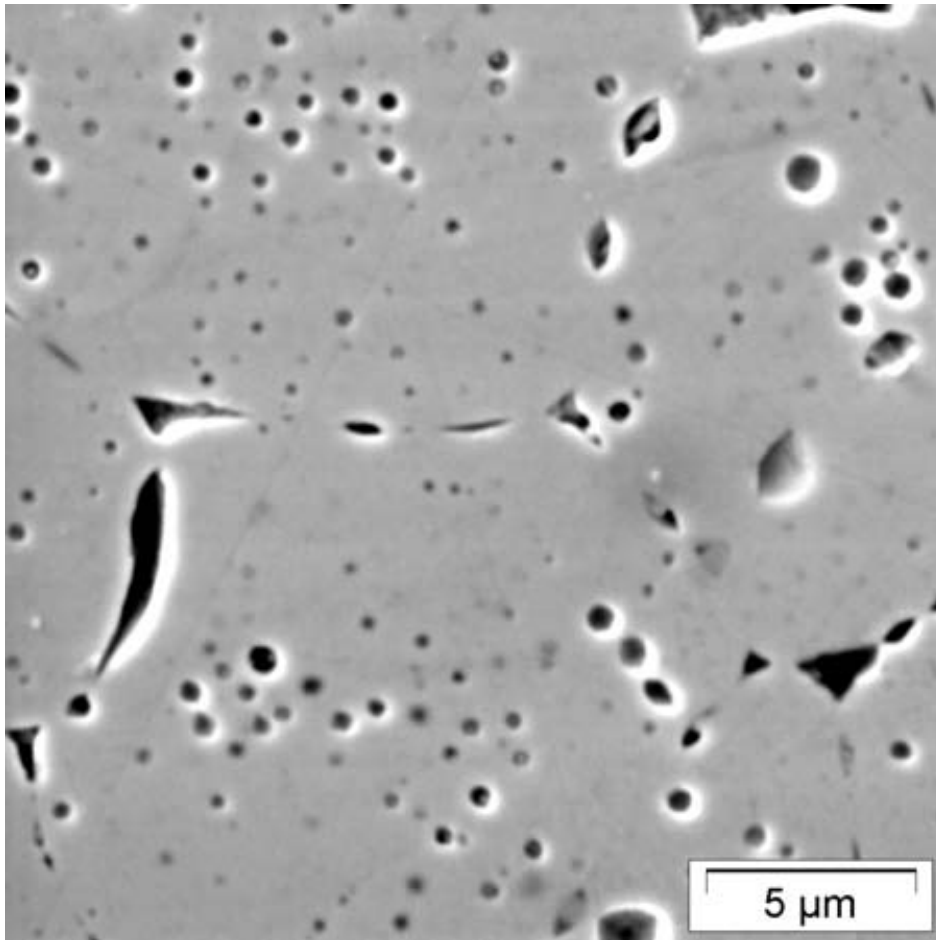


Fig. 10 : SEM image, detail at the centre of the pellet after the ramp test.

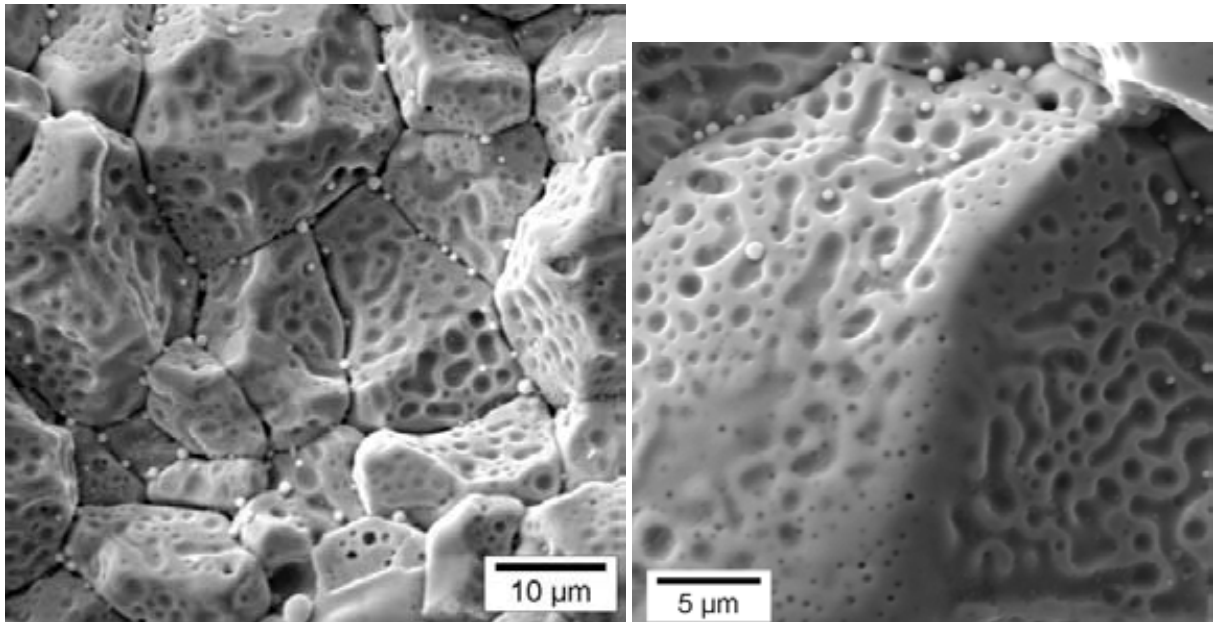


Fig. 11 : SEM fractographs at the center of the ramped fuel

The SEM fractographs Fig. 11 show on the contrary that in spite of the large covering of the grain boundaries by bubbles (more than 45 % of their surface) part of the intergranular bubbles appear still isolated from others that are interconnected.

An estimation of the molar volume of the fission gases is nevertheless possible since the SIMS shows that 0.22 weight % of xenon at least is in closed bubbles (intragranular + the smallest of the intergranular). This leads to estimate this molar volume between 1.8 and $2.8 \cdot 10^{-4} \text{ m}^3 \cdot \text{mol}^{-1}$ that is to say between 300 and $460 \text{ \AA} \cdot \text{at}^{-1}$ of xenon or krypton.

5. CONCLUSION

This paper had the purpose to show the capacities of our laboratory in term of fission gases behaviour evaluation. On two examples, one implying a simulated thermal transient, the other a ramp test, it showed the high interest of extended pre and post-test examination for a better understanding of the behaviour during the tests.

REFERENCES

-
- [1] Y. PONTILLON, J. BONNIN, B. CORNU, M.P. FERROUD-PLATTET, C. GONNIER, P.P. MALGOUYRES, C. ROURE, "Fuel Performance under different PWR conditions : An overview of the annealing test facilities at the CEA Cadarache" Water reactor fuel performance meeting, Kyoto (2005)
 - [2] L. DESGRANGES, M.H. FAURE, A. THOUROUDE "A new apparatus for determination of the free volume of a fuel using the double expansion method", Nuclear Technology Vol. 149 (2005) 14-21
 - [3] S. RAVEL, G. EMINET, E. MULLER, L. CAILLOT, "Partition of Grain Boundary and Matrix Gas Inventories: Results Obtained Using the ADAGIO Facility," *Proc. of the Fission Gas Behaviour in Water Reactor Fuels, Nuclear science OECD NEA*, p. 347, OECD, Cadarache, France (2000).
 - [4] S. KASHIBE, K. UNE, "Effect of external restraint on bubble swelling in UO₂ fuels" J. Nuc. Mater. 247 (1997) 138-146 ; S. KASHIBE, K. UNE, "Fission gas release from externally restrained uranium dioxide fuel", J. Nucl. Sci. Technol., Vol 37 n°6 p. 530-535 June 2000
 - [5] K. UNE, S. KASHIBE, K. HAYASHI, "Fission gas release behavior in high burnup UO₂ fuels with developed rim structure", Actinides 2001, Hayama, Japan, Nov 4-9 2001
 - [6] P. VON DER HARDT, A. TATTEGRAIN, J. Nucl. Mater., 188, 115, (1992) ; M. SCHWARZ, G. HACHE, P. VON DER HARDT, Nucl. Eng. Des., 187, 47, (1999).

-
- [7] C. POINSSOT, C. FERRY, P. LOVERA, J.M. GRAS, Proceedings of the 2004 Meeting on LWR Fuel performance, September 19-22, 2004 Paper 1107
- [8] M. VERWERFT, "Multiple voltage electron probe microanalysis of fission gas bubbles in irradiated nuclear fuel", Journal of Nuclear Materials, Vol. 282, Issues 2-3, Pages 97-111 (2000).
- [9] J. NOIROT, L. NOIROT, L. DESGRANGES, J. LAMONTAGNE, T. BLAY, B. PASQUET, E. MULLER, Proc. of the International topical meeting on LWR fuel performance, Orlando, USA Fl, 2004, Paper 1019 329.
- [10] F. HUET, J. NOIROT, V. MARELLE, S. DUBOIS, P. BOULCOURT, P. SACRISTAN, S. NAURY, P. LEMOINE; "Post irradiation examination on UMo full sized plates IRIS2 experiments" RRFM 2005 Budapest
- [11] F. HUET, V. MARELLE, J. NOIROT, P. SACRISTAN, P. LEMOINE; Full-sized plates irradiation with high UMo Fuel loading, Final results of IRIS 1 experiment; RERTR 2003 Chicago
- [12] M. NAGANUMA, J. NOIROT, D. LESPIAUX, S. KOYAMA, T. ASAGA, J. ROUAULT, G. CRITTENDEN, C. BROWN "High burnup irradiation performance of annular fuel pins irradiated in fast reactor PFR", MOX IAEA Symposium, May 1999
- [13] L. DESGRANGES, B. PASQUET, B. RASSER "Installation of a shielded SIMS in CEA Cadarache" IAEA-TECDOC-1277 (2002), Proceedings of a Technical Committee meeting on Advanced post-irradiation examination techniques for water reactor fuel, Dimitrovgrad, 2001
- [14] C. VALOT, J. LAMONTAGNE, L. DESGRANGES, B. PASQUET, J. NOIROT, T. BLAY, I. ROURE "Fission gases pressure evaluation in irradiated PWR fuels: complementarities of microanalyses techniques, SEM, EPMA and SIMS" Hot laboratories and remote handling Jülich (2006)
- [15] C. VALOT, L. DESGRANGES, B. PASQUET, J. LAMONTAGNE, J. NOIROT, T. BLAY, I. ROURE "Local Burn Up determination in UOx fuel rods using secondary ion mass spectroscopy" Hot laboratories and remote handling Mai 2005
- [16] J. LAMONTAGNE, J. NOIROT, L. DESGRANGES, T. BLAY, B. PASQUET, I. ROURE "Detection of gas bubbles by SIMS in irradiated nuclear fuel" EMAS 2003 + microchimica acta vol 145 p. 91-94 (2004)
- [17] L. DESGRANGES, C. VALOT, B. PASQUET "Characterisation of irradiated nuclear fuel with SIMS" Applied Surface Science, 252-19 (2006) 7048-7050
- [18] J. LAMONTAGNE, L. DESGRANGES, C. VALOT, J. NOIROT, T. BLAY, I. ROURE, B. PASQUET; "Fission Gas Bubbles Characterisation in Irradiated UO₂ Fuel by SEM, EPMA and SIMS" EMAS 2006 (Firenze) + Microchimica acta 155 (2006) 1-2 183 187
- [19] L. DESGRANGES, B. PASQUET, X. PUJOL, I. ROURE, T. BLAY, J. LAMONTAGNE, T. MARTELLA, B. LACROIX, O. COMITI, L. CAILLOT; "Characterisation of volatile fission products, including iodine, after a power ramp" PCI international seminar CEA/IAEA/OCDE Aix en Provence 2004
- [20] L. DESGRANGES, B. PASQUET; "Measurement of xenon in uranium dioxide (UO₂) with SIMS" Nuclear Instruments and Methods in Physics Research Section B: Beam Interactions with Materials and Atoms, Volume 215, Issues 3-4, February 2004, Pages 545-551
- [21] L. DESGRANGES, C. VALOT, B. PASQUET, J. LAMONTAGNE, T. BLAY, I. ROURE; "Quantification of total xenon concentration in nuclear fuel with SIMS and EPMA" Submitted to the Journal of nuclear Materials
- [22] Y. PONTILLON, M.P. FERROUD-PLATTET, D. PARRAT, S. RAVEL, G. DUCROS, C. STRUZIK, I. AUBRUN, G. EMINET, J. LAMONTAGNE, J. NOIROT, A. HARRER "Experimental and theoretical investigation of fission gas release from UO₂ up to 70 GWd/t under simulated LOCA type conditions: the GASPARD program" Proceedings of the 2004 International Meeting on LWR Fuel Performance, Orlando, Florida, September 19-22, 2004, Paper 1025
- [23] N. LOZANO, L. DESGRANGES, D. AYMES AND J.C. NIEPCE. "High magnification SEM observations for two types of granularity in a high burnup PWR fuel rim" *J. Nucl. Mater.* **257** (1998) 78.

Development of a Non-destructive Post-Irradiation Examination Technique using High-energy X-ray Computer Tomography

Kozo KATSUYAMA, Tsuyoshi NAGAMINE and Yasuo NAKAMURA

Fuel Monitoring Section, Fuels and Materials Department
O-arai Research and Development Center, Japan Atomic Energy Agency (JAEA)
4002 Narita-cho, O-arai-machi, Higashiibaraki-gun, Ibaraki-ken,
Japan, 311-1393

ABSTRACT

High-energy X-ray computer tomography (X-ray CT) is one of the most powerful non-destructive test tools for checking the inner condition of structure materials. This technique has been applied to the inspection of structure materials such as the booster rocket and the engine of automobile. However, the application of X-ray CT technique to the post irradiation examination (PIE) of nuclear reactor fuel was impossible due to the effects of gamma ray emissions from an irradiated fuel assembly. In order to minimize the effects of the gamma ray emissions from the irradiated fuel assembly, the 12 MeV X-ray pulse was used in synchronization with the switch-in of the detector, and then clear cross section CT image could be successfully obtained. This technique makes it possible to observe the inner condition of irradiated fuel assembly (maximum radioactivity: 2×10^{16} Bq) by non-destructive method for the first time in the world.

The measurement error for each defect is ± 0.3 mm and the difference of density distinguished down to $\pm 4\%$ in a material of density ~ 8 g/cm³. This technique allows non-destructive PIE to replace destructive PIE in some cases, and increases its efficiency and reduces radioactive wastes. This technique enables us to analyze overall fuel assembly performances such as central void distribution indicative of temperature distribution, wrapping wire distortion and bundle-duct interaction.

1. INTRODUCTION

X-ray computer tomography (X-ray CT) is one of the most powerful non-destructive test tools for characterizing the inner structure as used in medical field. Recently, this technique has been applied to the inspection of mechanical components such as a booster rocket and an automobile engine.

The application of X-ray CT technique was indispensable to observe inner condition of Fast Breeder Reactor (FBR) fuel assembly, because of visual observation was obstructed by the presence of the wrapper tube that completely surrounds the fuel assembly. However, it was thought that the application of X-ray CT technique to the post irradiation examinations (PIE) of irradiated nuclear fuel was impossible due to the effects of gamma ray emitted from the irradiated fuel assembly.

In this study, a pulsed high energy X-ray source synchronizing with the detection was utilized in order to reduce the effects of gamma ray emissions from an irradiated fuel assembly, and then clear cross section CT image could be successfully obtained[1].

This technique makes it possible to observe the inner condition of irradiated fuel assembly by a non-destructive method for the first time in the world, and to allow non-destructive PIE to replace destructive PIE in some cases.

In this paper, we describe following two items ;(1) Development of X-ray CT apparatus for PIE, and (2) Result of applying X-ray CT apparatus to an irradiated fuel assembly.

2. DEVELOPMENT OF X-RAY CT APPARATUS FOR PIE

2.1. X-ray CT apparatus

Fig.1 shows the outline of X-ray CT apparatus. The irradiated fuel assembly is inserted in the elevator in the hot cell and can be axially moved. The scanner that has an X-ray source and detector is put on the table rotating around the fuel assembly.

The X-ray intensity measured in the detector is converted to the X-ray CT image by the image-processing computer. All system of apparatus is controlled by the main computer and the X-ray CT image can be taken on any cross section.

Table 1 shows the main specification of X-ray CT apparatus. Main equipment is described in the following.

2.1.1. Scanner

Scanner is composed of an X-ray source and a detector. The X-ray detector measures X-ray transmitted through the fuel assembly.

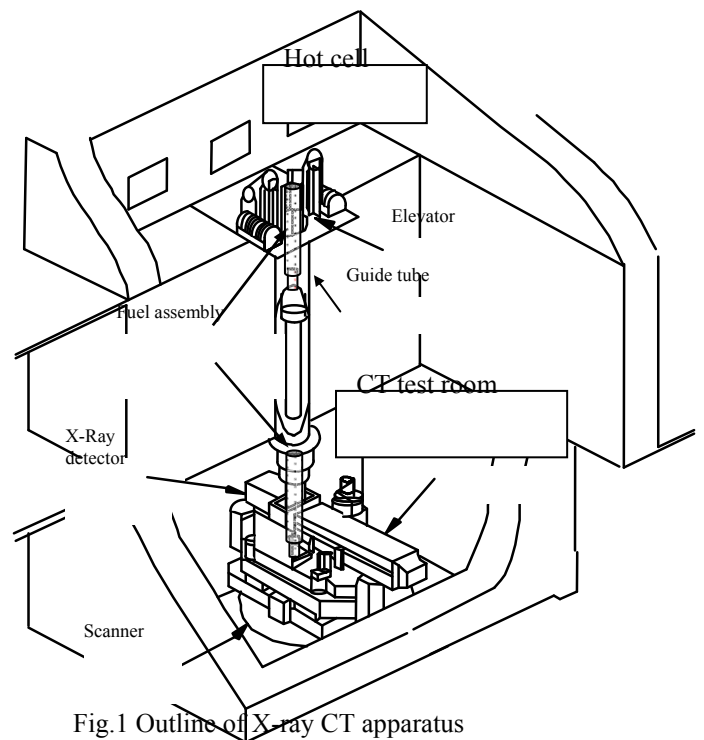


Fig.1 Outline of X-ray CT apparatus

(1) X-ray source

In order to obtain sufficient X-ray through the high-density specimens, high power and high energy (12MeV) X-ray, which is maximum in commercialized X-ray linear accelerator, was selected.

(2) X-ray detector

The X-ray detector was put in a scanner, and consists of a collimator and a scintillation detector. CdWO₄ was selected as the material of scintillation detector because of its high sensitivity.

2.1.2. Specimen drive unit

Specimen drive unit was consists of an elevator which loads an irradiated fuel assembly and a guide tube that is the boundary between the examination cell and CT test room. Irradiated fuel assembly is loaded on the elevator and transferred to CT test room though the duct tube.

2.2. Significant feature of apparatus

2.2.1. Detection system of pulsed X-ray source

A large problem is the disturbance to obtain clear CT image by the high level of gamma ray emitted from an irradiated fuel assembly. In order to solve the problem, the pulse of high energy X-ray that is generated by an accelerator was applied to the scanning. Detection of X-ray transmitted through the fuel assembly is synchronized with the pulse of high energy X-ray to minimize the disturbance of gamma ray from the fuel assembly.

X-rays pulse, which width is 4.5 microseconds, is generated every 10 milliseconds. The detection period is 10 microseconds synchronizing with X-ray pulse cycles. This improvement made it possible to reduce the amount of detected photon emitted from an irradiated fuel assembly (maximum radioactivity: 2×10^{16} Bq) to negligible level.

2.2.2. High performance of X-ray CT image

It was necessary to develop the X-ray CT apparatus that could be observed the wrapping wire (0.9mm) in the CT image. In order to improve the CT image, the collimators made of tungsten alloy, which has microscopic slit (width: 0.3mm/ height: 2mm), were prepared for this apparatus and these collimators were arranged in front of the detectors. Fig.2 shows the arrangement of X-ray source and collimators. Thirty scintillation detectors, which have collimators including slits, were arranged radially around the fuel assembly. The tungsten alloy was selected for the collimator material because of its high shielding effect. This system enables us to observe the wrapping wire in the CT image clearly.

2.3. Size measurement accuracy of X-ray CT image

A preliminary test was performed using a dummy fuel assembly of known dimension, in order to check the accuracy of this apparatus. This test showed that the

Table 1 Main specification of X-ray CT apparatus for PIE

Item	Contents
(1)CT scanning method	The second generation method (Traverse/Rotate)
(2) Scanner device	3-Axis drive system Rotation moving accuracy : 30sec Traverse moving accuracy : 0.02mm Up and down accuracy : 0.05mm
(3) X-ray source	Linear accelerator for Non-destructive Inspection Maximum electron energy : 12MeV Maximum power : 520mC/kg/min at 1m
(4) X-ray detector	Scintillates materials : CdWO ₄ Collimator slit size : 0.3mm ^(W) ×2mm ^(H) View pitch : 0.2deg Number of channel : 30 c h
(5) Translation pitch	Normal scanning : 0.3mm Low speed scanning : 0.03mm
(6) Measuring time (One Tomogram)	Normal scanning : 20min Low speed scanning : 40min

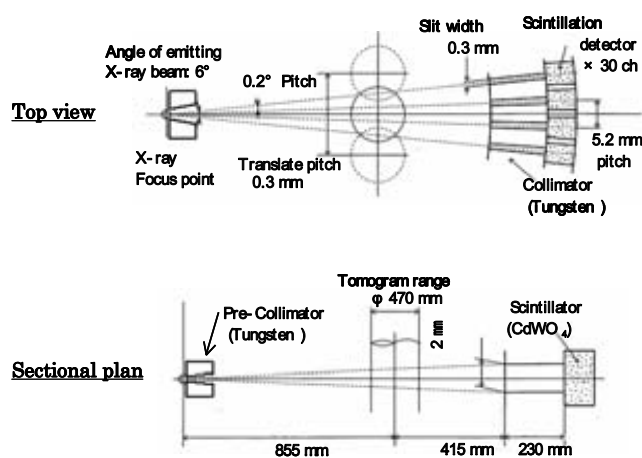


Fig.2 Arrangement of X-ray CT system

dimension could be measured within an error of 0.3mm.

From the preliminary test using a dummy fuel assembly, which had an artificial defect, it was confirmed that a slit defect with a 0.3mm width x 0.9mm length and a hole defect with 0.5mm were detected in the X-ray CT image.

3. RESULT OF APPLYING X-RAY CT APPARATUS TO IRRADIATED FUEL

3.1. Specimen

Fig.3 shows the fuel assembly used in this study, which was irradiated in the experimental fast reactor Joyo. The diameters of as-fabricated fuel pellets containing 21wt% plutonium oxide were around 5.42mm. The cladding, wrapping wire and wrapper tube were made of stainless steel. 61 fuel pins were loaded systematically in the assembly. The maximum calculated burn-up was 144GWd/t at the pellet peak.

3.2. Observation of cross section image

A typical cross section image obtained from the irradiated fuel assembly in the position of axial core center is shown in Fig.4. Clear cross section CT image could be successfully obtained by reducing the effects of gamma ray emissions from an irradiated fuel assembly.

In the left side figure, it can be seen that 61 fuel pins are arranged systematically in the hexagonal wrapper tube, and this observation makes it possible to grasp the displacement of fuel pin by analyzing of X-ray CT image [2]. Furthermore, in the closed up figure, the wrapping wire, cladding and MOX pellet with central void are distinguished respectively.

In the case of fast breeder reactor fuel, the central void is formed because of the influence of steep temperature gradient in radial direction of pellet. The central void diameter could be measured by analyzing of X-ray CT image[3]. Until now, the central void diameter has been measured by the metallurgical observation on the cross-section of the fuel after sectioning it. This technique made it possible to measure the central void diameters on the cross-section of all fuel pins included in the fuel assembly at same time without sectioning.

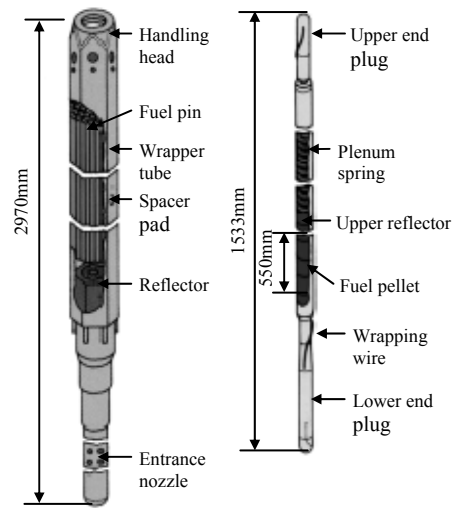


Fig.3 Outline of Joyo fuel assembly

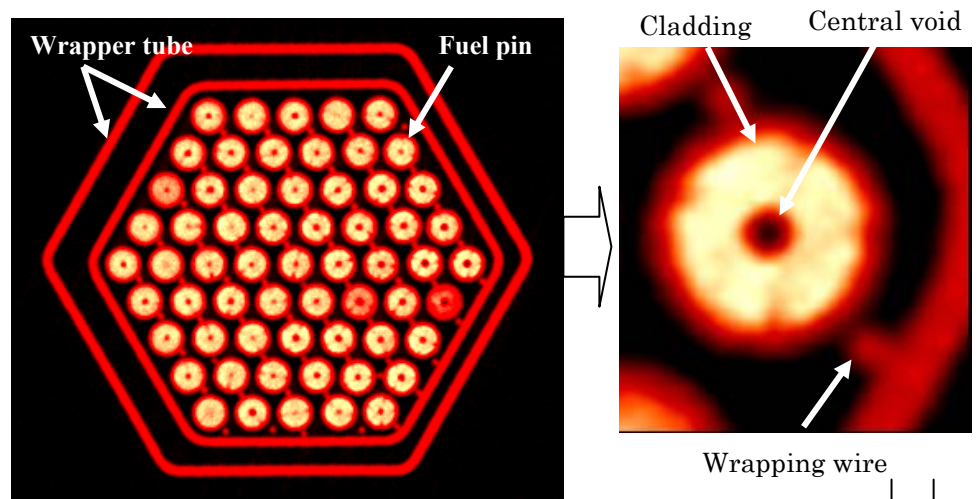


Fig.4 X-ray CT image for Joyo fuel assembly (Cross sectional view)

Using this technique, the central void diameter was determined within an error of ± 0.1 mm. Fig.5 shows the estimated result of central void diameters at the position of axial core center. The diameters increase toward the center of the reactor core. It is expected from this result that the temperatures of fuel pins and coolant in the fuel assembly increase as their positions approach the reactor center region.

3.3. Observation of the three dimensional image

When a number of X-ray CT images taken on the cross sections along the axial direction are synthesized, an X-ray CT image on the longitudinal cross section can be obtained.

Fig.6 shows three-dimensional (3-D) image for the top of fuel pin bundle. It can be seen that all of fuel pins arranged with regularity in the assembly. This observation permitted grasping the distribution of fuel pin elongation without dismantling a fuel assembly.

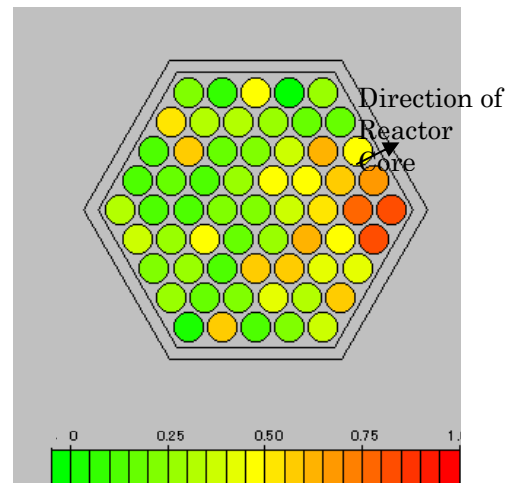


Fig.5 Distribution of central voids diameter in the fuel assembly

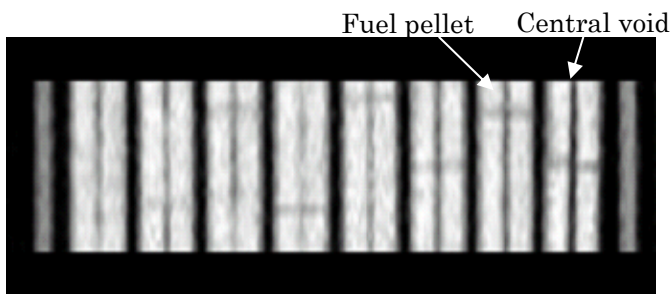


Fig.7 Longitudinal cross section image

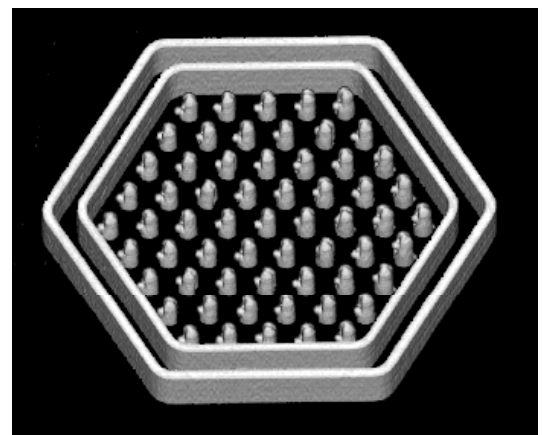


Fig.6 Observation for top of pin bundle

Fig.7 shows a longitudinal cross section image of the fuel pins around the region of mid-height of fuel assembly. This longitudinal cross sectional images show the inner structures of fuel pins located at the axial core center of fuel pins. This CT image makes it possible to grasp the change of central voids along the axial direction.

4. Conclusion

In this study, the non-destructive examination technique using X-ray CT was developed for the purpose of post irradiation examinations. This X-ray CT technique is characteristic of using a pulsed high energy X-ray source synchronizing with the detection in order to reduce the effects of gamma ray emissions from an irradiated fuel assembly, and then made it possible to obtain the clear cross section image.

This technique using the X-ray CT can eject destructive methods in many measurements. In addition, this technique also can be applied further to observation of high density and high radioactivity specimens, such as high-level radioactive wastes, activated equipment used in nuclear reactor and so on.

REFERENCES

- [1] S.IWANAGA, et al. " Large scale post irradiation examination facility for Monju fuel" , International Conference on Fuel Management and Handling, Edinburgh, U.K., Mar.20, (1995)
- [2] K.KATSUYAMA, et al. "Application of X-Ray Computer Tomography for Observing the Deflection and Displacement of Fuel Pins in an Assembly Irradiated in FBR" J. Nucl. Sci. Technol., Vol.40, No.4 (2003)
- [3] K.KATSUYAMA, et al. " Measurement of Central Void Diameter in FBR MOX Fuel by X-Ray Computer Tomography" Journal of Nuclear Science and Technology Vol.39, No.7(2002)

MODELLING OF V-HTR FUEL ELEMENTS AND COATED PARTICLES: NEEDS OF PIE IN SUPPORT TO THE EUROPEAN „RAPHAEL“ AND GEN-IV PROJECTS

G. Ruggirello^o and E.H.Toscano*

^o Comisión Nacional de Energía Atómica, UATEN, CAE

* European Commission, Joint Research Centre, Institute for Transuranium Elements, P.O.Box 2340, 76125 Karlsruhe, Germany

ABSTRACT

The fuel elements (spherical or compacts) of Very High Temperature Reactors (V/HTRs) are based on ceramic multilayer coated fuel particles, that represent the smallest constituent of the energy source in this type of reactors. As for the LWRs, the performance of the fuel element and its basic constituents has to be evaluated by modelling its behaviour under normal and accident conditions. In this context, the performance of the particle coatings (failure) and the consequent fission product release is of paramount importance. In the paper the main PIE-and characterisation methods needed to supply data for the current codes are described. The existing techniques and the main challenges for the future PIE needs in support of the European “Raphael” project and GEN-IV are presented.

Introduction

The fuel element in a modular High Temperature gas-cooled Reactor (HTR) is crucial for its safety and reliability. To this goal, ceramic multilayered coatings for nuclear fuel particles were developed for High Temperature Reactors. They are based on the synergy of the thermo-mechanical properties of silicon carbide (SiC) and pyrocarbon (PyC) to perform the coating of the fuel kernels, which should be able to retain most of the fission products release by the fuel during irradiation under normal and accident conditions.

Different types of nuclear fuel elements have been managed for the different HTRs developed all over the world in current reactor concepts and in the past. For example, pebbles (spherical fuel elements, 60 mm in diameter) are used in the Chinese reactor HTR-10. This was the concept developed in Germany in the nineteen sixties. On the other hand, the fuel is arranged in compacts (cylindrical fuel elements, approx. 26 mm in diameter, 39 mm in length) in the Japanese concept, which was also the concept for the reactor Fort St Vrain in USA.

In all reactor concepts, the coated particles constitute the basic energy producing unit, having the following coatings on the fuel kernel (see Fig.1) to retain the fission products:

- Buffer: porous pyrocarbon layer
- IPyC: internal, dense pyrocarbon layer
- SiC: Silicon carbide layer
- OpyC: external, dense pyrocarbon layer

Fuel kernels have been made of UO₂, UCO, UC₂, UO₂/ThO₂. Fuel kernels constitute the first barrier for the release of the fission products. The **buffer layer** provides space to accommodate fission gas and can be compared to the plenum in the fuel rods for LWRs. It absorbs the swelling of fuel kernels during irradiation and protects the inner dense PyC-coating from damage due to recoil from fission fragments. The **IPyC-layer** prevents the reaction between the kernel and chlorine compounds released during SiC-deposition. It constitutes the second barrier against fission product release. The **SiC-layer** is the main load bearing component of the coating and the main fission product barrier. Finally, the **OpyC-**

layer is meant to protect the SiC-layer from mechanical damage during the fuel manufacturing and provides an additional barrier against fission product release.

The present paper is a first attempt to review some of the most important Post-Irradiation Examinations (PIE)-methods applied in the past to coated particles. A simple model for the thermo-mechanical behaviour of the coated particles will be briefly discussed to introduce some of the main PIE to be performed in order to provide the necessary data to the modellers.

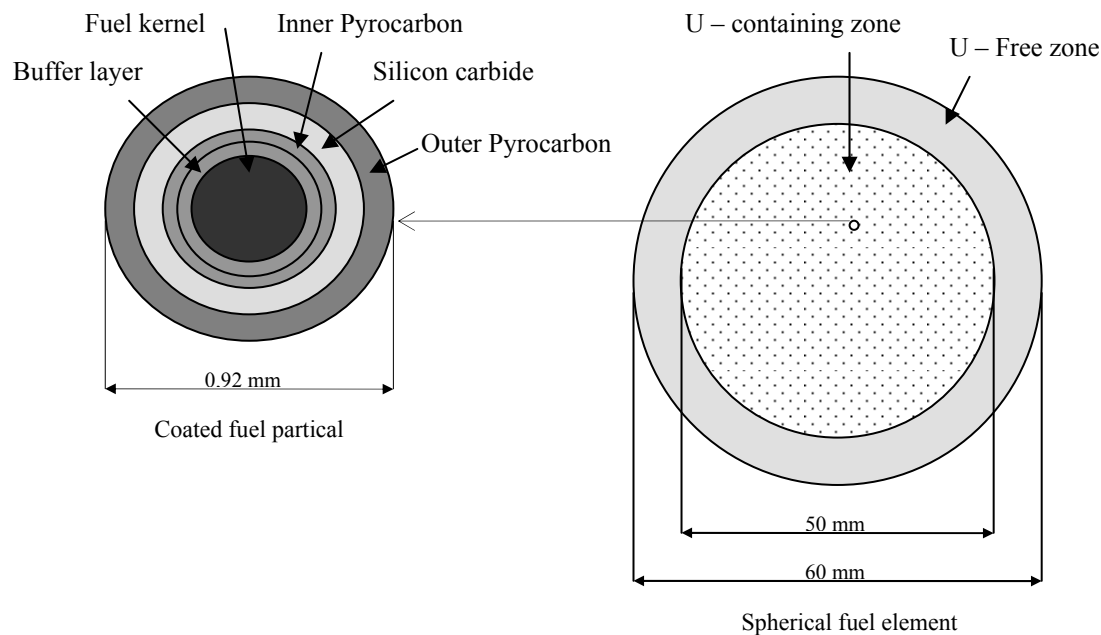


Fig. 1. Spherical fuel element for a High Temperature Reactor containing coated particles

1. Modelling

The principal mode of failure considered in the codes is the pressure vessel failure caused by the build-up of fission gas pressure in the kernel of the coated particle during irradiation (see, e.g., Ref. 1). In this model it is assumed that fission gas pressure builds up in the kernel and is partially released to the buffer layer regions. The IPyC, SiC and OPyC-layers act as structural layers to retain this pressure. The IPyC and OPyC-layers both shrink and creep during irradiation of the particle while the SiC exhibits only elastic response. Part of the gas pressure is transmitted through the IPyC to the SiC-layer.

Input parameters for the model include kernel diameter, buffer thickness, pyrocarbon and silicon carbide layer thicknesses, kernel and buffer densities and strength of the SiC-layer. A number of material properties have to be considered in the modelling of the particle behaviour under normal and abnormal irradiation conditions. In what follows, the main characterisation and PIE-methods will be described and the properties relevant for modelling purposes discussed.

2. Loss-of-Coolant-Accident (LOCA) simulation

The crucial aspect of the safety philosophy for a High Temperature Reactor (HTR) is the retention of fission products - particularly those of the iodine nuclides - in the fuel elements during operation and accidents. For this reason, the determination of the number of damaged particles constitutes the central objective of measuring the fission gas release in the reactor and also in the extensive post-irradiation examinations under accident conditions. In modern

production methodologies, the heavy metal contamination of fuel elements is kept very low. Consequently, solely the number of defective particles establishes fission gas or iodine release.

During a loss-of-coolant accident, the temperature in the core of a HTR will increase. The amount of this increase depends on the geometrical design of the reactor and the nature of the accident. For the extreme case of pressure loss in the core with the failure of all heat sinks, temperatures as high as 2000°C can be reached in a medium size HTR. On the other hand, for the case of small HTRs and the MODUL-concept in Germany, relatively low accident temperatures between 1400 and less than 1800 °C, typically 1620 °C, have been anticipated.

With the increase of the core temperature above normal reactor working temperature, fission products may be released from the fuel elements into the primary circuit and, eventually, into the environment. For a realistic assessment of the fission product release, the conditions in the reactor core during this accident scenario have to be simulated.

With the goal of simulate these accident conditions, the KÜFA (German acronym for “Cold-Finger Device”) was developed (see Fig. 2). The basic function of this device is to heat the fuel elements up to the expected temperature in a dynamic He-atmosphere, and then to

measure the fission product release. In the cold finger, protruding into the furnace, the solid fission products are plate-out whereas a continuous He-circulation through a cold trap allows the measuring of the gaseous fission products (⁸⁵Kr).

The device described has been already installed in a hot cell at the Institute for Transuranium Elements and has been thoroughly described in Ref. 2 and 3.

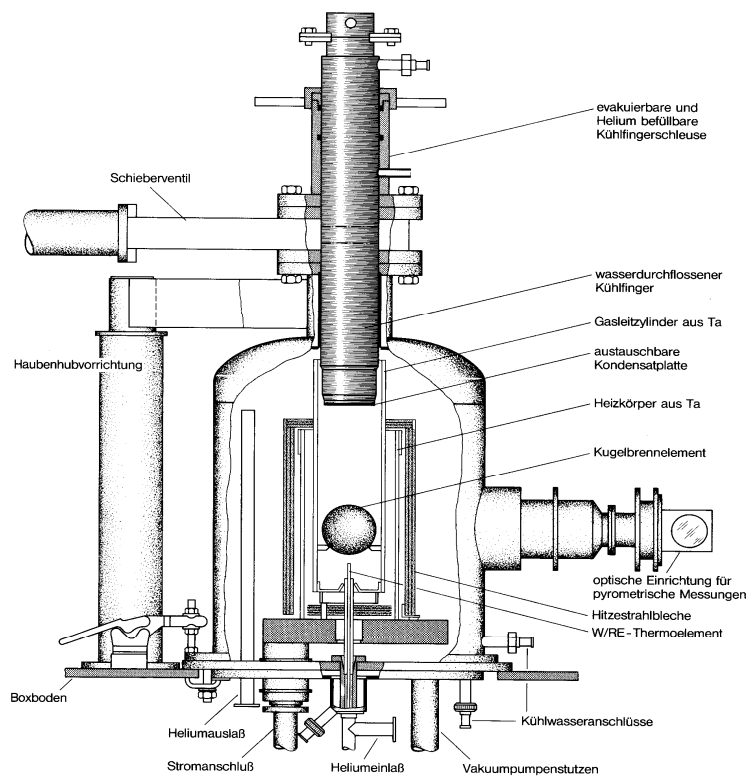


Fig. 2: Cold-finger installation for the simulation of the LOCA-accident

3. Deconsolidation

After irradiation or heat treatment in the KUFA-installation, an electrolytic process with the goal of obtaining individual coated particles has been developed to disintegrate fuel elements. The ultimate aim of the procedure is to be able to identify broken or damaged particles. The process is carried in two stages: In the first stage, the sphere (the method can be also applied to compacts) is partially deconsolidated to yield a cylinder through the centre of the fuelled region (Ref. 4). The second stage is to deconsolidate the previously obtained cylinder, stepwise, as schematically shown in Fig. 1. Each step gives rise to a sample of electrolyte solution, graphite matrix and the associated coated particles (CP). Each individual CP comprises, at this stage, the SiC and IPyC-layers and the kernel.

The method was developed by A.E.R.E.-Harwell and, with some modification, installed in the hot cell laboratory of the Kz-Juelich, Germany. The apparatus (see figure 3) consists of a motor to rotate the sample, which is attached to two holders connected to a direct current source, constituting the anode of the electrolytical system. The spherical fuel element is submerged in a beaker containing the cathode (a Pt-Ir net, having an approx. 10 mm mesh), immersed in the electrolyte ($2n \text{ HNO}_3$). The fuel element rotates at about 1 rpm.

During the procedure, the current is maintained at about 6 A. Through the anodic oxidation, the graphitic matrix is disintegrated during the process and the CPs fall to the lower part of the beaker. This process leaves a cylinder of about 20 mm in diameter in about 10 h. After that, this cylinder is placed vertical (see Fig.4), constituting again the anode, and disintegrated stepwise (2 to 5 mm disintegration steps), leaving typically 1.5 to 3 g of coated particles per step.

As already mentioned, the ultimate goal of this process is to obtain individual CPs, which can be tested to determine the damaged ones. To this goal, in several laboratories a method based on the gamma-spectrometric measurement of individual CPs was developed. The method was called IMGGA and allowed the identification of damaged particles.

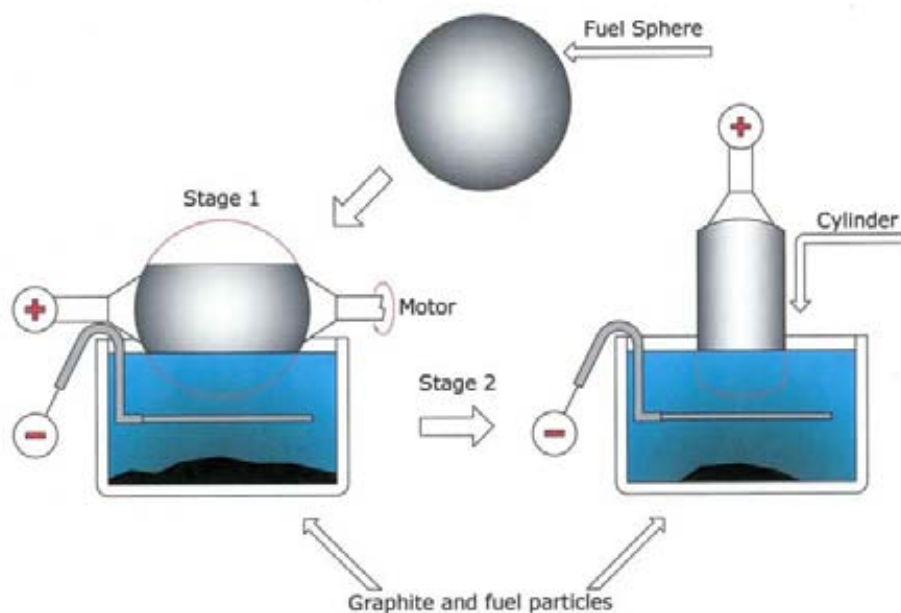


Fig. 3: Stepwise deconsolidation of a spherical fuel element.

4. Anisotropy of PyC-layers

Pyrocarbon is one of the key materials in the development of the coating of CPs. It has to be deposited (using Chemical Vapour Deposition (CVD)-technology) with two different densities onto two different substrates. The main challenge of this technology is the control of a perfect isotropic deposit, since this is crucial for an optimal sealing together with a perfect matching with the thermo-mechanical behaviour of the SiC-layer.

Carbon has hexagonal crystallography ($a = 2.461 \text{ \AA}$ and $c = 6.708 \text{ \AA}$) and is, hence, intrinsically anisotropic. Nevertheless, since graphitic carbon is not made of crystallites, but has a long range ordering that depends on the so-called graphene planes (graphene planes have the highest atomic density known in nature). The challenge is to develop at long range, a bulk isotropic material, starting from this highly anisotropic crystallographic unit cell. This can be accomplished by CVD in a fluidised bed, which significantly increases the surface/volume ratio, achieving high deposition rates.

Direct measurements of the degree of preferred orientation of the crystallites of pyrocarbon coatings deposited on spherical fuel particles have proved difficult. A first attempt was made by Bokros et al.^[5-10], using a modified X-ray diffraction technique to determine the so-called Bacon Anisotropy Factor (BAF) of strips of pyrocarbon removed from discs coated together with particles in the same fluidising bed. This is an index through which measurement ascertains the degree of anisotropy of a carbon deposit. It is derived from the pole figure method usually apply in XRD-measurements. Values of BAF increase from unity (ideal isotropic material) to higher values as the preferred orientation of the graphene layers increases. Regrettably, this method has proven to be very difficult to apply to coated particles.

For this reason, several laboratories all over the world have developed optical methods using reflected polarised light. As some of other physical properties, light reflection intensity varies with the absorption in the crystal, which is more important for the light rays perpendicular to the basal planes. In fact, when measured at a wave-length of 545 nm, the reflection parallel and perpendicular to the graphene planes are 32 and 9% of the incident intensity. This property is used to evidence the anisotropy of the graphite deposit.

The English Dragon project and CEA-France, developed in the pas the Degree of Anisotropy by Reflectance^[11] (DAR-index) as:

$$\mathbf{DAR} = \mathbf{R}_{90^\circ} / \mathbf{R}_{0^\circ}$$

where:

$$\mathbf{DAR} = (1 + \gamma + \mathbf{BAF}) / (2 + \gamma * \mathbf{BAF})$$

$$\text{and } \gamma = R_{\min} / R_{\max} = 9/32$$

The measurement is obtained by rotation of the analyser (without polarisation), parallel to the deposition plane. The optical window size can be varied but, typically, 25 μm is used.

In USA, GA developed the Optical Anisotropy Factor, or OAF-index^[12]. The photometry is the same except that the polarisation is rotated (without analyser) parallel or perpendicular to the deposit. In this case an oil objective has to be used. Again:

$$\mathbf{OAF} = \mathbf{R}_{90^\circ} / \mathbf{R}_{0^\circ}$$

With the following relationship between OAF and BAF index:

$$\text{BAF} \approx 1 + 0.77 (\text{OAF} - 1)$$

At ORNL^[13] and Jülich (FzJ)^[14], the developed the OPTAF-index, also defined as:

$$\text{OPTAF} = R_{\min} / R_{\max}$$

The optics for OPTAF is more complicated as for previously discussed indexes. A continuous cross-polar measurement is made during the rotation of the sample (under an oil objective), and the result is the maximum and minimum reflectance after disregarding the deposit plane.

Under fast neutron irradiation pyrolytic carbon undergoes densification and the coating shrinks. The shrinking of the pyrocarbon coating onto a stable substrate induces a tangential stress, which can be relaxed by irradiation creep and by re-orientation of the pyrocarbon crystallites. In order to calculate the steady state tangential stress in the pyrocarbon coating, reliable measurements of the overall dimensional changes and the preferred orientation of the crystallite are required. For this reason, comparative measurements before and after irradiation should be performed, using the same technique if possible.

5. Electron-Probe Micro-Analysis (EPMA)

One powerful tool to measure the distribution of the fission products in kernel and coating materials is the Electron Microprobe Analysis (EPMA). This technique provides also information on the chemical state of the fission products and their transport behaviour in the different coating layers.

Highly irradiated coated particles (50% FIMA) were analysed by Förthmann et al. (Ref. 15) using a CAMECA MS 46 electron microprobe analyser. As an example, in Fig. 4 some of the results that can be obtained using this technique are presented.

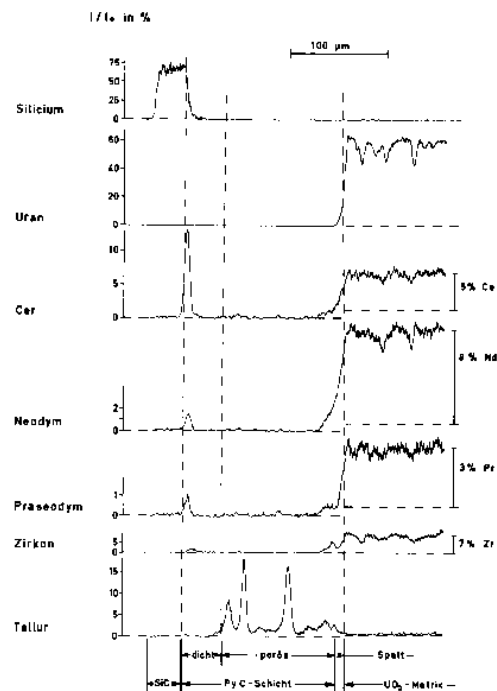


Fig. 4: Line scans of some fission products, matrix and layer components of the coated particles with UO₂-kernels (after Ref. 15)

The release of fission products from the coated particles depends on their chemical state in the kernel material and on the retention properties of the coating. A typical example is the different behaviour of the rare earths in oxide and carbide kernels. They are found in high concentrations in the oxide kernel matrix, forming solid solutions with very low vapour pressures. On the other hand, the rare earth carbides have relatively high dissociation pressures, resulting in a higher release of these fission products from carbide kernels.

The poor rare earth retention of the porous and dense pyrocarbon layers can be seen from the line scans in Fig. 4. Ce and Nd are collected at the boundary of the SiC-layer. On the other hand, Cs does not form stable compounds in either oxide or carbide kernels and, therefore, it shows the highest release from both oxide and carbide kernels but it is retained in the SiC-layer. Similar behaviour has been observed for Sr, Ba and I. Sr and Ba are not retained by the dense pyrocarbon layer but their release is lower than that of Cs because of the lower vapour pressures of SrO and BaO.

6. Fission gas release

As already stated, several mathematical models regard the particle coating as a miniature pressure vessel. For this reason, the knowledge of the actual pressure inside the particle coating is of paramount interest for the prediction of particle failure. In general, the value of the fission gas pressure is calculated from the amount of fission gas released by the kernel and the volume of the internal porosity in both kernel and buffer layer available to accommodate the gases.

The amount of gas can be measured by cracking the coating of an intact irradiated particle and measuring all the Xe, Kr, CO and CO₂, with a mass spectrometer. On the other hand, the porosity, which has to be calculated from the densities and dimensions of both kernel and coating are not very easy to measure and, since the dimensional and density changes during the irradiation are not very well known, the pressure inside a particle at a given burnup is substantially uncertain.

In Ref. 16, a direct method for the determination of the gas pressure inside fuel particles has been described. The method is based on the cracking of one particle by submitting it to hydrostatic pressure. Subsequently, the pressure is reduced until gas evolves from the cracks induced in the coating. The pressure at which this occurred can be read by observing when the bubbles begins to exude from the cracks.

The device was designed for pressures up to 10 Mpa (which is beyond the strength of the coatings and was enough to induce cracks on them) and was made of capillary borosilicate glass. The pressure was established by simply measuring the force apply to the liquid (heavy viscous liquid paraffin) in the capillary tube using a balance.

7. Strength of SiC

A method for measuring the strength of SiC-coatings using biaxial flexural tests of hemispherical samples obtained from coated particles was presented by Evans et al^[17]. The hemispherical samples used for this test were prepared by mounting the fuel particle in resin and, afterwards, polishing it down to its diameter. The UO₂-kernel was then removed and the remaining layers extracted from the resin. Afterwards, the PyC-layers could be removed by burning.

The loading of the hemispherical samples was performed using two different methods: the first loading the hemisphere with a loading sphere onto a support ring, the second, loading the hemispherical shell with a loading cylinder onto a plane base.

The flexural techniques have several advantages. The strengths of the outer and inner surface layers of the shells can be measured independently, tests can be performed at temperatures relevant to the reactor application, and good statistical strength data can be obtained (failure always occur from the inherent flaws and every specimen gives valid strength data.). On the other side, however, the tests do not give strengths that relate directly to the internal pressure conditions that apply during burnup, although the strengths under internal pressure can be evaluated with good accuracy from a statistical analysis.

Alternatively (Ref.18), ring samples were prepared by grinding the coated particles from two opposite sides nearly up to the equator, leaving a disc (typically some tens of microns thick) remains from which the kernel material can be removed mechanically. The method is called Brittle Ring Test and has several advantages according to the authors:

- Is based on a well established technique
- Gives values for the strength and Young's Modulus simultaneously
- Allows a simple analytical description of the deformation of the samples
- Is relatively easy to handle and, therefore, can be applied to a large number of samples
- Weibull statistics can be applied to the interpretation of the results, allowing the estimation of the influence of the geometry and strength distribution of the material

Using this technique also the mechanical properties of PyC-layers can be measured by producing "Biso" particles and then removing the buffer layer by chemical etching. In the case of the "Triso" particles the PyC-layers can be removed either by chemical etching (as reported in the paper) or by the burning as previously stated. Hence, entire or half-rings are tested by loading between two sapphire plates under a microscope. The load, the deflexion (strain) and the load at rupture are recorded.

8. Thermal Expansion Coefficient

One of the most challenging characterisation of coated particles is the measurement of the thermal expansion coefficient. The difficulty resides in the detail that CPs are, in fact, a composite material (PyC/SiC/PyC) in which is not easy to derive the corresponding properties from their constituents. An additional problem is represented by the small dimensions of the CPs with its consequent small coefficient of thermal expansion.

Experimental methods and results are described in Ref. 19 to 21. The experimental set-up is based on an interferometer, the so-called experimental Fizeau system, which allows the measurement of small variation in the coefficients of thermal expansion. Using this technique, the thermal expansion coefficient of PyC, SiC and PyC/SiC-coatings were measured.

9. Density measurements

Density measurements can be performed by a variety of methods but, under remote handling conditions, one of the most valuable (see e.g., Ref. 22) because of its rapidity and easy handling, is the sink-float method (Ref. 23). It is based on the principle that a linear density gradient can be established when two liquids, having different density, are properly mixed in a glass column. By introducing carefully calibrated standards, the correspondence between the height of the column (density of the liquid) and the density of the standards can be established. Afterwards, the density of the unknown samples can be easily determined by interpolation, reading the equilibrium position in the column, thus providing a reliable, easy to handle and very accurate method. The organic mixture consists, typically, of a-bromo-naphthalene, density about 1.49 g/cm³, and 1,1,2,2-tetrabromo-ethane, density about 2.97

g/cm³. Consequently, only densities lying between these two values can be measured. The apparatus is very stable and it meets the temperature and dimensional requirements of BS 3715 and ASTM D1505 – 60T.

In Fig. 5 the density as a function of the column height, as determined by using 6 different glass standards (crosses), is shown together with the density of three different types of active ²⁴⁴Cm-doped. It can be seen that a linear gradient could be established. This gradient could be maintained by holding the column at a constant temperature by immersion in a water bath. From such curves the density of the active glasses could easily be determined as a function of the cumulative dose, by just observing the position of active samples in relation to the standards.

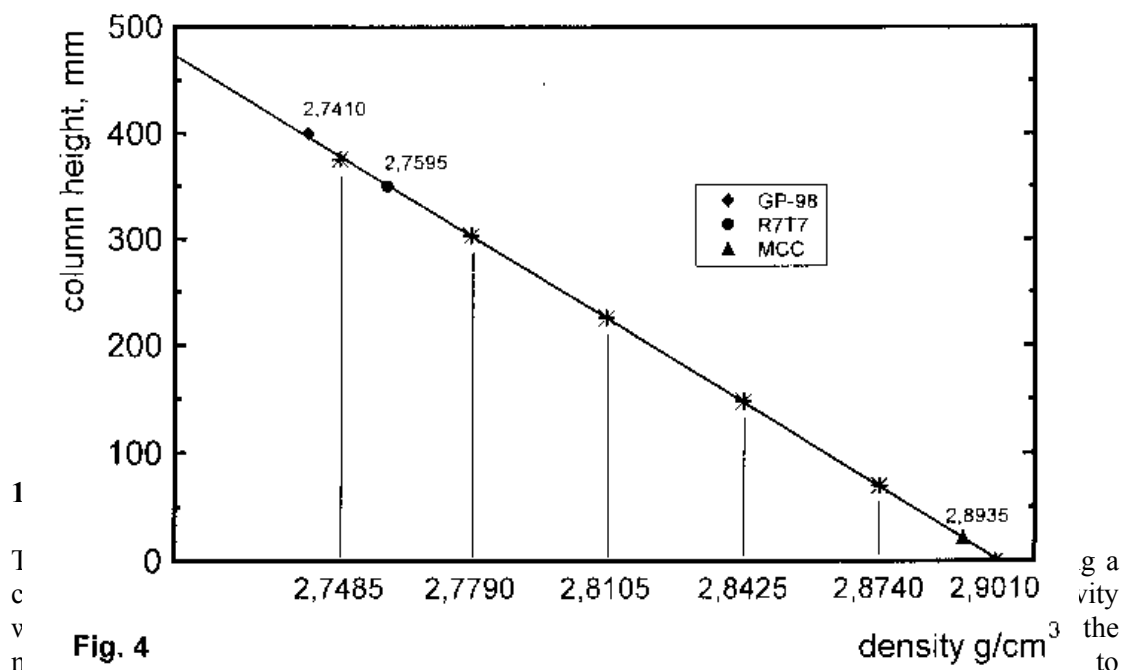


Fig. 4
 irradiation effects. On the other hand, the temperature variation across the buffer layers (estimated thermal conductivity about 1 W.m⁻¹.K⁻¹) can be most important, as well as the changes expected due to the gas release from the kernel (thermal conductivity of Xe ≅ 0.02 W.m⁻¹.K⁻¹).

11. Gen IV-Recommendations

A Gen-IV Fuel and fuel Cycle Project Management Board meeting was held to define PIE-techniques and the fuel properties that should be considered. In Table 1, the PIE-recommendations for Gen IV fuel development for the Very High Temperature Reactor (V/HTR) are gathered.

PIE both after irradiation and after KÜFA-tests	Scanning Electron Microscopy
Fuel Element Deconsolidation	Transmission Electron Microscopy
Fission gas and CO/CO ₂ -release	Electron-Probe Micro-Analysis
Anisotropy (comparison before and after irradiation)	Mean strength and Weibull's modulus of SiC
Dimensional changes	Thermal conductivity of the buffer layer
Irradiation induced creep of PyC	Density measurements

Elastic properties	KCMI (Kernel/Coating Mechanical Interaction)
Poisson's ratio (in creep)	Gamma spectrometry
Ceramography	Burnup determination

Table I: PIE-recommendations for Gen IV fuel development for V/HTR

CONCLUSIONS

In the present paper, some of the most important PIE-techniques historically and presently installed in hot cells have been briefly described in connection to modelling needs. One of the most important issues is constituted by the need of having representative samples to measure some of the key properties of coated particles. The broad field of characterisation (PIE) of fuel elements has not been treated. Standard measurements like gamma spectrometry, ceramography, burn up determination, etc., have not been considered in the present paper. From the micro-analytical techniques, only EPMA has been discussed. One useful technique, Secondary Ion Mass Spectrometry (SIMS) has not been mentioned but it is considered to be able to deliver valuable results in the future.

References

1. G.K.Miller, D.A. Petti, D.J.Varacalle and J.T.Maki, J. Nucl. Mater. 295 (2001) 205-212
2. H.Kostecka, J. Ejton, W.de Weerd and E.H.Toscano, Technical Meeting on "Current Status and Future Prospects of Gas Cooled Reactor Fuels, IAEA, Vienna, 2004
3. H.Kostecka, J. Ejton, W.de Weerd and E.H.Toscano, IAEA 2nd International Topical Meeting on High Temperature Reactor Technology, Beijing, 2004
4. Ch. Bauer, Technische Notiz IRW-TN-27/82, KFA-Juelich, 1982
5. J.C. Brokros and A.S. Schwartz, Trans.Met.Soc. A.I.M.E. 239 (1967)
6. G.E. Bacon, J. Appl. Chem. 6 (1956) 477
7. M. Pluchery, Mat. Res. Bull. 9 (1974) 251
8. P.A. Tempest, Carbon 16 (1978) 171
9. X. Bourrat, High Temperature Reactor School, Cadarache, France, 2002
10. J.C.Bokros, Nature 202 (1964) 1004
11. J. Holder and C. Braun, Measurement of the reflection anisotropy factor (DAR) on pyrolytic carbon, CR DMG 34/1972 or DPTN/302
12. Koss (Seibersdorf OSGAE) Doc. No. 901588 issue B, Doc. No. G.A. A13464
13. Bomar, Gray and Eatherly, Carbon coating Using Plane-Polarised Light, 885-897, 1968
14. Grübmayr and Schneider, An optical method for the determination of the local anisotropy of pyrolytic carbon layers and graphite, KFA RW597, 1969
15. Förthmann, H.Grübmaier, H.Kleykamp and A. Naoumidis, Proc. of IAEA Symposium on Thermodynamics of Nuclear Materials, Vienna, 21-25 October 1974.
16. G.W. Horsley, B.E. Sheldon and K.S.B.Rose, J.Nucl.Mater., 34 (1970) 345-347
17. A.G.Evans, C.Padgett and R.W.Davidge, J. Am. Ceram. Soc. 56 (1973) 36
18. K. Bongartz, E. Gyarmati, H. Schuster and K. Täuber, J. Nucl. Mater. 62 (1976) 123-137
19. A.F. Pojur, B. Yates and B.T. Kelly, J.Phys. D: Appl.Phys, 5 (1972) 1321
20. A.F. Pojur and B. Yates, J.Phys. E: Sci. Instrum. 5 (1972) 63
21. O.Pirgon, G.H.Wostenholm and B. Yates, J.Phys. D: Appl.Phys, 6 (1973) 309
22. Hj. Matzke and E.H.Toscano,
23. M.A. Knight, J. Am. Cer. Soc. 28 (1945) 297
24. D.G. Martin, private communication

FRACTURE SURFACE ANALYSIS OF AN IRRADIATED HAFNIUM CONTROL ROD BY METALLOGRAPHIC REPLICAS

Domizzi G., Ciriani D., Vigna G., Chomik E., Iorio. A.
U.A. Materiales. C.A.C. Comisión Nacional de Energía Atómica
Av. Gral Paz 1499. (B1650 KNA)
San Martín. Buenos Aires, Argentina

ABSTRACT

Two types of metallographic replicas were tested to reproduce the fracture surface of a failed hafnium rod. The deposition of replicating material was done in the alpha-gamma hot cell at CELCA facility in CNEA. The observation of replicas, in electronic microscopy, with low magnifications allows the identification of crack beginning even though the high activity of the rod damaged the replicas material, At high magnification, fracture hydride particle prints were observed on the fracture surface.

1. INTRODUCTION

In 1999, a task group was established to evaluate the cause of failure of hafnium control rods removed from service. Part of the work consisted in assessing the fracture mechanism and, for this purpose the observation of fracture surface was considered as a necessary step. At that time, the CELCA facility of CNEA did not count with scanning electronic microscope (SEM). For this reason, the preparation of metallographic replicas was considered as a valid alternative to observe the fracture surface by a conventional SEM.

The Materials Laboratory of CAC counts with a team which have wide experience in replica preparation on non irradiated components, but never before this technique had been tested on hot materials in CNEA. As a possible cause of failure of hafnium exposed to water corrosion at high temperature could be hydride precipitation, the Hydrogen Damage Group undertook the preparation of replicas and observation by SEM.

2. EXPERIMENTAL

The work has been developed in two stages:

The first stage was to evaluate the effectiveness of two different materials for replicating the fracture surface of non irradiated material. With this purpose, samples extracted from a hafnium rod were electrolytically hydrided and heat treated to produce a uniform hydride distribution [1]. Then, curved compact toughness specimens (CCT), analogous to ASTM E-399 standard [2], were machined from one section of the as received rod and from samples with 22 and 426 ppm of hydrogen. The specimens were fatigue pre-cracked and then tested until fracture in a servohydraulic universal testing machine. The observation of fracture surface of these specimens allowed the classification of different characteristics of fatigue and stable propagation of hafnium fracture, with and without hydrogen. Replicas of the fracture surface of non irradiated material were made in order to be compared with those of failed rod.

The second stage consisted in replicating the fracture surface of the irradiated rod at the beginning of the failure. A section of 27 cm long of the failed rod was introduced in the hot cell (Fig. 1). There, a small section of 50 mm in the axial direction by 4 mm in the circumferential direction by the rod thickness (3 mm) was cut and placed on a grooved plate, with the fracture surface side up in order to facilitate the replicating procedure.

The replicating materials used were:

1) An acetyl cellulose film of Bioden R.F.A. The replicating procedure is as follows: the plastic film is cut out into a little larger size than the specimen fracture surface. A small amount of methyl acetate, used as solvent, is dropped and spread on the surface. Before its volatilization, the film is laid over the specimen. After a few minutes the solvent is volatilized and the replica is carefully stripped off the specimen by picking it up with a tweezers. As this operation process had to be reproduced inside the hot cell on the fracture surface of the failed rod, a little device was constructed which facilitated the replica film manipulation with the telemanipulator. The device consisted of a metallic block (Fig. 2) where a slice of rubber, then two cellophane films and finally the Bioden film were deposited and attached with a clip. The rubber function was to act as a soft material between the replica and the hard metal, to ensure that all significant features of the fracture surface could be duplicated. The cellophane prevented the adherence of acetyl cellulose to the rubber.

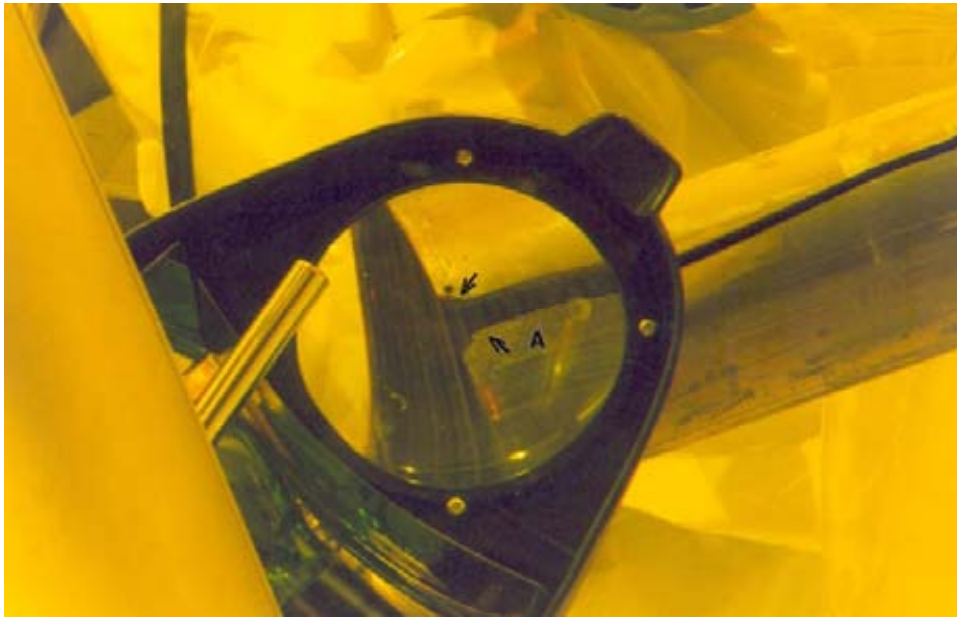
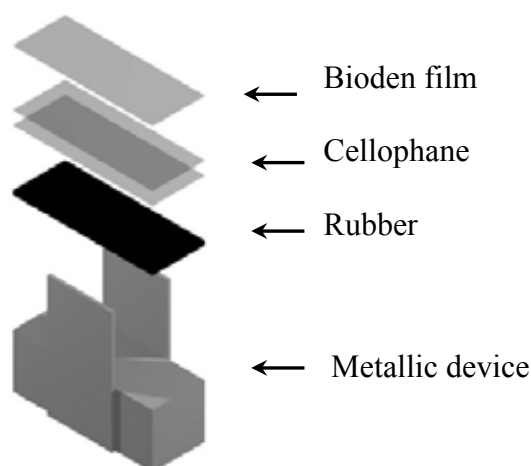


FIG. 1. Section of the failed hafnium rod. The arrows point a semicircular hole with a punch mark.

2) Technovit 3040 is a fast curing methyl methacrylate-based resin, it consists of two components: powder and liquid. The mixing ratio is approximately 2-3 parts per volume : 1 part per volume liquid. As the mix is viscous two barriers 2 mm thick made of plasticine mounted on steel plates were attached to both sides of the fracture to prevent it from pouring out of the fracture surface. Before pouring the Technovit on the surfaces, some drops of Pioloform (polyvinyl butyral) were deposited on the surface according to Siemens recommendation [3].



In order to remove the radioactive and foreign materials from the fracture surface and make clean replicas, several Bioden replicas were discarded, until the activity was low enough to take them out of the hot cell. Then, the Bioden extracted replicas were placed on a mirror and observed in the optical microscope to verify that they had not been damaged during stripping and the whole area of the sample had been properly copied. Both replicas, Bioden and Technovit were put into a vacuum evaporating equipment to receive gold evaporation which formed a conductor film in order to be observed by Scanning Electron Microscope out of hot cell.

3 RESULTS

3.1. Non irradiated material.

Fig. 3 shows the fracture surface of a non irradiated specimen without hydrogen. Fig. 3-a) corresponds to the fatigue pre cracked section with transgranular cleavage regions separated by areas of tearing and a few transgranular ductile zones. In the stable propagation zone (Fig. 3-b) transgranular ductile regions are bordered by small dimples and tear ridges, which is indicative of extensive ductility, similar to that observed in [4].

Fig. 4. corresponds to the specimen with 426 ppm of hydrogen. Both zones, fatigue and stable propagation present similar characteristics that the un-hydrised material but the aspect of the fracture is brittle due to the cracking of hydride clusters.

Bioden replicas seem to copy the fracture surface better than the Technovit replicas. With low magnification the fatigue zone was well differentiated from the stable propagation in the Bioden replicas but not so much in the Technovit replica (Fig. 5). The fracture surface of stable propagation. is rougher than that of the fatigue zone.

Fig. 6 is an example of Bioden replica made on the fracture surface of the specimen with 426 ppm, a) corresponds to the fatigue zone and b) to the stable propagation. As replicas are the negative of fracture surface, the negative of the photos are shown because they represent more accurately the fractograph of the specimen.

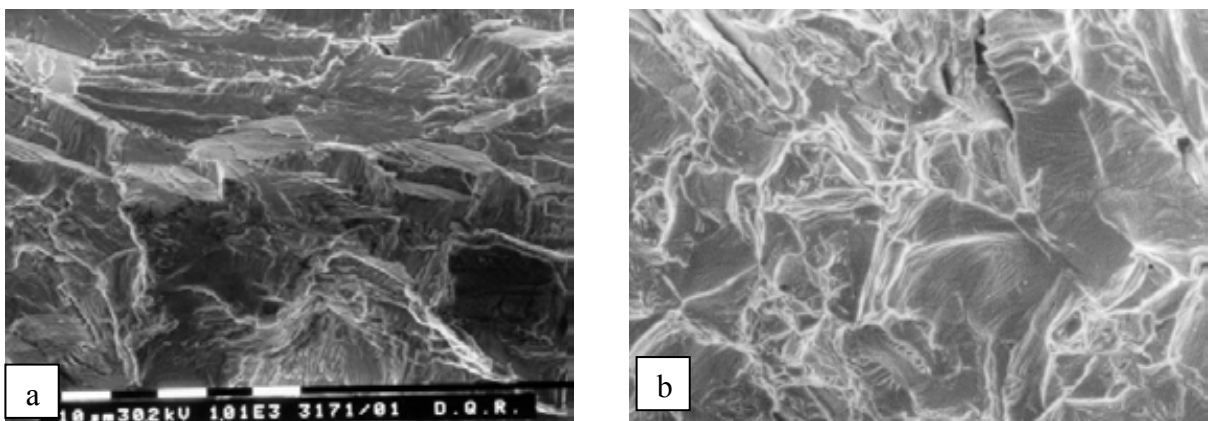


FIG. 3. Fractographies of non irradiated material without added hydrogen, a) Fatigue precracking zone: transgranular cleavage fracture containing cleavage feathers ; b) Stable propagation zone: transgranular ductile fracture with ripples, tearing and dimples.

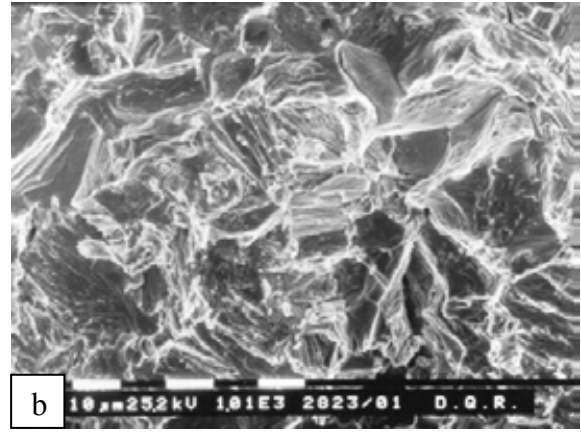
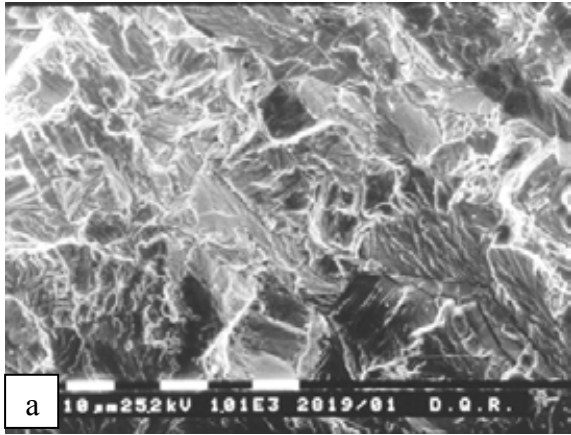


FIG. 4. Fracture surface of the sample containing 426 ppm. Brittle regions corresponding to cracked hydride clusters are observed in both zones: fatigue (a) and stable propagation zones (b).

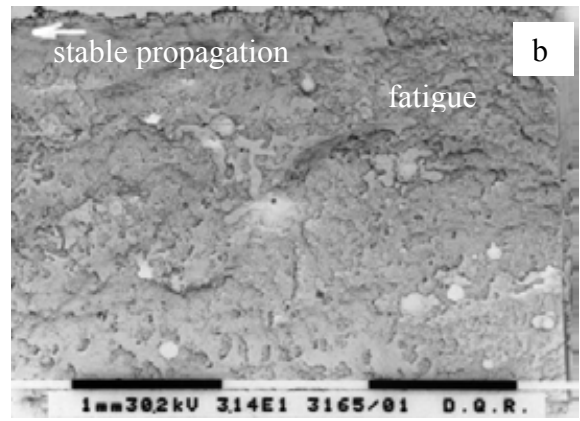
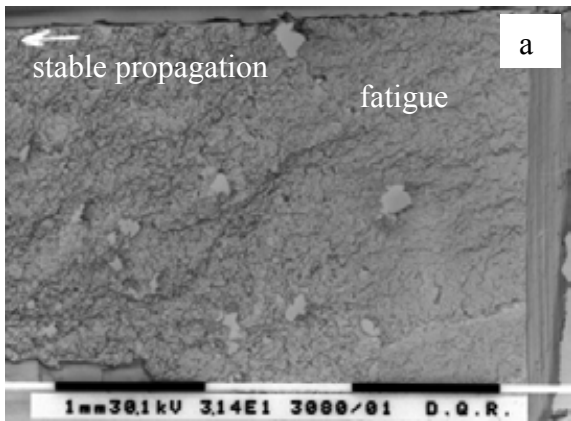


FIG. 5. Replicas made on the fracture surface of non irradiated non hydrided specimen. a) Bieden, b) Technovit.

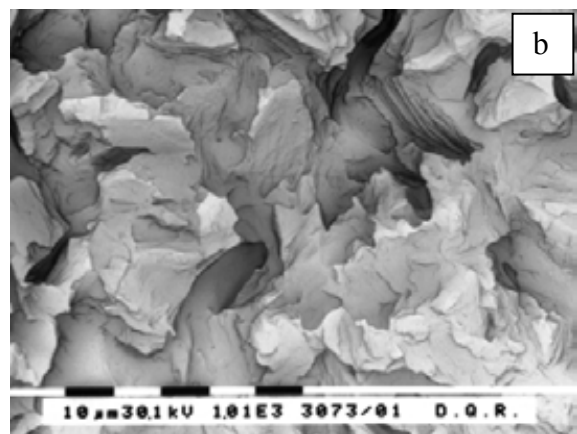
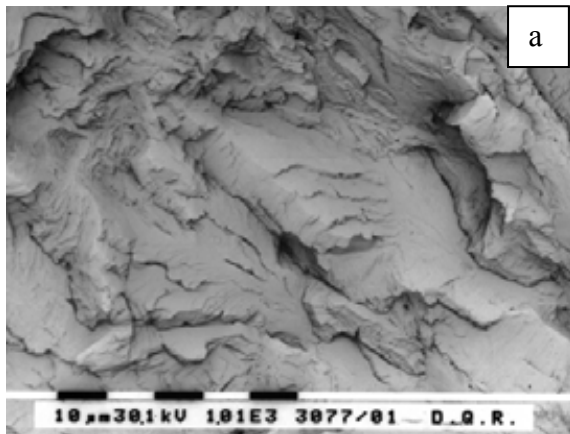


FIG. 6. Bieden replica made on the fracture surface of non irradiated specimen with 426 ppm. a) fatigue zone, b) stable propagation zone

3.2. Irradiated Material

Fig. 7 and 8 show the Bioden and Technovit replicas, respectively, obtained on the fracture surface of the failed rod. The location of the origin of the crack (pointed by the arrow) could be determined by the presence of a fibrous zone. As can be seen in the photograph of the rod at the beginning of the failure (Fig. 1) this region had a semicircular hole, where a mark was produced by a punch in order to fix the bolt that fastened the rod to the stainless steel plug.

As the rod was rolled over the stainless steel plug and irradiation reduced the rod diameter, circumferential stresses were developed through the wall. Under this condition the punch mark acted as a stress concentrator and could enhance the hydrogen diffusion and subsequent precipitation.

Replicas of the fracture were observed with higher magnification looking for prints of cracked hydrides. Fig. 9 shows a detail of the Bioden replica near the fracture origin. Some brittle zones can be observed that may have been produced by hydrides cracking. In the same Figure some marks pointed by the arrows are attributed to irradiation damage of the cellulose.

Any mechanism of fracture involving fatigue is rejected because the replicas show a fracture surface too rough compared with that of fatigue pre-cracked specimens.

4. CONCLUSIONS

The replication technique represented a valid alternative to observe fracture surface of a failed irradiated rod in Scanning Electronic Microscope outside the hot cell.

The methodology of replicating fracture surface was developed on non- irradiated fractured specimens and implemented inside hot cell using telemanipulators.

In spite of the damage that irradiation produced on the cellulose and the resin material, the quality of the replica was good enough to allow the crack origin identification and some details of fracture surface.

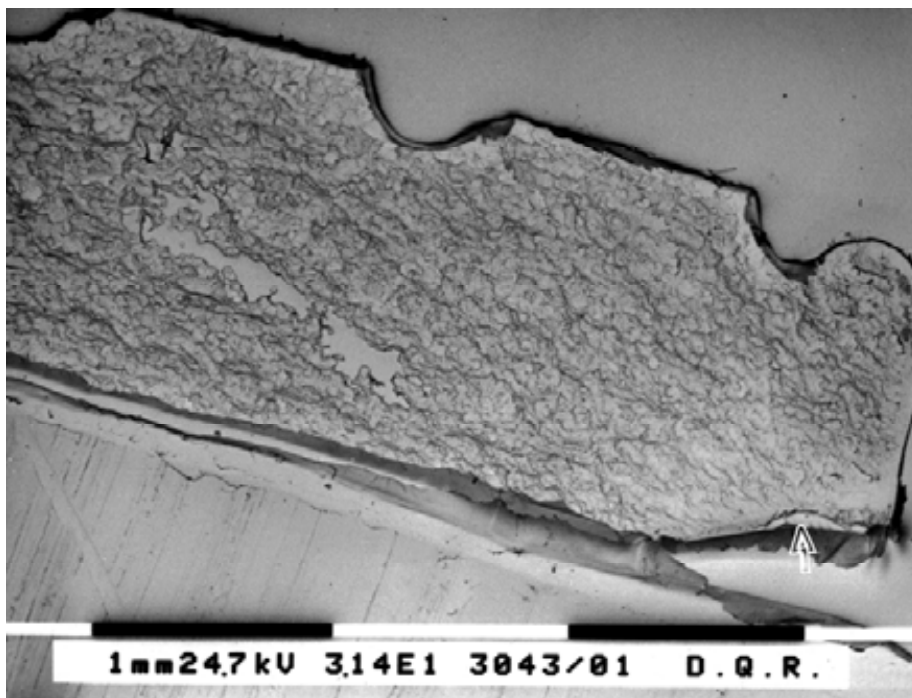


FIG. 7. Bioden replica of the fracture surface of the failed rod

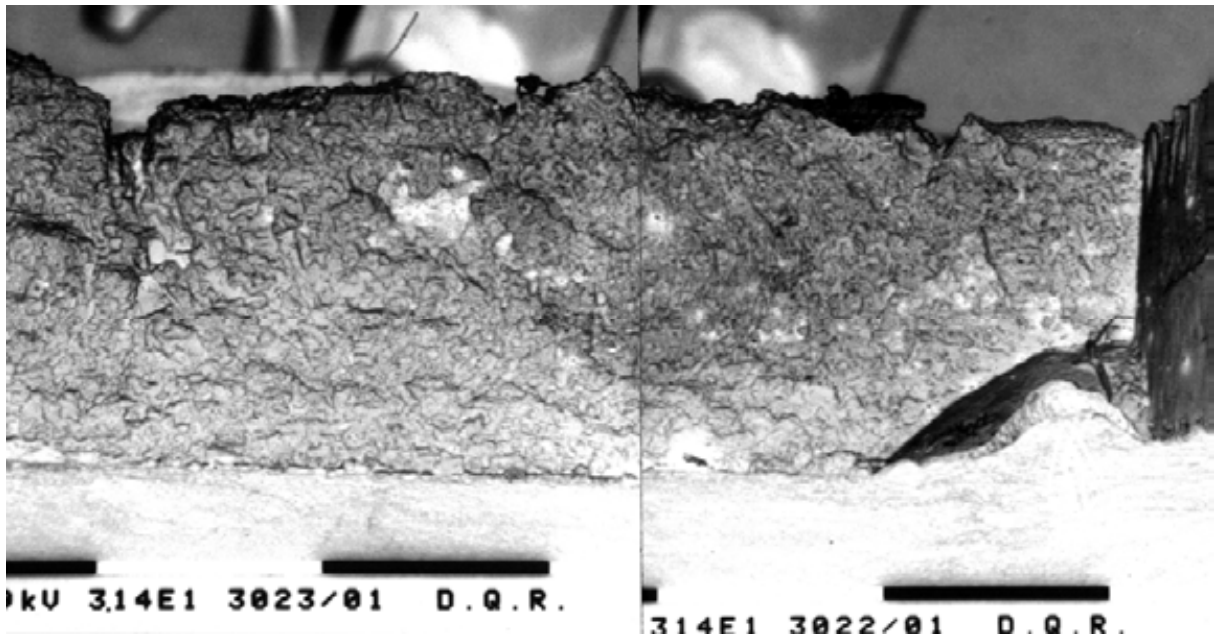


FIG. 8. Technovit replica of the fracture surface of the failed rod

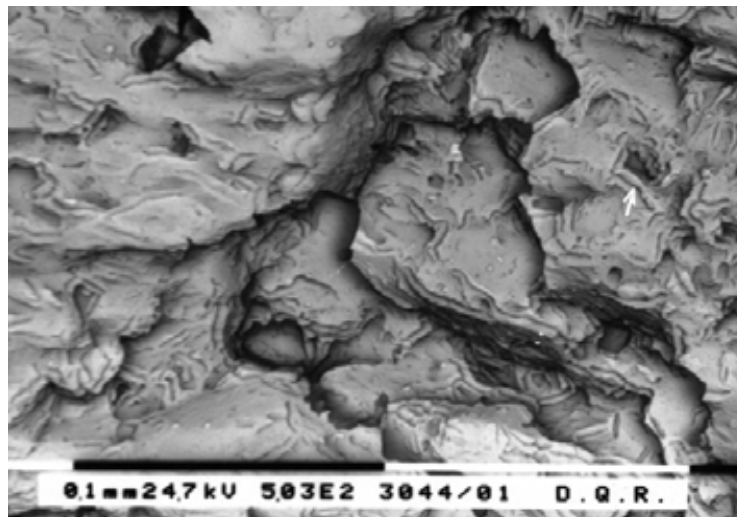


FIG.9. Detail of the fracture surface of failed rod near the origin of crack. Arrow points the damage produced on the replica by the irradiation.

REFERENCES

- [1] Domizzi G., Vigna G., Chomik E., Ciriani D., Iorio. A. "Effect of irradiation and hydrogen concentration on fracture toughness of a hafnium control rod". Technical Meeting on "Hot Cell Post Irradiation Examination Techniques and Poolside Inspection of Water Reactor Fuel Assemblies" 27-30 November 2006 Buenos Aires, Argentina
- [2] Test Method for plane strain fracture toughness, ASTM Standard e 399-93.
- [3] Siemens KWU. NT11, Maussner Erlangen, 24.9.99.
- [4] M. Habermann, H. Kaiser and H. Kaesche. Zeitschrift für Metallkunde. **84**-12 (1993) 832..

EFFECT OF IRRADIATION AND HYDROGEN CONCENTRATION ON FRACTURE TOUGHNESS OF A HAFNIUM CONTROL ROD

Domizzi G., Vigna G., Chomik E., Ciriani D., Iorio. A.

U.A. Materiales. C.A.C. Comisión Nacional de Energía Atómica
Av. Gral Paz 1499. (B1650 KNA)
San Martín. Buenos Aires, Argentina

ABSTRACT

Hafnium, among other applications, is used for the production of control rods of nuclear reactors since it is an excellent absorber of neutrons. Besides good mechanical properties, it presents very high corrosion resistance, mainly at high temperatures. However, like other elements of group IV B (Zr and Ti) hafnium can absorb H (or Deuterium) at high temperatures. The precipitation of hydride particles during cooling produces embrittlement, loss of ductility or toughness decrease. Hafnium rods exposed to radiation during service in reactors suffer irradiation embrittlement too.

In this work the effect of hydrogen on the loss of the tenacity or cracking resistance was studied and compared with the properties of a failed hafnium control rod removed from the reactor. Different amounts of H were introduced, by electrolytic charge on the non-irradiated material. A uniform hydride distribution was obtained by heat treatment. The resistance to the crack propagation was evaluated by means of fracture mechanics tests.

The used methodology covers the determination of J-resistance curve (J-R curve) for the condition where the crack propagation is ductile, while in the case of occurring unstable propagation the stress intensity factor, KIC, was used.

1. INTRODUCTION

Hafnium is one of the materials used in the production of control rods of nuclear reactors. Besides its capability as thermal neutron absorber, hafnium has also good mechanical properties and high resistance to corrosion in water at high temperatures.

In spite of the good properties above mentioned, the rods could suffer certain deterioration during their life in the reactor owing to two fundamental causes: a) irradiation, that produces an embrittlement of the material and an increment in their density because of the transformation into tantalum, b) pick up of hydrogen, produced by the corrosion reaction: $\text{Hf} + 2\text{H}_2\text{O} \rightarrow \text{HfO}_2 + 4\text{H}^+$.

As other elements of the group IVb (Zr, Ti), Hf can dissolve hydrogen at high temperature; when the material cools down to room temperature the solubility falls notably and the excess of hydrogen precipitates as hydride particles [1]. The solubility of H in Hf at 300 °C is 0.6 at %. or 33.3 ppm in weight, according to the formula of Edwards and Veleckis [2]

$$\log_{10} N_H = 0.317 - 1459 / T \quad (1)$$

where

N_H is the atomic fraction of hydrogen in hafnium,

T is the temperature in K.

The presence of precipitated hydrides in Hf produces embrittlement with subsequent ductility loss [3] and toughness resistance decrease [4].

In this work the effect of hydrogen on fracture toughness and of a non-irradiated Hf rod was studied and compared with that of an irradiated failed rod.

2. EXPERIMENTAL WORK

The material used was extracted from two hafnium rods of 3 mm wall thickness and 80 mm diameter whose chemical compositions measured in ingot are shown in Table 1. Samples were cut from two different positions along the axial direction of the “hot” rod:

Position 1: 27 cm, exposed to the highest neutronic flux, near the origin of the crack in the bottom end of the bar

Position 2: 12 cm, at 100 cm of the bottom

Table 1. Chemical composition of Hafnium rods (ppm ,excepting Hf and Zr).

	irradiated	non irradiated
Hf	>95.3%	>95.3%
Zr	>4.5 %	3.20%
Al	<100	<35
C	<150	40
Cl	<500	--
Co	<10	<5
Cr	<200	<20
Cu	<100	<25
Fe	<750	--
H	<20	<5
Mg	<600	<10
Mn	<50	<20
Mo	<20	<5
N	<50	30
Nb	<100	<50
Ni	<50	<25
O	300-1500	--
Pb	<20	<5
Ta	<200	<100
Ti	<100	<25
Si	<50	28
U(gral)	<10	<10
U-235	<0.07	0.006

First, hydrogen was introduced in sections of 20 mm (axial direction) by 25 mm (circunferencial direction) cut of the non-irradiated material. For this purpose, the surface oxide film was removed in a solution of 45 nitric acid ml, 45 lactic acid ml and fluorhydric acid 6 ml). The charge of hydrogen was carried out in an electrolytic cell with solution of H₂SO₄ 0. 05M in water at 90-95°C. Using this hydriding method, a hydride layer is formed on the sample surface, whose thickness is enough to exceed the required hydrogen concentration.

Then, each section received one heat treatment whose objective was to get the hydride particles uniformly distributed inside the thickness The temperature of this heat treatment was chosen according to the expected hydrogen concentration using Equation (1). The samples were cooled down in air to prevent the formation of a non-hydrided layer under the hydride layer. After the first heat treatment, the remaining hydride layer was eliminated by grinding with emery paper and a second heat treatment was carried out with slow cooling (more approximated to the cooling of a rod in service) in order to produce a hydride distribution similar to that obtained during in service cooling . The heat treatment duration was calculated according to the thermal diffusion Equation (2) of Reference [5]:

$$D_H = 6.968 \cdot 10^{-3} \exp(-10,600/RT) \text{ cm/s}^2 \quad (2)$$

Where

R is the gas constant 1.987 cal/mol K
T is the temperature in K

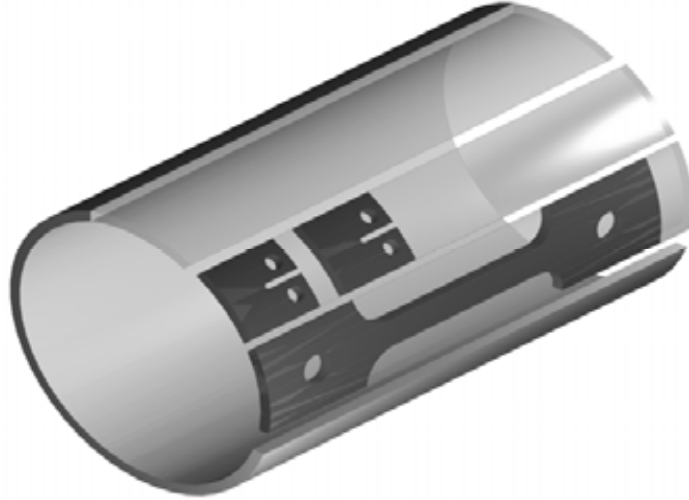


FIG. 1. Specimens extracted from the rod and used in tension and fracture mechanics tests.

The temperature and duration of heat treatments are presented in Table 2. Except for sample 4, that was encapsulated in atmosphere of argon to avoid oxidation, the other treatments were performed in the chamber of the furnace with static vacuum (10^{-2} torr. approximately).

Table 2. Heat treatments of hydrided samples.

Sample	First heat treatment		Second heat treatment	
	Temperature (°C)	Time (h)	Temperature (°C)	Time (h)
1	346 ± 4	6.25	375 ± 3	0.3
2	393 ±	20	390	
3	551 ± 2	18	574	0.5
4	747 ± 3	16	*	

*In this sample the hydride layer was quite dissolved during the first heat treatment and the sample was cooled in furnace.

The microstructure and hydride distribution was observed by optical microscope after polishing the samples in the same solution used for oxide film dissolution. The metallographic preparation of hot material was made inside the glove box facility at the CELCA laboratory in the Atomic Center Ezeiza, CNEA. The observations were made in a Leitz MM 5 RT optical microscope with remote control.

Then, specimens for tensile and fracture mechanics testing were prepared from the hydrided material and the irradiated rod, Figure 1 shows the orientation of specimens along the rods. The specimens were cut inside alpha beta gamma hot cell (CELCA) using a CNC milling machine Minuth electronic system. This task was made with the work place drowned under oil to reduce the production of volatile contaminants.

The mechanical properties of the materials were obtained through a tensile test according to the ASTM E8M-99 standard [6]. The fracture toughness was assessed following the usual methodology [7 to 9] that includes the determination of J - integral - resistance curve (J-R curve), for the condition when the crack propagation is ductile, and the stress intensity factor K_{IC} when the embrittlement is sufficient to prevent stable crack propagation. The curved compact specimens are similar to those used in the analysis of pressure tubes embrittlement of CANDU reactors. This methodology is applicable to the

present study because the dimensions of Hafnium rods and CANDU pressure tubes are alike. These tests were made with a servohydraulic - Universal testing Machine MTS 810, inside the beta gamma hot cell.

3. RESULTS

Figure 2 shows the microstructure of the irradiated rod at position 2 (a) and the non irradiated with 425 ppm. Hydride particles (white) are mainly distributed around grain edges. Position 1 could not be analysed because of the high dosis it had.

Table 3 reports the tensile test results, measured at room temperature. Specimens of irradiated material at Position 1 fractured outside the gage length because of the high embrittlement produced at this position by irradiation. Fig. 3 shows the stress - strain curves.

Table 3. Mechanical properties

	Non irradiated	irradiated Position 2	irradiated Position 1
Tensile strength (MPa)	475	796	> 717
Yield strength (MPa)	372.6	630	> 717
Percent elongation (%)	30.5	11.1	0
Reduction of area (%)	38.1	21.9	0

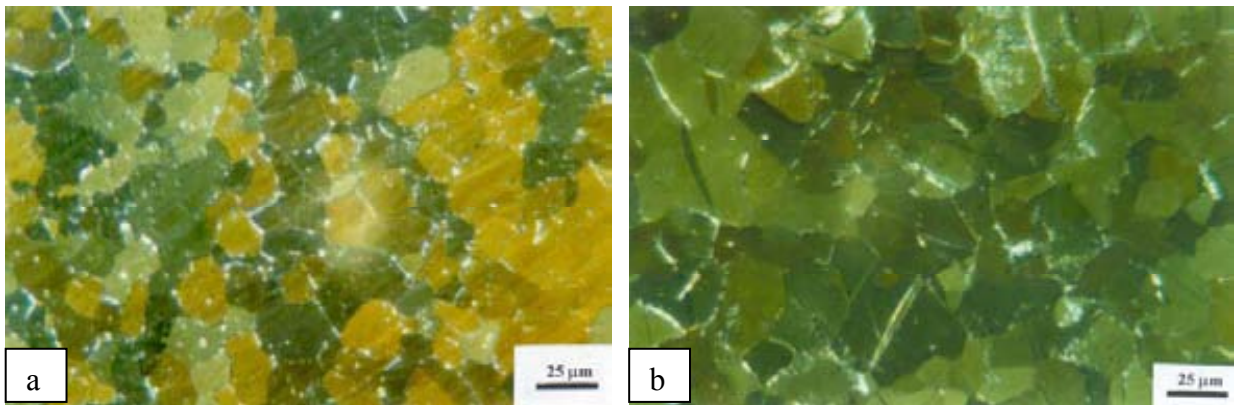


FIG. 2: Micrographs of Hf rods. a) irradiated position 2. b) non irradiated with 425 ppm of hydrogen

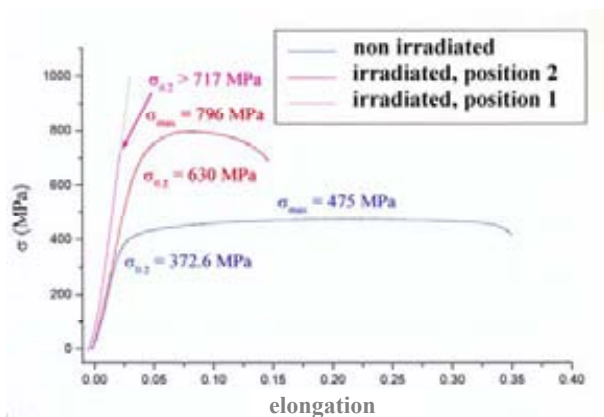


FIG. 4. Stress-elongation curves.

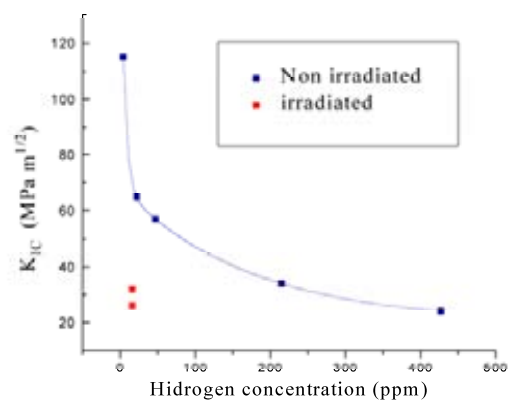


FIG. 5. Fracture Mechanics results.

Figure 5 presents the stress intensity factor as a function of hydrogen concentration for the non irradiated rod and the values measured for the irradiated rod at position 2. These results show that

hydride precipitation reduces the fracture toughness considerably. Nevertheless, in the hot material, the irradiation seems to play an important role in the material embrittlement. The embrittlement percentage can be calculated as:

$$F = (K_{IC}^0 - K_{IC}) / K_{IC}^0 \quad (3)$$

where

K_{IC}^0 is the stress intensity factor of the material without hydrogen and without irradiation. (115 MPa m^{1/2})

K_{IC} is the stress intensity factor of the material with hydrogen (71.7 MPa m^{1/2}) or with hydrogen and irradiation (29 MPa m^{1/2}).

Then, F of the “hot” material is 76.5% while F of the “cool” material with similar hydrogen concentration is 37.6%. If both effects are considered as additive, the irradiation (in position 2) adds 38.9% to the embrittlement caused by hydrides, i.e. both effects are in the same order. As the material of position 1 is even brittle than in position 2, the fracture test could not be carried out.

4. CONCLUSIONS.

The tensile and fracture test, performed on a “hot” hafnium rod and a similar “cold” rod hydrided until different hydrogen concentrations, showed that the failure was originated by a combined embrittlement effect produced by irradiation and hydride precipitation.

REFERENCES

- [1] M.H. Mintz. Hafnium-Hydrogen. Solid State Phenomena, 49-50, 331-354, 1942.
- [2] R.K. Edwards y E. Veleckis. Thermodynamic properties and phase relations in the system H-Hf. J, Phys, Chem, 66, 1657-1661, 1989
- [3] S.M. Seelinger y N.S. Stoloff. The effect of hydrogen on deformation and Fracture Processes in Hafnium. Metall. Trans.15, 1481-1484, 1971
- [4] M. Habermann, H. Kaiser y H. Kaesche. Wasserstoffeinfluß auf mechanische Eigenschaften von IVa- Metallen. Z. Metallkd, 84-12, 832-838, 1993.
- [5] Solid State Phenomena. **49-50**, 8 (1992).
- [6] Standard Test Method for Tension Testing of Metallic Materials [Metric], ASTM Standard E 8M 99
- [7] Standard Test Method for J_{IC} , A Measure of Fracture Toughness, ASTM Standard E-813-89.
- [8] Standard Test Method for Fracture Toughness of CANDU Pressure Tubes, COG-89-110-, September 1989.
- [9] Test Method for Plane Strain Fracture Toughness, ASTM Standard E 399-93.

SESSION 4: INTERNATIONAL PROJECTS AND DATA BASE

Chairpersons

Jean Noirot (CEA, France)

Jeffrey A. Fortner (USA)

THE EUROPEAN HOTLAB PROJECT AND ITS FUTURE, WITH EMPHASIS ON ITS INTERNET CATALOGUE

L. Sannen*, **W. Goll****, **J.Y. Blanc*****, **C. Verdeau*****

* SCK-CEN Mol, Belgium,

** Areva NP GmbH, Erlangen, Germany

*** DEN/DSOE, Bâtiment 121, CEA/Saclay, 91191 Gif-sur-Yvette Cedex, France

ABSTRACT

Started more than forty years ago, a conference on « Hot Laboratories and Remote Handling » is held each year in Europe to gather this scientific community. The 6th Framework Programme of the European Commission funded a “HOTLAB” project in 2004 and 2005 and this boosted new actions. HOTLAB included 19 organizations from 13 countries and was concentrated around three tasks. First a public web catalogue was designed to present capabilities of European hot laboratory facilities, their post irradiation examination techniques, and to provide contact points. This catalogue is based on the IAEA PIE database, but is focussed on European hot laboratory needs and extended by new tools. It is easy to use and to update, is open to public inclusive European hot laboratories that did not participate in the HOTLAB project. Secondly a report was written that surveys the present status of European hot laboratories and their future needs and evolution trends. This report is based on an enquiry at individual participating laboratories and was reviewed by some stakeholders (utilities, fuel vendors or safety organizations). The third task dealt with issues concerning nuclear transports and casks, as transports are essential for cooperation between labs and material testing reactors (MTR). About 20 technical data sheets on casks were added on the web catalogue. This paper presents the HOTLAB project with an emphasis on what was achieved in the web catalogue. HOTLAB should be considered as a starting point for more cooperative actions between hot laboratories and a way to enhance education and skills on nuclear materials research and laboratory techniques. New proposals have been and will be made for continuing collaboration through personnel exchanges, round robin tests, continuing work on transport issues, improving website and links with MTR. They represent the next steps towards more European integration in this field.

1. THE PANORAMA OF HOT LABORATORIES IN EUROPE

There are more than twenty national research hot laboratories in Europe, working for a safer and more economic production of nuclear energy and on technological and medical applications of radioisotopes. Most of them were built in the sixties when nuclear energy was beginning to develop. Since then, remotely operated research tools were continuously developed, implemented and applied. They supported successfully the implementation of nuclear power plants as demonstrated by the present day outstanding performance of European nuclear power plants.

The panorama of European hot laboratories has evolved as years were passing by [1]. On the one hand, as conventional reactors were performing very well, research in the area was decreased. In some countries, nuclear energy was abandoned or limited. This resulted in an appreciable downsizing of national hot laboratories. Some have already or are being closed down or considerably reduced, e.g. the Risø hot laboratory in Denmark and the Forschungszentrum Karlsruhe (FzK) hot laboratory in Germany. Economic optimisations have

also driven nuclear companies to reduce or concentrate their laboratories, as in France or in England. This trend was enhanced by more stringent requirements of regulatory authorities, leading to either refurbishing or closing aging facilities.

On the other hand, more than a third of western European electricity is provided today by conventional reactors and will still be for some decades, even in countries where a nuclear moratorium or phase-out has been decided (Sweden, Spain, the Netherlands, Germany, Belgium). Some other countries (Finland, Romania, France, Lithuania) are showing signs of a renewed interest for nuclear energy, e.g. to be more independent from oil or natural gas or decrease CO₂ production. This context will be favourable for hot labs with a need for more R&D on new fuels, core vessel steel studies, expertises and radio-isotope production.

The evolution is also noticeable in the field of examinations in hot cells, with higher demands for advanced research tools, to feed data to new simulation. Staff is evolving, with new but smaller generations of nuclear scientists, leading for a demand in nuclear training system. As a result, hot laboratories are facing more complex loads in a more stringent environment (i.e. more costly research assignments), with reduced funding and a restricted new crew.

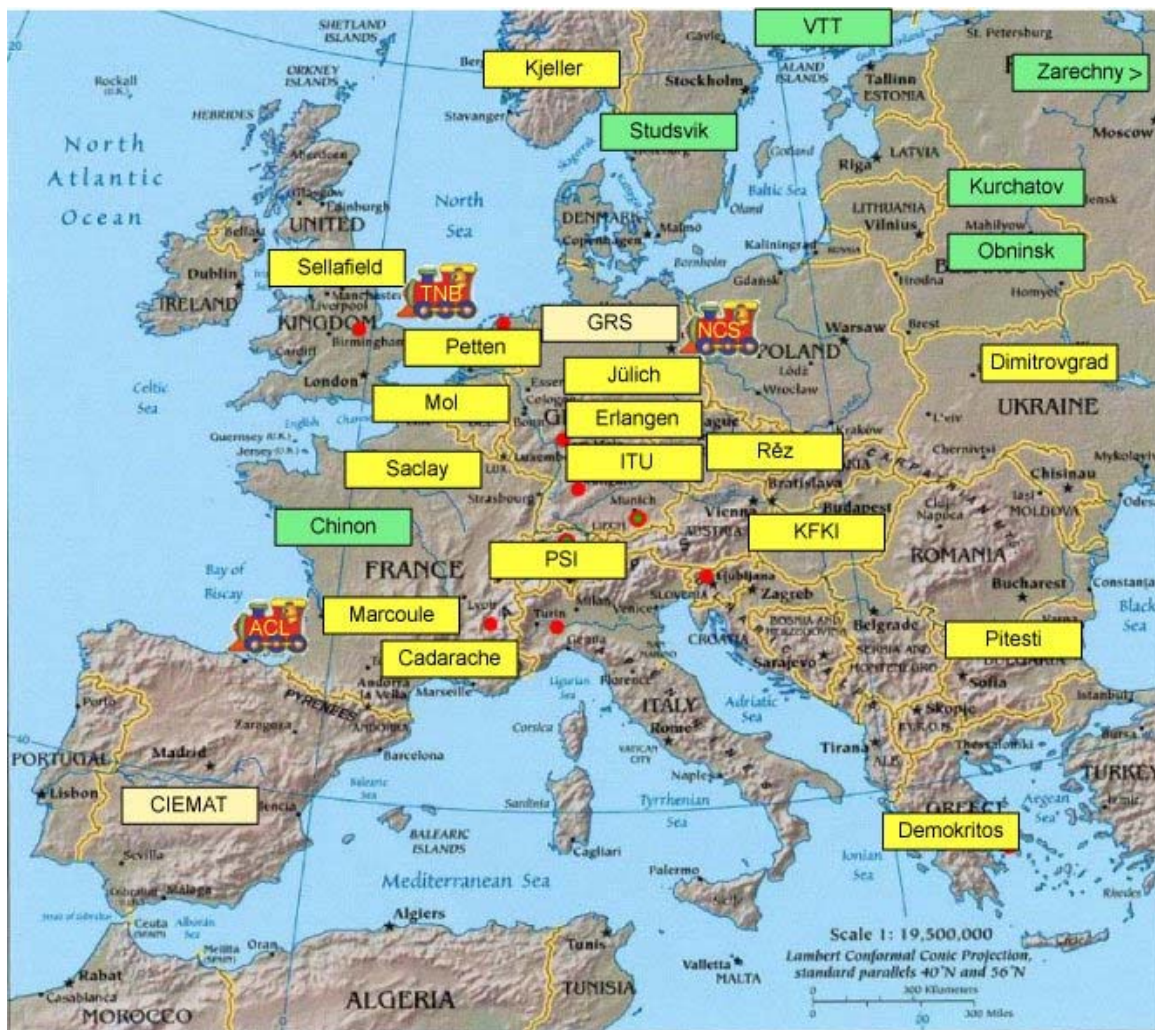


Figure 1: Map of main European hot labs. In yellow, HOTLAB participants with hot cells, in light yellow participants without hot cells. Trains are representing HOTLAB transport companies. In green, European hot laboratories which do not participate to HOTLAB.

2. THE HOTLAB PROJET

To gather this scientific community, a European Working Group on « Hot Laboratories and Remote Handling » was started more than 40 years ago (before 1963). On a yearly basis, a meeting is held hosted by a different laboratory each time.

But it was felt that this was not sufficient. So, inside the 6th Framework Programme of the European Commission, a Coordinated Action (CA) called “HOTLAB” was funded from January 1st, 2004 to June 30th, 2005 to launch new actions [2].

HOTLAB included 19 participating organizations from 13 countries. The consortium listed below gathered most European organizations disposing of hot laboratories. Additionally the project was supported by the nuclear supply industry for exploration of the needs, and by European nuclear transport companies for transport issue.

SCK•CEN – Nuclear Research Centre	Mol, Belgium
AREVA NP GmbH	Erlangen, Germany
CEA – Commissariat à l'Energie Atomique	Paris, France
PSI – Paul Scherrer Institut	Villigen, Switzerland
NRG – Nuclear Research & consultancy Group	Petten, The Netherlands
IFE – Institutt for energiteknikk	Kjeller, Norway
KFKI – AEKI – Atomic Energy Research Institute	Budapest, Hungary
BNFL – British Nuclear Fuel plc Nexia Solutions Ltd	Warrington, United Kingdom
CIEMAT – Centro de Investigaciones Energéticas Medioambientales y Tecnológicas	Madrid, Spain
NCSR – National Centre for Scientific Research "Demokritos"	Athens, Greece
FZJ – Forschungszentrum Jülich	Jülich, Germany
JRC – ITU – Institute for Transuranium Elements	Karlsruhe, Germany
NRI – Nuclear Research Institute Řež plc	Husinec-Řež, Czech Republic
RAAN – SCN – Nuclear Research Institute	Pitești, Romania
SCC – RIAR – Research Institute of Atomic Reactors	Dimitrovgrad, Russia
A.CL - Cogema Logistics	Saint-Quentin-en-Yvelines, France
NCS – Nuclear Cargo + Service GmbH	Hanau, Germany
TNB – Transnubel N.V.-S.A.	Dessel, Belgium
GRS – Gesellschaft für Anlagen- und Reaktorsicherheit mbH	Köln, Germany

Figure 2: Participants to the HOTLAB project.

The project was managed by a Steering Committee, with Leo Sannen, from SCK•CEN, Mol, Belgium as coordinator. The main events during the contract were two plenary meetings, during which all partners presented technical papers and gathered for their respective Core Team Meetings. According to available funding, the HOTLAB project was divided in three work packages (WP), managed by Core Teams.

WP1 was aimed at creating a highly dynamic internet based catalogue of hot laboratories incorporating appropriate functionality, allowing laboratory representatives to manage their part of the catalogue, and providing end-users with research tools provisions to retrieve information in this catalogue. This database both serves as easy input tool for consortium partners, both to build up the present day inventory and to maintain it in the future, and as an easy-to-use working platform (e.g. to search for synergies) and dissemination tool, also beyond HOTLAB project and consortium.

WP2 was focussing on present and future needs of experimental facilities for radiotoxic materials research to be operational in hot laboratories. The idea was to realize a survey of actual hot laboratory infrastructure solicitation by present research programmes. Then, starting from the estimated future research programmes being developed or announced, the survey has assessed the future near and long-term evolution of needs of existing hot laboratory infrastructures. These needs included:

- On the short term, material research, present day fuel licensing, reactor operation safety (e.g. Reactivity Initiated Accident, Loss Of Coolant Accident, higher burn-up, coolant chemistry), all aspects of the fuel cycle including fuel back end (i.e. spent fuel and waste conditioning, interim storage, up to final storage), non-proliferation, safeguards, medical & environmental activities,
- On the long term, new reactor types (e.g. Generation IV, like High Temperature Reactors, Accelerator-Driven Systems), new fuels, advanced fuel back end strategies (e.g. partitioning and transmutation), new nuclear applications (e.g. medical ones).

Inputs from relevant parties from outside the consortium (e.g. fuel vendors, utilities, safety authorities) were considered as very important to validate this survey.

WP3 was dealing with transportation of nuclear materials, which is essential to a closer co-operation between hot laboratories. And nuclear transportation is not a simple task at the moment. Hence an inventory on convenient nuclear transport means was also included in the digital platform. It contained both the characteristics of available transport casks and their application possibilities. The same functionality for remote updating by the competent actors and search-driven consultation by end-users has been incorporated.

3. THE INTERNET WEBSITE AND CATALOGUE

The HOTLAB web portal is in operation at <http://www.sckcen.be/hotlab/> (see Figure 3). It collects all project information with a home page accessible for general public that contains general information on the project and on events organized by the project that are open for participants from outside the consortium, and restricted pages for members only. Inside the portal, the project has designed a web application hosting a catalogue of hot laboratory facilities (<http://www.sckcen.be/hotlab/catalogue/>). This part is fully open to public.

To perform that, the Post Irradiation Examination Facilities Database (PIE), hosted by the Integrated Nuclear Fuel Cycle Information Systems at <http://www-nfcis.iaea.org/> was used as a starting point, with the help of V. Onufriev from IAEA in Vienna.

Our catalogue is hosting all European hot laboratories from the HOTLAB consortium, but the few laboratories which have not participated in the project have been invited to introduce their facilities in this catalogue as well (e. g. Studsvik and EDF Chinon).

HOTLAB - Microsoft Internet Explorer

Fichier Edition Affichage Favoris Outils ?

SCK·CEN.be **HOTLAB** **Sixth Framework Programme** 2006 Oct 23

[Restricted pages](#)
for members and partners
(password required)

[Contact](#)

Partners

1. SCK·CEN
2. FANP GmbH, Germany - FRAMATOME ANP
3. CEA, France
4. PSI, Switzerland
5. NRG (Petten, the Netherlands)
6. IFE, Norway
7. AEGK, Hungary
8. BNFL, United Kingdom
9. CIEMAT, Spain
10. Demokritos, Greece
11. FZ-Jülich, Germany
12. JRC-ITU, Europe
13. NRL, Czech Republic
14. RAAN-SCN, Romania
15. SCC-RIAR, Russia
16. Cogema Logistics, France
17. NCS, Germany
18. TNB, Belgium
19. GRS, Germany

Hot laboratories and remote handling

Plenary meeting 2006 (September 19-21), Jülich, Germany

[More info...](#)

HOTLAB - European Hot Laboratories Research Capacities and Needs

A European 6th FrameWork Programme Project


Abstract

The HOTLAB project was a coordination action sponsored by the 6th Euratom Framework programme, within the Euratom research and training programme in the field of nuclear energy (Contract number: F16O-CT-2003-508850).

The general objective was to assess the European hot laboratories research capacity and its aptitude for supporting the nuclear industrial and research community both at present and in the future. The ultimate goal is to preserve appropriate nuclear research infrastructure in Europe by combining the best available competences at the highest quality.

Within its 18 months running time, extending from January 2004 till June 2005, the collected European hot laboratories made up the inventory of the present research capabilities, in the form of an internet based highly dynamic permanent database, including the inter-laboratory transport facilities as well. An assessment of the present and future needs of nuclear research in terms of infrastructural facilities completed the basis to build upon a common strategy for durable integration in the longer term.

Results

- A digital web-based catalogue on hot laboratory facilities that can be maintained remotely by designated operators and that allows online searching by the general public
<http://www.sckcen.be/hotlab/catalogue/>
- The assessment of the present and future needs concerning the experimental techniques to be operational in hot laboratories
 [FI08HOTLAB022.pdf](#) (939 Kb)
- An up-to-date digital European transport cask inventory for inter-laboratory material exchange, presently confined to certified type B

Démarrer Paper2_Blanc_TCH_JAE... **HOTLAB - Microsoft In...** 10:54

http://www.sckcen.be - HOTLAB - Catalogue - Facilities - Microsoft Internet Explorer 10:54

Fichier Edition Affichage Favoris Outils ?

SCK·CEN.be **HOTLAB - Catalogue** **Sixth Framework Programme** [Hotlab main website](#) [Editors login](#)

[Home](#) | [Facilities](#) | [Statistics](#) | [Map](#)

Facilities (All topics...) (All techniques...) (All countries...)

1 2 3 >> >|

Facility name	Country	# of techniques
1. BNFL Windscale	United Kingdom	25
2. CEA - ATALANTE - alpha workshop, lab., analyses, transuraniens, reprocessing studies	France	20
3. CEA - LECA - Irradiated Fuel Examination Laboratory	France	17
4. CEA - LECT - Laboratory for Study of Irradiated Components	France	33
5. CEA - LEFCA - Laboratory for Study & Experimental Manufacturing of Advanced Fuels	France	10
6. CEA - STAB - Conditioning, Treatment & Cleaning Facility	France	7
7. Ciemat	Spain	17
8. EDF - AMI Chinon - Irradiated Material Workshop	France	23
9. Framatome ANP GmbH - Erlangen	Germany	22
10. FSUE-RIAR - Research Institute of Atomic Reactors	Russian Federation	37

[Privacy Statement](#) - [Disclaimer](#) webmaster@sckcen.be

Démarrer Paper2_Blanc_TCH_JAE... **HOTLAB - Microsoft Inter...** **http://www.sckcen.b...** 10:55

Figure 3 & 4: Front page of HOTLAB site and list of facilities (first page)

Hotlab main website
Editors login

Home | Facilities | Statistics | Map

Facility (All topics...) (All techniques...) (All countries...) Print this facility

General Additional info Techniques

FSUE-RIAR - Research Institute of Atomic Reactors
Russian Federation

Auger Spectroscopy	Hardness testing	Rod Puncture
Burnup	Helium Analysis	Scanning Electron Microscopy (SEM)
Clad Creep Testing	Hydrogen Analysis	Secondary Ion Mass Spectrometry (SIMS)
Clad-fuel Gap	Image Analysis	Spacer Grid Geometrical Parameters
Density	Impact testing (e.g. Charpy)	Specific Heat
Dilatometry	Leak Test	Tensile Testing
Eddy Current Testing (Integrity)	Length and/or Diameter	Thermal Diffusivity
Electric Resistance	Length and/or Diameter	Transmission Electron Microscopy (TEM)
Fracture Mechanics	Mechanical Fatigue Testing	Visual Examination
Fuel Assembly Top Nozzle Spring's Parameters	Micro Gamma-scanning	X-ray Diffraction
fuel rod volume	Optical Microscopy	X-ray Radiographs
Gamma Scanning	Oxide Thickness	Youngs Modulus
Guide Channel Inner Diameter		

Relaxo Statement - Disclaimer webmaster@sckcen.be

Hotlab main website
Editors login

Home | Facilities | Statistics | Map

Facility (All topics...) (All techniques...) (All countries...) Print this facility

General Additional info Techniques [Print this technique](#) [All techniques for this lab](#)

SCK•CEN - Laboratory for High and Medium Activity (LHMA)
Belgium

Technique name	Transmission Electron Microscopy (TEM)
Topics	Non-fuel materials PIE
Description	Transmission Electron Microscope
Equipment	JEM 3010 UHR Analytical TEM
Features	Specifications: High tension: 300 kV Resolution: 0.20 nm STEM capabilities and EDS detector.
Type of specimen	3mm discs of thickness <100µm
Standards	
Test parameters	
Measured parameters	Visualisation of the crystallographic structure, defect structure (e.g. dislocations) and morphology of the different phases in solids down to the atomic level. Local chemical composition.
Calculated parameters	Dislocation density.
References	
Contact	
Comments	
Related info&documents	

Links

<http://www.sckcen.be/microstructure/Infrastructuur>

Figures 5 & 6: List an detail of examination techniques available in a given hot laboratory

The catalogue gives the list of facilities (figure 4), the way to contact them, their general conditions for receiving nuclear materials, and the list of examinations they are able to perform (figure 5). Each examination has a file (figure 6) giving detailed description of how it is performed (machine, materials, standards, references). It is easy to make a search either from the list of facilities, countries, examination techniques, topics (fuel, radioisotopes, etc) or even by a name. The data can be easily printed, and laboratories have the possibility to add a brochure on their laboratory or on a technique, by a simple link in the page.

An important feature is that the base will be going on after the completion of the project, hosted by SCK-CEN in Mol. Its remote character allows it to be maintained in future, hence to serve as a basis for integration on the longer term.

4. PRESENT AND FUTURE NEEDS FOR HOT LABORATORIES

The general objective of HOTLAB was to assess research capacity of European hot laboratories and its aptitude for supporting nuclear industrial and research community at present and in the future. Results of WP2 are compiled in a global report, which encompasses both present and future needs, and provides a description of the actual scope and workload of hot laboratories and an estimation of near and long-term research objectives.

The work was structured in the following way. First, an enquiry was realized in all European hot cell laboratories that compiled their present situation by listing key themes, experiments, and infrastructure needed to achieve their individual objectives. It revealed that hot cell work could be categorised into the following areas: fuel cycle, material research, manufacturing, technical support, and new reactor systems. Main areas were gathered into key topics and supplemented by lists of techniques and infrastructure available in hot cells. Then, the Core Team tried to describe current trends in technique utilisation, elaborate general comments and preliminary conclusions and realized a first assessment on future needs. Doing that, it was considered as more efficient to gather present situation and future trends in the same document. Finally, the draft report was reviewed by all HOTLAB participating organisations and by specialists belonging to other companies, such as Belgonucléaire, AIB-Vinçotte Nuclear, Tractebel Engineering, Institute of Isotopes Co., Ltd. (Hungary), Cernavoda Nuclear Power Plant, National Agency for Radioactive Waste (Romania), Areva NP GmbH (Germany), Areva NC, EDF SEPTEN (France) and VGB PowerTech eV.

The main conclusions in regard to the present hot cell situation are as follows:

- Present hot cell work scope encompasses a broad range of activities dedicated to support safe and economic operation of nuclear power plants including initial work for new reactor systems. Emphasis is presently on work related to fuel cycle and life time assessment of structural core components (e.g. pressure vessel steel and steel internals)
- Though the total number of hot cell laboratories in Europe has been substantially reduced, many laboratories are now indicating high levels of utilisation of basic analytical techniques (e.g. optical microscopy, Transmission Electron Microscopy, Scanning Electron Microscopy, Microprobe Analysis (EPMA), X-ray diffraction, etc), thus implying a limited capacity to absorb any significant increase in demand.

Conclusions in regard to future hot cell utilisation:

- Near term utilisation of hot cell laboratories will be characterised by a continuation of present work scope, since the technique of commercial reactors will not change

significantly. Nevertheless, continuous efforts exist to improve safety and economy of reactors resulting in an ongoing utilisation of hot cell laboratories. On the other hand, one has to be aware that new programmes cannot be mathematically added to old ones without balancing changes of the utilisation level.

- Long-term utilisation of hot cell laboratories is strongly dependent on research scenarios towards new reactor systems envisaged to supplement or replace the present fleet of commercial reactors. However, it should be taken into account that most of future programmes will be organized on a world basis, and not on a 'European only' basis, which implies sharing tasks with non-European partners. This also means that future hot cell utilisation is even more dependent on progressing technical and political developments.

All these conclusions are broadly in agreement with the aims of European Research Area (ERA) initiative which aims to prevent duplication and fragmentation of resources to improve quality of European scientific output.

5. CASK AND TRANSPORT CATALOGUE

As for WP1, WP3 created a public catalogue of nuclear casks. This catalogue is hosted in the same site (<http://www.sckcen.be/hotlab/transport/>) and all relevant partners have been provided with an account and password to insert and edit their casks in an overview of casks available. It can be extended to other cask types, to facilitate exchange of materials between hot laboratories. The web site gives a list of 19 casks (by October 2006) with a detailed file sheet (Figures 7 & 8), contact names and search by cask provider. A useful tool is that a cask can be linked to a laboratory where it can be handled, leading to the hot lab catalogue elaborated by WP1. This link has only been implemented for a few casks.

More generally, activities of WP3 consisted in identification of common needs on transport casks and transport operations. The objective was to provide return of experience on radioactive material transport, to publish different reports concerning good practices either on design of transport cask or on transportation operation, and to initiate appropriate research programs if needed. In this frame, four axes of development were explored: provide exchange of good practices, address lessons learned from incidents or accidents occurring during transport (international data base, experience feedback, recommendations), share feedback on operational procedures (i.e. leak-tightness measurement, methods for radiation emission control), and initiate programs of research & development on specific topics.

WP 3 has identified several work items that seem to be relevant, with regard to the general scope (see Figure 9), but within 18 months, only three items have been achieved.

A code of good practices for measurement of neutron emission around transport packages was achieved. It recommended different techniques to achieve neutron emission measurements around a transport cask and gave relevant requirements for choosing an appropriate neutron dosimeter and achieving measurements in the best manner with regard to the sensitivity needed for that purpose.

Http://www.sckcen.be - HOTLAB - Transport - Cask - Microsoft Internet Explorer

Fichier Edition Affichage Favoris Outils ?

SCK•CEN.be **HOTLAB - Transport**
Sixth Framework Programme

Search

[View a printer-friendly version of this sheet](#)

Home
Providers
Casks
Hotlab main website
Editors login

This cask is referenced by
SCK•CEN - Laboratory for High and Medium Activity (LHMA)

RADIOACTIVE MATERIAL TRANSPORTATION PACKAGING DESCRIPTIVE FILE

BG 18

Provider: TRANSNUBEL	Purpose: Transport package for irradiated fuel rods from PWR and BWR reactors and for irradiated material
--------------------------------	---

CHARACTERISTICS


Type of loads: - Up to 30 fuel rods irradiated or not; heavy metal mass max. 43 kg - UO ₂ rods enriched up to 10 % U235 - MOX rods enriched up to 1,5 % U235 and 12% Pu fissile - Cooling time: min. 6 months	Classification: - Type B(U)F Licensing state: - Certificate: D/4197/B(U)F-05 (Rev.3) valid until 18.01.2008 - Validation: in CH, S, B, F
Mode of loading/unloading: - Vertical loading/unloading in pool - Dry horizontal loading/unloading by docking against hot cell wall	Available accessories: - Different internal arrangements such as baskets, on-site tools, ... - Auxiliary transport means (i.e. basket handling tool, transport frame, lifting beam, bling frame, ...) - Stability plate, drying and control module
Technical assistance provided: <input checked="" type="radio"/> Yes <input type="radio"/> No <input type="radio"/> Not specified	

DESCRIPTION

Main packaging characteristics:
- Total length

Technical assistance provided:
 Yes No Not specified

DESCRIPTION

Main packaging characteristics: - Total length - with shock absorbers: 6.865 mm - without shock absorbers: 5.611 mm - Effective cavity length: 4.550 mm - Effective cavity diameter: 162 mm - Diameter with shock absorbers: 1.200 mm - Diameter without shock absorbers: 775 mm - Weight without shock absorbers: 25 t - Weight with shock absorbers: 26,7 t - Weight in transport condition: 28 t	
Content characteristics: - Maximal activity - Neutron source strength: 1,0 100 n/s - Photon source strength: ca.2,0 1015 Bq/s (according to Energy spectra) - Maximal power for the whole package: 2400 W	Specific characteristics: - The BG 18 is a long cylindrical cask with an internal tight containment, particularly suited for full scale length fuel rods - The transfer of the load under water or against a hot cell proceeds through a shielded rotating plug - The minimum hot cell channel Ø required is 240mm
Mode of transportation: - On site: Dry - On public roads: Dry	References: - Germany (KGG, GKN, ITU) - Sweden: Studsvik - Norway: Halden - Switzerland (KKC, KKB, KKL, PSI) - Belgium (Tihange 1, SCK-CEN)

Contacts: Contacts: TRANSNUBEL S.A. Gravenstraat 73, 2480 Dessel, Belgium
Jurgen SPERLICH - Phone: +32 14 33 11 11; Fax: + 32 14 3189 48 - E-mail: jurgen.sperlich@transnubel.be

Private Statement - Disclaimer webmaster@sckcen.be

Figures 7 and 8: File sheet for a nuclear transport package inside the cask catalogue

Subject	Comments
1 – Exchange of good practices	
<ul style="list-style-type: none"> • Neutron emission measurement 	Results of neutron emission measurements are extremely dependent on the material used and on the location of the measurement point. So harmonized procedures are needed
<ul style="list-style-type: none"> • Contamination measurement 	Radioactive contamination measurements are extremely dependent on the technique used and on the location of the measurement point. So harmonized procedures are needed
<ul style="list-style-type: none"> • Techniques to ensure leak-tightness during transport of unsealed sources 	Different methods and techniques are worldwide in use to ensure leak-tightness during transport on non-sealed sources. Return of experience will be helpful.
2 – Lessons learned from incidents/accidents	Sharing experience feedback on this topic will be advised.
3 – Operational Procedures	
<ul style="list-style-type: none"> • Responsibilities 	Responsibilities of the different persons or organisations involved in a transport shall be defined and harmonized.
<ul style="list-style-type: none"> • Transport documents 	Due to the different practices in use, it will be helpful to harmonize the nature and the content of the different transport documents.
4 – Research & Development on transport of radioactive material	Research programs shall be initiated, especially in this field, in order to increase the knowledge in this area.
<ul style="list-style-type: none"> • Radiolysis phenomena • Characterization of the potential spectra of aerosols released during a transport accident 	

Figure 9: Identification of common needs on the design of transport casks and transport operations and possible topics.

A harmonized radiation protection control procedure for transport packages was written, to specify techniques for measurement of the different radiation emission occurring during a transport: external doses (including gamma as well as neutron emissions) and non fixed contamination levels at the surface of the transport cask. The objectives are to specify very clearly where measurement points have to be located, according to geometry and design of transport casks, in order to have an identical basis if contradictions appear between measurements made by the sender and the receiver.

Recommendations were drawn on techniques to ensure leak-tightness during transport of unsealed sources. This paper gives recommendations concerning: design and construction of different arrangements of internal envelopes contributing to primary containment system, and selection of applicable technique to be used to demonstrate the efficiency of this internal containment system in order to ensure safe transport of unsealed source.

Reports issued from WP2 and WP3 are available on the public part of the website.

6. GENERAL RESULTS FROM HOTLAB

Apart from results detailed above, success of both HOTLAB plenary meetings in Halden in 2004 [3] and in Petten in 2005 [4] was observed by the audience obtained. These meetings enable to discuss HOTLAB roadmap and progress and to have lecture sessions on hot laboratory topics (research and exploitation issues, re-fabrication and instrumentation, Post-Irradiation Examination, infrastructure, refurbishment and decommissioning, wastes, transport and even modelling: which data do code makers need?). Although these annual conferences are more than forty years old, the momentum given by this project was real. Both conferences had a participation of nearly sixty people coming from more than a dozen of countries (to be compared with about forty participants for similar conferences in 1998 and 1999).

Another success is an increase participation of Eastern European countries, such as Russia, the Czech Republic, Romania, Hungary and also Greece for the first time.

The most important thing is the mutual discussions that have been made possible through these common meetings. For instance, when one hot laboratory wants to buy a metallography system adapted to hot cell, contacts have been taken with a foreign laboratory that has just bought such a machine, giving good information about possible manufacturers and the best features to specify. Another example is a laboratory which wanted to buy a very specific electron microscope, and which performed and analysed the call for tender together with a specialist from another European laboratory. Other contacts have been taken to solve the problem of how to evacuate some unused nuclear materials stored in some countries, with practical results.

7. NEXT STEPS TO CONTINUE WITH HOTLAB

This project has always been considered as a starting point [5]. For example, hotlab.eu has been registered as a European web address. The last Steering Committee, in May 2005, decided to propose a follow-up to HOTLAB. But the difficulty is to choose the better tool within the 6th or 7th European Commission Framework Programmes (FP6 or FP7), and to bid accordingly to the call of tenders when they are open. To address that issue two possibilities have been identified: to propose a Specific Support Action (SSA) for the last FP6 call on April 11, 2006, called HOTLABSSA, or to propose an Integrated Infrastructure Initiative (I3) for FP7 starting in 2007, called HOTLABINST.

7.1 HOTLABSSA

Due to a limited amount of time and expected funding, the SSA proposal [6] was submitted with only five participants, either because they were highly involved in HOTLAB or particularly interested in one of the proposed tasks: SCK in Belgium, AREVA NP GmbH in Germany, RAAN-SCN in Romania, PSI in Switzerland and CEA in France.

The proposal was divided in four tasks or WP:

- To improve the existing website created in the HOTLAB coordinated action by giving more general information on hot laboratories especially for non specialist people (What is a hot laboratory? What it is used for? How to be protected from radiation or from contamination? What is the final destination of wastes?) and making the web site more visible and accessible by search engines.
- To list all the inter-laboratory tests comparisons (round robin) that could be carried out within the future I3 Project, to choose one of them and to launch the procedure for its practical realization (technological, legal and transport aspects). It will aim at improving the validation test methodologies applied hence improving the quality,
- To list all potential themes of collaboration where personnel exchanges between the different hot laboratories involved in the future I3 project could be implemented and to launch the procedure for practical realization of one of them (technological, legal aspects),
- To prepare the future I3 project by organizing some intermediate meetings and by finalizing the future FP7 proposal within a Topical Information Meeting which could be organized in parallel of the yearly conference “Hot laboratories and remote handling”, planned to be held in 2007 in Romania. This meeting would be opened to all HOTLAB participants, but also to other laboratories like VTT in Finland, Studsvik in Sweden, AMI Chinon in France, the COGEMA laboratory in Marcoule, France, etc.

The HOTLABSSA proposal was evaluated by the European Commission as above the threshold, but due to a global lack of funding for this call for tender, no money has been awarded to this proposal. Anyway, the yearly conference was held as usual on September 19 to 21, 2006 at Fz Jülich in Germany and hosted about fifty participants from a dozen of countries and nearly twenty papers were presented.

7.2 HOTLABINST

The proposed project intends to install a framework for the European hot laboratories in order to build a common strategy for future research capacity on radiotoxic materials R&D. It could be an Integrated Infrastructure Initiative (I3), which is a more ambitious tool than a Coordinated Action. It aimed to grow towards integration of laboratories, to achieve the first steps towards inter-operability, towards joint European research activities and towards an integrated strategy for scientific investments.

Some tasks have been identified, starting from previous proposals:

- Networking Activities fostering integration of hot laboratory community (open to non-HOTLAB participants) by organizing yearly conferences, improving the website, improving the report on inventory & needs, exchanging information, know-how cross-fertilization, exchanges of interdisciplinary personnel, professional training, working out on harmonized transport procedures and organizing round robin tests to benchmark the laboratories.
- Trans-national Access inside the hot laboratory consortium will be prepared.
- Joint Research Activities focusing on developments and fabrication of innovative PIE tests improving existing experimental capabilities to address safety issues, ageing management & optimisation of current power plants, fast neutron reactors with associated fuel cycle (sustainability, actinide management), and technologies for high temperature reactors (hydrogen economy). Examples of joint research activities can be: development of sub-size

specimens, clad corrosion & hydriding, study on radiolysis, compatibility of structural metals with liquid metals, etc.

8. CONCLUSIONS

Although limited in time and funding, the HOTLAB contract has been quite a success, with creation of a practical web portal giving useful information on European hot laboratories and technical files on nuclear casks, with some guidelines on good practices for international nuclear transports and with a report analysing future needs for participating European hot laboratories. Success of HOTLAB can also be measured by the audience at both plenary meetings held during the contract, with an increase participation of East European countries. But the most important success cannot be directly measured, because it results from better discussions between foreign laboratories.

All participants agreed in May 2005 to continue the action, in order to increase coordination inside European hot laboratories. A Specific Support Action HOTLABSSA was submitted in April 2006. Its evaluation was above threshold, but no funding was allowed. With the start of the 7th Framework Programme of the European Commission in 2007, a proposal for an Integrated Infrastructure Initiative should be considered. It is a more ambitious tool that can improve the tasks started in HOTLAB (website on examination techniques, ameliorations on international shipments and prospective studies for the hot lab needs), but also include exchange of staff, inter-laboratory tests and improved yearly conferences. If proposed and accepted, it will constitute a new and bigger step towards European integration.

ACKNOWLEDGEMENTS

This paper is indebted to many participants in HOTLAB: D. Gavillet (PSI), L.P. Roobol (NRG), B. Oberlander, H. Jenssen (IFE), F. Gillemot, U. Gabor (KFKI-AEKI), H.G. Morgan, R. Williamson (BNFL, Nexia Solutions), J. Quiñones (CIEMAT), I. Pirmettis (NCSR Demokritos), M. Rödiger, W. Kühnlein (FzJ), E. Toscano (ITU), P. Novosad (NRI), M. Parvan (RAAN-SCN), I. Gontcharenko (SSC-RIAR), D. Ohayon, J.-Y. Gayet (ACL), W. Bergmann, M. Mandla (NCS), J. Sperlich (TNB), F. Lange (GRS), A. Zurita, M. Hugon (EC) and special thanks to Gert Thys (SCK-CEN) who realized the web portal.

BIBLIOGRAPHY

- [1] Blanc J.-Y., "Les laboratoires d'examens", Conference SFEN "Les moyens de recherche en support à l'évolution des réacteurs de recherche", Paris 19-20 October 2005.
- [2] Sannen L. and al., Infrastructures for Nuclear Fission and Radiation Protection Research, HOTLAB – European Hot Laboratories Research Capacities and Needs, FISA-2003, Luxembourg, 10-13 November 2003.
- [3] Proceedings of HOTLAB Plenary Meeting 2004, Halden, Norway, 6-8 September 2004. (ISBN 82-7017-505-6), edited by IFE, Kjeller, Norway.
- [4] HOTLAB Plenary Meeting, 23 – 25 May 2005, Petten, The Netherlands, CD-ROM NRG.
- [5] Sannen L. et al., "European Network on Hot Laboratories (HOTLAB)", FISA-2006, Luxembourg, 13-16 March 2006.
- [6] Verdeau C. et al., "The EU 6th FPW Support Specific Action HOTLABSSA: A new step towards an European Network of hot laboratories", HOTLAB-2006, 19 – 21 September 2006, Jülich, Germany, CD-ROM to be published by FzJ.

STATUS OF THE iNFCIS IAEA PIE FACILITIES DATABASE

Håkon K. JENSSEN / IFE, Norway

Victor INOZEMTSEV, Mehmet CEYHAN / IAEA

Abstract

The number of hot cells in the world in which post irradiation examination (PIE) can be performed has diminished during last decades. This creates problems for countries that have nuclear power plants and require PIE for fuel development, surveillance and safety control. With this in mind, the IAEA initiated the issue of a catalogue within the framework of Coordinated Research Project (CRP) “Examination and Documentation Methodology for Water Reactor Fuel” compiling the PIE Facilities Catalogue, which was published as the IAEA Working Material in 1996 [1]. In 2002–2003, it was converted into a database and updated through questionnaires to the laboratories in the IAEA Member States. In 2005-2006, an interactive mode of the PIE Database was developed that allowed hot-lab managers to modify and amend its content in on-line internet regime at the IAEA Nuclear Fuel Cycle Information System web site <http://www-nfcis.iaea.org/>. The database consists of five main areas describing PIE facilities, i.e. acceptance criteria for irradiated components, cell characteristics, PIE techniques, refabrication/instrumentation capabilities and storage and conditioning capabilities. The content of the database represents the status of the participating laboratories and helps interested Member States to select PIE facilities most relevant to their particular needs. The database can also be used to compare the PIE capabilities worldwide with current and future requirements, as well as provide development incentives for laboratories with limited PIE techniques.

1. INTRODUCTION

The number of hot cells in the world in which post irradiation examination (PIE) can be performed has diminished during the last few decades. This creates problems for countries that have nuclear power plants and require PIE for surveillance, safety and fuel development. With this in mind and according to the recommendation by the Technical Working Group on Water Reactor Fuel Performance and Technology (TWGFPT), the IAEA initiated the issue of a catalogue within the framework of a coordinated research program (CRP), started in 1992 and completed in 1995, under the title of “Examination and Documentation Methodology for Water Reactor Fuel (ED-WARF-II)”. Within this program, a group of technical consultants prepared a questionnaire to be completed by relevant laboratories. From these questionnaires a catalogue was assembled that lists the hot laboratories and PIE possibilities worldwide in order to make it more convenient to arrange and perform contractual PIE on water reactor fuels and core components. The catalogue was published in 1996 as the IAEA Working Material [1].

The proposal to create an international database on PIE facilities/techniques was further discussed at the TM on advanced post-irradiation examination techniques for water reactor fuel held in Dimitrovgrad (2001), Russian Federation. The participants of this meeting agreed to convert the catalogue of PIE facilities into a database. PIE specialists from France, Germany, Norway and Russia volunteered to evaluate the possibility of creating an open database on the IAEA website. The group concluded that the scale of tasks and the number of PIE techniques have significantly increased since the beginning of the time of catalogue development. New materials and designs, including mixed oxide fuel, burnable absorber and other additive fuels, together with corrosion resistant claddings had become more prominent. PIE of lead test assemblies was completed with high burn-up test reactor experiments including re-fabricated fuel rods (made from irradiated commercial rods). Changes in composition, structure and properties of fuel and structural materials are to be investigated and understood in order to calculate, validate and forecast fuel operational margins and safety limits. Common approaches in PIE techniques allow comparison of results obtained in different countries and different laboratories that improve the trustworthiness of data used for fuel performance assessment and licensing. The group of PIE specialists agreed upon following basic principles of the database development: it should not interfere with commercial interests of participating organizations; the database should be regularly updated; all of the interested IAEA Member countries should have access

to the database. All previous activities in the area (e.g. PIE facilities catalogue) should be taken into account and the PIE database should be seen in co-operation with other related programmers and databases on nuclear fuel examinations. During 2002 and 2003, the catalogue was converted into a database and updated through questionnaires to the laboratories in the IAEA Member States.

The PIE specialist group worked under the co-ordination of Mr. V. Onufriev, IAEA, Nuclear Energy Department, Section of Nuclear Fuel Cycle and Materials, until his retirement in 2005. Now Mr. V. Inozemtsev is the administrator of the IAEA PIE database.

Upon recommendations from the PIE group IAEA IT specialist, Mr. M. Ceyhan, implemented and finalized the PIE database for the IAEA Integrated Nuclear Fuel Cycle Information System (iNFCIS) early in 2004. Figure 1 gives the general description of the iNFCIS database system. The database was further developed and improved during 2005. The most important improvement was the organization of interactive on-line access for registered hot-lab managers to edit facility data records. Then all modifications and new entries are checked by database reviewer Mr. H. Jenssen, IFE, Norway, and only afterwards they can be visualized on the iNFCIS web-site. The administrator, reviewer and facility coordinators have different roles and functions to perform that enable the interactive database desired levels of flexibility and reliability.

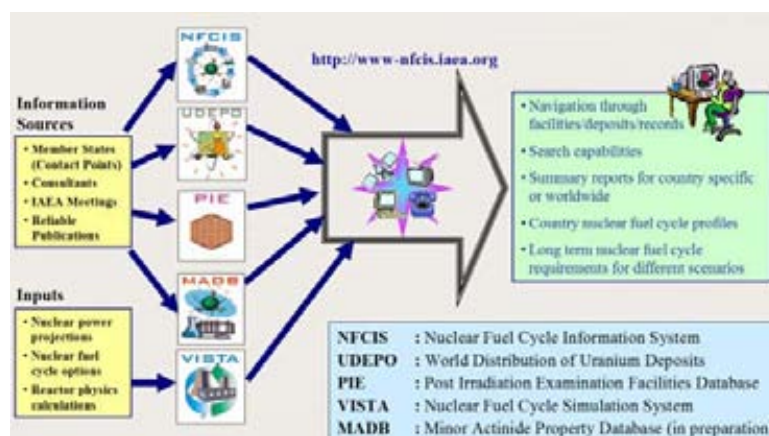


FIG. 1. Integrated Nuclear Fuel Cycle Information System of the IAEA.

2. BASIC FUNCTIONS AND MODULES OF THE IAEA PIE DATABASE

The IAEA operates a number of nuclear fuel cycle related databases and simulation systems for long-term projections of nuclear fuel cycle material and service requirements. Some of the databases and simulation systems are currently available online in iNFCIS web site at <http://www-nfcis.iaea.org/> where the PIE database is located. Their purpose is to provide the IAEA Member States and public users with current, consistent, and readily accessible information for planning activities related to the nuclear fuel cycle. For first login to this database system you must register there in order to get a UserID and a password. Necessary information will be then sent to your e-mail address and you will get access to all iNFCIS databases including the Post Irradiation Examination (PIE) Facilities Database.

The facilities included in the database are listed in the opening page. The selection of countries is linked to the various PIE techniques by the “technique” selection drop list. The general database user has the possibility to check the laboratories that perform for instance neutron radiography. The actual laboratories are listed if a search is performed on a specific technique. Listing of techniques linked to the specific laboratories is possible without extra navigations because the searching tools are always displayed at the database upper part. A user must only choose technique and country from the searching tool to list this information. The home and help buttons can also be reached without extra navigations, i.e. these links or “hand tool” buttons are always displayed in the title bar at the upper part of the database interface.

The database consists of five main areas or topics related to the PIE facilities, i.e. general/cell characteristics, acceptance criteria for irradiated components, available PIE techniques, refabrication

and instrumentation capabilities, and storage and conditioning capabilities. The general topic supplies facility name, the country where the facility is located, contact persons, phone and fax numbers, e-mail address, and link to the company/laboratory web page. The cell characteristics gives the main purpose of the facility, e.g. the specific materials that are examined in the laboratory, the number of cells and information of gamma activity limits for the concrete, steel and lead cells. The dimension of largest cell and the maximum fuel rod length that laboratory could receive are also important information given under this topic. Figure 2 gives an example of the general cell characteristics page of IFE/HRP facility.

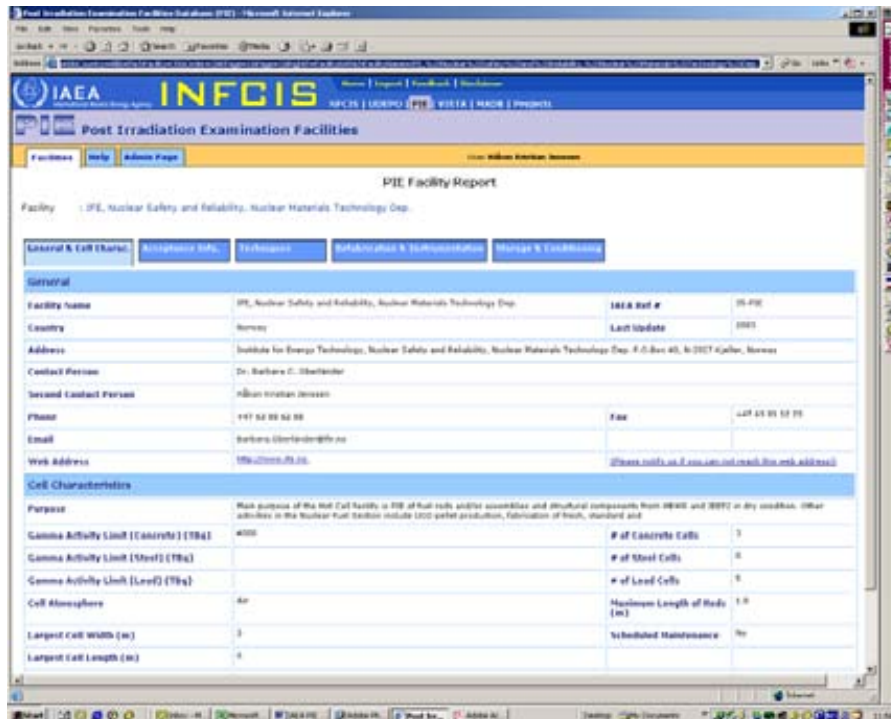


FIG. 2. An example of the General & Cell Characteristics page of the IAEA PIE Database

The acceptance topic gives information about acceptance type and condition, e.g. fuel rods, assemblies or structural components that could be received at the hot lab facility. Transfer mode, maximum cask length and weight are given to support information in relation to external transportations to the facilities. Maximum fuel enrichment and fissile weight, failed rod acceptance, eventual protection packing and a general comment field are also included under this topic.

The main advantages of the present PIE database comparing to the PIE catalogue (1996) are its open internet availability, simple interface, information volume and interactive on-line editing access for registered facility coordinators. Only actual PIE techniques were given in the catalogue, while essential technical PIE details are implemented in the new database. There are several predefined fields for detailed descriptions of the different PIE methods. The field layouts are similar for all different PIE methods to ensure a uniform structure of the database. With the adoption of a uniform database format for all laboratories and details of techniques, it is hoped that the IAEA Member States will be able to use the database to select laboratories most relevant to their particular needs. The database can also be used for comparison of PIE capabilities worldwide with current and future requirements. It is possible that the publishing of the database will provide an incentive for laboratories with limited PIE techniques to increase and improve their own capabilities.

The type of technique is given in the description, i.e. DT or NDT. There is also a field giving a short description of the techniques. One example of text in the description field under neutron radiography examination can be that neutron radiography is applied on irradiated and non-irradiated fuel rod internal components and material test samples. The "form of data presentation" field gives the format of the prepared data acquired under PIE, e.g. digital images and graphs. This is important information

since it influences the dataflow between the facility and the customer, e.g. digital images are possible to exchange by e-mail immediately after data acquisition while analogue images must be sent by traditional post. There are additional fields for general comments, references, equipment, standards and test parameters. The content of the “comment” field is decided by the facility staff involved in the description of the techniques. The test parameters are normally related to the ambient conditions under which the PIE is executed, e.g. sample temperature, atmospheric pressure and amount and strength of $\text{HNO}_3 + \text{HCl}$ acid. PIE details for type of specimen, measured and calculated parameters and features (e.g. measurement accuracy, microscope magnifications, etc.) are given in the respective fields of the various PIE techniques.

Refabrication and instrumentation possibilities of irradiated fuel rod are a separate topic. The information included hereunder is for instance fuel centre-line thermocouple, de-fuelling, welding of instrumented endplugs and pressurisation/leak testing, and other features. The last topic included in the PIE database is about storage & conditioning possibilities. Fields for description in relation to intermediate and long term storage and connection to reprocessing plants are implemented. There is a general reference field and also one for description of encapsulation purposes, e.g. in relation to reinsertion of fuel rod.

3. CONCLUSION

The PIE database was successfully implemented under the IAEA Integrated Nuclear Fuel Cycle Information System (iNFCIS) early in 2004. The iNFCIS database was given a new layout and it is also now possible for the facility coordinators to edit the PIE facilities data on the web page interactively. The number of visitors of the IAEA iNFCIS web site was 3350 and 4887 in 2004 and 2005 respectively. The number of visitors is nearly doubled in 2006 (6590 until 15 November).

The success of the database depends mainly on the quality of the data the IAEA receives from the hot laboratories and how frequent the editing and updating will be performed. The data transfer between the IAEA and the laboratories was in the beginning arranged by using Microsoft “Access” software. All relevant laboratories received an “Access” template with user instructions for filling out the PIE data and sending it back to the IAEA. The “Access” template was not always easy to use according to the lack of feedback from some hot laboratories, which had problems with data input through the “Access” software. These problems are avoided in the new upgraded IAEA PIE database, i.e. the coordinators of the PIE facilities are now able to modify their information directly online through the web site. The implementation of the “interactive” data input mode will ensure that the database should develop in a more flexible manner with minimum cost and efforts for both the IAEA and the PIE facilities. The updating of the IAEA PIE facility database with this new input mode started in 2005. The database usage is verified and ready for utilization and it is hoped that the hot laboratory coordinators will play an active role in developing the information’s contents of the database. The administrator and reviewer roles are to ensure that the coordinators maintain the facility data regularly.

A similar PIE facilities database, but only on the European PIE facilities, was constructed in 2005 at the LHMA-SCK-CEN hot laboratory in Belgium under sponsorship by the European Sixth Framework Programme and European Hot Laboratories Research Capacities and Needs. It also includes transportation issues, e.g. transportation gaskets, license issues, etc. It is necessary to secure the data similarity of the two databases to avoid confusion for the database users due to possible inconsistency of data for the same facility. The owners of the two databases should agree upon how to export and import data from one database to another and the reviewer’s role in this situation could include communication of necessary actions to be performed.

REFERENCES

- [1] INTERNATIONAL ATOMIC ENERGY AGENCY, Catalogue of PIE which can examine LWR fuel and structural components, Working Material IAEA-IWGFPT/46, limited distribution, IAEA, Vienna (1996).

**PART II. PROCEEDINGS OF THE IAEA TECHNICAL
MEETING HELD IN HALDEN, NORWAY 2007**

**SESSION 1: IRRADIATION TESTING TECHNIQUES – EXPERIENCE AND
DEVELOPMENT**

Chairperson

F. Klaasen (Netherlands)

FUEL IRRADIATION TESTING TECHNOLOGY AT SCK•CEN: EXPERIENCE AND DEVELOPMENTS

L. Vermeeren and J. Dekeyser

SCK•CEN, Boeretang 200, B-2400 Mol, Belgium

Abstract. Various instrumented and non-instrumented fuel irradiation test programs have been conducted at SCK•CEN during the past years and are scheduled for the near future. These tests include power transient tests, burn-up accumulation and dedicated irradiations for the detailed study of innovative fuel properties. Among the currently used irradiation devices in the BR2 reactor for fuel testing, PWR loops are operated which can contain up to 9 instrumented LWR fuel rods, as well as dedicated capsules containing a single rod in stagnant pressurized water.

A crucial parameter for all these types of irradiation is the (maximum) linear power generated in each of the test fuel segments. The maximum linear power is determined by measuring the enthalpy change of the cooling fluid passing through the device, corrected for axial/radial heat losses, and complemented by detailed full-core MCNP calculations. The full on-line fuel power determination procedure, including the full MCNP calculations, has been validated by a thorough analysis of a dummy rod irradiation and by several gamma spectrometry and radiochemical analysis campaigns.

Data from self-powered neutron detectors (SPND) placed in the vicinity of the test fuel rods provide reliable absolute thermal neutron flux values (after extensive detector modelling using MCNP), but the conversion from local neutron flux to maximum fuel rod power is not straightforward. However SPNDs have been successfully used to follow the fuel power evolution, especially to obtain more accurate data during the reactor start-up and to assess the effects of changing reactor core geometries.

Experience with instrumented fuel includes the monitoring of the central fuel temperature and of fission gas release by LVDTs positioned in a low flux region and connected to the fuel rods by a capillary tube. An innovative technique for in-pile dimensional measurements based on optical fiber technology is being developed.

For fuel transient tests, a new system is under development to replace the outdated He-3 based system: a combination of a screen with a boric acid solution at variable concentration (VANESSA) with a rotating device to be placed in a 200 mm diameter BR2 channel (RODEO).

1. INTRODUCTION

The BR2 reactor [1] has a long-standing experience in the irradiation of test fuel in various environments, both in steady state and in transient conditions [2]. To monitor the irradiation conditions and to maintain them within the preset margins, the power deposited in the fuel elements (total power and peak linear power) has always been determined on-line. For this purpose the enthalpy change in the coolant of the irradiation device is measured continuously and combined with information on power losses, heating of structure parts and spatial power profiles from mock-up test experiments and from calculations.

Until recently, mainly deterministic 1-D or 2-D codes were used to obtain the necessary theoretical input [3,4]. Due to the severe geometric approximations in the models, the calculated absolute fuel powers deviated significantly from the observed values. However, it turned out that the calculated power distribution over different fuel elements (and structure parts) was quite reliable and a procedure relying only on these relative power data yielded results in reasonable agreement with post-irradiation gamma spectroscopy analyses.

Since a few years Monte Carlo codes (MCNP) are used, describing the BR2 core in great detail for every reactor cycle with its specific core load: the fuel configuration (with the appropriate burn-up values) and the irradiation devices. These calculations not only yield reliable relative values, but also the calculated absolute local power values agree well with data from PIE analyses. Several methods were conceived to combine the experimental and calculated data for the on-line calculation of the local linear power in the fuel elements; their internal consistency and the consistency with gamma spectroscopy data was checked [5].

Complementary information can be obtained from self-powered neutron detectors (SPND) placed in the vicinity of the test fuel rods. They provide reliable absolute thermal neutron flux values (after extensive detector modeling using MCNP), but the conversion from local neutron flux to maximum fuel rod power is not straightforward. However SPNDs have been successfully used to follow the fuel power evolution, especially to obtain more accurate data during the reactor start-up and to assess the effects of changing reactor core geometries.

After a brief description of the fuel irradiation facilities at BR2, this paper describes in detail the on-line power determination procedure. Next the complementary input from SPNDs is discussed. Finally some information is given on the existing fuel instrumentation experience and ongoing developments in this field and on a new fuel ramp test facility for BR2 which is currently being designed.

2. FUEL IRRADIATION FACILITIES AT BR2

This BR2 Materials Testing Reactor is SCK•CEN's most important nuclear facility and was operated during the past forty-five years in the framework of many international programmes concerning the development of structural materials and nuclear fuels for the various types of nuclear fission reactors as well as in the frame of fusion reactor research. The qualities and particular features of the BR2 reactor also allowed performing experiments aiming at assessing and demonstrating the safety of nuclear cores.

The BR2 design (fig. 1) is optimized for these utilizations and offers:

- A core with a central vertical Ø200 mm channel, with all its other channels inclined to form a hyperboloidal arrangement around it. This geometry combines compactness leading to high fission power density with easy access at the top and bottom covers, allowing complex irradiation devices to be inserted.
- A large number of experimental positions, including 4 peripheral 200 mm channels for large irradiation devices. Through-loop experiments can be installed via penetrations in the bottom cover of the vessel.
- A remarkable flexibility of utilization: the reactor core configuration and operation mode are continuously being modified according to the experimental requirements.
- Irradiation conditions (temperature, pressure, environment, neutron spectrum...) representative for various power reactor types.
- High neutron fluxes, both thermal and fast (up to 10^{15} n/cm²·s).

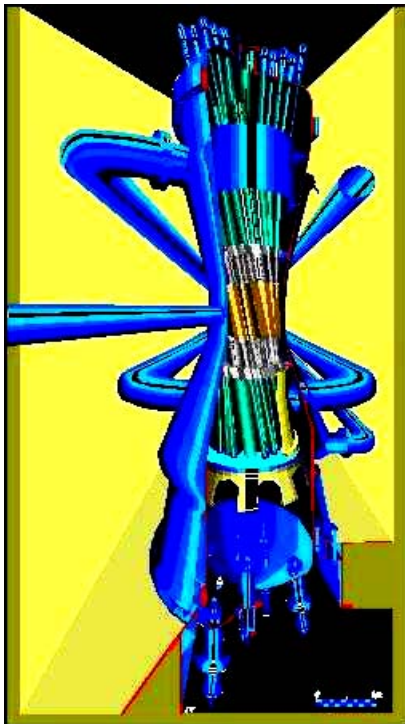


Fig. 1: Inside view of the BR2 reactor (left) and MCNP model representation of a horizontal cut 15 cm below midplane showing the hexagonal lattice with the various channels and their contents (right).

Currently two irradiation devices are in operation for the irradiation of test fuel: i) the PWC/CCD device for testing single fuel rods in a capsule, which can be loaded in a variety of BR2 channels, and ii) the CALLISTO PWR loop occupying three BR2 reactor channels offering a range of possible experimental conditions for the irradiation of up to 9 one-meter long fuel rods per channel.

2.1. PWC/CCD

The PWC/CCD irradiation rig [6], sketched in figure 2, consists of two parts: the PWC capsule and the CCD calorimeter.

The CCD (Calibration and Cycling Device) is a classic flow calorimeter allowing to monitor the thermal performance of the coolant flowing through it, using a diaphragm flow meter and thermocouples placed at inlet and outlet. The inside diameter of the stainless steel tube is about 34 mm. A 1 m high helium screen, placed on the outer surface of the CCD, serves as a thermal shield to reduce heat leaks. When using He-3 at a variable pressure it can also be used to vary the thermal neutron flux in the inner space of the CCD so as to adjust the fuel rod heating rate. This option is currently out of use due to tritium related maintenance; instead the gas gap is being filled with He-4. The fuel rod heating is adjusted by varying the BR2 reactor power during dedicated short reactor cycles. An alternative system based on a water loop with variable boric acid concentration is under development (see section 6).

The PWC (Pressurized Water Capsule) is an instrumented irradiation capsule for the test of single fuel rod segments with a diameter of 8-15 mm and an active length up to 1000 mm, under steady-state or transient conditions. The target fuel segment is placed into the stainless steel capsule filled with demineralised stagnant water. The water can be pressurized in the range of 0.1 to 16 MPa. The heat generated in the rod is dissipated radially through the stagnant water towards the outer surface of the pressure capsule by natural convection, with or without boiling, depending on the irradiation programme. The PWC capsule is cooled by the reactor water flow (at a typical temperature of 40-50 °C) passing through the CCD calorimeter. The normal flow rate is about 0.001 m³/s, leading to a heat transfer coefficient of about 20 W/(m²·K) on the outer surface of the capsule. Thermocouples have been installed to monitor the temperatures on the outer surface of the fuel rod at its midplane and in the stagnant water of the PWC. Water samples of the PWC water can be taken before, during and after reactor operation for monitoring the fission product activity in order to detect a possible fuel rod failure.

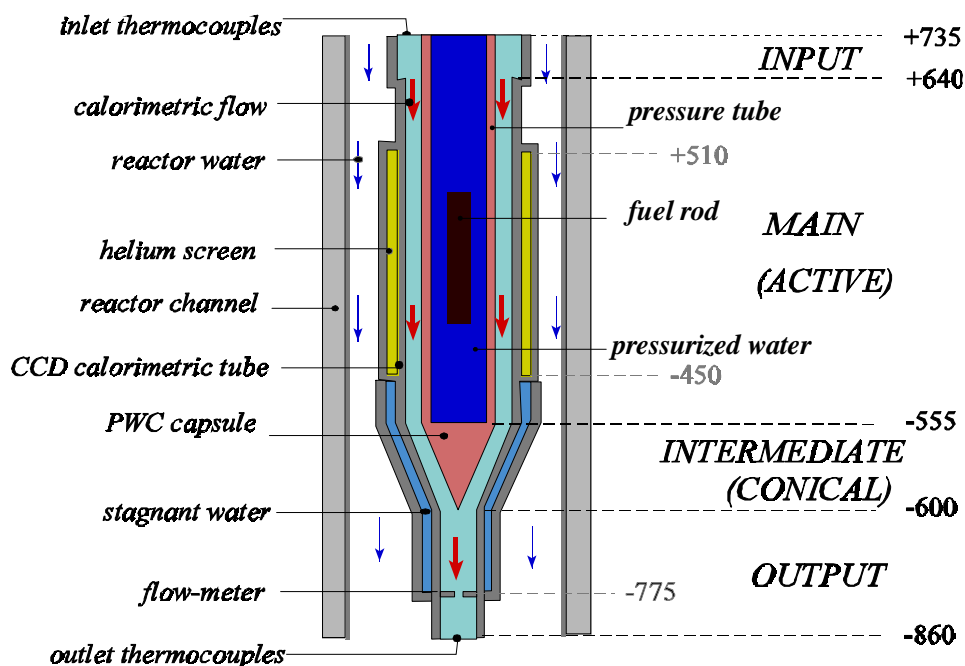


Fig. 2: Scheme of the PWC/CCD device with axial reactor coordinates in mm ('0' being the centre of the BR2 core).

2.2. CALLISTO

CALLISTO (figure 3) [7] is a PWR experimental facility for scientific in-pile studies. Three experimental rigs, called In-Pile Sections (IPS), are installed in three reactor channels to meet various irradiation conditions. They are connected to a common pressurized loop, which can deliver a wide range of pressure and temperature working regimes. These IPSs can be provided with dedicated instrumentation and be modified to perform many devoted irradiation studies, such as:

- the investigation of the behaviour of advanced fuel under representative PWR operating conditions and their qualification for safe, reliable and economical use in power reactors,
- the assessment of Irradiation Assisted Stress Corrosion Cracking (IASCC) phenomena in typical light water reactor materials,
- the study of corrosion processes in fusion candidate materials,
- the characterization of the performances of high neutron dose irradiated materials for light water and fusion reactors as well as for accelerator driven systems (ADS),
- the development and qualification of new on-line in-pile detectors (like neutron and gamma flux detectors, dissolved hydrogen sensors, electrochemical potential reference electrodes...) in a high neutron flux and in a relevant thermohydraulic environment.

From 1989 to mid-1992, the CALLISTO facility was designed, constructed, tested and fully licensed. In a second stage (mid-1992 to the end of 1994), 31 fuel rods (UO₂ and MOX) were irradiated at a peak linear power ranging from 225 to 430 W.cm⁻¹ reaching 57 GWd.t⁻¹ burn-up. In 1995, we started a scientific programme studying the PWR vessel steels behaviour under irradiation. After the BR2 refurbishment (1995 – 1996) one IPS, which was moved to a BR2 channel with higher thermal and fast fluxes, became especially dedicated for corrosion and material studies. From 1997 till now, many new applications in CALLISTO emerged, e.g.: fuel testing, fusion, PWR vessel steel and ADS materials studies, corrosion studies (crack initiation, crack propagation), basic mechanical material science and modelling, detectors testing, etc.

Each IPS is provided with a basket with a capacity of 40.5 x 40.5 x 1000 mm³. They can contain fuel rods or any other targets. Alternative basket geometries with similar volume are possible. Neutron flux and gamma heating data are summarized below (data at 100 % BR2 reactor power and at mid-reactor plane):

	Thermal flux (10 ¹⁴ n/cm ² .s)	Epithermal flux per unit lethargy (10 ¹⁴ n/cm ² .s)	Fast flux (> 100 keV) (10 ¹⁴ n/cm ² .s)	Fast flux (> 1MeV) (10 ¹⁴ n/cm ² .s)	Gamma heating (W/gAl)
IPS 1 & IPS 3	1.0 - 1.8	0.03 - 0.09	0.3 – 0.8	0.2 – 0.33	1.0 - 3.0
IPS 2	3.0 - 5.0	0.25 - 0.40	2.5 – 3.5	0.5 – 1.2	5.0 - 8.0

The axial distribution allows a 350 mm long basket section (centred around the mid-plane) to be irradiated at more than 80% of the maximum flux. Depending on the fuel composition and its enrichment, the maximum linear rod power (at peak pellet) ranges from 200 to 450 W/cm (in IPS1 and IPS3).

The CALLISTO loop is operated at the following thermohydraulic conditions: an IPS inlet temperature ranging from 80 °C to 300 °C, a coolant pressure between 1.0 MPa and 15.7 MPa and a flow rate in the IPS in the range from 1.8 kg/s to 2.5 kg/s. The chemical composition of the CALLISTO cooling water represents that of a PWR primary circuit. Typical conditions are (allowing some variation):

- Boron (boric acid): ± 400 ppm,
- Lithium (lithium hydroxide): 1.8 ppm ≤ [Li] ≤ 2.2 ppm,
- pH: 7.00 ≤ pH_{25°C} ≤ 7.08 or 7.26 ≤ pH_{300°C} ≤ 7.34,
- Dissolved hydrogen: 25 ccSTP/kg ≤ [H₂] ≤ 35 ccSTP/kg.

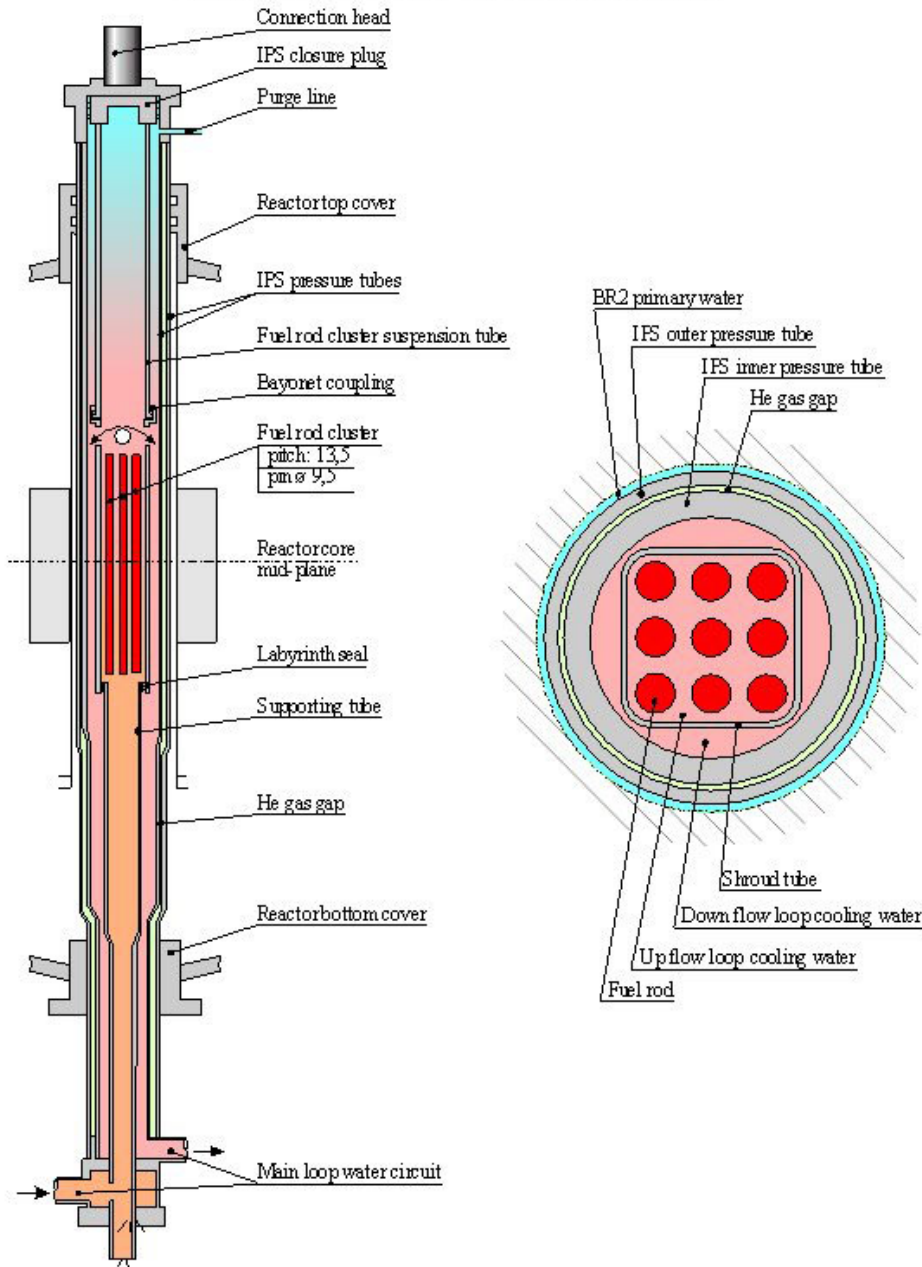


Fig. 3: Typical set-up of CALLISTO IPS for fuel irradiation tests

3. ON-LINE POWER DETERMINATION BASED ON THERMAL BALANCE

3.1. THERMAL BALANCE

The net heat flow rate to the coolant is represented by:

$$Q_{MEASURED} = G \cdot \underbrace{[h(T_{OUTLET}, P_{OUTLET}) - h(T_{INLET}, P_{INLET})]}_{\text{Enthalpy Variation}} - \underbrace{G \sum_i \frac{P_{OUTLET_i} - P_{INLET_i}}{\rho(T_{AVG_i}, P_{AVG_i})}}_{\text{Expansion Work}} - \underbrace{2G^3 \sum_i \frac{\zeta_i}{A_i^2 \rho(T_{AVG_i}, P_{AVG_i})^2}}_{\text{Friction Work}},$$

where Q is the power, G the mass flow rate, h the specific enthalpy, P the pressure, ρ the specific mass, F the specific friction work, T the temperature, A the cross section and ζ the dynamic friction loss coefficient. The last two terms in this expression are usually much smaller than the first one, so they can often be neglected. The pressure values are determined on the basis of the measured inlet pressure combined with a pressure drop along the device calculated with 1D routines.

In order to obtain the total incoming heat flow rate into the coolant during its passage through the rig, the heat losses between the coolant and the BR2 cooling water (between the inlet and outlet thermocouple positions) should be taken into account. In the case of the PWC/CCD device, these losses are very small due to the low water temperature and the presence of the He screen (and a stagnant water screen). A 2D axisymmetric thermal-hydraulic finite element calculation of all heat transfer coefficients leads to a relative loss of typically only 0.25 %.

For the CALLISTO loop, the losses can be much more important. The radial power loss is determined using an analytical model; it is essentially proportional to the temperature difference between the CALLISTO coolant and the BR2 cooling water, with a small correction term proportional to the average gamma heating rate in the device. The axial power loss at the head of the device is more difficult to model. Therefore, the total power loss is measured in the real configuration just before each irradiation cycle (at zero reactor power and as a function of the CALLISTO temperature) and corrected for the calculated radial power loss in order to obtain an empirical relation between the temperature at the highest point of the irradiation device and the axial power loss. Typical values are 10 kW for the radial power loss and another 10 kW for the axial power loss (with CALLISTO at 300 °C and the BR2 cooling water at 40 °C).

The total incoming heat flow rate into the coolant is finally determined as:

$$Q_{TOTAL} (W) = Q_{MEASURED} (W) + Q_{LOSS_TOTAL} (W)$$

3.2. POWER DEPOSITED IN STRUCTURE ELEMENTS

The power from the thermal balance method (Q_{TOTAL}) includes the heat generated not only in the fuel (Q_{FUEL}), but also in the structural parts of the device ($Q_{STRUCTURE}$). Both contributions must be disentangled in order to get information on the total fuel power:

$$Q_{FUEL} = Q_{TOTAL} - Q_{STRUCTURE}$$

During the last years significant progress was made in resolving this issue by combining detailed reactor physics calculations with experimental data from well-targeted mock-up irradiations.

Two distinct methods were implemented in the home-written on-line calculation software:

1. Determination of the power in the fuel from the computed relative power distribution in all parts of the rig and calibrated on the measured Q_{TOTAL} .
2. Determination of the power in the fuel from the thermal balance with the fuel loaded, after correction for the calculated heating in the structure parts (with the fuel rod loaded), the latter calculation being calibrated using the measured heating in the structure parts during a mock-up irradiation.

The two methods use different approximations and rely in a different way upon information from calculations and experiments. So, a critical evaluation of the correspondence between the results obtained with the two methods provides a powerful tool to assess the reliability of the methods.

First method

The first method consists in computing the relative power distribution in all parts of the device (with the fuel rod loaded) by the MCNP reactor physics code with best estimate modelling to take into account all particles transport and the delayed phenomena. Since the MCNP code outputs the results normalized per source neutron, the conversion to absolute power data is subject to additional uncertainties. Therefore, the *relative* MCNP results are considered to be more reliable.

Formally:

$$Q_{STRUCTURE} = W_{STRUCTURE} \times Q_{TOTAL}$$

$$Q_{ROD_i} = W_{ROD_i} \times Q_{TOTAL}$$

in which $W_{STRUCTURE}$ and W_{ROD_i} are the calculated relative power fractions in all structure parts and in fuel rod "i", respectively. In fact, the MCNP calculations are performed for a number of BR2 control rod

height values and W-values corresponding to the actual control rod height are obtained via interpolation. To obtain the average linear power of the fuel rod “i”, Q_{ROD_i} is divided by the length of the fuel rod.

Second method

The second method calculates $Q_{STRUCTURE}$ according to the following expression:

$$Q_{STRUCTURE} = Q_{STRUCTURE}^{MCNP} \frac{Q_{TOTAL_DUMMY}^{MEASURED}}{Q_{TOTAL_DUMMY}^{MCNP}}.$$

This expression can be interpreted in two ways. Primo, one can consider that $Q_{STRUCTURE}$ is taken as the calculated power deposited in the structure parts ($Q_{STRUCTURE}^{MCNP}$), but that possible systematic model errors are accounted for by multiplying with a calibration factor N, obtained from a mock-up irradiation:

$$N = \frac{Q_{TOTAL_DUMMY}^{MEASURED}}{Q_{TOTAL_DUMMY}^{MCNP}}$$

An alternative interpretation of the same formalism consists in taking $Q_{STRUCTURE}$ as the total measured heating in the dummy case, but accounting for the difference between both irradiations (mainly the rod material, but also details in the BR2 configuration) by multiplying with the appropriate ratio of power data from MCNP:

$$\frac{Q_{STRUCTURE}^{MCNP}}{Q_{TOTAL_DUMMY}^{MCNP}}$$

(after proper scaling of each of the power values, according to the actual total BR2 power). Also the contribution of the stainless steel rod heating to the experimental total dummy heating is properly taken into account in this way. Of course in this method it is crucial that both MCNP calculations (for the mock-up case and for the fuel irradiation) are carried out in a consistent way.

The influence of the reactor control rod height is taken into account by on-line interpolation between $Q_{STRUCTURE}^{MCNP}$ -values for various control rod heights. The semi-empirical factor N might also depend slightly on the control rod height; this dependence is determined before the fuel irradiation on the basis of the calculated and the measured data for the total dummy power at several control rod height values.

For the case of multiple fuel rod irradiation, the distribution of the fuel power over the respective fuel rods should be determined on the basis of the MCNP results for the relative powers, as in the first method.

3.3. AXIAL SHAPE FACTOR

For most experimental fuel irradiation programs, not the total power in each fuel rod (Q_{ROD_i}) itself, but rather the maximum linear power ($q_{ROD_i_MAX}$) is the crucial parameter. To access this parameter, information on the (instantaneous) axial power profile along the fuel rods is needed:

$$q_{ROD_i_MAX} = \frac{Q_{ROD_i}}{l} B_i,$$

with l the length of the active part of the fuel rod and

$$B_i = \frac{q_{ROD_i_MAX}}{q_{ROD_i_AVG}} \quad (12)$$

From BR2 reactor experience, some information is available on the typical axial power profiles. However, this profile depends on the reactor loading, on the positions of the control rods and on the specific properties of the irradiation device itself: the presence of the test fuel also influences the power profile. Therefore the determination of the maximum linear power in the fuel rod(s) is based on the relative power data obtained from the MCNP calculations.

The MCNP calculations yield data for the deposited power in the fuel, subdivided in axial segments of typically 1 to 2 cm length. If the resulting axial profiles for the fuel heating are sufficiently smooth, they can be fitted to determine the B-factors for every control rod position. The resulting values for B_i as a function of the control rod position are subsequently fitted with polynomial functions, which are implemented in the on-line power determination programme to determine instantaneous B_i -values and thus

deduce $q_{ROD_I_MAX}$ data from the Q_{ROD_i} values. In a fuel configuration in which the maximum linear power is reached at a rod extremity (due to a significant end peaking effect), fitting with a smooth function (a Gaussian or a cosine function) would systematically underestimate the B-factor. In that case, the B-factor is just determined as the calculated maximum (with its statistical uncertainty) divided by the average linear power.

3.4. UNCERTAINTY ASSESSMENT

Uncertainties on various parameters will have an effect on the accuracy of the obtained values for the (maximum) linear fuel power. Considering a simplified thermal balance calculation formalism

$$Q_{MEASURED} = GC_p (T_{OUTLET} - T_{INLET})$$

elucidates the most important experimental uncertainty sources:

- the differential temperature measurements: a typical uncertainty of 0.2 °C on the temperature difference between coolant inlet and outlet, i.e. a relative error of 1 to 2 % (depending on the actual differential temperature),
- the absolute coolant temperature measurement, resulting in an uncertainty of the deduced coolant heat capacity C_p of the order of 1.2 %,
- the coolant flow rate G , measured via a diaphragm flow meter with an accuracy of 2 %.

Quadratic addition of the uncertainties (considered to be independent) leads to an uncertainty on $Q_{MEASURED}$ of 2.5 to 3 %.

For the conversion to linear fuel power data, the following parameters cause additional uncertainties:

- the power loss from the irradiation device towards BR2, which is negligible in the case of PWC/CCD, but typically of the order of 20 kW (with an uncertainty of about 3 kW) for CALLISTO operating around 300°C,
- the relative MCNP results for the structure heating (in the case of the second method also influenced by the dummy irradiation data) and the average and maximum linear fuel rod powers: in view of the fair agreement of absolute MCNP power data with experimental results, the systematic error on the relative data is estimated to be at maximum 2 %. Statistical error margins on average fuel rod power data are of the order of 2 %, while those on the maximum linear power data vary between 3 and 6 % (depending on what degree of fitting can be applied).

Taking all these factors into account, one obtains a typical uncertainty of 4 to 6 % for the maximum linear power data and 3 to 5 % for the average linear power values.

3.5 MCNP CALCULATIONS

The calculations of specific heating are being performed by the Monte Carlo code MCNP-4C [8], using the cross section data from the ENDF/B-6 file. The geometry is modelled carefully in 3D (see figure 1): the BR2 reactor geometry is completely introduced, accounting even for the inclination of the channels. The relevant irradiation channel is even modelled in more detail: the irradiation rig geometry is fully incorporated. Refs. [9-11] provide extensive descriptions of state-of-the art applications of the MCNP code for the calculation of heating distributions in the BR2 reactor, including a validation with experimental data. The calculations take into account the heating contributions due to prompt and delayed neutrons, prompt and delayed γ - rays, as well as γ - rays released in neutron capture reactions (n,γ) on various materials in the BR2 reactor. The heating in the experimental device includes contributions from particles originating from all geometrical parts of the calculational model (from the irradiation channel itself, from all other channels in the reactor core, from the beryllium reflector, from all other experimental devices present during the irradiation, from the cooling water, etc.). This also holds for the calculated fuel power. Indeed, as the total fuel heating (and the fuel temperature) is a more important parameter for the fuel behaviour rather than the fission rate, we define the total fuel rod power as the thermal power leaving the rod through the cladding, or in other words, the power deposited in the rod by fission products, gammas, betas and neutrons from the rod itself, from a neighbouring test rod or from the BR2 reactor driver fuel.

MCNP-4C takes into account the transport of neutrons and photons (and, if relevant, electrons) and virtually all possible interactions of those particles; however, the code does not include processes in which delayed gammas (mainly released after β^- decay of fission products) are involved. Calculations of such contributions were performed by combining MCNP-4C with ORIGEN-S (SCALE4.3). Various modules of the SCALE4.3 system are used for the calculation of the gamma spectrum and the gamma source intensity in each fuel element (BR2 driver fuel and test fuel), with the appropriate fuel composition and burn-up. These calculated gamma spectra are consecutively introduced in a separate MCNP-4C input file as an external gamma source in the corresponding reactor channels, taking into account the radial and axial distribution of the fission power in the BR2 reactor. Finally the heating in the different parts of the experimental rig due to this gamma source is calculated.

MCNP-4C outputs heating data in terms of deposited energy per mass unit (MeV/g), normalized per Monte Carlo history, i.e. per source neutron. To convert the heating data into absolute power data, the following conversion factor is used:

$$\frac{Q_{BR2} \times \nu_f}{E_{f,BR2}}$$

in which Q_{BR2} is the BR2 reference power, ν_f the average number of neutrons emitted per fission (2.43 for BR2, as ^{235}U is by far the dominant fissioning isotope) and $E_{f,BR2}$ the energy deposited in the BR2 reactor per fission event. The latter is set equal to 196.4 MeV [9], the total fission energy minus the energy of the produced antineutrinos (escaping from the reactor without energy loss) plus the gamma energy released at neutron capture events in the reactor.

An important parameter in the calculation for the test fuel irradiations is the amount of energy deposited into the test fuel per fission event in this fuel – this number is needed to convert the fission rate (directly calculated by MCNP) into a value for the deposited power in the fuel. This parameter is determined using the known decomposition of the fission energy (for the relevant fissile nuclei) into its constituents: the kinetic energy of the fission products and of the emitted neutrons, betas and antineutrinos, and the energy of the prompt and delayed gammas emitted. It is assumed that the antineutrino energy is completely lost, while the kinetic energy of the fission products as well as the beta-particle energy is completely absorbed locally. Dedicated MCNP calculations are performed to determine the fraction of the gamma energy generated inside the test fuel that is also deposited inside. The standard “energy per fission” value is corrected for the lost energy assessed this way. On the other hand, gammas originating from outside the test fuel also deposit some power in the fuel, which is calculated separately (using the same calculation as for the gamma heating in the structure parts) and is included in order to obtain an effective value for the deposited energy per fission.

The statistical character of the Monte Carlo type calculations implies that the results are always subject to statistical uncertainties, which decrease only with the inverse square root of the number of source neutrons. If local information with high spatial resolution is needed (e.g. linear powers in fuel segments with dimensions of the order of 1 cm in the complete BR2 model covering about a cubic meter), the statistical errors can be significant. Typical relative statistical uncertainties are of the order of 5 % for $4 \cdot 10^7$ source neutrons (corresponding to a calculation time of the order of 2 days on present-day PCs or workstations).

3.6. VALIDATION: COMPARISON WITH GAMMA SPECTROSCOPY AND RADIOCHEMICAL BURNUP DATA

After the irradiation of each fuel segment and their removal from the reactor, gamma spectroscopy measurements can be performed. The measured activity of certain isotopes of suitable half-life (e.g. ^{140}Ba , ^{140}La), taking into account the relevant part of the irradiation history, provides data on the time-averaged fission rate during a certain period or on the instantaneous fission rate for a certain reference reactor power. Using the appropriate effective energy per fission these data can be converted to linear power data, which can be compared with the on-line linear power data. The validity of this method was certified by intercomparison with radiochemical methods, yielding a good mutual consistency.

The table below presents a comparison between data from gamma spectroscopy and from the on-line power determination for four fuel rod irradiations in the PWC/CCD device [12] and for a simultaneous irradiation of 8 rods in CALLISTO [13]. The average linear fuel power data from both methods are given and the percentage difference values are quoted in the last column. The data are in very good agreement,

especially in view of the assessed uncertainties of both methods: 4.2 % for the on-line power determination and 2.7 % for the gamma spectroscopy method.

Fuel rod	Reference BR2 power (MW)	Average linear fuel power after the transient (W/cm)		
		Gamma spectr.	On-line power det.	Difference (%)
PWC-1	14.0	301.3	297	+ 1.4 %
PWC-2	20.5	446.3	425	+ 5.0 %
PWC-3	20.7	423.5	426	- 0.6 %
PWC-4	16.6	388.7	369	+ 5.4 %
CALLISTO-1	52.4	237	238	- 0.4 %
CALLISTO-2	52.4	249	262	- 5.0 %
CALLISTO-3	52.4	231	227	+ 1.7 %
CALLISTO-4	52.4	259	256	+ 1.2 %
CALLISTO-5	52.4	237	244	- 2.9 %
CALLISTO-6	52.4	224	227	- 1.3 %
CALLISTO-7	52.4	226	232	- 2.6 %
CALLISTO-8	52.4	211	217	- 2.8 %

A comparison of the maximum linear fuel power is more difficult, since the gamma spectroscopy only yields time-integrated information and the axial power profile is expected to vary during irradiation, both with respect to width and to position of the maximum. Due to the resulting smoothed axial profile of the detected fission products, axial shape factors deduced from gamma spectroscopy will systematically be lower than the real instantaneous shape factors during the irradiation. Nevertheless, an attempt was made to reconstruct the integrated axial profiles by folding the calculated (control rod position dependent) profiles with the observed time evolution of the control rod position. The resulting axial shapes are in good agreement with the axial fission power profiles obtained by gamma spectroscopy: an average axial shape factor for the four tabulated PWC fuel rods of 1.072 was calculated, compared to an experimental value of 1.080 from gamma spectroscopy.

4. COMPLEMENTARY DATA FROM SELF-POWERED NEUTRON DETECTORS

In order to improve the monitoring of the irradiation conditions, the irradiation device can be equipped with self-powered neutron detectors and/or activation dosimeters. Self-powered neutron detectors (SPNDs) are small cylindrical sensors (length between 5 and 20 cm, diameter of 1.5 to 4 mm) that can be operated in in-core conditions. They output a current which is essentially a measure for the thermal neutron flux. Depending on the type of SPND the response is either immediate (with a sub-ms response time) or delayed (response time of the order of a few minutes). In the latter case the signal can be unfolded numerically using the known response function so as to obtain an effective response time of less than a second (at sufficiently high data acquisition rate).

The MCNP calculations that yield information on the deposited powers can simultaneously produce thermal neutron flux data at the locations of the SPNDs. Consequently the experimental SPND data can be used to verify the MCNP calculations: the calculated absolute flux/power in the irradiation device (normalized to reactor power) can be checked, as well as the dependence of (relative) local flux/power data on external parameters (changing control rod positions, modification of the reactor configuration, etc.). A typical example can be taken from an instrumented fuel irradiation in the CALLISTO device: data were collected on-line from three SPNDs (two with a rhodium emitter and one with a vanadium emitter) which were positioned in-between the fuel rods. We developed an MCNP-based model to convert the SPND currents into data on the neutron capture rates in the emitters (or, equivalently, conventional thermal neutron flux data), taking into account current contributions due to impinging gamma rays and due to high-energy beta rays directly from fission products in the test fuel (an effect which is especially important for the case of vanadium SPNDs positioned close to the fuel [14]). The resulting capture rate data were compared with MCNP data: the ratio between MCNP data and experimental results was found to be 0.95, 0.89 and 1.12 for the three SPNDs, respectively. In view of an estimated 10% uncertainty in the

conversion from SPND current to neutron capture rate and a similar total uncertainty on the MCNP capture rate data, the SPND data confirmed the validity of the MCNP calculations within these limits.

One of the advantages of SPNDs lies in the fact that the relative accuracy of their data is considerably higher than that of the power measurements (noise level below 0.1 % in typical conditions), so changing irradiation conditions can be followed more closely. This is illustrated in figure 4, representing partial data from the instrumented fuel irradiation mentioned above. The periodical movement of a strongly absorbing rig in a nearby BR2 channel (silicon doping device) induces small changes in neutron flux and fuel power in CALLISTO. These changes were recorded via the central temperature of the instrumented fuel rods, via the signals from two rhodium SPNDs (corrected for their delayed response) and via the measured thermal balance. Figure 4(a) shows a very good correlation between the central fuel temperature data and the thermal neutron flux data from the SPNDs (correlation coefficients of 0.95). On the other hand, the measured total rig power (thermal balance method) also follows somehow the same pattern, but is subject to much more noise (figure 4(b)), leading to a correlation coefficient with the central fuel temperature data of only 0.39.

When performing fast power transient experiments, SPND data will also provide data on the shape of the power ramp with a higher time resolution, since their response is faster than that of the measured thermal balance which involves the equilibration of temperature profiles.

Activation dosimetry wires on the other hand give information on time-integrated neutron fluxes which can be coupled to time-integrated power data using the MCNP calculation results. They provide an independent verification possibility of the integrated absolute power [15].

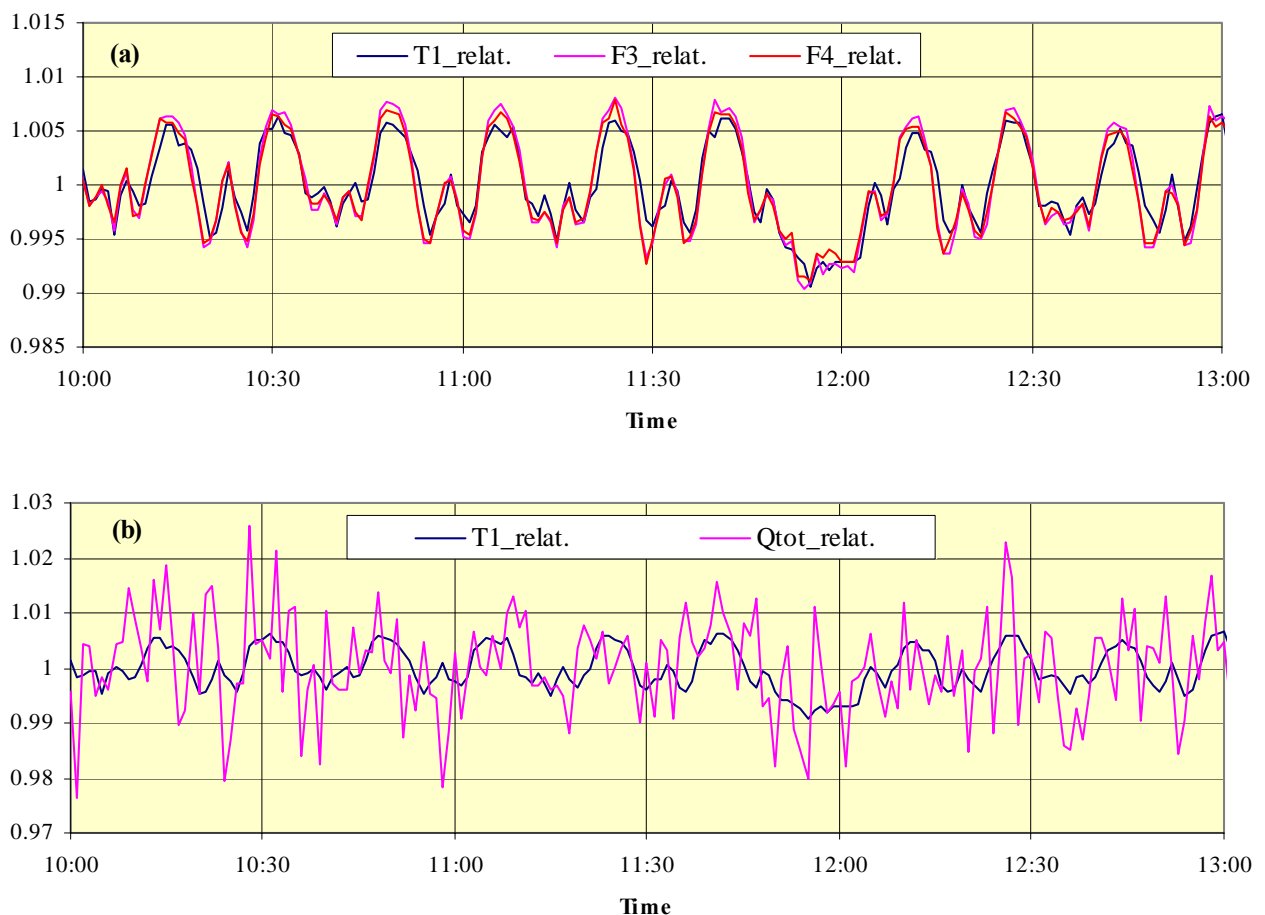


Fig. 4: Normalized data from instrumented fuel irradiation in CALLISTO: central fuel temperature data (T_1), rhodium SPND signals corrected for delayed response (F_3 , F_4) and total rig power data from the thermal balance (Q_{TOTAL}). The temperature and SPND data follow closely small changes in irradiation conditions, while the noise on the thermal balance data (also only of the order of 1%!) masks the detailed time evolution pattern.

5. EXPERIENCE WITH FUEL INSTRUMENTATION AND NEW DEVELOPMENTS

In the past, various programs involving instrumented fuel irradiation (central thermocouples) have been conducted at the BR2 reactor. More recently, from 2004 to 2006, eight instrumented rods with various compositions and fabrication procedures were irradiated simultaneously in one leg of the CALLISTO device (OMICO project [13]). Figure 5 shows a sketch of one of the fuel segments with a C-type (W5Re-W26Re) central thermocouple and the fission gas release measurement via an LVDT (purchased from the Halden Reactor Project) coupled to the fuel segment via a capillary tube. As an example of experimental results, figure 6 shows the recorded central fuel temperatures as a function of the measured total power of six fuel segments. The lower temperatures for the thorium oxide based fuel reflect the higher thermal conductivity.

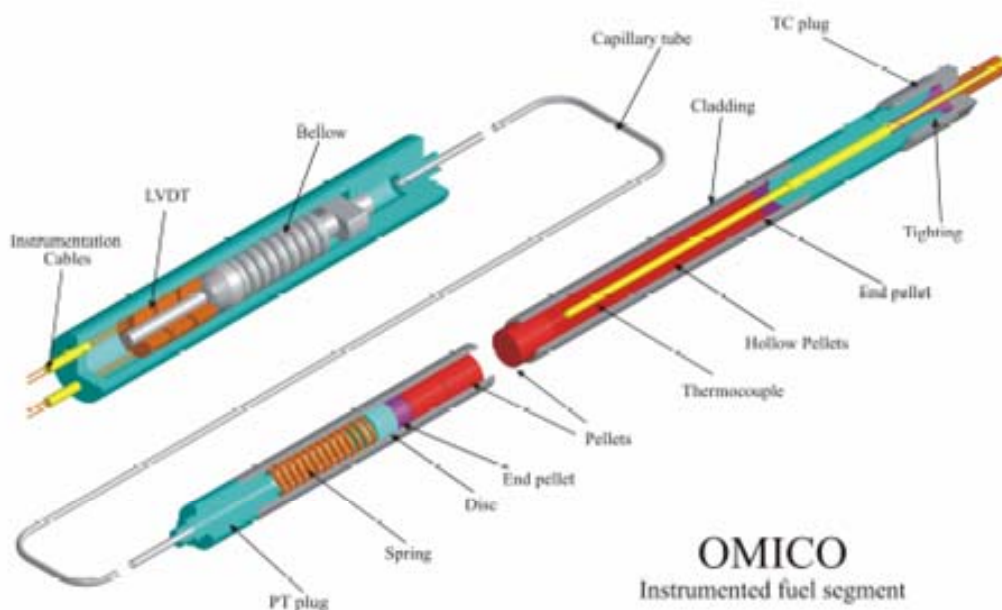


Fig. 5: Sketch of one of the OMICO fuel segments with thermocouple and pressure sensor

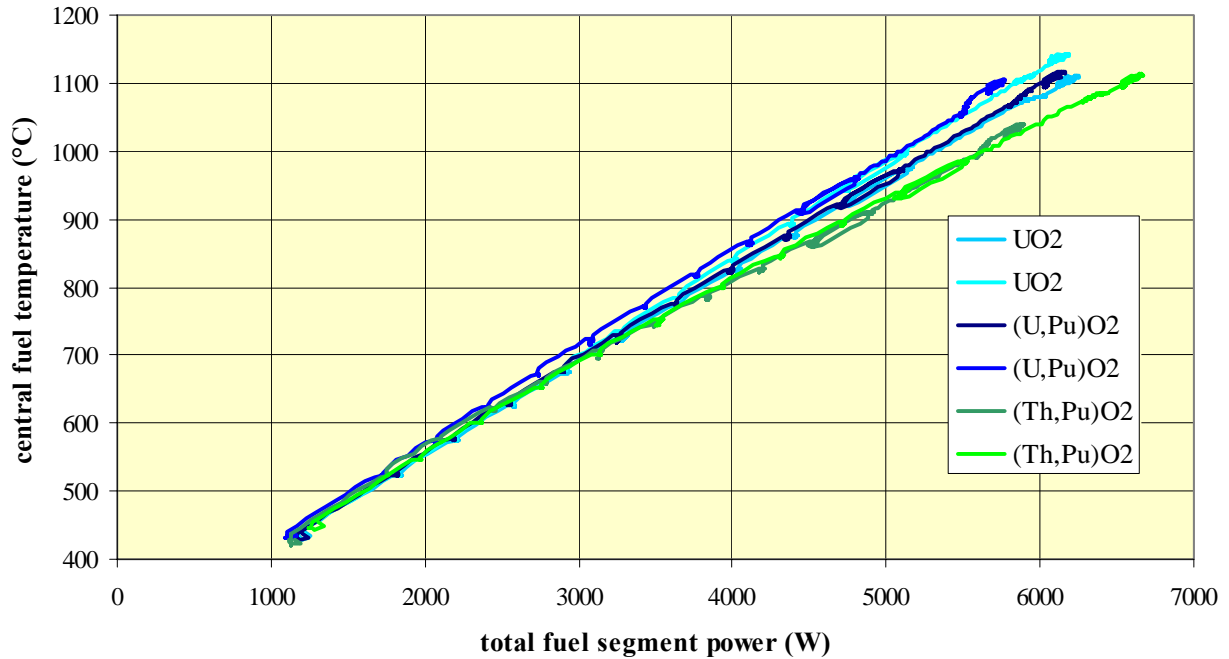
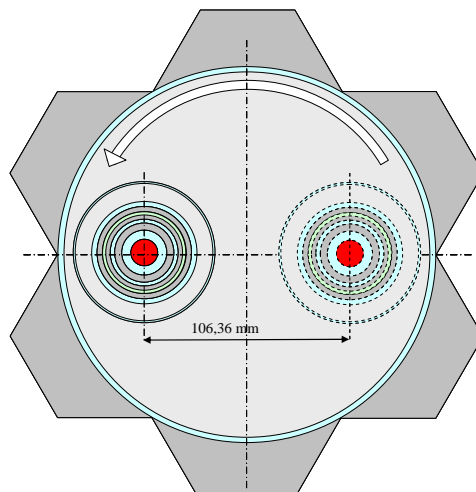


Fig. 6: Recorded central temperatures of OMICO fuel segments as a function of the measured total power in each segment.

Innovative in-pile instrumentation technologies are under development with possible applications to fuel rod measurements. For example dimensional measurement techniques based on optical fiber technology is being tested. Two candidate concepts, a Fabry-Pérot interferometer system and a fiber Bragg grating device, are under evaluation. The main remaining problem is the attachment of the fiber sensor to the surface of interest.

6. DEVELOPMENT OF ADVANCED FUEL TRANSIENT TEST FACILITIES

In order to increase the flexibility and efficiency of the PWC setup for fuel transient tests a new system is under design. It consists of two components: a variable neutron screen surrounding the PWC capsule, realized by a variable concentration boric acid solution (baptized as VANESSA) and a system to rotate the complete device within a 200 mm BR2 channel (RODEO). VANESSA not only provides the variable thermal neutron absorption, but the fluid in the device will also evacuate the heat and will serve to determine the fuel rod power via the thermal balance method. In principle, an unlimited number of transients with amplitude up to a factor two can be achieved by VANESSA. However, in order to reduce the complexity of the out-of-pile installation and to limit the amount of boric acid needed (and the waste) VANESSA will be designed to be compatible with the RODEO system. The RODEO concept is illustrated in figure 7. A rotating plug in a 200 mm channel allows to move a PWC capsule (possibly within VANESSA) across the flux gradient of the channel, yielding a maximum power increase factor of about 4,



depending on the BR2 configuration and on the boric acid concentration in VANESSA (assumed fixed). In this concept, VANESSA would serve to adjust the minimum power level and the ramp test would be accomplished by RODEO only. Of course any number of transients is possible with this system. Compared to the He-3 based ramp test technology, there is almost no production of waste. There is no production of tritium and the system availability problems linked to the tritium tightness are eliminated.

Fig. 7: Schematic representation of the RODEO/VANESSA system in a 200 mm channel of the BR2 hexagonal matrix.

7. CONCLUSIONS

BR2 is equipped with irradiation devices for irradiating test fuel in various environments, for long term burn-up accumulation tests as well as for ramp tests on fresh or pre-irradiated fuel elements. The desired irradiation regime is often specified by the client in terms of maximum linear power. Therefore the maximum linear fuel rod power is continuously monitored for properly piloting the experiments. We obtain the linear fuel rod power data via a measurement of the enthalpy change in the coolant of the irradiation device, combined with validated 3D Monte Carlo core calculations (MCNP). On-line power data from recent experiments have been confirmed by post-irradiation gamma spectroscopy experiments and radiochemical burn-up analysis, proving the validity of the on-line procedure.

SPNDs can provide reliable absolute thermal neutron flux values (after extensive detector modeling using MCNP), but the conversion from local neutron flux to maximum fuel rod power is not straightforward. However SPNDs have been successfully used to follow the fuel power evolution, especially to obtain more accurate data during the reactor start-up and to assess the effects of changing reactor core geometries.

Fuel segments instrumented with central thermocouples and pressure sensors by means of LVDTs have been irradiated in BR2. An innovative technique for in-pile dimensional measurements based on optical fiber technology is being developed.

A new system for fuel ramp tests is under development: a combination of a screen with a boric acid solution at variable concentration (VANESSA) with a rotating device to be placed in a 200 mm diameter BR2 channel (RODEO).

REFERENCES

- [1] J. Dekeyser, "The BR2 High Flux Reactor: A Versatile Tool for Neutron Irradiation and Materials Testing", VII CGEN, Belo Horizonte, Brasil, Aug. 31 – Sept. 3, 1999.
- [2] P. Gouat et al., "SCK•CEN: your partner in fuel research – Fuel irradiation testing in BR2 and related R&D: present and future capabilities", SCK•CEN-ER-15 (2006)
- [3] Ch. De Raedt, S. Bodart, B. Ponsard, M. Wéber, Th. Maldague, "Two-dimensional neutron and gamma calculations for devices irradiated in BR2 reflector positions", 8th ASTM-EURATOM Reactor Dosimetry Symposium, Aug. 29 – Sept. 3, 1993, Vail, Colorado, USA.
- [4] E. Malambu, Ch. De Raedt, M. Wéber, "Assessment of the linear power level in fuel rods irradiated in the CALLISTO loop in the high flux materials testing reactor BR2", 3rd Int. Topical Meeting on Research Reactor Fuel Management (RRFM), March 28-30, 1999, Bruges, Belgium.
- [5] L. Vermeeren et al., "Qualification of the on-line power determination of fuel elements in irradiation devices in the BR2 reactor", SCK•CEN-BLG-1006 (2005).
- [6] S. Bodart, Ch. De Raedt, B. Ponsard, "Single LWR fuel rod irradiations with power transients in BR2", Int. Conf. on Irradiation Technology, Saclay, May 20-22, 1992.
- [7] Ph. Benoit, C. Decloedt, J. Dekeyser, C. De Raedt, F. Joppen, A. Verwimp, M. Wéber, "CALLISTO: a PWR in BR2 – Design, construction and licensing", Int. Conf. on Irradiation Technology, Saclay, May 20-22, 1992.
- [8] J. Briesmeister, "MCNP – A General Monte Carlo N-Particle Transport Code – 4C, LA-13709-M (April 2000)
- [9] V. Kouzminov and E. Koonen, "Power distribution in MOX fuel rods – Benchmark calculation", SCK•CEN-BLG-951 (June 2003)

- [10] V. Kuzminov, M. Weber and E. Koonen, "Determination of the Linear Power in MOX Fuel Rods Irradiated at BR2 Reactor", Proc. on CD-ROM of PHYSOR-2004, Chicago, Illinois (U.S.A.), April 2004.
- [11] S. Kalcheva, E. Koonen and P. Gubel, "Assessment of Fuel Safety Margins with MCNP", Proc. on CD-ROM of Best Estimate 2004, Washington D.C., USA, November 14-18, 2004, p.288-301.
- [12] L. Borms, Y. Parthoens and A. Gys, "GERONIMO Third campaign: gamma spectroscopy PIE after ramp test on fuel segments GZR02, GZL33, GZL32 and GZR03", SCK•CEN-R-3783 (September 2004)
- [13] M. Verwerft et al., OMICO Final Report, 5th EURATOM Framework Programme Contract FIKS-CT-2001-00141, SCK•CEN-ER-42 (2007)
- [14] L. Vermeeren, to be published.
- [15] Ch. De Raedt, E. Malambu, S. Bodart, M. Wéber, M. Willekens, "Assessment of the fission power level in fuel rods irradiated in the high flux materials testing reactor BR2 with the aid of fluence dosimetry – Comparison with other methods", 10th International Symposium on Reactor Dosimetry (ISR D), Osaka (Japan), Sept. 12-17, 1999.

Instrumentation and Re-fabrication Techniques used for Fuel Rod Performance Characterization in the Halden Reactor

Christian Helsingreen
IFE, OECD Halden Reactor Project

ABSTRACT

The Halden Boiling Water Reactor (HBWR) is used for fuel irradiations in support of safe and reliable operation of nuclear power plants. One of the strengths of the HBWR is the capabilities that have been developed on-site for performing fuel irradiations with in-core instrumentation for on-line monitoring of key parameters. For basic fuel studies, instrumentation for monitoring fuel thermal and mechanical behaviour as well as fission gas release has been developed. In addition, instrumentation for monitoring the fuel pellet interaction with the cladding or for separately investigating the mechanical behaviour of the cladding can be utilized.

The different in-core instruments developed for use in the HBWR can be used with either un-irradiated or irradiated fuel rods and under steady-state or transient operating conditions. Purpose-built equipment has been designed and produced in order to attach instruments to re-fabricated segments taken from commercially irradiated fuel rods. Such instruments include fuel centreline thermocouples and in-rod pressure transducers, with all re-fabrication and instrumentation operations being carried out in hot-cell.

This paper describes the instrumentation that has been developed at Halden and how it is implemented for characterising fuel performance and behaviour under different testing conditions.

1. Introduction

The Halden Boiling Water Reactor (HBWR) started operation in 1958. The HBWR was built in order to demonstrate the usefulness of nuclear power as an energy source for the process industry. During its first years of operation the research programmes focused on studies of fuel performance at different heat-rates and on flow stabilities / in-stabilities (the HBWR is operated in natural circulation). The need for accurate in-core power calibration led to the development of in-core turbine flow meters (Figure 1). Based on similar principles, the development of a wide range of instruments continued.

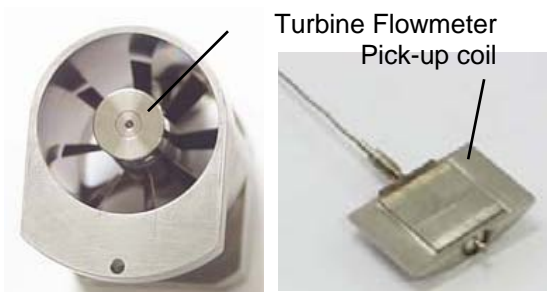


Figure 1, Turbine flowmeter

Today the Halden Reactor Project relies on extensive use of in-core instrumentation for both fuel and material testing in the HBWR. Separate loop systems have been installed in the reactor to simulate BWR, PWR, CANDU and AGR (Gas cooled) conditions.

Reliable in-core instrumentation has been developed for measuring all key parameters both for fuel and material such as fission gas release, fuel temperature, fuel swelling/densification, cladding creep etc¹. The different instruments can be attached to pre-irradiated fuel rods and material samples by using remote operated manipulators and purpose-built re-instrumentation equipment. To be able to measure the most important fuel performance parameters, the Halden Reactor Project has developed an instrument based on a Linear Voltage Differential Transformer (Figure 2).

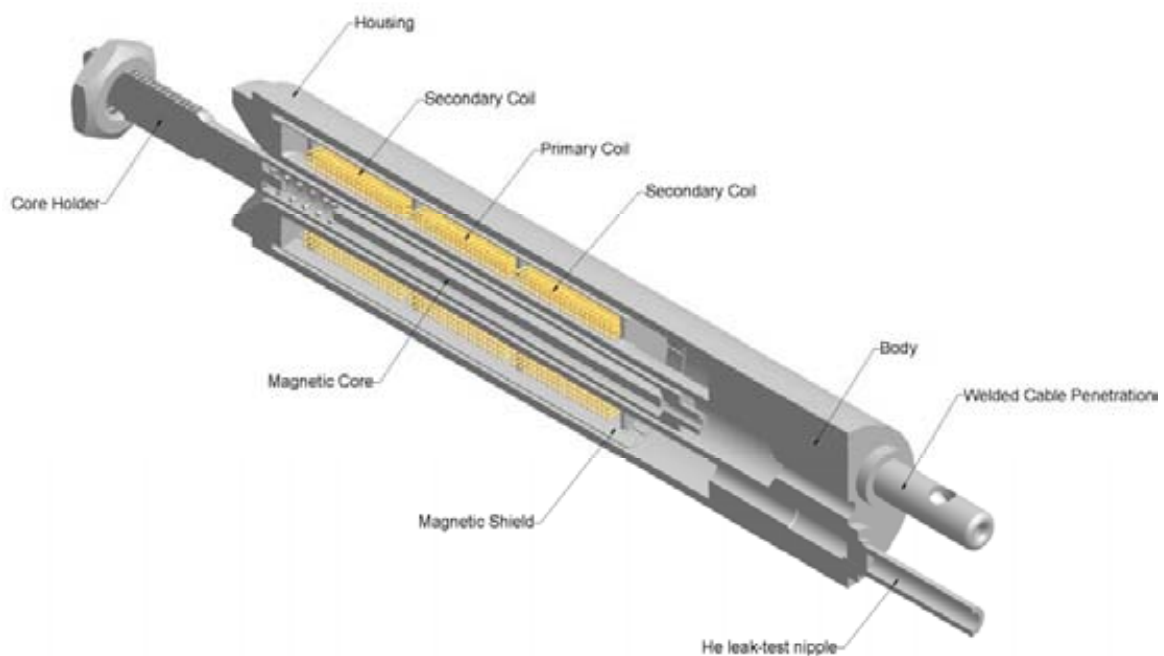


Figure 2, Principle design of a Linear Voltage Differential Transformer

The Linear Voltage Differential Transformer consists of one primary coil and two secondary coils. In the centre of the coil system there is a magnetic core. The primary coil is activated by a 400 Hz constant-current generator and the position of the magnetic core in relation to the primary coils affects the balance of the signal from the secondary coils. Thus the position of the magnetic core can be measured with an accuracy of $\pm 1 \mu\text{m}$. Since the Halden Reactor Project started with in-core measurements, more than 2200 Linear Voltage Differential Transformers of different types have been installed in test rigs in the HBWR. A failure rate of less than 10% after 5 year operation is expected for Linear Voltage Differential Transformers operating in BWR, PWR or CANDU conditions. A selection of the most important instrument combinations is described in the following sections.

2. Fuel rod pressure measurements

Fission gas release mechanisms and the fuel rod internal pressure are key issues for extending the burn-up of fuel in power reactors. Most licensing bodies have limitations on allowable fuel rod internal pressure in power reactors.

In order to study the fission gas release phenomena under different conditions the Halden Reactor Project has developed an in-core pressure sensor (Figure 3).

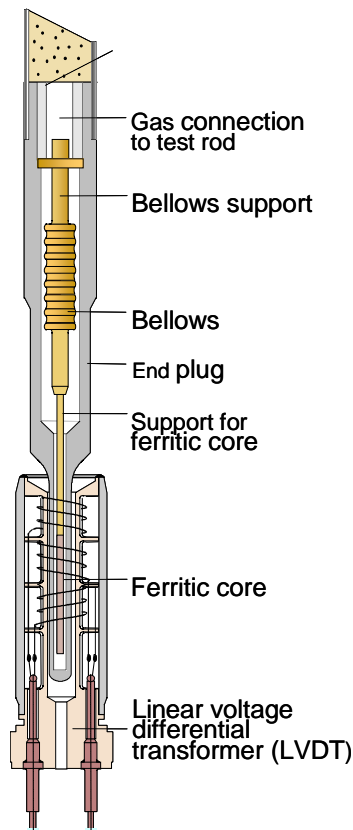


Figure 3, Pressure transducer

The pressure sensor consists of a miniaturised bellows assembly inserted into the plenum of the fuel rod.

One end of the bellows is fixed to the fuel rod end plug while the other end is allowed to move freely. A magnetic core assembly is attached to the free moving end of the bellows assembly. If the pressure in the fuel rod plenum increases, the bellows assembly will contract due to the increased outer pressure and the magnetic core will move accordingly. A Linear Voltage Differential Transformer is used for monitoring the position of the magnetic core and thus the fuel rod internal pressure can be interpreted.

3. Fuel centreline temperature measurements

Fuel centreline temperature measurements provide important information on the thermal performance of the fuel and in particular the fuel thermal conductivity. For monitoring fuel centreline temperatures, fuel thermocouples or expansion thermometers are utilized (Figure 4).

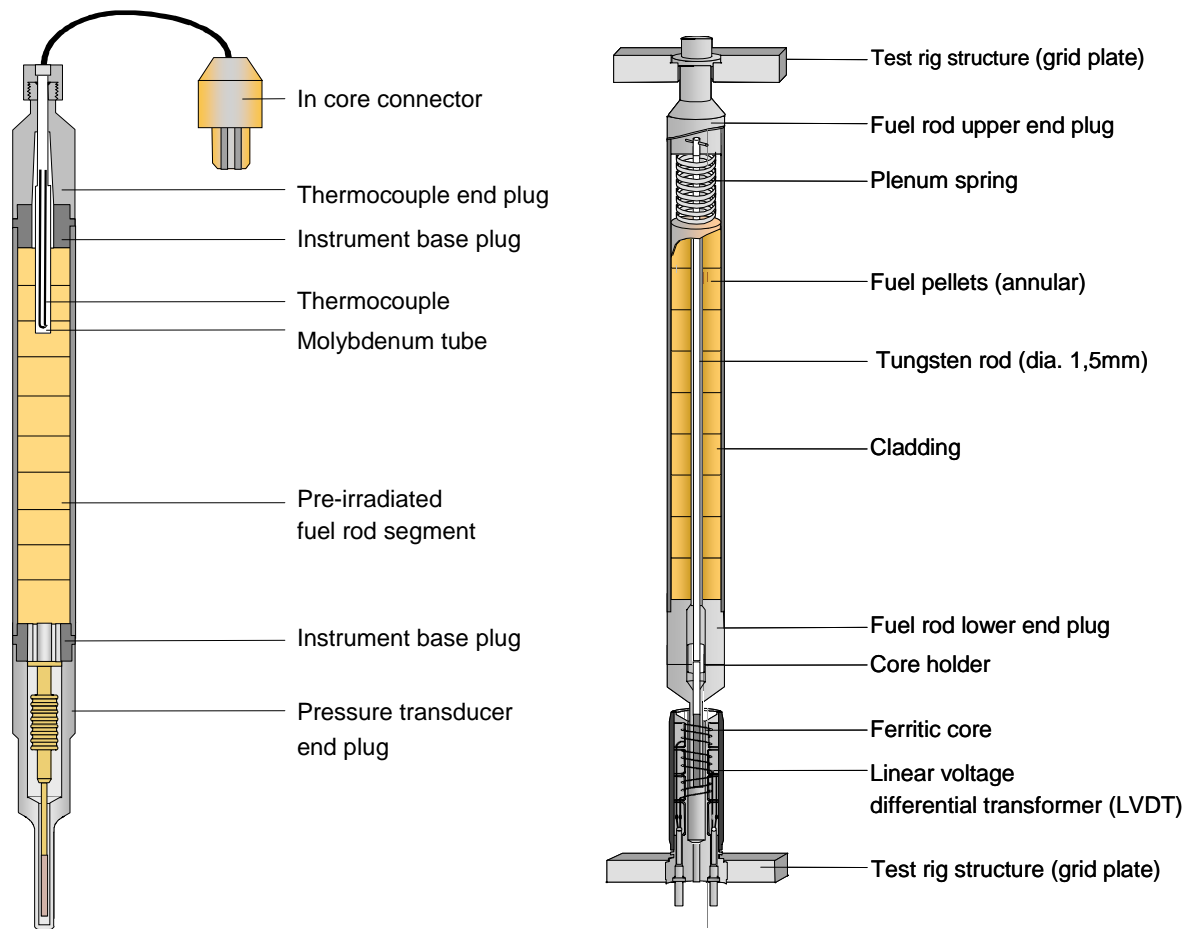


Figure 4, Fuel thermocouple and expansion thermometer

The fuel centreline thermocouple normally will be able to operate for several years in-core without failure, but the lifetime of the thermocouple will decrease with increasing fuel centreline temperatures. If the fuel centreline temperature exceeds 1400 – 1500 °C, the expected thermocouple lifetime typically is one year or less. For long term irradiation and TICs, decalibration due to transmutation of the T/C material needs to be accounted for.

The expansion thermometer is based on inserting an expansion rod made of tungsten

through a centre hole drilled in the entire fuel stack. The thermal expansion of the tungsten rod is measured by using a Linear Voltage Differential Transformer. The average fuel centreline temperature can be derived from the measured expansion of the tungsten rod. The expected lifetime of an expansion thermometer is longer than for a thermocouple, but the accuracy of the expansion thermometer due to the interpretation of the signal that is needed, is not as good as the accuracy of a thermocouple. There is also a risk that mechanical interaction between the fuel and the tungsten rod will affect the performance of the instrument.

4. Fuel densification / swelling measurements

The mechanical stability of nuclear fuels is an important performance parameter. For monitoring fuel stack length changes, an in-core fuel elongation detector is utilized (Figure 5).

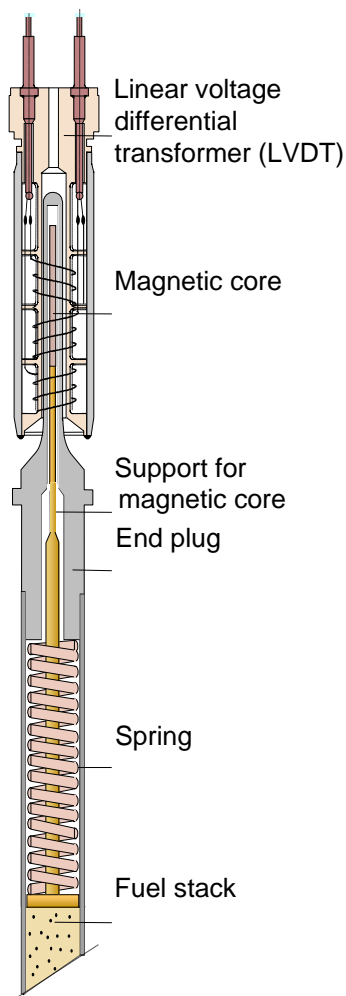


Figure 5, Fuel stack elongation detector

In order to measure fuel densification and swelling, the magnetic core of the Linear

Voltage Differential Transformer is attached to a spring loaded plate in contact with a fuel pellet in one end of the fuel stack. The magnetic core then will follow the expansion and contraction of the fuel stack and provide data on the mechanical behaviour of the fuel.

5. Cladding creep and pellet-cladding mechanical interaction (PCMI)

Cladding elongation and cladding diameter changes provide information on cladding creep, PCMI, fuel creep / relaxation and fuel rod crud deposits and are important performance factor. For monitoring cladding creep, PCMI and fuel rod crud deposits the Halden Reactor Project has developed an in-core cladding extensometer (Figure 6) and a diameter gauge (Figure 7).

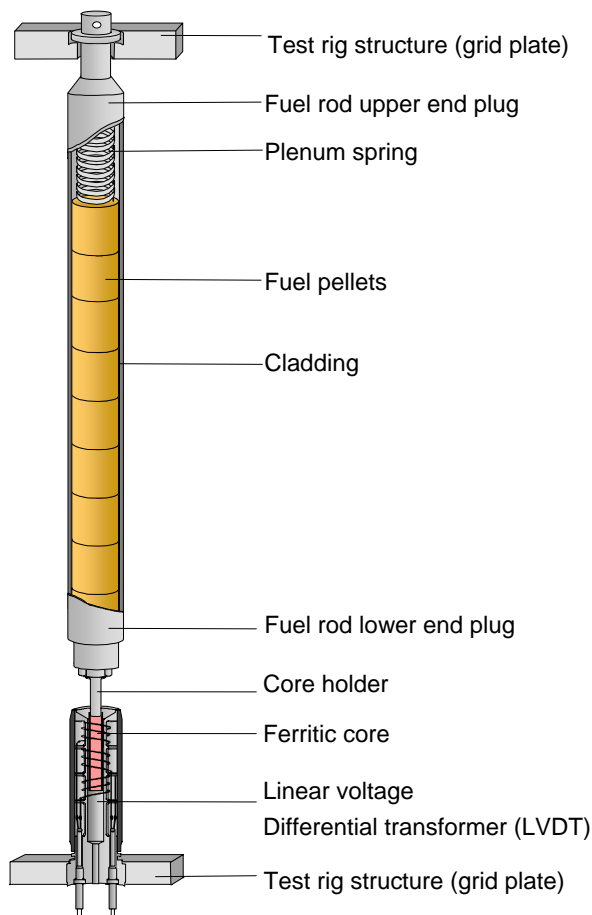


Figure 6, Cladding extensometer

In order to measure cladding elongation (Figure 6), the magnetic core of the Linear

Voltage Differential Transformer is attached to the end plug in one end of the fuel rod the magnetic core will follow the expansion or contraction of the fuel rod cladding.

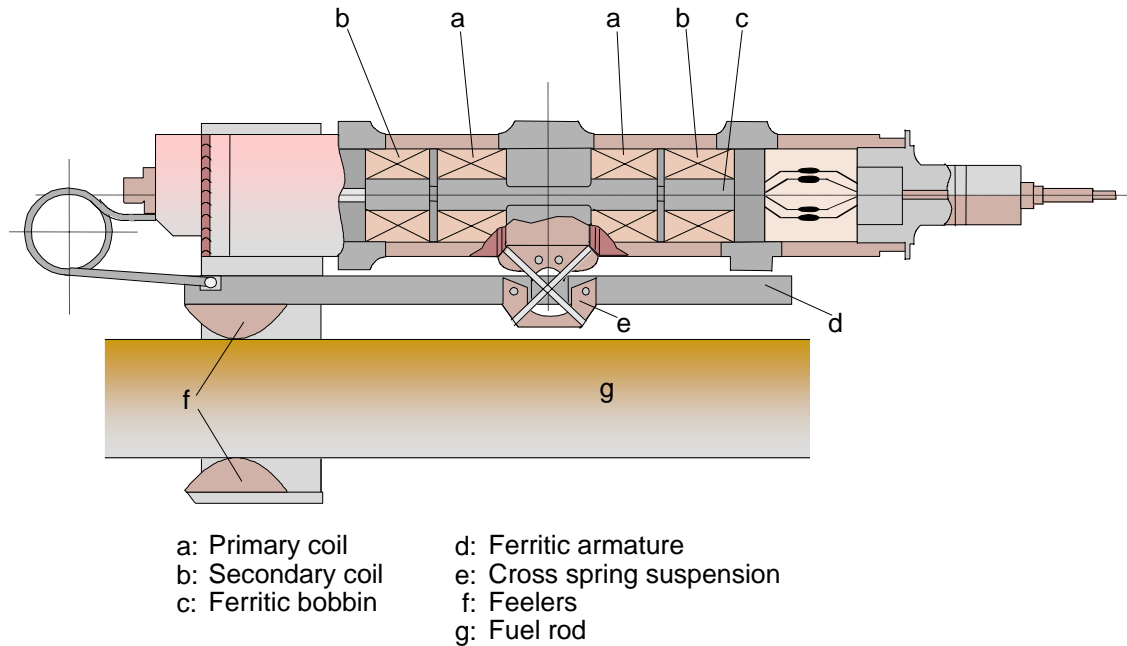


Figure 7, Diameter gauge

The diameter gauge is based on the Linear Voltage Differential Transformer principle. The diameter gauge travels along the fuel rod powered by a hydraulic drive and positioning system. It is possible to perform diameter measurements on a continuous basis (e.g. during power transients for measuring PCMI) or on a less frequent basis (e.g. once every month for monitoring crud build-up). The accuracy of the diameter-gauge is $\pm 1 \mu\text{m}$ and a calibration is performed in conjunction with each diameter trace by having calibration steps on both fuel rod end plugs.

6. Re-instrumentation

All the different fuel rod instruments developed by the Halden Reactor Project can be attached to both un-irradiated and pre-irradiated fuel rods. This means that it is possible to retrieve pre-irradiated fuel rods from power reactors (Figure 8) and re-instrument them before the irradiation is continued in the HBWR. The performance of fuel rods that have reached the current burn-up limit in a power reactor can then be studied at even higher burn-up in conjunction with e.g. an application for burn-up extension.

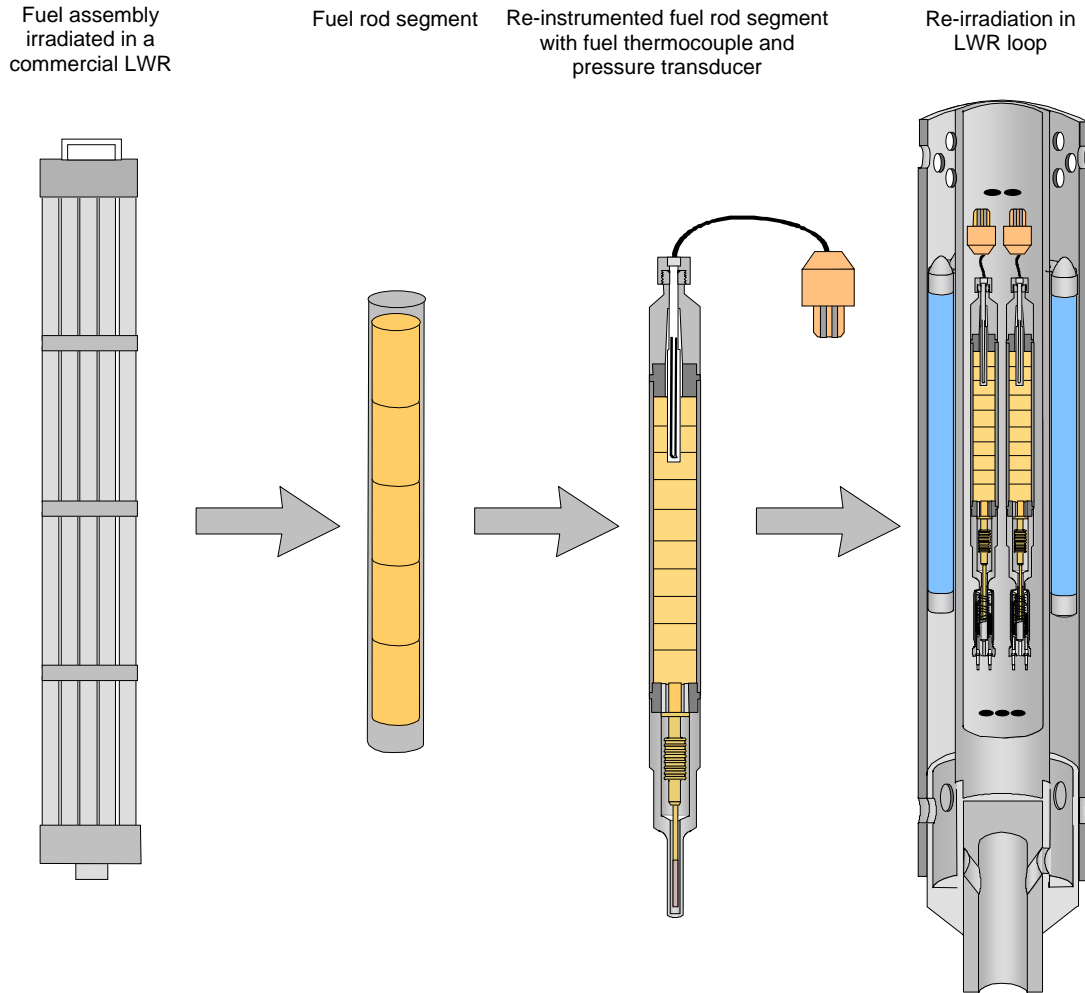


Figure 8, Re-instrumentation sequence

The re-instrumentation work must be performed in a hot-cell facility and purpose built re-instrumentation equipment must be used. Figures 9 and 10 show the re-instrumentation equipment developed by the Halden Reactor Project used to instrument pre-irradiated fuel rods. The equipment in Figure 9 is used to drill the hole in the fuel for insertion of a fuel thermocouple. Figure 10 shows the re-instrumentation equipment used for welding the instrumented end plugs to the fuel segment, leak testing and final checkout of the re-instrumented fuel rod. The instrumented end plugs may contain a thermocouple, pressure transducer, cladding elongation detector or a fuel stack elongation detector. The fuel segment is normally instrumented with a combination of a fuel thermocouple and a pressure transducer or cladding elongation detector.

Re-instrumentation procedure:

- Inspection of fuel rod (includes neutron radiography)
- Fuel rod cut to length
- De-fuelling of fuel rod ends
- Oxide layer removed from cladding ends
- End plugs welded to fuel rod (pressure transducer and thermocouple base plugs)
- Fuel rod filled with liquid CO₂ and frozen with liquid N₂
- Drilling of centre hole (vacuum process)
- Assembly of Mo-tube
- Fuel rod dried at 300 °C for 72 hours (vacuum)
- Second part of pressure transducer end plug welded to fuel rod
- Second part of thermocouple end plug welded to fuel rod
- Measurement of fuel rod free-volume and gas flow properties
- Fuel rod evacuated, filled with He and seal welded
- He leak-test of fuel rod
- Check-out / testing of fuel rod instrumentation
- Final inspection of fuel rod (includes neutron radiography)

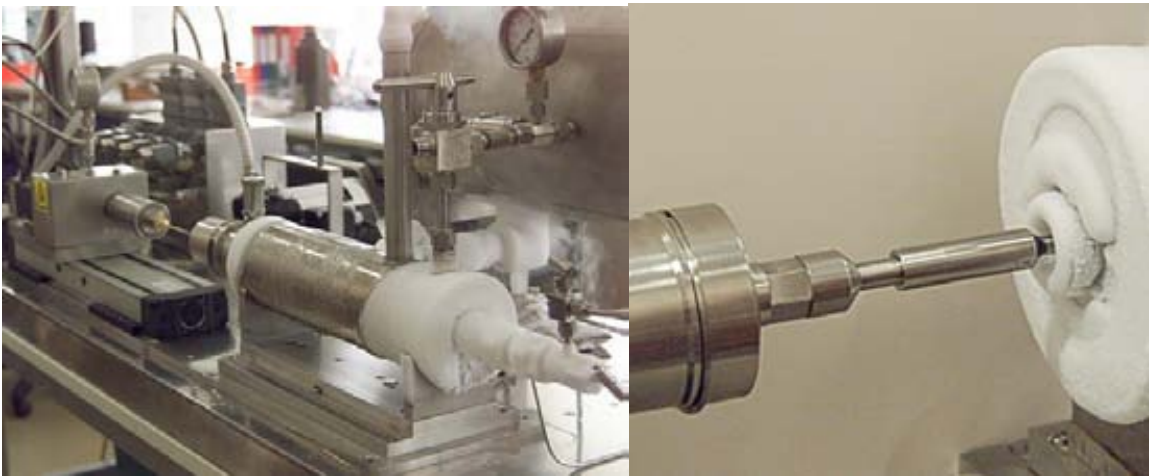


Figure 9, Re-instrumentation equipment used for drilling of thermocouple holes in pre-irradiated fuel rod segments

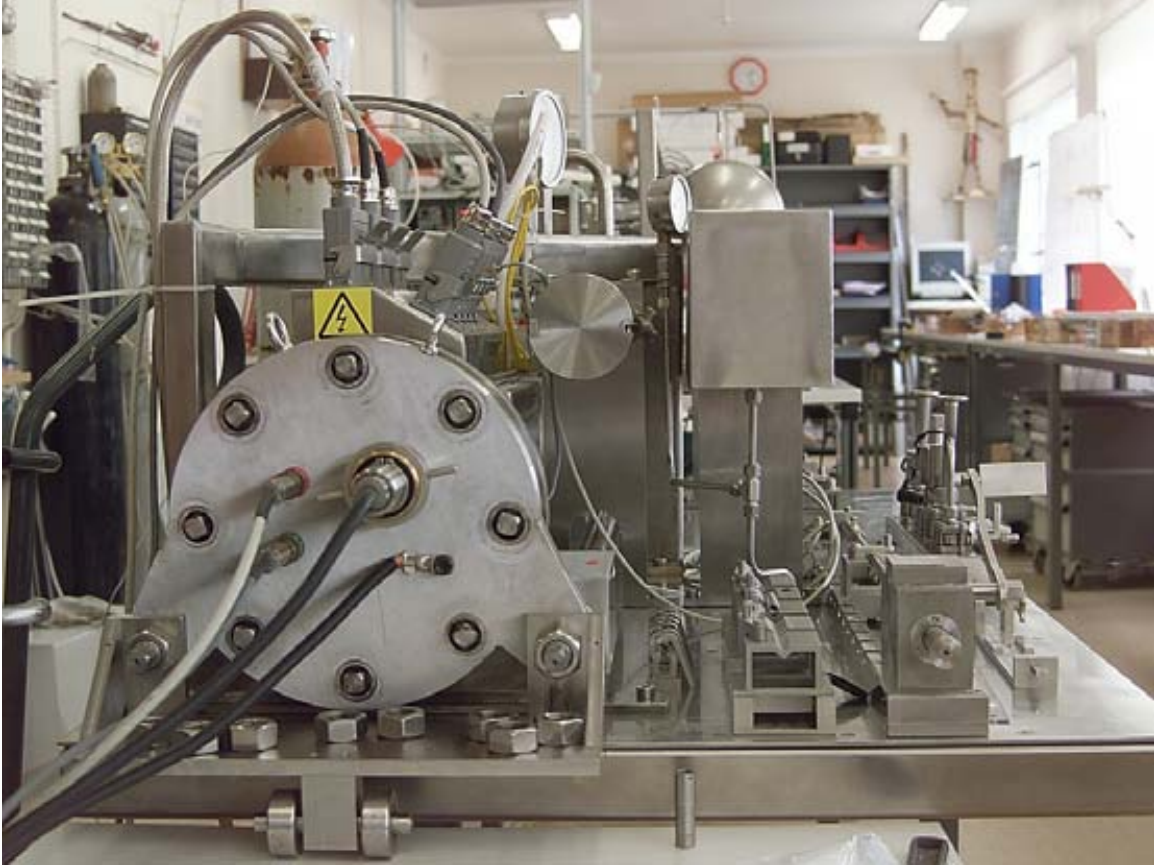


Figure 10, Re-instrumentation equipment used for welding of instrumented end plugs onto pre-irradiated fuel rod segments.

To be able to install a re-instrumented fuel rod with a thermocouple into a test rig, the Halden Reactor Project developed the in core connector (Figure 11). The in-core connector basically connects the cable from the fuel rod (thermocouple) to the designated cable in the test rig. The in-core connector can be used in PWR conditions.

The Halden Reactor Project re-instrumentation capabilities are quite extensive, the most common instruments are:

- Fuel thermocouple
- Rod pressure sensor
- Cladding elongation sensor
- Cladding thermocouple (LOCA or dry-out studies)
- Gas flow lines

The first re-instrumentation was done in 1991 on AGR rods for British Energy and more than 130 rods have been re-instrumented since then.

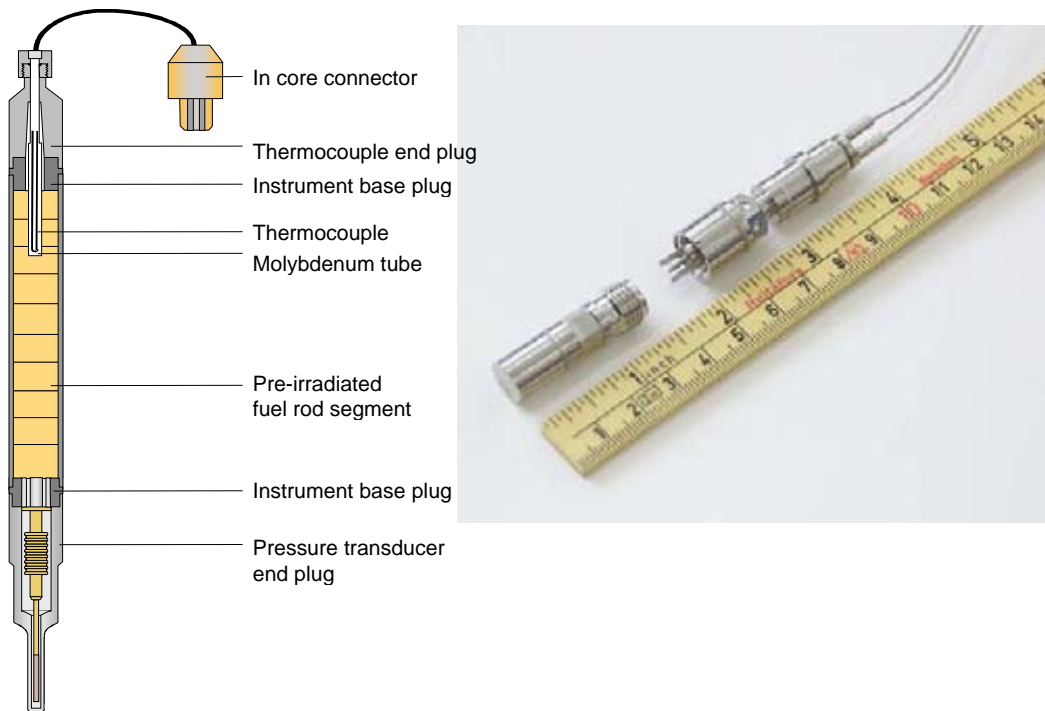


Figure 11, In-core connector

7. ECP reference electrodes

To understand behaviour of fuel or reactor materials can be improved by on-line measurements during operation, the Halden Reactor Project is developing ECP reference electrodes². There are ECP sensors on the market, but the transition between metal and the ceramic parts is normally brazed, which is sensitive to chemical environments. The ECP sensors developed at the Halden reactor project have mechanical sealing at the transition zone directly on the ceramic parts. The Halden platinum electrode (Figure 12) has proved reliable, but Pt electrodes do not give SHE values in oxygenated water. A Palladium electrode (Figure 12) shows promise for use in oxygenated water, but further testing and calibration is required. For reliable ECP measurements, two different reference electrode types should be used. Fe/Fe₃O₄ electrodes can be used in both hydrogenated and oxygenated water and a prototype Fe/Fe₃O₄ electrode (Figure 13) has been developed and is under testing. The results here show that further refinement and testing of this sensor is also needed.

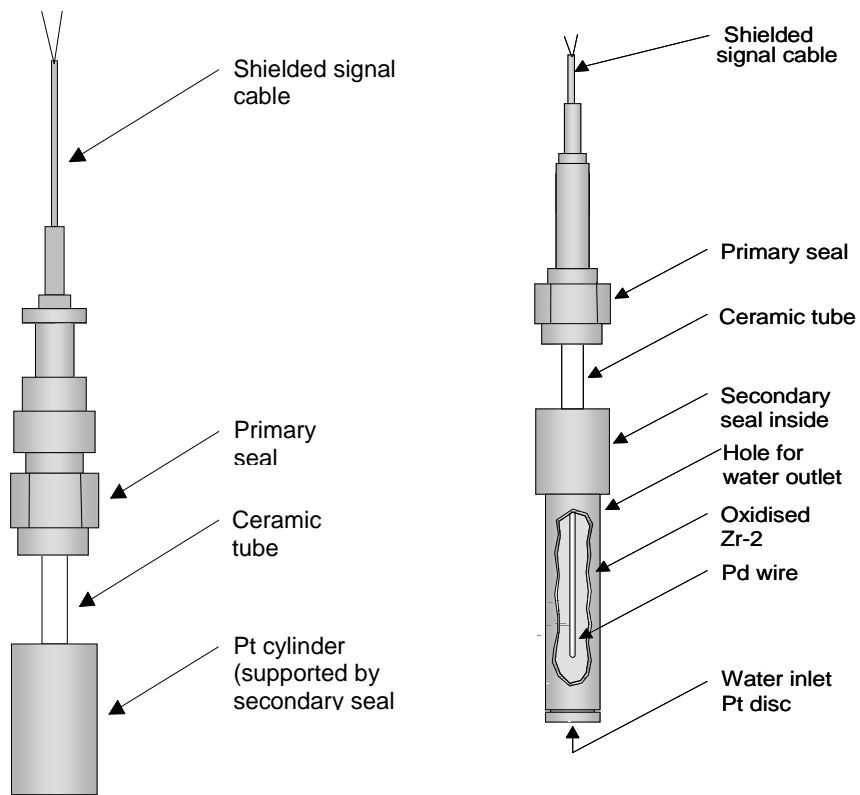


Figure 12, Pt and Pd ECP electrodes

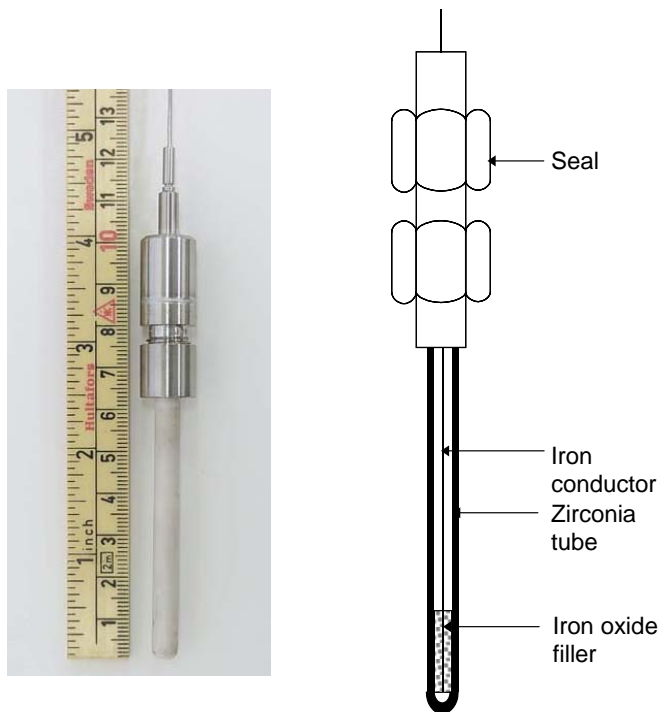


Figure 13, Fe/Fe₃O₄ ECP electrode

8. Summary

The Halden Reactor Project relies on the use of reliable and accurate in-core instrumentation to perform fuel and material irradiation programmes in the Halden Boiling Water Reactor. The possibility of attaching in-core instrumentation to pre-irradiated and un-irradiated fuel rods and material samples from power reactors is important for the nuclear industry. The Halden Reactor Project is refining its existing instruments (Figure 14) and is working with development of new instruments on a continuous basis.

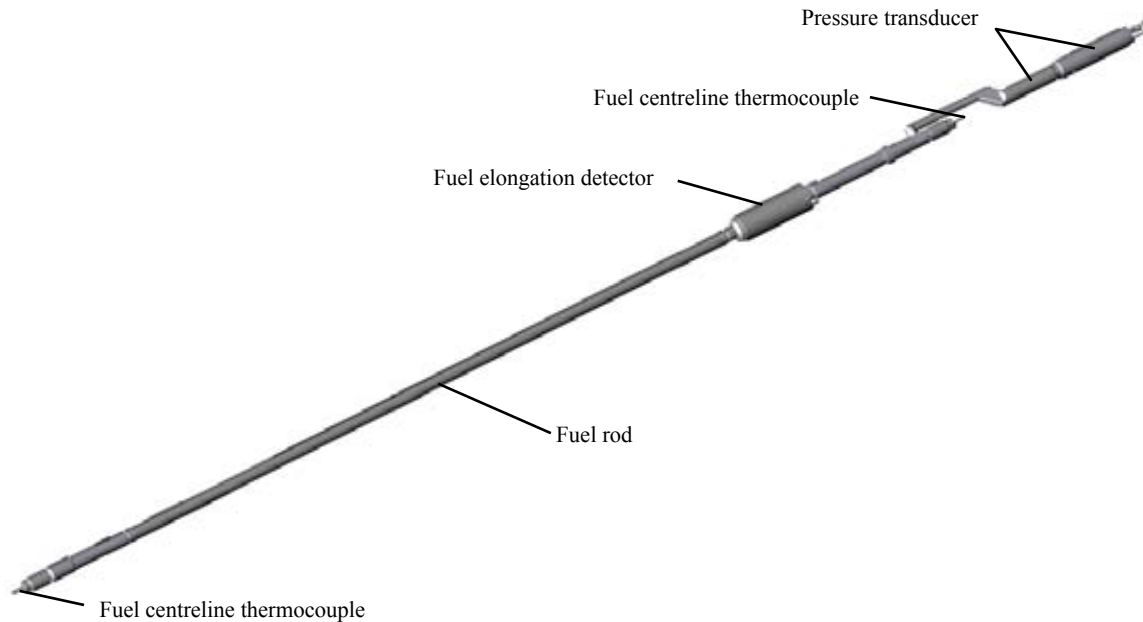


Figure 14, Fuel rod instrumented with several instruments in both ends

Development of new instruments will focus on Linear Voltage Differential Detectors for high temperature applications (above 400°C), on-line cladding corrosion detectors (potential drop, EIS / ECN), electrochemical sensors (ECP, conductivity etc.), in core Eddy-current techniques (e.g. for detecting cladding cracking / development of defects) and instrumentation for Generation IV applications (able to operate in liquid metals, supercritical “steam”, molten salt etc.).

References

-
- ¹ T. Tverberg, *In-pile fuel rod performance characterisation in the Halden Reactor*, This conference
- ² P. Bennet, *In-core measurements of fuel clad – coolant interactions in the Halden reactor*, This conference

Hard drilling technique for making a center hole of irradiated fuel pellets

Francis BERDOULA¹, Karl Silberstein
CEA / Cadarache / DEC / SLS / LIGNE
13108 St Paul lez Durance
France

Abstract :

The information on Fission gas pressure and centerline temperature of fuel pellets during power transient are important to study the FP gas release behaviour of high burnup LWR fuel rods. Beginning in 1999, CEA- LECA hot-lab developed a hard drilling technique for making a center hole of the irradiated fuel pellets for thermocouple insertion.

Various drilling tests were carried out using dummies of fuel rods consisted of zirconium alloy cladding and Ba sub 2 FeO sub 3 pellets. Diamond drills were used to make the center hole. These tests were completed successfully. A center hole, 59mm depth and 2.5mm diameter was realized by this method. Now, we are developing a mock-up machine to perform some drilling tests to make a center hole, 100 mm in depth and 2.5mm in diameter.

The purposes of the development program was to simplify the process and preserve integrity of the drilled fuel stack in order to qualify it on irradiated fuel. Metallographic exams confirm that the fuel microstructure is not significantly affected by the drilling operation.

The first objective was to drill the fuel without cryogenic cooling. Indeed, cryogenic freezing technique is not easy to work with in hot cells facility as liquid flux in and out of cells represents technological difficulties and safety risks. The new process has been qualified for different fuel types and burn up.

Below 2 irradiations cycle, fuel pellets can collapse during mechanical operations on the cladding. So, for basic re-fabricated rods we developed specific inside plugs to block the fuel stack.

A laser-based welding device provides the capability of "re-fabrication and instrumentation" of fuel rods in hot cells.

Keywords:

Experimental – hard drilling technique – Fuel pellets – Instrumentation - Thermocouple

1 Objective

In 1999, LECA Cadarache hot-lab decided to develop a machine tool (**figure 1**) able to drill a center hole in irradiated fuel pellets for thermocouple insertion. The purposes of the development program was to simplify the process and preserve integrity of the drilled fuel stack then to qualify it on irradiated fuel. The first objective was to drill the fuel without cryogenic cooling.

In order to do so centre fuel hole is realised with diamond drill tubes 2.2 mm diameter and 20 and 50 mm long. The rotational speed is around 10 000 rounds per minute and a 5 litres per minute argon flux inside the driller allows cooling of the diamond tube and avoid its filling up from fuel chips. The machine tool is a driller, which is commanded by remote control.

It allows to perform an unlimited number of cycles and modulates six parameters as well. Parameters are, length and speed advance, depth and speed pass, length and speed shrinkage, rotational speed, and number of cycles. The mechanical interaction between fuel stack and cladding induced by irradiation is absolutely needed otherwise the drill could carry the pellets out of the cladding. Thus, application of this process is devoted to a minimum of two cycles irradiated fuel rods.

¹ phone : (33) 04 42 25 34 21 ; fax : (33) 04 42 25 48 78 ; francis.berdoula@cea.fr

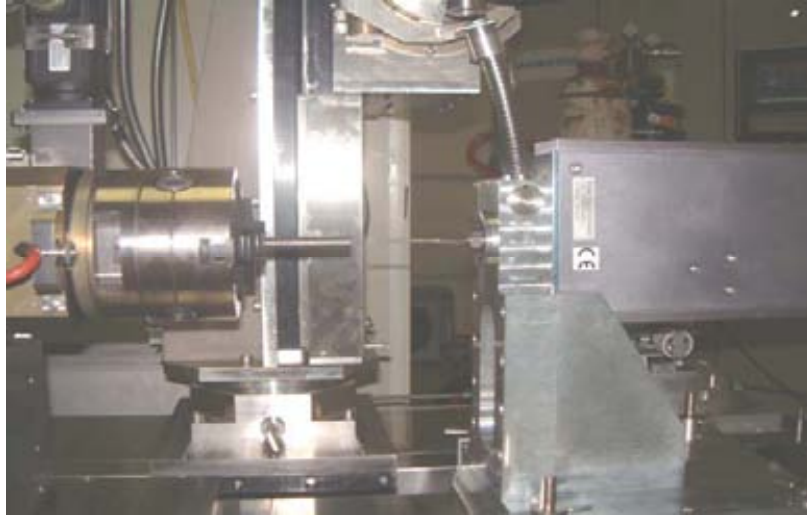


Fig.1 : boring module

After verification of length and depth of the hole, a 2.5 mm diameter molybdenum tube is introduced as the interface between fuel and thermocouple. The 2.5 mm diameter is the present lower limit due to drill mechanical resistance and rotation induced vibrations.

2 Comparison with state of the art cryogenic freezing process

The process presently used is the cold RISÖ process developed by Halden Reactor Project... The operation consists in filling the fuel rod with liquid CO₂ and subsequently freezing it down with liquid Nitrogen in order to stabilise the fuel for the purpose of drilling operation. CO₂ ice material at the outside of the rod is drilled out with a standard steel drill, then diamond drill tubes are used for the centre hole drilling.

Cryogenic freezing technique is not easy to work with in hot cells facility as liquid flux in and out of cells represents technological difficulties and safety risks.

In RISÖ process, the fuel rod must be dried in a 300 °C oven, which can affect the fuel microstructure and induce cracking during the drying operation, because of differential dilatation due to thermal gradients. This effect of the fuel cracking has not yet been quantified, but may have significant effect on fuel thermal behaviour.

The room temperature process allows accurate metrology measurement for the hole, in particular depth and diameter with standard metrology devices. In the RISÖ process, the molybdenum tube has to be inserted into the centreline hole directly after the drilling operation to provide mechanical support to the fuel. Thus metrology of the hole geometry is no more possible to perform.

The new process has been qualified for different fuel types and burn up. Metallographic exams confirm that the fuel microstructure (**figures 2 and 3**) is not significantly affected by the drilling operation.

Other dimensional exams provide important information such as concentricity and diameter of the hole. We have noticed, that the hole diameter is 15 % larger than drill diameter because of drilling vibrations. Accurate dimensions knowledge is particularly necessary for modelling the fuel behaviour with simulation tools.

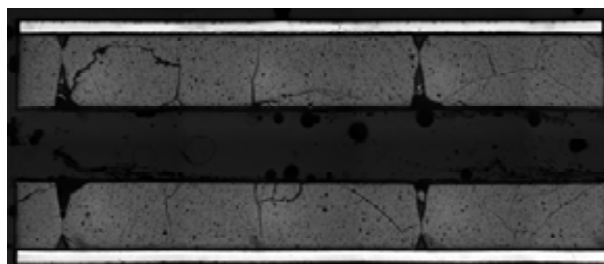


Fig 2: drilled pellets

RISÖ process is applicable for all fuel burn up values compared with the new process, which is valid for fuel rods with a minimum of two cycles irradiation.

To investigate the profile metrology hole, various techniques for postirradiation examination (PIE) are being developed in the LECA-STAR laboratory at the Cadarache CEA center which can be used for this application. They include visual inspections, diameter and length measurement, X-rays technique (**figure3**) as well as axial gamma scanning (**figure 4**) of fuel rods in order to determine the hole length and its reliable diameter.

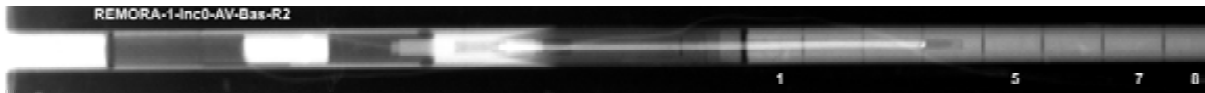


Fig.3 : X-rays radiographic film

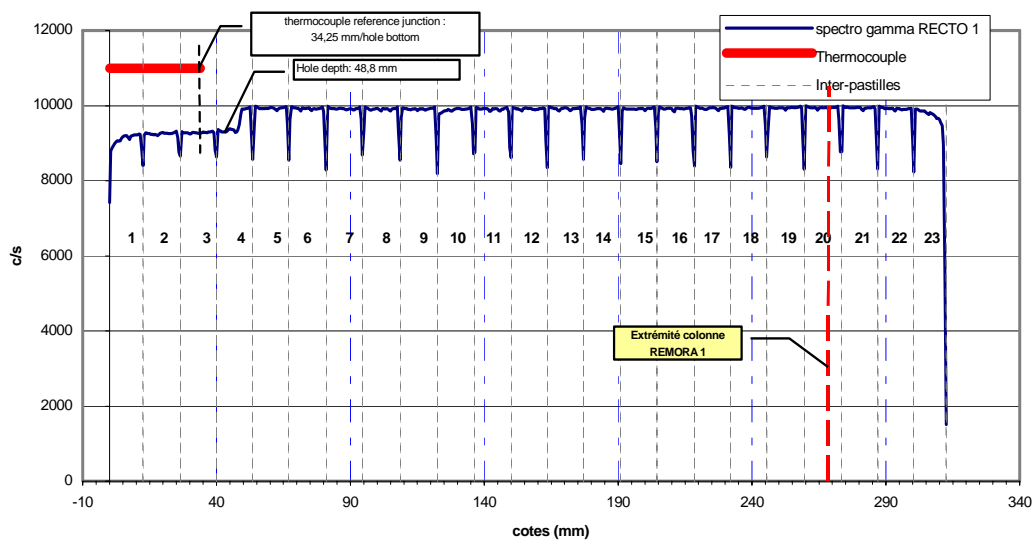


Fig.4 : gamma-scanning profile

So, our laboratory routinely employ the gamma-scanning technique to measure the radial distribution of fission products in fuel rods. The technique is reliable and gives accurate results, and confirms the other methods diagnosis.

3 Process qualification

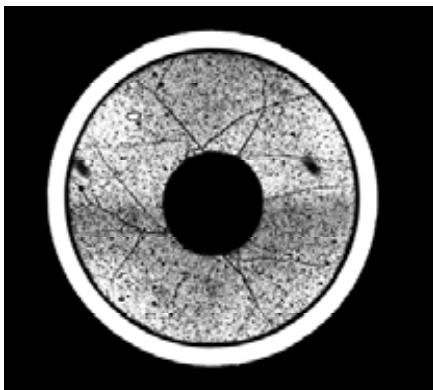
Chronological definition of tests has been chosen according to four parameters; “complexity of making use of the job”, availability of the different fuel rods, availability of the LECA hot-lab cells, and fuel type choice for the first instrumented fuel rod.

First tests have been performed in a glove box with non irradiated fuel in order to validate the capability of the driller to drill fuel pellet and also to get a first experience and provide orientation on parameters. Drills have been successfully manufactured.

The three next tests have been done in hot cell on a vertical simple concept machine tool. The target was to determine the kind of irradiated fuel we could drill, and also to know if we could drill a 50 mm deep hole. We worked on two irradiation cycle fuel and high burn up fuel. As results, we confirmed that we can drill from a two irradiations cycle fuel and also high burn up fuel, and the 50 mm deep hole target has been reached in both cases.

The two next tests have been performed with 70 GWd/t fuel. It has been chosen, because it is exactly representative of the first double instrumented rod fuel. Concentricity of the hole (**Figure 5**) has been obtained better than 0.1 mm with the pellets' axis, the entrance angle is less than 1° with the rod axis, the hole diameter is 2.6 mm for a 2.3 mm drill and the hole is 50 mm long.

At the end of the qualification program, we have realised a hole in the instrumented rod fuel, which was perfectly conform to our specification. The molybdenum tube and the thermocouple have been successfully adjusted for measurement optimisation.



Thermocouple sheath

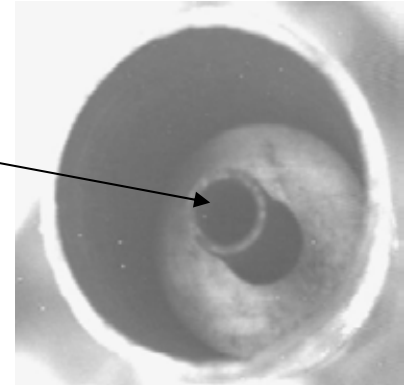


Fig.5 : centre hole

For low burn-up, below a two irradiations cycle fuel, we noticed fuel pellets can collapse when the rod was mechanically milled. So, for basic re-fabricated fuel rods without thermocouple, a specific pine is inserted in the cladding during the whole fabrication for stopping the fuel pellets move.

4 Perspectives

Now, we plan to perform some drilling tests to make a center hole, 100 mm in depth and 2.3 mm in diameter and to determine the optimum drilling condition.

We are testing a mock-up drilling machine which can drill the center on the irradiated fuel rod. Various drilling tests have already been carried out using ceramic rods. These tests were completed successfully. A center hole, 55 mm in depth and 2.5 mm in diameter, was realized by this method.

Following the development of a new prototype tool, it was designed and fabricated for testing in a mock-up area to check drilling process and remote operation, and provides actual hands-on training for operators. Recent tests with an appropriate diamond tool are encouraging.

The boring bench is already implanted in hot cell. We developed a new tool and adapted the drilling process (diamond drills set, improved drill guide, drill material enhancement). So, this technique can be carried out normally in hot cell.

Boring module

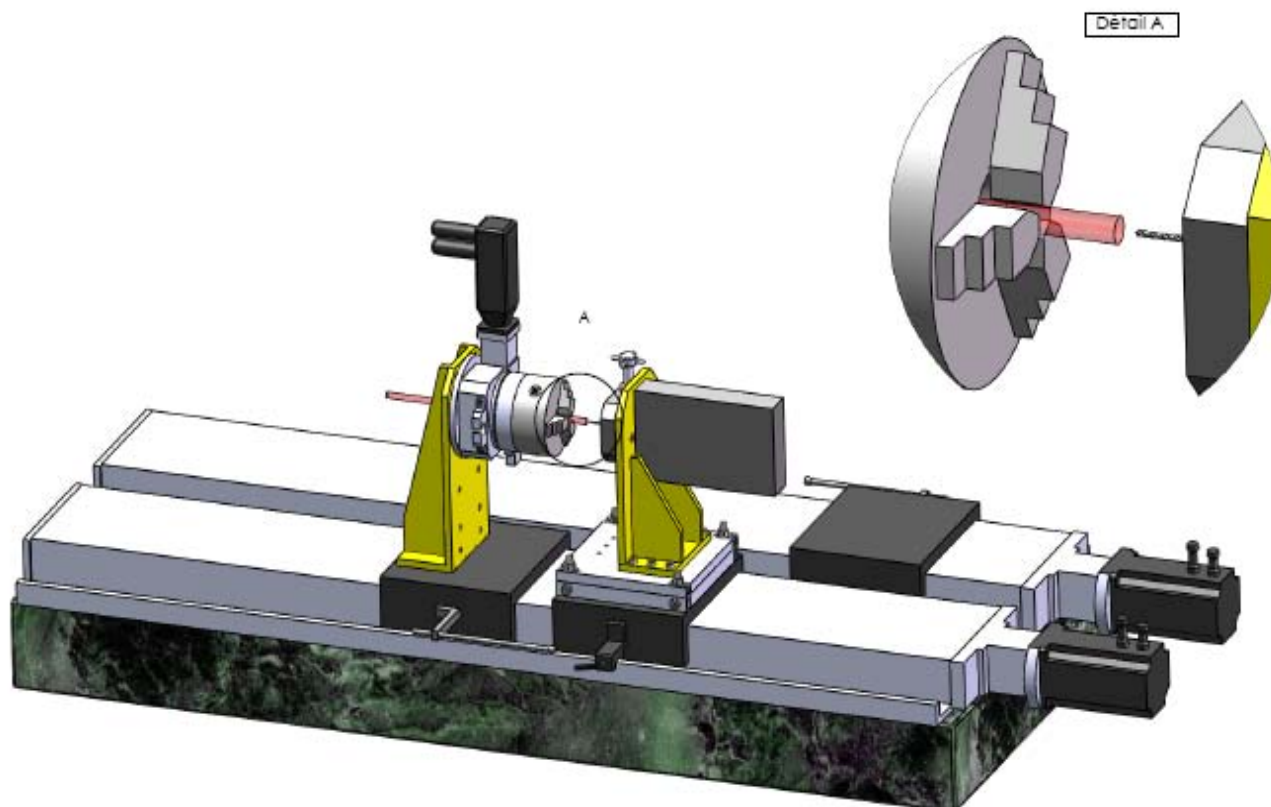


Fig. 6 : Boring module in multi-axes bench Coralie

Conclusion

This hard drilling process offers an accurate technique for making a center hole in fuel pellets, without altering the integrity of fuel pellets. Metallographic examination confirmed the overall satisfactory performance of the hard drilling technique and the absence of significant damage. Gamma-scanning and X-ray radiography were carried out to check the reliability of the diameter hole, as its length, the perfect parallelism between the hole and the cladding.

Operation drilling on large length are operating in a mock-up. It is difficult to drill holes over 50 mm in these materials by means of conventional tool. By improving the performances of the diamond tool, we reached recently the depth of 100 mm, 2,4 mm diameter in ceramic rod diameter of 9,5 mm. This technique can be easily integrated in hot cells on the device Coralie, our multi-axes bench (**Figure 6**) devoted for instrumentation of fuel rods.

Improving High-Temperature and Fission Gas Release Measurements in Irradiation Experiments

J-F. Villard^{1,3}, **D. Fourmentel**¹, **N. L'Hullier**¹, **T. Lambert**², **E. Muller**²

¹ *Commissariat à l'Energie Atomique, Saclay, F-91191 Gif-Sur-Yvette, France*

² *Commissariat à l'Energie Atomique, Cadarache, F-13108 St Paul Lez Durance, France*

³ Corresponding author - E-mail: jean-francois.villard@cea.fr

ABSTRACT

Monitoring irradiation experiments in Material Testing Reactors requires accurate and reliable in-pile instrumentation.

For some years, CEA (Commissariat à l'Énergie Atomique) has been managing a large research program to develop and qualify innovative in-pile instrumentation. The scope of these studies includes:

- Radiation measurements, for instance fast and thermal neutron flux and gamma heating. These parameters are crucial to improve the knowledge of MTR irradiation conditions.
- Measurements of physical parameters inside irradiation rigs, for example temperature, dimensions, fission gas release determination, etc.

An illustration of these developments is presented through two examples of rod instrumentations:

- New high-temperature thermocouples based on molybdenum and niobium thermo-elements, which have the propriety to remain nearly unchanged by neutron flux even during long-term irradiation, whereas in same conditions standard high-temperature thermocouples such as type C or type S are altered by significant drifts because of composition changes involved by material transmutations. For these reasons, this improvement is expected to have a remarkable impact on temperature measurement capabilities for future fuel irradiation experiments.
- Characterization of fission gas release. Successful results have been for example obtained for this purpose by measuring simultaneously the fuel temperature and the rod internal pressure, using a very accurate counter-pressure sensor developed by CEA.

1. INTRODUCTION

Nuclear research reactors are widely used around the World for very various purposes, such as irradiations of material or fuel samples, operation of reactor prototypes, safety studies, assessment of neutronic parameters, production of artificial radio-elements, etc.

Many experiments performed in these facilities require in-situ measurements to monitor and control the conducted tests. These needs are particularly critical in Material Testing Reactors (MTRs), which are specifically dedicated to the assessment of nuclear radiations effects on material or fuel samples proprieties. Irradiations carried out in MTRs come as crucial phases in most scientific programs regarding nuclear technologies, among which one can mention researches for the enhancement or qualification of nuclear fuels for current or future power reactors, as well as the assessment of reactors materials ageing for lifetime increase studies, in-pile tests of innovative devices for advanced reactors within Generation IV programs or material investigations for ITER project.

In France, the Commissariat à l'Energie Atomique (CEA) operates since 1966 the OSIRIS MTR in Saclay, near Paris, and is also preparing the construction of the Jules Horowitz Reactor (JHR). This 100 MW MTR of new generation will start in 2014 in Cadarache, in the South of France.

In MTRs, experiments are conducted in irradiation devices which are introduced inside or beside the core of the reactor, and contain material or fuel samples. The quality of these experiments depends for a large part on the measurements performed in the devices. Parameters measured in-situ are typically neutron flux, temperature, samples dimensions, fission gas release determination, etc.

These in-pile measurements require specific and high-quality sensors, which must satisfy the following features:

- (i) high reliability, because irradiated sensors can not be replaced or repaired easily;
- (ii) very fine accuracy, in order to satisfy scientific requirements continuously increasing;
- (iii) capability to operate in harsh nuclear environments (neutron flux and gamma radiation in MTRs can exceed respectively $4 \cdot 10^{18} \text{ n.m}^{-2}.\text{s}^{-1}$ and 1.5 MGy.s^{-1});
- (iv) capability to operate in pressurized water, liquid metals or high-temperature gas;
- (v) miniaturized body, to be implemented in small irradiation devices without altering the nominal thermal conditions of the samples.

In order to ensure the quality of its current and future MTRs experimental programs, the CEA has recently significantly strengthened its research and development activities about innovative in-pile instrumentation [1].

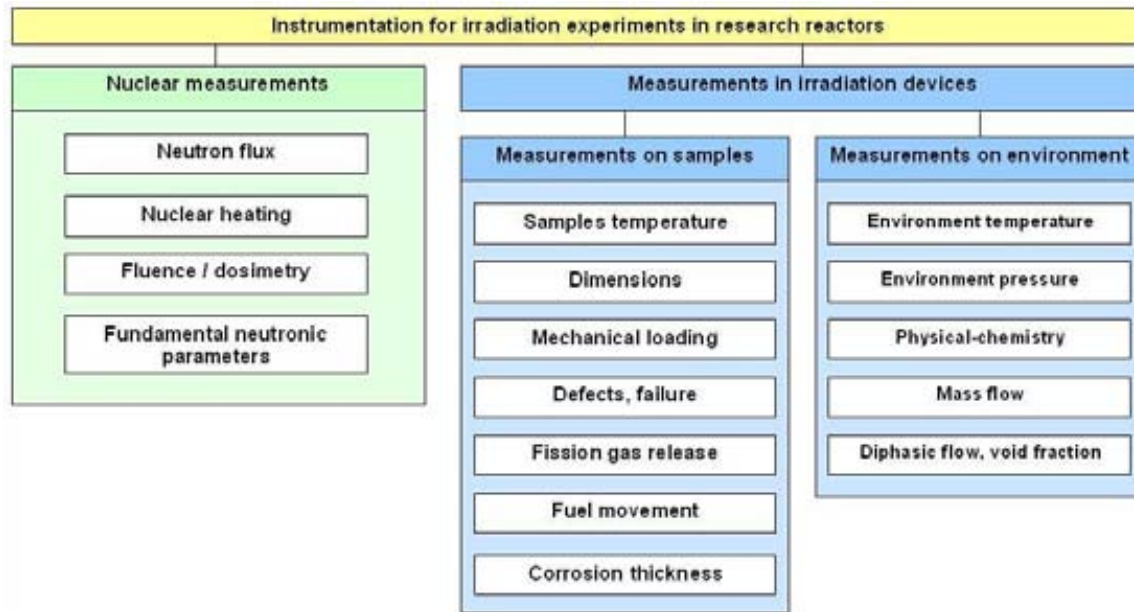


Figure 1 : global chart of in-pile measurements needs

Some of these developments have a strong impact on in-pile measurements capabilities for fuel studies and rod instrumentation. Among them, two examples are particularly relevant:

- innovative high-temperature thermocouples for enduring irradiations [2] [3],
- counter-pressure sensors for online determination of fission gas release [4].

2. INNOVATIVE HIGH-TEMPERATURE THERMOCOUPLES

2.1. Context of In-Pile Temperature Measurements

Samples temperature is definitely a key parameter for most irradiation experiments conducted in MTRs. In-pile temperature measurements have been being performed for decades with thermocouples having mineral insulation and metallic sheath.

For temperatures below 1000°C, needs are quite well satisfied using type K or type N thermocouples (Ni-Cr/Ni-Al or Ni-Cr-Si/Ni-Si), generally with alumina (Al₂O₃) insulation and 1 mm outer diameter stainless steel or Inconel sheath. These sensors have demonstrated an excellent behavior under irradiation regarding reliability and signal stability, even for very high integrated neutron fluxes, exceeding 10²⁶ n.m⁻² (thermal neutrons).

Major difficulties concern high-temperature measurements for long-term irradiations.

As type K and type N thermocouples fail frequently under irradiation above 1000°C (commonly admitted limit for type K is about 1080°C), in-pile temperatures measurements in this range, and more particularly fuel centre temperature measurements, have been achieved until now with type C thermocouples (W-Re alloys).

But under the influence of thermal neutron flux, type C thermo-elements transmute very rapidly. The susceptibility of an element to transmute can be characterized by its Neutron Absorption Cross Section (σ_n): the decrease of this component under irradiation is as faster as its σ_n is high. In type C thermo-elements, Tungsten and Rhenium, which σ_n are respectively

18 barns and 90 barns, are quickly transformed into mainly Osmium [5]. This significant change in the composition of the thermocouple wires causes an irreversible modification of its thermo-electric response, and finally induces a drastic and unacceptable signal drift, which can reach tens and even hundreds Celsius degrees after some weeks under MTR irradiation [6]. Furthermore, type S thermocouples (Platinum-Rhodium alloys), which could appear as an alternative for high-temperature in-pile measurements, are also affected by a decalibration even larger than the one of type C, because of very high Rhodium σ_n (145 barns).

Therefore, standard high-temperature thermocouples remain mainly unsuitable for long-term irradiations, and the need for the development of an adequate measurement system has become clearly strategic for a few years.

For this reason, the CEA started in 2003 a research program with the goal to develop innovative high-temperature thermocouples specially designed to satisfy MTRs requirements.

2.2. General approach

In the 70's, R. Schley initiated studies in CEA about innovative high-temperature thermocouples based on Molybdenum and Niobium thermo-elements [7]. Unfortunately these researches had not been totally concluded and the developments did not reach the industrial stage. However, as preliminary results appear promising for in-pile measurements, the CEA decided in 2003 to complete these studies, with the goal to define the appropriate sensor and assess its performances in nominal MTRs conditions.

2.3. Sensor development

2.3.1. Selection of materials

Materials for wires, insulator and sheath have been selected allowing for theoretical considerations, restrictions from experience and specific tests achieved within this study.

Key parameters taken into account for all materials are principally:

- (i) Melting temperature and mechanical properties (particularly ductility and corrosion resistance) at high temperature;
- (ii) Interactions between materials in the whole temperature range;
- (iii) Cost and availability.

Additional criteria have been considered for each part of the thermocouple.

Coupled materials for wires had to satisfy the following parameters:

- (i) Significant magnitude of the thermoelectric signal;
- (ii) Stability of the Electro-Motive Force (EMF) of the couple at high-temperature;
- (iii) Low susceptibility to transmutation (low σ_n);
- (iv) Compatible thermal expansions between coupled materials, in order to avoid fatal mechanical stress on hot junction when heated, because of different elongations.

For insulation material, the main parameter is the value of the insulation resistance in the whole temperature range, which must stay high enough to limit current leakage.

Sheath materials have to exhibit good machinability, and must also be compatible at high-temperature with materials that will be in contact with the sensor in final applications.

On a first technical step, wires, insulator and sheath materials have been selected allowing for results from previous studies [8] [9] and CEA's experience on in-pile applications. Table 1 resumes the considered materials.

One can note that Molybdenum and Niobium properties fully justify the interest of this development. With respective σ_n of 2.5 barns and 1.1 barns, these materials will remain almost unchanged by transmutation even for long-time in-pile applications.

On a first phase of these studies, only pure Mo and Nb have been considered, in order to promote long-term availability solutions and minimize dependency on material suppliers.

High-temperature compatibility tests have been performed in Thermocoax Laboratory in Flers (France), using a 2000°C induction furnace dedicated to high-temperature processes and calibrations (see Figure 2).

Several samples composed of wires, ceramic insulators and sheaths have been assembled on a graphite barrel then tested at 1600°C under Arcal 1 gas (Argon / Helium mixture) during 24 hours. Table 1 summarizes the results of this operation. A lot of severe interactions have been observed, and finally only 2 configurations appear as suitable for our application.

Consequently, first thermocouple prototypes have been defined and manufactured as following: pure Mo and Nb wires, HfO₂ insulator and Nb sheath.

Material	Neutron Absorption Cross Section ^a (barn)	Melting Temperature (°C)	Result of high-temperature compatibility test ^b	Observation
Wires				
Nb	1.1	2477	N/A	selected
Mo	2.5	2623	-	selected
Pt	10	1768	-	expensive
W	18	3422	-	difficult welding
Re	90	3186	-	expensive, high σ_n
Rh	145	1964	-	very expensive, very high σ_n
Sheath				
Ti	N/A	1668	important reaction (carburization + cracking)	
Nb	-	2477	light carburization	selected
Mo-Re 50%	-	> 2500	important reaction (carburization + cracking)	
Mo	-	2623	significant reaction (carburization)	
Ta	-	3017	light carburization	could be selected
Re	-	3186	light carburization	expensive, difficult machining

^a Neutron absorption cross section of main isotopes for thermal neutrons at 2200 m.s⁻¹, from literature values [10].

^b Results of 24 hours test at 1600°C under Argon / Helium mixture, performed on assemblies including Mo and Nb wires (0.2 mm diameter), HfO₂ insulation and sheath of the considered material, in contact with graphite.

Table I : Summary of main criteria for wires and sheath materials selection

2.3.2. Thermoelectric characterization of Mo-Nb couple

Using the same facility as for previous high-temperature compatibility tests, a complete calibration of the Mo-Nb thermocouple have been achieved, in order to assess its thermoelectric response in the considered temperature range.

The final signal has been obtained by comparison between the measured Mo-Nb EMF and the reference temperature given by a type S thermocouple, which response had previously been standardized by Thermocoax Calibration Laboratory.

Figure 2 shows the result of the Mo-Nb calibration from ambient to 1600°C. This sensor exhibits a reproducible response of about $14\mu\text{v}/^\circ\text{C}$ in the 1000-1600°C range. This signal is of the same order of magnitude as those of standard high-temperature thermocouples, and is definitely compatible with input ranges of conventional data acquisition systems.

The calibration curve obtained during this study is also consistent with results previously obtained at CEA and INEL [7] [9].

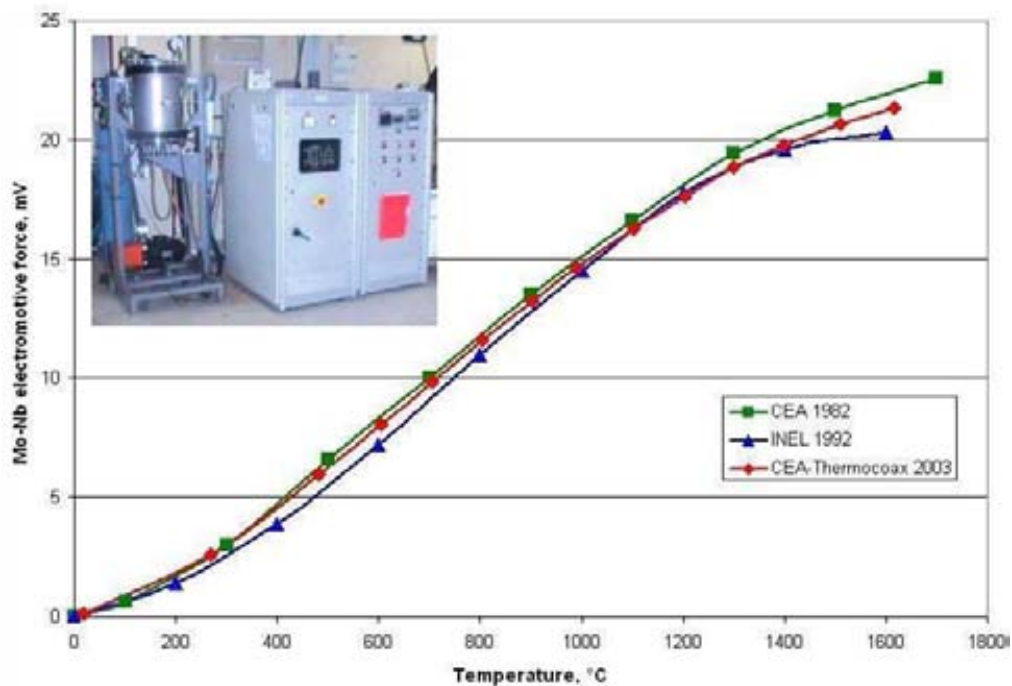


Figure 2 : Electromotive force of Mo-Nb thermocouples measured during calibration tests, compared with previous results obtained by CEA [7] and INEL [9]. In picture: the 2000°C calibration furnace

2.3.1. Prototypes manufacturing

As characteristics (geometry and purity) of the components have a significant impact onto the behaviour of this future thermocouple, the selection and the purchase of the raw materials were carefully managed. Pure Niobium (99.9%) tube, 1.6 mm outer diameter, was selected for the thermocouple outer sheath. Pure molybdenum (99.95%) and niobium (99.9%) wires were

selected and draw up to 0.23 mm diameter by Thermocoax Company. Hard fired hafnium oxide (99.9%) insulators with single and double holes were defined in order to be compatible with the outer tube and the wires.

The typical process used to fabricate thermocouples includes:

- (i) cleaning the sheath outer tube by high-temperature heat treatment under neutral gas,
- (ii) cleaning the thermoelectric wires with solvents and bake out process,
- (iii) baking insulators beads,
- (iv) welding closure cap on the sheath outer tube,
- (v) stringing insulator beads on thermoelectric wires and laser welding the hot junction,
- (vi) stringing a single hole insulator on the hot junction,
- (vii) introducing all parts into sheath tube up to closure cap,
- (viii) vacuum backing and helium filling,
- (ix) sealing end tip with temporary resin, before assembling a prolongation cable,
- (x) controls by radiography.

The thermoelectric signal of a thermocouple must be stable and repeatable on the whole temperature range. Calibration tests performed on Mo-Nb thermocouples up to 1600°C demonstrated that these thermocouples are not stable and not repeatable without initial thermal stabilisation. Parasitic thermal drifts are principally attributed on one hand to migrations of chemical elements around the hot junction, and on the other hand to annealing of mechanical stresses induced during manufacturing by mechanical operations. Therefore an adequate stabilisation process by heat treatment under neutral gas was investigated and defined, then applied onto Mo-Nb thermocouples prototypes.

2.4. Enduring High-Temperature Tests

A major phase in the qualification of the selected prototype is the enduring high-temperature tests. The goal is to assess both reliability and stability of the finalized sensor when used in nominal conditions (except nuclear radiations).

A specific bench-test based on a high-temperature electric furnace has been assembled and operated in Thermocoax Laboratory. Thermocouples have been exposed to a regulated temperature of 1100°C, in low flow neutral gas, while positioned in contact with nuclear-grade graphite. These conditions were chosen to be as close as possible to the first scheduled applications of these sensors (i.e. HTR irradiation experiments in OSIRIS reactor). This test has run during 2500 hours, with an intermediate visual examination after 500 hours. A large variety of sensors has been tested simultaneously, including types K, N, C and Mo-Nb prototypes.

Figure 3 exhibits main results of this 2500 hours operation. Best stability is obtained with type N and type K thermocouples, especially with large diameters (1.5 mm). The well-known quality of these sensors must not hinder that they can not be suitable at higher temperatures, particularly for in-pile use. Above 1100°C, only type C or Mo-Nb will remain usable for in-pile measurements. Moreover, if out-of-pile behaviour of type C is recognized to be excellent

(as measured during this test), one must remind that the expected drift of this sensor under irradiation will finally ban their use of in-core long-term measurements. As an indication, Figure 3 includes a representation of the supposed in-pile drift of a type C thermocouple when exposed to a thermal neutron flux of $4.10^{18} \text{ n.m}^{-2}.\text{s}^{-1}$, which is typical of a MTR core environment (this calculation is based on literature values from in-pile measurements reported for example in [6] and [11]).

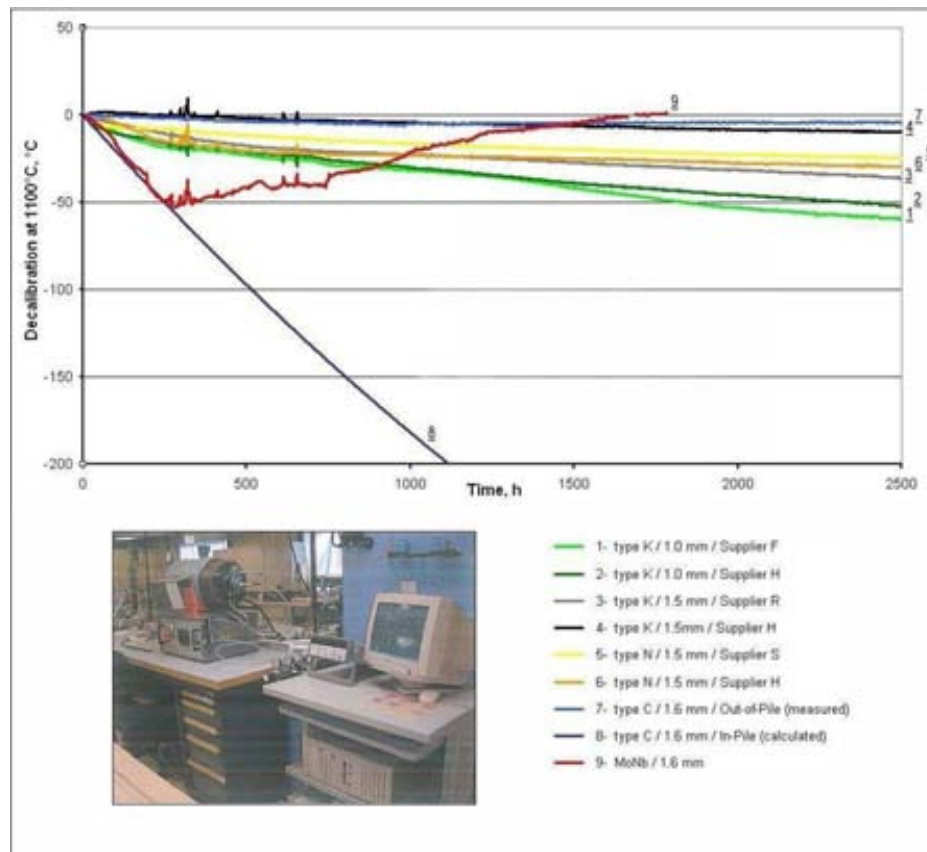


Figure 3 : Evolution of the signal measured by different thermocouples during the enduring test at 1100°C, and indication of the expected in-pile drift of type C thermocouple under a constant thermal neutron flux of $4.10^{18} \text{ n.m}^{-2}.\text{s}^{-1}$ (this last calculation is based on literature values from in-pile measurements reported for example in [6] and [11]). In picture: the specific high-temperature bench-test

The Mo-Nb prototype failed after 1800 hours, and during the first 50 hours at high-temperature its signal was affected by a negative drift up to -50°C (i.e. 4.5 %), then it evolves positively. Such response demonstrates that different and successive phenomena have occurred on this thermocouple during this operation. Finally, this prototype exhibits a very small residual drift of less than 2°C (i.e. $< 0.2 \%$) at the end of its running time, but its behaviour is obviously not yet fully satisfactory.

2.5. Current improvements and perspectives

Some improvements are now being experienced in order to increase reliability and stability of Mo-Nb prototypes. The first enhancement consists in changing the geometry of the ceramic insulation, with the goal to reduce mechanical pre-machining on wires during sensors assembly. A second progress should come from the use of Mo and Nb alloys instead of pure metals. Advantages of alloys have been largely recognized for standard thermo-elements both for reliability and for stability.

First in-pile uses of pure and alloyed Mo-Nb thermocouples are already scheduled during 2008 in different European Material Testing Reactors.

3. IMPLEMENTATION OF FUEL CENTRE THERMOCOUPLES

The implementation of high-temperature thermocouples in pre-irradiated fuel rods is a key point for high-performance irradiation programs in Material Testing Reactors. An innovative technique has been recently developed in CEA.

For the introduction of the thermocouple, the fuel segment is centre drilled over around four end pellets using a fuel drilling process without cryogenic cooling. This technique has been firstly qualified for different fuel types and burn-ups (from fresh and irradiated fuels up to 70 GWd/tM) in order to check if any change or crack in fuel microstructure was induced, which could result in a modification of the fuel thermal conductivity. Both the drilling characteristics (diameter, concentricity) and the state of the fuel microstructure have been controlled by metallographic examinations.

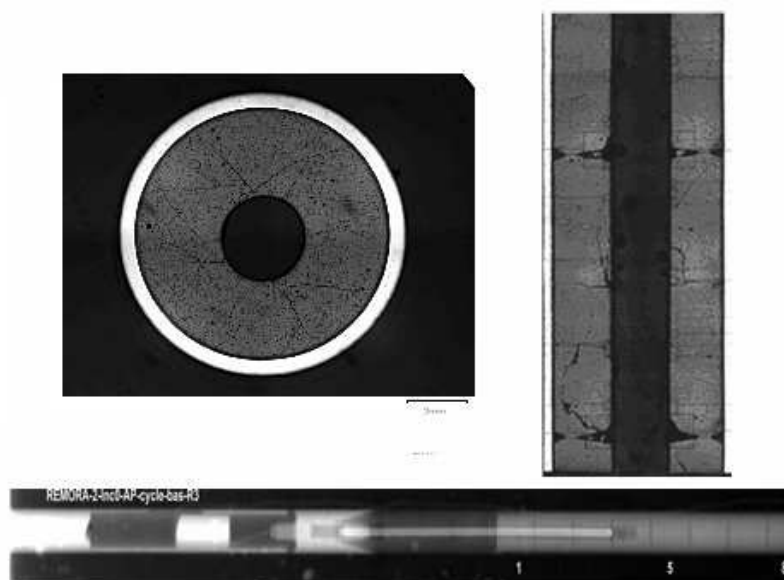


Figure 4 : Various views of pre-irradiated (62 GWd/tM) advanced PWR fuel rod drilled by CEA's innovative technique, then instrumented with a high-temperature thermocouple

This drilling technique has been successfully employed for the fabrication of the instrumented fuel rods of the REMORA experiments in 2005 and 2006 [12]. The fuel rods were re-fabricated from segments of high burn-up UO_2 fuel rods previously irradiated in power reactor up to a burn-up of 60 GWd/tM for the first experiment and up to 70 GWd/tM for the second one.

4. COUNTER-PRESSURE SENSOR FOR ROD PRESSURE MEASUREMENTS

4.1. Description of the sensor

A specific sensor for online measurement of the fuel rod internal pressure during irradiation experiments has been developed by CEA. The sensor is designed to be set up on a pre-irradiated PWR fuel rod and to operate under severe irradiation environments, which means very high neutron flux and gamma radiation, high temperature (up to 350 °C) and heavy external pressure (up to 150 bar). In order to be less intrusive as possible in the experiment irradiation device, this sensor has the same diameter as the fuel rod (approximately 10 mm), and is roughly 250 mm long.

It is based on the reliable and drift-less counter-pressure principle. It consists of two gas cavities, separated by a double bellow (see fig. 5). The first cavity communicates with the fuel rod. The second cavity is connected to an external helium circuit, which is called “counter-pressure” circuit.

The imbalance between the internal rod pressure and the counter-pressure is accurately detected by two electric contacts, activated by the motion of the bellows. This imbalance can be automatically compensated by inflating or deflating the counter-pressure.

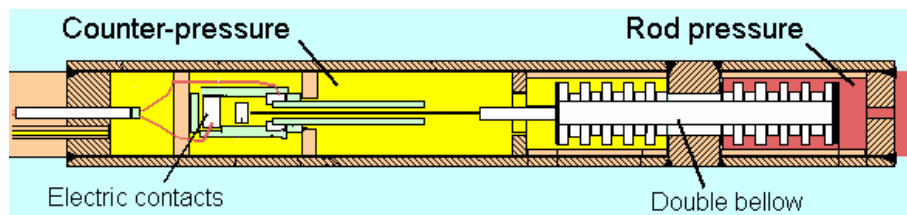


Figure 5 : Simplified drawing of the counter-pressure sensor

This system provides a very accurate online measurement of the internal fuel rod, through the simultaneous knowledge of the imbalance detection signals on the one hand, and the online out-of-pile measurement of the counter-pressure on the other hand.

Making transfer operations and transport easier has been a priority at each step of the design of this instrument. The lower part of the measurement system, including the two cavities and the fuel rod, is linked to the upper part of the sample holder through a specific connector, providing both the electric and the gas transmissions. This connector is also designed to be easily handled by telemanipulators. Once it has been set up on the pre-irradiated fuel rod, the

sensor can thus be linked to the sample holder, and then inserted into the irradiation device, before being transferred in the reactor area.

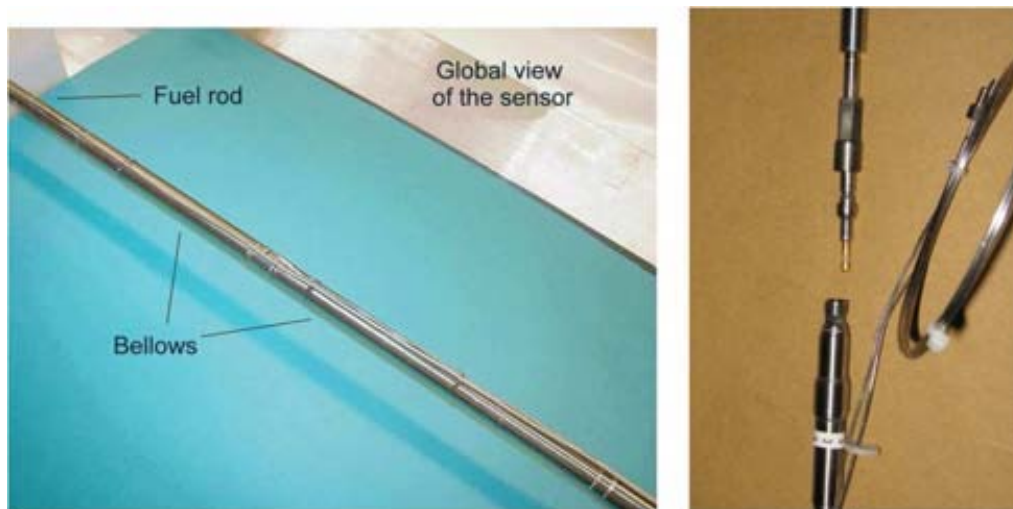


Figure 6 : Views of the counter-pressure sensor and its electric/gas connector

4.2. In-pile performance

The physical principle of the counter-pressure avoids any drift phenomenon due to nuclear radiation. During its in-pile qualification in 2003 in the OSIRIS reactor, this sensor exhibited an accuracy better than $\pm 0,5$ bar (with the confidence of 95 %) up to 120 bars, while no signal drift could be observed up to a integrated thermal neutron flux of 1.5×10^{24} n.m⁻² [4].

In 2006, the sensor was used successfully during REMORA in-pile experiment [12]. A pre-irradiated (5 cycles - 62 GWd/tM) advanced UO₂ PWR fuel rod was instrumented in CEA Cadarache with both a high-temperature thermocouple and a counter-pressure sensor, and then transferred to CEA Saclay in the GRIFFONOS pressurized water loop of OSIRIS reactor. The irradiation scenario included power ramps up to 360 W/cm. Online measurements were accurately achieved during the whole in-pile sequence.

Moreover, the final rod internal pressure was also measured by a post-irradiation destructive method (rod puncture) and compared to the counter-pressure sensor signal at the end of the irradiation. Taking into account the free volumes in the rod and the quantity of fission gases released from the fuel, the determined value (43.2 bars) was very close to the online measurement (43.3 bars), corroborating the very good in-pile performance of this new pressure transducer.

Finally the fission gas release was obtained by using:

- (i) the internal pressure measurement,
- (ii) the evolution of the internal free volume obtained by calculation and corroborated by measurements before and after the in-pile experiment,
- (iii) the internal gas average temperature obtained by a preliminary in-pile calibration phase.

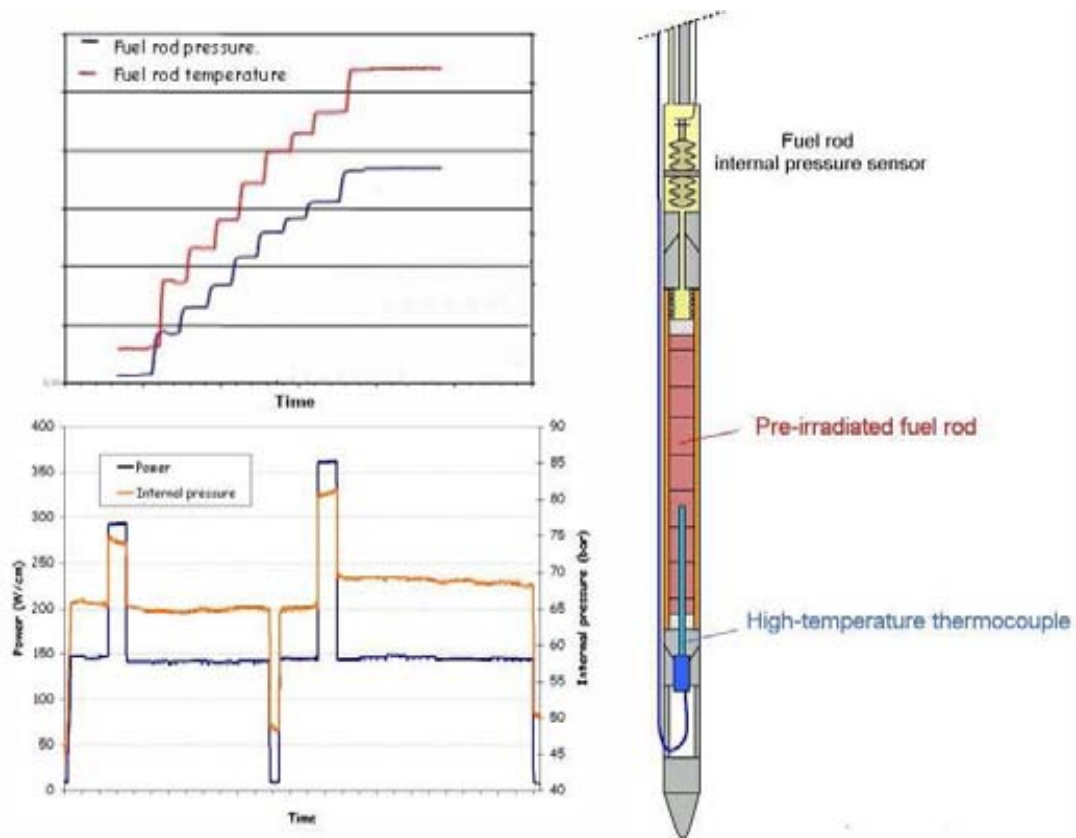


Figure 7 : REMORA experiment : global design of the instrumented fuel rod and examples of online measurements

5. CONCLUSION

Significant improvements in rod instrumentation capabilities have been recently achieved in CEA, making possible the execution of high-performance irradiation experiments on advanced PWR fuels in OSIRIS reactor.

A large research and development program related to innovative in-pile measurements is still in progress, and further beneficial impacts are expected in the coming years, with for example the qualification of a new high-temperature thermocouple with enhanced stability under irradiation.

Moreover, a major step will be soon got over regarding the characterization of fission gas release kinetics, with the possibility to implement acoustic measurements on refabricated fuel rods. An acoustic sensor, using a high-frequency echography technique to measure the acoustic wave's velocity in the gas contained inside the fuel rod, is currently under development. Such a system will allow the online and simultaneous measurements of the pressure and of the composition of the gas inside the rod. This ongoing study is carried out in the framework of the CEA-SCK·CEN Joint Instrumentation Laboratory, and in collaboration with the French National Centre for Scientific Research [1] [13] [14].

REFERENCES

1. J-F. Villard, "Innovative In-Pile Instrumentation Developments for Irradiation Experiments in Material Testing Reactors", at *10th International Group on Research Reactors meeting* (IGORR, Gaithersburg, 2005)
2. J-F. Villard, S. Fourrez, D. Fourmentel, A. Legrand, "Improving High-Temperature Measurements in Nuclear Reactors with Mo-Nb Thermocouples", at *10th International Symposium on Temperature and Thermal Measurements in Industry and Science* (TEMPMEKO, Lake Louise, 2007)
3. J-F. Villard, S. Fourrez, "High Temperature Measurement Needs for Irradiation Experiments in Material Testing Reactors: Development of a New Type of Thermocouple and Interest of High Temperature Fixed Points for its Characterization and In-Pile Qualification" at *Physikalisch-Technische Bundesanstalt Seminar on High-Temperature Fixed-Points for Industrial and Scientific Applications* (Berlin, 2005)
4. J-F. Villard, G. Lemaitre, J-M. Chaussy, F. Lefèvre, "High Accuracy Sensor for Online Measurement of the Fuel Rod Internal Pressure during Irradiation Experiments", at *7th International Topical Meeting Research Reactor Fuel Management* (RRFM, Aix-en-Provence, 2003)
5. W.E. Browning, C.E. Miller, "Calculated Radiation Induced Changes in Thermocouple Composition", in *Temperature: Its Measurement and Control in Science and Industry*, Vol. 3, Part 2 (AIP, New York, 1962), pp. 265-276
6. F.A. Johnson, A.J. Walter, and R.H. Brooks, "Tungsten-Rhenium Thermocouple Drift Under Irradiation" in *International Colloquium on High-Temperature In-Pile Thermometry* (Petten, 1974), pp. 579-584
7. R. Schley, G. Metauer, "Thermocouples for Measurements under Conditions of High-Temperature and Nuclear Radiation", in *Temperature: Its Measurement and Control in Science and Industry*, Vol. 5, Part 2 (AIP, New York, 1982), pp. 1109-1113
8. R. Schley, J-P. Leveque, C. Lavoine, G. Metauer and M. Gantois, "Technological Improvements of High-temperature thermocouples used in Nuclear reactors", at *7th European Thermophysical Properties Conference*, (Anvers, 1980)
9. S.C. Wilkins, "Characterization and Material-Compatibility Tests of Molybdenum/Niobium Thermocouples", in *Temperature: Its Measurement and Control in Science and Industry*, Vol. 6, Part 1 (AIP, New York, 1992), pp. 627-630
10. G. Pfennig, H. Klewe-Nebenius, W. Seelmann-Eggebert, *Chart of the Nuclides*, 6th edition, 1995, revised reprint 1998, Forschungszentrum Karlsruhe GmbH
11. C. Vitanza and T.E. Stien, "Assessment for Fuel Thermocouple Decalibration During In-Pile Service", in *Journal of Nuclear Materials*, 139 (1986), pp. 11-18
12. E. Muller, T. Lambert, N. L'Hullier, K. Silberstein, C. Delafoy, B. Therache, "Thermal Behavior of Advanced UO₂ Fuel at High Burnup", at *International LWR Fuel Performance Meeting* (San Francisco, 2007)
13. J-Y. Ferrandis, G. Leveque, F. Augereau, E. Rosenkrantz, D. Baron, J-F. Villard, "An ultrasonic sensor for pressure and fission-gas release measurements in fuel rods for pressurized water reactors", at *9th International conference on CANDU fuel* (Belleville, 2005)
14. D. Baron, P. Chantoin, J-M. Saurel, J-F. Villard, "Micro-acoustic methods applied to nuclear materials examination", at *6th International Conference on WWER Fuel Performance, Modelling and Experimental Support* (Albena, 2005)

SESSION 2: IRRADIATION TESTING FACILITIES AND CAPABILITIES

Chairperson

R. Van Nieuwenhove (Norway)

INSTRUMENTATION TECHNIQUES IN NSRR EXPERIMENTS

Y. MURAMATSU, Y. UDAGAWA¹

NSRR Operation Section, Department of Research Reactor and Tandem Accelerator
Japan Atomic Energy Agency
Tokai-mura, Ibaraki-ken
Japan

Abstract

The Japan Atomic Energy Agency has performed a great number of pulse irradiation experiments of light water reactor (LWR) fuel rods using the Nuclear Safety Research Reactor (NSRR) since 1975, in order to study fuel behavior under reactivity initiated accident (RIA) conditions. Through a great number of pulse irradiation experiments both for fresh and irradiated fuel rods, experiences for measurements of very fast transient under strong irradiation condition have been accumulated and unique instrumentation techniques, as spot-welding of thermocouple to achieve quick response or water column velocimeter to evaluate generated mechanical energy at fuel failure, have been developed. The results have been utilized to establish safety evaluation guidelines for RIA in some other countries as well as in Japan.

1. INTRODUCTION

The Japan Atomic Energy Agency (JAEA) has conducted experimental and analytical studies of light water reactor (LWR) fuel behavior under accident conditions. One of the most important accidents to assess is the reactivity initiated accident (RIA) which could cause fuel failure and consequent damages to the reactor vessel and to the core internal structure. JAEA started an experimental program of RIA-simulating pulse irradiation on LWR fuels using the Nuclear Safety Research Reactor (NSRR) in 1975.

The first phase of the NSRR program was conducted with fresh, i.e. unirradiated, LWR fuels. Over 1200 pulse irradiation experiments were parametrically performed under standardized test conditions. Fuel states during the pulse irradiation, including cladding temperature, rod pressure and so on, were measured and the results were presented mainly as a function of peak fuel enthalpy. The Nuclear Safety Commission (NSC) of Japan utilized the experimental results to establish safety evaluation guidelines for reactivity insertion events at LWRs [1]. For fresh fuel experiments, test capsules for specific purposes have been developed, such as a visual observation capsule with a periscope and a high-speed camera [2][3]. Research reactor fuels, including silicide [4] and TRIGA [5] fuels, were tested as well. Unirradiated MOX fuel tests were also carried out [6].

The second phase of the NSRR program started in 1989, which was intended for irradiated fuel experiments. Prior to the experiments, the NSRR facilities were modified to enable handling and testing of high burnup fuels. Experiments were carried out on LWR fuel rods, which were irradiated in a commercial BWR/PWR or in the Japan Materials Testing Reactor (JMTR). Regarding irradiated MOX fuels, tests of prototype ATR (advanced thermal reactor) Fugen fuel rods have been performed since 1996 [7]. Results of irradiated fuel experiments have shown that high burnup fuel rods have a different failure mode from those of fresh rods. In failure of high burnup fuel rods, the key phenomenon is the pellet cladding mechanical interaction (PCMI) and the failure threshold in terms of peak fuel enthalpy decreases with burnup, mainly due to degradation of the cladding mechanical strength resulting from hydride precipitation [8][9]. These experimental results were reflected in safety evaluation guidelines for RIA of high burnup fuels, which was established by the NSC of Japan in 1998 [1]. The burnup of test fuel rods is being raised in response to the worldwide trend of burnup extension.

Instrumentation techniques in NSRR experiments have been developed mainly through the experience of many experiments with fresh fuels in the first phase program. Since quick response and stability under strong irradiation are required for sensors in NSRR experiments, methods and materials have been tried and selected to satisfy these requirements. Almost all instrumentation which had been developed in the first phase program is used also in the second phase program and providing successful measurements. Since the number of irradiated fuel experiments is limited mainly due to their large cost compared to fresh fuel experiments, the reliability of measurement have become more important and so improvement of instrumentation technique is continued. This paper introduces the NSRR facilities and the test procedure, and then provides significant information on the instrumentation techniques. Basic specifications are described for the main instrumentation and, for some of them, detailed mechanisms and examples of measurement results are explained.

¹ Nuclear Safety Research Center, JAEA

2. FACILITIES AND TEST PROCEDURE

2.1. NSRR

Figure 1 shows vertical and horizontal cross sections of the NSRR. The NSRR is a modified TRIGA[®] Annular Core Pulse Reactor (ACPR). The TRIGA type reactor is known for the unique nature of the strong negative feedback to reactivity insertion. The NSRR, in particular, is a modified type with enhanced negative feedback. The stainless cladding of the driver core fuel rod is dimpled to make circular protuberances on the inner surface of the cladding, which in turn keeps the fuel-clad gap open and reduces the thermal conductance. Therefore, the peak fuel temperature is preserved, resulting in the enhanced temperature feedback. Such techniques enable the NSRR to produce a high power pulse reaching ~23 GW safely.

Figure 2 shows typical histories of reactor power and fuel temperature in the NSRR experiments. Most of the NSRR experiments have been performed with the natural pulse operation mode, as shown in Fig. 2, to simulate power excursion in RIA. The pulse shape, which is specified with height and width, depends on the total energy release (i.e. time-integrated power). The full width at half maximum and the power peak are approximately 4 ms and 23 GW, respectively, for a total energy release of 130 MJ.

In addition to the operational capability, the NSRR has a large experimental cavity at the core center as shown in Fig. 1, which enables insertion of a test capsule with a diameter up to 200 mm into the reactor core and permits flexible design of the test capsule. JAEA has taken advantage of the NSRR features to carry out accident-simulating experiments under various conditions.

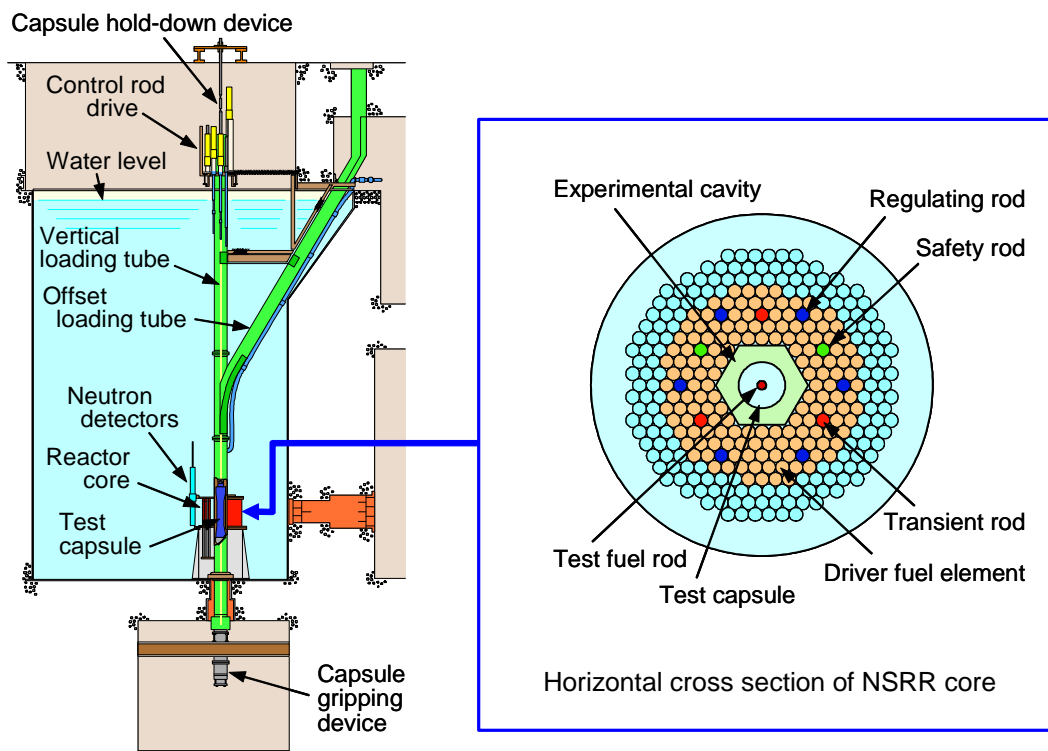


Fig. 1. Vertical and horizontal cross-section of NSRR

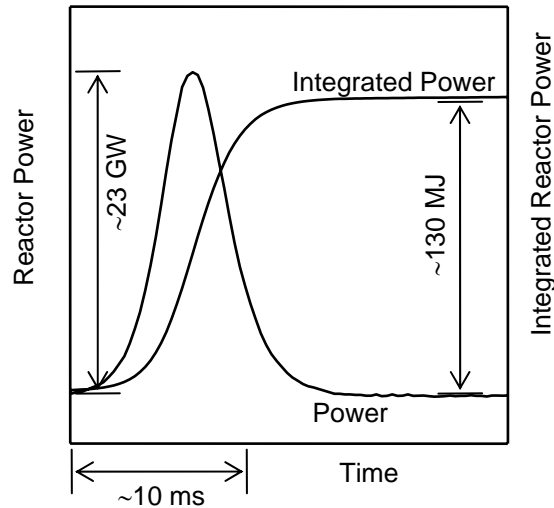


Fig. 2. Typical history of reactor power and fuel temperature in NSRR experiments

2.2. Test capsules

JAEA has developed several types of capsules to test various fuels under different coolant conditions. Test fuels are presently categorized into UO_2 , MOX, silicide and TRIGA fuels. Pulse irradiation tests are performed at room temperature (~ 20 degrees C) and atmospheric pressure (~ 0.1 MPa) condition, with stagnant coolant water in a test capsule.

2.2.1. Test capsules for fresh fuels

Figure 3 shows the atmospheric test capsule for fresh UO_2 fuel rods, which is made of stainless steel and has an inner diameter of 120 mm. Most of fresh fuel tests were performed with this capsule containing stagnant water at room temperature and atmospheric pressure. Various equipment can be installed in the capsule according to need, including an electric heater to raise water temperature, an electric pump for forced convection, flow channel tube to adjust hydraulic diameter, etc. Bundled rods can also be tested with this capsule to compare fuel failure threshold between single rod and bundled rods systems.

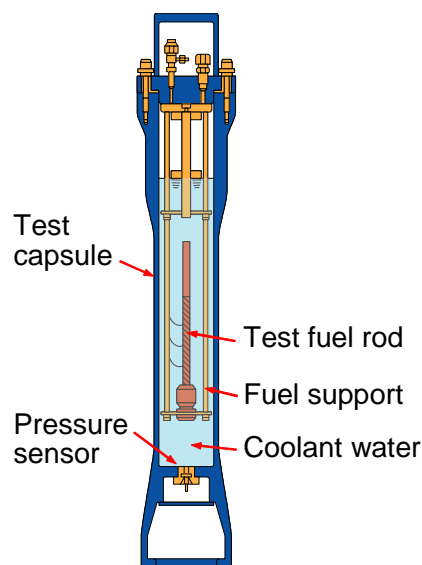


Fig. 3. Test capsule for fresh UO_2 fuel

JAEA has also developed test capsules for specific purposes. A visual observation capsule which is equipped with a periscope and a high-speed camera enabled visualization of fuel behavior under RIA conditions for the first time in the world [2].

Test capsules for fresh MOX, silicide and TRIGA fuels have been individually designed, but the bases are common to that of the fresh UO₂ test capsules.

2.2.2. Test capsules for irradiated fuels

Test capsule for irradiated fuels has a double container structure to assure pressure-resistance and airtightness for radioactive materials. A schematic of the irradiated fuel test capsule is shown in Fig. 4. The test section is smaller than those of fresh fuel test capsules, but the same kind of equipment and sensors can be installed. Coolant conditions for this capsule are normally room temperature and atmospheric pressure. The coolant temperature can be raised up to ~90 degrees C using an electric heater. This type of capsule is available for irradiated UO₂ and MOX fuels.

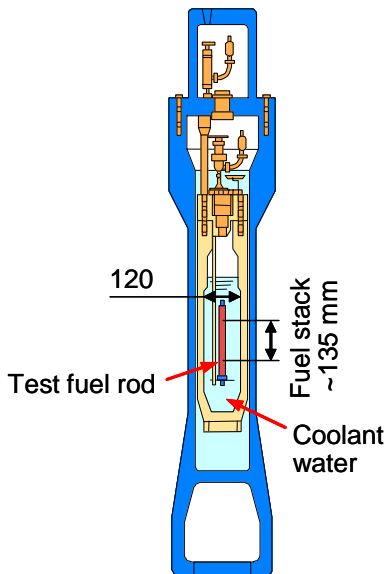


Fig. 4. Irradiated fuel test capsule

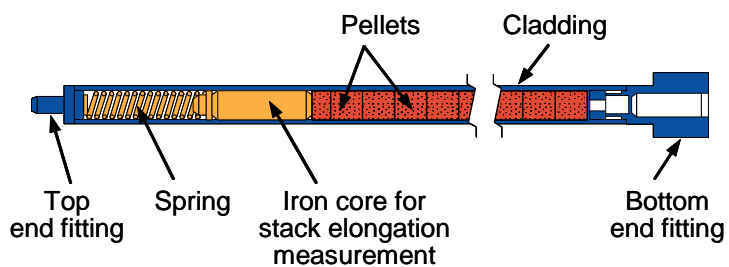


Fig. 5. NSRR standard test fuel rod

Irradiated fuel rods for the NSRR tests are categorized into two types; the NSRR standard test rods irradiated in the JMTR, and shortened and re-fabricated segments of fuel rods irradiated in commercial BWR/PWR or in ATR. Basic designs of rod end plugs and other parts are common to those for the NSRR standard test fuel rod shown in Fig. 5.

3. INSTRUMENTATION

3.1. Main instrumentation

The following sensors can be installed on the test rods or test capsule.

- * Cladding surface thermocouple
- * Coolant water thermocouple
- * Capsule pressure sensor
- * Rod internal pressure sensor
- * Cladding elongation sensor
- * Pellet stack elongation sensor
- * Water column velocimeter
- * Cladding surface strain gauge

Signals from all sensors are pre-amplified and sent to the NSRR data acquisition system. Data had been recorded to a magnetic tape using a high-speed analog recorder until 1999. The present system has a real-time A/D converter, which digitizes signals with a 16-bit resolution at sampling frequencies up to 200 kHz. Figure 6 shows examples of layout for these sensors. Elongation sensor and water column velocimeter can not be used in one test because each of them requires the space above test fuel rod. Generally, water column velocimeter is used in case fuel failure is expected and elongation sensor is used in case fuel is expected to survive. The detailed information for each sensor

is described below.

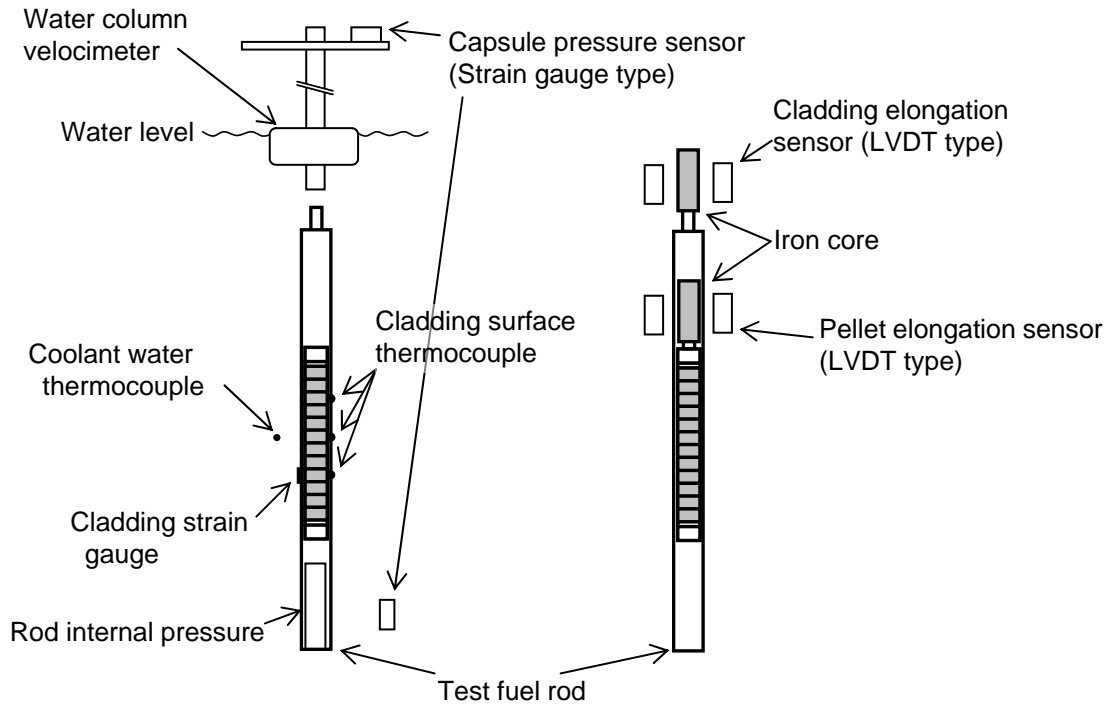


Fig. 6. Instrumentations in NSRR tests

3.1.1. Cladding surface thermocouple

Cladding surface thermocouple is to measure cladding surface temperature of test fuel rod. This sensor is attached to the cladding surface in the axial range of pellet stack, as shown in Fig. 6. In the measurement of cladding surface temperature in the NSRR tests, quick response of thermocouple is required to follow the fast transient, so thin (diameter : 0.2 mm) wire is used and bare wire of thermocouple is directly spot-welded on the cladding surface. R-type thermocouple (Pt and Pt/13%Rh) wires are employed to cover high temperature range.

For irradiated fuel rods, which have oxide layer at the cladding surface, partial removal of oxide layer is needed before the spot-welding to ensure electric conductivity between the thermocouple wire and cladding surface. Ensuring radioprotection, remote control technique is needed for removal of oxide layer and spot-welding. Figure 7 shows the procedure of oxide removal. In the NSRR hot cell, test fuel rod is fixed and its oxide layer is partially removed with remotely controlled grinder. The removal of oxide layer is confirmed with visual inspection and electric conductivity check. Figures 8 and 9 show schematics of spot-welding device and spot-welding procedure, respectively. Bare wires of thermocouples are supplied from the nozzles of two TC cartridges for Pt wire and Pt-Rh wire. The TC cartridges are remotely controlled so that the tip of nozzle contacts with the surface of oxide-removed zone of cladding. Bare wire of thermocouple is first welded to cladding and then welded to terminal which is positioned beside test fuel rod in test capsule. Since the direct output of cladding surface thermocouple reflects the temperature gap between cladding surface and terminal, terminal temperature is necessary to decide the absolute value of cladding surface temperature. Practically, water temperature, obtained with coolant water thermocouple, is used as terminal temperature to decide cladding surface temperature. Welded wire on terminal is cut by melting. Figure 10 shows examples of aspect and cross section of cladding after spot-welding.

Figure 11 shows examples of measured history of cladding surface temperature. As shown in Fig. 11, with spot-welded thermocouple, cladding surface temperature is successfully measured and DNB behaviors have been observed in numbers of NSRR tests.

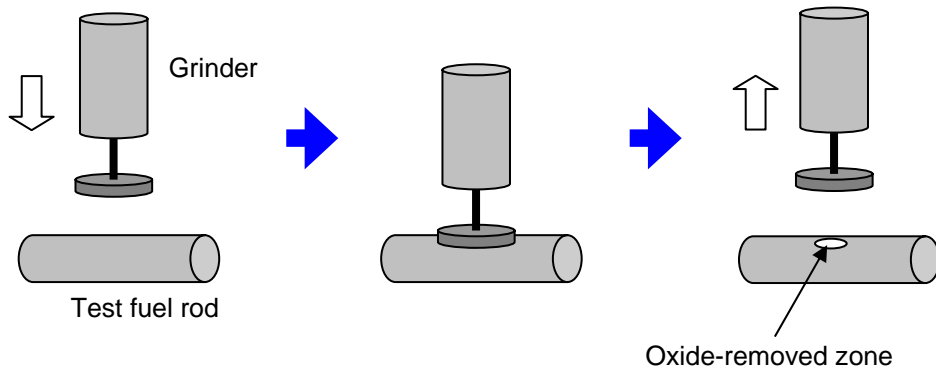


Fig. 7. Removal procedure for cladding surface oxide layer

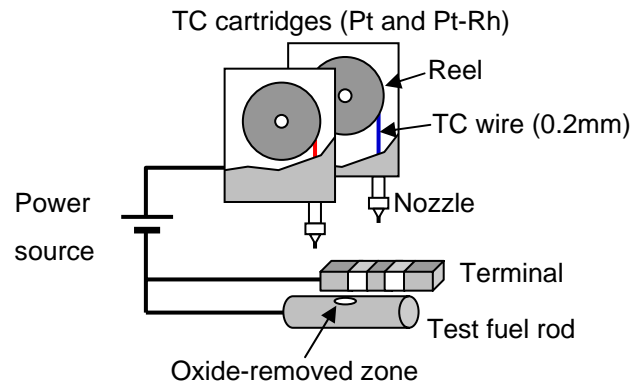


Fig. 8. Schematic of spot-welding device for cladding surface thermocouple

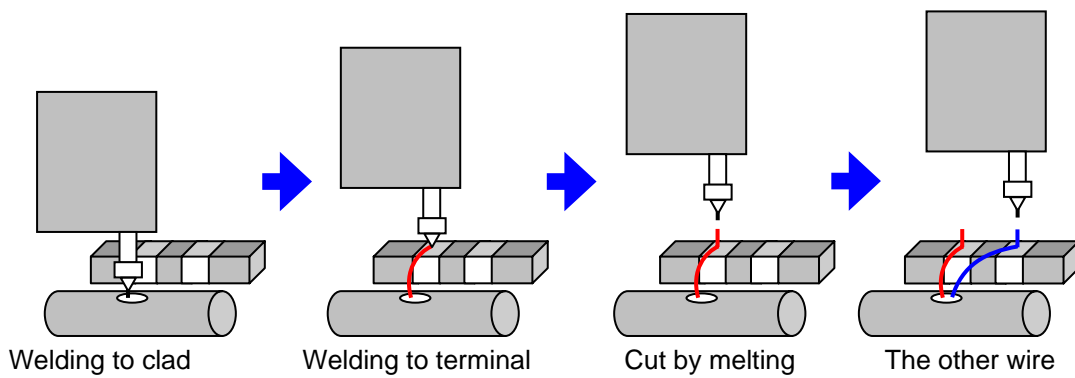


Fig. 9. Spot-welding procedure for cladding surface thermocouple

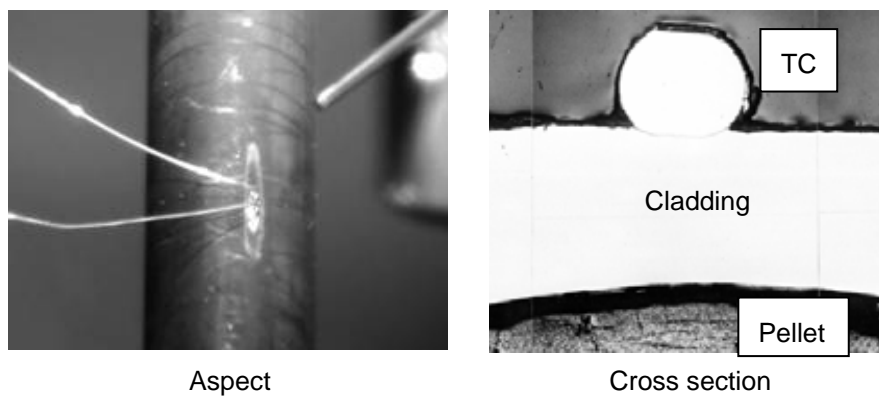


Fig. 10. Aspect and cross section of cladding after spot-welding of thermocouple

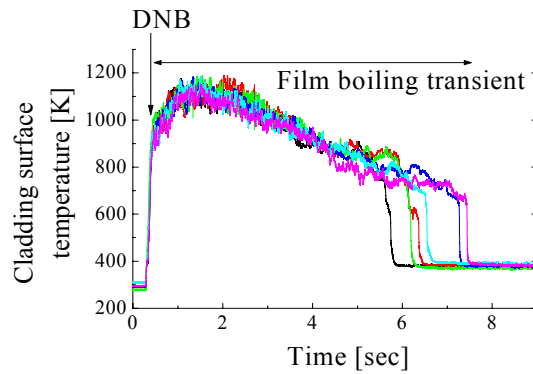


Fig. 11. Cladding surface temperature measured by cladding surface thermocouple

3.1.2. Coolant water thermocouple

Coolant water thermocouple is to measure water temperature in test capsule. This sensor is put within 10 mm from the center of test fuel rod in axial direction and with distance more than 10 mm from the surface of test fuel rod in radial direction, as shown in Fig. 6. K-type (chromel-alumel) thermocouple is used with sheath of 1.0 mm diameter.

3.1.3. Capsule pressure sensor

Capsule pressure sensor is a strain gauge type pressure sensor and used in two ways. One is to detect fuel failure and decide failure time. The other is to evaluate mechanical energy generated at fuel failure. In the former case, sensor is put at 130 mm lower position from the center of pellet stack in axial direction and 18 mm from the center of test fuel rod in radial direction, as shown in Fig. 6. At fuel failure, pressure wave is generated at the fractured part, propagates in coolant water and detected by capsule pressure sensor as a spike signal. The spike signal is reliable information to detect fuel failure and decide failure time. In the latter case, sensor is put above the water level as shown in Fig. 6. At fuel failure, fragments of fuel pellet are released into coolant water and steam is instantaneously generated. The upper part of coolant water forms water column and this water column compresses the plenum gas of test capsule. The capsule pressure sensor, put above the water level, detects the pressure rise of plenum gas and the measured pressure history data is used to evaluate generated mechanical energy.

3.1.4. Rod internal pressure sensor

Rod internal pressure sensor is a strain gauge type pressure sensor and used to measure pressure history in the lower plenum of test fuel rod. This sensor contains a diaphragm, on which strain gauges are attached, and is connected to the lower edge of test fuel rod, as shown in Fig 6. In fresh fuel experiments, a sensor of commercially designed type, which is composed of stainless steel parts, is available. An adaptor with an O-ring as a gasket is used to attach this sensor to a fresh fuel rod. On the other hand, in irradiated fuel experiments, welding of a sensor to a test fuel rod is required because an irradiated fuel rod contains fission products and needs to be sealed. Since stainless steel can not be welded to Zircaloy cladding, rod internal pressure sensor for irradiated fuel experiments is manufactured with Zircaloy parts.

3.1.5. Cladding elongation sensor

Cladding elongation sensor is a LVDT type sensor and used to measure transient elongation behavior of whole test fuel rod. Iron core is connected to the upper edge of test fuel rod and differential transformer is put beside the iron core as shown in Fig 6. This sensor detects the axial movement of the connected iron core induced by cladding thermal expansion and PCMI. In order to follow the fast transient during pulse irradiation, the excitation frequency of primary voltage should be set as high as possible. The main limitation of the excitation frequency comes from the influence of eddy current which is generated in iron core and affect sensitivity. Through characteristic tests, the excitation frequency was determined 7 kHz for fresh fuel experiments and 3 kHz for irradiated fuel experiments.

3.1.6. Pellet stack elongation sensor

Pellet stack elongation sensor is a LVDT type sensor and used to measure transient elongation behavior of pellet stack. Iron core is put on pellet stack inside test fuel rod and differential transformer is put beside the iron core as

shown in Fig 6. This sensor detects the axial movement of the iron core induced by pellet thermal expansion. Usually the specifications are identical to cladding elongation sensor.

3.1.7. Water column velocimeter

Water column velocimeter is to measure the water level movement, which gives information on mechanical energy generation at fuel failure. Figure 12 shows a schematic of water column velocimeter. As shown in Fig. 12, this sensor consists of two parts; movable float and fixed shaft. Float is made from polyethylene and includes a ring-shape magnet. Shaft contains a coil whose winding direction is inversed with every 6 or 3 mm interval (l in Fig. 12). At fuel failure, water column jumps up induced by the pressure of generated steam, as described in 3.1.3., and float jumps up with water column. Figure 13 schematically shows the phenomenon at fuel failure. When float jumps up and pass along the coil in shaft, sign-shaped electromotive force is generated in the coil by electromagnetic induction.

There are two ways to evaluate water column velocity with the output sign-wave of water column velocimeter. The first is with the frequency of the output sign-wave. Through some characteristic tests for water column velocimeter, it was confirmed that the electromotive force becomes zero when the magnet is axially at the center position of a region where the winding direction of coil is uniform, regardless of the magnet velocity. Hence, dt in Fig. 13 is the time which the magnet needed to move the distance from the axial center of one interval to the next, i.e., 6 or 3 mm. Based on these understandings, water column velocity can be calculated as $v = l / dt$. The second is with the amplitude of the output sign-wave. With a calibration result of the correlation between sign-wave amplitude and velocity, the history of water column velocity can be directly obtained by extracting the extreme values from the sign-wave. Basically the first method is employed to decide water column velocity because it doesn't need any calibration process.

Figure 14 shows examples of the output of water column velocimeter and the water column velocity calculated by using the velocimeter output, with the histories of the reactor power and the integrated reactor power. In the case shown in Fig. 14, failure time is around 10 ms and the velocimeter output shows significant response after 10 ms. The sign-wave of velocimeter output is partially flattened because of the limit of measurement range, +50 mV and -50 mV. In such a case, only the first method, which uses the frequency of the sign-wave, is available to evaluate water column velocity. The velocity history in Fig. 14 is based on the frequency, which reaches 15 m/s around at 15 ms.

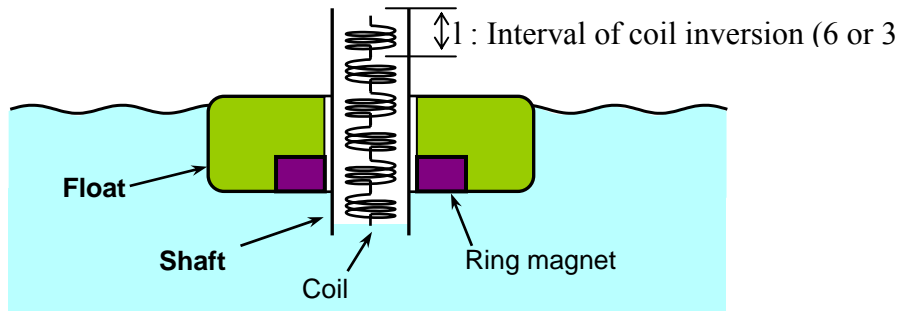


Fig. 12. Schematic of water column velocimeter

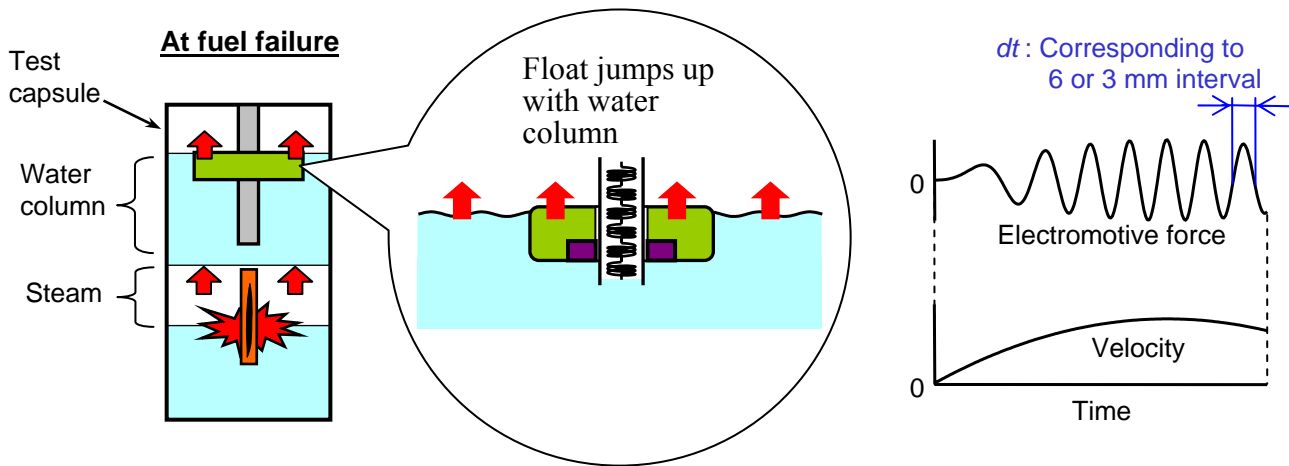


Fig. 13. Move and response of water column velocimeter at fuel failure

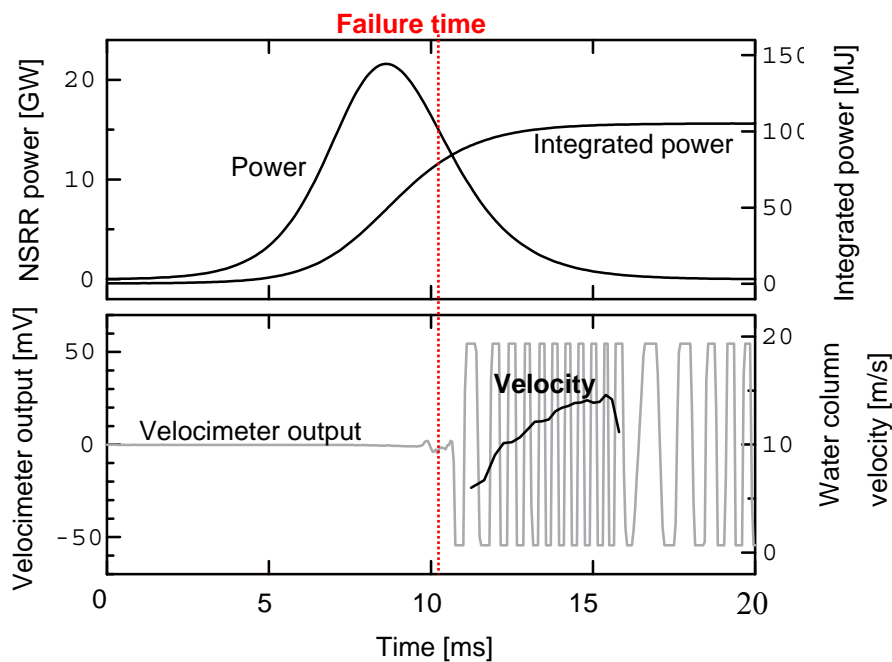


Fig. 14. Water velocimeter output and the water column velocity calculated with the velocimeter output

3.1.8. Cladding surface strain gauge

Cladding surface strain gauge is used to measure transient deformation of cladding tube. It is a foil type strain gauge, which is commercially designed, and attached to cladding surface with instantaneous adhesive, cyanoacrylate. In case cladding surface thermocouple is welded to the test fuel rod, strain gauge is attached to the opposite side of the welded thermocouple, as shown in Fig 6. Since the usable temperature range is not wide (from -30 to +70 degrees Celsius), this sensor is applicable only to investigate the cladding deformation behavior before significant temperature rise of cladding surface.

3.2. Measurement under high temperature and high pressure condition

As described above, high burnup fuel tests have shown the hydride-assisted PCMI failures at low fuel enthalpies. However, some cladding might survive if the tests had been performed at high temperatures, because the hydrogen solubility limit in the cladding increases with temperature. To clarify the high temperature effect on the PCMI failure limit, a new capsule is being developed for irradiated fuel experiments. A schematic of the high-temperature/high-pressure test capsule is given in Fig. 15. This capsule is equipped with an electric heater to produce BWR operating temperatures and pressure. The main objective is to test the temperature effect above ~200 degrees C. Therefore, high pressure is not the primary interest and the PWR operation conditions are not targeted.

The practical coolant condition is 559 K and 7 MPa.

In order to ensure integrity under high temperature and high pressure condition, the axial size of inner capsule is inevitably smaller than that of the ordinary irradiated fuel test capsule for room temperature and atmospheric pressure. Due to this limitation of test section, elongation sensors and water column velocimeter is not available. Cladding surface strain gauge is not available, either, because the adhesive, cyanoacrylate, for attachment of strain gauge to cladding surface is not usable in high temperature water. In some tests, which were carried out so far, availability of cladding surface thermocouple, coolant water thermocouple and capsule pressure sensor have been confirmed.

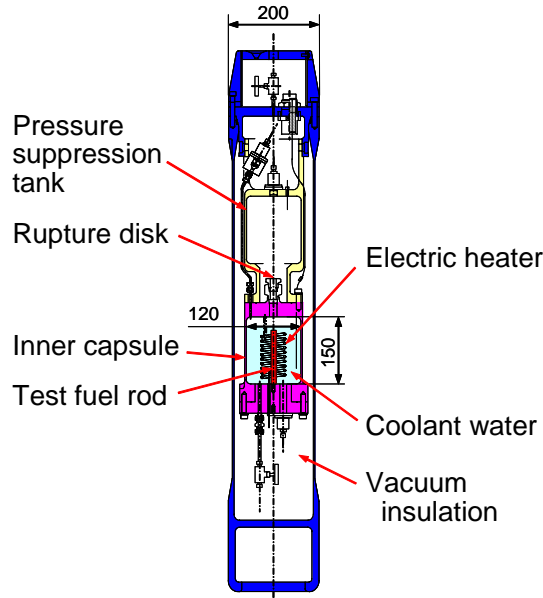


Fig. 15. High-temperature/high-pressure test capsule

5. CONCLUSIONS

JAEA has utilized the NSRR to perform accident-simulating experiments of light water reactor fuels since 1975. Over 1200 experiments have successfully been carried out with fresh fuel rods to clarify fuel behavior under RIA conditions and to obtain fuel failure limit. After the modification of the NSRR facilities for high burnup fuel tests, more than 70 experiments have been performed with irradiated fuel rods so far since 1989. In order to achieve successful measurement, instrumentation methods and materials have been tried and selected continuously through these many experiments, aiming for quick response and stability under strong irradiation. Unique instrumentation techniques as spot-welding of thermocouple to cladding surface or water column velocimeter have been developed and, with accumulated experiences and developed sensors, a great deal of data has been obtained. The results have been reflected in safety evaluation guidelines for RIA in some other countries as well as in Japan. Further safety researches using the NSRR are expected to support fuel burnup extension and MOX fuel introduction. In order to meet the requirements, the capability of the NSRR facilities is being extended and improvement of instrumentation technique is continued.

ACKNOWLEDGEMENTS

The authors are indebted to the engineers, technicians, and researchers in Japan Atomic Energy Research Institute (presently, JAEA), who have worked on the development of the NSRR facilities and equipments since the construction. Especially the technical advises and supports by the members of NSRR operation section and Fuel Safety Research Group are greatly acknowledged.

REFERENCES

- [1] NUCLEAR SAFETY COMMISSION OF JAPAN, Safety Evaluation Guidelines, 10th Edition, (2000) (in Japanese).
- [2] SAITO, S., et al., "Development of In-reactor Fuel Behavior Observation System", J. Nucl. Sci. Technol., Vol. 18, No. 6, pp. 427-439 (1982).
- [3] KOBAYASHI, S., et al., "RIA Fuel Behavior under High Pressure and High Temperature Cooling Conditions", Proc. ANS-ENS Topical Mtg. on Reactor Safety Aspects of Fuel Behavior, Sun Valley, U.S.A.,

(1981).

- [4] FUKETA, T., et al., "Fragmentation and Mechanical Forces Generation in In-pile Power Burst Experiment with Uranium Silicide Miniplate", Proc. 8th Int. Top. Mtg. on Nuclear Reactor Thermal-Hydraulics (NURETH-8), Kyoto, Japan, (1997).
- [5] SASAJIMA, H., et al., "Behavior of Uranium-Zirconium-Hydride Fuel under Reactivity Initiated Accident Conditions", Proc. ENS 7th International Topical Mtg. on Research Reactor Fuel Management, Aix-en-Provence, France, March 2003, pp. 109-113 (2003).
- [6] ABE, T., et al., "Failure Behavior of Plutonium Uranium Mixed Oxide Fuel Under Reactivity-Initiated Accident Condition", J. Nucl. Mater., 188, pp. 154-161 (1992)
- [7] SASAJIMA, H., et al., "Behavior of Irradiated ATR/MOX Fuel under Reactivity Initiated Accident Conditions", J. Nucl. Sci. Technol., Vol. 37, No. 5, pp. 455-464 (2000).
- [8] FUKETA, T., et al., "Behavior of High Burnup PWR Fuel Under a Simulated RIA Conditions in the NSRR", Proc. CSNI Specialist Mtg. on Transient Behavior of High Burnup Fuel, Cadarache, France, September 12-14, 1995, NEA/CSNI/R(95)22, pp. 59-85 (1996).
- [9] FUKETA, T., et al., "Behavior of High-burnup PWR Fuels with Low-tin Zircaloy-4 Cladding under Reactivity-Initiated-Accident Conditions", Nuclear Technology, Vol. 133, No. 1, pp. 50-62 (2001).
- [10] NAKAMURA, T., et al., "Irradiated Fuel Behavior under Power Oscillation Conditions", J. Nucl. Sci. Technol., Vol.40, No.5, pp.325-333 (2003)
- [11] OCHIAI, M., "WTRLGD – A Computer Program for the Transient Analysis of Waterlogged Fuel Rods under the RIA Condition", Nucl. Eng. Design, Vol. 66, No. 2, pp. 223-232 (1981).
- [12] SAITO, S., et al., "Effects of Rod Pre-Pressurization on Light Water Reactor Fuel Behavior during Reactivity Initiated Accident Conditions", J. Nucl. Sci. Technol., Vol.19, No.4, pp.289-306 (1982).
- [13] MACDONALD, P.E., et al., "Assessment of Light-Water-Reactor Fuel Damage During a Reactivity-Initiated Accident", Nuclear Safety, Vol. 21, No. 5, pp. 582-602 (1980).
- [14] SCHMITZ, F., et al., "New Results from Pulse Tests in the CABRI Reactor", Proc. 23rd Water Reactor Safety Information Mtg., Bethesda, Maryland, October 23-25, 1995, NUREG/CP-0149, vol. 1, pp. 33-43 (1996).
- [15] SUGIYAMA, T., et al., "Mechanical Energy Generation during High Burnup Fuel Failure under Reactivity Initiated Accident Conditions", J. Nucl. Sci. Technol., Vol. 37, No. 10, pp. 877-886 (2000).

Test methods of VVER fuel with simulating transitive and emergency modes in the MIR reactor

A.L. Izhutov, A.V. Burukin, V.V. Kalygin, V.A. Ovchinnikov, V.N. Shulimov

*State Scientific Centre of Russia Research Institute of Atomic Reactors,
433510, Dimitrovgrad, Ulyanovsk region, Russia*

ABSTRACT

The MIR reactor is mainly designed for testing fragments of fuel elements and fuel assemblies (FA) of different nuclear power reactor types under normal (stationary and transient) operating conditions as well as emergency ones in a certain project. At present six test loop facilities are being operated (2 PWR loops, 2 BWR loops and 2 steam coolant loops). The majority of current fuel tests is conducted for improving and upgrading the Russian PWR fuel, such as: long term tests of short-size rods with different modifications of cladding materials and fuel pellets; further irradiation of NPP refabricated and full-size fuel rods up to achieving 80 MW-d/kg U; experiments with leaking fuel rods at different burn-up and under transient conditions; continuation of the RAMP type experiments at high burn-up of fuel; in-pile tests with simulation of LOCA and RIA type accidents. Testing of the LEU research reactor fuel is conducted within the framework of the RERTR programme. The quoted information touches upon goals and methods of loop tests in the MIR research reactor with the purpose of VVER fuel elements serviceability study in transitive and emergency modes (power cycling, RAMP, LOCA, RIA). Loop installations characteristics and their instrumental equipment are represented. The applied irradiation devices and sensors for measuring and determination of experimental parameters are listed. The developed instrumentation and installations are available for testing of VVER-type fuel at transient and project emergency conditions.

1. Introduction

The MIR reactor is a heterogeneous thermal reactor with a moderator and a reflector made of metal beryllium [1]. It has a channel-type design and is placed in the water pool. The frame of the core is made up of hexagonal beryllium blocks with width across flats of 148,5. In the central axis holes of the blocks channel bodies are installed for operating FAs (37 pcs); combined operating FA with absorber (12 pcs); experimental loop channels (11 pcs). The maximum diameter of experimental channels is up to 148 mm, height of core 1000 mm.

At present 6 loop facilities (PV-1, PVK-1, PV-2, PVK-2, PVP-1, PVP-2) are being in operation and 2 facilities (PG, PM) have not been used for the last 15 years (table 1).

No	Parameters, unit	Loop facilities							
		PV-1	PVK-1	PV -2	PVK -2	PVP-1	PVP-2	PG	PM
1.	Coolant	water	boiling water	water	boiling water	water, steam	water, steam	nitrogen, helium	heavy metal
2.	Number of test channels	2	2	2	2	1	1	1	1
3.	Maximum channel power, kW	1500	1500	1500	1500	100	2000	160	500
4.	Maximum coolant temperature, C°: -in outlet of channel, -in outlet of device	350 350	350 350	350 350	365 365	500 500	550 1100	500 1000	550 550
5.	Maximum pressure, MPa	17,0	17,0	18,0	18,0	8,5	15,0	20,0	1,7
6.	Maximum coolant flow rate through the channel, m ³ /h	16,0	16,0	13,0	13,0	0,6	10,0		5,0

Table 1. Key parameters of loop facilities

Water and boiling water high-temperature loop facilities provide necessary coolant parameters for WWER fuel testing. Lay-out of control rods of the reactor and loop facilities in the core makes it possible to perform several testing programs simultaneously at different values of neutron flux density in the loop channel (they differ by a factor of 5 to 10). A high neutron flux density (up to $\sim 5 \cdot 10^{18} \text{ m}^{-2} \cdot \text{s}^{-1}$) allows repeated irradiation of standard or experimental fuel rods from the WWER fuel assemblies up to a burnup of $\sim 80 \text{ MWd/kgU}$ and higher. The main purpose of loop testing is experimental examinations of fuel rod new modifications serviceability and reliability at different normal and accidental operating conditions. These operating conditions include in particular the following: long-term operation under nominal parameters with allowance for tolerance; daily power cycling with a fast power change (power ramping); design-basis accidents followed by heat-transfer drop (coolant loss, burn-out), positive reactivity insertion and operation with leaking fuel rods.

The presented in this paper programs and techniques for in-pile examination of the WWER fuel are aimed at obtaining experimental data that are necessary to provide conformity of the WWER fuel with licensing requirements such as: total pressure of helium and fission gas under the cladding; plastic strain of the cladding as a result of its interaction with fuel; temperature, strain and integrity of claddings in case of design-basis accident with loss of coolant (LOCA); local depth of cladding oxidation; value of fuel enthalpy under design-basis reactivity increase accident (RIA); permissible number of leaking fuel rods in the core and others.

2. Experimental techniques for WWER fuel testing in the MIR reactor

Comparison of the WWER fuel operating conditions with characteristics of the MIR water-coolant loop facilities (table 2) testify their conformity.

Parameter	WWER	MIR
Maximum LP, kW/m	≤ 44.7	Higher values are possible
Pressure, MPa	≤ 17.7	≤ 18.0
Maximum coolant temperature inlet / outlet, °C	290 / 340	325 / 350
Coolant-chemical conditions Boric acid concentration, g/kg	Ammonia-boric-potassium Up to 10	Provided Up to 10*
Coolant velocity, m/s	5.7	Provided
Burn-up, MWd/kgU	~ 55	Up to 100
Start time of fuel rod leaking	Impossible	Possible
Increase of liner power	Impossible	Possible
Intermediate control of fuel rod status	NA	Possible in the pool and shielded hot cell
Control and change of water chemistry	NA	Possible

Table 2. The WWER fuel operating conditions and characteristics of the MIR loop facilities

Several types of irradiation devices have been designed for testing of the WWER-type fuel rods [2]:

- the module type, dismountable device for testing short-size ($\leq 250 \text{ mm}$) fuel rods, up to 4 such rigs can be installed one over another in the loop channel;
- dismountable and instrumented device for testing fuel rods $\sim 1000 \text{ mm}$, containing up to 19 fuel rods;
- device for combined irradiation of non-instrumented refabricated ($\leq 1000 \text{ mm}$) and full-size fuel rods ($\leq 3500 \text{ mm}$) taken from spent NPP with WWER fuel assemblies;
- device for tests of instrumented refabricated fuel rods ($\leq 1000 \text{ mm}$) and full-size fuel rods ($\leq 3500 \text{ mm}$);
- dismountable devices for power cycling and RAMP experiments of instrumented fuel rods by displacement or rotation of the absorbing screens in the experimental channel;

- instrumented devices for simulation of RIA and LOCA conditions (fuel rod drying and overheating);
- devices and equipment for leaking fuel rods testing.

Types and characteristics of instrumentation for in-pile measurements of coolant, cladding and fuel pellet temperatures; fuel rods elongation, change of cladding diameter; gas pressure inside fuel rods, neutron flux and stem content in coolant are given in table 3.

Parameter	Transducer	Measurement range	Measuring error	Sensor dimensions, mm	
				Diameter	Length
Coolant (T_c) and cladding temperature (T_{cl})	Chromel-alumel thermocouple	up to 1100 °C	0.75%	0.5	
Fuel pellet temperature (T_f)	Chromel-alumel thermoprobe	up to 1100 °C	0.75%	1...1.5	
	W-Re thermoprobe	up to 2300 °C	~ 1.5%	1.2...2	
Cladding elongation (δL)	Liner differential inductosyn transducer (LDIT)	(0...5) mm	$\pm 30\mu\text{m}$	16	80
Diameter change (δD)	LDIT	(0...200) μm	$\pm 2\mu\text{m}$	16	80
Gas pressure inside of fuel rod (P_f)	Bellows rolling diaphragm + LDDT	(0...20) MPa	~ 1.5 %	16	80
Neutron flux (F)	Rh-, V-, Hf - direct-charge detector	$10^{15} \dots 10^{19} \text{ m}^{-2} \text{ s}^{-1}$	~ 1%	2...4	50...100
Volume steam content in coolant (β)	Cable-type resistivity sensor	20...100%	10%	1.5	

Table 3. Characteristics of instrumentation for in-pile measurements

3. The program and main results of WWER fuel testing in the MIR reactor

3.1. Irradiation of refabricated and full-size WWER fuel rods

The test objective is to investigate the behavior of fuel under higher burn-up and to achieve higher burn-up for preparation of RAMP, LOCA and RIA tests (table 4).

Type of fuel rod	Number of fuel rods	Length of fuel rods, m	Initial burnup, MWd/kgU	Final burnup, MWd/kgU	Liner power, kW/m
WWER-1000	2	3.53	49...50	62...63	18...30
WWER-1000	1	0.95	49	63	19...31
WWER-440	2	2.42	61	72	17...28
WWER-440	1	0.94	60	72	19...31
WWER-1000	5	3.53	53...55	74...75	18...24
WWER-1000	3	0.4	53...58	74...78	18...24

Table 4. General data on irradiation of the WWER refabricated and full-size fuel rods

3.2. Testing under power ramping conditions

By now 14 RAMP tests with the WWER fuel rods have been performed in the MIR reactor. Experimental fuel rods of different modifications, as well as full-size and refabricated fuel rods were tested at burn-up values from ~ 10 MWd/kgU up to ~ 70 MWd/kgU. In figure 1 are illustrated the main results of experiments - range of liner power (LP) changing and state of cladding after power ramp.

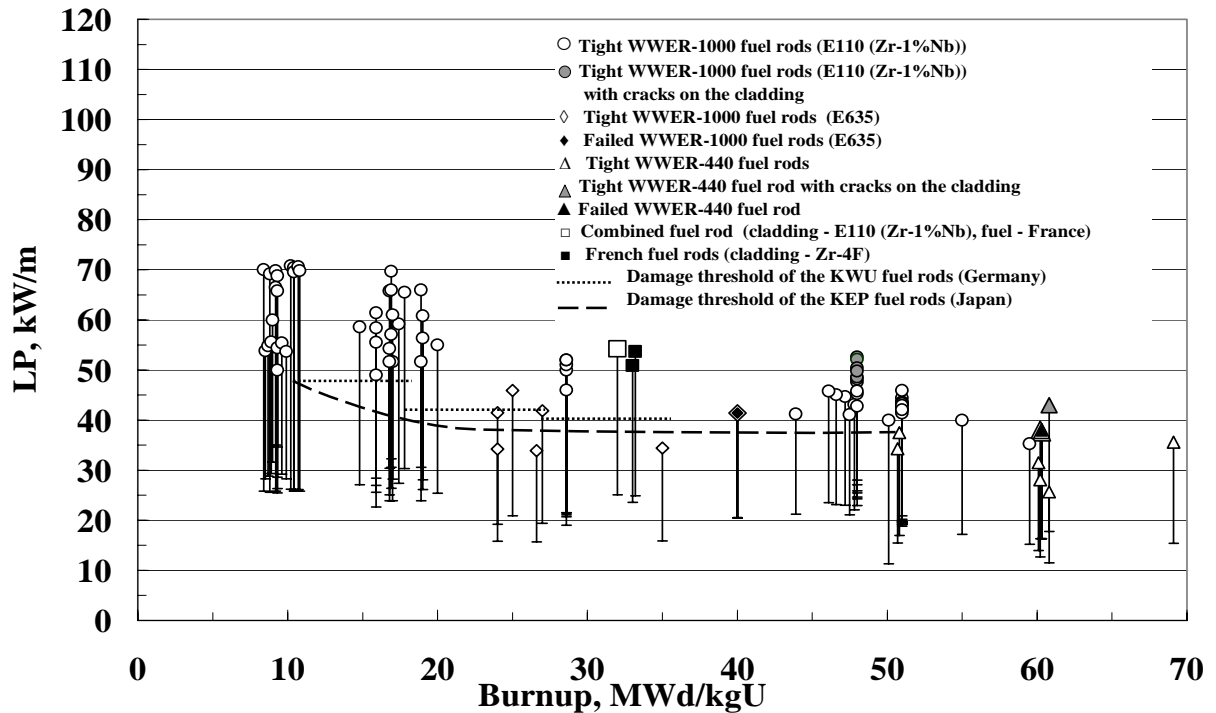


Figure 1. RAMP tests liner power amplitudes versus WWER fuel rods burn-up

In 2008 it is planned to finish RAMP experimental program for WWER-1000 fuel with high burn-up ~ 80 MWd/kgU.

3.3. Testing under power cycling conditions

The objective of testing is to obtain experimental data that characterize a change in the cladding strain, gas pressure in the free volume of a fuel rod, fuel temperature in course of daily power cycling. The fuel rod power changed within (20...30) minutes, exposure at the stable power level makes up ~ 6 hours. Data on tests are presented in table 5.

Type of fuel rod	Number of fuel rods	Instrumentation	Burnup, MWd/kgU	Initial LP, kW/m	LP increase step, kW/m	LP increase rate, kW/m/min
WWER-440	1	$P_f, \delta L, \delta D$	51	19	10	0.3
WWER-440	5	T_f	51...60	15...19	8...10	~ 0.3
WWER-440	4	T_f	52...61	18	11	~ 0.9
WWER-1000	2	T_f, L	49...50	21; 21*	9; 21*	0.6; 0.9*
WWER-1000	2	$P_f, \delta L$	49...50	21	9	0.6

Table 5. The main data of power cycling tests

Power cycling tests will be continued for WWER-1000 fuel rods with burn-up ~ 60 MWd/kgU and higher in 2007-2008.

3.4. Testing under fuel rod drying, overheating and reflooding conditions (LOCA)

A series of tests was performed with the WWER-440 and WWER-1000 multi-element fuel assembly fragments under different phases of design-basis LOCA conditions [3]. The objective of the tests is to verify or refine serviceability criteria of fuel rods and fuel assemblies, determine ultimate parameters, which allow disassembling of the core after operation under deteriorated heat transfer conditions, and to obtain data for code verification and improvement. The main parameters of experiments are given in

Experiment	Number of fresh fuel rods	Number/ burn-up, of irradiated fuel rods, MWd/kgU	Pressure in loop, MPa	Implemented temperature range, °C	Instrumentation	Fuel rod status	
						Non-failed	Failed
SL-1	18	-	12	530...950	T _c , T _{cl} , T _f , F, β	+	
SL-2	19	-	12	Up to 1200	-//-		+
SL-5	6	1/52	4.9	750...1250	-//-		+
SL-5P	6	1/49	6	700...930	-//-	+	
SL-3	19	-	4	650...730	T _c , T _{cl} , T _f , F, P _f	+	
LL-1	19	3/50	4	550...850	-//-	+	

Table 8. The main parameters of LOCA experiments

LOCA experiments will be continued for WWER-1000 fuel rods with burn-up ~ 60 MWd/kgU and higher in 2007-2008.

3.4. Testing of the WWER-1000 high burn-up fuel rods under design-basis RIA conditions

Calculation data show that the WWER-1000 reactor parameters of the design-basis RIA conditions are as follows: power ratio in impulse ~ 2, half-width of impulse – (2...2.5)s, power rise duration ~ 1s. The program and techniques were developed for tests performed in the MIR loop facilities to obtain experimental data on behavior of high burn-up fuel rods under the above-mentioned conditions [4]. In the MIR loop channel it is possible for high burn-up fuel to provide a rising of liner power in impulse up to ~ 4.0 times and to control power rise duration from ~ 0.5s and more. In 2006 was started experimental program and were provided 2 experiments for WWER-1000 fuel rods with burn-up ~ 50 MWd/kgU, in 2007-2008 the program will be continued.

3.5. Leaking high burn-up fuel rods testing

Taking into account the state of the WWER fuel rods with a burn-up of above ~ (45...50) MWd/kgU, new experimental data are necessary for the development and verification of computer codes, validation of safe operation criteria for WWER reactors in case of leaking fuel rods appearance, as well as for prediction of a change in their state and radiation situation. For this purpose, a testing program was developed and a series of tests is being prepared now to be performed in the MIR loop facilities with refabricated fuel rods claddings some of which have artificial defects. In 2006 first experiment was conducted, in 2007-2008 the program will be continued.

4. Conclusion

Several types of irradiation devices have been designed for testing WWER-type fuel rods under steady state parameters; daily power cycling with a fast power change (power ramping); design-basis accidents have been developed. The current fuel tests program aimed at improving the Russian operating WWER-440 and WWER-1000 fuel should be finished in the MIR reactor in 2008.

At present prospective program of fuel testing for evolutionary design of WWER with improved economics and safety (project AES-2006) is being created. The testing program of upgrading fuel AES-2006 reactors will start in 2008.

In the MIR reactor will be continued testing of the LEU research reactor fuel within the framework of the RERTR program, and in March 2007 will be started testing of 4 full-scale IRT-4 type fuel assemblies.

Upgrading of gas cooled PG-1 loop with increasing coolant outlet temperature up to 1100 °C for in-pile investigations HTGR fuel and steam cooled PVP-2 loop with increasing the pressure up to 22.5 MPa for testing fuel and constructive materials sub-critical water-cooled reactor are scheduled.

5. References

- [1] A.L.Ijoutov et al, «Experiences of Exploitation Research reactors SSC RIAR», Proceedings of the 12th Annual Conference of the Nuclear Society of Russia "Research Reactors: Science and High Technologies", Dimitrovgrad, Russia, June 2001.
- [2] A.V. Burukin, V.A. Ovchinnikov, V.A. Tsykanov et al., «Testing of the instrumented fuel rods of the power reactors in the MIR research reactor. Status and development prospects», Proceedings of the VII Russian Conference on Reactor Material Science, RIAR, September 8–12, 2003r, Dimitrovgrad, Russia. V. 2, P. 3. Dimitrovgrad, 2004.
- [3] I.V. Kiseleva, V.M. Makhin, V.N. Shulimov et al, «Integrated reactor testing of multielement fragments of the WWER-440 and WWER-1000 fuel assemblies under coolant loss accident. Summary of the Small LOCA experiment cycle», Atomic Science and Engineering. Issue: Nuclear reactor physics. I. 2, P. 29-38, Moscow, 2004.
- [4] A.V. Alekseev, I.V. Kiseleva, V.N. Shulimov. «Study of behaviour of the WWER-440 and WWER-1000 fuel rods under RIA conditions» // Proceedings of the IV International scientific and technical conference «Safety assurance of nuclear power plants with WWER reactors», EDO Gidropress, May 23-26, 2005, Podolsk, Russia. Podolsk, 2005.

IRRADIATION FACILITY PROJECT

O. Beuter - S. Halpert – A. Marajofsky – L. Vázquez
National Atomic Energy Commission of Argentina
Av. Gral. Paz 1499, (1650) San Martín, Buenos Aires
Argentina

Abstract

The objective of this project is the design, fabrication, set up and installation in the RA-3 reactor of a device to irradiate nuclear power plants fuel rods, under total or partial operation conditions, in order to study their behavior. In order to qualify the design it is planned to construct a full scale facility mock-up with electrical heater and to operate this mock-up in normal & some transient conditions in order to set up all of the involved systems, to perform the procedures of installation, assembly, disassembly & transport and to train operators.

1. INTRODUCTION

In Argentina there are many facilities related to the nuclear fuel cycle. They include, among others, NPP & MTR fuel elements fabrication, hot cells for post-irradiation examination, an experimental hydraulic loop at high pressure and temperature, as well as instrumentation laboratories and facilities for thermal/hydraulic studies. However, Argentina has not irradiation devices to simulate power fuel elements behavior in research reactors.

Besides a few years ago the RA-3 research reactor power increased to 10 MW and it became an excellent tool to install a high pressure irradiation loop. At present, this reactor is used for radioisotope production and materials basic research.

A Technical Cooperation Project between the International Atomic Energy Agency (IAEA) and the National Atomic Energy Commission (CNEA) ARG/4/087 is being carried out to design, fabrication and assembling of an irradiation facility (LOOP) in the RA-3 reactor.

The objective of the LOOP is to irradiate power reactors fuel rods under total or partial operational conditions in order to study their behavior. It is proposed that the operation conditions (pressure, temperature, velocity and chemistry of the coolant) of the Argentine NPP Atucha I (CNAI), Atucha II (CNAII), Embalse (CNE) and CAREM reactor shall be established in the LOOP.

The results of post-irradiation studies to be performed in fuel rods would be used in design review and fuel fabrication. A better knowledge of the nuclear fuels behavior will contribute to improve the security and efficiency of those currently in use and contribute in the design of possible new fuels.

2.- DESCRIPTION OF THE FACILITY

The facility will consists of three main parts:

- *Irradiation module* emplacement of the fuel rods to be irradiated, located in a site of the RA-3 grid in the place of a reflector. This position belongs to the core external corona normally completed with graphite.
- *System*: those systems that fix and control the pressure, temperature, flow and chemistry conditions of the coolant that shall be placed in the reactor loops room.

- *Interphase*: pipelines, shielding, etc. that will connect the device within the reactor pool with the loops room outside the pool.

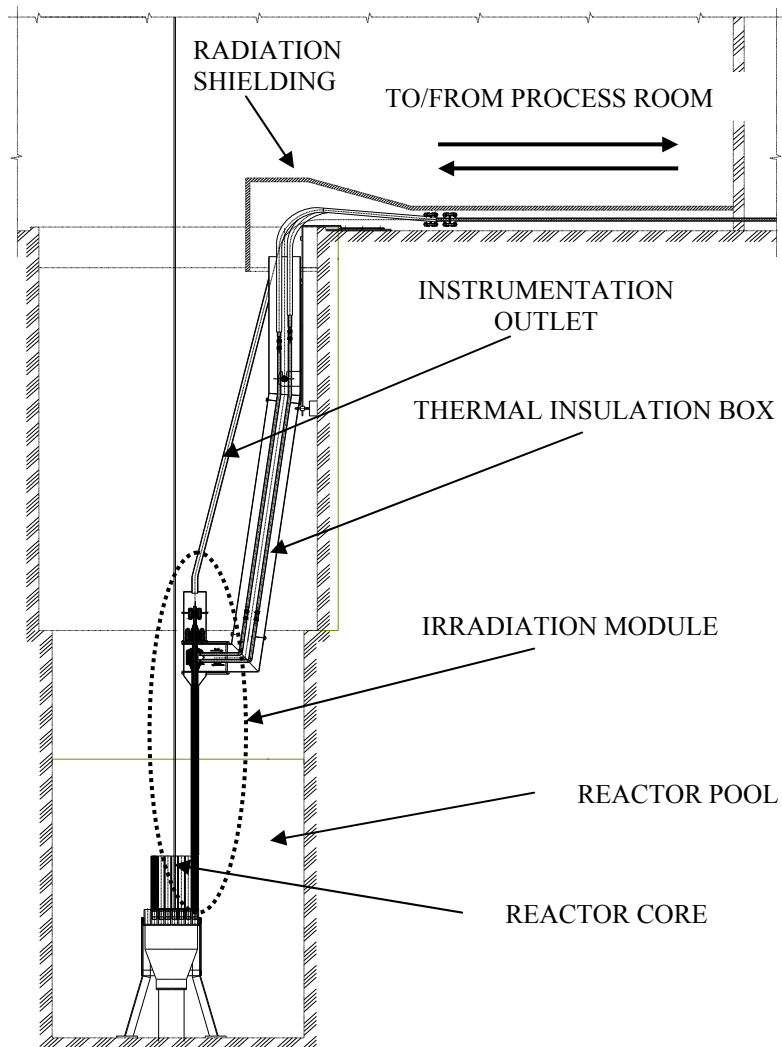


Figure 1: Irradiation Module and Interphase

2.1.- Irradiation Module

It is composed mainly of three concentric tubes of approximately 2 m long. The two external tubes act as pressure vessels and the inner tube divides the coolant flow (Figure 2 and 3).

The external tube, called safety tube, has two functions according to the operation condition of the facility.

- Normal operation. To form, together with the pressure tube, an external gap to locate the gas that will act as thermal barrier between reactor pool water (approximately at 40°C) and irradiation module coolant (approximately 300°C).
- Pressure tube rupture accident: it will act as last pressure limit.

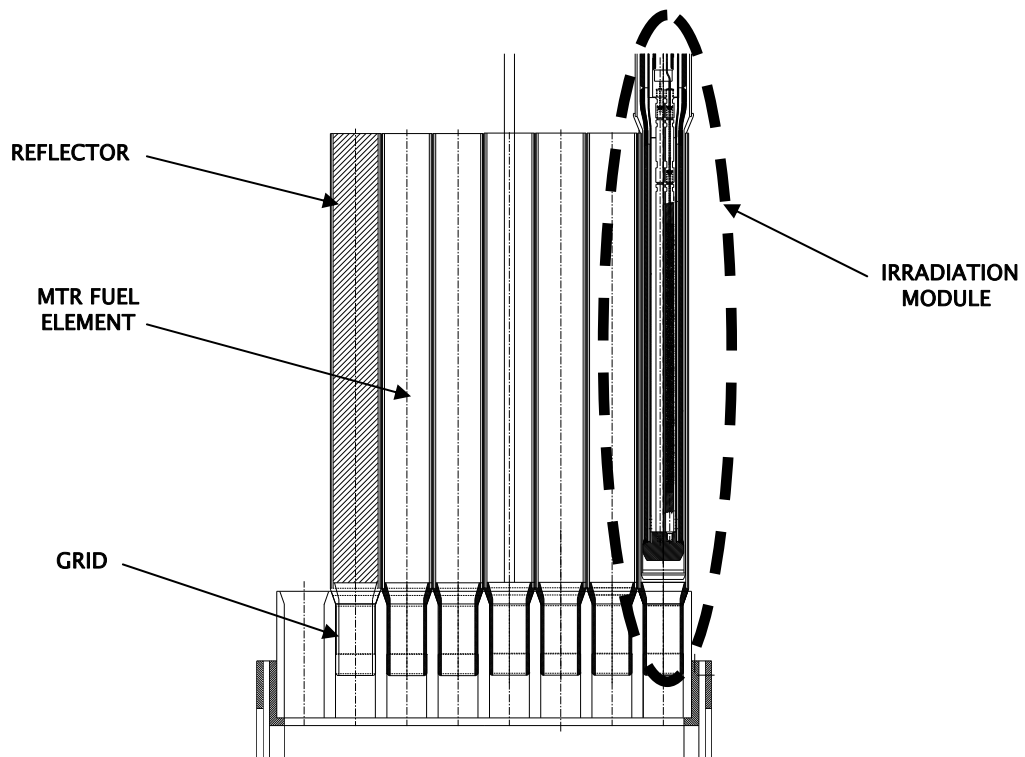


Figure 2: Irradiation Module Location in Reactor Core

The intermediate tube, called pressure tube, has also two functions but in this case always under normal operation conditions.

- To act as pressure limit.
- To form a down comer, together with the inner tube, through which the coolant will circulate downwards when it enters the irradiation module.

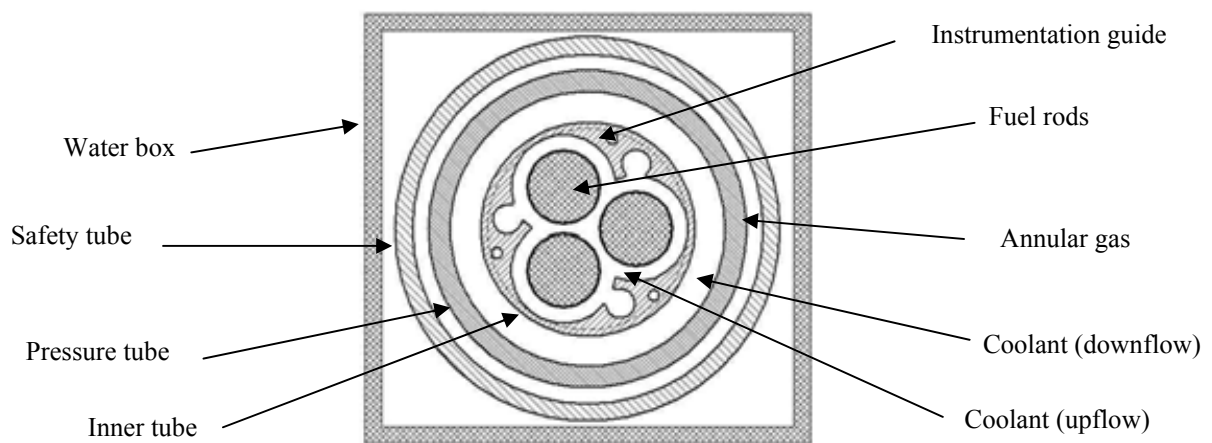


Figure 3: Irradiation module cross section (at reactor core zone)

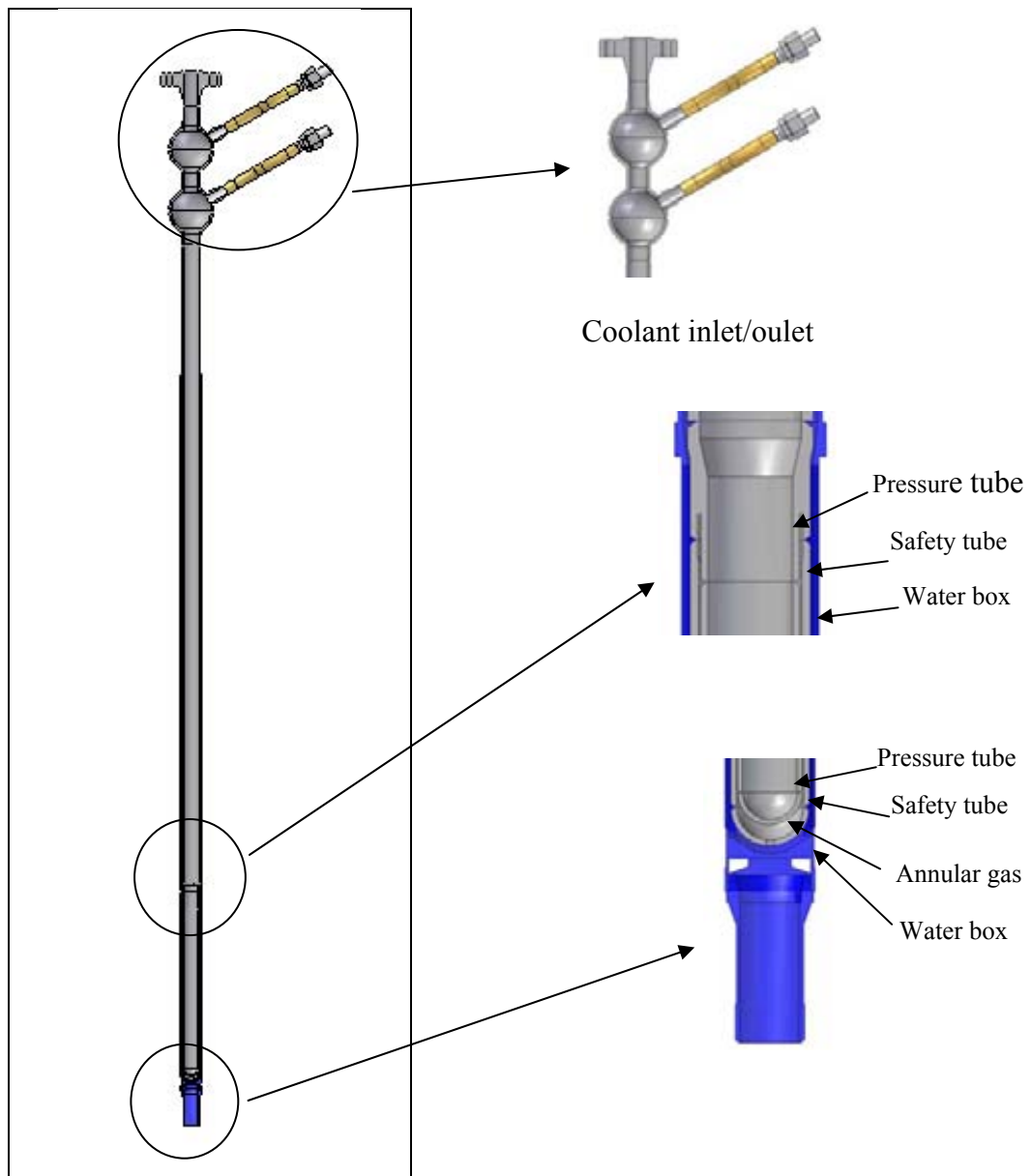


Figure 4: Irradiation module

The irradiation module will be instrumented in order to measure: coolant inlet and outlet temperature, coolant flow, fuel cladding temperature, pellet centre temperature, neutron flux, fission, gas pressure and rods elongation.

2.2.- Interphase

The interphase connects the irradiation module with *The System* that shall be located in the loops room. It consists basically of two tubes: one the coolant inlet to the irradiation module (System inlet) and the other the outlet (System outlet). At a relatively short distance of the of reactor tank water level the rigid pipes are connected to flexible pipes and these pipes, in turn, are connected to other rigid pipes, which run across the wall to the loops room. The entire place under water shall be thermally isolated and the water of the reactor tank shall act as radiological shielding. The pipelines and equipment outside the reactor tank shall be thermally isolated and protected by radiological shielding.

2.3.- System

It shall be placed as above mentioned within the loops room of the RA-3 reactor. As shown in

Figure 4, it will have the following main subsystems: primary heat transport system, pressurization system and pressure control, system for continuous purification of water, intermediate heat treatment system, energy coolant system and auxiliary systems.

The primary heat transport system will consist at least of a centrifugal pump, a heat exchanger, a preheater, pipelines, valves, accessories and instrumentation. It shall be capable of controlling the coolant flow and temperature at the core inlet.

The pressure control system shall have a pressurizer, a degasification vessel – condenser, pipelines and valves (Figures 4). The pressurizer will have electric heaters, connection with the degasification – condenser through purge valves, level control, pressure control (by switching the heaters or opening the purge valves).

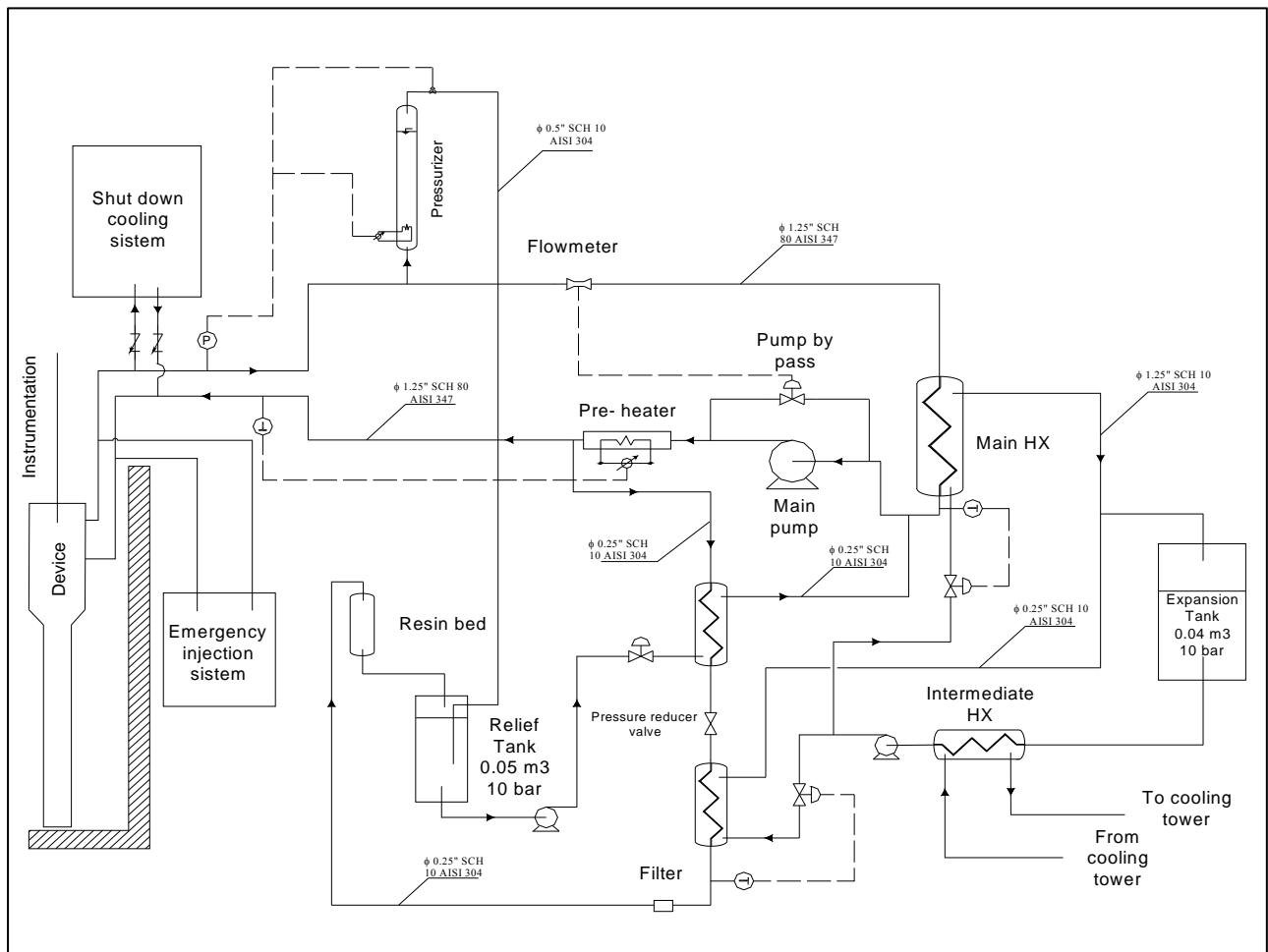


Figure 3: The System

3.- LOOP CHARACTERISTICS

The basic thermohydraulic characteristics of the device are summarized in the following table:

Maximum massic flow [kg / s]	2
Coolant temperature at channel inlet [°C]	260 / 300
Coolant temperature at channel outlet [°C]	≤ 310
Design temperature [°C]	330
Increase of coolant temperature [°C]	8 / 16
Coolant pressure at the outlet [MPa]	10.00
Design pressure [MPa]	13
Maximum working pressure [MPa]	12
Maximum linear power [W / m]	600
Rods length [m]	0.4
Power by fuel rod [W]	25000
Number of rods	3
Total power [W]	75000
Coolant velocity [m / s]	8.5
Position in the RA-3	In-Core

4.- OUT OF PILE TASK AND TRAINING

In order to qualify the design it is planned:

- ✓ To construct a full scale facility mock-up with electrical heater. The majority of its components will be the same that will be used in the in-pile facility
- ✓ To operate this mock-up in normal & some transient conditions in order to set up all of the involved systems:
 - ❖ Instrumentation & Control
 - ❖ SDCS
 - ❖ Emergency
- ✓ To construct a structure simulating part of the reactor pool in order to perform the procedures of installation, assembly, disassembly & transport.
- ✓ To train operators in operation, assembly, disassembly & transport steps.

Remote on-line measurement of fission gas release during irradiation testing

F.C. Klaassen^{1,*}, M.A.C. van Kranenburg, K. Bakker¹, R.P.C. Schram¹

¹ Nuclear Research and consultancy Group, P.O. Box 25, 1755 ZG Petten,
Netherlands

ABSTRACT

One of the most important aspects of the proper performance of nuclear fuel, is the fission gas behaviour, or, more specifically, the release of fission gas during irradiation. Although techniques exist for the in-pile measurement of fission gas release, the application of sensitive instrumentation in a strong neutron and gamma radiation environment is not straightforward.

At the High Flux Reactor in Petten, a 45 MWth materials test reactor, a technique was developed to measure the in-pile behaviour of (fission) gas during fuel testing, but with the instrumentation applied out of pile. In this approach, the irradiation capsule, for example containing the nuclear fuel under investigation, is connected with a capillary tube to a gas panel, in which various types of instrumentation, such as pressure transducers, can be applied. The advantage of this alternative approach is 1) a wider range of pressure transducers can be applied for the irradiation test; 2) out of pile space requirements provide generally less limitations; 3) if the pressure transducers would fail, these can be easily replaced.

In this paper, the implementation of this technique of remote fission gas release measurements will be explained, with special emphasis on the correct interpretation of the pressure data. This interpretation is not straightforward, as the instrumentation is applied out-of-pile, whereas the gas release occurs at higher (in-pile) temperatures.

As an example of the successful application of the technique, a transmutation experiment of iodine will be discussed. Iodine-129 is one of the most cumbersome long-lived fission products in spent nuclear fuel, but it can be transmuted to Xe-130. In this irradiation experiment both NaI pellets and NaI powders were irradiated. The transmutation of iodine to xenon and the release of xenon during transmutation were measured for both capsules. It appeared that the xenon release in powders was much higher and occurred continuously during irradiation, whereas the NaI pellets showed a lower and more step-wise release of xenon.

Although the example discussed does, strictly speaking, not involve nuclear fuel testing, the application of out-of-pile pressure measurements can be easily extended to test the fission gas release in (light) water reactor nuclear fuels under various conditions.

* Corresponding author; tel. +31224564131, fax +31224568608, email: klaassen@nrg-nl.com

SESSION 3: ON-LINE MONITORING SYSTEMS

Chairperson

L. Vermeeren (Belgium)

**TECHNICAL MEETING
ON
“FUEL ROD INSTRUMENTATION AND IN-PILE MEASUREMENT
TECHNIQUES”**

**3 - 5 September 2007
Halden, Norway**

In-core measurements of fuel clad – coolant interactions in the Halden reactor

**Peter Bennett
Halden Reactor Project**

Abstract

As reactor operators implement longer fuel cycles and power upratings, problems associated with accelerated fuel clad corrosion and creep and crud deposition can be encountered. Changes in water chemistry conditions can be implemented to mitigate specific corrosion phenomena, while new fuel cladding alloys offering improved corrosion and creep performance are under constant development. In-core testing of the corrosion/creep performance of new alloys or the effect of new water chemistry regimes in a test reactor may be required, by licensing authorities, vendors and utilities, before they can be implemented in commercial power plants.

Such studies require representative light water reactor (LWR) conditions, which are achieved by installing test fuel in pressure flasks that are positioned in fuel channels in the reactor and connected to dedicated water loops, in which boiling water reactor (BWR), pressurised water reactor (PWR) or pressurised heavy water reactor (PHWR) conditions are simulated. This paper describes how thermal hydraulic and water chemistry conditions are controlled in the loop systems, and gives details of the techniques currently used, and under development, to provide on-line, in-core corrosion/creep and water chemistry monitoring data.

1. Introduction

As reactor operators implement longer fuel cycles and power upratings, the corrosion/creep behaviour of the alloys used for in-core structures and fuel rod cladding must be studied under the new operating conditions. New cladding alloys offering improved performance are under constant development; while in conjunction, changes in water chemistry conditions can be implemented to mitigate specific corrosion phenomena. An understanding of the mechanisms that lead to material degradation can help to improve and optimise materials properties and to define and qualify water chemistry changes. Studies should be performed under representative conditions to ensure the validity of the data.

The Halden boiling water reactor (HBWR) has been in operation since 1958. It is a test reactor with a maximum power of 18 MW and is cooled and moderated by boiling heavy water, with a normal operating temperature of 230°C and a pressure of 34 bar.

The reactor has been predominantly used for investigation of important fuel properties (temperature, pressure, fuel pellet dimensional changes, etc), where the overall aim has been to assess the performance of current and advanced fuel under normal, abnormal and accident conditions. The results are used for fuel behaviour model development and verification, and in safety analyses [1].

In the past 15 years increasing emphasis has been placed on materials testing, both of in-core structural materials and fuel claddings [2,3]. These tests require representative light water reactor (LWR) conditions, which are achieved by housing the test rigs in pressure flasks that are positioned in fuel channels in the reactor and connected to dedicated water loops, in which boiling water reactor (BWR), pressurised water reactor (PWR) or pressurised heavy water reactor (PHWR) conditions are simulated.

Understanding of the in-core behaviour of fuel or reactor materials can be greatly improved by on-line measurements during power operation. The Halden Project has performed in-pile measurements for a period of over 35 years, beginning with fuel temperature measurements using thermocouples and use of differential transformers for measurement of fuel pellet or cladding dimensional changes and internal rod pressure [4]. Experience gained over this period has been applied to on-line instrumentation for use in materials tests [5]. This paper describes how thermal hydraulic and water chemistry conditions are controlled in the loop systems, and gives details of the techniques currently used, and under development, to provide on-line, in-core corrosion and water chemistry monitoring data.

2. Description of experimental systems

2.1 Test rigs

Test rigs for corrosion studies are positioned in a pressure flask which is loaded into an individual irradiation position in the HBWR. A cross-section of the upper part of an irradiation position is shown in Figure 1.

As an example, the design of a PWR clad corrosion test rig (IFA-638) is shown in Figure 2. The irradiation rig consists of several main components: the top seal assembly, which serves as the main pressure boundary; the manifold assembly, which routes the coolant water to the test section and connects the test section to the top seal assembly; the test section, which contains the test rods together with the instrumentation for thermal-hydraulic and neutronic measurements; and the bottom cone, which routes the coolant water through the test section and serves as a guide when the irradiation rigs are loaded into the pressure flask assemblies. The construction materials are stainless steel, Inconel and zirconium alloys.

The top seal assembly (Figure 3) constitutes the upper part of the irradiation rig and is the pressure boundary between the environment inside the high pressure loop and the environment outside the reactor pressure vessel. The top seal serves three functions: (i) sealing against the high pressure flask; (ii) sealing of instrument signal cables; and (iii) connection of inlet and outlet flow tubes from the rig to the external loop system. The seal between the top seal assembly and the high pressure flask consists of a conical sealing surface which seals against a conical insert in the high pressure flask (see Figure 1). The top seal assembly is forced against the conical seat in the high pressure flask by means of a threaded nut.

The seal between the signal cables and the top seal assembly consists of a compressed graphite seal (see Figures 1 and 3). The signal cables are protected by flexible protection tubes / hoses made from a double braided stainless steel mesh. The flexible cable protections cover / protect the signal cables over the distance from the top seal assembly to the permanent signal cable connections in the reactor hall. These flexible cable protections used are a standard Halden Project design.

The flow tubes in the top seal assembly are the connection between the external loop system and the irradiation rigs. A section of the inlet and outlet flow tubes are welded to the bottom end of the top seal assembly as shown in Figure 3. Above the top seal assembly the inlet and outlet flow tubes are connected to the external loop system with mechanical seals consisting of conical seals loaded by threaded nuts. The top seal flow tube connectors are a standard Halden Project design. The lower end of the inlet flow tube is connected to the upper end of the manifold assembly with a tube extension (see Figures 1 and 3).

The manifold assembly connects the top seal assembly with three downcomer tubes and a signal cable tube in the test section. The downcomer tubes and the signal cable tube constitute the lower structural part of the rig. The downcomer tubes route the coolant water to the bottom of the rig, where the inlet section is located. The inlet section routes the coolant water through the test section where it flows over the test rods. After the coolant water has passed through the test section, it is routed into the manifold assembly again (the outlet ports) and leaves the irradiation rig through the top seal assembly. The cable tube first routes the signal cables through the test section into the manifold assembly and then to the top seal assembly.

For temperature monitoring, three inlet coolant thermocouples and three outlet coolant thermocouples are installed. Thermocouples can also be positioned in the downcomer tubes for the power calibration that is done at the start of irradiation. The test rig is also instrumented with four self-powered neutron detectors (vanadium-type) for measuring thermal flux, which can be related to fast flux by neutronic calculations. The flux can be verified by analysis of fluence monitor wires installed in the test rig. Three different fluence monitor wires can be installed in the test rig - iron and nickel wires for measuring fast neutron fluence and cobalt wires for measuring thermal neutron fluence. The fluence monitor wires can be analysed in conjunction with interim inspections. The fluence monitor wires cover the full length of the test section in the irradiation rig.

The flasks are often surrounded by highly enriched (10 - 13 % wt% ^{235}U) booster fuel rods, for increasing the fast neutron flux to levels typical of those in commercial LWRs.

2.2 LWR loop systems

A schematic drawing of a loop system is shown in Figure 4. Specific BWR, PWR or PHWR conditions can be simulated by varying the pressure and the temperature of the coolant and the concentrations of dissolved additives and gases. Each loop consists of three main sections: the loop itself, the purification system and the sampling system. Other components include the main circulation pump, heaters/coolers and valves. Main thermal-hydraulic operating parameters, such as temperature, pressure and flow rate are automatically controlled within specified limits by the use of Programmable Logic Control (PLC).

The loops are constructed from 316L stainless steel and have a volume (including the purification system) of between 60 and 120 litres. The loop circulation pumps have capacities from 100 litres to 10 tons per hour, and electric heating is used to ensure that the desired temperature can be maintained in the test section.

Chemistry conditions in the loop are controlled by additives and by the purification plant. Impurities are removed by lithium, boron or mixed bed ion exchange units, or by cartridge filters. Under normal operation the flow through the purification plant is approximately 1 to 2 loop volumes per hour. Figure 5 shows the loop diagram for a PWR loop.

The sampling system is used to obtain representative water samples from the loop, to monitor continuously conductivity and dissolved oxygen and hydrogen concentrations in the coolant and to provide a facility for the controlled injection of impurities into the loop. The flowrate through the sample loop is normally in the range from 20 to 50 l h⁻¹. The full loop pressure is maintained in the sampling line, however the coolant temperature is quickly reduced to room temperature to ensure that the samples are representative. A drawing of a loop sampling system is shown in Figure 6.

2.3 Chemistry control

Grab samples of the coolant are analysed using inductively coupled plasma mass spectrometry (ICPMS) to determine the concentrations of soluble transition metal cations, and by capillary electrophoresis for analyses of dissolved anions. Dissolved oxygen and hydrogen gases are monitored by Orbisphere detectors placed in series in the sampling system. Conductivity is also measured on-line. Filter packs, mounted in parallel before the gas analysers, are used to determine integrated concentrations in the coolant of both soluble and insoluble corrosion products and radioactive transition metal species. Approximately 20 litres of coolant are concentrated onto the packs, which contain a Millipore filter (to retain insoluble material) and ion exchange membranes (to retain soluble cationic and anionic species). The filters are subsequently analysed using x-ray fluorescence spectroscopy (XRF) and gamma spectrometry.

Limits are defined for the concentrations of many species in the loop coolant, including both species that effect safety (e.g. chloride ions) and chemicals that are added to the water to simulate LWR conditions (e.g. lithium hydroxide in PWR primary coolant). Procedures to be followed if concentrations are outside of the prescribed limits are defined. These include, for example, coolant water replacement if lithium concentrations are outside specification.

3. In-core monitoring

3.1 Creep of Zircaloy fuel cladding

Creep deformation of LWR fuel cladding during in-reactor service is driven by the net pressure differential across the fuel rod wall, which depends on rod internal pressure (affected by fuel swelling and fission gas release, (FGR)) and the coolant pressure. When fuel is first loaded, rod internal pressure is exceeded by coolant pressure and the clad starts to creep down onto the fuel. Eventually, with fuel-clad gap closure, the creep response of the clad is dictated by the behaviour of the fuel and clad creep-out (tensile creep) occurs as the fuel swells due to formation of fission products. With variations in reactor power, both tensile stress increments and stress reversals can occur, due to the induced thermal expansion/contraction of the fuel. Eventually, at high burn-up, FGR will start to play a role with the possibility that excessive FGR may cause the cladding to lift-

off the fuel, re-opening the fuel-clad gap at power. This is undesirable for both fuel thermal performance and safety considerations. The situation is further complicated by concurrent fast neutron irradiation leading to accumulation of radiation damage in clad material, thereby influencing creep behaviour. Creep data on LWR fuel cladding are required in fuel performance modelling; in-pile data are particularly needed from modern cladding materials exposed to high fast fluence and tested under well defined conditions representative of those within commercial reactors.

Fuel rods for creep testing normally contain two clad segments. End-plugs, with gas line connections, are TIG welded to each segment, which are then joined by a mid-plug. The mid-plugs can either be hollow such that both segments in a given test rod are equally affected by internal gas pressurisation, or solid so that pressure within each segment can be varied independently. The end and mid-plugs are made from Zircaloy and have 50 μm calibration steps machined on them for on-line calibration of the diameter gauges (see below). The segments contain either hollow, fresh UO_2 pellets or Zircaloy filler pellets, depending on the clad temperature required. Fuelled samples are required for testing under PWR conditions, whereas the coolant in a PWR loop gives clad temperatures representative of BWRs if the segments are unfuelled. Clad-fuel diametral gaps are normally 400 μm - large enough to allow for appreciable clad creepdown without pellet-cladding mechanical interaction (PCMI).

A diagram of a diameter gauge is shown in Figure 7. The gauge consists of a differential transformer with primary and secondary coils arranged symmetrically on an E-shaped ferritic core. A ferritic armature is arranged along the face of the E, and is pivoted in the middle. Two or three feelers at different radial positions on a fuel rod transmit diameter variations to the armature. A fixture with three spring loaded fingers keeps the differential transformer in position close to the rod.

A schematic diagram of a cladding creep test rig is shown in Figure 8. Stress is applied by internal gas pressurisation of the fuel rods and diameter changes are measured on-line using diameter gauges. Both internal and external rod pressure are monitored on-line and the data used to calculate the applied circumferential or hoop stress (σ_c) in the clad segments. A wide range of compressive and tensile stresses can be applied to the specimens and changes in stress level can be effected both rapidly and repeatedly. On-line monitoring of the clad diameter can be carried out as often as every 10 minutes and to an accuracy of approximately 2 μm .

Diameter traces are obtained by moving the gauges axially along the rods, including the end plugs. This generates a complete profile, in arbitrary units, of each rod diameter. A sinusoidal position indicator attached to the piston records the axial location of each diametral measurement.

Some results showing the creep behaviour of a Zircaloy-2 clad segment are shown in Figure 9 [6]. The clad was retrieved from a test rod that had been irradiated in a BWR at a temperature of 285 - 290°C to a fast neutron fluence of $6 \times 10^{21} \text{ n cm}^{-2}$. The final steps in the rod manufacture consisted of a 70 per cent reduction by cold work followed by a

576°C anneal for three hours, which resulted in a fully recrystallised microstructure. The tube was received with a 10 µm oxide layer on the outside, with a hydrogen content of about 60 ppm. For creep testing in the HBWR, the rod was unfuelled. The internal pressure of the rod was changed nine times during the experiment, and the total diameter change during each stress period is shown in Figure 9. On changing the applied stress, there was an immediate step change in measured diameter due to change in elastic deformation. The plot indicates subsequent primary creep (creep rate decreasing with time), followed by secondary creep (constant creep rate).

3.2 Fuel clad corrosion

Traditionally, corrosion of fuel rod cladding in reactor cores has been studied by taking measurements of oxide thickness or sample weight during reactor shutdowns. The main limitation of this method is that only average corrosion rates can be determined. The use of on-line measurements would deliver more information on corrosion processes and would assist in the determination of corrosion mechanisms. Two in-core techniques that would provide on-line data are currently under development, as described below.

(i) On-line potential drop corrosion monitor

The dc potential drop method, which has been developed and used to measure crack growth on-line in the Halden irradiation assisted stress corrosion cracking (IASCC) programme [2], has been adapted for on-line measurement of cladding corrosion. Current and potential wires are attached to the end plugs of a fuel rod, and potential drops caused by the passage of an applied current are measured at different positions on the end plugs (Figure 10). The potential drops are related to cladding thickness through out-of-pile calibration. With this technique, cladding thickness and thus oxide formation can be measured to an accuracy of ± 2 µm.

Qualification and testing of the method under in-core conditions will be conducted. Oxide thicknesses will be compared with measurements performed using standard techniques such as eddy current and SEM.

(ii) Electrochemical impedance spectroscopy

In electrochemical impedance spectroscopy (EIS) measurements, a variable (ac) voltage is applied to the sample and its impedance (ratio of voltage to current) is measured as the frequency of the applied voltage changes. The technique possesses several advantages. Methods using ac use low perturbation signals that do not disturb the system under test, as do direct current (dc) methods. The technique can be used in low conductivity media, such as BWR type coolant, and is non-destructive. EIS is a powerful technique that can measure a wide range of kinetic phenomena in one test, including information on surface films, diffusion and corrosion rates.

Preliminary development work, in conjunction with the University of Gothenburg, Sweden, was conducted in an autoclave to assess the feasibility of monitoring oxide growth on Zircaloy fuel cladding on-line. Measurements were taken using cable lengths of up to 20 m to study any adverse effects caused by the large separation of the sample and measuring equipment. Oxide thicknesses were calculated from an equivalent electrical circuit, in which the insulating ZrO_2 is modelled by a capacitor with plate separation equal to the oxide thickness.

Initial in-core measurements will be performed under PWR conditions, i.e. in water with a relatively high conductivity. The sample (or working electrode) will consist of either a coupon or a tube placed inside a cylindrical platinum mesh counter electrode. Platinum reference electrodes will also be installed. The measurements will be conducted using commercial computer software loaded onto computers located in the reactor hall. This technique has been used for previously in Halden for studies of Zircaloy-4 corrosion in LiOH solutions [7], in which it was shown that reliable measurements can be obtained using the long signal cables necessary for in-core measurements. PIE showed that the relative corrosion rates of the five samples agreed well with the in-core EIS measurements.

Provisionally, it is proposed to test Zircaloy-4 and Zircaloy-2. The former will allow comparison of the corrosion rate data with corrosion models, while use of the two materials will allow demonstration of the effects of material composition on corrosion behaviour. Other alloys, either those used currently in LWRs or under development, can also be tested. Further experiments will be conducted under BWR water chemistry conditions.

3.3 *Crud effects*

Crud is the term given to corrosion product deposits on fuel cladding and primary system surfaces. It is produced from dissolved and particulate corrosion products in the coolant, and consists mainly of iron (and in PWRs, nickel) oxides. The primary driving force for crud deposition is the thermal electromotive force on heated surfaces, and the major factors determining crud deposition are thought to be the heat flux at the clad surface, coolant corrosion product concentrations and steam void fraction along the clad surface.

Many nuclear power plants are attempting to increase efficiency by operating at higher power and coolant temperatures than were common previously. Such operation increases the probability of crud-related problems.

3.3.1 PWR AOA studies

Many PWRs have suffered from the axial offset anomaly (AOA) since the early 1990s. AOA is a phenomenon associated with localised boron hideout in corrosion product deposits (crud) on fuel surfaces formed because of the presence of sub-cooled nucleate

boiling. Since boron absorbs neutrons, the reactor experiences a shift in power output towards the bottom of the core. AOA has caused one plant to de-rate and forced other utilities to design less efficient cores to avoid the phenomenon.

Several mitigation approaches have been developed or are underway to either delay the onset of AOA or avoid it entirely, including use of enriched boric acid (EBA) in the reactor coolant [8]. The boric acid used as a soluble reactivity control agent in PWRs contains approximately 20 percent ^{10}B . Use of EBA will allow the total amount of soluble boron (and LiOH) to be lower. However, due to the significant capital investment associated with converting a plant to EBA, it is prudent to first demonstrate in a research reactor that EBA would be successful. Prior to this, it is necessary to prove that the same facility can develop the symptoms of AOA under proto-typical or near proto-typical PWR conditions. IFA-665 was the first phase in an experimental program to investigate whether AOA can be delayed or avoided by using EBA [9]. The objective of the experiment was to entrain boron within fuel crud deposits and measure the resulting flux depression under proto-typical PWR conditions.

The test fuel comprised a bundle of eight rods, each with an active length of 60 cm. One of the test requirements was that no boiling should occur along the lower section of the fuel rods and that sub-cooled nucleate boiling was required along the upper section. Hence, the lower (20 cm) and upper (40 cm) sections of the test rods were fuelled with UO_2 with different enrichments. The fuel bundle was contained in a pressure flask, and loop system supplied PWR-type coolant and enabled chemical additions to be made (as described in Section 2).

One of the test rods could be hydraulically withdrawn into the upper part of the pressure flask and scanned by a diameter gauge to detect crud deposition. Neutron detectors (NDs) and coolant differential thermocouples (DTs) were employed to detect neutron flux/power depressions. The NDs were positioned, at three axial positions, on the outside of the pressure flask and in the centre of the test rig. The DTs were positioned, in groups of four, at four axial levels. The intention was to study power reductions from a comparison of the signals from the NDs in the test rig and on the pressure flask. A flux depression due to loss of power in the test rig would affect the rig NDs, while the sensors on the pressure flask, which will also be influenced by the flux from neighbouring test rigs, should show a different response. A reduction in power should also be seen from the DT measurements, as the coolant temperature increase should be lower. The lower ND in the test rig was employed as a control: crud was not expected to deposit over this portion of the fuel, and hence AOA symptoms should be absent. Unfortunately, at the start of the second cycle, this ND became faulty. Hence, another method of assessing the neutron flux behaviour was used, which involved use of the ND signals from three neighbouring test rigs.

In order to increase concentrations of Fe and Ni in the coolant, an Fe-Ni-EDTA (EDTA = Ethylene Diamine Tetra Acetic acid) solution (15 per cent in EDTA with 125 ppm each of Fe and Ni) was injected continuously into the loop coolant. Since EDTA has a strong chelate effect and forms stable complexes with transition elements in solutions up to 250

- 260°C, soluble Fe and Ni were transported at high concentrations to the test rig. At higher temperatures, or in a gamma/neutron field, the complex decomposes and releases its central ion. Such a release of Fe and Ni in the in-core section of the test rig at concentrations above their solubilities should result in deposition on the fuel cladding. Measured concentrations of soluble Fe and Ni increased from 3.5 and 0.3 ppb to 13 and 1.8 ppb as a result of the injections.

Crud deposition was observed on-line from diameter measurements (Figure 11). This figure shows three diameter traces. The first trace was taken at the start of the experiment, and shows the expected flat profile, with the measured diameter close to the nominal value of 9.5 mm. The second trace, taken after 232 days at power, shows a reduction in diameter, indicating clad creepdown. In the third measurement, taken 25 FPD later, the traces from the lower third of the rod are similar, whereas along the upper section, the later trace has moved upwards relative to the earlier, which (from the magnitude of the calibration steps) is indicative of deposition of a crud layer of approximately 10 - 20 µm.

Evidence of a power depression was obtained from the ND signals, while coolant chemistry measurements gave support to boron hide-out. Figure 12 shows the ND signals from the test rig and the pressure flask normalised to the signals from the NDs at corresponding axial locations in three neighbouring test rigs. The normalised signals from the bottom section of the pressure flask show no downward trend. This indicates that power variations measured by these sensors were similar to those in the other rigs. For the middle and upper sections of the pressure flask, a reduction was seen from 33 days. However, for the test rig signals, a strong downwards trend was seen, showing that the upper section of the fuel bundle was losing power relative to the three surrounding rigs.

During the shutdown at the end of the cycle, the loop chemistry was maintained alkaline with the objective of minimising dissolution of any fuel crud. The reactor was shutdown with a planned scram. The rig temperature decreased by 40°C over a period of five minutes, and by a further 25°C during the following hour. The coolant Li content increased from 3.04 to 12.38 ppm during this period (Figure 13). This large increase in Li during the shutdown, which has not previously been observed in PWR loops in the Halden reactor, is similar to the behaviour observed in PWRs that have experienced AOA, and is caused by dissolution of fuel crud as the coolant temperature decreases.

3.3.2 BWR crud thermal conductivity studies

In BWRs, formation of a hard impervious crud layer, by preventing free flow of coolant to the fuel clad surface, results in a large rise in clad temperature. This leads to increased cladding corrosion and to a higher probability of clad failure.

Several BWRs are currently operating with a water chemistry regime that includes addition of hydrogen and zinc, together with noble metal chemical addition (NMCA) during shutdown periods. It is known that zinc injection may result in formation of an impervious crud layer, while the combination of Zn and NMCA requires investigation.

The purpose of the IFA-698 experiment is to investigate the impact of this chemistry regime on the heat transfer from the fuel to the coolant, i.e. on the thermal conductivity of the oxide-crud layer.

The test rods utilise refuelled, pre-irradiated clad segments taken from fuel rods irradiated in the US Hatch BWR. Two test rods are included in the test: a reference rod, with no significant crud deposits, and one rod with a thick ($> 20 \mu\text{m}$) tenacious crud layer. Each test rod consists of two short segments (approximately 14 cm each) connected by a mid plug. The rods have been re-fuelled and fitted with extensometers for measurement of cladding elongation. The thermal conductivity of the tenacious crud layer is determined by measuring the change in clad elongation with heat rate during power ramps of the two test rods.

Operating conditions have been chosen to be representative of those under which the fuel rod operated in the Hatch BWR. Specifically, the conditions at the axial location with the maximum crud thickness have been chosen. These are an average fuel linear heat rate of 20 – 23 kW/m, with the coolant void fraction in the range from 0 to 10 per cent. The test has been conducted in a loop operating with hydrogen water chemistry.

Figure 14 shows on-line data obtained during a power ramp, including the coolant temperature and the elongation of the reference and crudded rods. A clear difference in behaviour between the two test rods is observed.

3.4 *In-core water chemistry monitoring*

Many aqueous corrosion processes are strongly affected by the pH of the corroding solution, concentrations of dissolved oxygen gas and concentrations of ionic species, which can be measured as the solution conductivity. Although on-line methods of measuring these parameters have been developed mainly in order to study corrosion of reactor structural materials, they are also of use when the effects of water chemistry on fuel clad corrosion and crud formation and deposition are studied. As described in Section 2, conductivity and oxygen/hydrogen concentrations are measured on-line in the Halden reactor, although the loop coolant is cooled to room temperature first. In-core, on-line measurements can aid in interpretation of corrosion results, and two such techniques are described below.

3.4.1 In-core ECP measurements

The electrochemical corrosion potential (ECP) of a corroding metal is the potential difference between it and the standard hydrogen electrode (SHE). ECP is determined by measuring the potential between the sample and a reference electrode, and adding the (calculated) potential versus SHE of the reference electrode. A reference electrode is a half-cell that produces a stable and reproducible potential. For in-core measurements of

ECP, reference electrodes must be capable of withstanding the high temperatures and pressures, and neutron and gamma fluxes within the reactor core.

The ECP is one of the most important measures of a corrosive environment, and is determined by a combination of the surface conditions of the specimen and concentrations of dissolved oxidants. The ECP is a key measurement when the performance of reactor structural materials is to be assessed or measures taken to optimise their integrity - many BWRs now inject hydrogen in order to maintain the ECP of in-core stainless steel components below the "IASCC threshold" of $-230 \text{ mV}_{\text{SHE}}$.

Perhaps the most critical aspect of the design of a reference electrode is the seal between the potential sensing element and the signal cable, which must be water resistant. Temperature changes will cause mechanical stress on the electrode seals, signal cables etc, and it can be assumed that the electrode lifetime will be dependent on the number of reactor power or loop operations causing large temperature changes in the loop coolant. In the electrodes designed and produced in Halden, the seal is constructed from two metal (Inconel) sub-units connected by a ceramic tube and has main dimensions of length 80 - 100 mm and diameter 12 mm. No ceramic-to-metal brazing is required [10].

To obtain reliable ECP measurements it is recommended that two different types of reference electrode be used. In Halden, palladium (Pd) and iron/iron oxide (Fe/Fe₃O₄) electrodes are being developed for use under oxidising conditions; in addition, Pt electrodes can be used under reducing conditions.

The Halden platinum (Pt) electrode [11, 12] is shown in Figure 15. The potential-sensing element consists of a Pt cylinder and end plate. The large surface area of the platinum serves to reduce the effect of any mixed potentials caused by the other metal components.

Figure 16 shows an example of ECP data measured with Pt electrode under PWR water chemistry conditions (3 ppm LiOH, 1000 ppm B as boric acid (H₃BO₄), 2-4 ppm H₂ and conductivity 25-30 $\mu\text{S}/\text{cm}$). The electrode gave reliable signals over the duration of the test, 340 full power days. This period included four reactor cycles, with several heating and cooldown periods within each, and shows that the seal arrangement is satisfactory. The measured potential between the stainless steel pressure flask (used as the sample) and the reference electrode was, as would be expected under reducing conditions, of the order of a few millivolts, i.e. both metals were at similar potentials. Under such conditions, the ECP of stainless steel primarily reflects the thermodynamic potential of the H₂/H₂O reaction, and values in the range from -770 to $-830 \text{ mV}_{\text{SHE}}$ were obtained.

The Halden/VTT palladium reference electrode [13] is shown in Figure 17. The potential-determining reaction of the palladium hydrogen electrode is similar to that of the platinum hydrogen electrode or SHE [14]. In the SHE, hydrogen is introduced from an external source and the electrode potential is determined by the H₂ partial pressure and the pH of the electrolyte. Palladium differs from platinum in that it can hold hydrogen within its lattice; in aqueous solutions, hydrogen can be produced by cathodic charging of the Pd. When sufficient hydrogen is loaded, some will diffuse to the surface of the Pd,

which can thus function as a hydrogen electrode. Hence, the advantage of the Pd electrode over the Pt electrode is that it can be used in oxygenated water. The Pd electrode is suitable for in-core measurements since the potential-determining species (H_2/H^+) are stable over the temperature range of interest and do not contaminate the environment (as would happen, for example, if an Ag/AgCl reference electrode were to fail).

The Pd electrode must be calibrated against another type of electrode in order to determine the surface coverage of palladium with hydrogen atoms. The surface coverage is analogous to the H_2 partial pressure used in the calculation of the potential of platinum electrodes, and thus allows calculation of the potential of the electrode.

Initial in-core results [13] showed that the Pd electrode can produce a stable reference potential in oxygenated water (5 ppm O_2) (Figure 18), and that it can measure changes in ECP due to changes in oxidant concentration. ECP measurements with the Pd electrode have also been performed in hydrogenated water; Figure 19 shows the effect of coolant temperature on the surface coverage of hydrogen atoms on palladium [15].

Metal/metal oxide electrodes have been used for many years, and development of Fe/Fe₃O₄ electrodes has commenced at Halden. Whereas many designs use a ceramic tube made from yttrium partially stabilised zirconia (Y PSZ), the Halden studies have focused on magnesium partially stabilised zirconia (M PSZ) due to its higher strength, which should make it easier to construct a reliable seal. Tests have shown that M PSZ works as an oxygen conducting membrane and that the internal resistance of Mg-PSZ (Fe/Fe₃O₄ electrode) is low enough to allow in-pile measurements. A prototype electrode is shown in Figure 20.

3.4.2 In-core conductivity measurements

The inter-relationship between ECP and conductivity, and hence between conductivity and crack propagation in reactor materials, is well established. Most on-line techniques for monitoring water quality are designed for use at room temperature. However, room temperature measurements may not be representative of the conductivity at elevated temperature. Although high-temperature conductivity can be modelled, the calculations require as input the high temperature concentrations of dissolved ions, which may not be available. Hence, the advantages in measuring conductivity at the temperature of interest, for both precise determination of water quality and to study the effect of impurities on corrosion, are clear.

A novel conductivity electrode (Figure 21) has been developed that can be installed in in-core pressure flasks and hence measure conductivity at operating temperature and pressure, and in the presence of water radiolysis products. The sensor is a modification of the Halden platinum ECP electrode, in which the Pt sensing element is surrounded by a second Pt cylinder. An additional signal cable is fitted through which a current is passed, and the conductivity of the coolant is determined from the measured voltage difference

between the two Pt cylinders. Use of the Halden leak-tight mechanical seal enables the monitoring of conductivity in-core. It is envisaged that the sensor will give the most useful data under BWR conditions, since impurity leakages are more readily monitored at high temperature, due to increased ionic mobilities. Under PWR conditions, conductivity is dominated by LiOH and boric acid, and the effects of impurities may not be distinguishable.

The prototype cell functioned reliably in a test conducted under PWR conditions (2 ppm LiOH, 1200 ppm B, 2.5 - 3 ppm H₂) for a period of 45 days (Figure 22). A solution conductivity of approximately 200 $\mu\text{S}/\text{cm}$ was measured at 335°C; the corresponding low temperature conductivity, measured in the loop sampling system, was approximately 20 $\mu\text{S}/\text{cm}$. The measured conductivity agreed well with literature data of the high temperature conductivity of LiOH solutions.

The sensor may give more useful data under BWR conditions, where water radiolysis products will have a larger effect on the in-core conductivity. Chemical additions to the coolant are planned in several forthcoming BWR IASCC studies; conductivity measurements in these experiments will be conducted to investigate whether the cell gives useful results in water with a lower conductivity than that of PWR coolant.

4. Summary

Loop systems allow tests to be conducted under LWR thermal-hydraulic and water chemistry conditions. In-core, on-line instrumentation is flexible and can be used for several purposes – for example, diameter gauges can be used to obtain creep data and to detect crud deposition of fuel cladding.

Instrumentation developed for studies of corrosion of plant materials, for example electrochemical corrosion potential (ECP) electrodes, are also valuable in fuel clad corrosion/crud studies where the water chemistry conditions have a large effect on fuel-coolant interactions.

In-core, on-line techniques are under development to allow investigation of fuel clad corrosion.

References

- [1] T Tverberg, *In-pile fuel rod performance characterisation in the Halden reactor*, This conference.
- [2] T. M. Karlsen and E. Hauso, *Qualification and application of instrumented specimens for in-core studies on cracking behaviour of austenitic stainless steels*, Proc 9th Int. Conf. On Environmental Degradation of Materials in Nuclear Power Systems - Water Reactors, Newport Beach, California, USA, August 1999, NACE, Houston, USA.
- [3] T. M. Karlsen, M. McGrath and E. Kolstad, *Halden research on Zircaloy cladding corrosion*, in Water chemistry and corrosion control of cladding and primary circuit components, Proceedings of a Technical Committee meeting, Vltavou, Czech Republic, 28 September - 2 October 1998, IAEA-TECDOC-1128.
- [4] C Helsingreen, *In-pile instrumentation and re-fabrication techniques of the Halden Reactor Project*, This conference.
- [5] P. J. Bennett, E. Hauso, N-W. Høgberg, T. M. Karlsen and M. A. McGrath, *In-core materials testing under LWR conditions in the Halden reactor*, Proc. Chimie 2002, 22 - 26 April 2002, Avignon, France, SFEN, 2002.
- [6] M A McGrath, *In-reactor creep behaviour of Zircaloy cladding*, ANS Top Fuel meeting, Park City, Utah, USA, April, 2000.
- [7] D M Rishel, K L Eklund and B F Kammenzind, *In-situ EIS measurements of irradiated Zircaloy-4 post transition corrosion kinetic behaviour*, 15th International Symposium on Zirconium in the Nuclear Industry, ASTM, 2007.
- [8] P L Frattini, J Blok, S Chauffriat, J Sawicki and J Riddle, *Axial offset anomaly: coupling PWR primary chemistry with core design*, Water chemistry of nuclear reactor systems 8, 22 - 26 October 2000, Bournemouth, UK, (BNES, London, UK, 2000).
- [9] P J Bennett, B Beverskog, R Suther and J Deshon, *Demonstration of the PWR AOA in the Halden Reactor*, International conference on water chemistry of nuclear reactor systems, Korean nuclear Society, 2006.
- [10] B. Beverskog, L. Lie, N-W. Høgberg and K. Mäkelä, *Verification of the miniaturised in-core Pd reference electrode operation in out-of-core and in-core location at Halden*, Proc. Water Chemistry of Nuclear Reactor Systems 8, 22 - 26 October 2000, Bournemouth, UK, BNES, 2000.
- [11] P. J. Bennett, B. Beverskog, N-W. Høgberg, T. M. Karlsen and H. Thoresen, *In-core ECP measurements under LWR conditions in the HBWR*, Tenth Int. Conf. on Environmental Degradation of Materials in Nuclear Power Systems - Water Reactors, NACE, USA, 2001.

- [12] P J Bennett, M McGrath, K Bagli and M Dymarski, *Measurements of carbon steel ECP and critical deuterium concentration under CANDU conditions in the Halden Reactor*, 12th Int. Conf. on Environmental Degradation of Materials in Nuclear Power Systems - Water Reactors, NACE, USA, 2005.
- [13] P J Bennett, *In-core ECP measurements in oxygenated water in the Halden Reactor using a palladium reference electrode*, Int. conf. on water chemistry of nuclear reactor systems, EPRI, San Francisco, 11 - 14 October 2004.
- [14] R. W. Bosch, R. van Nieuwenhove, W. F. Bogaerts and F. Moons, *Development of high temperature, high pressure reference electrodes for in-pile use*, EUROCORR '98, 28 September - 1 October 1998, Utrecht, Netherlands, EFC, 1998.
- [15] P J Bennett, *In-core ECP measurements under PWR conditions using a palladium reference electrode*, Fontevraud 6, SFEN, 18 – 22 September 2006.

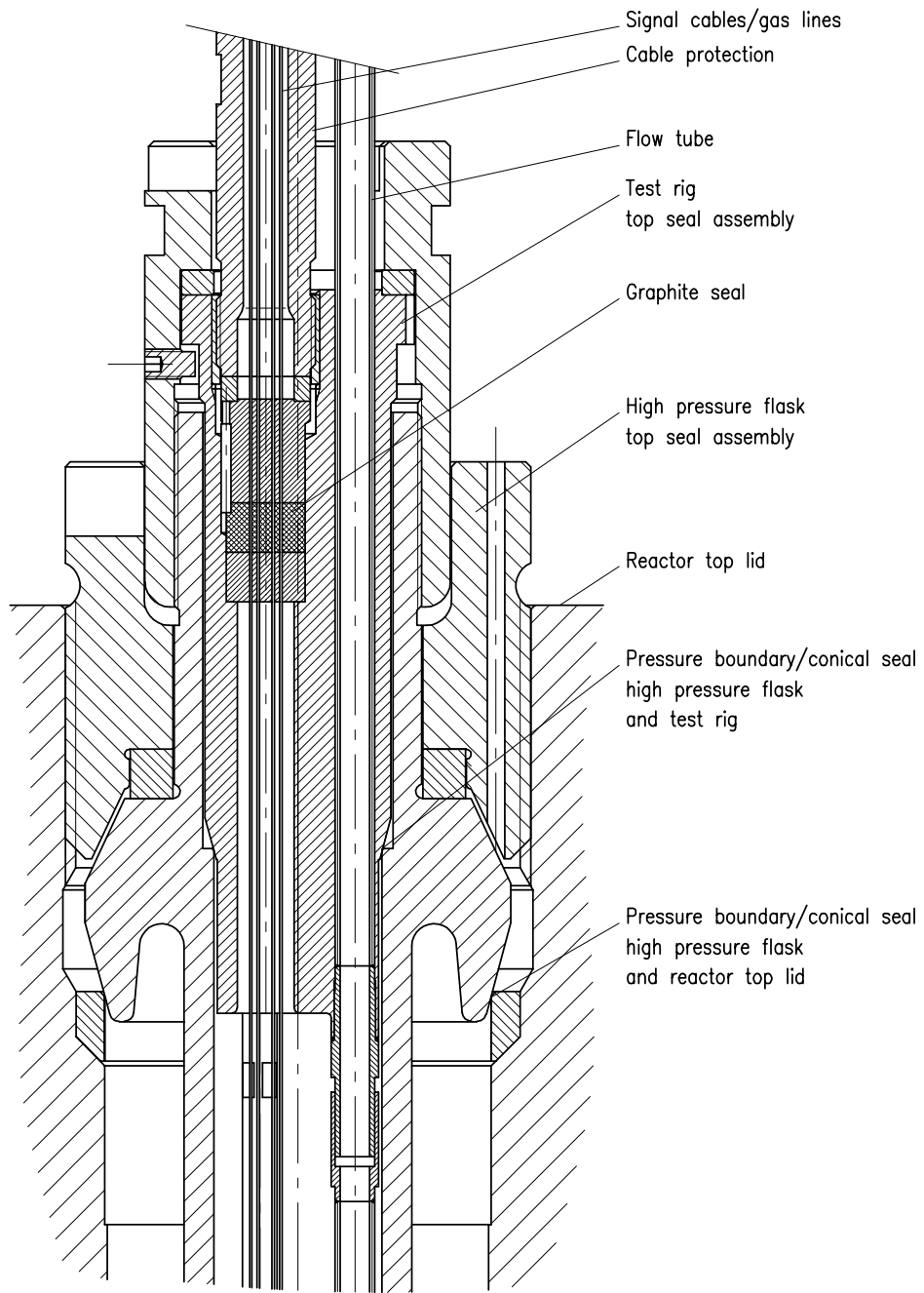


Figure 1. Outline of a typical irradiation position

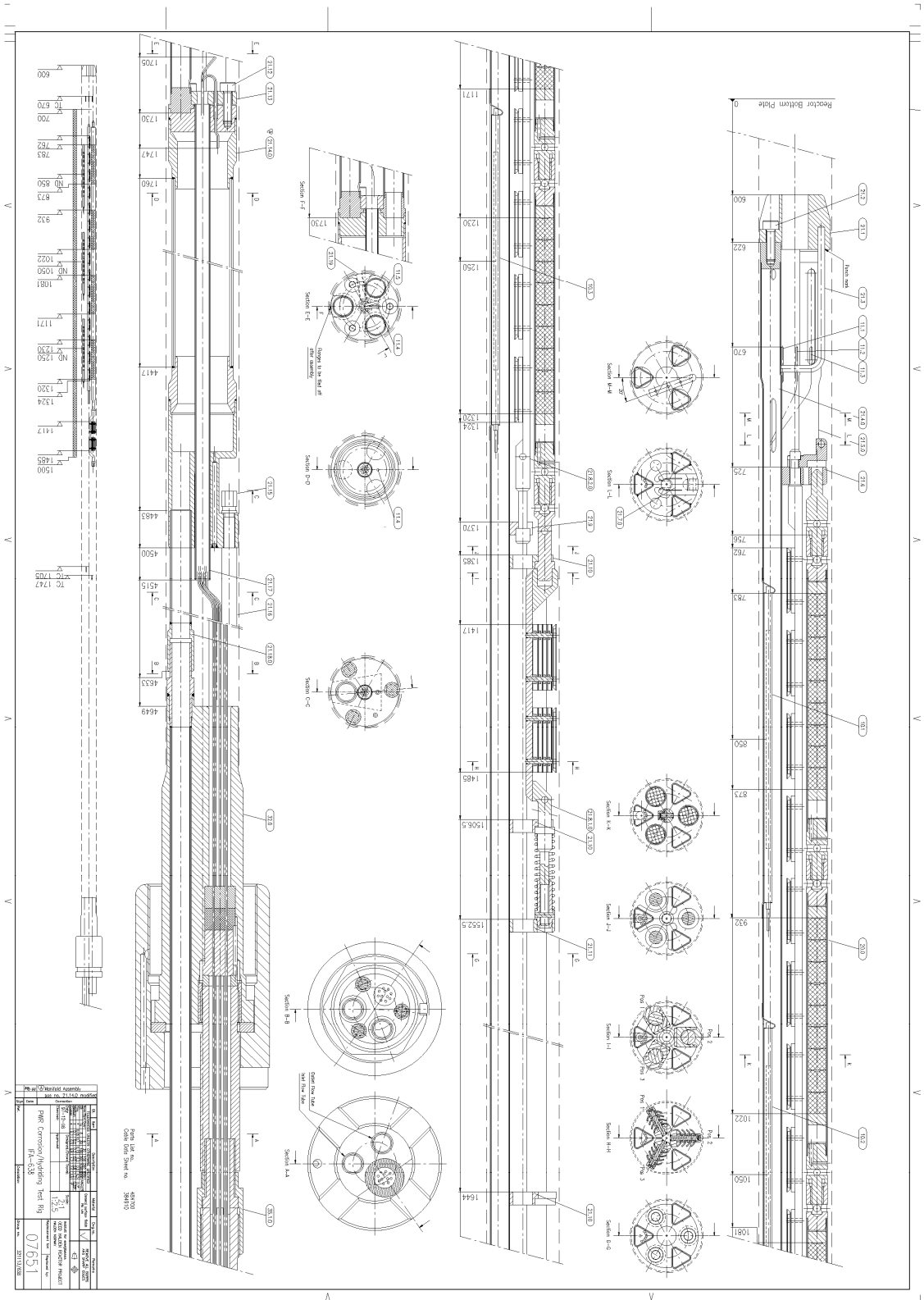
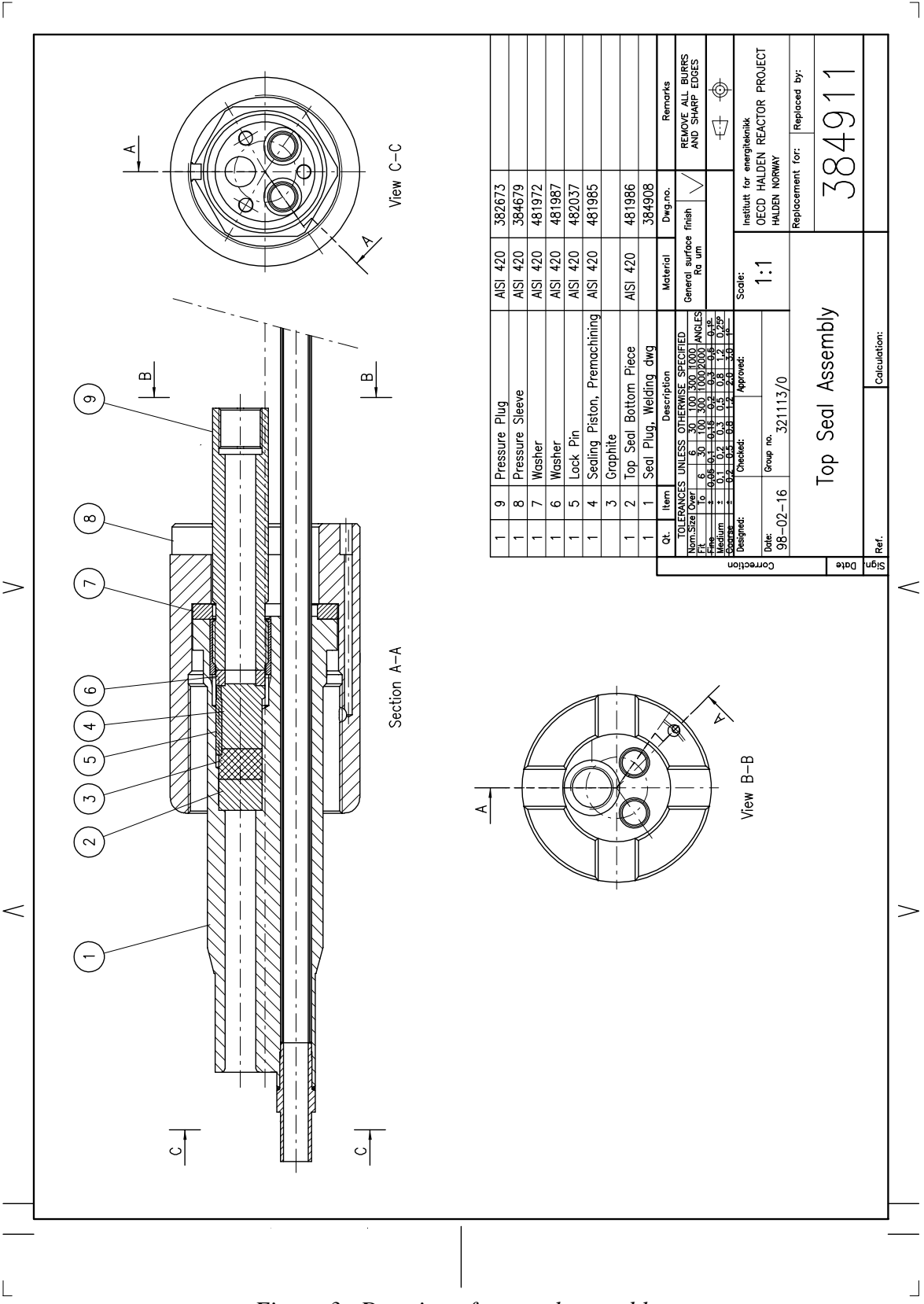


Figure 2. Drawing of clad corrosion test rig IFA-638



Qt.	Item	Description	Material	Dwg.no.	Remarks
1	9	Pressure Plug	AISI 420	382673	
1	8	Pressure Sleeve	AISI 420	384679	
1	7	Washer	AISI 420	481972	
1	6	Washer	AISI 420	481987	
1	5	Lock Pin	AISI 420	482037	
1	4	Sealing Piston, Premachining	AISI 420	481985	
	3	Graphite			
1	2	Top Seal Bottom Piece	AISI 420	481986	
1	1	Seal Plug, Welding dwg		384908	

TOLERANCES UNLESS OTHERWISE SPECIFIED	
Norm Size Over	6 30 100 300 1000 2000
F.F.	0.012 0.015 0.02 0.03 0.04 0.05
Free	0.015 0.02 0.03 0.04 0.05 0.06
Finish	0.02 0.03 0.04 0.05 0.06 0.08
Surface	0.2 0.3 0.4 0.5 0.6 0.8

Design:	Checked:	Approved:	Scale:	1:1
Date:	98-02-16	Group no.:	321113/0	
Institutt for energiteknikk OECD HALDEN REACTOR PROJECT HALDEN NORWAY				
Replacement for:	384911			
Replaced by:				

Figure 3. Drawing of top seal assembly

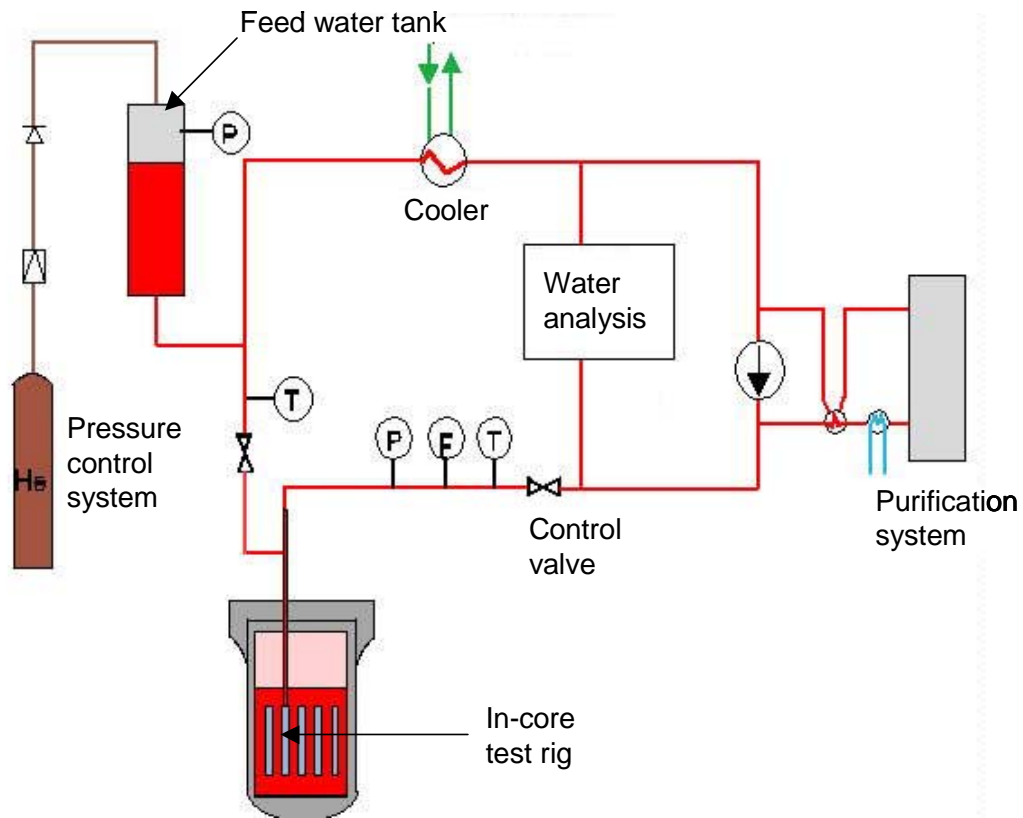


Figure 4. Schematic drawing of loop system

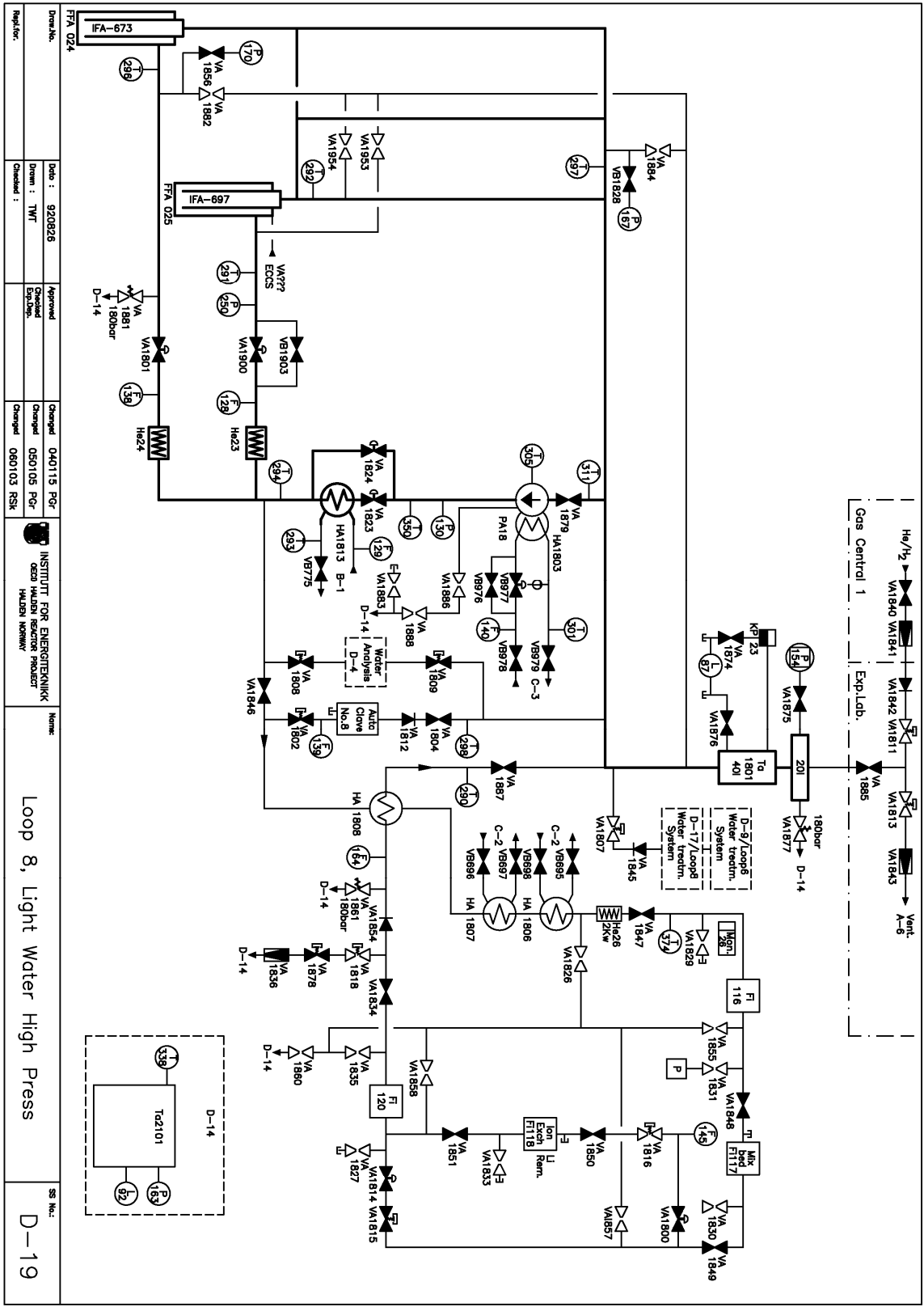


Figure 5. Drawing of a PWR loop system

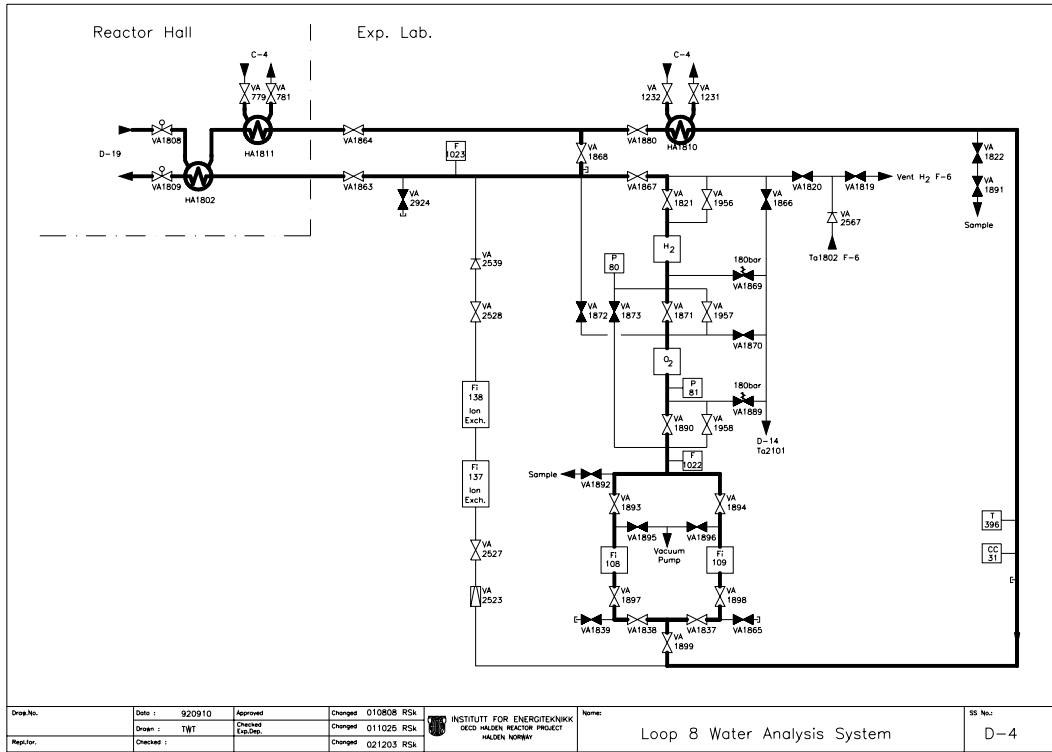
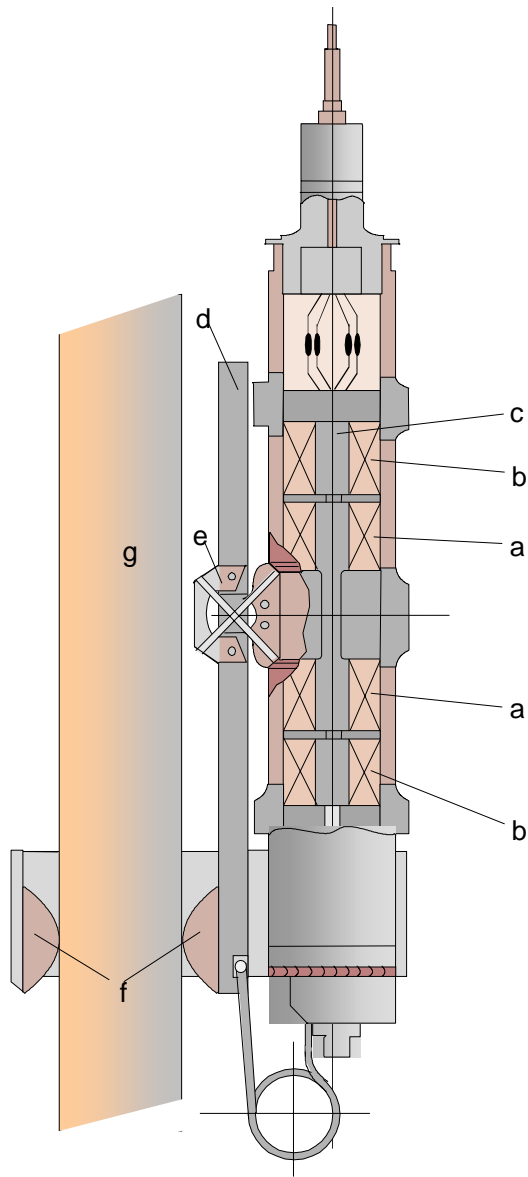


Figure 6. Drawing of loop sampling system



- a: Primary coil
- b: Secondary coil
- c: Ferritic bobbin
- d: Ferritic armature
- e: Cross spring suspension
- f: Feelers
- g: Fuel rod

Figure 7. Schematic of diameter gauge

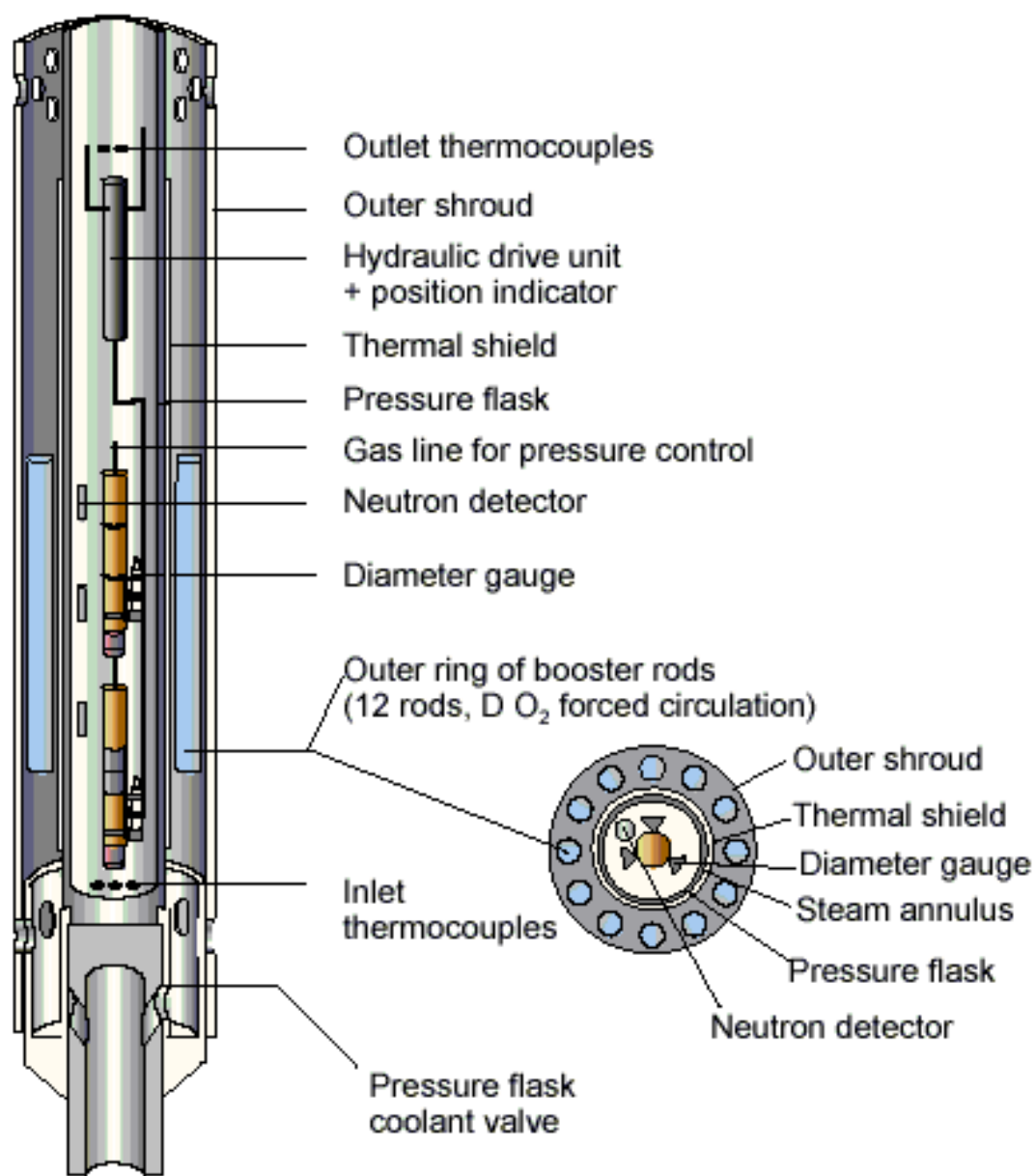


Figure 8. Schematic of cladding creep test rig

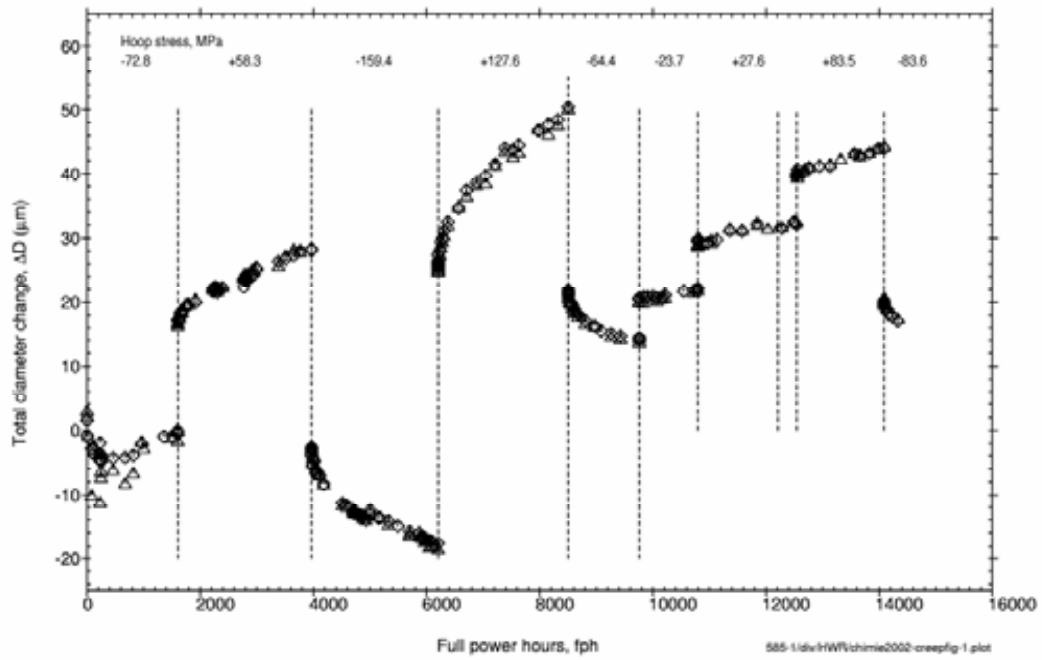


Figure 9. Diameter changes of a Zircaloy-2 clad tube

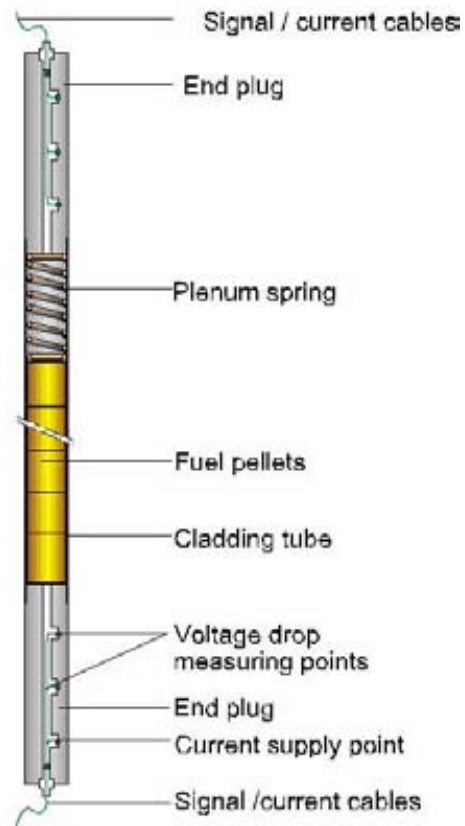


Figure 10. On-line potential drop corrosion monitor

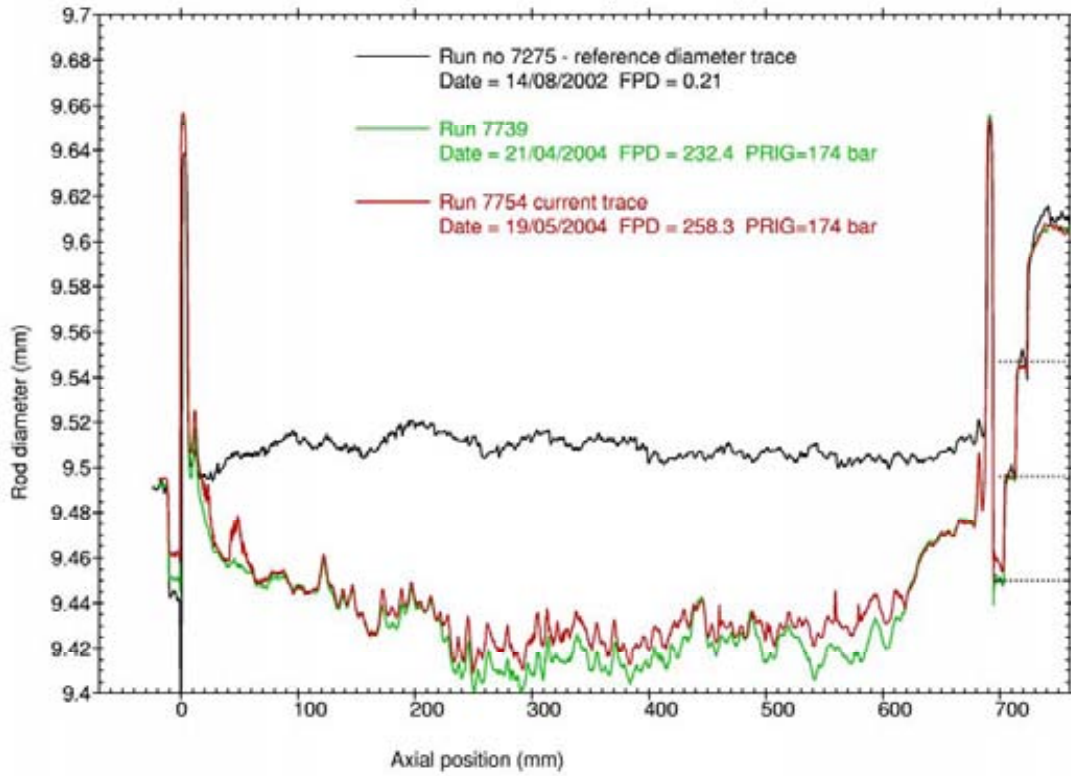


Figure 11. On-line diameter measurements indicating crud deposition (PWR AOA test, IFA-665)

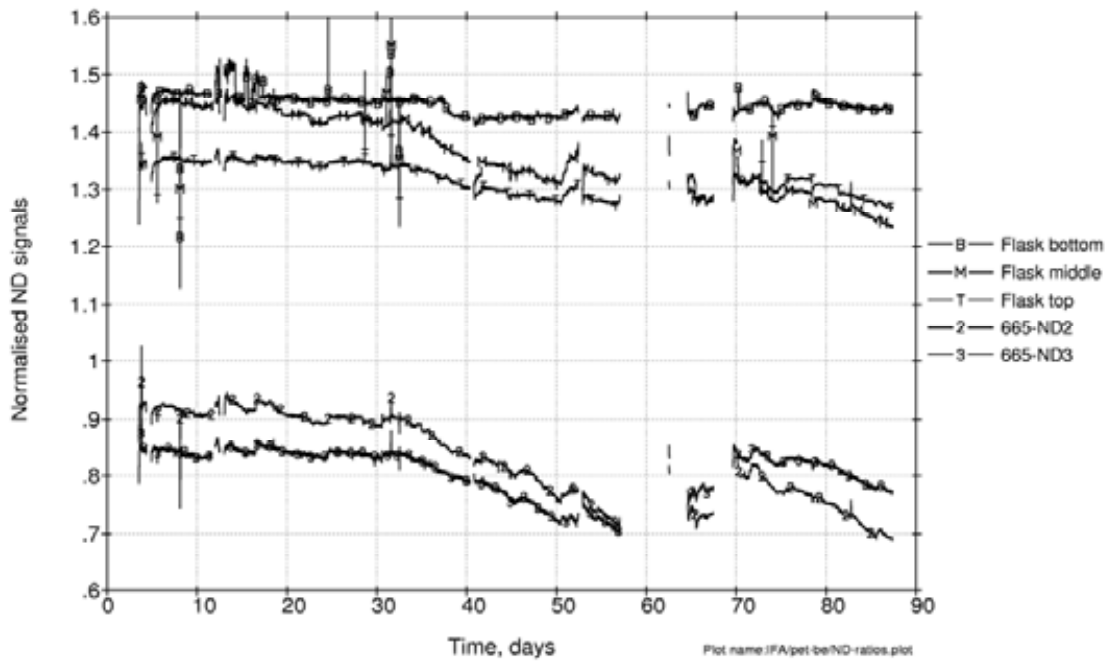


Figure 12. Test rig and pressure flask ND signals normalised to neighbouring test rig ND signals, showing evidence of power suppression (PWR AOA test, IFA-665)

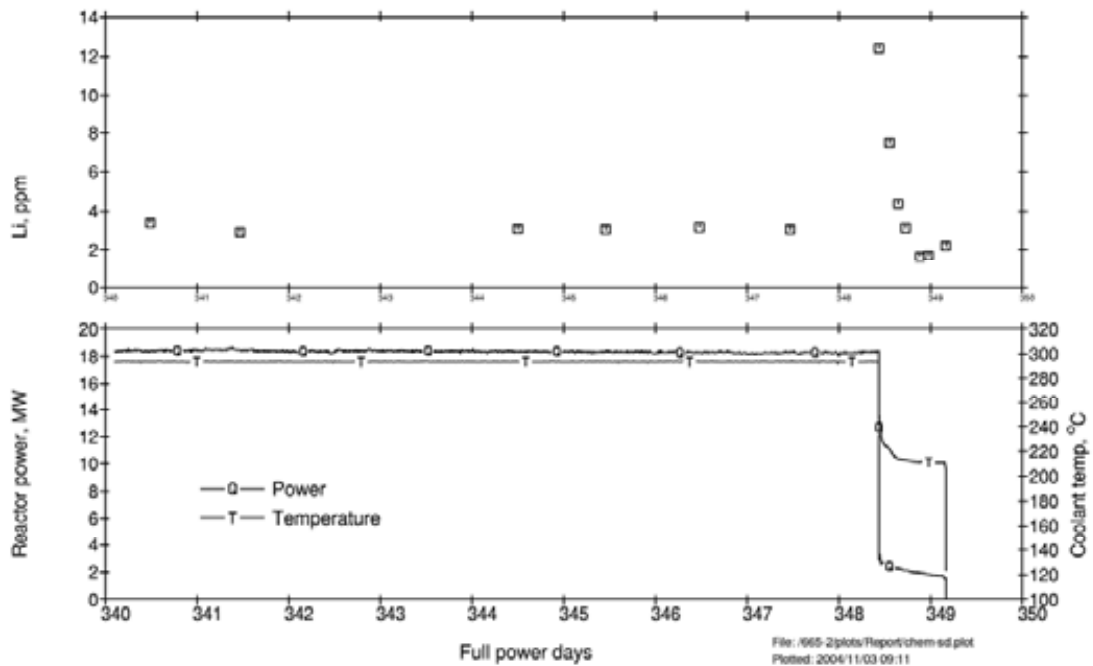


Figure 13. Coolant lithium return during shutdown (PWR AOA test, IFA-665)

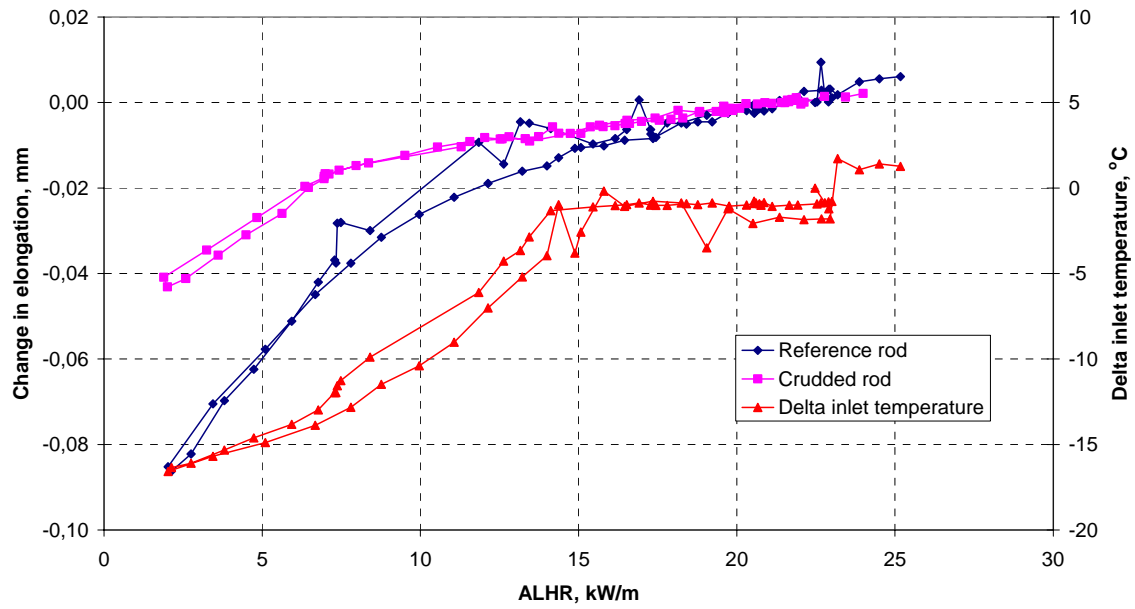


Figure 14. Coolant temperature and rod elongation measurements during a power ramp (BWR crud thermal conductivity test, IFA-698)

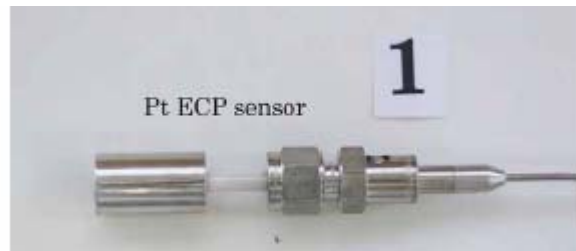


Figure 15. Halden platinum ECP reference electrode

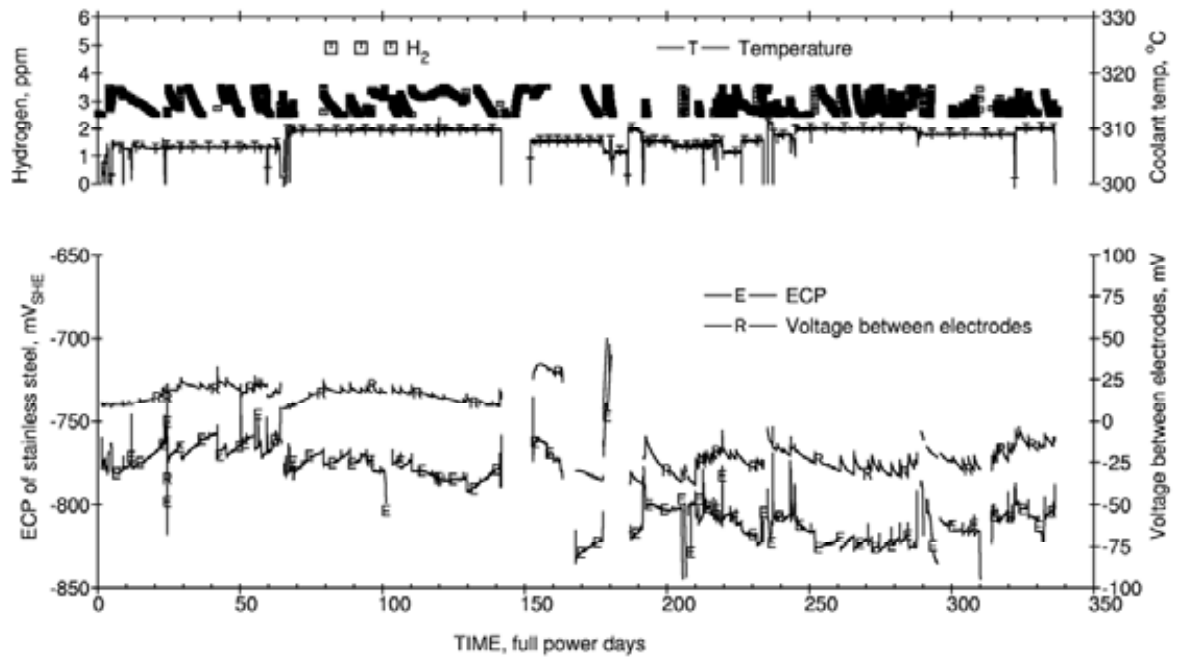


Figure 16. ECP of stainless steel under PWR conditions (3 ppm LiOH, 1000 ppm B), measured with a Pt reference electrode



Figure 17. Halden/VTT palladium ECP reference electrode

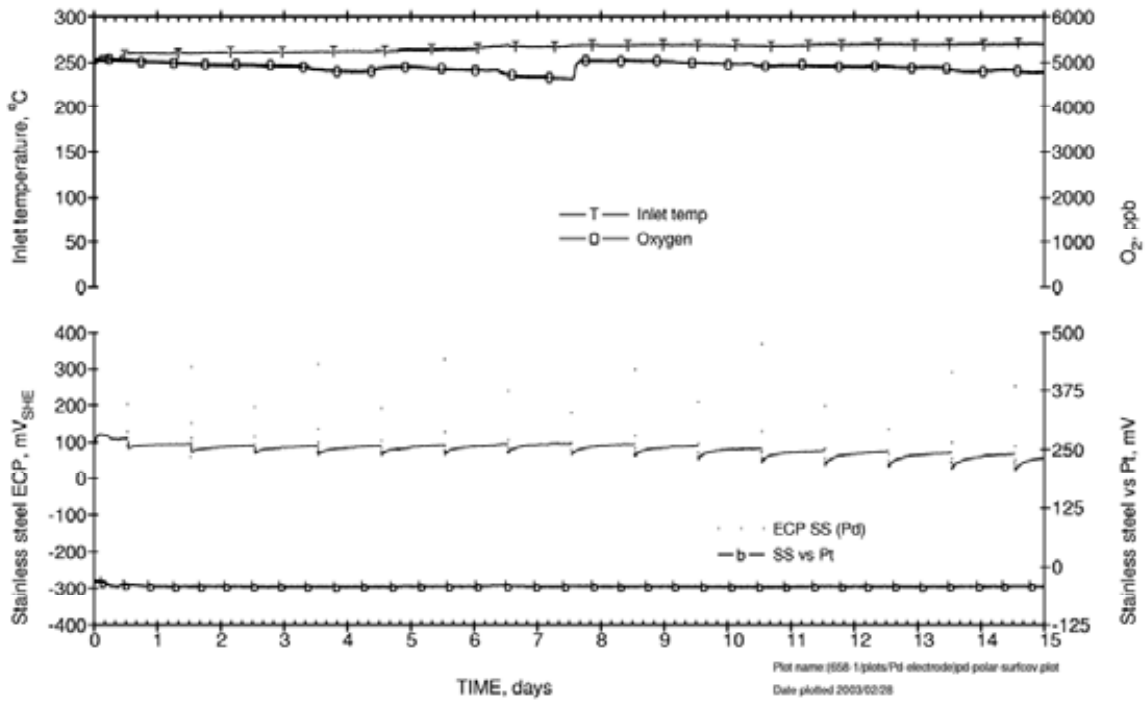


Figure 18. ECP of stainless steel, measured with a Pd electrode, during steady state operation

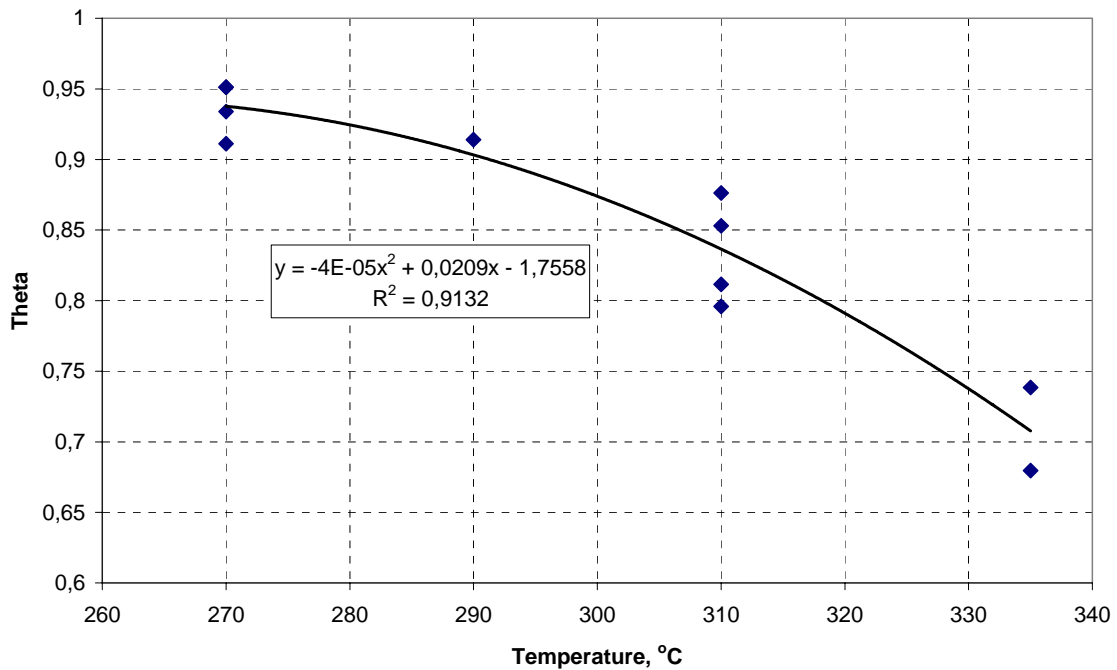


Figure 19. Surface coverage of hydrogen on palladium versus temperature for hydrogenated water chemistry (250 ppb LiOH, 5 ppm H₂)



Figure 20. Prototype Fe/Fe₃O₄ ECP reference electrode



Figure 21. In-core conductivity cell

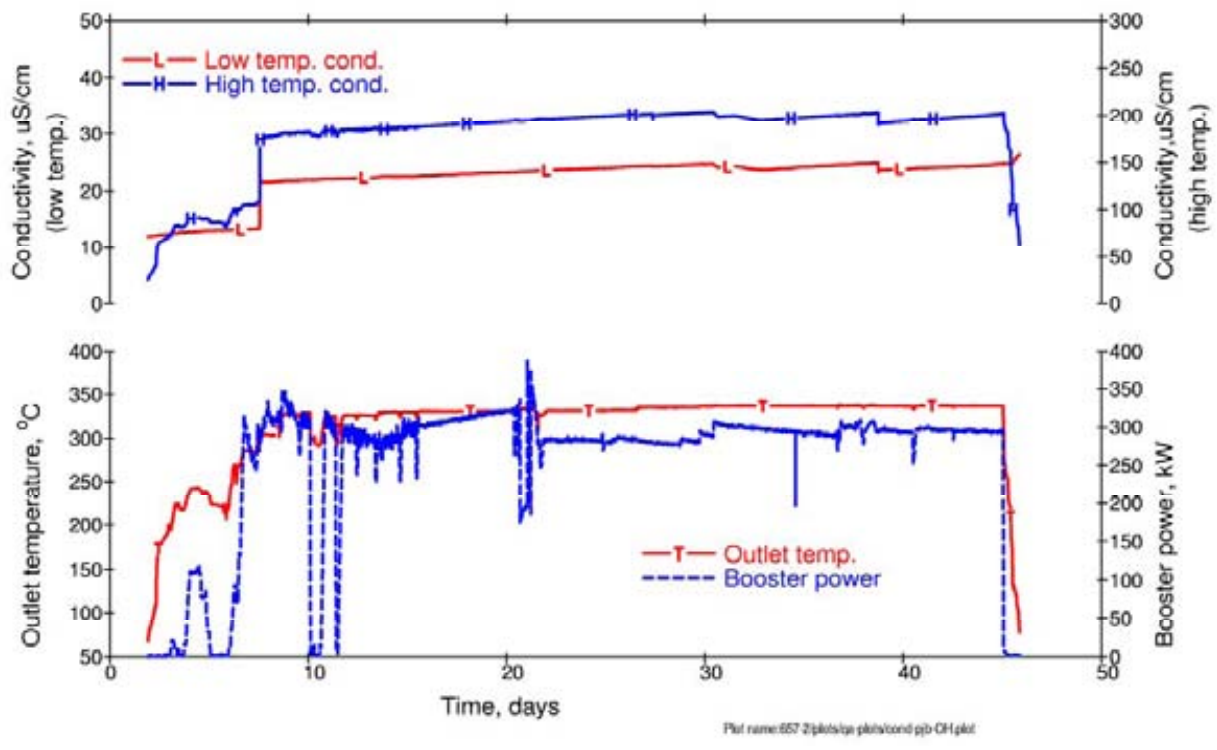


Figure 22. Conductivity measurements, showing in-core (high temperature) and out-of-core (low temperature) data

Flux Mapping and Channel Temperature Monitoring System for Tapp3&4

R. K. Patil
E&I Group
Bhabha Atomic Research Centre

Flux Mapping System

Introduction

TAPP 3 & 4 reactor core requires on-line computation of the in-core flux profiles using a dedicated in-core Flux Mapping System (FMS). This system monitors the in-core detector signals located at different locations in the core and generates neutron flux profiles, 14 zonal powers and other related information. This information is generated using predefined matrices for known reactor states. The zonal powers generated by FMS are used to calculate the correction factors for the zonal powers as calculated by reactor regulating system and send these correction factors to reactor regulating system for computation of flux tilts and maintain required flux profiles. In order to meet the system requirements, redundant computer based Flux Mapping System with fault tolerant optical network connectivity is used. The paper describes the system requirements, system configuration, hardware used at different levels of the Flux Mapping system along with the dual fault tolerant optical link between various nodes of the system, and normal / diagnostic mode of operation of the system.

System Description

Flux mapping system for TAPP 3 & 4 consists of 102 numbers of vanadium Self Powered Neutron Detectors (SPND) located in different vertical flux units inside the reactor core. FMS receives these detector signals and computes the thermal neutron flux at various points in the core including the thermal neutron flux in each of the fourteen zones of the reactor core. The system also calculates the correction factors for the zonal power as measured using in-core Cobalt Self Powered Neutron Detectors of reactor regulating system. These correction factors are communicated to Reactor regulating system over isolated RS232 serial interface link. The system also computes the build-up and burn-up for all the detectors by making use of this flux profiles and stores it in the database on daily basis. Additionally Flux mapping system also consists of low power flux logger unit that is used during phase B experiments of reactor start-up. This unit receives and scans data from Cobalt as well as Vanadium Self Powered Neutron Detectors along with various input contacts at a scan rate of 20 milliseconds and stores this data for further analysis later. Flux mapping system incorporates suitable diagnostic features for early detection of malfunction / failure and subsequent early corrective actions. Diagnosed malfunctions / failures are prompted by appropriate messages on the operator console and necessary indicators / alarms on different alarm panels.

System Configuration and Architecture

The flux mapping system has been configured using industrial grade rugged PC based hardware having built-in diagnostic features. The overall system architecture consists of following:

1. 102 nos. of Vanadium Self Powered Neutron Detector Amplifiers.
2. Three numbers of Input Signal Processing (ISP) nodes located in the reactor building.
3. Two numbers of Flux Mapping Processor (FMP) nodes located in the Control Equipment room.
4. Two numbers of Operator Consoles- one located in Control Equipment room and the other located in shift-charge engineer's room.
5. One number of Low-power Flux Logging computer node along with its operator console located in Control Equipment room during Phase-B experiments.

Individual SPND amplifiers amplify the 102 detector signals. The SPND amplifiers are distributed in three ISP node panels. The signals generated by each of these amplifiers are fed to the front-end processing units on ISP. Each of these ISP nodes consists of three independent CPU modules, called ISP sub nodes and each of these CPU modules caters to maximum of 12 detector signals (amplifier outputs). Each of these ISP nodes is connected to two identical Flux Mapping Processor nodes located in Control equipment room, through fault tolerant dual fiber optical cable links. Each ISP node CPU scans and sends the amplifier data, status / health information of SPND's to FMP nodes upon receipt of data request from FMP. ISP also receives request for testing of SPND amplifiers, design parameter changes from FMP node and respond to the request from FMP node over the dual fault tolerant network link. The local 320 * 240 pixel graphic LCD panel display associated with each of ISP sub node provides the information of all the amplifiers, design parameters, IP address, Watch dog timer status, power supply status of the other ISP nodes and the connected bin identification

FMP nodes are configured in master mode and each of the ISP sub nodes sends the scanned data on receiving the requests from FMP nodes. Both the FMP nodes under the requests issued either by FMP node 1 or FMP node 2 acquires data from the ISP nodes. The ISP scan cycle (for all the 102 detector signals) requests are initiated either by FMP node 1 or FMP node 2 alternatively. This scheme ensures that both the FMP nodes are utilized alternately. FMP nodes also make the request on both the dual fiber optical links alternatively to ensure healthiness of both the links at all times. In normal mode of operation both the FMP nodes collect data from ISP nodes by alternately using the two redundant links. The FMP nodes also communicate among themselves through the network links for scanning synchronization, data validation, etc. The scanning synchronization of the FMP nodes is ensured to decide the link mastership of FMP –ISP communication before start of the data collection from ISP nodes. Central Clock System (CCS) is used for RTC synchronization of both the FMP nodes periodically. The FMP nodes use data acquired from the ISP nodes to compute the flux profile. When RRS requests a particular FMP node for correction factors, the FMP node computes the zone-power correction factors using the most recent collected data from ISPs and the other relevant data received from RRS, and sends the computed correction factor to the requesting RRS node within the required time response (2 seconds of nominal response

time). Each FMP node has isolated serial communication links (RS232) with the both main processor nodes of RRS.

These FMP nodes also have Ethernet connectivity on dual redundant link to remotely located two operator's consoles. These consoles provide human interface with FMS and also send FMS data to COIS through Ethernet. Operator Console provides operator interface to issue test commands, to change design parameters for ISP's through FMP's etc. It also provides the necessary operator information and also maintains database for collected flux data, static data like design parameters of the SPND amplifiers, limits of correction factors etc. The dynamic database mainly comprise of readings from 102 Vanadium detectors, data contained in the packet received from RRS and alarms messages history. FMS user database contain the passwords for administrators.

Diagnostic features have been incorporated on each nodes/hardware for early detection of malfunction/failure and subsequent early corrective actions. This is prompted by appropriate message on the PC console/Operator's console and necessary indications on respective panels.

The overall scheme is as shown in the figure 1.

Hardware Description

The FMS hardware is distributed in five functional nodes and two operators' consoles. A separate node connected temporarily serves the function of Low Power Flux logging. The nodes are geographically distributed within reactor building and control equipment room.

Input Signal Processing Nodes

There are three numbers of input signal processing nodes located at three different locations within the reactor building. Each node receives signals from 34 in-core detectors. The total hardware for one ISP node is mounted in a 600mm(w) x 2024mm(h) x 800mm(d) standard 19'' rack. Each ISP rack contains 3 numbers of SPND amplifiers power supply bins, 3 numbers of SPND amplifier bins, 3 numbers of processor bins and network accessories like hubs etc. One processor bin is interfaced to one SPND amplifier bin catering to maximum of 12 detectors. The detail of each of this hardware is described below:

SPND AMPLIFIERS

SPND amplifier bins consist of 12, 11 & 11 number of single width amplifier modules respectively. These amplifiers incorporate a circuit to measure the on-line insulation resistance (IR) between emitter and collector (body) of the detector along the detector cable. Each SPND amplifier can be set to operate in low / high power mode of operation, test / operate mode of operation locally or remotely. Thus each SPND amplifier along with analog outputs give IR, low / high power mode of operation, test / operate mode of operation status to its processor bin. Each amplifier bin also gives unique 4-bit bin identification number to its processor bin.

SIGNAL PROCESSORS

Each signal processor bin consists of 7-width processor module, 3-width relay & watchdog timer module and 2-width power supply module. Each processor module consists 8 slots PCI back-plane and houses half size 16 bits 16 / 8 channel single ended / differential analog input cards, 48 bit digital input / output cards, fan less single board computer (SBC) and 10 / 100 MBPS network interface cards. SBC is based on Geode GXI 300 MHz processor and consists of 128 MB SDRAM, 256 MB of disk on chip. 3-width relay module provides potential free contacts as well as indication for watchdog failure; SPND amplifier power supply failure and diagnostic fail. Signal processors can be reset locally or remotely.

NETWORK CONNECTIVITY

Each processor bin consists of two 10/100MBPS network interface card (NIC). Network interface cards are connected to the respective hubs located in the network accessories bin through a UTP cable. NIC-1 is connected to link1 and NIC-2 is connected to link2 of the dual Ethernet link. Each ISP can send detector and amplifier data, status or health information and also, receive design parameters from FMP nodes. The ISP nodes only respond to the request from FMP nodes at every second. The remote testing/diagnostic of ISP nodes is also possible over the dual fault tolerant (Ethernet/fiber optic) network link through FMP nodes.

Flux Mapping Processing Node

There are two numbers of Flux Mapping Processor (FMP) nodes, located in the control equipment area. Each FMP node computer is based on Industrial grade PC chassis that houses 14-Slot Passive back plane (6 ISA, 7 PCI & CPU), P4, 1GHz SBC with 512 MB DDR SDRAM, 256 MB Disk on chip; 10 / 100 MBPS Ethernet cards, 64 channel isolated digital input / output card and isolated dual RS 232 / 485 serial interface card. Both the FMP nodes are connected to the 3 ISP nodes by a dual fault tolerant fiber optic link. For this connectivity there are six hubs, six media adapters, three Light Interface guide units (LIUs) located in ISP racks. On FMP side, two LIUs are located in the FMP racks and third LIU is located at other panel (Channel-C). Each FMP rack also houses 2 numbers of media adapters and one number of hubs. Each LIU receives one 2 numbers of twelve core Fiber optic cable from ISP side. Through two media adapters located close to each LIU, UTP cables provide the connection between media adapter, hub and the respective FMP nodes. Both the FMP nodes communicate with RRS on serial link using RS232. Both the RRS main processor nodes are connected to both the FMP nodes. RRS receives the information from the requested FMP node. The FMP nodes also communicate with two operator consoles for operator information on a dual fault tolerant Ethernet Links via hubs. In this configuration, the FMP nodes act as master for all the ISP nodes. FMP nodes control the data request periodicity on the ISP network and the other remote test features of ISP. A separate signal conditioning and relay bin interfaces with the FMP node to give visual alarm indications and potential free contacts for remote indication.

Operator Consoles

There are 2 operator consoles for operator information and for providing human interface with FMS. The operator consoles are configured using 2 industrial grade PC's. These 2

Operator consoles are connected to FMP nodes via separate dual Ethernet links. Each OC is also connected to COIS through another dedicated Ethernet link. Operator consoles maintain the entire database for the FMS, communicate alarms and messages to COIS, compare the outputs from FMP nodes to RRS, enable / disable either or both FMP nodes; send commands to ISP nodes via FMP, calculate and maintain database for build-up, burn-up of the detectors on daily basis and display information of ISP nodes, FMP nodes with diagnostic report and alarm messages. Operator Consoles also display on demand 2D / 3D flux profile, on demand trend of the detector signals etc. Operator consoles incorporate appropriate security measures to access various databases for entry / modification of parameters, ISP diagnostic commands and FMP enable / disable command etc. At any time only one operator console carries out these secured operations and is governed by master pass keyword authorization by the administrator.

FMS LOGGING MODES

FMS operates in two data acquisition modes referred to as logging modes of FMS:

1. Low power logging mode (LPLM): In this mode of operation all the SPND amplifiers operate in low power mode
2. Normal power flux logging mode: In this mode of operation all the SPND amplifiers operate in high power mode.

Mode of operation of individual SPND amplifiers can be changed locally or remotely.

ISP NODE MODE OF OPERATION

ISP sub nodes operate in one of the two modes: Normal or Diagnostic mode. Under regular operation ISP sub nodes operates in normal mode. However authorized personnel can put ISP sub nodes in the diagnostic mode via OC or locally connected laptop to the network through local hub ports. In normal operating mode each ISP sub node scans and processes analog, digital inputs connected to the sub node at a scan rate of 100 ms, periodically refreshes the 320 * 240 graphic LCD at an update rate of 5 seconds, performs on-line self diagnostics checks on all the boards and services asynchronous request received from FMP via network links. Requested ISP sub node sends response packet to both the FMP nodes that include scanned data, status of SPND amplifies, report of self-diagnostic tests, operating mode information etc. Apart from periodic self- diagnosis, authorized personnel can also put ISP sub nodes in on-demand diagnosis to test the SPND amplifiers and network connectivity in the normal mode of operation of ISP sub node. Administrator can also put a particular ISP sub node in special diagnostic mode wherein administrator can conduct tests on all the hardware components such SPND amplifier, ADC / DAC, Digital I /O, network cards. When an ISP sub node is operating in special diagnostic mode it is treated as unavailable for carrying out normal expected node functions.

FMP NODE MODE OF OPERATION

The FMP nodes implement the main functionality of the FMS to compute and convey zonal power correction factors to RRS. FMP nodes also operate in one of the two modes: Normal or Diagnostic mode. In normal operating mode, FMP nodes periodically (1 second) collect scanned data from all the ISP sub nodes over dual fault tolerant optical

network link, perform alarm checks and generate alarm / message report that is sent to operator console for operator information, carry out on-line self diagnostics checks on all the boards, respond to asynchronous RRS request received once in 2 minutes over isolated RS232 serial link, synchronize their RTC with plant clock and achieve synchronization between themselves over the network link. FMP nodes can also be put in on-demand diagnosis to test the network connectivity between FMP and OC during normal mode of operation. Administrator can also put a particular FMP node in special diagnostic mode wherein administrator can conduct tests on all the hardware components such Digital I /O, network cards. In this special diagnostic mode the FMP node gets disabled for carrying out normal expected functions.

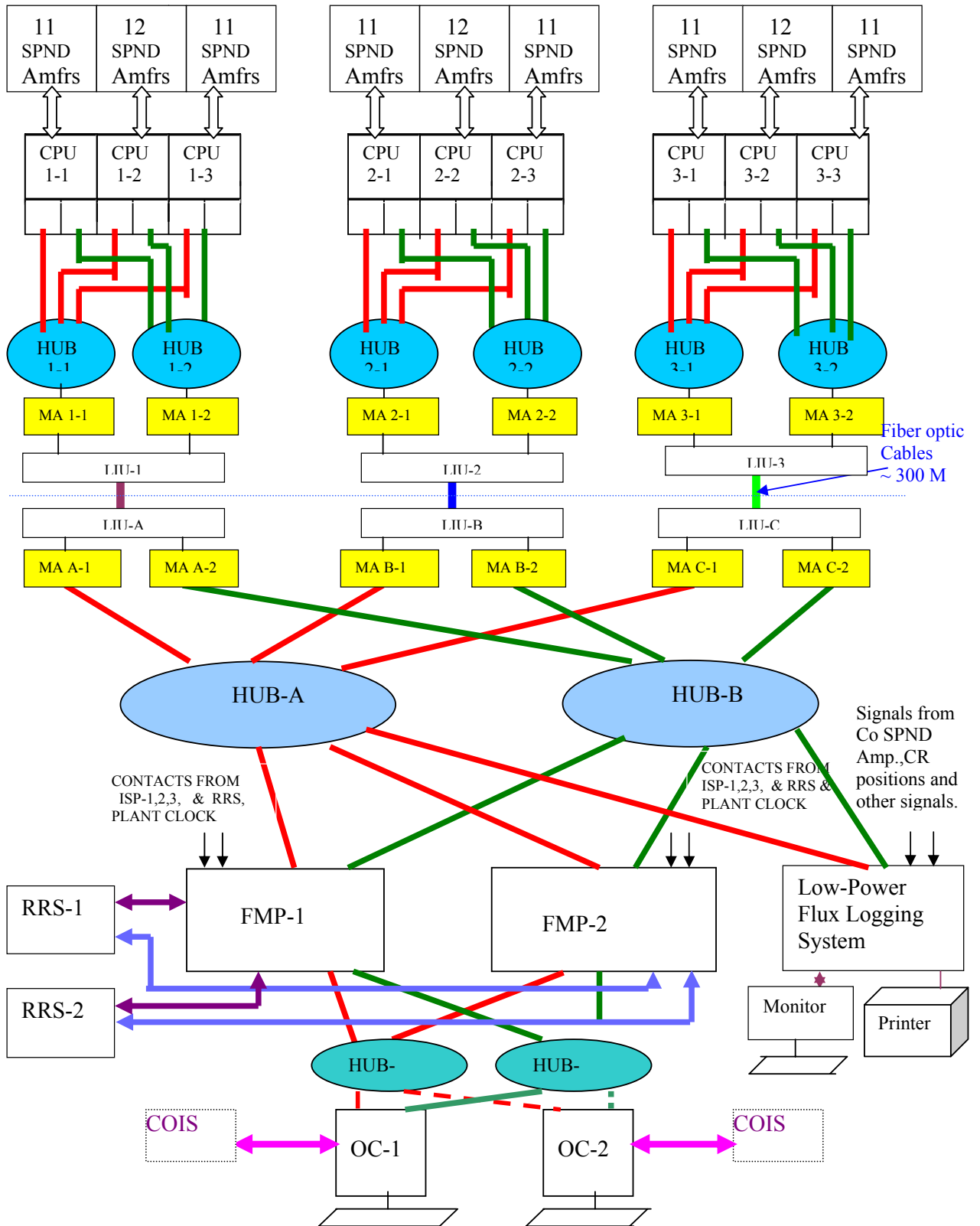
The FMP nodes store all the pre-computed matrices for fuel state and flux modes relevant to reactor that are used for generating the 2D / 3D flux profiles, zonal powers, global power and correction factors etc. The reactor operating state as provided by the RRS, fuel state and number of flux modes as specified by operator through operator console enable the FMP node to select the appropriate stored pre-computed matrices and compute the 2D / 3D flux profiles, zonal powers, global power and correction factors etc. Computation also takes into account any ISP sub node fault, SPND / SPND amplifier fault, non-availability of information etc. The FMP node computes correction factor by comparing the computed zonal power values with the corresponding values as sent by the RRS. RRS send request for correction factors every 2 minutes and FMP node responds in sending the correction factor maximum in 2 seconds.

Software

Software for ISP, FMP nodes are developed using VC++ and runs under embedded XP, while Operator console software runs under normal XP. It is presented in another paper.

Conclusion

Accurate and detailed information of core condition is indispensable in order to make the best use of core and fuel capability and also to achieve flexible and efficient operation. From this point of view Flux Mapping System helps in validating the reactor core design parameters by continuously measuring three dimensional power distribution and other related parameters. Thus Flux Mapping system will help the operator in core monitoring, analysis and its well-designed graphical user interface will help site engineers in analyzing and evaluating core conditions under different operating conditions of reactor core & fuel utilization. Flux mapping system being an on-line system eliminates the need for an off-line flux map code analysis. The system also allows operator to quickly and accurately monitor the current core conditions & predict the future core conditions.



Note: The dashed lines shown on HUB-OC1 & OC2 will be coaxial, if the distance is more than 100 meters otherwise CAT-V.

Figure 1: Overall Scheme for Flux Mapping System



Figure 2: Flux Mapping System for TAPP

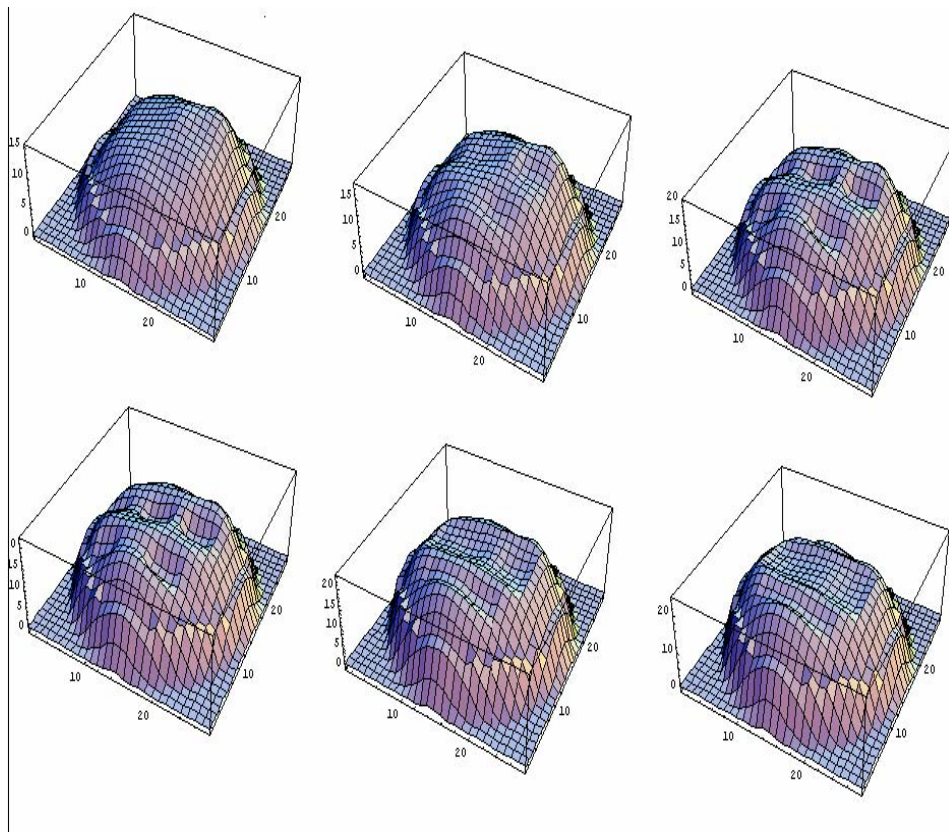


Figure 3: Flux Maps

Computerised Channel Temperature Monitoring System

Introduction:

The channel temperature monitoring (CTM) system forms one of the important surveillance and protective functions in Indian pressurized heavy water reactors (PHWR). Any excessive rise in coolant outlet temperature of any channel is indicative of inadequate cooling of the channel. Since flow measurement in all coolant channels are not performed, CTM system is designed to detect excessive rise in any coolant channel outlet temperature and apply corrective action for safe operation of the reactor. Since boiling is not permitted in the present generation of Indian PHWRs accurate measurement of temperature is essential. Further, accurate measurement of channel outlet temperature helps in maintaining differential temperature across each channel to a maximum safe limit, thereby maximizing the reactor power output. It also helps in efficient fuel management by computing the thermal power generated and thereby estimation of the burn-up.

Abnormal rise in PHT temperature reflects the presence of abnormal situation in reactor operation, which can be either due to low coolant flow or high reactivity changes. If such abnormal situation is allowed to exist without plant trip or any corrective action like 'setback', it may lead to unsafe conditions like damaging fuel or its cladding. Reactor trip is initiated by 'High N' trip in the case of high reactivity changes and by 'High PHT pressure' trip in the case of sudden flow reduction to 30% normal flow. Under this situation CTM system provides back-up protection only. But excessive rise in PHT temperature of a particular channel cannot be detected by either 'High N' trip or 'High PHT pressure'. Only CTM system can detect such abnormality and provides setback action so that the PHT temperature is not allowed to rise beyond its boiling point.

Sensor Details

For the purpose of measuring the temperature at the coolant outlet, two Resistance Temperature Detectors (RTD) are mounted on stubs of Reactor Outlet Header. Surface mounted type, strap-on RTDs are selected to avoid large number of penetrations for thermo-wells in high pressure and high temperature PHT boundary. The RTDs have Pt-200 elements, which are highly accurate, stable, reliable and sensitive sensors. Calibration of RTDs is reproducible over a long period of time.

Pulsed Current Source:

In order to reduce the self heating error (due to RTD bridge excitation), it was decided to pulse the current (sufficiently large to produce a high level output) for a short duration through each RTD. Passing the current for 20 millisecond duration through each RTD once every 4 sec. (typical scan rate) has virtually eliminated the error due to self heating. The accuracy of the measurement now depends on the stability of the current source and its value at any given moment. For this reason, the same current source is passed through high precision resistors (equivalent to 0 and full scale). This could be achieved under the control of a microprocessor.

TAPS-3&4 CCTM System:

Computerised Channel Temperature Monitoring System (CCTM) for TAPS-3&4 monitors the temperature of the coolant (PHT) at the outlet of all 392 coolant channels of the 540MWe reactor. If the outlet temperature crosses a set alarm limit (309 Deg. C) the system detects it and initiates reactor setback.

The CCTM System consists of two functionally identical, independent and galvanically isolated computer based installations. Each CCTM system installation is designed as an embedded system configured around microprocessor based CPU boards. Each installation acquires 392 COT inputs from an independent set of 392 RTDs. These inputs are processed independently. The two installations then exchange COT Very High (VHI) alarm status information with each other over dual redundant RS232C serial communication links. They then check for coincidence of COT VHI alarm for a channel on both the installations. If a coincident Very High alarm is detected then reactor setback contact output is given for generation of reactor setback. Each installation of CCTM provides a CRT based user friendly HMI for displaying essential CCTM data and for allowing the operator to change system setpoints and system mode of operation under password and passkey control. The two CCTM installations communicate to a gateway over Ethernet link, each sending values of all channels and diagnostics information to the gateway. This information is further forwarded to the COIS for further use and presentation through several formats to the operator.

CCTM System functions are:

1. Acquire Channel Outlet Temperature of 392 coolant channels
2. Process these inputs
3. Generate alarm outputs
4. Generate SETBACK on coincidence of VHI alarm
5. Provide operator interface through CRT
6. Communicate acquired information to the COIS through the gateway.

Conclusion:

The CTM systems from MAPS to TAPS have continuously evolved in functionality. The system has evolved from a simple monitoring system to a safety related system generating setback for NPP. The system has also used the advances in technology to improve its hardware and software. The hardware used in the system has evolved from 8 bit CPU (5MHz) at MAPS to 32 bit CPU (20MHz) at TAPP. The software for TAPP-4 has been developed to the required quality standards for an IB system.

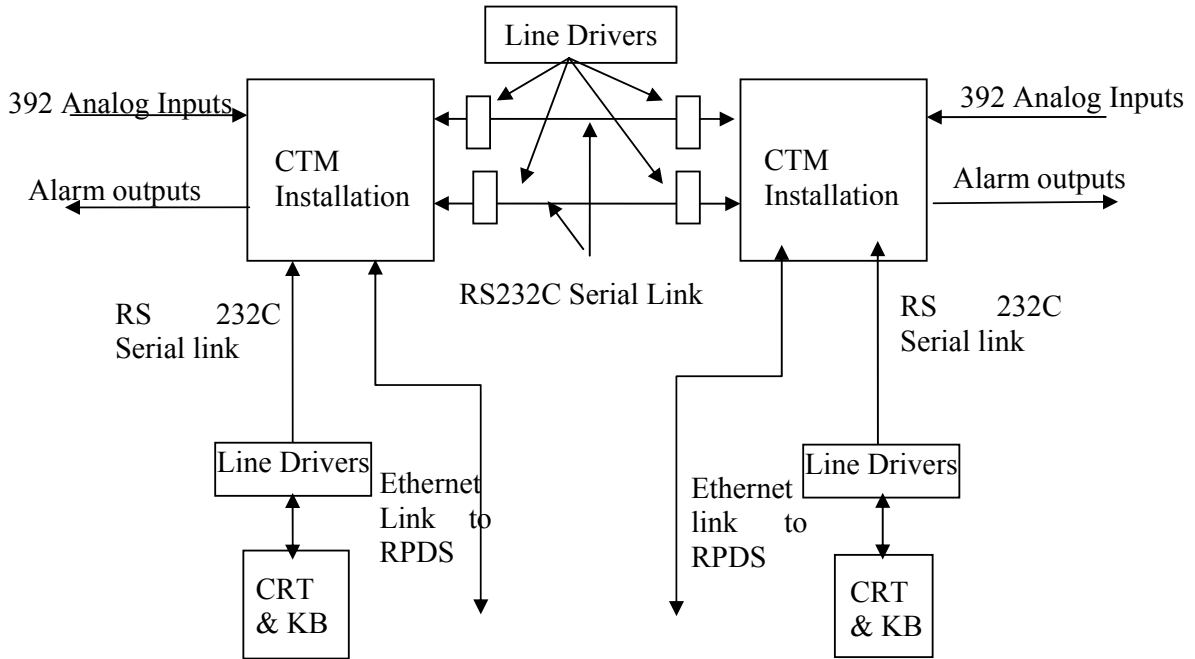


Figure 4: TAPS-3&4 CCTM SYTEM

Design of the on-line fission gas release analysis system in the High Flux Reactor Petten

M. Laurie, A. Marmier, G. Berg, M. A. Fütterer

European Commission
Joint Research Centre - Institute for Energy
P.O. Box 2, NL-1755 ZG Petten, Netherlands

Abstract. Within the European High Temperature Reactor Technology Network (HTR-TN) and related projects a number of HTR fuel irradiations are planned in the High Flux Reactor Petten (HFR) with the objective to explore the potential of recently produced fuel for even higher temperature and burnup. For these irradiation tests a specific installation was designed and installed, dubbed the “Sweep Loop Facility (SLF)”. The SLF is tasked with three functions, namely temperature control, surveillance of safety parameters and analysis of fission gas release for three individual capsules in two separate experiments. This paper describes the gas activity measurement technique and shows how qualitative and quantitative analysis of volatile fission products can be performed on-line. The fractional release of these fission products, defined as the ratio between release rate of a gaseous fission isotope (measured) to its instantaneous birth rate (calculated), is a licensing-relevant experimental result of HTR fuel irradiation experiments, because it determines the operational (as opposed to accidental) source term for radioactivity release. The newly developed data acquisition system allows for higher measurement frequencies if activity values increase, thus enabling follow-up of transients. The SLF is designed to deal with a wide range of activities by modification of the distance between detectors and gas samples.

1. Introduction

The main objective of HTR fuel irradiations in the HFR is to explore the potential for high temperature performance and high burn-up for existing and newly developed fuel, in the frame of the European program, for the Chinese HTR-10, the South African PBMR, and for the Generation IV VHTR concept. Irradiating this fuel under defined conditions to extremely high burn-ups will provide a better understanding of fission product release and failure mechanisms if particle failure occurs.

Each of these irradiation tests will be connected to the Sweep Loop Facility (SLF) which fulfils three specific tasks:

- Maintenance of constant irradiation conditions (temperature, hygrometry, gas flow etc.);
- Surveillance of fission gas release by purging capsules with inert gas thus enabling qualitative and quantitative calculation of fission gas release rates;
- Monitoring of safety-relevant operating parameters, namely the dose rate in the gas lines, glove boxes and working area. If predefined thresholds are exceeded, automatic actions are triggered to put the installation into a fool-proof safe condition.

The SLF is based on an earlier system used for the qualification of the German HTR fuel until the early 1990s.

2. Experimental possibilities

The SLF enables continuous and independent surveillance of all in-pile and rig head containments. The release of volatile fission products of the in-pile experiments is monitored by continuous gas purge of the containers. The purge gas is mainly used for temperature control by the He/Ne mixture technique.

All gas lines containing radioactive gases are double contained to prevent leakage into the working area. The high purity gas supplied by the standard HFR gas system flows through the capsules in a defined direction. The purge gas (helium/neon) is to sweep all gaseous fission products coming from damaged particles or from contamination around intact fuel particles.

The SLF design features 12 GM tubes, 3 NaI detectors and 3 HPGe detectors. All operating parameters, pressure, gas flow, humidity, and gamma activity are monitored and stored to be further analyzed. A specific removable gas container (100 cm³) equipped with snap-tight connectors enables gamma spectrometry analysis of the released gas. This container is seen by an HPGe detector equipped with a Lynx system based on digital signal processing techniques. The calibrated spectrometer performs the measurement of at least five different isotopes, namely ^{85m}Kr, ⁸⁷Kr, ⁸⁸Kr, ¹³³Xe and ¹³⁵Xe.

Geiger-Müller counters monitor the downstream effluents and are part of the SLF safety instrumentation. Excessive radioactivity level in the exhaust line of the SLF isolates the concerned capsule by triggering closure of several solenoid valves.

Three NaI spectrometers are dedicated to the on-line purge gas measurement for three different capsules. Each of the three capsules are monitored for fission product release. NaI crystals are positioned as close as possible to the measuring volume (15 cm³) but can be moved away in defined distances from this volume to reduce the detector counting rate. They are adjusted within a 40 keV window in order to be able to measure ⁸⁸Kr. The total count rate within this energy window for each capsule is measured and recorded continuously during irradiation. A gamma peak of ⁸⁸Kr is chosen such that the signal is not dominated by Compton effects of ²³Ne and interference with other gamma emitters at the same energy is avoided. The NaI detectors are shielded with 10 cm of lead to minimize gamma background coming from the HFR.

Considering the flow of the gas purge and the volume to be filled before reaching the measuring volume, only a few fission gases are detectable at this point. The capsule release rate is a relatively slow process which is why only released isotopes with decay half lives over several minutes can be seen. Three processes must be taken into account: diffusion through the SiC coating, transit time of the sweep gas from each capsule to the measuring chamber (about 4.5 min using a low flow rate of 50 cm³/min) and the limit of detection of the gamma detector. The list concerning established tracers of particle integrity is given in Table1.

Nuclide	Half life	Detectable daughter products (gamma emitters)
^{85m} Kr	4.48 h	
⁸⁷ Kr	1.27 h	
⁸⁸ Kr	2.84 h	⁸⁸ Rb
⁸⁹ Kr	3.16 min	⁸⁹ Rb
¹³⁵ Xe	9.14 h	
^{135m} Xe	15.29 min	¹³⁵ Xe
¹³⁸ Xe	14.08 min	¹³⁸ Cs

Table 1: Tracers of particle integrity

Together with the known gas flow, pressure and temperature, the fission gas release rate R could be determined and related to the birth rate B from neutronics calculations. The R/B value is considered as a good health indicator of coated particles.

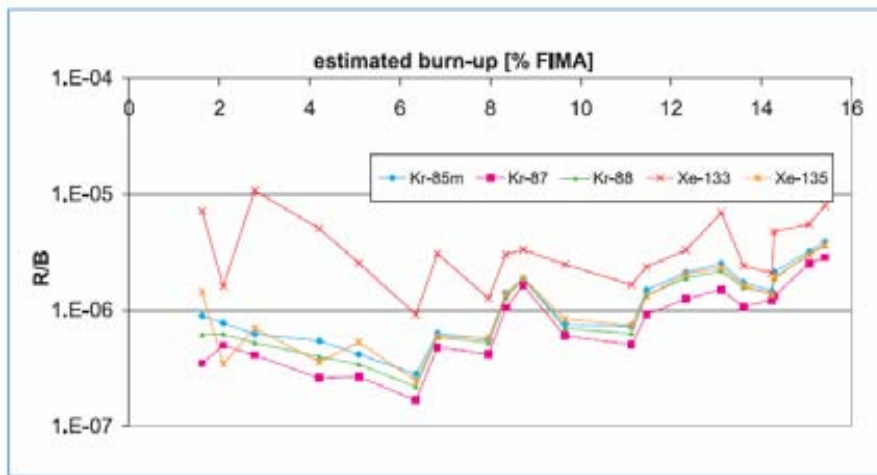


Figure 1: Preliminary results R/B vs. burn-up for the HFR-EU1bis irradiation

For example, at the end of the irradiation HFR-EU1bis an R/B of approximately 4×10^{-6} was measured^[1]. This figure is five times lower than the theoretical R/B from complete failure (100% release) of a single particle in the experiment. In the earlier experiments HFR-K5 and HFR-K6, R/B values of 5×10^{-7} had been measured on fresh fuel.

The Booth model is most commonly taken to determine the ratio of release rate to the birth rate (R/B) considering Kr and Xe. The Booth model is applicable to diffusive release of fission products from kernels^[2].

$$R/B = \frac{3}{x} \left(\coth x - \frac{1}{x} \right)$$

$$\text{With } x = \sqrt{\frac{\lambda}{D'}}$$

λ is the decay constant [s^{-1}]

D' is the apparent fission gas diffusivity [s^{-1}]

D' is temperature dependent and geometry dependent

$$\text{If } x \gg 1 \text{ then } R/B = 3 \sqrt{\frac{D'}{\lambda}}$$

at constant temperature we can derive: $\ln(R/B) = K - n \ln(\lambda)$

In the Booth model $n = 0.5$. Experimentation, however, yields a range of n values between 0.1 and 0.5.

$n < 0.2$ for graphite contamination

$0.2 < n < 0.3$ commonly encountered

$n > 0.5$ in case of particle bursts

Consequently, when plotting the individual $\ln(R/B)$ against $\ln(\lambda)$ the result should be a straight line with the negative inclination: n . This method was applied to each gas sample. A typical result is given in Figure 2^[1].

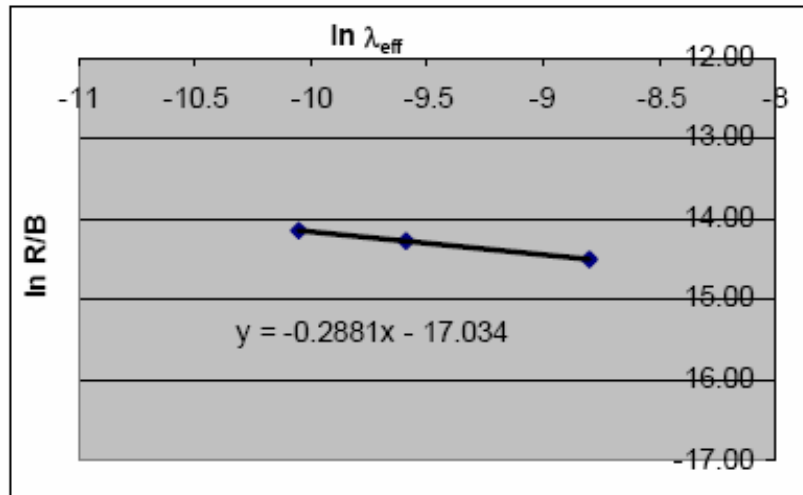


Figure 2: Typical $\ln R/B$ vs. $\ln \lambda_{\text{eff}}$ plots for $^{85\text{m}}\text{Kr}$, ^{88}Kr and ^{87}Kr gas release measurements (HFR-EU1bis)

3. Design features of the Sweep Loop Facility

Internal gas pressure inside the fuel particles increases with burn-up. The combination of high burn-up and high temperatures may result in pressure-induced failures. If an experiment is driven with conditions beyond the fuel performance limits, some particles may leak and on-line gamma spectrometry may detect a sudden burst of activity. With the new SLF we have sufficient sensitivity to detect failure of a coated particle and to perform measurements at low count rates. At the beginning of the experiment, the release rate is very low (only heavy metal contamination will be detected) and the system is also able to perform an accurate measurement in the reactor building background.

The newly implemented on-line gamma spectrometry enhances the number and quality of batch analyses.

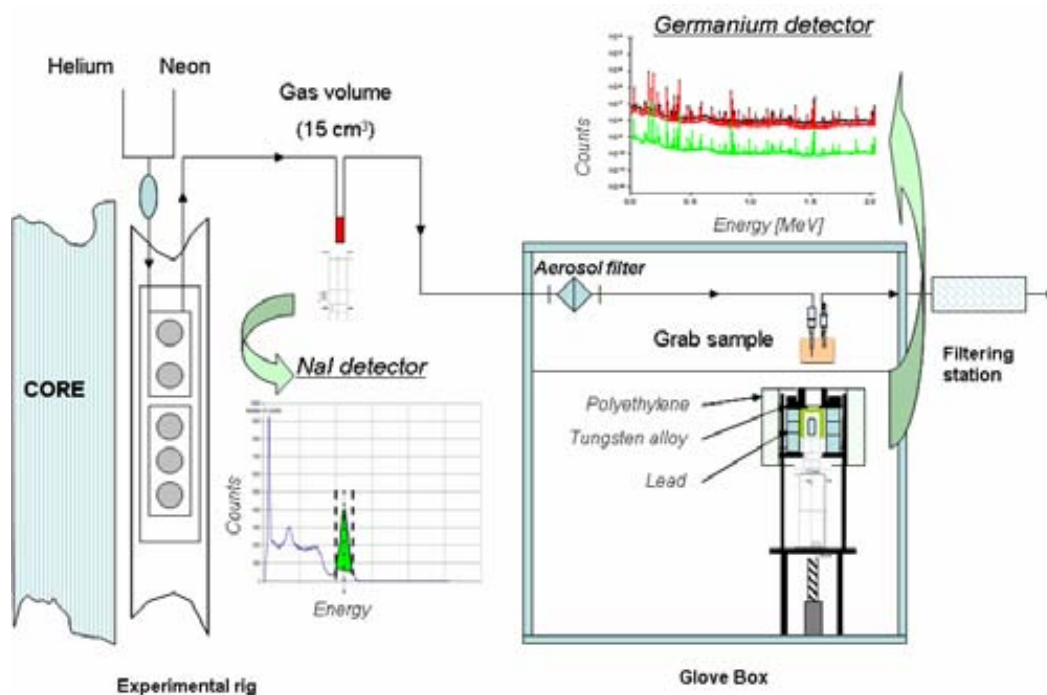


Figure 3: SLF gamma spectrometry measurement train

3.1. Particle filter

A particle filter is mounted upstream of the sampling device (see Figure 3) to prevent aerosols from contaminating the sampling vessel. A bypass is kept available. A specific detector is devoted to detect a sudden burst of activity on this filter. In order to perform gamma spectrometry measurements, this filter is made removable. As ^{131}I , ^{137}Cs are known to be good indicators concerning the level of heavy metal contamination (of the graphite matrix) and afterwards of a coated particle failure, suspected particle failure may be confirmed by the presence of large amounts of these radionuclides on the filter.

3.2. Measurement system

The sweep gas from each capsule flows to a gross radiation monitor and a gamma-ray spectrometer. Geiger Müller counters provide a first indication concerning the released radiation levels. NaI spectrometers dedicated to ^{88}Kr perform one-line qualitative measurement of the activities.

The sampling lines enter a shielded glove box for gamma measurements.

Contrary to GM and NaI detectors in the safety panels yielding continuous signals and more qualitative results, high precision data can be obtained from a multi-channel analyzer connected to an HPGe detector. The sweep gas is routed through a grab sample of 100 cm^3 seen by the HPGe detector. This sample usually remains in position and is only occasionally removed for external cross check measurements.

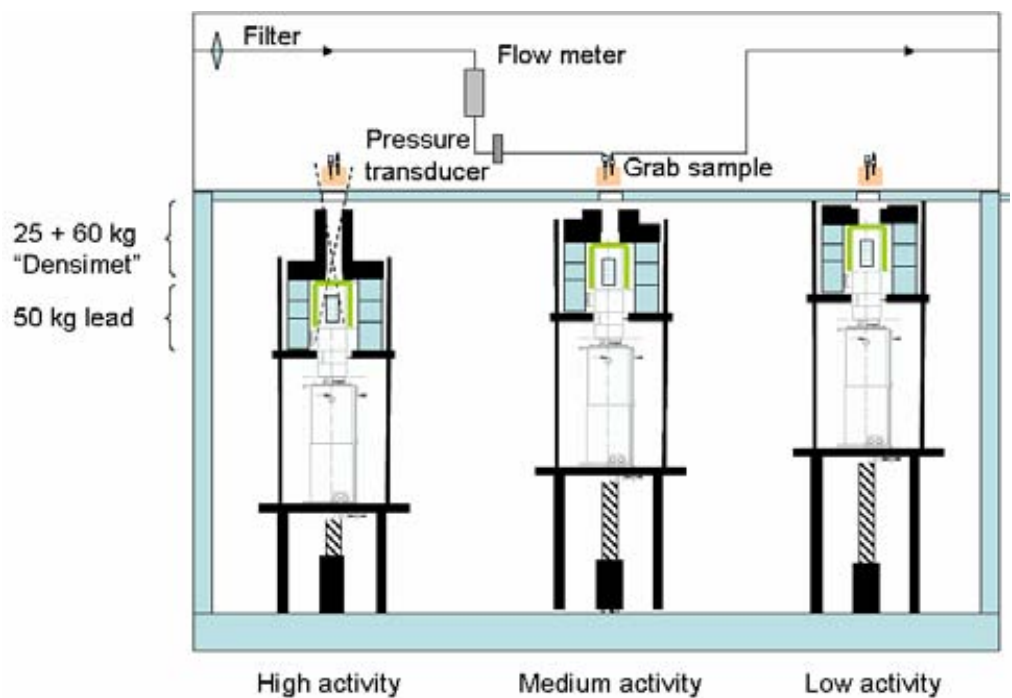


Figure 4: Glove Box with HPGe detectors

Considering that an HTR fuel irradiation experiment requires a wide range of counting rates (from the beginning of an experiment where releases are due to heavy metal contamination to possibly damaged fuel with cracked particles towards the end of irradiation), the measuring system has to be as flexible as possible. The shielded spectrometer can adopt three specific geometries (cf. Figure 4). The first position is expected to be as close as possible to the gas sample. The second requires an extra collimator for intermediate count rates. In case of particle failure, the gamma spectrometer can be recessed up to 200 mm.

A special effort has been made to minimize the effect of background radiation. The glove box is shielded with at least 5 cm of lead. The cold head of the detector is equipped with a removable shield system as close as possible to the cold head to reduce the required amount of lead. In order to avoid interference from other radiation sources, the detector is collimated using various custom-made tungsten alloy cylinders. Without this set of collimators, all radioactive equipment located 150 mm around the gas capsule would be seen in the most recessed position (cf. Figure 5).

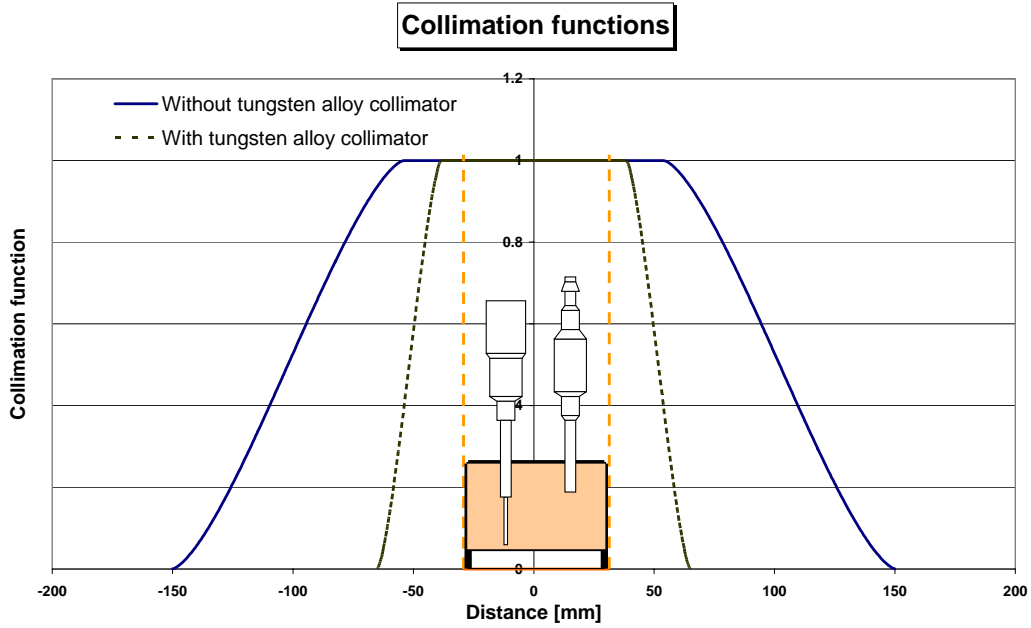


Figure 5: Collimation function for the withdrawn position

The analysis of the spectra is performed and displayed by the Canberra Genie™ 2000 software. The gamma ray spectrometers are supported by commercial electronic components. Due to a space limitation in the existing glove box, a small cryogenic cooler was preferred to a liquid nitrogen system. Its innovative system prevents vibrations in the cold head and avoids degradation in resolution.

3.3. Efficiency curve

Gamma detectors have to be calibrated for each geometry to obtain quantitative results. Calibration can be performed by using standards as close as possible to the sample to be measured. All aspects of the measurement (shielding thickness, geometry, misalignment etc.) must be taken into account. A configuration dealing with a gas sample is relatively difficult to accomplish. There are only a few radioactive gases that could be used for gamma calibration and most of them have relatively short half lives. We have chosen a different way by filling our gas sample with e.g. ^{152}Eu contained in a very low density polymer.

The proportionality between the area measured under the peaks of the obtained gamma ray energy spectra and the activity of the corresponding gamma emitter is to be calculated. For the low-density standards generated within the sealed gas counting container, activity A is given by using the general expression below:

$$A = \frac{S}{\tau_E \varepsilon \int e^{-\lambda t} dt}$$

with :

S : net area under the peak for given energy [counts]

τ_E : emission yield at given energy

ε : efficiency of the γ -spectrometer at given energy

$e^{-\lambda t}$: radioactive decay during measurement

The efficiency curve can be easily deduced. For example, an expected efficiency curve for the intermediate level geometry is given in Figure 6. Considering the low density of the radioactive source, differences in self-absorption in the standard as compared to the gas capsule can be neglected.

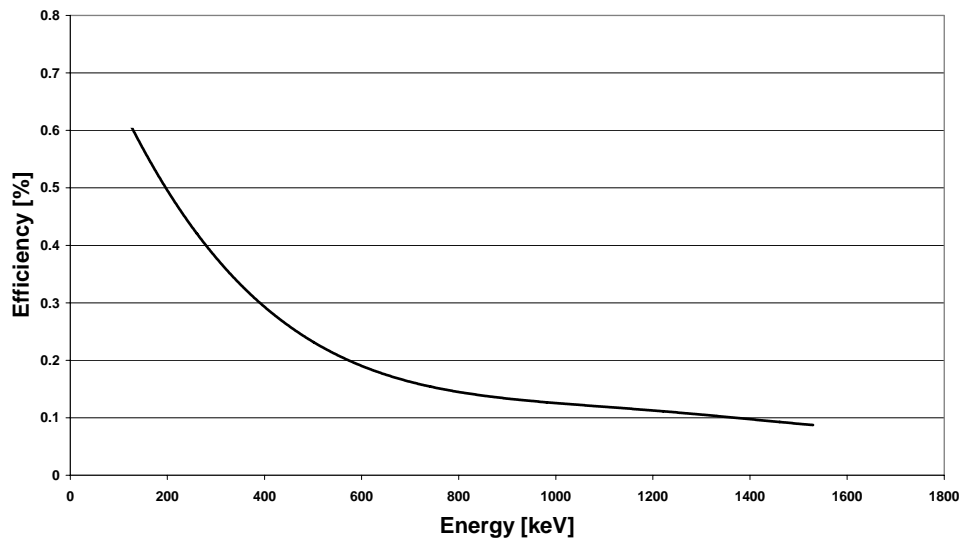


Figure 6: Efficiency curve for the intermediate position

4. Conclusion

In order to explore the potential high performance of HTR fuel in terms of high temperature and burn-up, a specific facility for current and upcoming tests at the HFR Petten has been developed. The Sweep Loop Facility operates the in-pile irradiation capsules at the required operating conditions and features temperature control, on-line surveillance of fission gas release and safety functions. The newly developed system allows on-line gamma spectrometry measurements and is flexible enough to consider either low or high count rates during the lifetime of an irradiation test while minimizing the effect from background radiation in the reactor building. This system provides a relatively large number of spectra with high quality and permits post-measurement analysis in case of specific events. The frequency of the measurements can be adequately adapted in case of increased release of fission gases or multiple transients.

REFERENCES

- [1] M. A. Fütterer, G. Berg, A. Marmier, E. Toscano, K. Bakker, Irradiation result of AVR fuel pebbles at increased temperature and burn-up in the HFR Petten, Proc. HTR 2006, Johannesburg, South Africa, 1-4 October 2006.
- [2] Fuel performance and fission product behaviour in gas cooled reactors, IAEA TECDOC-978, ISSN1011-4289, November 1997.
- [3] M. A. Fütterer, H. Lohner, R. Conrad, K. Bakker, S. de Groodt, C. M. Sciolla. Irradiation of high temperature reactor fuel pebbles at VHTR conditions in the HFR Petten, Proc. HTR 2004, Beijing, China, 22-24 September 2004.
- [4] D. Freis, R. Nasyrow, E. Toscano, Burn-up determination of high temperature reactor spherical fuel elements by gamma specrometry, HTR 2006, Johannesburg, South Africa, 1-4 October 2006.

SESSION 4: HOT CELL FACILITIES AND PIE

Chairperson

Y. Goncharenko (Russian Federation)

RIAR HOT CELLS MATERIAL TESTING COMPLEX, METHODOLOGICAL POSSIBILITIES

Y.D. Goncharenko, V.N. Golovanov, A.E. Novoselov, V.D. Risovany
Federal State Unitary Enterprise, "State Scientific Center of Russian Federation
Research Institute of Atomic Reactors",
Ulyanovsk region, Dimitrovgrad, Russia

ABSTRACT

The RIAR material science complex was commissioned at the beginning of 1964. For more than 40-year period of existence of the material science complex several generations of its main and auxiliary research equipment have changed. The specialists have gained great experience in conducting examinations of irradiated materials, methods that are the most suitable for investigation of such materials have been selected. Current methodical possibilities of RIAR Material testing complex represented in this report.

1. INTRODUCTION

Research Institute of Atomic Reactors is the largest hot laboratory in Russia. The RIAR material science complex that was commissioned at the beginning of 1964 was created to solve the following main tasks:

- organization and conducting of material science investigations prior to and after irradiation of fuel elements, fuel assemblies, control rods, fuel, absorber and structural materials of the cores of various purpose and other materials and products of nuclear engineering;
- conducting of investigations in the field of radiation damage physics;
- conducting of investigations to validate long-term storage of spent nuclear fuel, develop utilization technologies of irradiated materials and products;
- physical modeling of behavior of core materials and elements for nuclear reactors;
- development of techniques for post-irradiation examination;
- organization and conducting of material science supervision of the Institute and NPP reactors;
- development and manufacture of irradiation rigs, fuel and absorbing compositions, fuel elements, fuel assemblies and control rods, accumulation targets of radiation sources and other products of nuclear engineering;
- development of process equipment and production processes of reactor materials;
- development of production processes of transuranium elements (TUE) and alloys on their basis, study of their properties;
- widening of application scope of the developed technologies, materials and products in all branches of industry;
- participation in the development and implementation of federal and branch scientific-technical programs;

For more than 40-year period of existence of the material science complex several generations of its main and auxiliary research equipment have changed. The specialists have gained great experience in conducting examinations of irradiated materials, methods that are the most suitable for investigation of such materials have been selected.

2. RIAR MATERIAL TESTING COMPLEX

RIAR Material testing complex houses 64 hot cells and 60 heavy-duty boxes and consists of three buildings:

- for non-destructive analysis of full-scale fuel rods and fuel assemblies (measurements of fuel rod parameters; visual examinations; gamma scanning; vortex-current defectoscopy, etc);
- for destructive analysis (burn-up, fission products release; gamma scanning; metallography and micro-hardness; density and porosity; thermal conductivity and electric resistance; X-ray analysis; dilatometry; TEM, SEM, EPMA, AES, SIMS; mechanical testing (tensile, compression, bending, impact, etc.);
- for technological engineering programs;

2.1. Non-destructive analysis of full-scale fuel rods and fuel assemblies

There are two large hot cells in the first building (these big hot cells designed for operations with full-scale fuel assemblies for commercial reactors are 7.5 m long, 4.0 m wide and 7.2 m high) and five hot cells of the smaller size. These five hot cells are 5.0*1.8*2.6 m in size.

We have a system for fuel rod diameter measurement and eddy-current defectoscopy, a fuel rod gamma-scanning system and a system for dimensional measurements of fuel assembly wrappers in the first large hot cell of this building.

In the second large hot cell we have a leak testing system, a fuel assembly and fuel rod cutter, a system for visual inspection of fuel assemblies and fuel rods, an express eddy-current defectoscope and fuel rod storages. In other five hot cells of the smaller size we have:

- a fuel rod cutter;
- a system for fuel assembly re-assembling.

- a fuel rod X-ray system;
- an automated system for fuel rod gamma-scanning;
- a system for measurements of fuel rod total activity;
- an autoradiographic system;
- a computer gamma-tomographic system.

- an automated system for fuel rod diameter measurement and eddy-current defectoscopy;
- a system for visual inspection of fuel rods;
- a system for fuel-to-cladding gap measurements;
- facility to measure fuel rod volume.

- a system for laser puncture and analysis of under-cladding gas volume and composition;
- a system for thermal testing of fuel rods;
- a system for cladding testing by gas pressurization;
- a machine for crust removal and fuel rod surface cleaning;
- facility for mechanical clearing of fuel rod surface.

2.2. Destructive analysis

The scheme of the second building approximately can be divided into eight sections intended for:

- mechanical tests;
- dismantling of capsule assemblies, fuel assemblies and other irradiated products;
- x-ray and element-fractographic examination;
- metallography examination;
- production of gamma-, beta- and neutron sources;
- investigation of physical-mechanical properties and TEM-examination;
- study on the damage nature and local element - isotopic composition of irradiated specimens;
- study of the element composition of irradiated specimens by the microprobe analysis.

2.2.1. Mechanical testing area

The most commonly used techniques of determining mechanical properties in our hot laboratory are:

- Technique for growing preliminary fatigue crack in compact specimens and Charpy-type specimens;
- Technique of post-irradiation examination of crack resistance based on the three-point bending test of specimens manufactured from technological channels and control rod channels of the RBMK-type reactors;
- Technique of remote instrumented impact toughness tests;
- Test technique of irradiated specimens to determine fracture toughness of material for the RBMK reactor channel tubes;
- Technique for definition of growth rate of fatigue crack during cyclic loading of 0.5 C(T)-type compact specimens
- Technique for definition of short-term mechanical properties of irradiated materials;
- Bending test technique at decreased room temperature and elevated temperatures;
- Technique for definition of creep and long-term strength of irradiated materials;
- Technique for definition of crack resistance parameters of irradiated zirconium alloys during three-point bending test of specimens (5x5x35 mm) with a fatigue crack;
- Measurement technique of crack resistance parameters of cladding tube (5.8x0.5 mm diameter) material using a composite flat specimen;
- Estimation technique of dynamic toughness using Charpy specimens with a fatigue crack during testing at the instrumented impact testing machine with falling weight;
- Comprehensive techniques for tensile test of cladding materials;
- Techniques based on resonance-acoustic method for definition of elastic constants of materials.

Additional information about mechanical testing in RIAR material testing complex are presented in report [1].

2.2.2. X-ray and element-fractographic examination area

There are two x-ray remote handling diffractometers DARD and one scanning electron microscope Phillips XL 30 ESEM-TMP in this area.

Technical characteristics of the remotely controlled diffractometers do not differ from those of the general-purpose ones:

- accuracy of diffraction angle measurements ($d\theta = 0.005^{\circ}$)
- power of X-ray tube (2.5kW)
- maximum diffraction angle ($2\theta = 164^{\circ}$).

Technical characteristics of the remotely controlled scanning electron microscope Phillips XL 30 ESEM-TMP and some examples demonstrating the microscope possibilities are resulted in [2], [3].

2.2.3. Metallographic examinations area

The hot cells for metallographic analysis are equipped with:

- UMSD, MIM-7, MIM-8, MIM-10 and MIM-15 microscopes;
- micro-hardness meters PMT-3 and PMT-6;
- polishing machines and other auxiliary equipment;
- microscopes MMD-1M.

Irradiated specimens are examined in the hot cells by remotely controlled equipment.

2.2.4. TEM-examination area

We have two transmission electron microscopes in this area: JEM 2000 FX II and EM-125.

2.2.5. Surface element - isotopic composition examination area

There are two differential scanning auger electron spectrometers: ESO-3 and ESO-5 (electron beam energy up to 10 keV, ion beam energy up to 10 keV also), one scanning electron microscope and one secondary ion mass-spectrometer MS-7202M (ion beam energy up to 10 keV) in this area. Usually we use the techniques from this area for examinations of the isotope and elemental surface composition. For example, for examinations of the grain boundary surface elemental composition of the different alloys, for examinations of the elemental and isotope composition of any corrosion surfaces, sometimes for the examinations of the isotope and elemental composition of the cross-sections of any absorbing and fuel elements. Some results of such examinations are adduced in [4, 5, 6, 7].

2.2.6. Microprobe examination area

There are X-ray micro analyzer MAR-4 and laser atomic-fluorescent analyser LAFA-1 in the hot cell of this area. Technical characteristics of the remotely controlled micro analyzer MAR-4 do not differ from those of the general-purpose ones.

Laser atomic-fluorescent analyser LAFA-1 is intended for local spectral qualitative analysis of elemental composition (from hydrogen to californium). Some results of fuel examinations are adduced in [8].

There are many other facilities in RIAR Hot Laboratory:

- Mass-spectrometer MI-1201. MI-1201 is designed for determination of helium content in alloys;
- Emission plasma spectrometer "Spectroflame Modula S". It is intended for qualitative elemental analysis of water solutions of different materials (more than 70 elements);
- Gas Analyzer OH-900. The ELTRA gas analyzer is intended for determination of oxygen and hydrogen concentration in steels, zirconium, and other irradiated materials;
- and so, so on.

REFERENCES

1. O. Makarov, A. Postyanko, A. Fedoseev, C. Petersen. Mechanical Testing Methods in RIAR Hot Cells for Sub sized Specimens of Fusion Reactor Materials, paper presented at Plenary Meeting 2006 of European Working Group "Hot Laboratory and Remote Handling" at Julich, Germany, 19 - 21 September, 2006.
2. V.N. Golovanov, A.E. Novoselov, S.V. Kuzmin, V.V. Yakovlev, Possibilities and prospects of investigation of irradiated structural and fuel materials using scanning electron microscope PHILLIPS XL 30 ESEM-TMP located in the hot cell, paper on Plenary Meeting 2004 of European Working Group "Hot Laboratory and Remote Handling", Halden, Norway, 6 - 8 September, 2004, p. 121-126.
3. S.V.Kuzmin, F.N.Kryukov, V.V.Yakovlev, A.E.Novoselov and V.N.Golovanov, Electron probe microanalysis of fuel using scanning electron microscope XL30 ESEM TMP, paper on Plenary Meeting 2005 of European Working Group "Hot Laboratory and Remote Handling", Halden, Norway, 23 - 25 May, 2005.
4. Yu. D. Goncharenko, L. A. Evseev, V. D. Risovany, New possibilities of the isotope distribution examination in irradiated absorbing materials using secondary ion mass spectrometry method, paper on Plenary Meeting 2004 of European Working Group "Hot Laboratory and Remote Handling", Halden, Norway, 6 - 8 September, 2004, p. 127-131.
5. Yu.D. Goncharenko, L.A. Evseev, V.A. Kazakov, F.N. Kryukov, SIMS – an effective addition to the traditional SEM and EPMA methods for examination of irradiated oxide fuel, paper on Plenary Meeting 2003 of European Working Group "Hot Laboratory and Remote Handling", Saclay, France, 22 - 24 September, 2003, p. 19 – 24.

6. Yu. D. Goncharenko, L. A. Evseev. Application of SIMS and SEM methods to study CRUD materials, Annual Meeting on Nuclear Technology 2005, Nuremberg, May 10-12, Germany, p.647-650.
7. Yu. D. Goncharenko, V.A. Kazakov, V.K. Shamardin, A.M. Pechyorin, G.V. Filyakin, Z.E. Ostrovsky, Irradiation-assisted intergranular stress corrosion cracking of the austenitic stainless steel in steam-water mixture, Annual Meeting on Nuclear Technology 2002, Stuttgart, May 14-16, Germany, p.605-609.
8. F.N. Kryukov, G.D. Lyadov, O.N. Nikitin, V.P. Smirnov, A.P. Chetverikov, Radial distribution of plutonium burn-up and content in the VVER fuel pellets, Atomic energy, v. 100, No. 1, 2006 p. 3–8. (in Russian)

Diffusion of Xenon Gas in Nuclear Fuels with Oxygen Potentials in 0.1 MWd/t-U of a Burnup

Heemoon Kim, Kwangheon Park*, Bong Goo Kim, Yong Sun Choo, Woo Seog Ryu

Korea Atomic Energy Research Institute, Daejeon, Republic of KOREA

*Dept. of Nuclear Engineering, Kyung Hee University, Yong-In, Kyunggi, Republic of KOREA
hkim1211@kaeri.re.kr

Abstract

Post irradiation annealing tests were performed to obtain the Xe-133 diffusion coefficients in a UO_2 , $(\text{Th,U})\text{O}_2$ and SIMFUEL. Samples were fabricated as a single crystalline UO_2 powder, polycrystalline UO_2 , $(\text{Th,U})\text{O}_2$ and SIMFUEL. Each 300mg specimen was irradiated in the HANARO research reactor for up to a 0.1 MWd/t-U burnup. Post irradiation annealing tests were carried out at 1400°C, 1500°C and 1600°C. The f^2 .vs. t ratios were plotted to obtain the value of a slope at each temperature. Diffusion coefficient at each temperature was obtain by using the value of a slope. Flowing gases(He, He+H₂(1%), He+H₂(10%)) were used to change the oxygen potential condition, where the oxygen potentials were -370 kJ/mol in He+H₂(10%), -250 kJ/mol in He+H₂(10%) and -110 kJ/mol in He. The xenon diffusion coefficients for the near stoichiometric single crystalline UO_2 agree well with the data of others. The xenon diffusion coefficients in the polycrystalline $(\text{Th,U})\text{O}_2$ and SIMFUEL were lower than those in the polycrystalline UO_2 by one order of a magnitude and 3 times, respectively. The xenon diffusion in a fuel seems to be controlled by a cation vacancy concentration which is related to the melting point and valence of a matrix. Its diffusion coefficient in fuels increases with an increasing oxygen potential of the ambient gas.

Keywords : Xe-133, Booth model, Fission gas release, Diffusion coefficient, Post irradiation annealing, Diffusivity, Oxygen potential

1. Introduction

Fission gas release is the most important behavior for a fuel performance. Many models have been published to explain this mechanism. The models start from the diffusion theory in a spherical geometry. Exact diffusion coefficient is needed in this theory. Therefore, a diffusion coefficient is dominant factor for a fission gas release. Especially, a lattice diffusion is a basal movement of gas atom such as a fission gas produced by a fission event. Many experiments have been carried out to obtain a diffusion coefficient in UO_2 by tracing xenon or krypton[1,2,3,4,5,6].

Generally, a considerable amount of the data for the diffusion coefficient of Xe-133 still shows a large scattering due to the effects of a porosity, stoichiometry, and burnup. Higher porosity and burnup should retard a fission gas release by a gas atom trapping while a higher stoichiometry should enhance a fission gas release.

To observe only a lattice mobility of a gas atom without a bubble creation, fuel sample must be a low burnup because a diffusion of a fission gas at a high burnup is more complicated due to a bubble formation/resolution at intragranular and intergranular grains as well as a lattice diffusion.

Diffusion in UO_2 fuel must be changed with the valences of fission products; higher in 5+ valent elements and lower in 3+ valent elements. To establish the effects of fission products in the past, the tests for doped UO_2 were carried out one by one with different valent additives.

In this study, pure UO_2 and $(\text{Th,U})\text{O}_2$ were made as a powder and polycrystal, and a SIMFUEL was also made with natural elements to simulate a spent fuel corresponding to a declared burnup.

Diffusion of xenon in the fuel samples was measured to establish the xenon's mobility in a matrix with fission products. It will be useful information to compare each other with the data for pure UO_2 .

2. Experimental

2.1 Specimen preparation

Four kinds of samples were prepared; single-grained UO_2 (powder) and polycrystalline samples (UO_2 , $(\text{Th,U})\text{O}_2$, SIMFUEL). Fig. 1 shows the resulting single grains of UO_2 in the powder after a nuclear grain growth process.

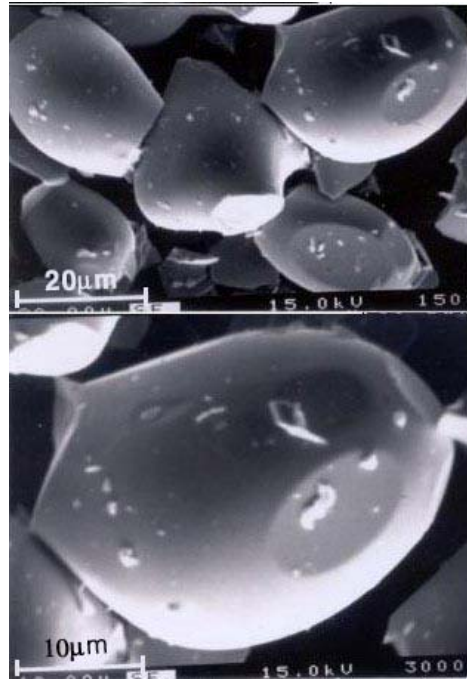


FIG. 1. Single grained UO_2 observed by SEM.

The polycrystalline $(\text{Th,U})\text{O}_2$ specimens were made by mixing ThO_2 with UO_2 at a 35%/65% ratio. To make the SIMFUEL with a given burnup(27,300 MWd/t-U), all the compositions and amounts were obtained by using the ORIGEN-2 code. The SIMFUEL in this study was fabricated with 13 dominant compositions as shown in Table I. The polycrystalline UO_2 , $(\text{Th,U})\text{O}_2$ and SIMFUEL were made by a pelletizing process (power mixing, green packing, then sintering). Then all the polycrystalline samples were cut into 2x2x2 mm (8mm^3) cubes. The theoretical densities of the polycrystalline samples were almost 97%. The properties of the specimens in this study are shown in Table II.

Table I.. Compositions of the SIMFUEL(27,300 MWd/t-U) based on a calculation.

Oxide	mg	Oxide	mg
Rb	0.095	PdO	0.34
SrO	0.171	TeO ₂	0.126
Y ₂ O ₃	0.12	BaCO ₃	0.57
ZrO ₂	1.04	La ₂ O ₃	0.42
MoO ₃	1.055	CeO ₂	1.99
RuO ₂	0.825	Nd ₂ O ₃	1.46
Rh ₂ O ₃	0.11	UO ₂	300
Total	308.35		

Table II.. Properties of the samples used for the irradiation / annealing experiments.

Specimens	Type	Irrad. Time	Density	Grain size
Single grained UO ₂ (S-1,S-2)	Powder	20 min.	99%	23±2 μm
Polycrystalline UO ₂ (P-U-1,P-U-2,P-U-3)	3 Cubes	20 min.	97%	8.1±0.5 μm
Polycrystalline (Th,U)O ₂ (P-Th-1,P-Th-2)	2 Cubes	30 min.	97%	7.5±0.5 μm
Polycrystalline SIMFUEL(SIM-1,SIM-2)	3 Cubes	20 min.	97.5%	10±0.5 μm

To obtain a diffusion coefficient(D) with the Booth model, the radius('a') of a equivalent sphere must be measured by a surface to volume ratio(S/V) in a sphere model[7]. In the case of UO₂ powder, the grain shape is not exactly spherical, but appears ellipsoidal as shown in fig. 1. We set this radius as similar to one that gives the same surface to volume ratio. An ellipsoidal grain has two minor axes and one major axis. For a simplicity, we assumed that the radii of the two minor axes are the same. In this case, the radius of an equivalent sphere using the surface to volume ratio can be obtained by Eq. (1).

$$\frac{3}{a} = \frac{4\pi xy}{4/3\pi x^2 y} = \frac{3}{x} \quad (1)$$

where, 'x' and 'y' are the radii of the minor and major axes, respectively. In this case the radius 'a' of the minor axis becomes the radius, 'a' of an equivalent sphere. The radius of the minor axis was measured by SEM, and the equivalent radius turned out to be 23μm ±2μm (95% confidence level). At the surface of the grains, small chips (2~3μm) were observed as shown in fig. 1.

The radius of an equivalent sphere for a polycrystalline sample is usually obtained from a measurement of the surface-to-volume ratio. The surface to volume values of the samples used in our experiment were not measured. Considering a low porosity (less than 3%) and a low surface roughness, the radius of an equivalent sphere would be about 1 mm by using a specimen's dimensions.

Each fuel specimen was contained in a sealed quartz tube, placed into a double-layered aluminum capsule for a thermal safety during an irradiation, and it was irradiated in the HANARO research reactor up to a burnup of 0.1 MWd/t-U. After an irradiation, the specimen was cooled for 10~11 days to reduce the irradiation exposure level. We used 300mg of fuel for each irradiation and annealing test.

2.2 Apparatus of the Post Annealing Experiments

The experimental apparatus is shown in fig. 2. The furnace was made by a high-grade, pure Al₂O₃ tube with heater wires of U-shaped MoSi₂. An oxygen sensor was installed at the top of the furnace to measure the voltage difference between the inner and outer atmosphere conditions. Then, partial oxygen pressures could be obtained by using the voltage difference of the sensor. The filtration system was designed to catch the released gases such as Kr and Xe. The filter material was granular activated carbon which was placed inside a glass cylinder. This glass cylinder was placed into a beaker filled with liquid nitrogen and surrounded by a lead box.

Liquid nitrogen was used as a cryogenic agent in order to convert the xenon gas to a solid. A Ge detector was installed through a hole in the lead box of the filtration system and it measured the gamma rays from the trapped fission gases. Helium gas flowed through the system to transport the released fission gases into the trapping system. The helium was mixed with hydrogen in order to

change the oxygen potential of the gas(He, He+H₂(1%) and He+H₂(10%)). The flow rate of the helium was fixed at 100 ml per minute during the annealing tests.

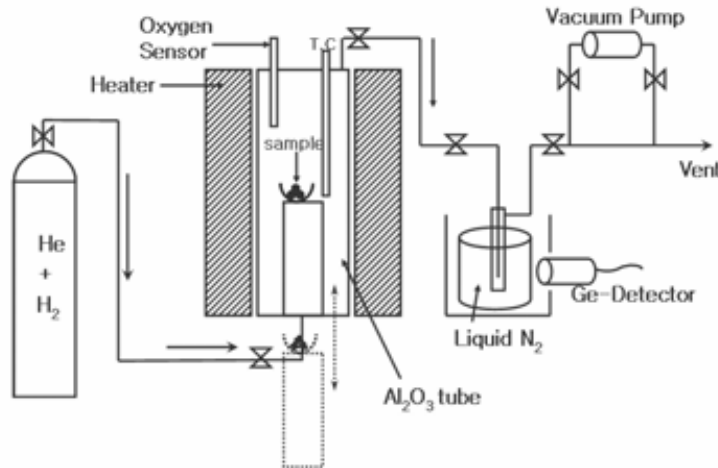


FIG. 2. Schematic of the annealing apparatus.

3. Results

The fraction(*f*) of the fission gases released from a given sample was obtained from the measurements of both the total amount of fission gases produced in the specimen and the amount collected in the trapping system. Since the peak of Xe-133 (81 keV) is located in a low energy region where the background noise is relatively high for a gamma scanning of a sample, the peak of Xe-133 is not accurate enough to be used as a produced radioactivity. Hence, the accurate radioactivity of Xe-133 in the samples was calculated from the exact burnup of the specimen that was obtained from the absolute activities of I-132 and La-140. ORIGEN-2 was used for the calculation of the burnup and the Xe-133 amount. The radioactivity of the released Xe-133 was directly measured in the filtration system by the Ge-detector, where the absolute radioactivity was obtained from a calibration by using a reference source(Ba-133 with a similar peak energy of Xe-133) in the filtration geometry.

We used Booth's model[7] to determine the diffusion coefficients of the fission gases from the fractions released from the specimens with respect to time. Eq. (2) can be approximated for small values of '*f*' (*f*≤0.3) at a fixed temperature,

$$f^2 = \frac{36}{\pi} D't, \quad D' = \frac{D}{a^2} \quad (2)$$

Matzke [8] introduced a plot of a squared fraction (*f*²) with time to produce a more straightened slope at each temperature rather than a plot of '*f*' with *t*^{1/2}. Une [9] performed post-annealing experiments with a stepwise change of the temperature, and obtained reasonably good diffusion coefficients. But, Eq.(2) includes lattice and grain boundary diffusions for polycrystalline samples(except S-1,S-2). Fig. 3, fig.4 and fig.5 show the measured release-fractions of the fission gases for the fuel samples with low oxygen potentials. The annealing temperature was changed stepwise to a fixed value during an experiment. Table III shows the Xe-133 diffusion coefficients(*D*) for all the specimens used in our experiments, based on a slope analysis with Eq.(2). We neglected the burst behavior that appeared at a given temperature change. Oxygen potentials in this annealing atmosphere were -370 kJ/mol in He+H₂(10%), -250 kJ/mol in He+H₂(10%) and -110 kJ/mol in He, which can be converted to O/U ratios of 2.0005, 2.01 and 2.16, respectively by the data in Lindemer's paper [10].

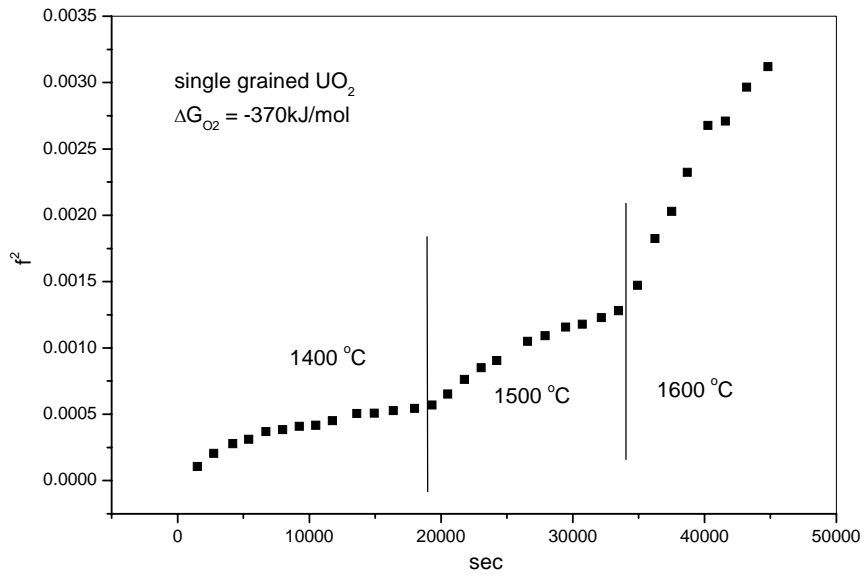


FIG. 3. Released fractions with the annealing time for the single grained UO_2 (S-1)

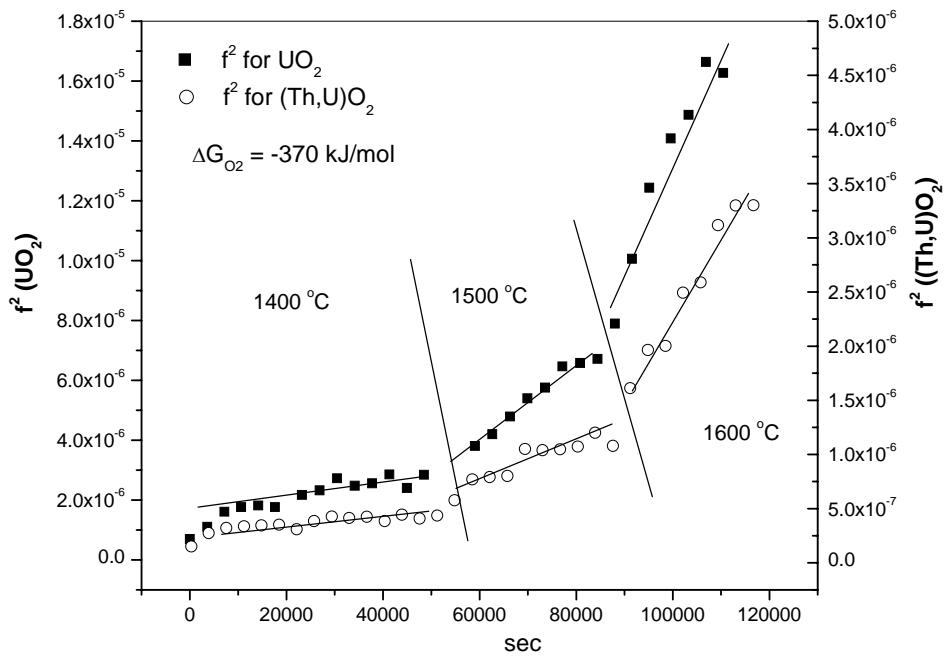


FIG. 4. Released fractions with the annealing time for the polycrystalline specimens (P-U-1, P-Th-1)

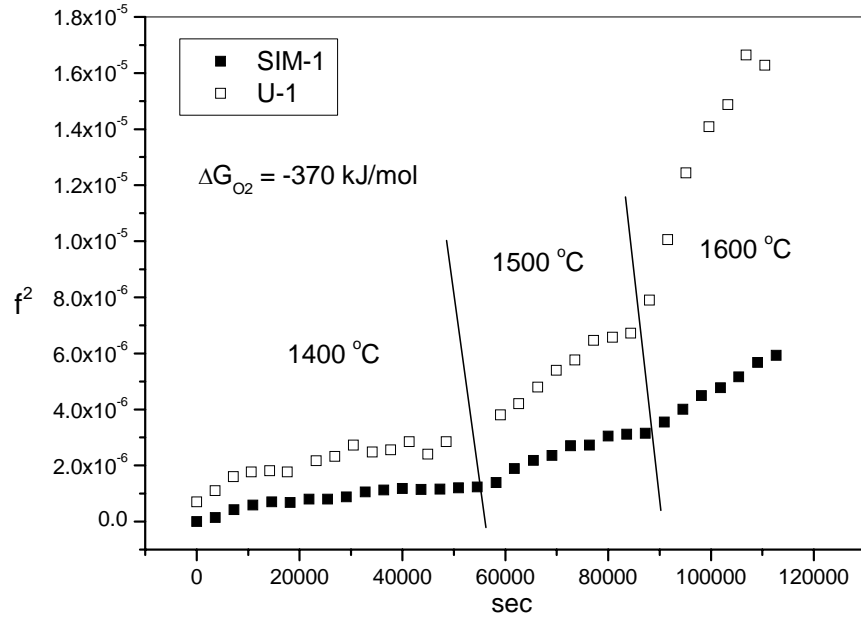


FIG. 5. Release fractions with the annealing time for the SIMFUEL(SIM-1)

Table III.. Diffusion coefficients of Xe-133 in all samples at each temperature and oxygen potential

Specimen notation	Oxygen potential	Diffusion coefficient (m ² /s)*		
		1400 °C	1500 °C	1600 °C
S-1	-370kJ/mol	1.89 X10 ⁻¹⁹	5.35 X10 ⁻¹⁹	1.91X10 ⁻¹⁸
S-2	-110kJ/mol	1.1 X10 ⁻¹⁷	3.45 X10 ⁻¹⁷	1.95 X10 ⁻¹⁶
P-U-1	-370kJ/mol	3.27 X10 ⁻¹⁸	1.13 X10 ⁻¹⁷	3.45 X10 ⁻¹⁷
P-U-2	-250kJ/mol	3.58 X10 ⁻¹⁷	8.15 X10 ⁻¹⁷	2.37 X10 ⁻¹⁶
P-U-3	-110kJ/mol	6.32 X10 ⁻¹⁵	1.13 X10 ⁻¹⁴	1.46 X10 ⁻¹⁴
P-Th-1	-370kJ/mol	2.45 X10 ⁻¹⁹	1.7 X10 ⁻¹⁸	6.45 X10 ⁻¹⁸
P-Th-2	-250kJ/mol	5.02 X10 ⁻¹⁸	1.68 X10 ⁻¹⁷	6.03 X10 ⁻¹⁷
SIM-1	-370kJ/mol	1.6 X10 ⁻¹⁸	4.5 X10 ⁻¹⁸	9.1 X10 ⁻¹⁸
SIM-2	-250kJ/mol	8.1 X10 ⁻¹⁷	2.8 X10 ⁻¹⁷	4.3 X10 ⁻¹⁷

* measured diffusion coefficient(lattice and grain boundary) contains less than 20% error

All the fuel samples with higher oxygen potentials showed a higher gas release of Xe-133. Diffusion coefficient of the polycrystalline specimen (P-U-1) is about 20 times larger than that of the single grained specimen (S-1). It would be affected by a grain boundary diffusion. The diffusion coefficients for the (Th,U)O₂ and SIMFUEL with a low oxygen potential were lower than the diffusion coefficients for the pure UO₂ by one order of a magnitude and 3 times, respectively. Released fraction of Xe-133 in SIM-2 showed a bursting motion at the initial time of 1400 °C, and it was assumed that

the xenon gas had already been released below this temperature. Data of the released fractions were difficult to analyze with a low reliability, even the diffusion coefficient at 1600 °C was too high. In spite of a low accuracy and abnormal results, it is clear that a higher diffusion coefficient was observed.

4. Discussion

The single-grained UO_2 data from this experiment was compared with other data [11,12,13] in fig. 6. The available diffusion data from single-grained near stoichiometric UO_2 samples are dispersed over a relatively large range, with up to 3 orders of a magnitude variation. Our measured values from the specimen with a near stoichiometry(S-1) are relatively close to those of Davies and Long [11]. Une's data [13] is about one order lower than ours. Une explained that his relatively low diffusion coefficients were a result of a burnup effect(4MWD/t-U). McEwan and Stevens[2] noticed that the release of fission gases during annealing tests tends to be saturated after a certain value of a burnup (0.4 MWD/t-U), resulting in a decrease of the diffusion coefficient due to a higher inventory of the fission gases in a higher burnup fuel.

This retarding effect is apparently due to a trapping of the gases by irradiation induced defects. The burnup in this experiment is about 0.1 MWD/t-U thus a defect trapping may not have occurred. Davies and Long used fuel specimens with 0.8 MWD/t-U, which apparently explains the similarity between our data and those of Davies and Long. The activation energy of Baker and Killeen's data is quite different from the other data, indicating a different release mechanism in their high burnup fuel sample (38,000 MWd/t-U).

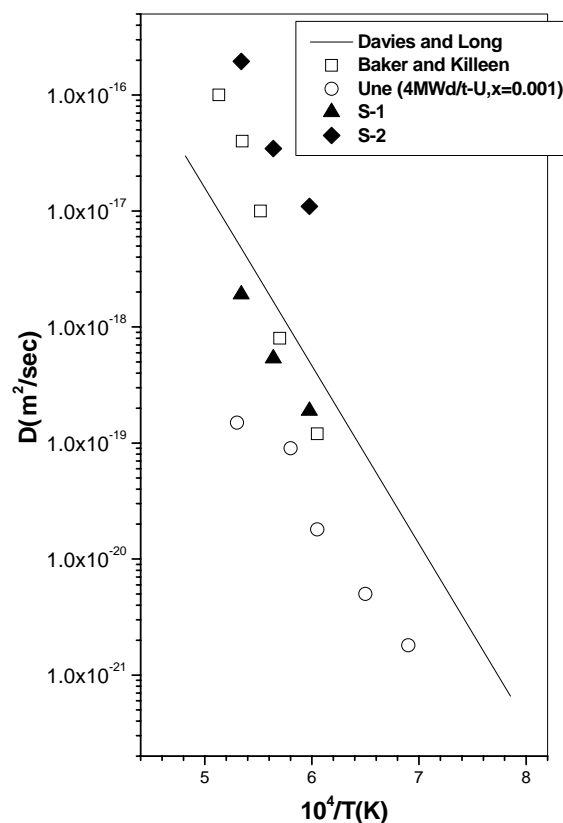


FIG. 6. Diffusion coefficients of the single-grained UO_2

Diffusion mechanism of xenon in a fuel matrix depends on the cation vacancy concentration. It means that a higher cation vacancy concentration causes a higher diffusivity level. In some experiments with a doped UO_2 sample, diffusion coefficients are different with valence of additives which are able to

change the cation vacancy concentration [9,13]. Doped tri-valent additives in UO_2 retards a fission gas release due to a reduced concentration of the cation vacancy while penta-valent additives enhance a fission gas release by an increase of the concentration of the cation vacancy.

Matzke[14] proposed a mechanism for an xenon diffusion via an neutral tri-vacancy cluster(one cation vacancy and two anion vacancies). This proposition was deduced from doping experiments in which the diffusion rate of the xenon was not different in the undoped and the doped UO_2 in a low concentration but sufficiently different in a high concentration. This implies that xenon does not migrate via uranium vacancies only. The diffusion of fission gases is considered to be strongly related to the concentration of the cation vacancies in a fuel. But in the hyper-stoichiometric state (UO_{2+x}), Grimes produced theoretical data in which xenon moved via a uranium vacancy not a tri-vacancy cluster[15].

In this study, the diffusion coefficients in $(\text{Th,U})\text{O}_2$ and SIMFUEL were elucidated with a valence of additives or fission products. In the case of $(\text{Th,U})\text{O}_2$, a change of the valence of thorium is not easier than that of UO_2 where compared to uranium, so, its binding energy is stronger. Stronger binding energy, and a higher melting point, makes it hard for a gas atom to migrate. That's the reason that the diffusion coefficient in $(\text{Th,U})\text{O}_2$ is lower than that in UO_2 .

In the case of the SIMFUEL, it included various valent additives but the tri-valent additives were dominant based on the composition of the SIMFUEL. It means that the concentration of the cation vacancies in the SIMFUEL was lower than that in UO_2 , even though it is complicated to deduce the actual mechanism due to so many additives being present. It was assumed that the grain boundary diffusion in both of them was the same.

As for the results of the samples with higher oxygen potentials such as S-2, P-U-2, P-U-3, P-Th-2 and SIM-2, they showed the same behaviors in that the oxidation enhanced the concentration of the cation vacancy(Uranium ion vacancy) then, it increased the released fraction of the xenon gas and the diffusion coefficient.

5. Conclusions

Post irradiation annealing tests were carried out to observe the diffusion of Xe-133 in fuel samples. Samples of UO_2 , $(\text{Th,U})\text{O}_2$ and a SIMFUEL(27,300 MWd/t-U) were prepared as a powder and polycrystal shape. After an irradiation in the HANARO research reactor, annealing tests were carried out. The measured diffusion coefficients in the samples were compared to those in pure UO_2 . Post irradiation annealing tests were carried out at 1400°C, 1500°C and 1600°C. The f^2 .vs. t values were plotted to obtain the value of a slope at each temperature. Diffusion coefficients at each temperature were obtain by using the value of a slope.

The xenon diffusion coefficients for the near stoichiometric single grained UO_2 agreed well with the data of the others. Difference in the diffusion coefficients for the single grained UO_2 and polycrystalline UO_2 could have resulted from a grain boundary diffusion. The xenon diffusion coefficients in the polycrystalline $(\text{Th,U})\text{O}_2$ and SIMFUEL at -370 kJ/mol were lower than those in the polycrystalline UO_2 by one order of a magnitude and 3 times, respectively. The xenon diffusion in a fuel seems to be controlled by the cation vacancy concentration which is related to the melting point(binding energy) and the valence of the additives. Diffusion coefficient in the samples increased with an increasing oxygen potential of the ambient gas.

Acknowledgement

This work was supported by the Ministry of Science and Technology of the Republic of Korea under the Long- and Mid-term development of Nuclear Energy.

REFERENCES

- [1] R.M.Cornell, Phil.Mag. "The growth of fission gas bubble in irradiated uranium dioxide.", 19 , 539 (1969)
- [2] J. R. MacEwan and W. H. Stevens, "Xenon diffusion in UO_2 ", J. Nucl. Mater., 11 , 77 (1964)
- [3] J. C. Killeen, J. A. Turnbull, "An experimental and theoretical treatment of the release of Kr-85 from hyperstoichiometric uranium dioxide.", Proc. Sym. on chemical reactivity of oxide fuel and fission product release, Berkeley, UK (1987)
- [4] Hj. Matzke, Radiation Effects, "Radiation enhanced diffusion in UO_2 and $(\text{U,Pu})\text{O}_2$ ", 75 , 317 (1983)
- [5] J. A. Turnbull, C. A. Friskney, J.R.Findlay, F.A.Johnson, A.J.Walter, "The diffusion coefficients of gaseous and volatile species during the irradiation of uranium dioxides.", J. Nucl. Mater., 107 , 168 (1982)
- [6] W. Miekeley, F. W. Felix, "Effect of Stoichiometry on Diffusion of Xenon in UO_2 ", J.Nucl.Mater. 42(1972)297
- [7] A. H. Booth, "A Method of Calculating Fission Gas Diffusion from UO_2 Fuel and Its Application to The x-2-f Loop Test.", CRDC-721 (1957)
- [8] Hj. Matzke, Radiation Effects, "Gas release mechanisms in UO_2 -A critical review.", 53 , 219 (1980)
- [9] S. Kashibe and K. Une, "Effect of additives (Cr_2O_3 , Al_2O_3 , SiO_2 , MgO) on diffusional release of Xe-133 from UO_2 fuels.", J. Nucl. Mater., 254 , 234 (1998)
- [10] T.B.Lindemer, T.M.Besmann, 'Chemical thermodynamic representation of UO_{2+x} .', J.Nucl.Mater. 30, 473-488 (1985)
- [11] D. Davies and G. Long, AERE Report No.4347 (1963)
- [12] C.Baker, J.C.Killeen, Proc. Int. Conf. On Materials for Nuclear Reactor Core Applications, Bristol UK,(1987) BNES, p.153
- [13] K. Une, I. Tanabe, and M. Oguma, "Effects of Additives and The Oxygen Potential on The Fission Gas Diffusion in UO_2 Fuel.", J. Nucl. Mater., 150 , 93 (1987)
- [14] Hj. Matzke, "Diffusion in Doped UO_2 .", Nuclear Applications, 2 , 131 (1966)
- [15] R.W.Grimes, C.R.A.Catlow, 'The stability of fission products in uranium dioxide', Phil. Trans. R.Soc.Lond. 335 (1991) 609

Post Irradiation Examinations of a Pakistani Fabricated Fuel Bundle Irradiated at Karachi Nuclear Power Plant

***Muhammad Sajjad Zaheer**

ABSTRACT

Pakistani fabricated fuel bundles which were irradiated at KANUPP have been studied at Post Irradiation Examination facility of Pakistan Institute of Nuclear Science and Technology (PINSTECH) for many years. The results of one such bundle having its end plates in damaged condition are being represented in this paper. This fuel bundle was of typical CANDU type and consisted of nineteen fuel pins. Each fuel pin was composed of sintered UO_2 fuel with Zircaloy-4 cladding. This bundle had an irradiation history of about five years in reactor and had maximum burn-up of 6917 MWD/TeU. The examinations comprised of visual examination, metrology, gamma scanning, fission gases collection, spectro-chemical analysis, metallography and autoradiography. The visual inspection showed that its end plates were in damaged condition and some fuel pins were found detached. The integral gamma scanning revealed uniform distribution of gamma activity along the length of all fuel pins whereas point spectra analysis depicted the presence of radionuclides like $\text{Zr}^{95}/\text{Nb}^{95}$, Ru^{106} , Cs^{137} and Eu^{154} . No significant bending/bowing was detected during metrology. The analysis of the fission gases of selected fuel pins showed their low percentage release of the order of 4-6% of total produced gases, which indicated low temperature (i.e. maximum 1600°C) achievement during total irradiation period. The metallographic and auto radiographic study revealed the structural features characteristic of normal irradiated CANDU fuels. There were some evidences of marginal increase in grain size in certain regions of the fuel. The hydridation effect was found on end plate material. The burn-up determinations confirmed that its burn-up value was close to the respective simulated one at KANUPP.

*Chief Engineer, PINSTECH

P.O. Nilore, Islamabad (Pakistan).

1. **Introduction**

KANUPP has been operating on Pakistani fabricated CANDU type fuel bundles for more than three decades. PAEC planned that post irradiation examination of some damaged fuel bundles be carried out at PIE facility of PINSTECH. Therefore a fuel bundle which had an irradiation history of about five years was received at PINSTECH for detailed examinations. The examinations of this fuel bundle and its individual fuel pins were carried out and the work was completed during period of more than two years. Various radio nuclides like Zr^{95}/Nb^{95} , Cs^{137} , Cs^{134} , Ru^{106} , Ce^{144} and Eu^{154} were detected during gamma scanning. Some fuel pins were subjected to puncturing and fission gases analysis which revealed the low percentage of gas release, The presence of slight increase in grain size, distribution of metallic fission products and radial cracking which are features characteristic of irradiated fuel were noticed during micro structural study. The results of various examinations have been discussed in this paper.

2. **Irradiation Data and Fabrication History of fuel Bundle.**

The irradiated fuel bundle under study was fabricated at fuel fabrication plant (KNC-1) of PAEC. It was CANDU type fuel bundle and consisted of nineteen (19) fuel pins arranged in a geometrical pattern of 1, 6 and 12 Nos. Each fuel pin was fabricated of sintered uranium dioxide fuel pellets with zircaloy-4 cladding. The bundle was irradiated in KANUPP for a period of five years under total fluence of 1.7274 n/KB up to burn-up of 6917 MWD/TeU.

3. **Visual Examination**

The visual examination imparts information like micro cracking, oxidation and corrosion effects, crud formation and fretting phenomenon. This fuel bundle was received with its end plates in damaged condition. Both the end plates had some fuel pins in detached condition (fig.1 and 2). Each end plate had some mechanical scratches and shining surfaces at some of its regions whereas one end plate had some detached material from internal side of its outer periphery.

The observations made on fuel pins are summarized as below:

All the fuel pins were found in perfectly sound conditions. Black colour rings were seen around areas of bearing pads and spacers on cladding of all; fuel pins. There were the portions

were observed in two or three fuel pins especially on their bearing pads. Some fretting scratches were found mainly on fuel pins of outermost layer. However, pins of intermediate layer and innermost fuel pin had very rare presence of such scratches. The end plugs, spacers and bearing pads of all fuel pins were found to be very much intact and in integral condition.

4. **Metrology**

Metrology is meant to determine the extent of deformations in length, diameter and profile of irradiated fuel bundle. The results have been described in following paragraphs.

4.1 **Fuel Bundle**

Generally there existed no considerable variation in length of fuel bundle due to irradiation. Mechanically deformed areas were found on both the end plates. The lateral variation was in the range from 435 microns to 1560 microns. The diametrical and profile measurements of fuel bundle showed variation with in range of two microns.

4.2 **Fuel Pins**

Generally there existed no change in diameter of all nineteen fuel pins. A small change in profile in the shape of bowing with one transducer and bending with the other one was observed in the range from 50 microns to 550 microns. The overall behaviour of all fuel pins was similar in both diametrical and the profile variation measurements.

5. **Gamma Scanning**

Gamma scanning has got great importance in post irradiation examination of fuel pins because it provides direct guideline for further destructive tests like metallography and spectrochemical analysis. Three examinations were carried out during gamma scanning of all nineteen fuel pins. (a) Integral gamma scanning in order to study the gross gamma activity effect along fuel pins, (b) Isotopic gamma scanning along length of fuel pins in order to study the behaviour of fission products like Zr^{95}/Nb^{95} , Cs^{137} , Cs^{134} and Ru^{106} , and (c) point spectra analysis in order to study distribution of various fission products at particular point of fuel pin.

Observations made during gamma scanning are summarized below:

5.1 **Integral Gamma Scan**

gamma scan showed similar behaviour in all 19 fuel pins. No irregular behaviour in trace of any fuel pin was observed.

5.2 Isotopic Gamma Scan

Isotopic gamma scan of various fission products like Zr^{95}/Nb^{95} , Cs^{134} , Cs^{137} , Ru^{106} , Ce^{144} and Eu^{154} were taken for all fuel pins. There was slight depletion of Cs^{137} at one end of all fuel pins. Behaviour of all other radioisotopes was almost uniform.

5.3 The Point Spectra Analysis

Gamma spectra at three points (both ends and centre) were taken for all fuel pins. The radioisotopes identified were Zr^{95}/Nb^{95} , Cs^{137} , Cs^{134} , Cs^{134} , Ru^{106} , Ce^{144} and Eu^{154} (fig.3). It was found that gamma activity at various points was mainly due to activity of Cs^{137} , Cs^{134} and Ru^{106} . All the nineteen fuel pins behaved in a similar manner.

6. Puncturing of and Fission Gas Collection from Fuel Pins

The Xenon and Krypton are the most abundant elements present among the fission products of irradiated fuel. The production and release of these gases from fuel pin and their further effect on fuel integrity are of prime importance in reactor fuel design. Therefore, four fuel pins from this fuel bundle were selected for puncturing & fission gases collection;

Theoretical calculations were carried out to assimilate the volume and activity of produced fission gases (Table I). These were compared with the volume and activity of released gases. The pressure measurement of released fission gases and pin free volume determinations were carried out for each fuel pin and enlisted in Table II. Low volume, percentage of released fission gases of the order of below 5.5 percent and low pressure in the range from 2941 to 3257 m bar were observed.

7. Microstructural Study

7.1 Structural Analysis of Fuel

7.1.1 The Grain Size

The polished as well as etched specimens did not show any presence of columnar grain region. The literature study shows that columnar grain's are formed only when the threshold temperature (1600 °C) required to form such regions has reached [1]. The origin of columnar grain growth is the migration of pores along thermal gradient by the evaporation/condensation

evidence of columnar grain region in any of the sectioned fuel pin specimens. It confirmed that the temperature responsible for the initiation of columnar grains was never achieved during irradiation. The grain size of fuel pellets of this bundle was determined to be in the range from 9 to 15 microns. Examples of equiaxed grain region were very rare in this bundle.

7.1.2. **Porosity Distribution**

The uniform distribution of porosity along transverse section of fuel in addition to presence of radial cracks showed that no restructuring phenomenon took place during irradiation. The distribution of porosity was in the range from 7.0 to 8.0 percent.

7.1.3. **Fuel/Clad Gap**

Fuel/clad gap observed in all specimens was in the range from 20 to 40 microns. It is assumed to be a little higher than foreseen during fabrication of fuel pins for KANUPP. This fuel/clad gap has thus been formed due to shrinkage of the fuel from cladding during irradiation.

7.1.4. **Behaviour of Metallic Fission Products**

The presence of metallic fission products was rare. An example of metallic inclusions is given in fig.4. The size analysis showed that metallic fission inclusions were in the range from 2 to 4 microns.

7.1.5. **Cracking Behaviour in Irradiated Fuel**

Macro cracks were present in all the specimens. Almost all cracks radiated from center to the outer surface of fuel. Some cracks crossed each other in the central region of fuel pellets. The grain growth was observed in some areas adjacent to the crack length which clearly showed the migration of pores towards the cracks (fig. 5).

7.2. **Behaviour of Cladding and End Plates**

The cladding of fuel pin should be compatible with UO₂ fuel and the performance of fuel pin depends on cladding performance as well. The etched fuel specimens did not show any fuel cladding interaction. No micro crack was observed in the cladding wall. The etching of transversely sectioned end plug specimens showed normal welded and heat affected areas. Main areas of stud were hydridation effect and oxide layer thickness measurement in the end plate material.

7.2.1. Hydridation Effect

The hydridation effect on cladding and end plate material of various specimens of this fuel bundle was studied. It was observed that radial hydrides were present in reasonable quantity in end plates because of F_n factor being greater than 0.3. Whereas there was presence of mainly circumferential hydrides only in cladding

7.2.2. Oxide Layer Thickness

The oxide layer thickness was almost uniform in cladding and end plate material. The oxidation layer was determined to be in the range from 15 to 50 microns in thickness in end plate material.

7.2.3. Microstructure of Weldments (End plugs with Cladding)

The welded zones of various transversely sectioned specimens of end plugs of fuel pins were studied. The microstructure revealed heat affected areas and weld lines typical of zircaloy welds (fig.6). The perfect sound condition of welds after irradiation was revealed during their microstructural study.

8. Authoradiography

Alpha autoradiography of all sectioned specimens of this fuel bundle was successfully carried out. No presence of alpha particle concentration within cracks was observed. However, cracking behaviour of fuel could apparently be seen in alpha autoradiographs. There was evidence of slight concentration of alpha emitting fission fragments near the periphery of fuel as compared to its central area.

9. Burn-up Measurements

The burn-up determination of various selected samples of this fuel bundle was carried out by radiochemical analysis of gamma fission products like Cs^{137} , Cs^{134} , Ce^{144} , and Eu^{154} etc. using gamma spectrometry, The burn-up determinations showed that the values were close to the estimated ones of KANUPP (Table III).

10. Discussions

This fuel bundle had an irradiation history of a period of more than five years in KANUPP. It had a cooling time of more than two years before it was received at PINSTECH for detailed study. The post irradiation examinations of such CANDU type bundles have

As far as the performance of nuclear fuel is concerned, UO_2 has behaved well in pressurized heavy water reactors. The similar behaviour of fuel was observed well in this case as well. There was found to be no abnormal crud formation, oxidation and corrosion effects on cladding material. This depicted that cladding was inert to the coolant's effect.

The metrology of fuel bundle and its fuel pins did not reveal any abnormality except some deformation end plates. This was of the order of 1560 microns. This deformation might have taken place during post irradiation handling of fuel bundle. However, diameter, length and profile measurements revealed the variations to be within permissible tolerance for all fuel pins. This confirmed their integrity during irradiation cycle of fuel bundle.

The fission gases analysis of selected fuel pins which were subjected to puncturing showed that there was low volume and low pressure of released fission gases. It confirmed that the maximum temperature at centre of fuel remained below 1600°C during irradiation history and in turn suppressed the release of produced fission gases.

Low temperature of fuel was further confirmed during micro structural study when no columnar grain region was found while rare evidences of equiaxed grain region were observed [1, 2]. This demonstrated that the threshold temperature for columnar grain region (1600°C) was never achieved. However, the grain size of fuel was determined to be in the range from 10 to 15 microns. It revealed a marginal grain growth in fuel which has already been reported [3, 6].

The presence of radial hydrides in end plate material with F_n - Factor in the range from 0.28 to 0.36 was observed whereas oxide layer thickness in end plate material was up to 45 microns. This excessive hydridation and oxidation effect might have caused the damage in end plates of bundle.

The results of various fuel samples showed that burn-up value was close to simulated value as determined by KANUPP.

11. **Conclusion**

The detailed post Irradiation examinations of this fuel bundle can be summarized as below:

1. The low percentage release of fission gases confirmed that the temperature inside fuel

confirmed by the metallographic examination.

2. Hydride determination has revealed that no excessive hydrogen has been picked up by the cladding material to enhance its brittleness. However there was reasonable hydridation effect in end-plate material which might have damaged end-plates of bundle.
3. The uniform distribution of volatile Cs¹³⁷ and Cs¹³⁴ along fuel pins confirmed that there was more or less uniform temperature in axial direction during irradiation period.
4. The microstructures of irradiated fuel revealed that no appreciable grain growth took place during irradiation period. It indicated that temperature of fuel did not rise above threshold level so as to allow restructuring to take place.
5. The burn-up measurements of fuel bundles by gamma spectrometry revealed that its values were close to estimated ones by KAN'UPP.

12. **Acknowledgment**

The study of first post irradiation examinations has been completed with the help of a large number of colleagues from various groups of PINSTECH. The contributions made by the technical staff of our Post Irradiation Examination Group over the years and also during this work are recorded with satisfaction.

Thanks are also due to Member Technical PAEC for this help extended in carrying out our various assignments at PINSTECH. The work was undertaken under the direct guidance of Chairman PAEC. His personal interest almost its day to day progress in this assignment and his encouragement during the course of this work are acknowledged with profound gratitude.

References

1. Nichols, "Theory of Columnar Grain Growth and Central Void formation in Oxide Fuel Rods", Journal of Nuclear Materials 22(1967)214-222.
2. J. R. Mac Ewan "Grain Growth in Sintered UO₂" I. Equiaxed Grain Growth, "II Columnar Grain Growth". AECL, Chalk River, Canada No.37-42.
3. I. J. Hastings, J.A. Scoberg, K Mackenzie and W.W. Alden "Grain Growth in UO₂ Studies at Chalk River Nuclear Laboratories" A.E.C.L.-6411.
4. M. Zafarullah, D.Geithoff and P.Weimar "The Specifications, Design, Irradiation and Post Irradiation Examinations of a Mixed Oxide Pin of the Mol-SC-Series (Pin No.5) "KFK-2221" (1975).
5. K.C.Sahoo, K.S.Sivaramakrishnan and G. Ganguly "Post Irradiation Examination of Fuels of Madras Atomic Power Station "Page 270-281, Proceeding of Second Internal Conference on CANDU fuels w.e.f. 1-5th Oct. 1989, Penbroke-CANDU. Edited by I. J. Hastings, Published by the Canadian Nuclear Society, 1989.
6. P. T. Truant and R. D. McDonald, "Documentation and Post Irradiation Examination of Canadian Nuclear Fuel" AECL-MISC-250(Rev.1). Edition.
7. Data Provided by KNC-1 and KANUPP (Personnel communications).

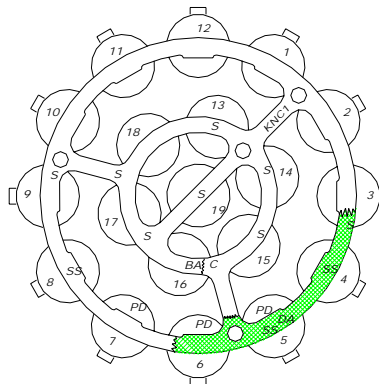


Fig. No.1 ENDPLATE NO I OF FUEL BUNDLE

NOTE	
ABBREVIATION	DETAIL
S	SCRATCHES
SS	SHINY SURFACE
C	CRACKS
DA	DEPRESSED AREA
PD	PIN DETACHED FROM END PLATE
BA	BENT AREA
1 TO 19	FUEL PIN NUMBERS

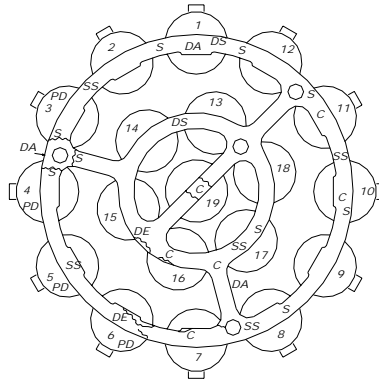


Fig. No.2 ENDPLATE NO II OF FUEL BUNDLE

NOTE

ABBREVIATION	DETAIL
S	SCRATCHES
SS	SHINY SURFACE
C	CRACKS
DA	DEPRESSED AREA
PD	PIN DETACHED FROM END PLATE
BA	BENT AREA
DE	DETACHED EDGE
DS	DEEP SCRATCHES
1 TO 19	FUEL PIN NUMBERS

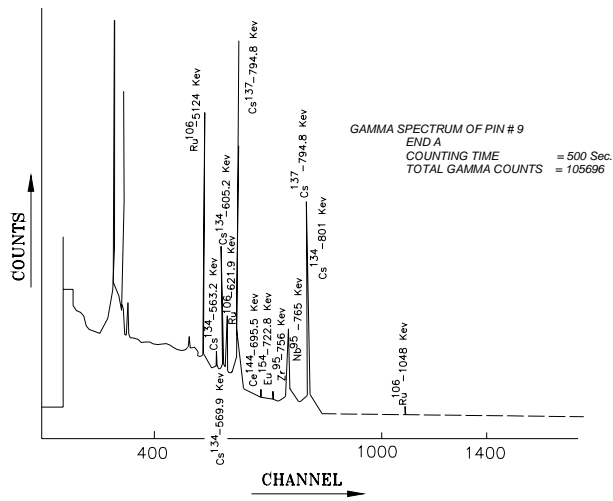


FIG. 3 POINT SPECTRA ANALYSIS OF A FUEL PIN

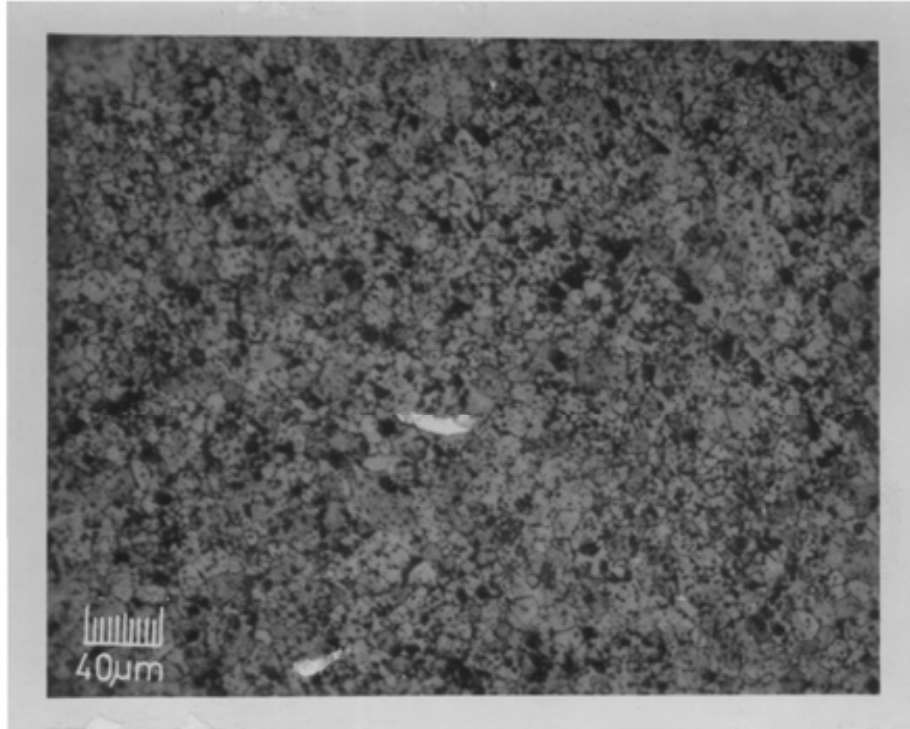


Fig. No. 4: Metallic (Fission Product) inclusion in Irradiated Fuel.

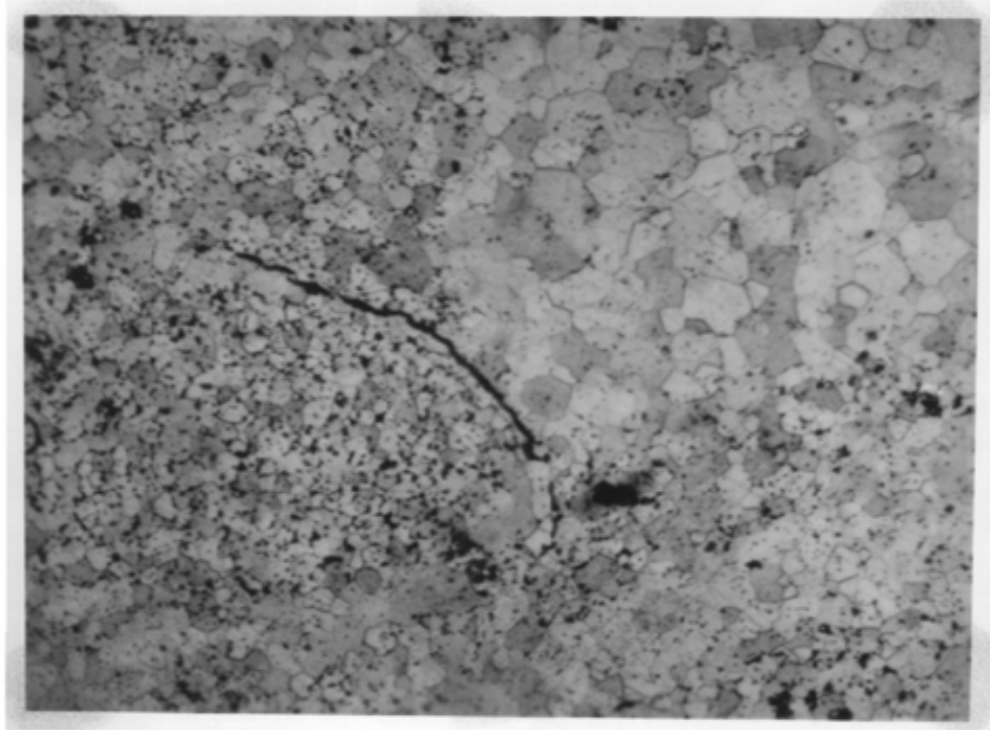


Fig. 5: Grain Growth in Crack's Adjacent Area in Irradiated UO₂ Fuel Mag 250 X.

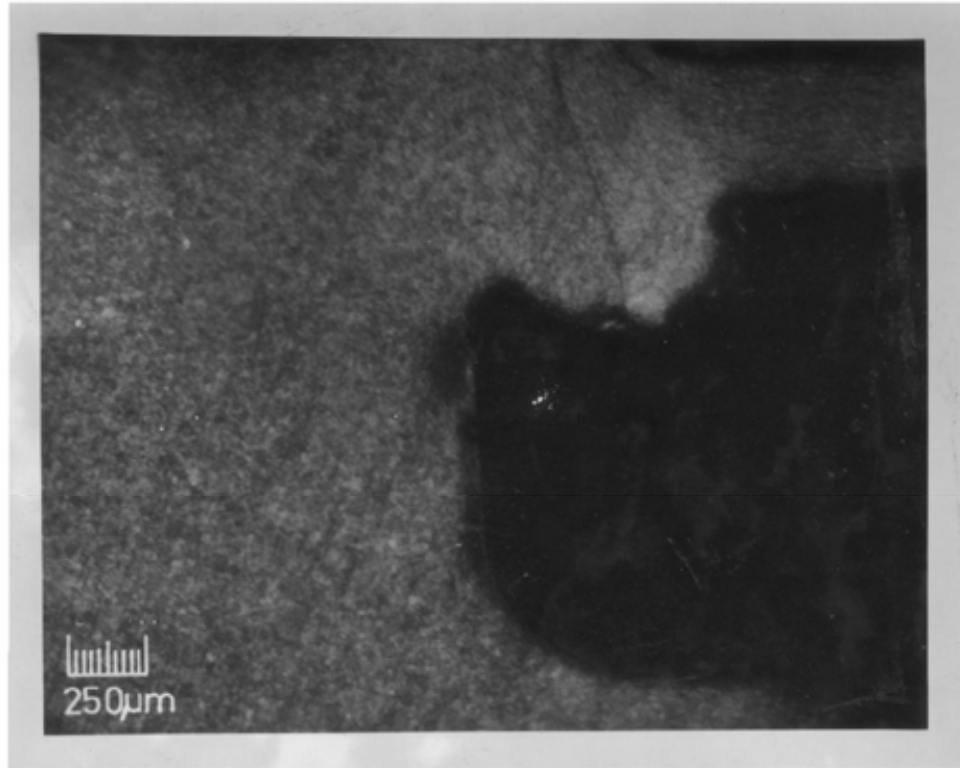


Fig. No. 6: Photomicrograph showing Heat-affected Zone and Weld Line Defect in end-plug's weld area. Mag 40X.

Table I

**FISSION GASES CALCULATIONS OF PUNCTURED
FUEL PINS OF FUEL BUNDLE**

. No.	Fuel pin No.	Cooling time (Sec)	P _{sdp} [*] (m bar)	V _p (Cm) ³		V _F	P _p (m bar)	Released percentage (%)	Activity of released Kr ⁸⁵ (μCi)
				sing	sing				
)	6	8.13 × 10'	9.5	.89	.94	6.4 7	314 3.0	5.16	391
)	1	8.90 × 10'	8.8	.83	.92	5.9 9	294 1.5	4.78	356
)	18	9.27 × 10'	9.2	.77	.88	6.2 6	314 0.4	4.99	369
)	13	9.47 × 10'	10.	.05	.00	6.8 8	325 7.0	5.49	404

P_{sdp}* = Pressure of fission gases noted in V_{sdp}

V_p = Pin free volume

V_F = Volume of fission gases

P_p = Pressure of fission gases is in free volume

Table II

VOLUME CALCULATIONS OF PRODUCED FISSION, GASES OF FUEL BUNDLE

S. No.	Isotope	Fission Yield		Volume per fuel pin (cm ³)
		(%)	(Fraction)	
1.	Kr-83	0.54	0.0054	2.696
2.	Kr-84	1.00	0.0100	4.993
3.	Kr-85	2.28	0.0028	1.398
4.	Kr-86	1.97	0.0197	9.835
5.	Xe-131	2.88	0.0288	14.379
6.	Xe-132	4.30	0.0430	21.469
7.	Xe-134	7.80	0.0780	38.944
8.	Xe-136	6.31	0.0631	31.506

Total Krypton = 18.920cm³

Total Xenon = 106.296 cm³

Total Xe + Kr = 125.216 cm³

Table III

BURN-UP DETERMINATION OF IRRADIATED FUEL BUNDLE

Sample No.	Fuel Wt. dissolved (g)	Activity in KBq/ml						Burn up % in MWD/ TeU Gamma
		^{144}Ce	^{134}Cs	^{137}Cs	^{137}Cs	^{154}Eu	Using ^{137}Cs as monitor	
1) (Pin-6)	05- 574	4553	427	25	814	134	8107	
2) (Pin-6)	04- 551	820	960	20	673	108	8057	
3) (Pin-6)	04.915 8	930	030	00	743	137	8119	
4) (Pin-13)	05- 1809	870	260	00	660	102	6884	
5) (Pin-i3)	04- 2868	340	690	40	484	740	6144	

Remarks: Average burn up for bundle as calculated KANUPP Engineers was 6917 MWD/t of U.

SESSION 5: PRACTICAL USES OF IN-PILE AND PIE DATA

Chairperson

T. Nemeč

Fuel failure and reconstitute in Qinshan nuclear power plant

Xue Xincan

Qinshan Nuclear Power Company

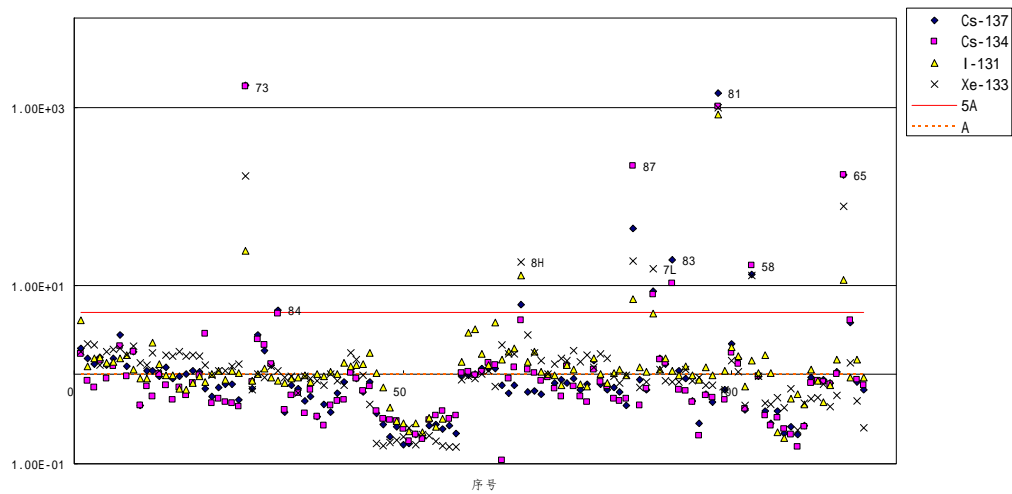
1、 Introduction

Fuel failure in nuclear power plant is fatal considering radiation protection and economical operation. In the operation history of Qinshan nuclear power plant, fuel failure has occurred several times. Based on evaluation of coolant activity during operation, it was confirmed that there were fuel leaking in cycle -4, cycle-5 and cycle -6. Also during fuel loading in cycle -7 two fuel assemblies were damaged.

2、 Root cause analysis of fuel failure

In order to analyse the root cause of fuel failure, poolside inspection for unloading fuel assemblies were performed during outage including sipping test, eddy current detection, oxide thickness measurements, and visual inspection.

For sipping test, wet sipping was used in Qinshan nuclear power plant. Sipping test is performed immediately after fuel unloading (normally 7 to 9 days after shutdown). All the fuel assemblies unloaded from the core were tested by sipping. According to measurement and evaluation of gamma spectrum of the fission nuclide in sipping sample total 11 fuel assemblies (9 in cycle 4, 1 in cycle 5 and 1 in cycle 6) were identified to be failure. Figure 1 shows the sipping samples analysis result for the cycle 4 fuel assemblies.



The fuel failure assemblies identified by sipping test were disassembled so that fuel rod examination could be performed by eddy current detection. Total 1836 fuel rods were detected and 23 fuel rods were identified to be defective at the position of lower end plugs based on the EC signal analysis (see Fig.2).

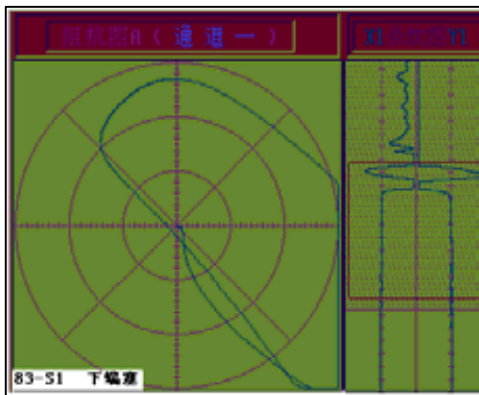


Fig.2 EC signal of defective fuel rod

Fig.3 Defective in fuel rod near lower end plug

Among the 23 defective fuel rods there were 11 fuel rods with through hole near the lower end plug according to the EC signal, these were confirmed by visual inspection using under water TV camera (see Fig. 3) Before the fuel assemblies were disassembled, visual inspection was

spacer near the bottom. Debris was also found in the core bottom plate (see Fig 4). So it is sure that the fuel failure is due to debris fretting.



Fig. 4 Debris in the fuel assembly and fretted hole in fuel rod

During eddy current testing it was found that in some fuel rods there were EC signal located at the height of 60%--70% full fuel rod from the lower end. It was inner signal and all the rods with this kind of signal were confirmed that they had fretted hole near the lower end plug.

So we thought this kind of EC signal was due to the secondary hydriding (see Fig.5)

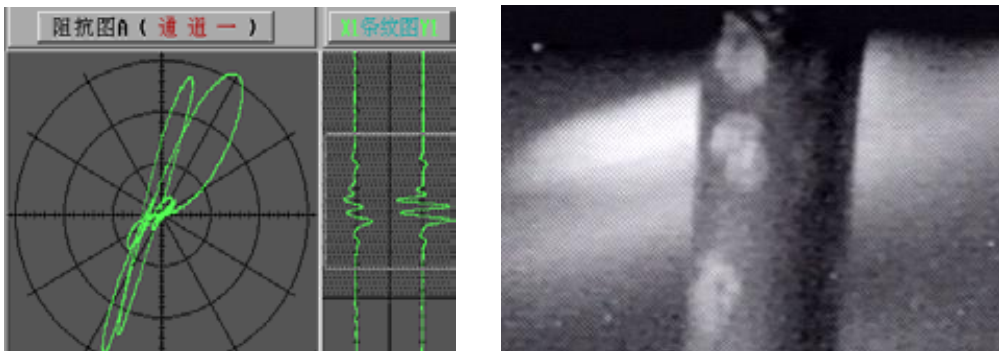


Fig.5 Fuel rod with inner EC signal

For other fuel rods no clad defect was found by eddy current testing, there was no evidence of grid-fretting on the surface of fuel rod.

Oxide thickness measurements showed the maximum oxide thickness was about 40um under the burn-up of 40000MWD/TU thinner than the

At sixth refueling outage (in 2002), two fuel assemblies were damaged (see Fig.6) during the fuel loading when the fuel was inserted into the core. It was due to human error.

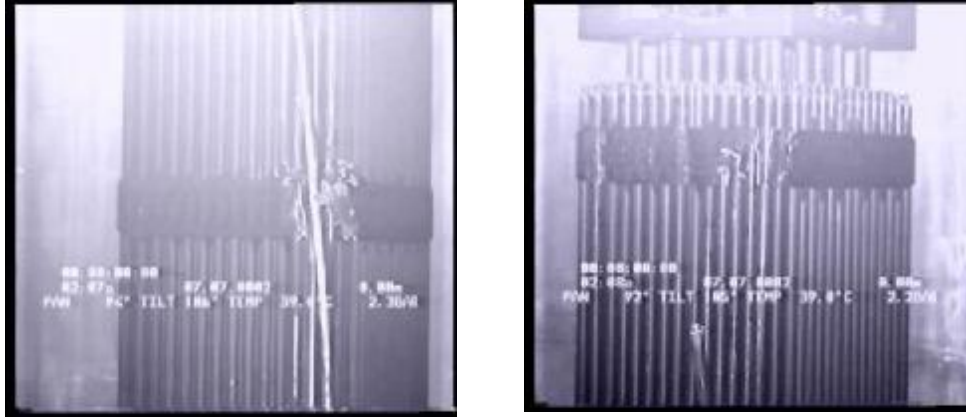


Fig.6 Fuel damage due to fuel handling

3、 Reconstitute of defective fuel assembly

The failure of fuel assembly not only seriously affect the safe operation of nuclear power plant, but also bring about big economic loss, According to Qinshan nuclear power plant condition, if one fuel assembly can not be refueled due to failure, another three fuel assemblies laid with the failure fuel assembly symmetrically in the core also can not be reused. Thus the core fuel loading map has to be redesigned, it may lead to prolong the outage time. So if the failure fuel assembly can be reconstituted then reused, it will be of great signification to the nuclear power plant.

There were two ways of failure fuel reconstitute used in Qinshan nuclear power plant. In refueling outage 4、 5 and 6, seven failure fuel assembly which would be refueled were reconstituted by exchanging the defective fuel rods with new fuel rods, and during the fuel loading in cycle 7 the fuel failure happened not only in fuel rod but also in grid spacer, so they

were reconstituted by exchanging the defective rods and damaged skeleton.

The reconstituted fuel assemblies were used in following cycle and no abnormal phenomena appeared in operation.

4、 Corrective action for fuel failure

Based on the fuel failure experience in Qinshan nuclear power plant, the major cause of fuel assembly defective is debris fretting. To prevent fuel failure some corrective actions have been taken as follow:

- Establish the debris prevention management program to prevent debris producing during maintenance and operation;
- Establish debris inspection and cleanup program to insure there is no debris in fuel assemblies and in reactor core.
- Modify the fuel assembly design applying filters in the bottom tie plate.

A Negative Void Reactivity PHWR Fuel Element for Extended Burnup: Design, Modelling, Experimental Support and a Proposal for an Irradiation Test

Armando C. MARINO
Daniel O. BRASNAROF
Héctor A. LESTANI
Pablo C. FLORIDO

Comisión Nacional de Energía Atómica
División DAEE, Departamento TECNIN
Centro Atómico Bariloche
R8402AGP Bariloche
Argentina

Abstract

CARA is an advanced PHWR fuel element designed to fit the Argentinean fuel-cycle requirement for Atucha I, II, and Embalse NPP's. The CARA fuel element can be used in both reactor types and substantially it improves the competitiveness of the nuclear option, keeping the same operational conditions. At present the most interesting goal reached for CARA is its negative void reactivity and to improve the safety margins of the PHWR technology. The design and analysis of the expected performance and behaviour under operation of the CARA fuel is made with the BaCo code and its 3D tools. In order to test the capabilities of BaCo, we participated in the CRP FUMEX II of the IAEA. These exercises were the preview of a proposal for a programme of experimental irradiations. In this paper we present the CARA basic design, the BaCo code and exercises of code validation. We emphasize our participation in the CRP FUMEX II and the extensive use of the Halden irradiations tests in order to show the demanding conditions of the designers and modellers before the preparation of an experiment of irradiation as the CARA ones.

1. INTRODUCTION

The National Atomic Energy Commission of Argentina (CNEA, “Comisión Nacional de Energía Atómica”) is developing the CARA advanced fuel element for Argentinean PHWR, specially designed to fit the Argentinean fuel-cycle requirement for Atucha I and II (pressure vessel type, Siemens designs), and Embalse (CANDU type) NPP's. The CARA fuel element can be used in both reactor types and substantially improves the competitiveness of the nuclear option, keeping the same operational conditions for both NPP's. These are the coolant flow and hydraulic channel pressure drop, and the mechanical compatibility of the refuelling machine of the vertical and horizontal channel reactors [1, 2].

This design is very innovative (doubling length of the CANDU type, few welding on sheaths, spacer grids) in respect to previous ones, allowing extended burnup by the use of slightly enriched uranium (SEU) and burnable poison, with good thermal hydraulic margins using a single fuel rod diameter. An additional assembly system enables its use into PHWR vertical channel reactors.

Typically, the PHWR NPP's fuelled with natural uranium has positive void reactivity. The CARA improves it to robust safety design, based on negative void reactivity, by the use of SEU and burnable poison. Depending on the enriched uranium composition in the different rings and the burnable poison level in the central rods, the void reactivity can be near zero or negative, the with exit burnup up to 20000. Nevertheless we could find good neutronic performance up to 24000 MWd/tonU.

The BaCo code (“Barra Combustible”, Spanish expression for “fuel rod”) was developed at CNEA for the simulation of the behaviour of nuclear fuel rods under irradiation. The development of BaCo is focused on PHWR fuels as the CANDU and Atucha ones but we keep a full compatibility with PWR, BWR, WWER and PHWR MOX among advanced, experimental and/or unusual fuels as the Halden irradiation cases. BaCo is being used in the CARA Project for the fuel design, the analysis of the expected performance and the development of a future irradiation test [3, 4].

In this paper we present the CARA fuel element, the keys of the design showing the criteria adopted and the mechanical solution proposed, the use of the BaCo code for the modelling and simulation of our PHWR fuels, the validation of our results with our participation in the CRP FUMEX II of the IAEA and by

using old irradiation tests performed at the Halden Reactor, and finally a proposal for an irradiation test. We intent to demonstrate how the use of old experiments of irradiation stored at the Halden Reactor Project, and the international projects as the CRP FUMEX of the IAEA, can be joined with advanced development as our new PHWR fuel and a frame for a proposal of an experiment for irradiation in order to validate the CARA concept [5, 6, 7].

2. THE CARA FUEL

The main characteristics of the CARA are: 52 equal fuel rods (collapsible under the operational reactor pressure) about 1 meter length fasten by three spacer grids (similarly to PWR ones). This minimizes the welding on claddings instead of the classical CANDU sheath welded appendix “spacer”, keeping the original cladding microstructure for extended burnup by the use of slightly enriched uranium (SEU).

The rods are only welded at both ends on two end-plates (similarly to CANDU fuel). The bundle has a cluster array with four rings, having 4-10-16-22 fuel rods respectively. For Atucha it is necessary to join five CARA fuel elements by means of an additional coupling system external to the fuel bundles, by using the slightly greater channel diameter of this NPP (5 mm greater than Embalse, which is 103 mm).

The geometry and fuel dimensions of the CARA FE (Fuel Element) are as follows:

- Number of fuel rods per FE: 52
- Number of spacer grids per FE: 3
- Total length: ~1000 mm
- Fuel element diameter: ~100 mm
- Clad external diameter: ~11 mm
- Clad thickness: ~0.35 mm
- Pellet radius: ~5 mm
- Pellet length: ~12 mm

From the beginning, the CARA design was done having in mind a versatile bundle allowing the improvement of all the major performances in the PHWR fuel technology. New fuel reaches higher burnup and thermal-hydraulic safety margins, together with lower fuel pellet temperatures and Zry/HM mass ratio. Moreover, it keeps the fuel mass content per unit length and the channel pressure drop by using a single diameter of fuel rods.

A base design was done having in mind our experience on the use of fuel elements with 0.85% SEU. The estimated CARA cost is lower as compared with actual PHWR fuel produced in Argentina. It was estimated a reduction in the generation cost between 20 to 25 % in respect to the present one if we use 0.90% SEU. With these results a new design was focused on safety improvements.

The PHWR NPP’s fuelled with natural uranium have positive coolant void-reactivity. During postulated initiated events such as a large break loss of coolant accident (LOCA), the reactivity insertion is very large and the safety systems need to be designed in order to shut down the reactor in a very short time. If the fast shutdown system fails in the Atucha II, the reactor could reach a prompt supercritical state. The Atucha II NPP has large vertical channels and a CANDU reactor has horizontal ones. A CANDU divides the primary circuit in two loops to mitigate the void effect. The new CARA design can simultaneously enhances the above-mentioned requirements and uses this handicap to enhance the safety of PHWR NPP for large-LOCA, towards a robust inherent safety design, especially for large LOCA scenarios. It is based on negative or near zero coolant void reactivity in any plant condition, by the use of SEU and burnable poison such as dysprosium [8]. Depending on the enrichment uranium composition in the different rings and the burnable poison level in the central rods, the void reactivity calculated with WIMS-D5 [9] can be near zero or negative, with exit burnup from 15000 to 24000 MWd/TonU (see table 1).

	Base case bundle	Low void reactivity bundle
1 st ring (inner)	0.9 SEU	Nat U + Dy (7 to 8%)
2 nd ring	0.9 SEU	1,2 to 1.7 % SEU
3 rd ring	0.9 SEU	1.6 to 2 SEU
4 th ring (outer)	0.9 SEU	1.3 to 1.6 SEU
Bundle max. power peak factor	1.15	1.15 to 1.34
Extraction Burn up	15000 MWd/tonU	17000 to 24000 MWd/tonU
Average Void coefficient	6.6 mk	-1 to -2 mk

Table 1: CARA pellet compositions and neutronic data.

On August 2006 our government announced a launch of an 8 years nuclear programme where the key will be the finalization of Atucha II NPP. The CARA project is under restudying in order to complete the development program, according this new horizon by considering the safety as the main task.

3. THE BACO CODE

The BACO code structure and models in its present versions have already been described in references [3], [4] and [2]. A complete application example of BaCo for PHWR fuel design is included in reference [2]. The strategy for the development of the code is presented in reference [4] with a brief description of the code. Statistical analysis, data post-processing and 3D tools improves the code's performance and analysis of results [10, 11].

On modelling the UO_2 pellet behaviour, phenomena such as elastic deformation, thermal expansion, creep, swelling, densification, restructuring, cracks and fission gas release, are included. For the Zry cladding, the code models the elastic deformation, thermal expansion, anisotropic plastic deformation, and creep and growth under irradiation. The modular structure of the code easily allows to add different material properties. It can be used for any geometrical dimensions of cylindrical fuel rods with UO_2 pellets (either compact or hollow, with or without dishing) and Zry cladding.

BACO assumes azimuthal symmetry in cylindrical coordinates for the fuel rod; the model is bidimensional and angular coordinates are not considered. However, angular dependent phenomenon, as well as radial cracking, is simulated via some angular averaging method [12]. For the numerical modeling the hypotheses of axial symmetry and modified plane strains (constant axial strain) are adopted. The fuel rod is divided in axial sections in order to simulate its axial power profile dependence. The mechanical and thermal treatment and the pellet, cladding and constitutive equations are available from reference [3].

3.1. CARA Fuel Behaviour

The analysis of the CARA fuel rod behaviour starts with the definition of a power history. We extrapolate a history from one of the most demanding scenario found at a normal fuel in the Atucha I NPP. We accommodated the burnup and the power level to the new situation. The power history used for a CARA fuel in the Atucha I NPP is an extension in power and burnup of a real power history (see figure 1). The reduction in the linear power is ~ 140 W/cm. The time for the irradiation in order to reach 20000 MWd/tonU is ~ 660 days.

The figure 2 shows the pellet centre calculation of the BaCo code. We find a reduction of $\sim 350^\circ\text{C}$ from the original fuel filled with natural UO_2 or SEU [13]. The curve of the Vitanza threshold shows us than the FGR (Fission Gas Release) must be more than a 1 %. The calculated FGR at EOL (End of Life) was 1.6 % in agreement with the empirical correlation of the Halden Reactor. The figure 3 shows the dynamics of the free fission gases. We included in that plot the produced gases, the gas at the grain boundary, the grain at the UO_2 matrix and the gas released. The figure 4 includes the gas composition of the free gases. The fresh fuel is filled with He at 1 atm of pressure. The relative contributions to the gap conductance of Xe and Kr are greater than in the normal Atucha fuel. We calculate that the ~ 90 % of the free gases at EOL are Xe and Kr, and the thermal conductance in the pellet-cladding gap is reduced to a ~ 50 % of the conductance at BOL (Beginning of Life) where all the gas was He. The gas pressure at EOL appears less than the coolant pressure (see figure 5).

We calculated a small growing of equiaxed grains at the centre of the pellet (up to a radius of the forth of the original pellet radius). No columnar grains and central hole were found from our calculations in agreement with the temperatures that we find with the CARA fuel. The calculation of the fuel stresses shows a negative hoop stress in the cladding (tangential stress at the inner surface) during all the time of the irradiation. That means that the cladding is under compression.

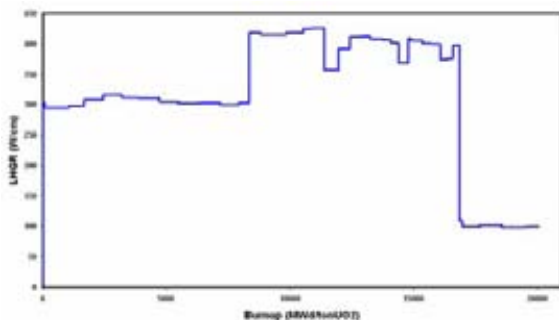


Figure 1: Power history for a CARA fuel in the Atucha I NPP.

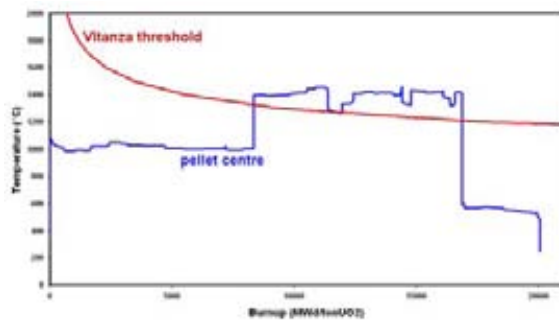


Figure 2: Pellet centre temperature and the Vitanza threshold.

The figure 6 shows the evolution of the pellet and cladding radius (where we include the original radius as a reference value). We mention that the CARA fuel has a collapsible cladding. That concept is done based the small thickness of the cladding and the low pressure of the filling gas. The expected collapsibility was not found at BOL and after the down power ramp (at ~ 17000 MWd/tonU). The cladding had a plastic deformation during the high power step of irradiation (between ~ 7000 and ~ 17000 MWd/tonU). That deformation keeps open the pellet-cladding gap. A value of $\sim 25\%$ over the original Embalse fuel is obtained for the axial deformation of the CARA fuel rod due to the increment in burnup.

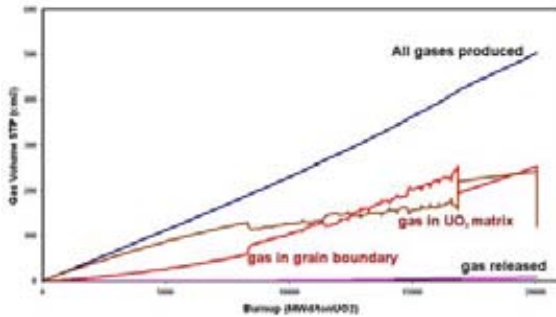


Figure 3: Dynamics of the gases in the fuel rod.

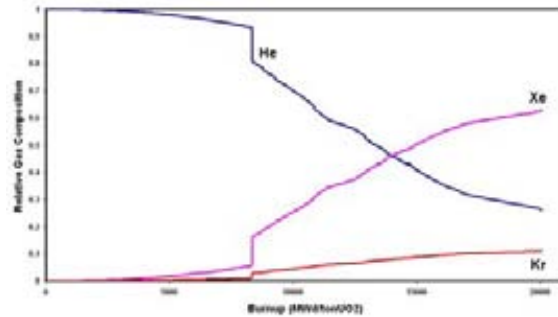


Figure 4: Relative composition of the free gases in the fuel.

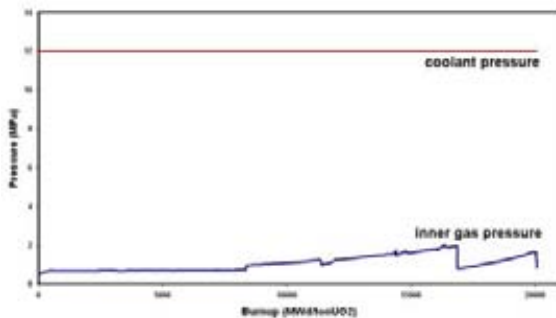


Figure 5: Inner pressure of the free gases in the fuel rod.

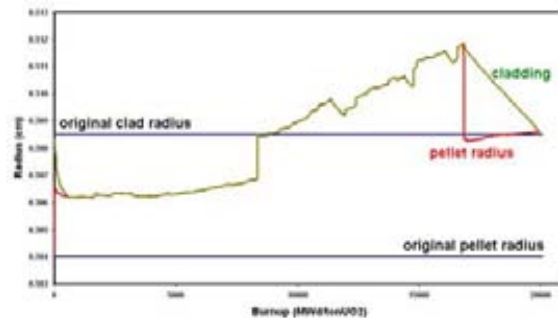


Figure 6: Pellet and cladding radius evolution of a CARA fuel rod.

The result of the calculation of the cladding radius at EOL appears similar to the original ones at EOL (see figure 6). The radial and axial deformations of the cladding were less than $\sim 0.5\%$ during the most demanding condition.

The calculated values with BaCo of the CARA fuel rod behaviour show conservative trends and good safety levels in order to use these results as a seed for an irradiation proposal.

3.2. BaCo Test (CRP FUMEX II Halden Cases)

In order to illustrate the BaCo code capabilities with LWR fuel rods we present an exercise of comparison with experimental data. These irradiation tests are included in the CRP FUMEX II (Co-ordinated Research Project on “Improvements of models used for fuel behaviour simulation”) organized for the IAEA (International Atomic Energy Agency) [14] where BaCo is one of the participants. A previous version of the CRP was organized for the IAEA from 1993 to 1996, the reference [15] includes the BaCo code performance among the others participants. All the cases included in the first CRP FUMEX were experimental irradiation of the HRP (Halden Reactor Project). The main characteristics of the cases were: blind test, PWR, and too complicated and detailed power histories. At present these set of experiments remain as a key for modellers and programmers.

The Halden irradiations are usually recorded on their Test Fuel Data Bank with measurements recorded every 15 minutes of reactor time. The histories are condensed to manageable size by amalgamating adjacent data points if the power changed by less than 1 kW/m. Care is taken that the resulting condensed history faithfully represented the raw data. However a discrepancy between calculated burnup and the data could be done due to the sparse information of the base irradiation, the long extension of the Halden irradiation and the final condensed history. Also, the in-pile measurements of rod internal pressure are usually given as a function of burnup as well as a conversion to FGR versus burnup. This treatment was done

to the Halden cases of the CRP FUMEX I and II. We solve the uncertainty of the burnup calculations including the time and burnup simultaneously as input data for each time-burnup step of the BaCo code.

After calculation we analyze the BaCo results by following these steps: (1) evaluation of the burnup (or time), (2) thermal calculation, (3) stress-strain calculation, and finally (4) coupled issues. We appreciate that a wrong evaluation of burnup produces a wrong results for FGR, grain size and so on. A wrong evaluation of the stress-strain state produces a wrong results for free volume in the rod. The evaluation of the inner pressure is a result of the coupling of free volume, FGR and temperature. Then we accept a good result when the previous steps were acceptable values. A good result of gas pressure is not so good with a wrong result of FGR; a good result of FGR is not so good with a wrong result of burnup; and so on. And finally a good result at EOL is not so good when the way to reach that value is deficient.

3.2.1. CASE 1 & 2, HALDEN IFA 534.14, RODS 18 & 19

The assembly IFA-534 contained 4 rods base irradiated for 4 cycles in the Swiss Goesgen PWR, up to a burnup of ~52 MWd/kg. The rods were re-instrumented with either pressure transducers or clad elongation detectors and re-irradiated between January and May 1998, at the Halden HBWR, to a final discharge burnup of ~55 MWd/kg (see the figure 1.1). The purpose of the experiment was to investigate the effect of fuel grain size on irradiation performance. The rods included in this data sets are the rods 18 (22 micron grain size) and 19 (8.5 micron grain size) fitted with pressure transducers from which Fission Gas Release (FGR) was measured both in-pile and during final PIE (“Post Irradiation Examination”).

The results of the experiment successfully demonstrated the effect of grain size on FGR. Nevertheless a third case with an intermediate grain size at BOL between 8.5 and 22 μm could be plausible in order to improve the FGR and grain size modelling [16]. At present the fission gas release model of BaCo does not include the influence of the grain size. Likewise BaCo is not including the modelling of a HBS. We find some differences between cases 3 and 4 due to the influence of grain size in other fuel phenomena but not for the FGR modelling.

	Data	BaCo
Average Burnup at EOL [MWd/kgU ₂]	~52	55.05
FGR [%] (from Halden Data)	3.05	1.24
FGR [%] (from PIE)	4.68	
Free volume [cm ³]	5.21	5.03
Gas Pressure at EOL [MPa]	2.347	2.90
Grain size in the intermediate zone [μm]	~24	~22
Grain size in pellet centre [μm]	25-31	~22

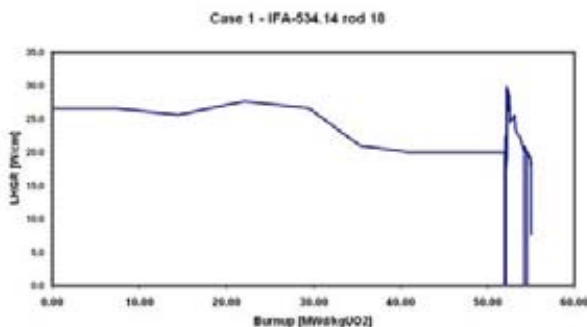


Figure 7: Power history for the rod 18 of IFA 534.14. (Power against Burnup).

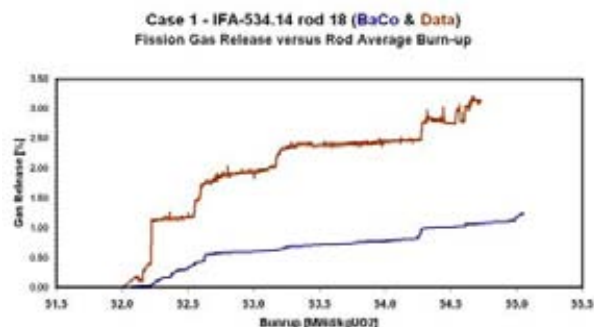


Figure 8: Fission gas release at the last step of the irradiation. Data (upper curve) and BaCo code calculation (lower curve) for the rod 18 of IFA 534.14.

3.2.1.1. Case 1, Halden IFA 534.14, rod 18

The pellets of the rod 18 from the IFA 534.14 had a grain size of 22 μm and the burnup at EOL was ~52 MWd/kgUO₂. The measurements used for the comparison were: Fission gas release and gas pressure at

EOL; pore distributions and free volume data are available. The table 1 shows the main results of the first case of CRP FUMEX II. The calculated burnup agrees very well with the experimental estimation (see table 1 and figure 7). Good agreements were found for grain size at EOL and the free volume in the fuel rod (see table 1). We under predict the FGR and over predict the inner gas pressure but an acceptable agreement was obtained (see figures 8, 9 and 10 and table 1). However there are two experimental values for FGR: the FGR estimated from gas pressure at the Halden reactor or the FGR from PIE. It was not clear that difference.

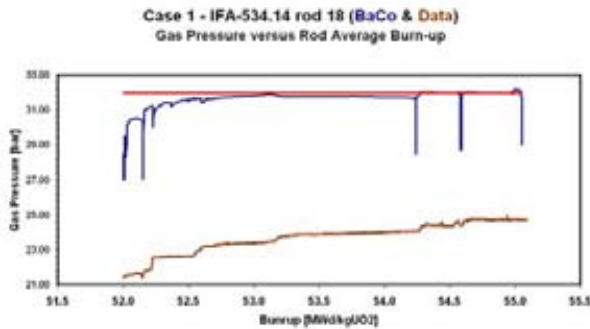


Figure 9: Gas pressure at the last step of the irradiation. Data (lower curve) and BaCo code calculation (upper curve) for the rod 18 of IFA 534.14 and coolant pressure (red curve).

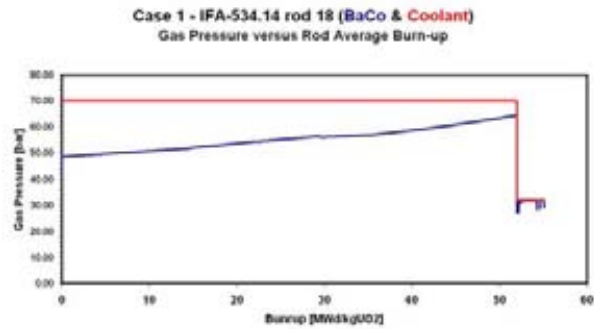


Figure 10: BaCo code calculation of the Gas pressure during the irradiation for the rod 18 of IFA 534.14 and coolant pressure (red curve).

3.2.1.2. Case 2, Halden IFA 534.14, rod 19

Measurements made for comparison: Fission gas release and gas pressure at EOL. Likewise grain size, pore distributions and free volume data are available. Main characteristics: Grain size 8.5 μm , Burnup at EOL ~ 52 MWd/kgUO₂.

Table 3: Case 2 comparisons		
	Data	BaCo
Average Burnup at EOL [MWd/kgUO ₂]	~ 52	55.05
FGR [%] (from Halden Data)	9.14	0.62
FGR [%] (from PIE)	8.89	
Free volume [cm ³]	5.35	5.03
Gas Pressure [MPa]	2.603	2.90
Grain size in the intermediate zone [μm]	~ 10	~ 8.5
Grain size in pellet centre [μm]	11-14	$\sim 8,6$

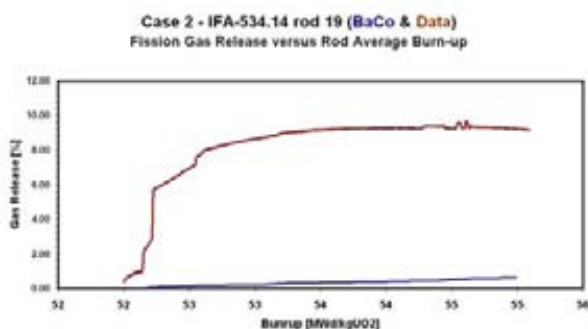


Figure 11: Fission gas release at the last step of the irradiation. Data (upper curve) and BaCo code calculation (lower curve) for the rod 19 of IFA 534.14.

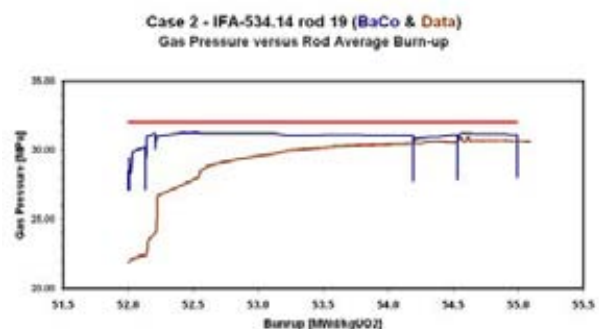


Figure 12: Gas pressure at the last step of the irradiation. Data (lower curve) and BaCo code calculation (upper curve) for the rod 19 of IFA 534.14 and coolant pressure (red curve).

The table 2 shows the main results for the second case of CRP FUMEX II. The calculated burnup agrees very well with the experimental estimation (the power history for the case 2 looks similar to 7). A good agreement was found for the inner gas pressure (see figure 12), grain size at EOL and the free volume

in the fuel rod (see the table 3). We under predict the FGR and a very low value was obtained (see figure 11). There are two experimental values for FGR. Both values appear to be equivalent with a reasonable uncertainty. The inner gas pressure at EOL appears as the best result for this case (see table 3). But it do not agree with the under prediction of FGR and the good result for the free volume. An under prediction of the inner gas pressure could be a best result by taking into account the coupling among inner pressure, FGR and volume.

3.2.2. CASE 3 & 4, HALDEN IFA 597.3, RODS 7 & 8

The fuel segments for the high burnup integral rod behaviour test IFA-597 were taken from a commercial fuel rod, which was irradiated in the Ringhals 1 BWR for approximately 12 years. A final rod averaged burnup of 52 MWd/kgUO₂ was achieved. The burnup at the location of the Halden segments was estimated as 59 MWd/kgUO₂, well beyond the formation of a HBS at the pellet rim. At the rim, the burnup was estimated as 130 MWd/kgUO₂. After commercial irradiation, PIE was performed at Studsvik.

Rods 8 and 9 were in IFA-597.2 (second loading) and irradiated in Halden for some 20 days in July 1995. After a small number of power ramps, rod 9 failed and the assembly withdrawn. During this time, useful data were generated on centreline temperature as a function of power.

Rod 9 was removed and replaced by rod 7. The assembly was returned to the reactor as IFA-597.3 (third loading); the irradiation started in January 1997 and continued to May of that year. Data obtained included, centreline temperature as a function of power and burnup, (rod 8), FGR from the increase in rod internal pressure (rod 8) and clad elongation (rod 7).

The assembly was discharged and transported to Kjeller for PIE. FGR values of 12.6 % and 15.8 % were measured from puncturing and gas extraction from rods 7 and 8 respectively.

3.2.2.1. Case 3, Halden IFA 597.3, rod 7

The table 3 shows the main results of the third case of CRP FUMEX II. The calculated burnup agrees very well with the experimental estimation (see figures 13). We use as input data the coupling of time-burnup against lineal power. We obtained good results for fission gas release, inner gas pressure and the free volume in the fuel rod (see the table 4).

We over predict the value for the clad elongation during irradiation (see the figures 14). The hypothesis of axial symmetry and modified plane strain (constant axial strain) produces a weak BaCo development when an axial strain is required. The quasi bidimensional approach does not reflect the pellet to pellet axial interaction. Due to those reasons we assumed that the present prediction is a good estimation of the cladding elongation.

Table 4: Case 3 comparisons

	Data	BaCo
Average Burnup at EOL [MWd/kgU]	61.62	61.62
FGR [%]	12.60	7.14
Gas Pressure [MPa]	1.68	3.20
Clad elongation	see plots	
Free volume [cm ³]	6.18	4.85

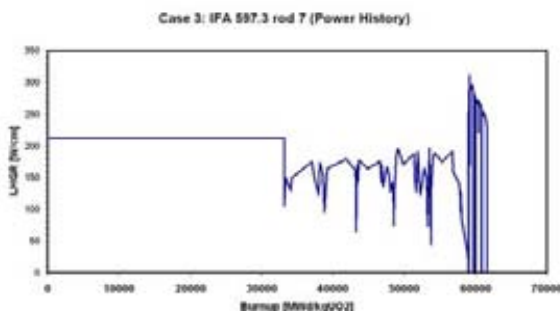


Figure 13: Power history for the rod 7 of IFA 597.3 (Power against Burnup).

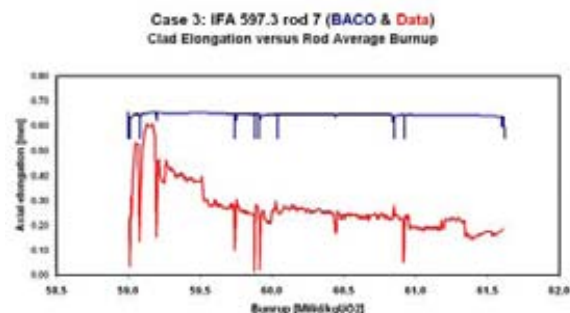


Figure 14: Clad elongation for the rod 7 of IFA 597.3 during the last step of the irradiation. BaCo calculations (upper curve) and experimental data (lower curve).

3.2.2.2. Case 4, Halden IFA 597.3, rod 8

The table 5 shows the main results of the fourth case of CRP FUMEX II. The calculated burnup agrees very well with the experimental data. We use the coupling of time-burnup against lineal power as input data. We find an excellent agreement between the measurements of the pellet centreline temperatures and our predictions (see the figures 15 y 16). We obtain good results for the inner gas pressure (see the figures 18) and for the free volume in the fuel rod.

The figure 17 shows the fission gas release calculated with the BaCo code and the data. The results at EOL agree very well with the experimental one. Nevertheless the data of that was derived from rod internal pressure measurements and that data are unreliable above 60.2 MWd/kgU₂ because its pressure limits was reached (see figure 18). The calculation and the derived data of FGR show different ways of converge for both curves to the derived value for FGR. The FGR after PIE at the Kjeller facilities, Norway, presents a value of 15.8 % (see the table 5).

	Data	BaCo
Average Burnup at EOL [MWd/kgU]	61.67	61.67
FGR [%] derived from measurements	7.55	7.08
FGR [%] PIE at Kjeller	15.80	
Gas Pressure [MPa]	2.06	2.58
Pellet centre temperature	see plots	
Free volume [cm ³]	5.93	5.54

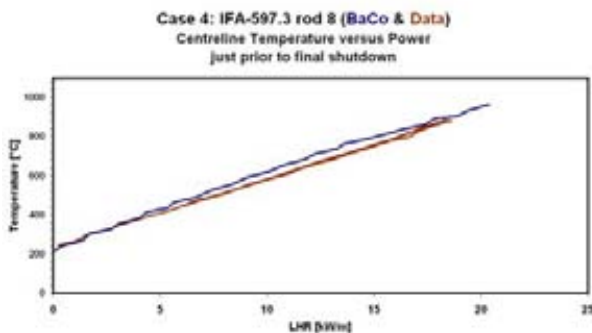


Figure 15: Centreline temperature versus linear power just prior to final shutdown for the rod 8 of IFA 597.3. BaCo calculations and Halden data.

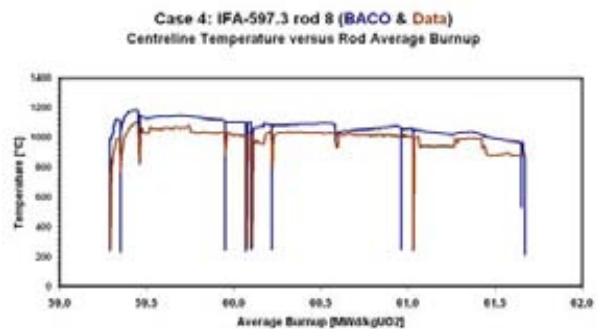


Figure 16: Centreline temperature during the second loading at the Halden reactor (rod 8 of IFA 597.3). BaCo calculations (upper curve) and Halden data.

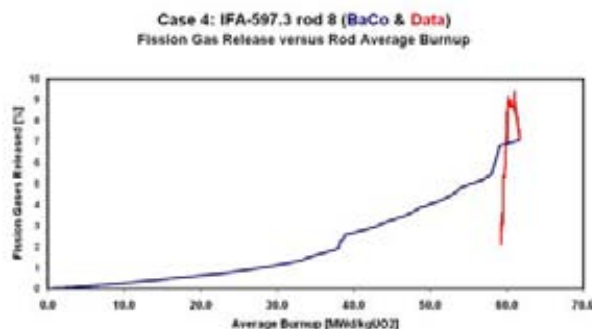


Figure 17: Fission gas release calculated with the BaCo code (blue curve) and data (red) during irradiation for the rod 8 of IFA 597.3

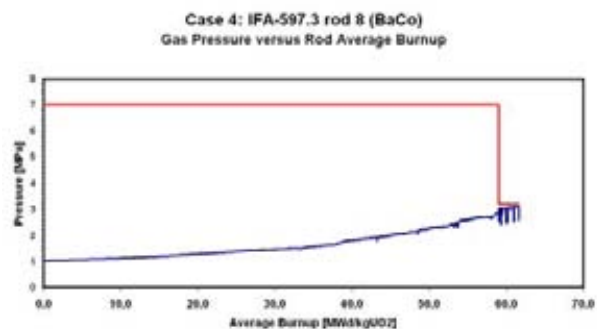


Figure 18: Gas pressure in the rod 8 of IFA 597.3 calculated with BaCo. Coolant pressure (red line) as reference.

3.2.2.3. Case 3 & 4, Conclusions

The BaCo code predictions are in good agreement with the measurements for the fuel rods of the IFA 597 (cases 3 and 4). The pellet centreline temperature looks as the strong point in these cases. Likewise we found reasonable good results for the requirements (FGR and gas pressure) in both cases. Nevertheless it was clearly shown how the final results of a calculation could be the consequences of different behaviours

where the ways followed by the modelling is not exactly the same that the measured during the irradiation. These kinds of results could be present when just is available the PIE at EOL.

3.2.3. CASE 5 & 6, HALDEN IFA 507, TF3 & TF5

At the Halden reactor a test at a power of ~15 MW, a test was performed to study the transient temperature response of the two thermocoupled rods for a rapid power increase. At the time of the experiment the burnup of these rods was ~18 MWd/kgUO₂. The experiment consisted of two parts, first to establish the steady state relationship between fuel temperature and shield position and secondly, a rapid withdrawal of the shield and continuous monitoring of the dynamic fuel temperature changes versus both shield position and time.

The approach adopted in the second part of the test was to lower the shield pass the thermocouple tips (~10 cm below) to suppress the local rating at these locations and pull it rapidly upwards to uncover the portion of the fuel column containing the central oxide thermocouples.

The rods were subjected to a reactor SCRAM and temperatures monitored by the two thermocouples. The 6 rod cluster in IFA-507 was surrounded by a moveable silver shield encased in stainless steel which was capable of reducing the power to about 50% of the full power rating. The rods in the cluster were of the BWR design with Zr-2 cladding two of which contained centreline thermocouples designated TF3 and TF5. The data are particularly valuable for modelling fuel transient temperatures during power increase.

3.2.3.1. Case 5, Halden IFA 507, TF3

We obtained a good result for the pellet centre temperature up to a power of 130 W/cm (~700°C) where the discrepancy is increased up to a value of $\Delta T < 200^\circ\text{C}$ at the top of the power ramp (see the figures 19 and 20). We appointed that our results are in a good correspondence with the measurements at BOL. We included in the figure 20 the temperatures during all the irradiation.

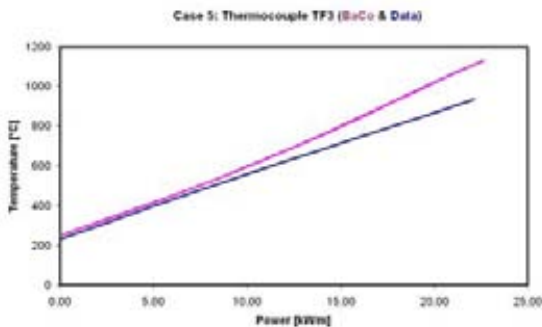


Figure 19: Steady state relationship between thermocouples and power for IFA-507. Data digitised from figure 2 of HWR-120. Thermocouple TF3 (Case 5). Fuel filled with 30% He and 70% Xe.

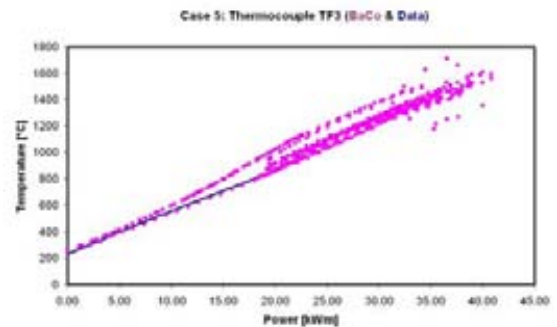


Figure 20: idem figure 19 including all the calculated points for the BaCo code during the irradiation.

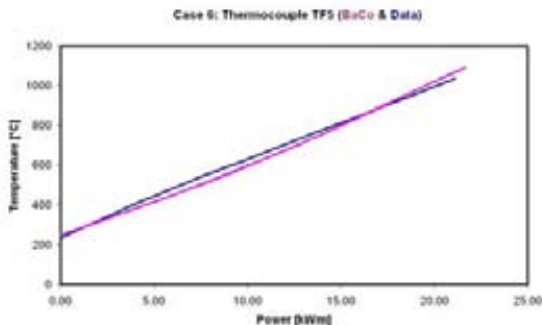


Figure 21: Steady state relationship between thermocouples and power for IFA-507. Data digitized from figure 2 of HWR-120. Thermocouple TF5 (Case 6). Fuel filled with 30% He and 70% Xe.

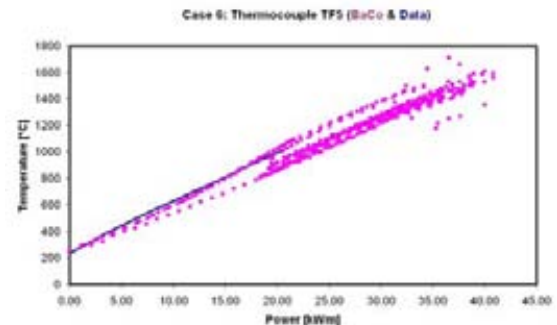


Figure 22: idem figure 21 including all the calculated points for the BaCo code during the irradiation.

3.2.3.2. Case 6, Halden IFA 507, TF5

We obtained an excellent agreement between the data and BaCo. No discrepancies were found between them (see the figures 21 and 22). We include in the figure 6.2 the temperatures during all the irradiation process. We obtained a very good agreement between the data and the code predictions. BaCo can reproduce with reasonable accuracy these types of transients.

3.2.4. OVERVIEW OF THE BACO CODE TEST CASES

We were pushing the limits of the BaCo code in order to estimate its present range of applicability. We need to keep the compatibility with the "Argentinean" fuels defined above, to test the real capabilities of our code and modelling in order to prepare BaCo for the challenge of the near future as the fuels for the CAREM reactor [17] and the Atucha II [13], the CARA fuel for the Argentinean reactors [1] and the next CRP FUMEX III of the IAEA, among others.

4. A 3D ANALYSIS – BACO + THE MECOM TOOLS

We complemented the BaCo results with 3D finite element (FEM) calculations. For this purpose we used two software packages developed at the Computational Mechanics (MeCom) Division at the Bariloche Atomic Centre (CAB), CNEA. One package, named "acd95" [18, 19] is a set of tools to generate two and three dimensional linear tetrahedral meshes we used to perform the discretization of the pellet volume. It contains also a set of programs to visualize scalar and vector fields on these meshes. These fields are the finite element solution obtained with the other package, "gpfep99" [20]. This is a software system written in FORTRAN 77 distributed in source form that allows the user to generate a FEM solver. With "gpfep99", the user has only to write a block of code in a subroutine to implement the physical model of interest. This block of code computes the FEM elemental matrix. In our case, we wrote approximately 300 lines of code to perform the calculation of the elastic displacements, the stresses and the von Mises equivalent stress. Some of the physical data needed to perform the FEM calculation are material parameters while others are obtained from the output of BaCo, like the temperature profile, the inner gas pressure, pellet to pellet axial stresses and main parameters of the pellet geometry. The coupling of BaCo, a quasi 2D code based on a finite differences scheme, and the MeCom tools, based on the method of finite elements, constitutes a complete system for 3D analysis of the stress-strain state of a nuclear fuel under irradiation.

We calculate the 3D stress-strain state of the UO₂ pellet at each time step calculation of the BaCo code. We obtain the stresses and the geometry of a fuel rod (that includes radial profiles and the shape). We obtain a good agreement between experiments of irradiation and calculations particularly for the pellet radial profile after irradiation [21]. We can define an "ad hoc" 3D pattern of cracks based on BaCo calculation and experimental data in order to enhance the results [11].

The BaCo code includes time dependent phenomena as creep and the opening, closure and healing of cracks in the fuel pellet during the irradiation among others. The creep of UO₂ and the dynamics of the cracks are the main mechanisms in BaCo to release stresses at the fuel pellet. The MeCom tools include the same laws for elasticity and thermal expansion than the BaCo code. A first approximation of the fuel rod behaviour is made by using the BaCo code. The treatment is quasi-bidimensional at this stage but using the complete set of models and options of BaCo. We generate the input data for the MeCom tools, in particular the geometry of the pellets and the boundary conditions for a particular time of the irradiation. The geometry of the pellet includes the evolution of the shape of the dishing, the shoulders, central hole and the deformations calculated by BaCo (see figure 23), and also we can included a crack pattern.

We assume that the cladding follows the pellet deformation at the points where we find contact between pellet and cladding. Here the assumption is that the cladding deformations are irreversible ones and the cladding do not return to its previous shape when the radial pellet deformation is reduced due to thermal changes (or power rate changes). Then the fuel rod profile is the cladding profile at the end of the irradiation. Nevertheless a good approach is done if we consider just the pellet radial profile and we assume a direct translation of the pellet shape to the cladding surface. This approach is a very good model for CANDU fuel where the cladding is collapsible by design and a pellet-cladding contact is done during all the irradiation.

The boundary conditions for the pellets are: 1) the pressure of the free inner gases in the fuel rod calculated with BaCo (also for the dishing of the pellet, the central hole and the inner surface of the cracks), 2) the coolant pressure, a datum for the lateral surface of the cylindrical pellet, and 3) the axial stresses calculated by BaCo for the pellet shoulders (see the Figure 23).

The temperature field is an input data. Porosity, crack pattern and thermal conductivity can be included into MeCom for a best estimation of its thermal behaviour. The result is the 3D deformed geometry of the pellets and cladding and the 3D maps of stresses and strains. At present, we are including elasticity, thermal expansion and cracks into the FEM solver (Finite Element Method solver included in the MeCom package).

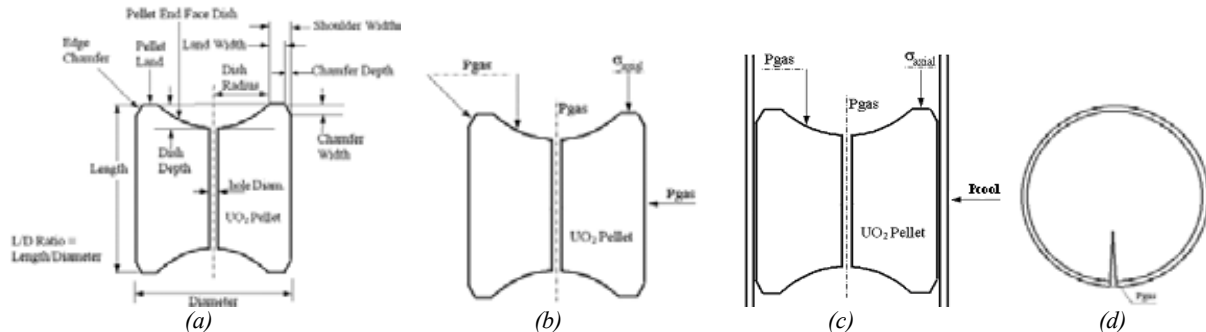


Fig. 23: (a) A fuel pellet and its main geometric parameters. (b) We show the boundary conditions condition of a fuel pellet without contact with the cladding and (c) when pellet-cladding are in contact. Where, P_{gas} is the pressure of the inner gases of the fuel rod, P_{cool} is coolant pressure and σ_{axial} is the axial pellet to pellet stress. (d) The last draw shows that at the inner surface of a crack the boundary condition is the gas pressure. We can include several radial cracks as the previous one in the pellet.

Taking into account the 3D simulation of a fuel pellet we perform a parametric analysis of the influence of the boundary conditions in the final result of the calculations. We vary the radial stresses at the lateral surface of the pellet among reasonable values over and under the inner gas (P_{gas}) and the coolant (P_{cool}) pressures. Likewise, we included the influence of an axial constrain, we do not allow the axial deformation of the pellet. We found that the influence of those variations produces a negligible influence in the pellet shape. The values of the ridging and the radial deformations show a small variation, for example the pellet ridge height results less than 1 μm of difference respect the original boundary conditions.

4.1. Analysis of the Fuel Pellet Geometry of WWER fuels

We can find the stresses and the radial profiles of a fuel rod and the shape of the cracked pellet under irradiation showing the bamboo effect and others 3D effects as the presence of the secondary ridge. Figure 24 shows four different pellets. The first one is the WWER fuel pellet of the cases 9 to 12 of the CRP FUMEX II [22]. The second one is the same cylinder without the central hole. The third is the previous one with dishing and chamfers at the top and at the bottom. And, finally, we repeat the third pellet including a central hole.

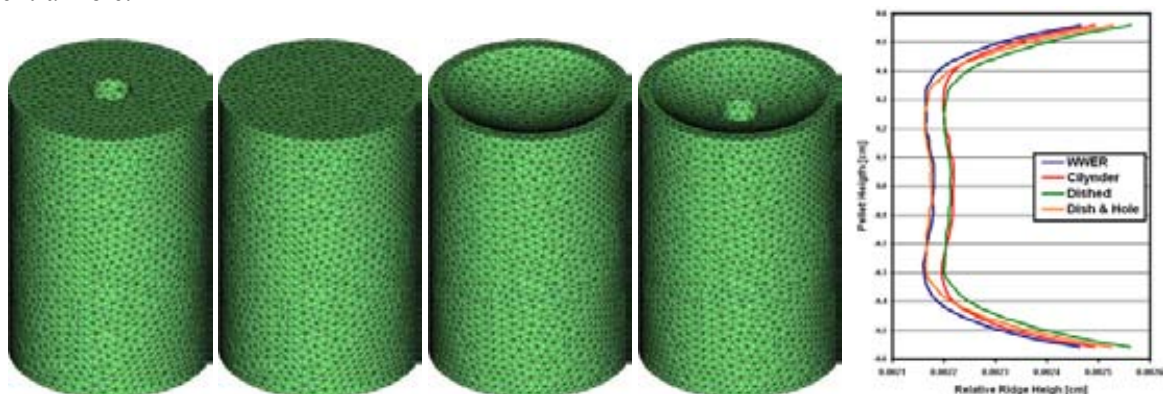


Fig. 24: Meshes for different pellets in order to start the analysis of the best geometric shape for a WWER fuel.

As interesting examples by using BaCo + MECOM we find the mentioned secondary ridge and the “bamboo” effect plus (see figure 19): (a) the reduction of the deformation when a hole is included in the centre of the pellets, and (b) the increment of ridging when a dishing is present. The WWER fuel pellet appears with minor ridging and radial deformations.

Figure 25 includes several cuts of the 3D maps for the deformations and the stresses of the same WWER fuel pellet. Here we see more clearly the reduction in the radial deformation, the reduction in the ridging among a decrement in the radial stresses between pellet and cladding and the secondary ridge. The von Mises equivalent stresses are greater at the lateral surface and at the hole of the pellet. Positive values of the tangential stresses (that means traction) are found at the periphery of the pellet (top, bottom and lateral surfaces with light colours) and negative ones (compression) at the central zone of the pellet (dark colours).

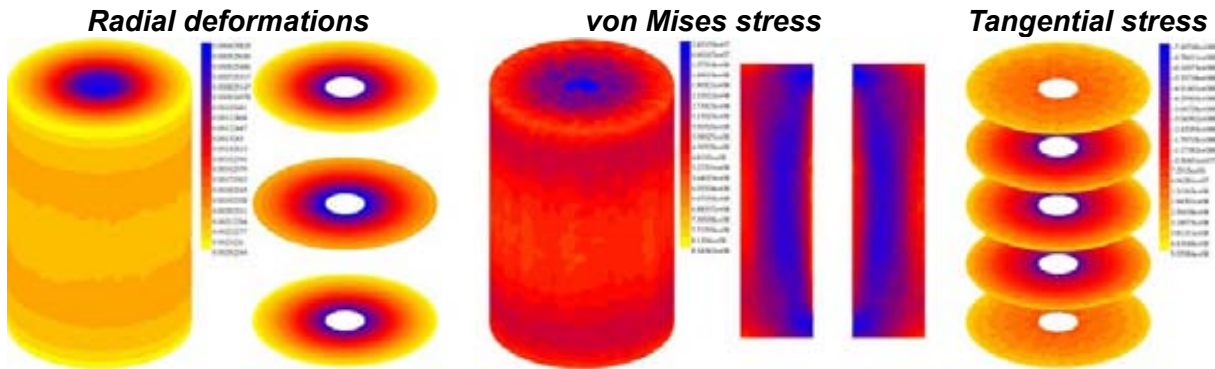


Fig. 25: Radial deformation from two different options of viewing, von Mises stresses (two point of view) and tangential stresses of a WWER fuel pellet.

We mentioned above that the optimization of fuel pellet geometry could be approached with the finding of the best l/d relation (length/diameter). It is confirmed by the agreement with several experiments present in the literature [23, 24]. We find as a result of BaCo that the ridging is reduced when l/d is reduced with a perfect agreement with experimental observation, at least for a qualitative purpose, including the presence or not of shoulders and/or chamfers in the pellet [25].

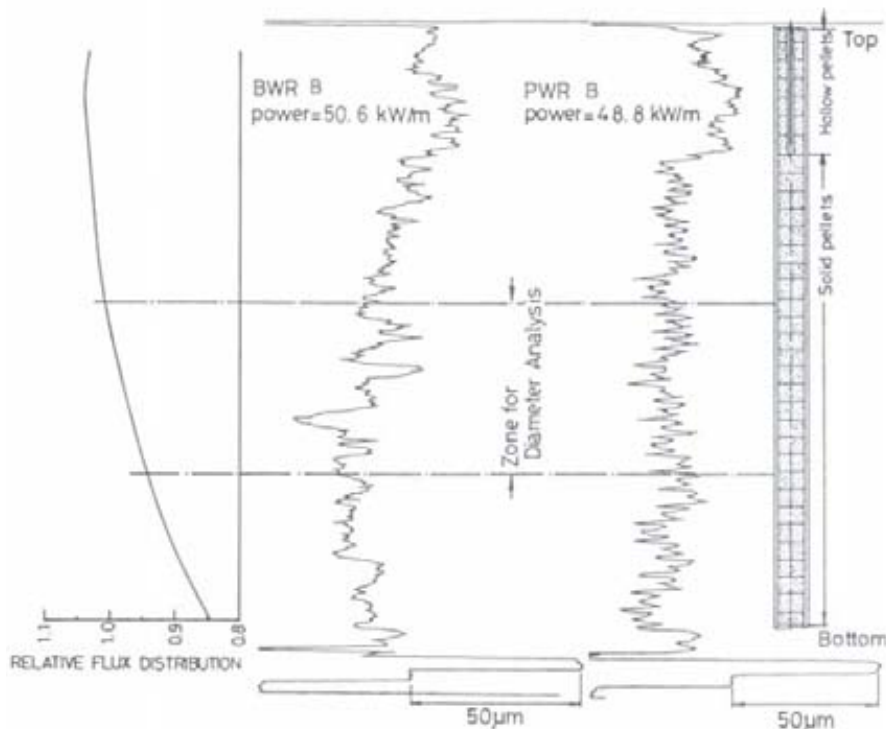


Figure 26: Rod profile of an experimental fuel at the Halden Reactor. At the top hollowed thermocoupled pellets are present [26].

4.2. 3D Test Cases

As an exercise of validation of our calculation we show in the figure 26 the radial profile of two experimental fuel rods irradiated at the Halden reactor [26]. Those rods have some hollowed pellets at the top of the fuel with the purpose to include a thermocouple. The figure includes the power profile of the rods. We see that the power is slightly greater than in the rest of the rod. Nevertheless we observe a reduction of

radial deformation of the fuel diameter and a reduction of the ridges height as we calculate with BaCo. It is interesting to mention that this validation test is obtained by using a non specific experiment. We observe the same behaviour at the figure 22 where an experimental comparison of hollow and solid pellets is included. Here PCMI is much reduced in the hollow pellet rod and, unlike the solid pellet rod, results in no plastic permanent deformation of the clad [27, 28].

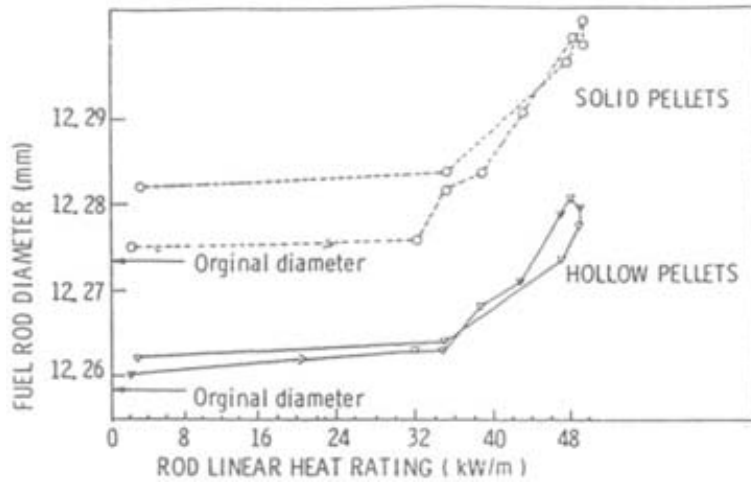


Figure 27: Clad average diameter versus linear heat rate for hollow and solid pellet rods in IFA-509 during a ramp at 3.0 MWd/kgUO₂ [27, 28].

4.3. Modelling cracks with BaCo and MeCom

The pellet is allowed to crack radially and axially; circumferential cracks are not included in the mechanical modelling but may be considered in the temperature calculation using relocation of pellet fragments and gap heat conductance. The criterion adopted for crack opening is that the pellet cracks when the tensile stress (radial or axial) is greater than the fracture strength σ_{fr} of the material [29]. As the description of the pellet has an axial symmetry and no dependence on the axial coordinate (at each axial section), cracks are smeared in the pellet [12]. By using this approximation we calculate the cracks evolution with BaCo and we determine the depth of cracks in the fuel in order to fix the 3D pellet geometry for MeCom. The figure 28 is an example of the crack depth evolution for an Atucha I fuel [13].

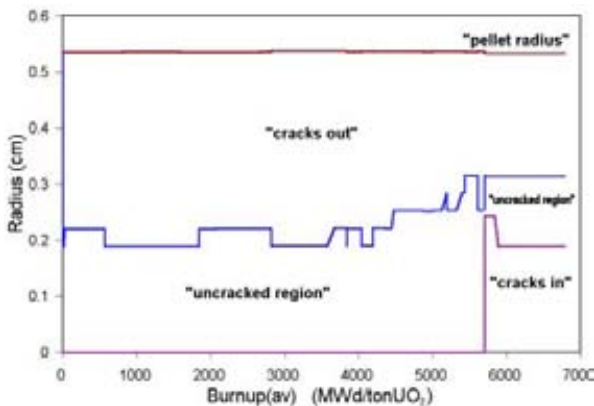


Figure 28: Depth of pellet cracks opened from the surface of the pellet (*cracks-out*) and cracks opened from de centre of the fuel (*cracks-in*).

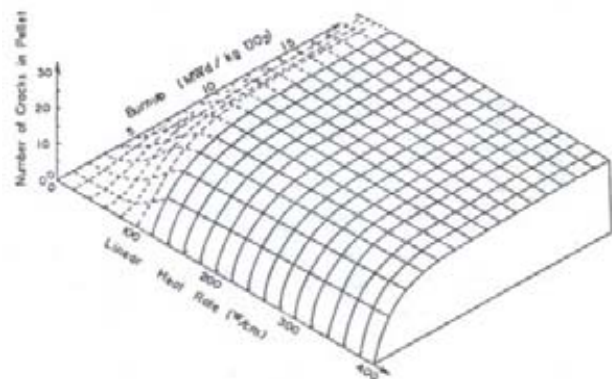


Figure 29: Numbers of cracks in pellet vs. burnup and linear heat rate [30].

It was experimentally defined the maximum number of cracks present in a fuel during irradiation, see figure 29 [30], and a common pattern adopted for the cracks (see figure 30) at different steps of the irradiation. This pattern and amount of cracks were enough to release stresses via fracture of the UO₂ pellet [30]. In the references [11] and [12] we showed that the presence of a single crack at the top of the pellet reduces stresses at the pellet surface, concentrate stresses at the vertex of the cracks and increase the pellet ridging with an improvement of the accuracy of the comparison between experimental data and our

calculations. The figure 29 includes the plot with the number of cracks present in a fuel pellet as a function of the power and the burnup [30]. We see saturation when stress release is done due to cracking of the pellet. The figure 30 shows the progression of a pellet cracks for three different stage of irradiation and the progress of an empirical cracks pattern based on the Halden experience [30]. These radial cracks are the basics of our “ad hoc” 3D crack pattern. The figure 7 shows the pellet profile calculated with a single crack and without one.

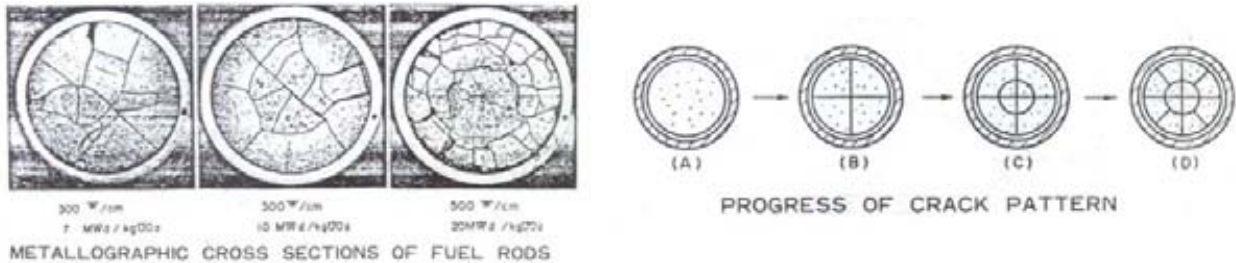


Figure 30: Experimental crack pattern at different irradiation and an empirical progression of the pattern based on the HRP experience (HPR-229/23, [30]).

At present we are defining a mesh for the 3D calculation with the inclusion of radial cracks in order to reduce the pellet stresses. The figure 31 shows the meshes used for the analysis of the influence of cracks on a fuel pellet. The first cylindrical pellet is a reference. The dished pellet shows an increment in the ridge height but it reduces the pellet to pellet interaction. It is clearly shown the reduction of the radial deformation and ridge height of the hollowed pellet. The single crack at the top of the pellet produces an increment of the ridging close to the crack. The pellet with a transversal crack keeps the maximum value of radial deformation as the previous pellet but it increments the deformation at the middle of the pellet. It looks as a translation of the first cylinder. The last pellet introduces 7 cracks at the top and 7 cracks at the bottom (rotated the half of the angle between the cracks of the top). The result is a realistic pellet ridging.

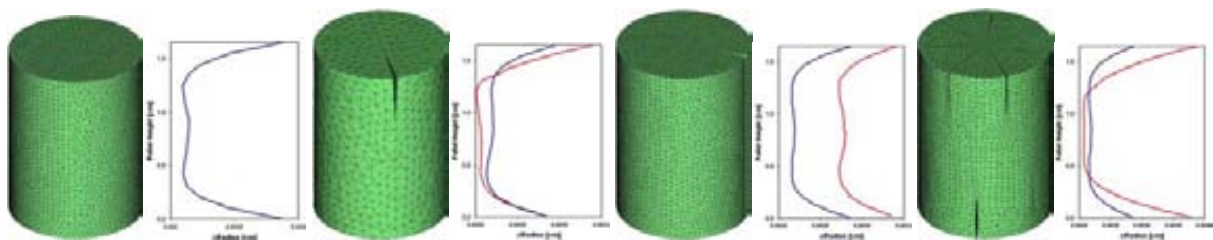


Figure 31: Meshes for different pellets and different crack approach and its radial profile. The red curves are the pellet profile for each pellet and the blue one is the profile of the cylindrical pellet as a reference.

We start with 1 crack and we increase by 1 the number of cracks in order to obtain a hoop stress (or tangential stress) under the σ_{fr} of the UO_2 . The figure 32 includes a curve of the maximum hoop stress calculated by using a mesh with pre-defined number of cracks from 0 to 7. We find that 6 is the number of radial cracks enough to reduce hoop stress under the value of the σ_{fr} .

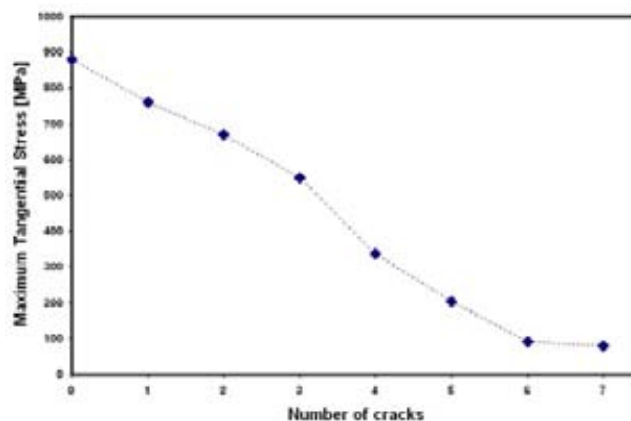


Figure 32: Maximum tangential stress in the pellet against the number of radial cracks in the pellet.

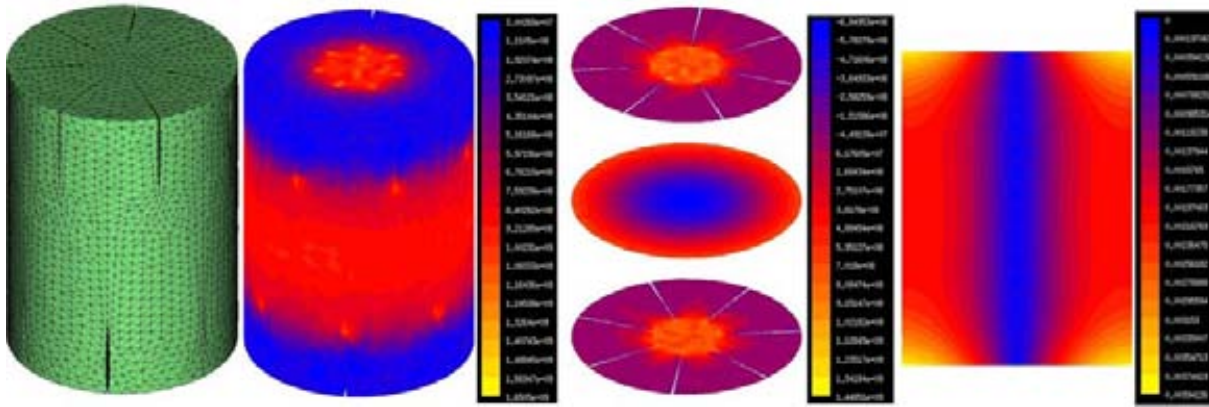


Figure 33: Finite element mesh, von Mises equivalent stress, tangential stresses (hoop stress) at three heights and radial deformation for a cracked fuel.

The details of the calculations made by using a fuel pellet with 7 cracks (at the top and 7 at the bottom) produce the 3D map of stresses of the figure 33. The stress release produced for these realistic “ad hoc” cracks is represented for the von Mises equivalent stress and the hoop stress of the figure 33. The influence of the cracks is of most importance in the 1/3 top and at the 1/3 bottom of the pellet. We see that the stress in those regions where the cracks are opened presents a maximum value under the σ_r of the UO_2 . The axial profile obtained with this assumption is the 3D radial map of deformations of the figure 33. The pellet ridge height is greater than the value obtained without the stress release via cracks [11] as we expected.

5. EXPERIMENTAL SUPPORT OF THE CARA FUEL DESIGN

We mention as the BaCo code can be used as a frame for the analyses of experiments and for “computational experiments”. Then the first steps of an experimental support can be assisted by a digital tool as the BaCo code [4]. We identify the first steps of the experimental support of the CARA fuel design as follows:

- a) the identification of the weak points of the design,
- b) to identify the most demanding condition of the real operation,
- c) the searching of similar irradiations of our design in the open literature, international programs or institutions,
- d) the simulation with the code of the weak points under demanding conditions,
- e) to define a set of irradiations in order to check the weak points (a) under the most demanding conditions (b),
- f) to analyze the irradiation by comparison with our code simulation,
- g) to tune the code with the new experimental data,
- h) to include the experiment in our database of irradiations (and analyze to share the irradiation with the open database as the IFPE).

Nevertheless the result of the previous step could be that we do not need to perform an irradiation experiment in order to test the fuel rod or at least a strong reduction of the number of irradiations. An example of the application of the BaCo code in the fuel rod design of an advanced PHWR MOX fuel is included in the reference [31] where MOX prototypes were irradiated in the Petten reactor. The preparation of the irradiation, the analyses of the performance and the PIE were made with BaCo.

The CARA fuels reduce the temperature of operation. Then a decrement of the stresses in the fuel rod with respect to the present Atucha and Embalse ones is done. Then we could assume that we do not need graphite at the inner surface of the cladding in order to reduce the tangential stress over the inner surface of the cladding (or as a getter for fission products) and to neglect a PCS-SCC failure. The parametric analysis of the CARA fuel rods performed with the BACO code shows that the pellet radius is the most sensitive parameter. The variations in the pellets radius, when we are taking into account the tolerances of the Atucha I and Embalse NPPs, results in a maximum dispersion of pellet centre temperature, deformations, pressure and stresses, specially the hoop stress between pellet and cladding. Therefore, we must study the influence of these variations of parameters and its relation with the failure mechanisms and SCC-PCI

(“Stress Corrosion Cracking – Pellet Cladding Mechanical Interaction”) during irradiation in order to determine if we need to cover with graphite the inner surface of the cladding.

After some analyses of the most complete set of irradiation experiments of the CARA fuel [5], a more realistic proposal of an experimental support was analyzed with the OECD Halden Reactor Project (Norway) [6]. At present we are evaluating a similar proposal of the irradiation of four CARA fuel rods from a set of eight rods. The set of fuel prototypes for the first experiments of irradiation of CARA fuel rods were to simulate extreme conditions of irradiation. Four fuel rods will be kept under a base irradiation of 20 days including power cycle. The base power level and the cycling will be enough to assert that stress reversal at the inner surface of the cladding. A power ramp will be performed after the preconditioning irradiation. The maximum power level will be up to a value of 430 W/cm. That value is comparable to the most severe power ramp in Atucha I (see figure 1).

First experiment (a test rig with two fuel rods):

- 1) A normal CARA fuel rod with a length and an enrichment according with the irradiation device.
- 2) A fuel rod as the last one with a pellet radius enough to simulate the swelling at end of life (~20000 MWd/tonU) including Xe as filling gas (80 % Xe and 20 % He) in order to simulate the influence of fission gas release in thermal conductivity of the gap pellet-cladding (see figure 4).

Second experiment (a test rig with two fuel rods) depending of the results of the first experiment (with or without graphite):

- 1) A normal fuel rod as (1) with dense (or normal) pellets, Xe as filling gas and synthetic products (CsI and Mo) in order to simulate the corrosive material at end of life (~20000 MWd/tU).
- 2) A fuel rod similar to the rod (3). The pellets will include failures (like “chips”) in the surface and dishing enough to reproduce an extreme cracking in order to enhance the production of cracks in the cladding.

Centre pellet temperature and axial deformations will be monitored during irradiation. The experiments must include a complete PIE after irradiation. After those irradiations we will analyze the irradiation of single rods up to ~20000 MWd/tonU or to go for the irradiation of a complete CARA bundle [7].

6. CONCLUSIONS

We find an excellent agreement with experimental data for the calculation of burnup, fission gas release and inner gas pressure. A good agreement is found for dimensional changes as the diameter and the length of the fuels. Then we can assume that the physical laws included in BaCo and the boundary conditions that we will use constitute a reasonable approach as a seed for the 3D calculations of fuel rods with the MeCom tools. The main assumption for the analyses of the 3D pellet simulation is that we have a direct translation from the pellet profile to the cladding one. Here we find an excellent qualitative agreement in particular for the pellet ridging and the secondary ridge. The inclusion of a pattern of crack in order to release stresses in the pellet enhance our simulation providing an excellent agreement with the experimental data due to the increment of the pellet ridging. We are obtaining a very good dimensional agreement taking into account experiments of irradiations from the Halden Reactor Project.

It is interesting to mention that the variation of the classical WWER fuel pellet shape, as dishing and a solid centre does not mean an improvement of the stress-strain behaviour. This analysis is being taken into account in the design of our CARA and CAREM fuels for Argentine reactors as Atucha I, Embalse and CAREM NPP's. The BaCo code appears as good tools for the fuel rod design.

The goal of the CARA fuel element is the performance improvement for those reactors and the enhancing of their normal operative conditions. The mechanical solution proposal by the CARA design is very innovative (doubling length, not welding on sheaths) respect to the evolutionary solution proposal by CANFLEX. Indeed, the CARA open a new way for built FE for PHW reactors, allowing extended burnup, thermal-hydraulic margins and a negative void reactivity.

An experimental support for the CARA fuel design was presented in order to perform a strong test of behaviour under irradiation and a specific validation of BACO. We want to check the needs of CANLUB® when we reduce the linear power of the fuel. The decrement of linear expansion and deformations, the stability of the pellet geometry, the absence of a central hole and columnar grains during irradiation, indicate us that we could to reject an internal covering of the cladding with graphite keeping the safety margins.

All these advantages push to a new version of the CARA fuel with a near zero or negative void coefficient. The restart of the Atucha II NPP project requires updated safety system in agreement with the best international practices and the broadly accepted design approaches.

We mentioned the use of the BaCo code as a frame for the analysis of irradiation test. We presented Halden cases in order to illustrate the direct applicability in our fuel development of the lessons from our participation international round robin test as the CRP FUMEX I and II. We included in the paper the troubles that we found in the interpretation of irradiation data and PIE for the direct use of the code. Likewise the applicability of specific irradiation of the HRP in different areas that the original ones.

An approach to the troubleshooting and the hopes of the designers, code programmers, modellers and code users was presented in this paper with the simple intention to contribute with a different point of view in the area of the experimental irradiation tests and advanced instrumental devices.

ACKNOWLEDGEMENTS

Halden Reactor Project who kindly made available for us its valuable experimental data.

CNEA and IAEA for the continuous support.

Dr. H. E. Troiani who review this paper and made several suggestions.

REFERENCES

- [1] D. Brasnarof, A.C. Marino, P.C. Florido, J. Bergallo, H. Daverio, H. Gonzalez, A. Martín Ghiselli, H.E. Troiani, C. Muñoz, D. Bianchi, D. Banchick, M. Giorgis, M. Markiewicz, “*CARA development: An Argentinean fuel cycle challenge*”, 9th International Conference on CANDU Fuel, Ramada on The Bay, Belleville, Ontario, Canada, September 18-21, 2005.
- [2] A. C. Marino, and D.O. Brasnarof, “*Modelling and Design of advanced PHWR fuels*”, IAEA’s Technical Meeting on “Pressurised Heavy Water Reactor (PHWR) Fuel Modelling”, Mumbai, India, December 5-8, 2006.
- [3] A. C. Marino, E. J. Savino and S. Harriague, “*BACO (BARRA COMBUSTIBLE) Code Version 2.20: a thermo-mechanical description of a nuclear fuel rod*”, Journal of Nuclear Materials, Vol. 229, April II, p155-168 (1996).
- [4] A.C. Marino, “*Strategy for the Development of BaCo: a Fuel Rod Behaviour Simulation Code*”, International Conference on Advances in Nuclear Materials: Processing, Performance and Phenomena (ANM 2006) & Conference on “Materials Behaviour: Far from Equilibrium” (MBFE), Mumbai, India, December 12-16, 2006. To be published in Journal of Nuclear Material.
- [5] A.C. Marino and J.E. Bergallo, “*Propuesta de irradiación de barras combustibles CARA*”, XXVI Reunión Científica de la Asociación Argentina de Tecnología Nuclear (AATN 99), November 9-12, 1999, Bariloche, Argentina.
- [6] A.C. Marino, J.E. Bergallo and F. Barrera, “*Irradiación experimental de barras combustibles CARA en el Reactor OECD Halden*”, paper 68, XXVII Reunión Científica de la Asociación Argentina de Tecnología Nuclear (AATN 2000), September 22-24, 2000, Buenos Aires, Argentina.
- [7] A.C. Marino, J.E. Bergallo and P. Adelfang, “*Irradiación experimental de un elemento combustible CARA en el Reactor NRU (Canadá)*”, paper 124, XXVII Reunión Científica de la Asociación Argentina de Tecnología Nuclear (AATN 2000), November 22-24, 2000, Buenos Aires, Argentina.
- [8] S.J. Palleck, K-S. Sim, M.R. Floyd, J.H. Lau and F.J. Doria, “*Bruce CANFLEX-LVFR fuel qualification*”, 9th International Conference on CANDU Fuel, Ramada on The Bay, Belleville, Ontario, Canada, September 18-21, 2005.
- [9] “*WIMS-D: A Neutronic Code for Standard Lattice Physics Analysis*”, AEA Technology, 1986.
- [10] A. C. Marino, “*Probabilistic Safety Criteria on High Burnup HWR Fuels*”, IAEA Technical Committee Meeting on "Technical and Economic Limits to Fuel Burnup Extension", IAEA-TECDOC-1299, Bariloche, Argentina, November 15-19, 1999.
- [11] A. C. Marino and G. L. Demarco, “*3D Assessments of the Cracked UO₂ Pellets Behaviour*”, 2006 International Meeting on LWR Fuel Performance, "NUCLEAR FUEL: Addressing the future", Top-Fuel 2006, Salamanca, Spain, October 22-26, 2006.
- [12] A.C. Marino, “*Crack and dishing evolution models and PCI-SCC considerations for fuel pellets in a quasi-bidimensional environment*”, Les Journées de Cadarache 2004, International Seminar on Pellet-Clad Interaction in Water Reactor Fuels, Aix en Provence, France, March 9-11, 2004.
- [13] A.C. Marino and P.C. Florido, “*High Power Ramping in Commercial PHWR Fuel at Extended Burnup*”, Nuclear Engineering & Design 236 (2006) 1371-1383.

- [14] J. Killeen, V. Inozemtsev and J. Turnbull, “*Fuel Modelling at Extended Burnup: IAEA Coordinated Research Project FUMEX-IP*”, 2006 International Meeting on LWR Fuel Performance, "NUCLEAR FUEL: Addressing the future", Top-Fuel 2006, Salamanca, Spain, October 22-26, 2006.
- [15] “*Fuel modelling at extended burnup*”, Report of the Co-ordinated Research Programme on Fuel Modelling at Extended Burnup – FUMEX, 1993-1996, IAEA, IAEA-TECDOC-998.
- [16] W. Hering, “*The KWU fission gas release model for LWR fuels rods*”, Journal of Nuclear Material 114 (1983) 41-49.
- [17] “*Status of advanced Light Water Reactor designs, 2004*”, IAEA-TECDOC-1391, May 2004.
- [18] M. de Oliveira et al., “*An Object Oriented Tool for Automatic Surface Mesh Generation using the Advancing Front Technique*”, Latin American Applied Research 27 pp. 39-49 (1997).
- [19] P. Zavattieri, G. Buscaglia and E. Dari, “*Finite element mesh optimization in three dimensions*”, Latin American Applied Research, 26 pp. 233-236 (1996).
- [20] G. Buscaglia et al., “*Un programa general de elementos finitos en paralelo*”, 6° Congreso Argentino de Mecánica Computacional, MECOM'99, Mendoza, Argentina, September 1999.
- [21] A.C. Marino, G.L. Demarco and P.C. Florido, “*3D Assessments for Design and Performance Analysis of UO₂ Pellets*”, 9th International Conference on CANDU Fuel “Fuelling a Clean Future”, 2005 September 17-21, Ramada Inn on the Bay, Belleville, Canada.
- [22] A.C. Marino and G.L. Demarco, “*An approach to WWER fuels with BaCo*”, 7th International Conference on WWER Fuel Performance, Modelling and Experimental Support, September 17-21, 2007, Albena near Varna, Bulgaria.
- [23] I. J. Hastings, T.J. Carter, R. Da Silva, P.J. Fehrenbach, D.G. Hardy and J.C. Wood, “*CANDU fuel performance: Influence of fabrication variables*”, IAEA-CNEA International Seminar on Heavy Water Reactor Fuel Technology, AECL MISC 250 (1983), S. C. de Bariloche (1983).
- [24] T.J. Carter, “*Experimental Investigation of Various Pellet Geometries to Reduce Strains in Zirconium Alloy Cladding*”, Nuclear Technology 45 pp. 166-176 (1979).
- [25] A.C. Marino, G.L. Demarco and P.C. Florido, “*3D Assessments for Design and Performance Analysis of UO₂ Pellets*”, 9th International Conference on CANDU Fuel “Fuelling a Clean Future”, 2005 September 17-21, Ramada Inn on the Bay, Belleville, Canada.
- [26] M. Ichikawa et al., “*Preliminary results from power ramping experiments by LWR Rigs*”, Enlarged Halden Programme Group Meeting, Løen, Norway, HRP-305/8, 1985.
- [27] H.U. Stall, “*Radial and Axial Deformation Behaviour of Solid and Hollow Fuel Rods during Base Irradiation and Power Ramp in IFA-509.2*”, HWR-49 May 1982.
- [28] OECD Documents, Review of Nuclear Fuel Experimental Data prepared by J. A. Turnbull, January 1995 (<http://www.oecdnea.org/html/science/docs/pubs/nea0197-fuel.pdf>).
- [29] J.R. Matthews, “*Mechanical properties and diffusion data for carbide and oxide fuels. Ceramic data contribution*”, Atomic Energy Research Establishment, Harwell, UKEA, AERE-M 2643 (1974).
- [30] S. Shimada et al., “*Analysis of fuel relocation using in-pile data from IFA-211 and IFA-410*”, Enlarged Halden Programme Group Meeting, Hankø, Norway, 1979, HRP-229/23.
- [31] A.C. Marino, E.E. Pérez & P. Adelfang, “*Irradiation of Argentine MOX fuels. Post-irradiation results and experimental analysis with the BACO code*”, J.Nuc.Mat. Vol. 229, April II, 1996.



Where to order IAEA publications

In the following countries IAEA publications may be purchased from the sources listed below, or from major local booksellers. Payment may be made in local currency or with UNESCO coupons.

Australia

DA Information Services, 648 Whitehorse Road, Mitcham Victoria 3132
Telephone: +61 3 9210 7777 • Fax: +61 3 9210 7788
Email: service@dadirect.com.au • Web site: <http://www.dadirect.com.au>

Belgium

Jean de Lannoy, avenue du Roi 202, B-1190 Brussels
Telephone: +32 2 538 43 08 • Fax: +32 2 538 08 41
Email: jean.de.lannoy@infoboard.be • Web site: <http://www.jean-de-lannoy.be>

Canada

Bernan Associates, 4611-F Assembly Drive, Lanham, MD 20706-4391, USA
Telephone: 1-800-865-3457 • Fax: 1-800-865-3450
Email: order@bernan.com • Web site: <http://www.bernan.com>

Renouf Publishing Company Ltd., 1-5369 Canotek Rd., Ottawa, Ontario, K1J 9J3
Telephone: +613 745 2665 • Fax: +613 745 7660
Email: order.dept@renoufbooks.com • Web site: <http://www.renoufbooks.com>

China

IAEA Publications in Chinese: China Nuclear Energy Industry Corporation, Translation Section, P.O. Box 2103, Beijing

Czech Republic

Suweco CZ, S.R.O. Klecakova 347, 180 21 Praha 9
Telephone: +420 26603 5364 • Fax: +420 28482 1646
Email: nakup@suweco.cz • Web site: <http://www.suweco.cz>

Finland

Akateeminen Kirjakauppa, PL 128 (Keskuskatu 1), FIN-00101 Helsinki
Telephone: +358 9 121 41 • Fax: +358 9 121 4450
Email: akatilaus@akateeminen.com • Web site: <http://www.akateeminen.com>

France

Form-Edit, 5, rue Janssen, P.O. Box 25, F-75921 Paris Cedex 19
Telephone: +33 1 42 01 49 49 • Fax: +33 1 42 01 90 90 • Email: formedit@formedit.fr

Lavoisier SAS, 14 rue de Provigny, 94236 Cachan Cedex
Telephone: + 33 1 47 40 67 00 • Fax +33 1 47 40 67 02
Email: livres@lavoisier.fr • Web site: <http://www.lavoisier.fr>

Germany

UNO-Verlag, Vertriebs- und Verlags GmbH, August-Bebel-Allee 6, D-53175 Bonn
Telephone: +49 02 28 949 02-0 • Fax: +49 02 28 949 02-22
Email: info@uno-verlag.de • Web site: <http://www.uno-verlag.de>

Hungary

Librotrade Ltd., Book Import, P.O. Box 126, H-1656 Budapest
Telephone: +36 1 257 7777 • Fax: +36 1 257 7472 • Email: books@librotrade.hu

India

Allied Publishers Group, 1st Floor, Dubash House, 15, J. N. Heredia Marg, Ballard Estate, Mumbai 400 001,
Telephone: +91 22 22617926/27 • Fax: +91 22 22617928
Email: alliedpl@vsnl.com • Web site: <http://www.alliedpublishers.com>

Bookwell, 24/4800, Ansari Road, Darya Ganj, New Delhi 110002
Telephone: +91 11 23268786, +91 11 23257264 • Fax: +91 11 23281315
Email: bookwell@vsnl.net • Web site: <http://www.bookwellindia.com>

Italy

Libreria Scientifica Dott. Lucio di Biasio "AEIOU", Via Coronelli 6, I-20146 Milan
Telephone: +39 02 48 95 45 52 or 48 95 45 62 • Fax: +39 02 48 95 45 48

Japan

Maruzen Company, Ltd., 13-6 Nihonbashi, 3 chome, Chuo-ku, Tokyo 103-0027
Telephone: +81 3 3275 8582 • Fax: +81 3 3275 9072
Email: journal@maruzen.co.jp • Web site: <http://www.maruzen.co.jp>

Korea, Republic of

KINS Inc., Information Business Dept. Samho Bldg. 2nd Floor, 275-1 Yang Jae-dong SeoCho-G, Seoul 137-130
Telephone: +02 589 1740 • Fax: +02 589 1746
Email: sj8142@kins.co.kr • Web site: <http://www.kins.co.kr>

Netherlands

Martinus Nijhoff International, Koraalrood 50, P.O. Box 1853, 2700 CZ Zoetermeer
Telephone: +31 793 684 400 • Fax: +31 793 615 698 • Email: info@nijhoff.nl • Web site: <http://www.nijhoff.nl>

Swets and Zeitlinger b.v., P.O. Box 830, 2160 SZ Lisse
Telephone: +31 252 435 111 • Fax: +31 252 415 888 • Email: info@swets.nl • Web site: <http://www.swets.nl>

New Zealand

DA Information Services, 648 Whitehorse Road, MITCHAM 3132, Australia
Telephone: +61 3 9210 7777 • Fax: +61 3 9210 7788
Email: service@dadirect.com.au • Web site: <http://www.dadirect.com.au>

Slovenia

Cankarjeva Založba d.d., Kopitarjeva 2, SI-1512 Ljubljana
Telephone: +386 1 432 31 44 • Fax: +386 1 230 14 35
Email: import.books@cankarjeva-z.si • Web site: <http://www.cankarjeva-z.si/uvoz>

Spain

Díaz de Santos, S.A., c/ Juan Bravo, 3A, E-28006 Madrid
Telephone: +34 91 781 94 80 • Fax: +34 91 575 55 63 • Email: compras@diazdesantos.es
carmela@diazdesantos.es • barcelona@diazdesantos.es • julio@diazdesantos.es
Web site: <http://www.diazdesantos.es>

United Kingdom

The Stationery Office Ltd, International Sales Agency, PO Box 29, Norwich, NR3 1 GN
Telephone (orders): +44 870 600 5552 • (enquiries): +44 207 873 8372 • Fax: +44 207 873 8203
Email (orders): book.orders@tso.co.uk • (enquiries): book.enquiries@tso.co.uk • Web site: <http://www.tso.co.uk>

On-line orders:

DELTA Int. Book Wholesalers Ltd., 39 Alexandra Road, Addlestone, Surrey, KT15 2PQ
Email: info@profbooks.com • Web site: <http://www.profbooks.com>

Books on the Environment:

Earthprint Ltd., P.O. Box 119, Stevenage SG1 4TP
Telephone: +44 1438748111 • Fax: +44 1438748844
Email: orders@earthprint.com • Web site: <http://www.earthprint.com>

United Nations (UN)

Dept. 1004, Room DC2-0853, First Avenue at 46th Street, New York, N.Y. 10017, USA
Telephone: +800 253-9646 or +212 963-8302 • Fax: +212 963-3489
Email: publications@un.org • Web site: <http://www.un.org>

United States of America

Bernan Associates, 4611-F Assembly Drive, Lanham, MD 20706-4391
Telephone: 1-800-865-3457 • Fax: 1-800-865-3450
Email: order@bernan.com • Web site: <http://www.bernan.com>

Renouf Publishing Company Ltd., 812 Proctor Ave., Ogdensburg, NY, 13669
Telephone: +888 551 7470 (toll-free) • Fax: +888 568 8546 (toll-free)
Email: order.dept@renoufbooks.com • Web site: <http://www.renoufbooks.com>

Orders and requests for information may also be addressed directly to:

Sales and Promotion Unit, International Atomic Energy Agency

Vienna International Centre, PO Box 100, 1400 Vienna, Austria
Telephone: +43 1 2600 22529 (or 22530) • Fax: +43 1 2600 29302
Email: sales.publications@iaea.org • Web site: <http://www.iaea.org/books>